

AD-A062 790

TRW DEFENSE AND SPACE SYSTEMS GROUP REDONDO BEACH CALIF F/G 9/1
PROCESS-ORIENTED, HIGH-INJECTION CIRCUIT MODELS FOR INTEGRATED --ETC(U)
JAN 78 J CHOMA

N00014-77-C-0043

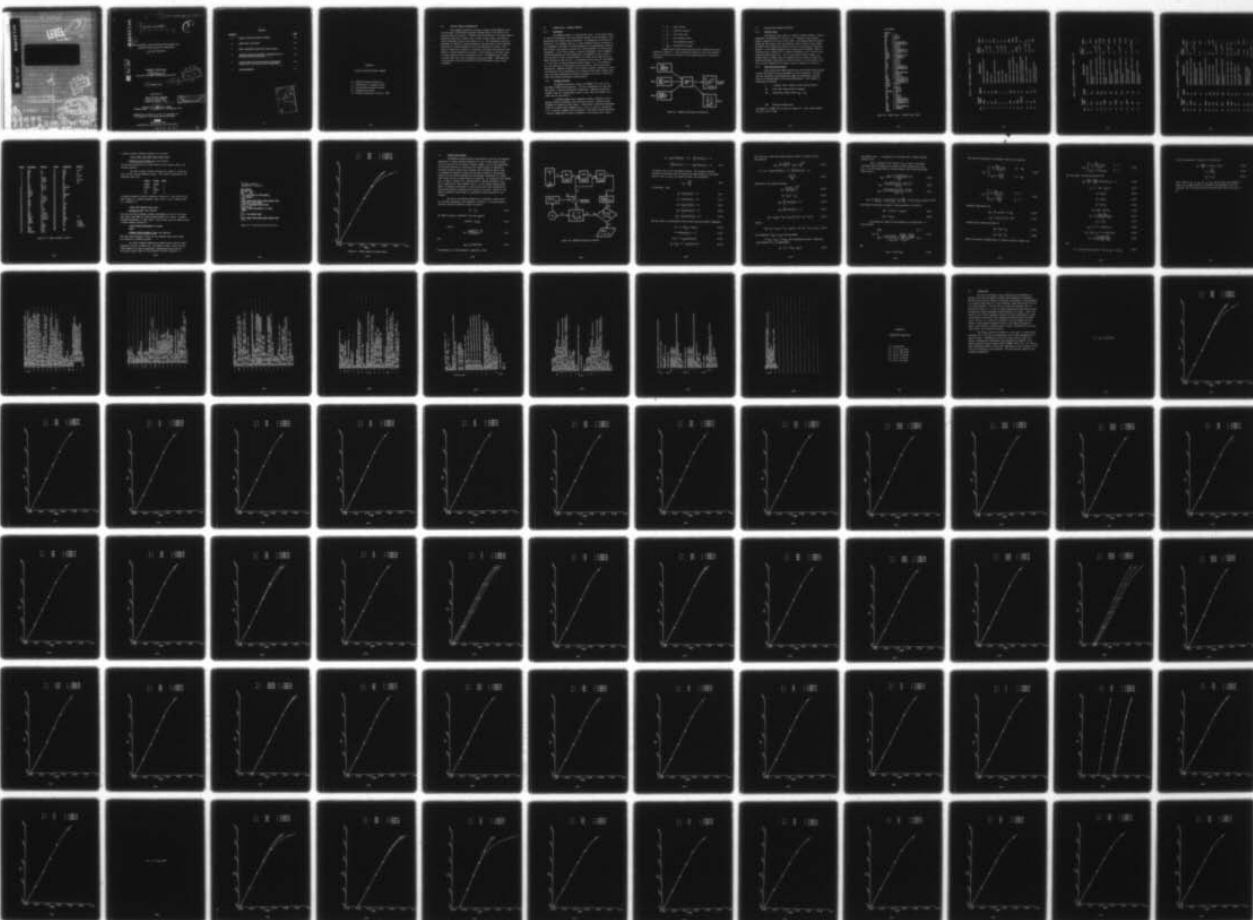
UNCLASSIFIED

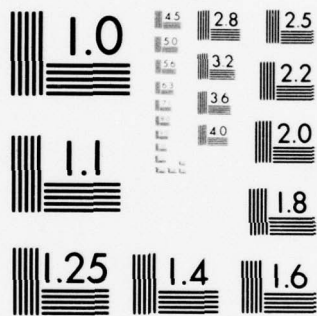
TRW-78.4734.7-023-PT-2-V0

NL

1 OF 4

AD
A062790





TRW

AD A062790

DDC FILE COPY

LEVEL

Bo25 833

3



DDC
JAN 2 1979
F

DISTRIBUTION STATEMENT A
Approved for public release
Distribution Unlimited

TRW

Code 427
NR.

14 TRW- 78.4734.7-023 - PT-2-VOL-2

AD A062790

9

FINAL REPORT.

21 Jan 77-28 Feb 78

3

PROCESS-ORIENTED, HIGH-INJECTION CIRCUIT MODELS FOR
INTEGRATED BIPOLAR JUNCTION TRANSISTORS.

PART II. - VOLUME II.

DDC FILE COPY

PRINCIPAL INVESTIGATOR

10 Dr. John Choma, Jr

Electronic Systems & Technology Department

DDC
JAN 2 1978
F

11

January 1978

12 304p.

Executed for

OFFICE OF NAVAL RESEARCH
800 North Quincy Road
Arlington, Virginia 22217

DISTRIBUTION STATEMENT A
Approved for public release;
Distribution Unlimited

15

Contract No. N00014-77-C-0043
CONTRACT DATES: 21 January 1977 - 28 February 1978

Reproduction in whole or in part is permitted for
any purpose of the United States Government.

TRW

DEFENSE AND SPACE SYSTEMS GROUP

ONE SPACE PARK • REDONDO BEACH • CALIFORNIA 90278

409 637

LB

CONTENTS

APPENDIX

PAGE

A	<u>EQSOLVE (EQUATION SOLVER) PROGRAM</u>	A-1
B	<u>SENSITIVITY CURVE SETS</u>	B-1
C	<u>PAREV (PARAMETER EVALUATION) CODE LISTING</u>	C-1
D	<u>TRANSIENT RADIATION RECOVERY CHARACTERISTICS OF BIPOLAR JUNCTION TRANSISTORS</u> , and	D-1
E	<u>CIRCUIT MODEL FOR NEUTRON-INDUCED PERFORMANCE DEGRADATION IN BIPOLAR JUNCTION TRANSISTORS</u> ,	E-1
F	ACKNOWLEDGEMENTS	F-1

ACCESSION for

NTIS ☐ Write Section ☐

DDC ☐ Bull Section ☐

UNCLASSIFIED ☐

for file

DO NOT WRITE IN THESE SPACES

SPECIAL

A

APPENDIX A

EQSOLVE (EQUATION SOLVER) PROGRAM

- A.0 EQSOLVE Program Documentation
- A.1 Introduction — Program Overview
- A.2 Detailed Main Program Structure
- A.3 Program Calculations
- A.4 Detailed subroutine structure — GRIM

A.0 EQSOLVE PROGRAM DOCUMENTATION

This appendix describes a software program called EQSOLVE, which was developed at TRW Defense and Space Systems Group for the ONR in conjunction with this contract. EQSOLVE accepts parameters of the Choma Bipolar Transistor model and a tabular list of base current values, and produces device performance curves such as Beta vs. I_c . The performance curves are presented in families, allowing parametric variation with a third parameter which may be a model parameter or the collector-emitter voltage. This allows a sensitivity analysis of transistor operating characteristics with respect to model parameters and allows a "fine tuning" of the model based on easily observed device performance curves. The EQSOLVE code is made to accept model data from a companion code called PAREV. PAREV generates from electrical and processing data the model parameters used as input to EQSOLVE.

A.1 INTRODUCTION - PROGRAM OVERVIEW

A.1.1 Objectives

The EQSOLVE program is a dual-purpose code. In the early stages of contract performance, the code provided insight into development of test methodology for specific model parameters. By examination of Calcomp plot families of, for example, Beta vs. I_C with extrinsic emitter resistance R_e as a parameter, the effect of model parameters on test-generated curves is made evident, and insight is gained into testing methods for various model parameters. In the later stages of contract performance, after parameter testing methodology has been established, the EQSOLVE is code is used to fine tune and to verify the performance of a given device model prior to model release for CAD activity. An additional future goal for the EQSOLVE is in the area of computer-assisted device design, i.e., the process of using an ideal set of performance characteristics to direct the device fabrication. EQSOLVE provides a link allowing software comparison of ideal and predicted device performance in an iterative improvement feedback loop that can produce masking and diffusion information for device fabrication based upon desired performance characteristics.

A.1.2 Program Structure

The EQSOLVE program is written in FORTRAN IV for use on the CDC 6000 or CYBER series machines. The core requirements are less than 60K (octal) to insure interactivity capability. Expected interactive terminal time for a single graph output is less than five minutes with a total cost of less than \$5.

A multiple graph output capability exists, allowing a user to generate several performance curve families on which a different model parameter is varied for every family. Additionally, different performance curves for a given model parameter (e.g., f_T vs. I_C with R_C varying and β vs. I_C with R_C varying) can be generated. Each family request generates a list of common device values in addition to the Calcomp plot, namely:

1. I_B - Base current
2. I_C - Collector current
3. h_{FE} - DC current gain
4. B_F - Base pushout factor
5. f_T - Gain bandwidth product
6. V_{BE} - Base-emitter voltage

Program input-output interaction and user interaction are summarized in figure A-1. User interaction consists of real time requests, wherein the details and contents of the Calcomp families of curves are stipulated.

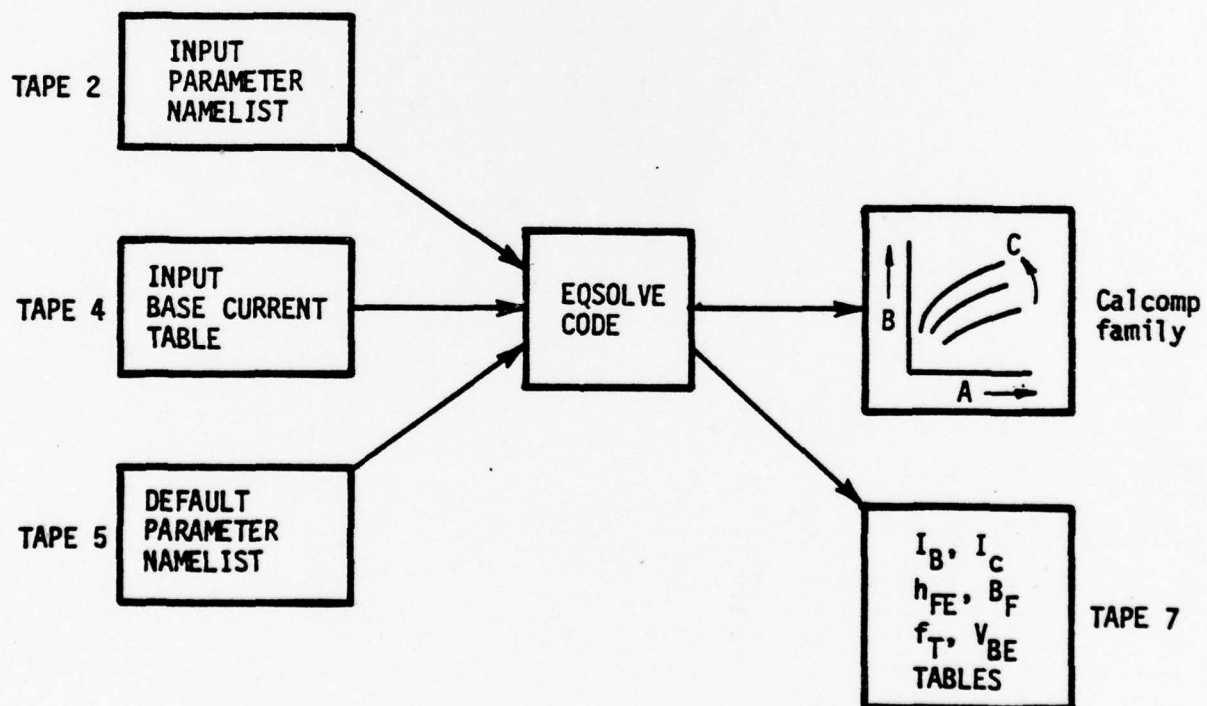


Figure A-1 EQSOLVE Input-Output Interaction

A.2 DETAILED MAIN PROGRAM STRUCTURE

A.2.1 Namelist Input

The namelist input works in a default override fashion. Default parameters corresponding to the model of a 2 Gigahertz small geometry bipolar transistor are used on input TAPE5. The program reads the default values and then reads in any user-supplied update values on input TAPE2. The TAPE2 values replace the default values for the duration of the user session. If the PAREV companion code is used prior to EQSOLVE, TAPE2 is available with a complete set of updated parameters, and it totally overwrites the TAPE5 default set. This is the expected mode of usage. An example TAPE2 for PAREV output and EQSOLVE input is shown in figure A-2. Detailed parameter explanation is found in Section 2 of this report, and a list of input parameters with default values is supplied in table A-1.

A.2.2 Base Current File Input

Base current file TAPE4 contains the list of base current points at which the bipolar device performance is to be calculated. The user thus has flexibility in selecting the range and coarseness of Calcomp output by tailoring TAPE4 to his own specifications. Input format is free-format as follows:

```
N      < integer value = number of base current points >
IB1    First base current point in amperes
IB2    Second base current point ( $I_{B2} > I_{B1}$ )
      .
      .
      .
IBN    Nth base current point
```

An example of a TAPE4 file is given in Figure A-3. Base current points are from .1 μ A to 1.0mA.

[LIST,TAPE2

1\$TRANS

RBO = 1.8,
RBB = 1.5E+02,
RE = 5.0E-01,
RCC = 0.,
BS = 3.33333333E-01,
BC = 3.33333333E-01,
BE = 5.0E-01,
CSO = 2.0E-12,
CEO = 8.998858595E-13,
CCO = 7.999348551E-13,
PHISS = 9.0E-01,
PHICO = 9.004004474E-01,
PHIEO = 1.200517562,
ISR = 3.0E-12,
IS = 3.2E-16,
IER = 3.0E-14,
IDR = 3.0E-13,
VER = 2.196833685E+01,
VCR = 6.056999515E+01,
NC = 1.8,
VT = 2.587500647E-02,
VTS = 3.0E-02,
QFN = 6.178E-16,
QRN = 2.261411812E-12,
TAUFO = 1.275024046E-10,
TAUR = 4.667132469E-07,
BETA0 = 5.5E+01,
BETAR = 1.5,
AE = 9.8E-07,
XO = 2.7E-04,
WCPRIME = 3.0E-04,
NE = 1.5,
KR = 5.0E-01,
BF2 = 1.4E+01,
VB = 1.368120028E+01,
VF = 2.587500647E-02,
FF = 1.027800526E-14,
VCE = 5.0,
IDB = 1.380000345E-03,
PC = 3.25E-03,
\$END

Figure A-2 PAREV Output — EQSOLVE Input TAPE2

TABLE A-1 INPUT PARAMETER LIST -- SEGMENT 1 OF 3

No.	Program Name	Symbol	Description	TAPE 5 Default	Units
1	RHOB	ρ_B	Extrinsic Base Resistivity	.009	ohms
2	TE	t_E	Emitter Depth	1×10^{-4}	cm
3	AB	A_B	Base Area	5×10^{-7}	cm^2
4	RBO	R_{BO}	Extrinsic Base Resistance	0.	ohms
5	L	L	Emitter Width	6×10^{-5}	cm
6	H	h	Emitter Length	6×10^{-5}	cm
7	W	W	Base Width	6×10^{-5}	cm
8	RBB	R_{BB}	Intrinsic Base Resistance	0.	ohms
9	RE	R_E	Extrinsic Emitter Resistance	0.5	ohms
10	RHOC	ρ_C	Collector Resistivity	.00325	ohm-cm
11	WCPRIME	W'_C	Distance from Collector-Base Junction to Buried Layer	3×10^{-4}	cm
12	XO	X_0	X_0/W'_C is a parametric ratio	2.7×10^{-4}	cm
13	AE	A_E	Area of Emitter	9.8×10^{-7}	cm^2
14	RCC	R_{CC}	Low Injection Extrinsic Collector Response	7.0	ohms

TABLE A-1 INPUT PARAMETER LIST - SEGMENT 2 OF 3

No.	Program Name	Symbol	Description	TAPE 5 Default	Units
15	T	T	Junction Temperature	27.	°C
16	VTS	V_{TS}	Substrate Junction Voltage Parameter	.03	volts
17	ISR	I_{SR}	Substrate Saturation Current	3×10^{-12}	amps
18	CSO	C_{SO}	Substrate Zero Bias Capacitance	2×10^{-12}	farads
19	PHISS	ϕ_{SS}	Substrate Built-In Junction Voltage	0.9	volts
20	CEO	C_{EO}	Emitter Junction Zero-Bias Capacitance	9×10^{-13}	farads
21	PHIEO	ϕ_{EO}	Emitter Junction Built-In Junction Voltage	.9	volts
22	CCO	C_{CO}	Collector Junction Zero-Bias Capacitance	8×10^{-13}	farads
23	PHICO	ϕ_{CO}	Collector Junction Built-In Junction Voltage	1.2	volts
24	IER	I_{ER}	Nonideal Emitter Diode Satur- ation Current	3.2×10^{-14}	amps
25	NE	η_E	Nonideal Emitter Exponent Multiplier	1.5	----

TABLE A-1 INPUT PARAMETER LIST - SEGMENT 3 OF 3

No.	Program Name	Symbol	Description	TAPE 5	
				Default	Units
26	IS	I_S	Forward Saturation Current	3.2×10^{-16}	amps
27	BETAO	β_o	Maximum Forward Current Ratio	55	----
28	IBR	I_{BR}	Nonideal Collector Diode Saturation Current	$3. \times 10^{-13}$	amps
29	NC	η_C	Nonideal Collector Diode Saturation Current	1.8	amps
30	BETAR	β_r	Reverse Maximum Current Ratio	1.5	----
31	VER	V_{ER}	Forward Early Voltage	20.	volts
32	VCR	V_{CR}	Inverse Early Voltage	60.	volts
33	QFN	Q_{FN}	Normalized Forward Injection Coefficient	1.5×10^{-16}	----
34	QRN	Q_{RN}	Normalized Reverse Injection Coefficient	1.5×10^{-12}	----
35	TAUFO	τ_{FO}	Forward Base Transit Time	1.59×10^{-9}	sec
36	TAUR	τ_R	Reverse Base Transit Time	1.27×10^{-9}	sec
37	KR	K_R	AC Crowding Parameter	0.6	----
38	VT	V_T	Junction Diode Exponent Coefficient	0.0259	volts
39	VB	V_B	Mathematical Fitting	17.79	volts
40	BF2	B_{F2}	Parameters for Base	13.64	----
41	FF	F_F	Pushout Simulation	1.336×10^{-14}	----

```

17
.1E-6
.2E-6
.4E-6
.7E-6
1.0E-6
2.0E-6
4.0E-6
7.0E-6
10.E-6
20.E-6
40.E-6
70.E-6
.1E-3
.2E-3
.4E-3
.7E-3
1.E-3

```

Figure A-3 TAPE4 - Base Current Input File Example

A.2.3 Tabular Output

Local file TAPE7 is written at every I_B point with the variables V_C , I_B , I_C , h_{FE} , B_F , f_T , and V_{BE} . TAPE7 may be listed at the termination of an interactive session to supplement the Calcomp printer plots. An example TAPE7 partial listing is shown in Figure A-4.

A.2.4 Calcomp Output

Examples of Calcomp output graphs are shown in the sensitivity curve sets of Appendix B.

A.2.5 User Interaction - Sample Session

The interactive session using EQSOLVE requires user input in response to terminal prompts for specification of Calcomp output details. The first request identifies the independent (x-axis), dependent (y-axis), and parametric variables by name and index number. Index number is the relative position of the variables within a COMMON block called PRAMTRS, and is used for internal program identification only. Parameter name is used for axis labeling and may be specified by alpha-numeric string less than eight characters without altering graphical output. Index values are tabulated, including default values, in Figure A-5.

[LIST,TAPE7

VCPRIME = -4.572E+00 IB = 1.000E-07 IC = 1.276E-06
HFE = 1.276E+01 BF = 1.000E+00 FT = 4.639E+06
VBE = 5.713E-01

VCPRIME = -4.554E+00 IB = 2.000E-07 IC = 3.212E-06
HFE = 1.606E+01 BF = 1.001E+00 FT = 1.143E+07
VBE = 5.953E-01

VCPRIME = -4.536E+00 IB = 4.000E-07 IC = 7.890E-06
HFE = 1.973E+01 BF = 1.003E+00 FT = 2.719E+07
VBE = 6.186E-01

VCPRIME = -4.522E+00 IB = 7.000E-07 IC = 1.600E-05
HFE = 2.286E+01 BF = 1.006E+00 FT = 5.298E+07
VBE = 6.370E-01

VCPRIME = -4.514E+00 IB = 1.000E-06 IC = 2.491E-05
HFE = 2.491E+01 BF = 1.009E+00 FT = 7.939E+07
VBE = 6.485E-01

Figure A-4 TAPE7 Partial Output List

<u>Index</u>	<u>Parameter</u>	<u>Default</u>	<u>Index</u>	<u>Parameter</u>	<u>Default</u>
1	RBO	9.	35	NDC	1.E16
2	RBB	150	36	PHIC	.7
3	RE	.5	37	DNC	48.
4	RCO	5.	38	XO	1.2E-4
5	PC	.00325	39	KR	.4
6	BS	.33333	40	TD	20.E-12
7	BC	.33333	41	M	2.0
8	BE	.5	42	NE	1.5
9	CSO	2E-12	43	IB	
10	CEO	.9E-12	44	VCPRIME	
11	CCO	.8E-12	45	IBB	
12	PHISS	.9	46	QF	
13	PHICO	.9	47	QR	
14	PHIEO	1.2	48	LAMBDAB	
15	ISR	3.E-12	49	ISS	
16	IS	3.2E-16	50	IN	
17	IER	3.2E-14	51	II	
18	IBR	3E-13	52	IO	
19	VER	20.	53	ILIM	
20	VCR	60.	54	BF	
21	NC	1.8	55	QBN	
22	VT	.0259	56	VBE	
23	VTB	.03	57	IC	
24	QFN	1.5E-16	58	HFE	
25	QRN	1.5E-12	59	FT	
26	TAUFO	159.E-12	60	VCE	5.0
27	TAUR	1270E-12	61	BETAB	
28	BETAO	55.	62	BF2	13.64
29	BETAR	1.5	63	VB	17.793
30	W	.6E-4	64	VF	2.59E-3
31	AE	9.8E-7	65	FF	1.336E-14
32	VLIM	6.E6	66	F	
33	DNB	22.6	67	BFO	
34	WCPRIME	3.E-4			

Figure A-5 Common Parameter Indices

A typical prompter-response dialogue is as follows:

ENTER, IDNME, INDEX, DPNME, INDEX, PARNME, INDEX

? *VBE*,56,*IC*,57,*RBO*,1 ← user supplied

The dialogue requested an IC versus VBE plot with resistor RBO as the varying parameter.

The next dialogue requests Calcomp type, number of curves per plot, and the varying parameter values. Curve type is specified by the following index list:

<u>X-Axis</u>	<u>Y-Axis</u>	<u>Index</u>
LINEAR	LINEAR	1
LINEAR	LOG	2
LOG	LINEAR	3
LOG	LOG	4

A prompter-response dialogue requesting a linear (x) - log (Y) plot with three values of a varying parameter equal to 90, 9, and .9 (RBO values) is: (NCURVES ≤ 5)

ENTER, TYPE, NCURVES, PARAM VALUES

? 2,3,90.,9.,.9 ← user supplied

The third and final dialogue requests adjustments in size of the x-axis and y-axis, and number of points between symbols on a curve. A sample dialogue requesting a 6 inch x-axis, 7 inch y-axis, and plot symbols every 3 points (default values) is:

UPDATE XINCH, YINCH, MARKS(5) IF REQD

\$CURV

YINCH=7, XINCH=6, MARKS=3,3,3 ← user supplied

Note that three entries of three (3) are required since three curves are requested by NCURVES prompter.

An actual teletype session for Calcomp output using the above dialogues is given in Figure A-6. The default x-axis, y-axis size and symbol density are used by supplying a terminating dollar sign (\$). An actual Calcomp output for this session is given in Figure A-7.

07/13/77. 10.37.10.
TRW/TSS C174 - 07/11/77.

USER NUMBER:
JOB NAME PLRG.
PORT 220.
[GET,TAPE4,EQSOLVE,TAPE5=EQDATA1
[RX,I=EQSOLVE
[LGO
ENTER INDNME,INDEX,DPNME,INDEX,PARNME,INDEX
? *VBE*,56,*IC*,57,*RBO*,1
ENTER TYPE,NCURVES,PARAM VALUES
? 2,3,90,.9,9
UPDATE YINCH,XINCH,MARKS(5) IF REQD
\$CURV
? \$
TYPE 1 FOR ANOTHER CASE
? 1
ENTER INDNME,INDEX,DPNME,INDEX,PARNME,INDEX
<etc.>

Figure A-6 Interactive Session Printout

■ --	RBO	=	9.000E+01
+ --	RBO	=	9.000E-01
0 --	RBO	=	9.000E+00

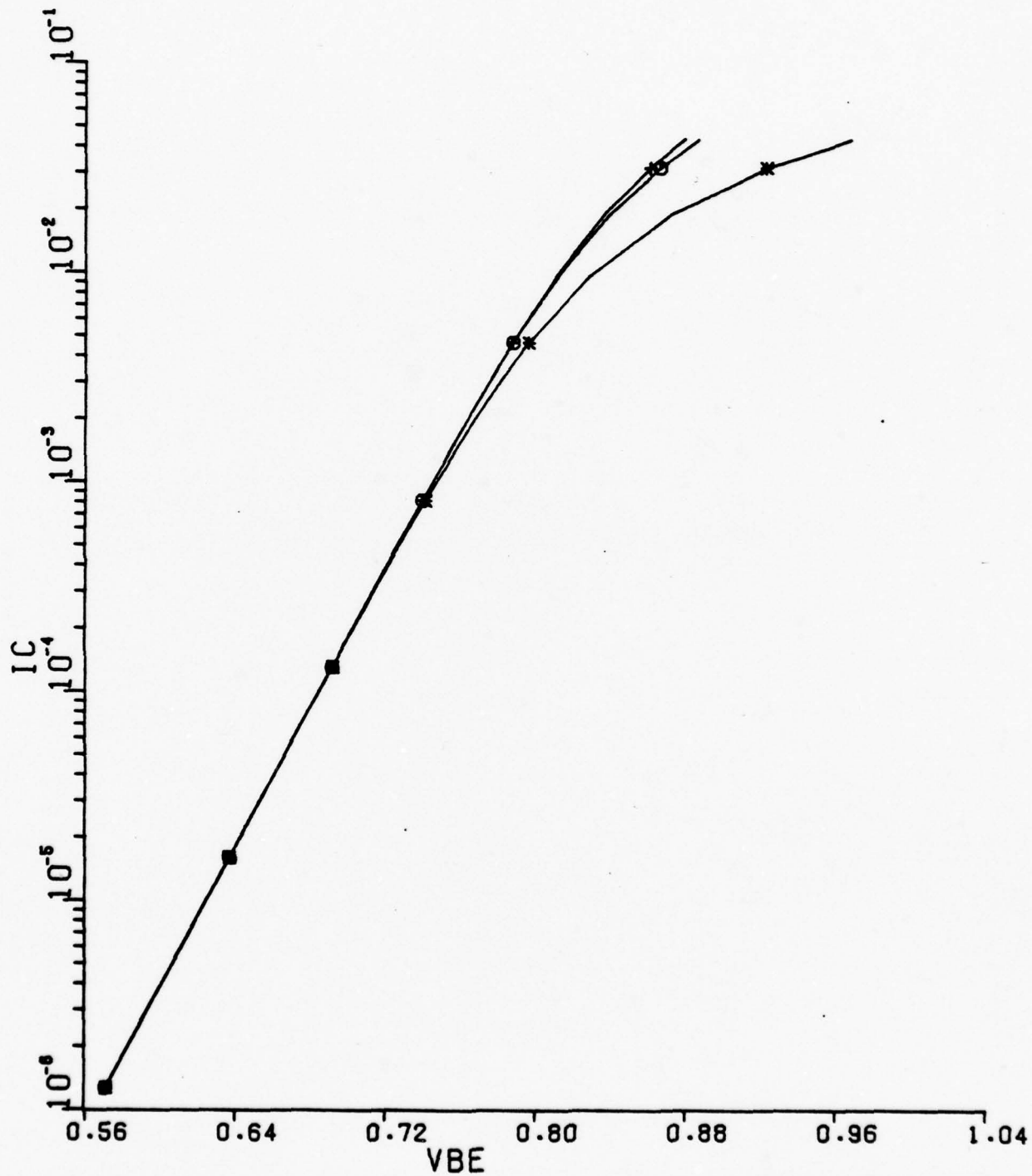


Figure A-7 Sample Session Calcomp Output

A.3 Program Calculations

The EQSOLVE program performs calculations of internal and external parameters of a given modeled transistor at a set of base current values and at a fixed VCE in the normal (forward) regime. Due to the dependencies of the model equations, a nonlinear root finder routine is required to calculate internal currents and voltages, and an iteration path is used to converge the internal currents and junction voltages to values which satisfy both the model equations and the external constraints of a fixed base current IB and collector-emitter voltage VCE. An overview of the program flow is shown in Figure A-8, illustrating the internal variables Z, V_E , and I_C generated by three separate calls to a root finder routine called GRM. An auxiliary subroutine is used in each call, which describes the controlling equation containing the variable to be found. Details of the GRM and auxiliary subroutines are explained in other sections of this document.

The set of calculations begins with a requested current point, I_B , and model parameters (user supplied or default). An initial guess of collector junction intrinsic voltage is given as

$$V_C' = -V_{CE} \quad (A-1)$$

and GRM is called to evaluate Z from the equation

$$Z \tan(Z) = I_B / I_{BB} \quad (A-2)$$

Given Z,

$$R_B = \frac{R_{BB} [\tan(Z) - Z]}{4 \cdot Z \cdot \tan(Z)} \quad (A-3)$$

and

$$A_{EF} = A_E \cdot \sin(2Z) / 2Z \quad (A-4)$$

The estimate V_C' is now required to compute V_E' from

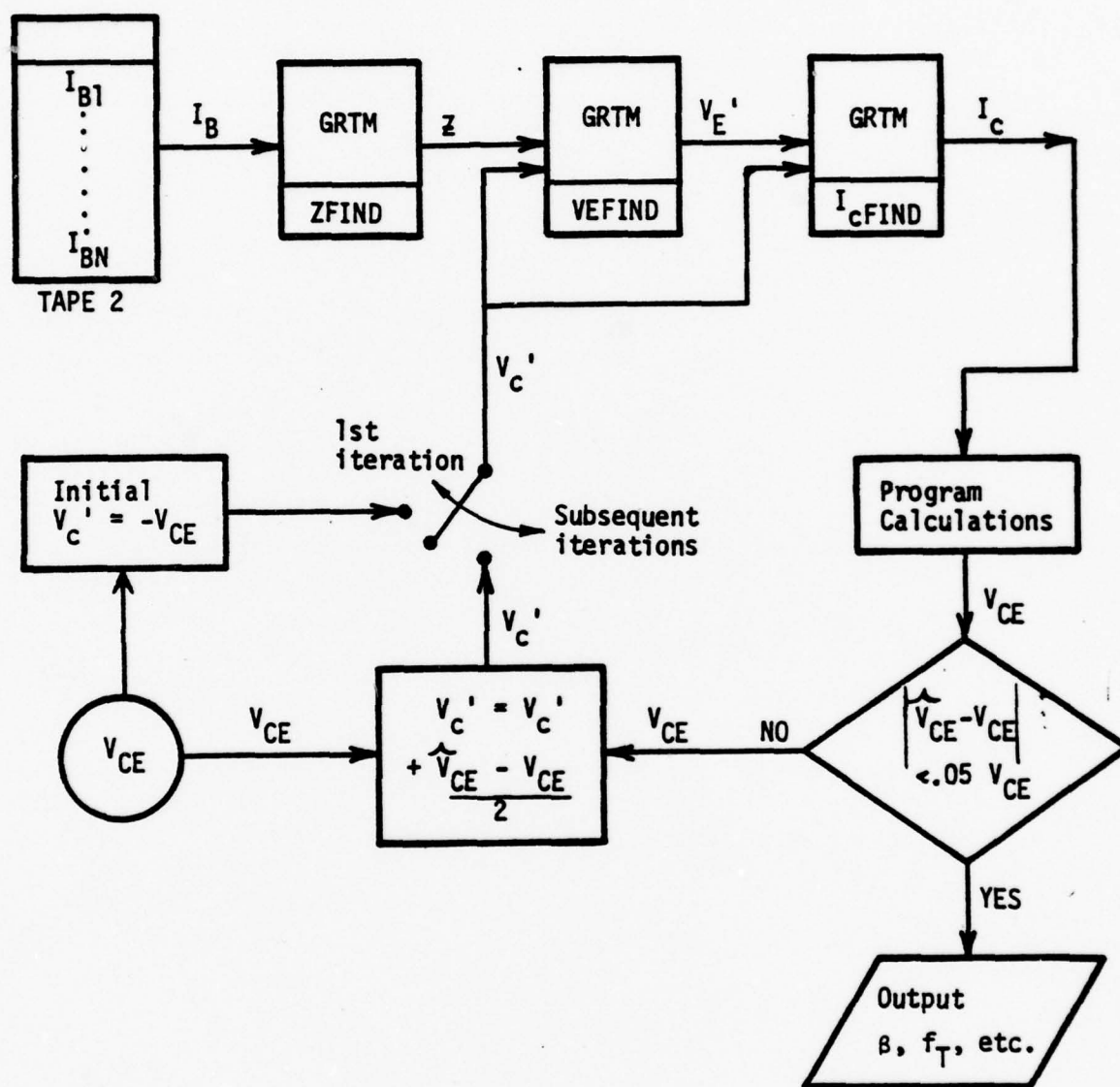


Figure A-8 EQSOLVE Program Flow Diagram

$$\begin{aligned}
I_B = & I_{ER} [\exp(V'_E/N_E V_T) - 1] + \frac{I_S}{\beta_O} [\exp(V'_E/V_T) - 1] \\
& + \frac{I_S}{\beta_F} [\exp(V'_C/V_T) - 1] + I_{BR} [\exp(V'_C/N_C V_T) - 1] \quad (A-5)
\end{aligned}$$

by another call to the root finder routine. The intrinsic junction voltages are now known, and the current and charge terms are calculated. Prior to this, if R_{CC} is not given as input, the calculation

$$R_{CC} = \frac{\rho_C W'_C}{A_{EF}} \quad (A-6)$$

is performed. Then,

$$I_N = I_S [\exp(V'_E/V_T) - 1] \quad (A-7)$$

$$I_I = I_S [\exp(V'_C/V_T) - 1] \quad (A-8)$$

$$Q_F = Q_{FN} [\exp(V'_E/V_T) - 1] \quad (A-9)$$

$$Q_R = Q_{RN} [\exp(V'_C/V_T) - 1] \quad (A-10)$$

$$I_{SS} = I_{SR} [\exp(V'_C/V_{TS}) - 1] . \quad (A-11)$$

The next block of calculations is Early effect and base pushout parameters.

$$\lambda_E = 1 + V'_E/V_{ER} + V'_C/V_{CR} , \quad (A-12)$$

$$F = FF [\exp(V'_E/V_F) - 1] , \quad (A-13)$$

$$B_{FO} = 1 + B_{F2} [\exp(V'_C/V_B)] , \quad (A-14)$$

$$B_F = B_{FO} + (1 - B_{FO}) [(\exp(-F))] . \quad (A-15)$$

The third call to the root finder routine is made to evaluate I_C from the equations

$$Q_{BN} = \frac{\lambda_E}{2} + \left[\left(\frac{\lambda_E}{2} \right)^2 + B_F Q_F + Q_R \right]^{1/2} \quad (A-16)$$

$$I_C = I_{SS} - I_{BR} [\exp(V'_C / N_C V_T) - 1] - \frac{I_S}{\beta_F} [\exp(V'_C / V_T) - 1] + \frac{I_N - I_I}{Q_{BN}} \quad (A-17)$$

Additionally, the program evaluates

$$\lambda_{CC} = \frac{X_O}{W_C} \left(\frac{B_F - 1}{B_{F2}} \right)^{1/2} \quad (A-18)$$

$$R_C = R_{CC} (1 - \lambda_{CC}) \quad (A-19)$$

$$I_{BE} = \frac{I_S}{\beta_O} [\exp(V'_E / V_T) - 1] \quad (A-20)$$

$$I_{BC} = \frac{I_S}{\beta_F} [\exp(V'_C / V_T) - 1] \quad (A-21)$$

$$V_{BE} = I_B \cdot R_{BO} + (I_{BE} + I_{BC}) \cdot R_B + V'_E + (I_B + I_C) \cdot R_E \quad (A-22)$$

Finally,

$$\hat{V}_{CE} = V_X = I_C \cdot R_{CO} + (I_C - I_{SS}) \cdot R_C - V'_C + V'_E + (I_B + I_C) \cdot R_E \quad (A-23)$$

The comparison of \hat{V}_{CE} to V_{CE} is now performed.

If $|\hat{V}_{CE} - V_{CE}| \leq .05 V_{CE}$, the calculations proceed. Otherwise, a new estimate of V'_C is generated by

$$\hat{V}'_C = V'_C + (\hat{V}_{CE} - V_{CE})/2 \quad (A-24)$$

and program control is transferred to the second call to GRTM following equation (A-5).

Once a "suitably close" value for \hat{V}_{CE} is found, the program calculates several parameters of interest at the operating point (I_B , V_{CE}). The first quantities are the base pushout and forward base charge sensitivities,

$$S_{BE} = \frac{(B_{FO} - 1) \cdot FF \cdot \exp(V'_E/V_F - F)}{B_F \cdot V_F} \quad (A-25)$$

$$S_{BC} = \frac{B_{F2} \cdot \exp(V'_C/V_B) \cdot [1 - \exp(-F)]}{B_F \cdot V_B} \quad (A-26)$$

$$S_{QE} = \frac{[I_C \cdot B_F \cdot Q_{FN} / (I_S \cdot V_T)] (1 + V_T \cdot S_{BE})}{2 \cdot Q_{BN} - \lambda_E} \quad (A-27)$$

$$S_{QC} = \left(\frac{1}{2 \cdot V_{CR} \cdot Q_{BN}} + \frac{1}{2 \cdot V_{CR} / (2 \cdot Q_{BN} - \lambda_E)} \right) \left(\frac{\lambda_E}{Q_{BN}} + 2 \cdot V_{CR} \cdot B_F \cdot Q_{FN} \cdot I_C \cdot S_{BC} / I_S \right) \quad (A-28)$$

The forward and reverse incremental transconductances are given by

$$gm_f = (I_C / V_T) \cdot (1 - S_{QE} / V_T) \quad (A-29)$$

$$gm_r = I_C \cdot S_{QC} \quad (A-30)$$

The program now checks if base pushout is inevidence ($B_F > 1$) and calculates

$$R_{OC} = \begin{cases} R_{CC} & B_F = 1 \\ R_C - \frac{I_C \cdot R_{CC} \cdot (X_O / W'_C) \cdot \left(\frac{B_F \cdot S_{BE}}{gm_f} - \frac{B_F \cdot S_{BC}}{gm_r} \right)}{2 \cdot B_{F2} \cdot [(B_F - 1) / B_{F2}]^{1/2}} & B_F > 1 \end{cases} \quad (A-31)$$

and

$$R_{OB} = 2 \cdot V_T / (3 \cdot I_{BB}) \quad (A-32)$$

The junction capacitances are assigned values by the equations

$$C_{jE} = \begin{cases} \frac{C_{EO}}{(1 - V'_E/\phi_{EO})^{B_E}} & V'_E < \phi_{EO} \\ C_{EO} \cdot (1 + \frac{B_E \cdot V'_E}{\phi_{EO}}) & V'_E > \phi_{EO} \end{cases} \quad (A-33)$$

$$C_{jC} = \begin{cases} \frac{C_{CO}}{(1 - V'_C/\phi_{CO})^{B_C}} & V'_C < 0 \\ C_{CO} \cdot (1 + \frac{B_C \cdot V'_C}{\phi_{CO}}) & V'_C > 0 \end{cases} \quad (A-34)$$

Diffusion capacitances are

$$C_{DE} = B_F \cdot \tau_{FO} \cdot (gm_f + I_C \cdot S_{BE}) \quad (A-35)$$

$$C_{DC} = B_F \cdot \tau_{FO} \cdot (I_C \cdot S_{BC} - gmr) \quad (A-36)$$

yielding total capacitances given by

$$C_{TE} = C_{DE} + C_{jE} \quad (A-37)$$

$$C_{TC} = C_{DC} + C_{jC} \quad (A-38)$$

Substrate voltage is assumed equal to collector junction voltage, and

$$C_{SS} = \begin{cases} \frac{C_{SO}}{(1 - V'_C/\phi_{SS})^{B_S}} & V'_C < 0 \\ C_{SO} \cdot (1 + B_S \cdot V'_C/\phi_{SS}) & V'_C > 0 \end{cases} \quad (A-39)$$

The time moment calculations proceed with

$$g_{BE} = \frac{I_{BE}}{V_T} + \frac{I_{ER}}{\eta_E \cdot V_T} \cdot [\exp(V'_E/\eta_E \cdot V_T) - 1] \quad (A-40)$$

$$F_E = 1 + (gm_f + g_{BE}) \cdot R_E \quad (A-41)$$

$$g_B = g_{BE}/F_E \quad (A-42)$$

$$C_E = C_{TE}/F_E \quad (A-43)$$

$$go = gmr/F_E \quad (A-44)$$

$$gm = (gm_f - gmr)/F_E \quad (A-45)$$

$$R'_L = \frac{R_{OC} + R_{CO}}{1 + go \cdot (R_{OC} + R_{CO})} \quad (A-46)$$

$$r_{11} = 1/g_B \quad (A-47)$$

$$r_{22} = R'_L + (1 + gm \cdot R'_L) \cdot r_{11} \quad (A-48)$$

$$r_{33} = R_{OB} + r_{11} + (1 + gm \cdot r_{11}) \cdot R'_L \quad (A-49)$$

$$r_{44} = \frac{(1 + go \cdot R_{OC}) \cdot R_{CO}}{1 + go \cdot (R_{OC} + R_{CO})} \quad (A-50)$$

and

$$T_1 = r_{11} \cdot C_{TE} + K_R \cdot r_{22} \cdot C_{TC} \cdot (1 - K_R) \cdot r_{33} \cdot C_{TC} + r_{44} \cdot C_{SS} \quad (A-51)$$

The final parameters of interest are calculated as

$$\beta_F = \left(\frac{g_m}{g_B}\right) [1 + g_o(R_{OC} + R_{CO})] \quad (A-52)$$

$$f_T = \frac{\beta_F}{2 \cdot \pi \cdot T_1} \quad (A-53)$$

$$h_{FE} = I_C / I_B \quad (A-54)$$

After output of I_B , I_C , h_{FE} , B_F , f_T , V_{BE} , and any other user-requested values, the program control is returned to the beginning of the calculations, and the calculations are performed again with a new value of I_B .

A.4 Detailed Subroutine Structure - GRTM

A.4.1 Module Usage and Interface

GRTM is a general root finder routine which is called three times during a pass through the EQSOLVE equations. It is called to determine the onset parameter Z , V_E' , and I_C . Linkage into GRTM is accomplished by providing auxiliary subroutines which contain an equation that evaluates to zero for the proper value of the variable to be found. The auxiliary subroutine names and equations used in EQSOLVE calls are as follows:

<u>Name</u>	<u>Equation</u>
ZFIND	(A-2)
VEFIND	(A-5)
ICFIND	(A-17)

A.4.2 Subroutine Input

Input to GRTM is the auxiliary function name, an initial guess of roots requested, and an iteration convergence value described in section 4.1.4.4. The maximum iteration value is set at 50 and a convergence criteria of 1×10^{-6} is used for EQSOLVE.

A.4.3 Subroutine Output

The onset parameter Z , intrinsic base-emitter voltage V_E' , and collector current I_C , are outputs of GRTM when called from EQSOLVE.

A.4.4 Subroutine Calculations

GRTM uses Muller's method to find the roots of $f(x)$. This method is detailed in Section 4.3.2.

A.5 EQSOLVE CODE LISTING

```

PROGRAM EQSOLVE(INPUT,OUTPUT,TAPE4,TAPE2,TAPE6,TAPE7,TAPE20,
* TAPE3=INPUT)
C PROGRAM WILL SOLVE A SERIES OF EQUATIONS TO DETERMINE THE EFFECTS
C OF PROCESS PARAMETER VARIATION ON SEMICONDUCTOR DEVICES.
COMMON /DATA/ FX(500,3), X(500,3), CGVAR(5), CGLBL, DPEND,
* INDPEND, TYPE, NPIS, NCURVES, YINCH, XINCH, MARKS(5)
COMMON /PARAMS/ RBO, RBB, RE, RCO, PC, BS, BC, BE, CSO, CEO,
* CCO, PHISS, PHICO, PHIEO, ISR, IS, IER, IBR, VER, VCR, NC, VT,
* VTS, QFN, QPN, QNF, TAUF, TAUR, BETAD, BETAR, W, AE, VLIM, DNB,
* WCPRIME, NDC, PHIC, DNC, XO, KR, ID, M, NE, IB, VCPRIME, IBB,
* QF, QR, LMBDAE, ISS, IN, II, IO, ILIM, BF, OBN, VBE, IC, HFE,
* FT, VCE, BETAF, BF2, VB, VF, FF, F, BFQ
DIMENSION LINK(67)
NAMELIST /CURV/ YINCH, XINCH, MARKS
REAL IBB, IB, ISR, IS, IER, IBR, KR, M, NC, NE, IO, ILIM, NDC,
* IN, II, ISS, IBE, IBC, KI, K2, LPBDAE, IC, LMBDACC, LASTZ,
* LASTVE, LINK
EQUIVALENCE (RBO, LINK(1))
NAMELIST /TRANS/ RBO, RBB, RE, RCO, BS, BC, BE, CSO, CEO,
* CCO, PHISS, PHICO, PHIEO, ISR, IS, IER, IBR, VER, VCR, NC, VT,
* VTS, QFN, QPN, QNF, TAUF, TAUR, BETAD, BETAR, AE,
* WCPRIME, XO, NE, KR, BF2, VB, VF, FF, VCE, IBB
1 FORMAT(//,5X,VCPRIME = *,E10.3,5X,*IB = *,E10.3,5X,*IC = *,
* E10.3,5X,*HFE = *,E10.3,5X,*BF = *,E10.3,5X,*FI = *,
* E10.3,5X,/,5X,*VBE = *,E10.3)
INTEGER TYPE, YPTR, XPTR, CGPNTR, GRAPHS
EXTERNAL ZFIND, VEFIND, ICFIND
CALL NHLEOF
REWIND 50
CALL LOOK(50)
CALL PLOT(0,1,,231)
16 REWIND 2
4 READ(2,TRANS)
IF(EOF,2) 5,4
5 XINCH=6. $ YINCH=7. $ MARKS(1)=MARKS(2)=MARKS(3)=3
DISPLAY *ENTER INDCME,INDEX,DPNME,INDEX,PARNME,INDEX*
ACCEPT INDPEND,XPTR,DPEND,YPTR,CGLBL,CGPNTR
DISPLAY *ENTER TYPE,NCURVES,PARA VALUES*
ACCEPT TYPE,NCURVES,(CGVAR(1),1=1,NCURVES)
DISPLAY *UPDATE YINCH,XINCH,MARKS(5) IF REQD*
READ(3,CURV)
LASTZ = 1.0

```



```

LASTVE = .755555
Q = 1.602E-19
EPSILON = 1.062E-12
PI = 3.14159
GRAPHS = 0
NPASS = 0
REWIND 4
ACCEPT(4) NPTS
GRAPHS = GRAPHS + 1
LINK(CGPNT) = CGVAR(GRAPHS)
6 ACCEPT(4) IB
IF(EOF(4)) 7,8
8 VALUES = LASTZ
VCPRIME = -VCE
NPASS = NPASS + 1
CALL GRM(1,VALUES,0.50,ZFIND,0.1,E-6)
2 = LASTZ = VALUES
RB = (RBB + (TAN(Z) - Z)) / ((4.0 * Z) + (TAN(Z)*2))
AEF = AE + SIN(2.0 * Z) / (2.0 * Z)
14 VALUES = LASTVE
CALL GRM(1,VALUES,0.50,VEFIND,0.1,E-6)
VEPRIME = LASTVE = VALUES
RCC = (PC + VCPRIME) / AEF
IN = IS + (EXP(VEPRIME/VT) - 1.0)
II = IS + (EXP(VCPRIME/VT) - 1.0)
QF = QFN + (EXP(VEPRIME/VT) - 1.0)
QR = QRN + (EXP(VCPRIME/VT) - 1.0)
ISS = ISR + (EXP(VCPRIME/VIS) - 1.0)
LMBDAE = 1.0 + VEPRIME/VER + VCPRIME/VCR
F = FF + (EXP(VEPRIME/VF) - 1.0)
BFD = 1.0 + BF2 + EXP(VCPRIME/VB)
BF = BFD + (1.0 - BFD) + EXP(-F)
VALUES = IO
CALL GRM(1,VALUES,0.50,ICFIND,0.1,E-6)
IC = VALUES
LMBDACC = (XO/VCPRIME) + ((BF-1.)/BFD2)**.5
RC = RCC + (1.0 - LMBDACC)
IBE = (IS/BETAD) + (EXP(VEPRIME/VT) - 1.0)
IBC = (IS/BETAR) + (EXP(VCPRIME/VT) - 1.0)
VBE = IB + RBO + (IBE + IBC) + RB + VEPRIME + (IB + IC) + RE
VX = IC + RCO + (IC - ISS) + RC - VCPRIME + VEPRIME +
+ (IB + IC) + RE

```

```

IFABS(VX-VCE) .LE. .05*VCE) GO TO 13
VCPRIME = VCPRIME + ((VX-VCE)/2.0)
GO TO 14
13 SBE = ((BED - 1.0) * FF * EXP(VEPRIME/VF - FI)) / (BF * VF)
SBC = ((BF2 * EXP(VCPRIME/VB) * (1.0 - EXP(-FI))) / (BF * VB)
SDE = ((IC * BF * QFN / (IS * VT)) * (1.0 + VT * SBE) /
* (2.0 + QBN - LMBDAE)
SOC = (1.0 / (2.0 + VCR * QBN)) * ((1.0 / (2.0 + VCR) /
* (2.0 + QBN - LMBDAE)) * ((LMBDAE/QBN) + (2.0 + VCR * BF * QFN
* (IC * SBC / IS)))
GMF = ((IC/VT) * (1.0 - (SDE * VT)))
GMR = IC * SOC
RDC = RCC
IF(BF.GT.1.)RDC=RC-IC*RCC*(XO/WCPRIME)*(BF*SBE/GMF-BF*SBC/GMR)/
* (2.*BF2*((BF-1.)/BF2)+.2)
ROB = 2.*VT/(3.+IBB)
IFVEPRIME .LT. PHIEO) CJE = CED/((1.0 - VEPRIME/PHIEO)*SBE)
IFVEPRIME .GE. PHIEO) CJE = CED * (1.0 + BE * VEPRIME/PHIEO)
IFVCPRIME .LE. 0.0) CJC = CCO/((1.0 - VCPRIME/PHICQ)*SBC)
IFVCPRIME .GT. 0.0) CJC = CCG * (1.0 + BC*VCPRIME/PHICQ)
CDE = BF * TAUFQ * (GMF * IC * SBE)
CDC = BF * TAUFQ * (IC * SBC - GMR)
CJE = CDE * CJE
CTC = CDC * CJC
IFVCPRIME .LE. 0.0) CSS = CSO/((1.0 - VCPRIME/PHISS)*SBS)
IFVCPRIME .GT. 0.0) CSS = CSO * (1.0 + BS*VCPRIME/PHISS)
GBE = IBE/VT * IER/(NE * VT) * (EXP(VEPRIME/(NE * VT)) - 1.0)
FE = 1.0 + (GMF * GBE) * RE
GB = GBE/FE
CE = CTE/FE
GD = GMR/FE
GM = (GMF - GMR)/FE
RLPRIME = (ROC + RCO)/((1.0 + GD * (RGC + RCO)))
R11 = 1.0/GB
R22 = RLPRIME * (1.0 + GM * RLPRIME) * R11
R31 = ROB + R11 * (1.0 + GM * R11) * RLPRIME
R44 = ((1.0 + GD * RCO) * RCO)/(1.0 + GD * (ROC + RCO))
T1 = R11 * CTE * NR * R22 * CTC + (1.0 - KR) * R33 * CTC +
* R44 * CSS
BETAF = (GM/GB)/(1.0 + GD * (ROC + RCO))
FT = BETAF/(2.0 * PI * T1)
HFE = IC/IB

```

```

WRITE(7,1) VCPRIME, IB, IC, HFE, BF, FI, VDE
FX(INPASS,GRAPHS) = LINK(XPTR)
X(INPASS,GRAPHS) = LINK(XPTR)
IF(INPASS .LT. NPTS) GO TO 5
IF(IGRAPHS .LT. VCURVES) GO TO 9
7 CALL PLTEXEC
  DISPLAY = TYPE 1 FOR ANOTHER CASE
  ACCEPT III
  IF(III.EQ.1) GO TO 16
  CALL PLOT(0,0,999)
  STOP
END
SUBROUTINE ZFIND(Z,FZ)
ZFIND CALCULATES Z AS A FUNCTION OF THE TANGENT OF ITSELF.
COMMON /PPRATRS/ SKIP1(42), IB, SKIP2, IB8, SKIP3(22)
REAL IB, IB8
FZ = Z + TAN(Z) - (IB / IB8)
RETURN
END
SUBROUTINE VEFIND(VEPRIME,FVE)
VEFIND CALCULATES THE VARIABLE IB BASED ON SOME ASSUMED VALUE OF
VEPRIME.
COMMON /PPRATRS/ SKIP1(15), IS, IER, IAR, SKIP2(2), NC, VT,
+ SKIP3(5), BETAD, BETAR, SKIP4(12), NE, IB, VCPRIME, SKIP5(23)
REAL IER, IS, IAR, NC, NE, IB
TERM1 = IER + (EXP(VEPRIME/(NE*VT)) - 1.0)
TERM2 = (IS / BETAD) + (EXP(VEPRIME/VT) - 1.0)
TERM3 = (IS / BETAR) + (EXP(VEPRIME/VT) - 1.0)
TERM4 = IAR + (EXP(VCPRIME/(NC*VT)) - 1.0)
FVE = TERM1 + TERM2 + TERM3 + TERM4 - IB
RETURN
END
SUBROUTINE ICFIND(IC,FIC)
ICFIND CALCULATES THE VALUE FIC WHICH IS DEPENDENT UPON IC. THE VALUE
IC AND FIC MUST BE EQUAL UPON CONVERGENCE.
COMMON /PPRATRS/ SKIP1(15), IS, SKIP2, IBR, SKIP3(2), NC, VT,
+ SKIP4(6), BETAR, N, SKIP5(2), DNB, NCPRIME, SKIP6(2), DNC,
+ SKIP7(6), VCPRIME, SKIP8, QF, QR, LMBDAE, ISS, IN, II, IO, IILM,
+ BF, GBH, SKIP9(12)
REAL IC, IO, IILM, IS, ISS, IBR, NC, II, LMBDAE, IN
QBH = LMBDAE/2.0 + (LMBDAE/2.0)**2 + BF + QF + QR)**.5
TERM1 = IAR + (EXP(VCPRIME/(NC*VT)) - 1.0)

```



```

        LOOPS = NCURVES
        YMINALL = 1.E200
        DELYALL = YMAXALL = -1.E200
        CALL YSCALE(FX(BASE),YINCH,NPTS+INC,1)
        IF(TYPE.EQ.1.OR.TYPE.EQ.3) YMAX = FX(BASE+NPTS+INC) +
        + YINCH + FX(BASE+NPTS+INC+1)
        IF(TYPE.EQ.2.OR.TYPE.EQ.4)
        + CALL FORMAX(FX(BASE+NPTS+INC),FX(BASE+NPTS+INC+1),YMAX,YINCH)
        IF(YMAXALL.LT.YMAX) YMAXALL = YMAX
        IF(YMINALL.GT.FX(BASE+NPTS+INC)) YMINALL = FX(BASE+NPTS+INC)
        IF(DELYALL.LT.FX(BASE+NPTS+INC+1)) DELYALL = FX(BASE+NPTS+INC+1)
        LOOPS = LOOPS - 1
        IF(LOOPS.EQ.0) GO TO 7
        BASE = BASE + 500
        FX(BASE+NPTS) = YMINALL
        FX(BASE+NPTS+1) = YMAXALL
        INC = 2
        GO TO 6
7      CALL YAXIS(0.0,0.0,DPEND,10,YINCH,90,YMINALL,DELYALL)
C
C      X AXIS PREPARATION
C
        BASE = 1
        INC = 0
        LOOPS = NCURVES
        YMINALL = 1.E200
        DELXALL = XMAXALL = -1.E200
        CALL XSCALE(X(BASE),XINCH,NPTS+INC,1)
        IF(TYPE.EQ.1.OR.TYPE.EQ.2) XMAX = X(BASE+NPTS+INC) +
        + XINCH + X(BASE+NPTS+INC+1)
        IF(TYPE.EQ.3.OR.TYPE.EQ.4)
        + CALL FORMAX(X(BASE+NPTS+INC),X(BASE+NPTS+INC+1),XMAX,XINCH)
        IF(XMAXALL.LT.XMAX) XMAXALL = XMAX
        IF(XMINALL.GT.X(BASE+NPTS+INC)) XMINALL = X(BASE+NPTS+INC)
        IF(DELYALL.LT.X(BASE+NPTS+INC+1)) DELXALL = X(BASE+NPTS+INC+1)
        LOOPS = LOOPS - 1
        IF(LOOPS.EQ.0) GO TO 9
        BASE = BASE + 500
        X(BASE+NPTS) = XMINALL
        X(BASE+NPTS+1) = XMAXALL
        INC = 2
        GO TO 8
9

```

```

9 CALL XAXIS(0.0,0.0,INDPEND,-10,XINCH,0.0,XMINALL,DELXALL)
C
C GENERATE CURVES AND PLOT LEGEND
C
BASE = LOOPS = 1
IF(LOGTYPE .GT. -2) GO TO 3
C
C LINEAR/LINEAR PLOT
C
13 FX(BASE+NPTS) = YMINALL
FX(BASE+NPTS+1) = DELYALL
X(BASE+NPTS) = XMINALL
X(BASE+NPTS+1) = DELXALL
CALL CURVES(X(RASE),FX(BASE),NPTS,1,MARKS(LOGPS),CHRINDX(LOOPS))
IF(LOOPS .EQ. NCURVES) GO TO 4
LOOPS = LOOPS + 1
BASE = BASE + 500
GO TO 13
C
C ONE OR BOTH AXES ARE LOG
C
3 FX(BASE+NPTS) = YMINALL
FX(BASE+NPTS+1) = DELYALL
X(BASE+NPTS) = XMINALL
X(BASE+NPTS+1) = DELXALL
CALL CURVES(X(BASE),FX(BASE),NPTS,1,MARKS(LOGPS),CHRINDX(LOOPS),
+ LOGTYPE)
IF(LOOPS .EQ. NCURVES) GO TO 4
LOOPS = LOOPS + 1
BASE = BASE + 500
GO TO 3
C
C ANNOTATE LFEND
C
4 LOOPS = NCURVES
YCORD = YINCH + .6
14 ENCODE(40,1,TITLE) CHARS(LOOPS), CGLBL, CGVAF(LOOPS)
CALL SYMBOL(1.5,YCORD,.1,TITLE,0.0,40)
LOOPS = LOOPS - 1
IF(LOOPS .EQ. 0) RETURN
YCORD = YCORD + .2
GO TO 14

```

```

END
SUBROUTINE FORMAX(MINVAL,DELTA,MAXVAL,AXLENGTH)
C   FORMAX DETERMINES THE MAX VALUE OF THE INFORMATION JUST SUBMITTED
C   TO THE SCALING ROUTINE.
REAL MINVAL, MAXVAL, LGMIN
LGMIN = ALOG10(MINVAL)
MAXVAL = 1.0 + 10.0**((AXLENGTH * DELTA + LGMIN)
RETURN
END

```

APPENDIX B

SENSITIVITY CURVE SETS

- B.0 Introduction
- B.1 I_B vs. V_{BE} Curves
- B.2 I_C vs. V_{BE} Curves
- B.3 H_{FE} vs. I_C Curves
- B.4 F_t vs. I_C Curves
- B.5 B_F vs. I_C Curves

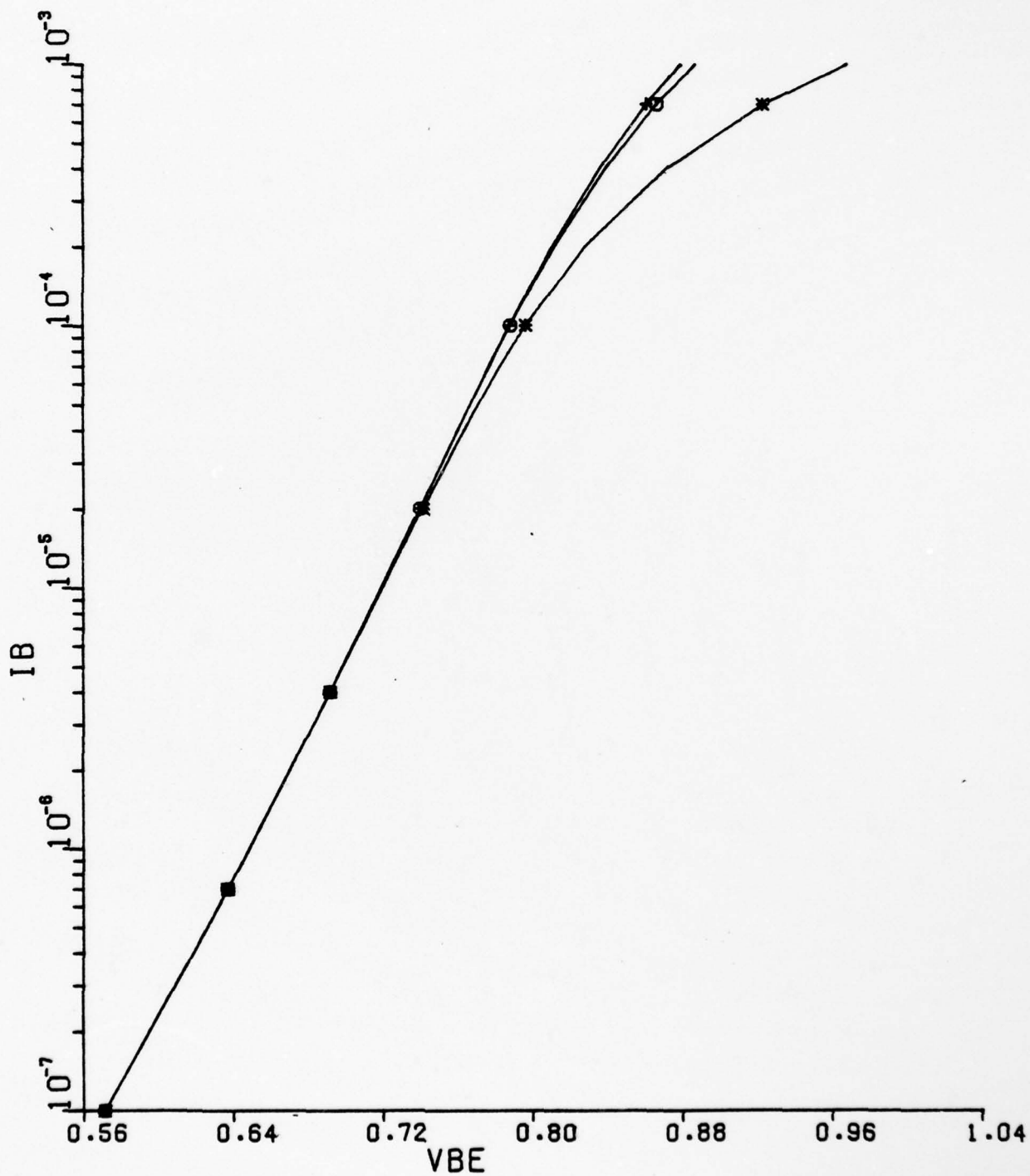
B.0 INTRODUCTION

The sets of parametric curves comprising this appendix are Calcomp output from the EQSOLVE software code documented in Appendix A. The curve sets show the change in functional relationship of two-parameters of the Choma LSBJT model of a 2 GHz transistor under perturbation in value of a third parameter. The five sets of curves are selected, with the exception of the B_F vs. I_C set, as useful design-type curves which provide the essential device performance characteristics at a glance. Hence, the effects of the "third" parameter variation on these characteristic curves are produced by varying the third parameter above and below the nominal value. The B_F vs. I_C curves are included to provide insight into the effects of base pushout parameter values on the complex mathematical model of base pushout, an effect which is vital to understand for precise, large signal, high injection modeling.

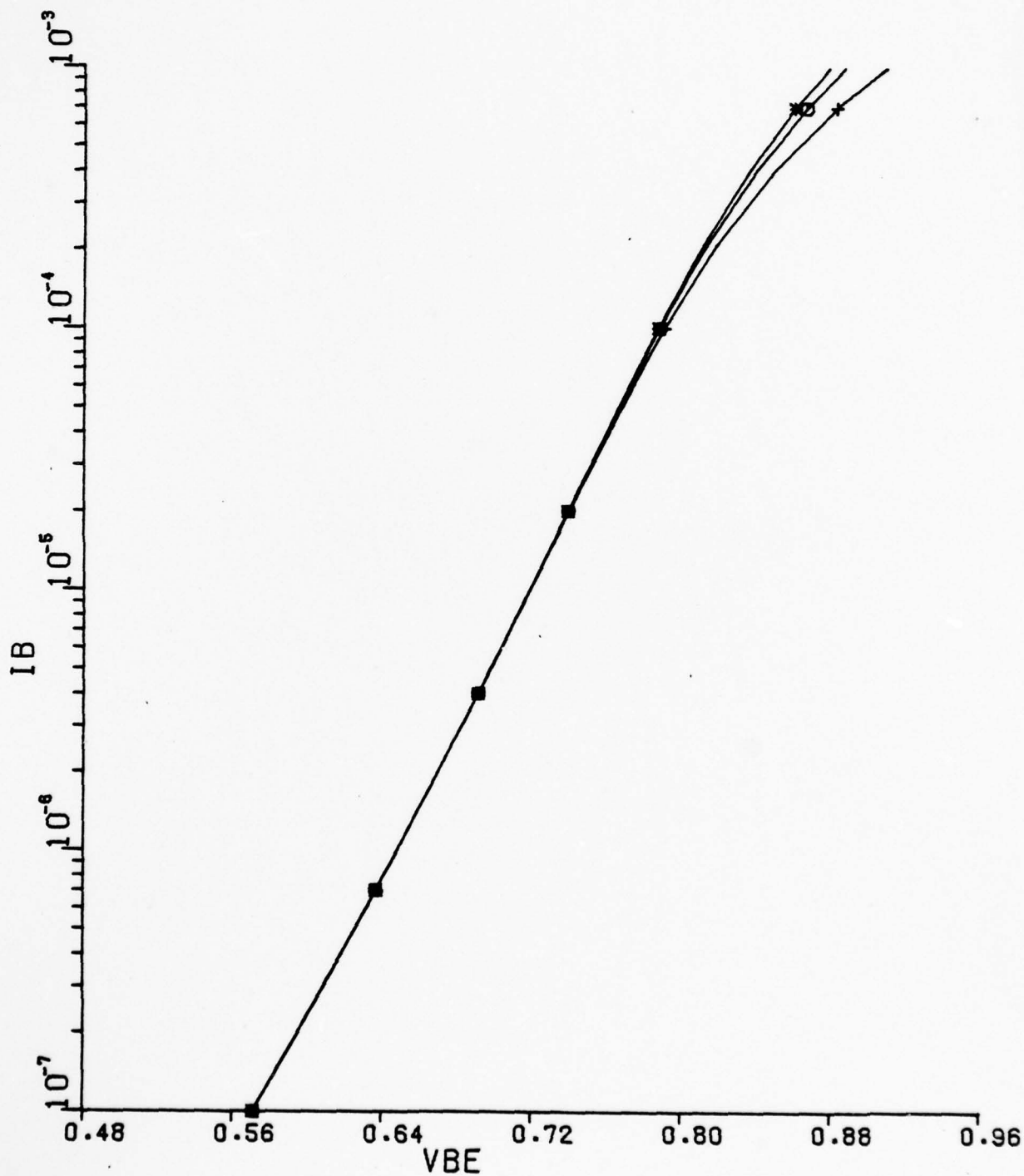
The design curves are included as a last step, or "fine-tuning" capability for a user who has determined a set of model parameters for a specific device. Comparison of device test data curves or other CAD values to mathematical performance curves generated by EQSOLVE or any general modeling software package (ECAP, SCEPTRE, SPICE, etc.) will produce curve differences similar to the curve differences on one or several of the curve sets contained in this appendix. The user then has insight on the erroneous parameter(s).

B.1 I_B vs. V_{BE} Curves

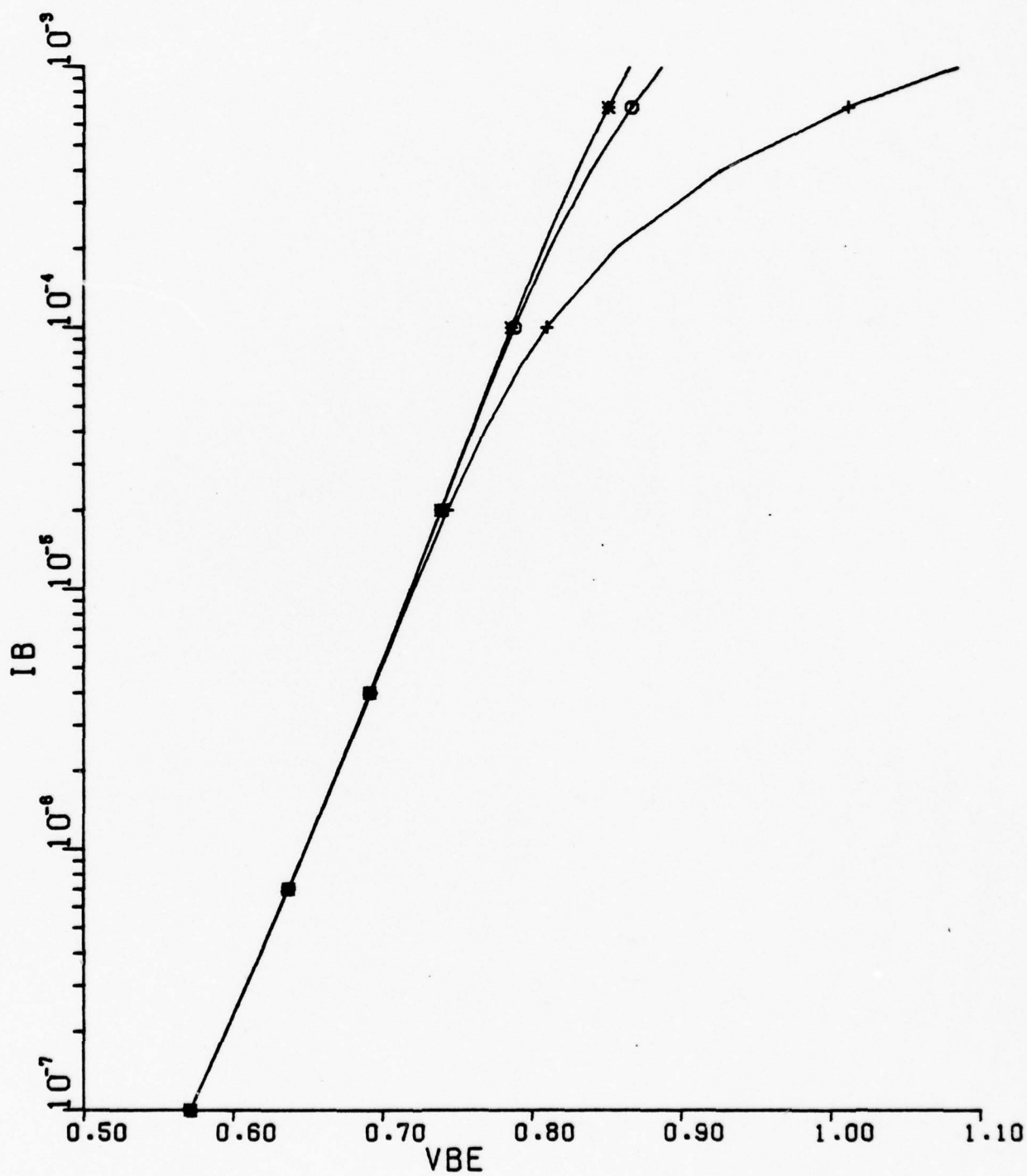
■ --	RBO	=	9.000E+01
+ --	RBO	=	9.000E-01
0 --	RBO	=	9.000E+00



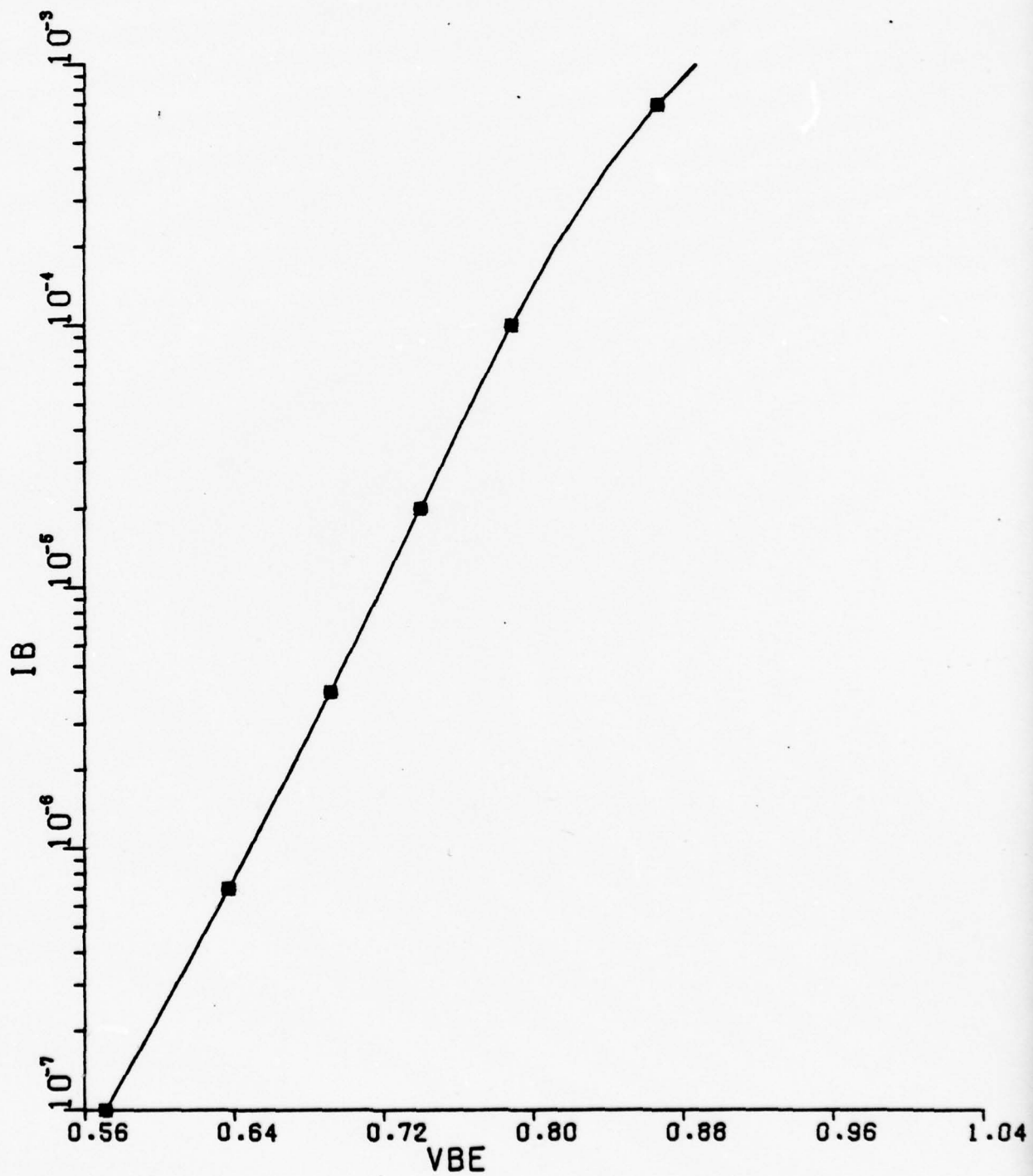
■ --	RBB	=	1.500E+01
+ --	RBB	=	5.000E+02
0 --	RBB	=	1.500E+02



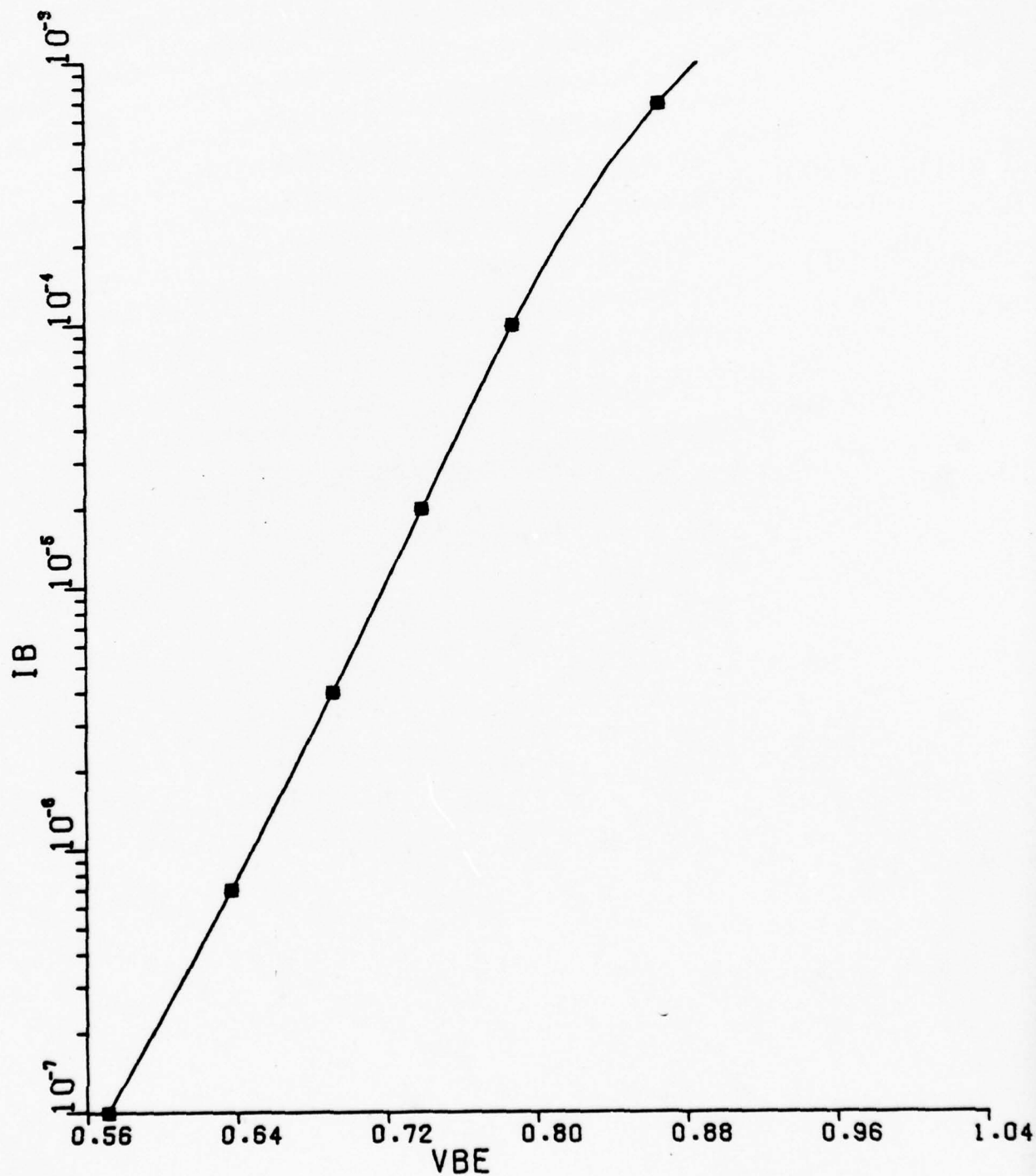
* --	RE	= 1.000E-02
+ --	RE	= 5.000E+00
o --	RE	= 5.000E-01



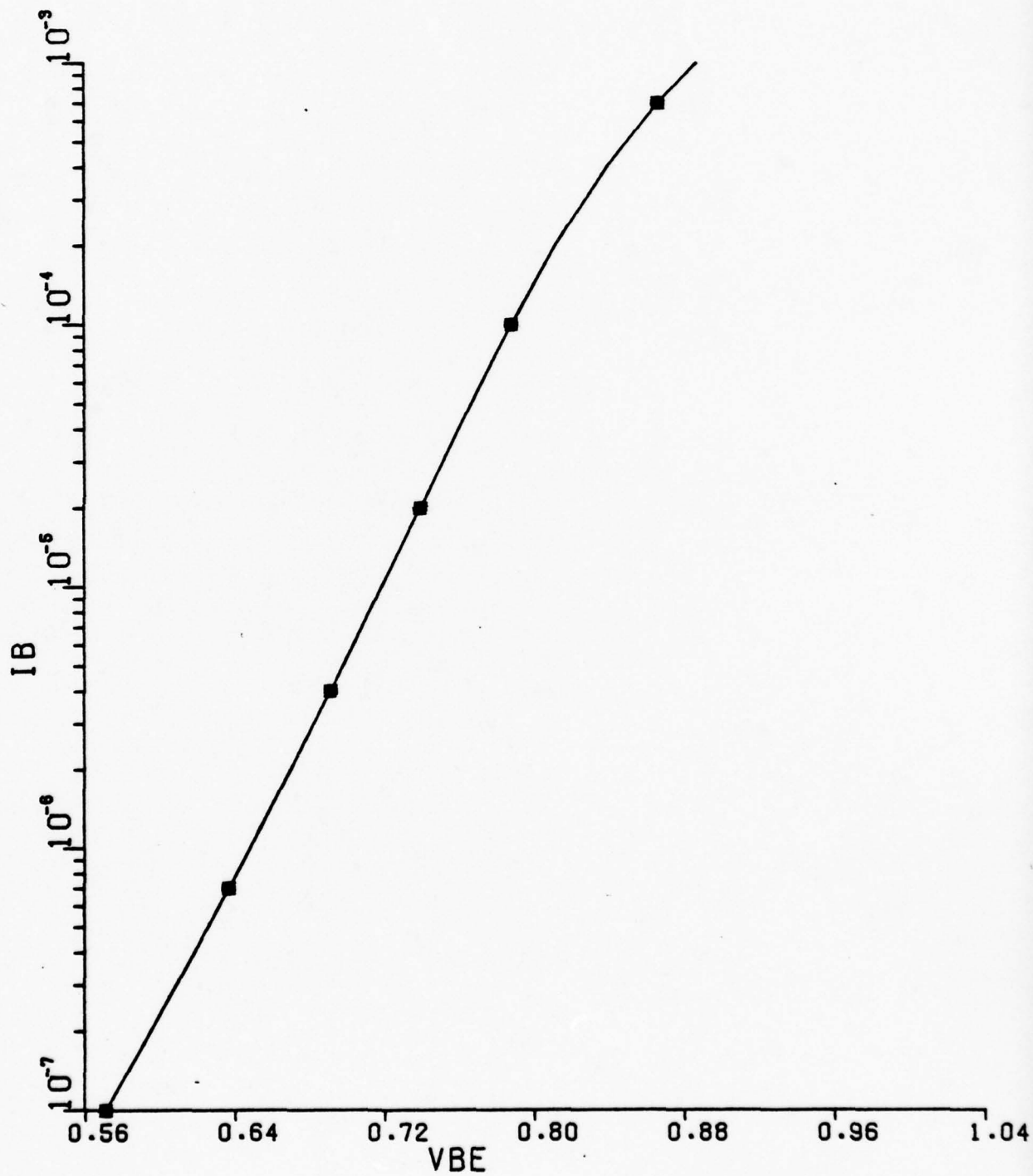
■ --	RCO	=	1.000E+00
+ --	RCO	=	5.000E+01
0 --	RCO	=	5.000E+00



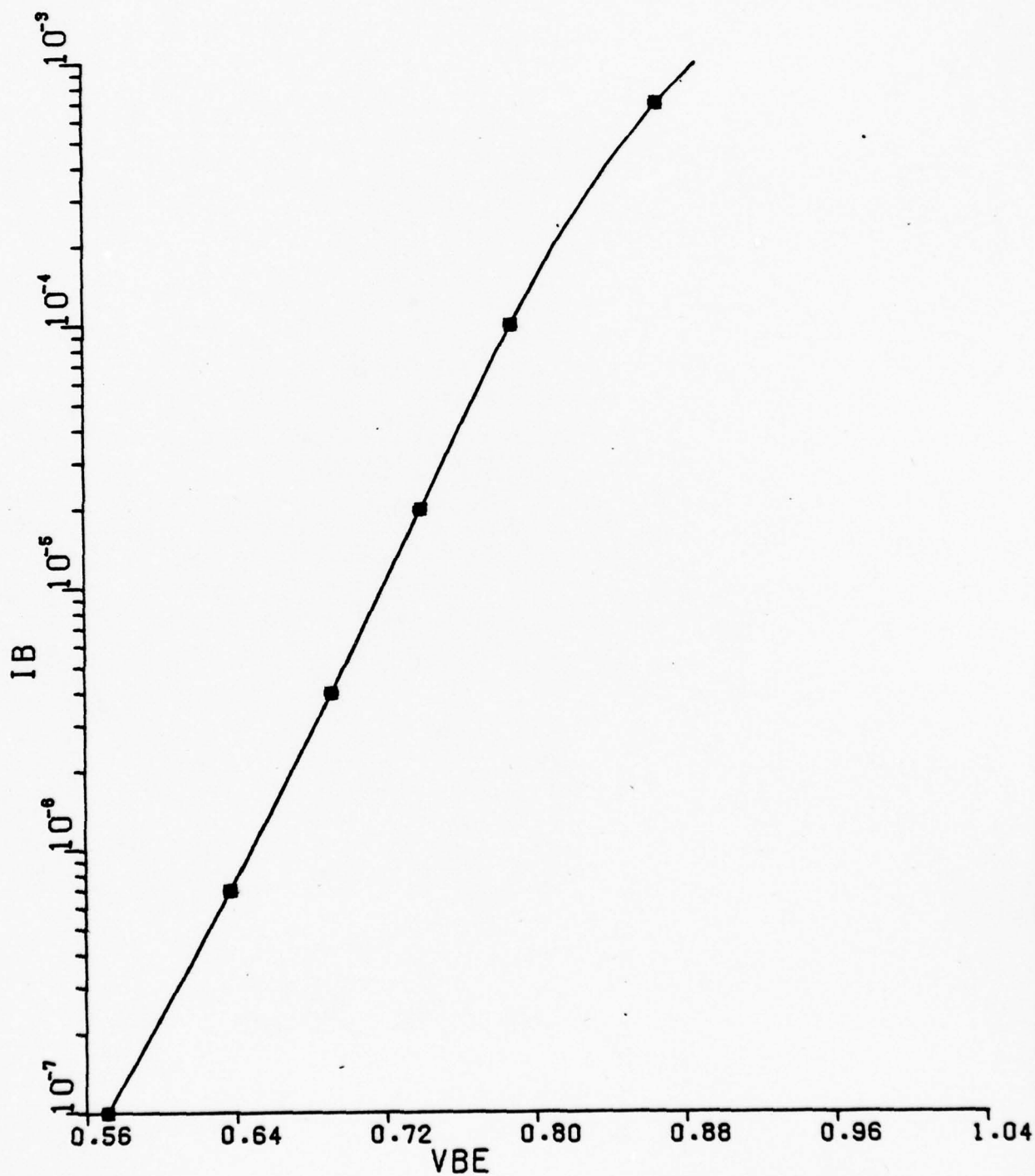
■ --	PC	=	6.000E-03
+ --	PC	=	1.000E-03
0 --	PC	=	3.250E-03



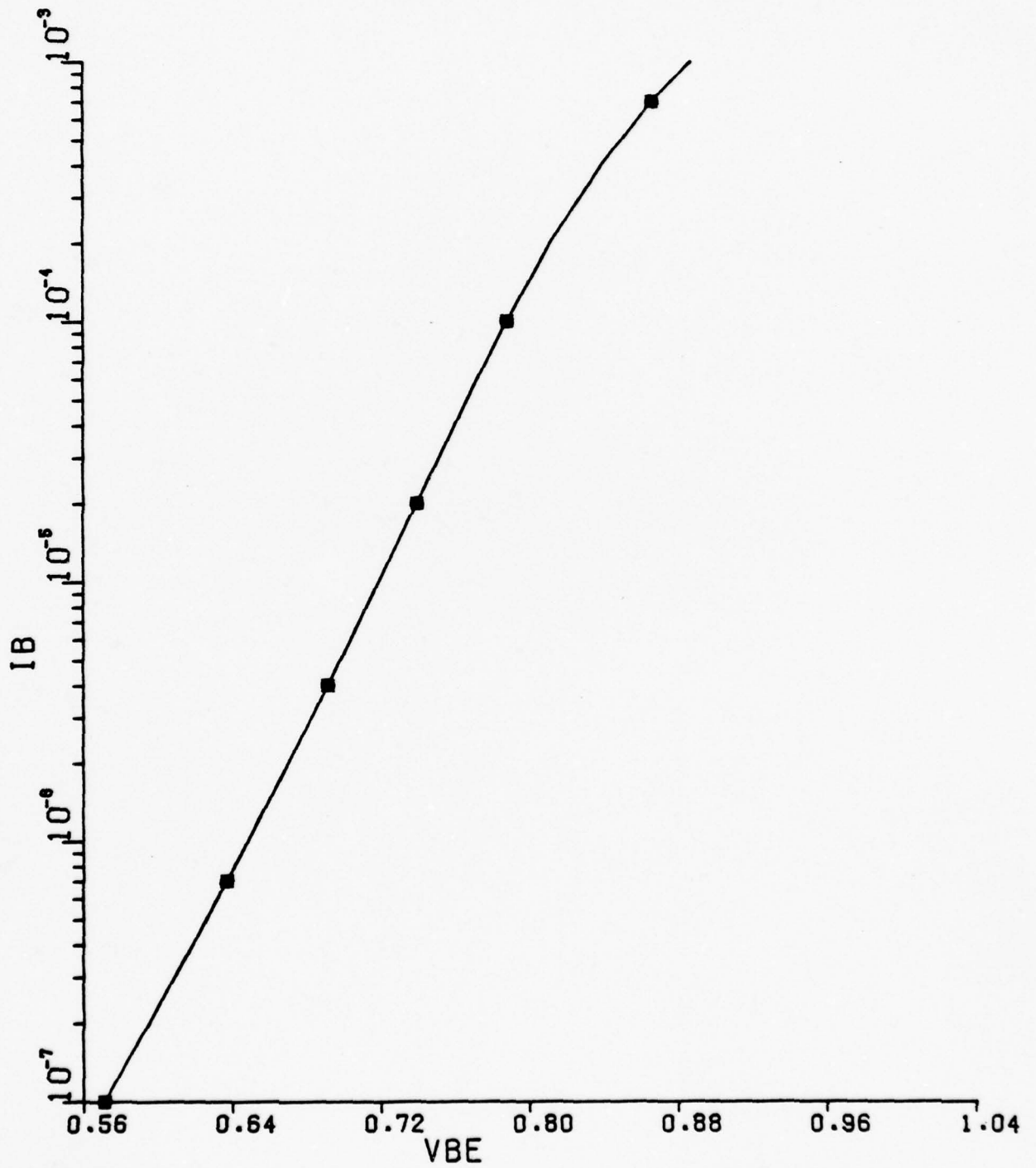
■	--	BS	=	2.500E-01
+	--	BS	=	5.000E-01
0	--	BS	=	3.333E-01



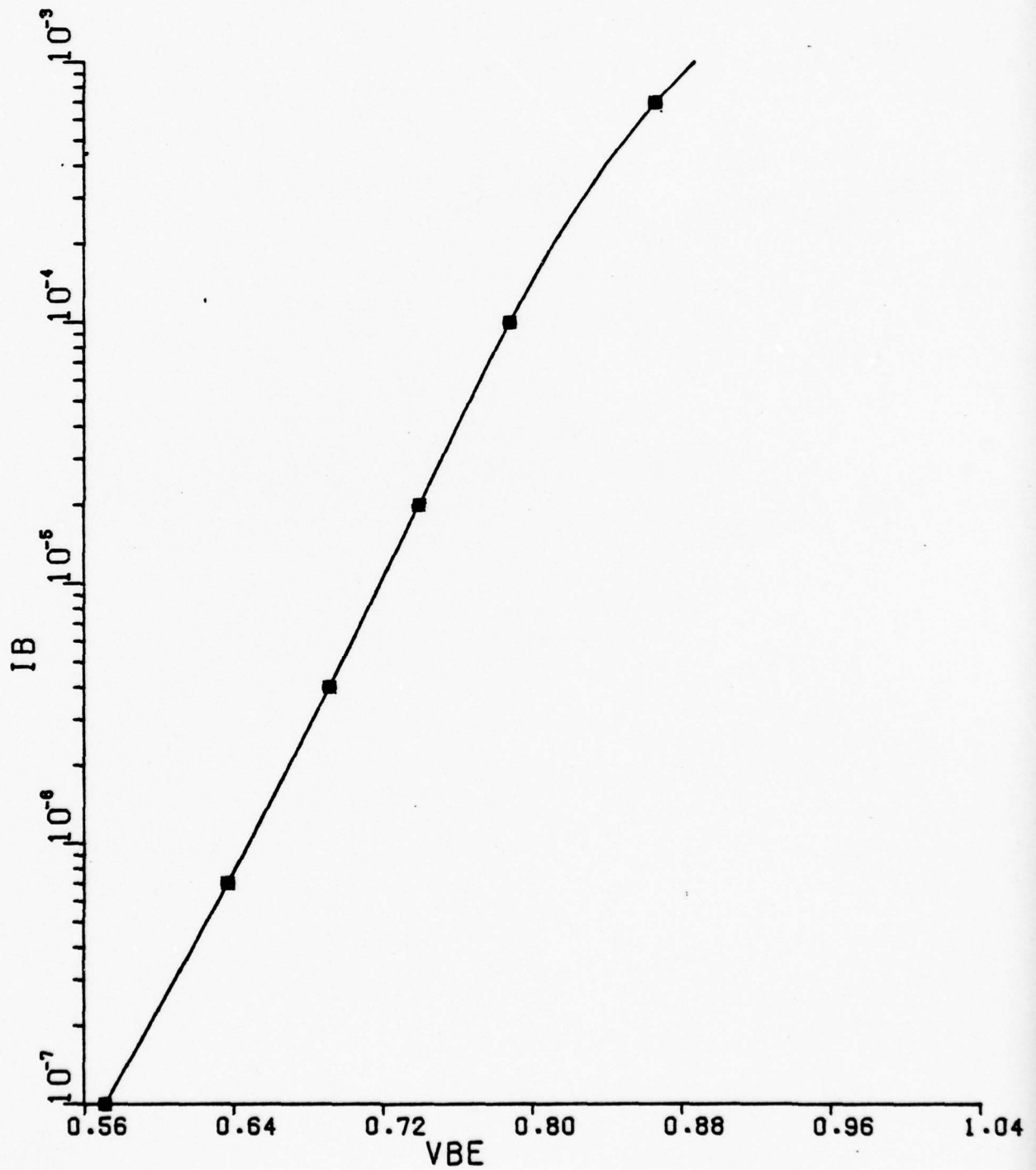
■ --	BC	=	2.500E-01
+ --	BC	=	5.000E-01
0 --	BC	=	3.333E-01



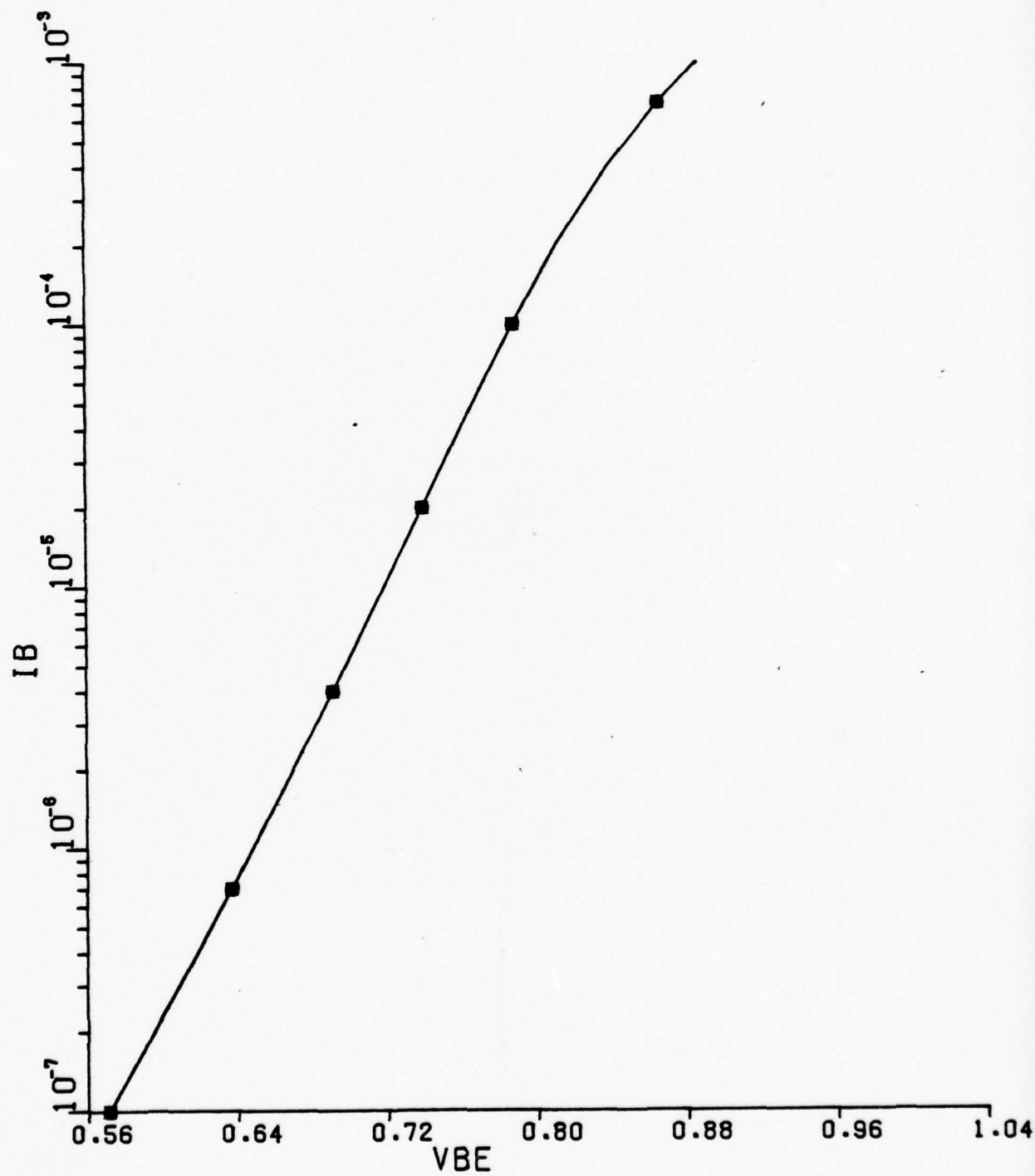
■ --	BE	=	2.500E-01
+ --	BE	=	3.333E-01
0 --	BE	=	5.000E-01



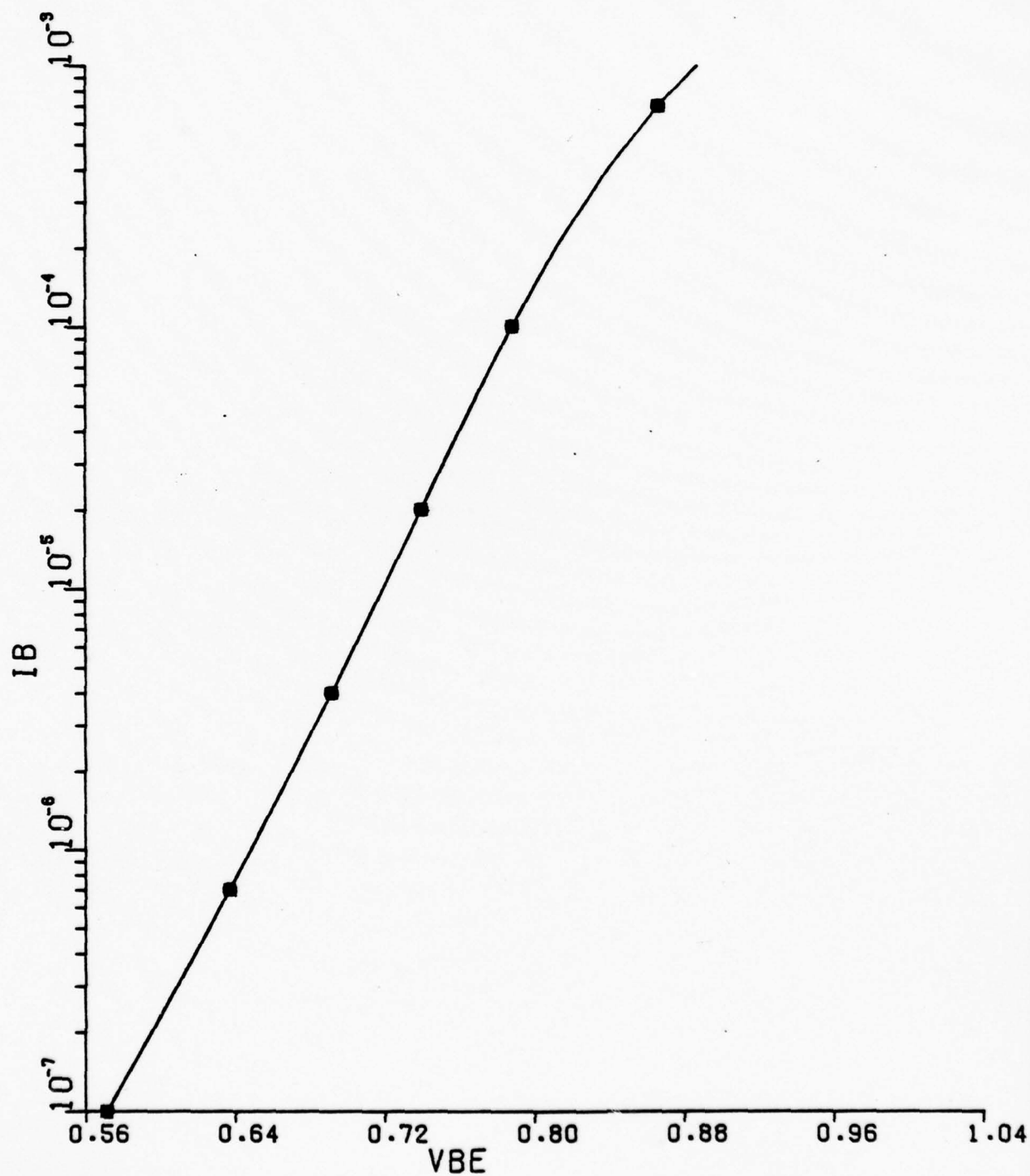
■ --	CS0	=	4.000E-13
+ --	CS0	=	1.000E-11
0 --	CS0	=	2.000E-12



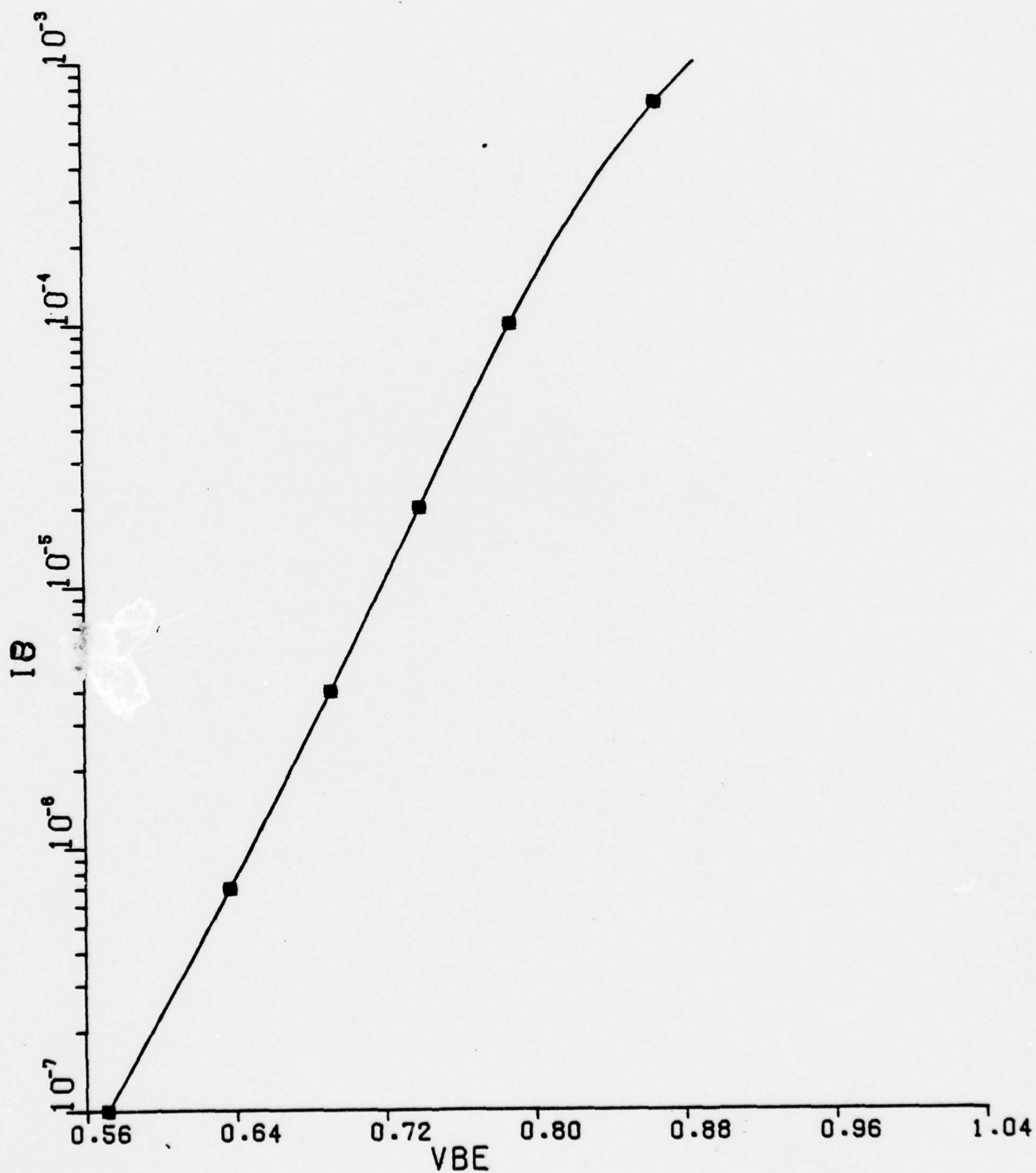
■ --	CEO	=	4.000E-13
+ --	CEO	=	1.000E-11
0 --	CEO	=	9.000E-13



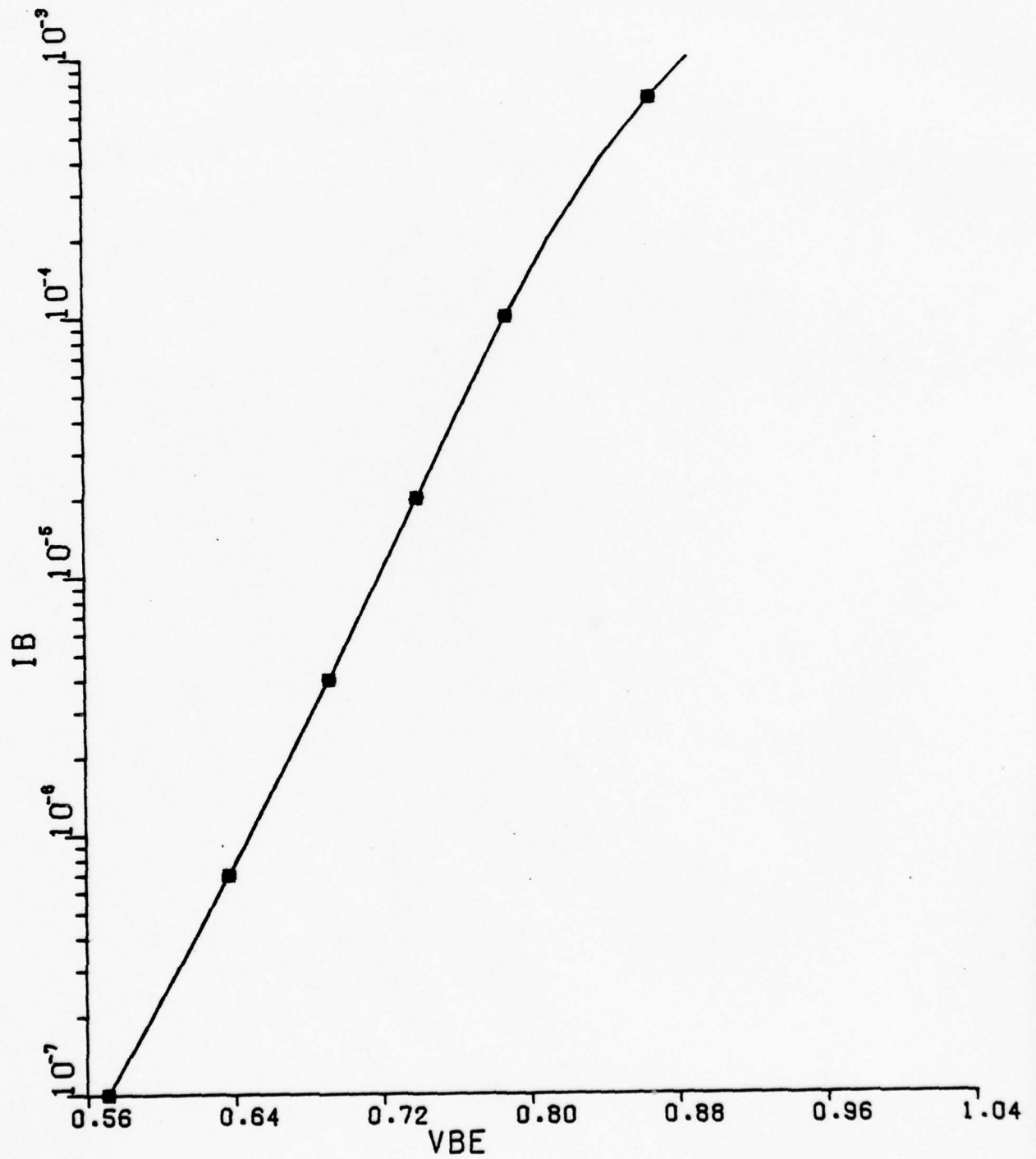
* --	CCO	=	4.000E-13
+ --	CCO	=	1.000E-10
0 --	CCO	=	8.000E-13



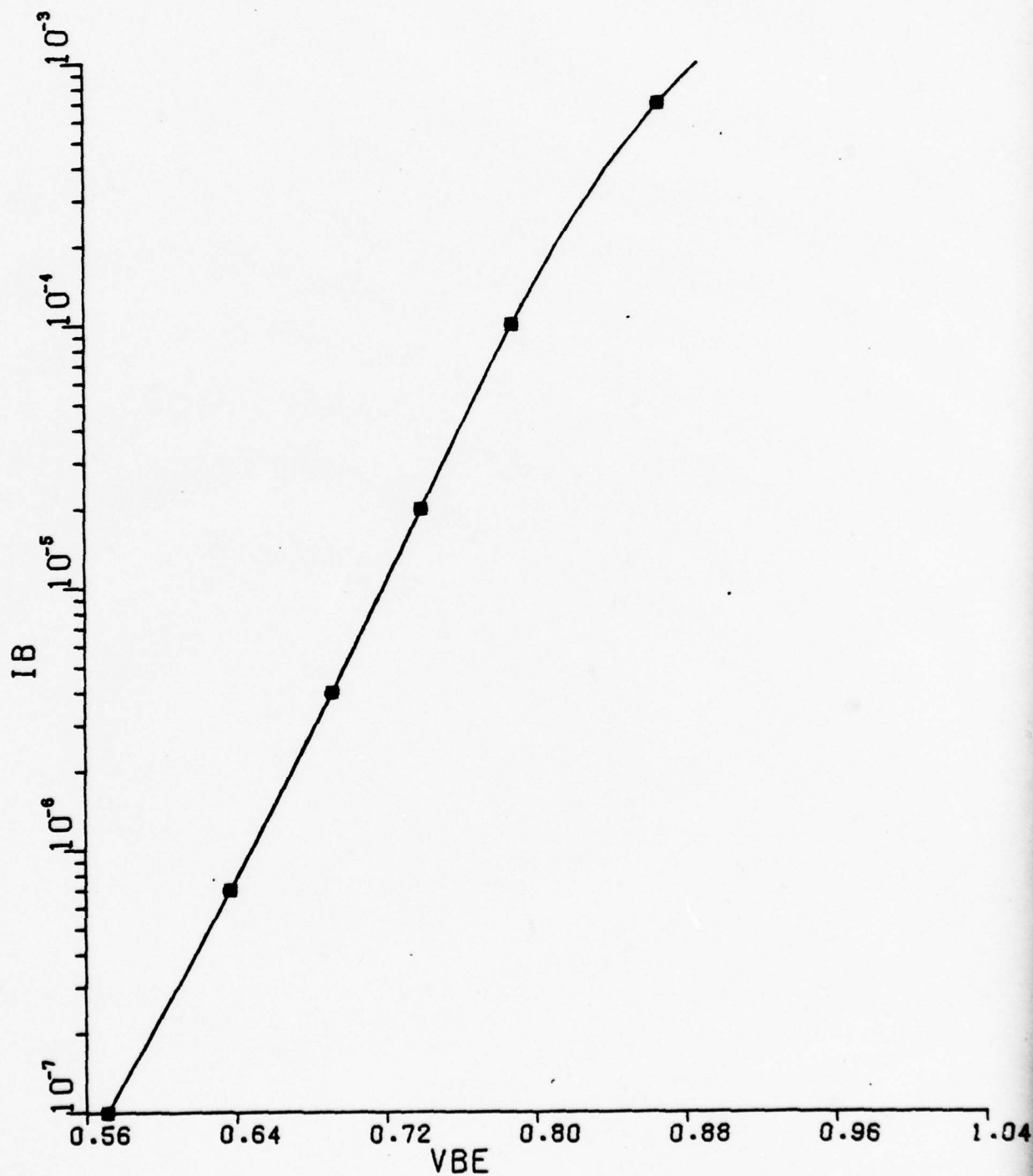
■ --	PHISS	=	5.000E-01
+ --	PHISS	=	1.200E+00
0 --	PHISS	=	9.000E-01



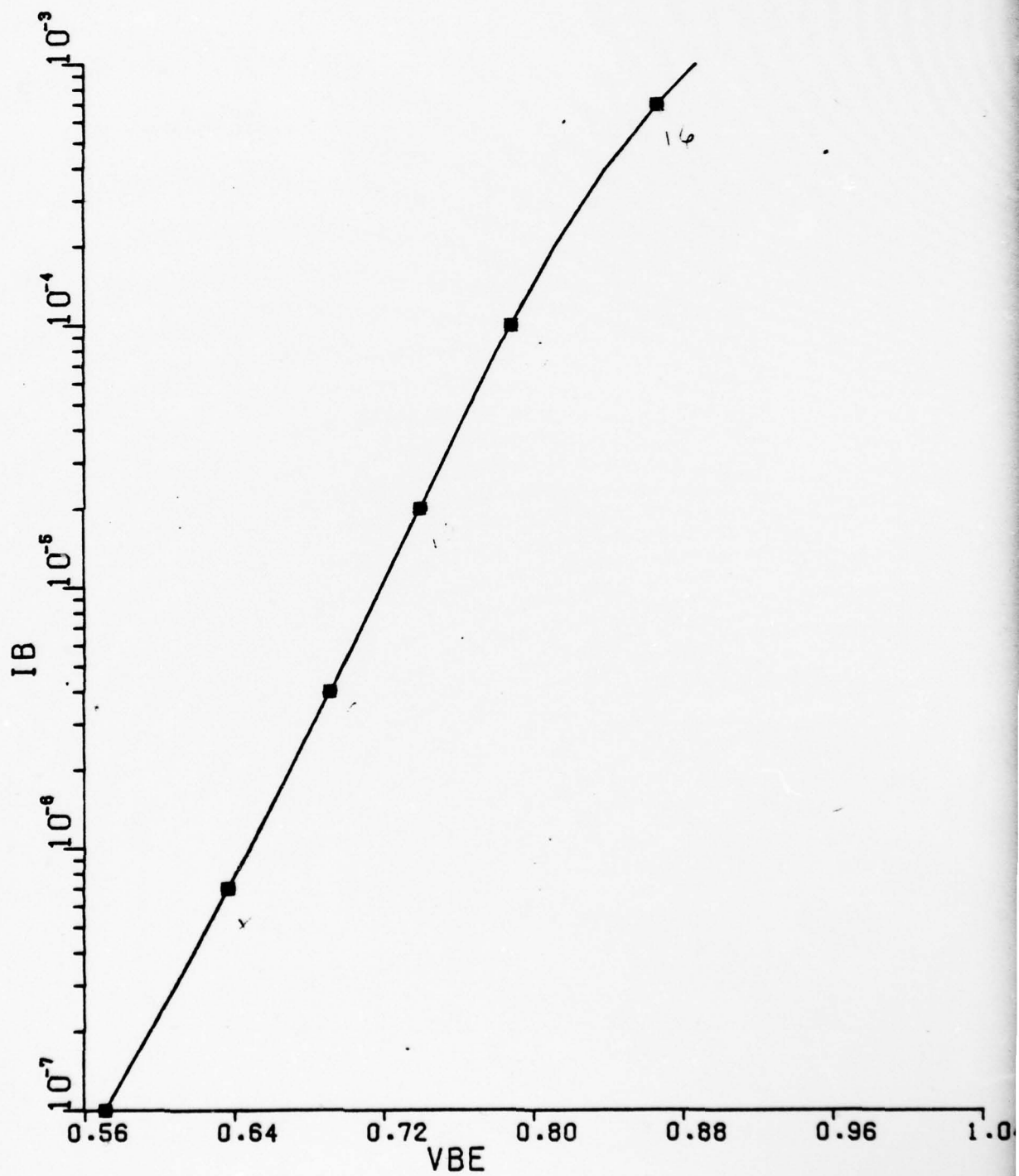
■ --	PHICO	=	5.000E-01
+ --	PHICO	=	1.200E+00
0 --	PHICO	=	9.000E-01

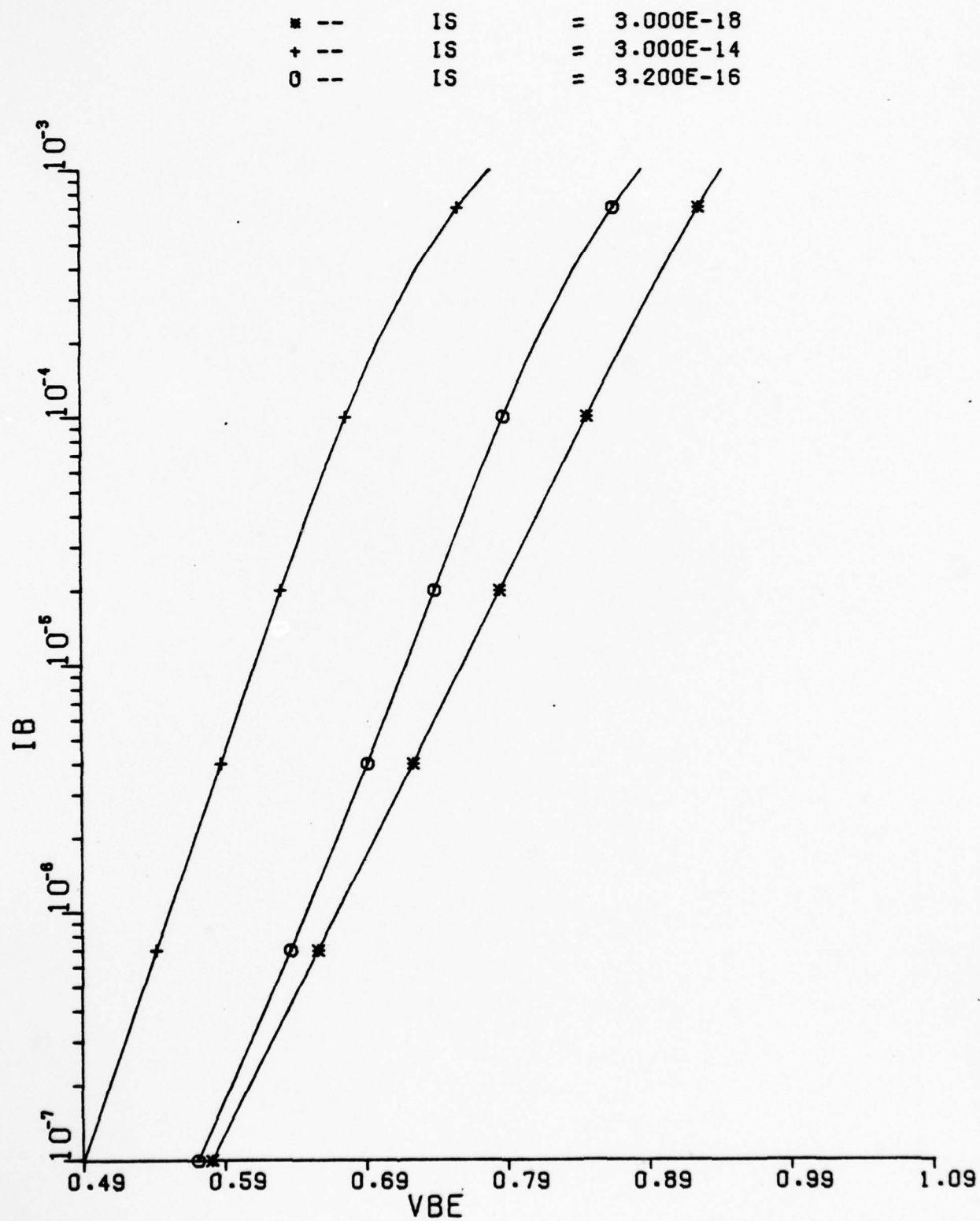


■ --	PHIE0	=	5.000E-01
+ --	PHIE0	=	1.500E+00
0 --	PHIE0	=	1.200E+00

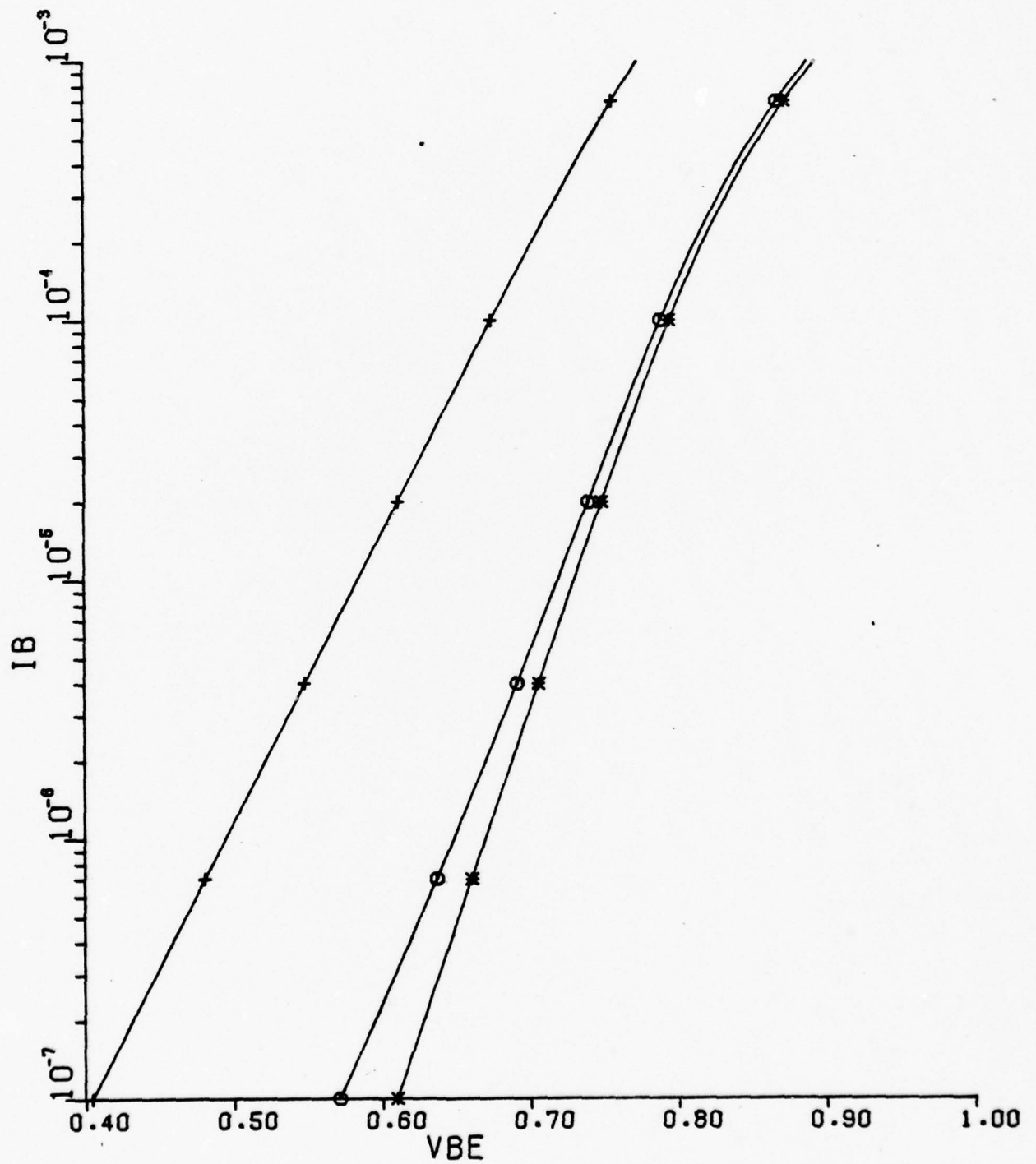


■ --	ISR	=	3.000E-13
+ --	ISR	=	3.000E-11
0 --	ISR	=	3.000E-12

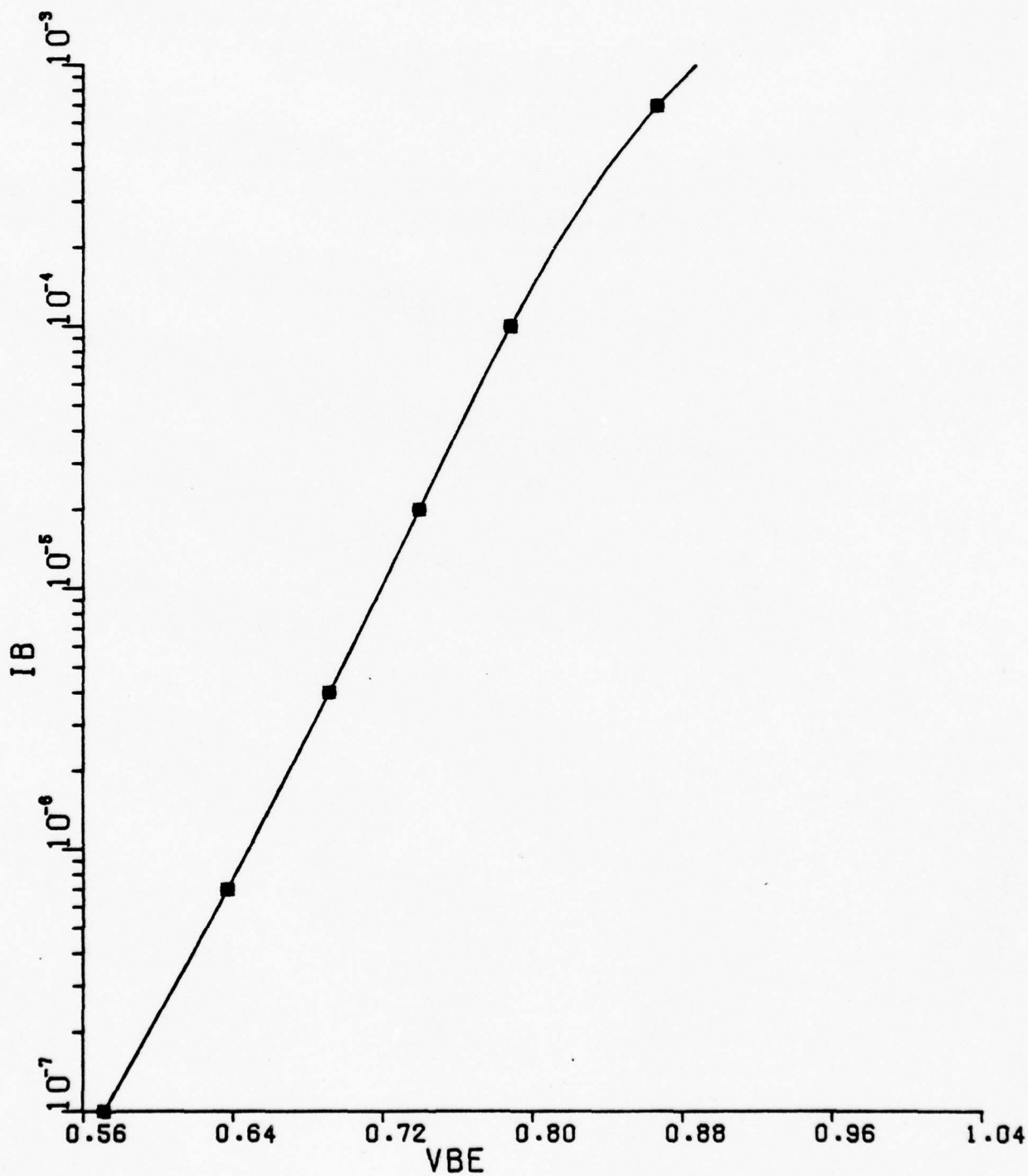




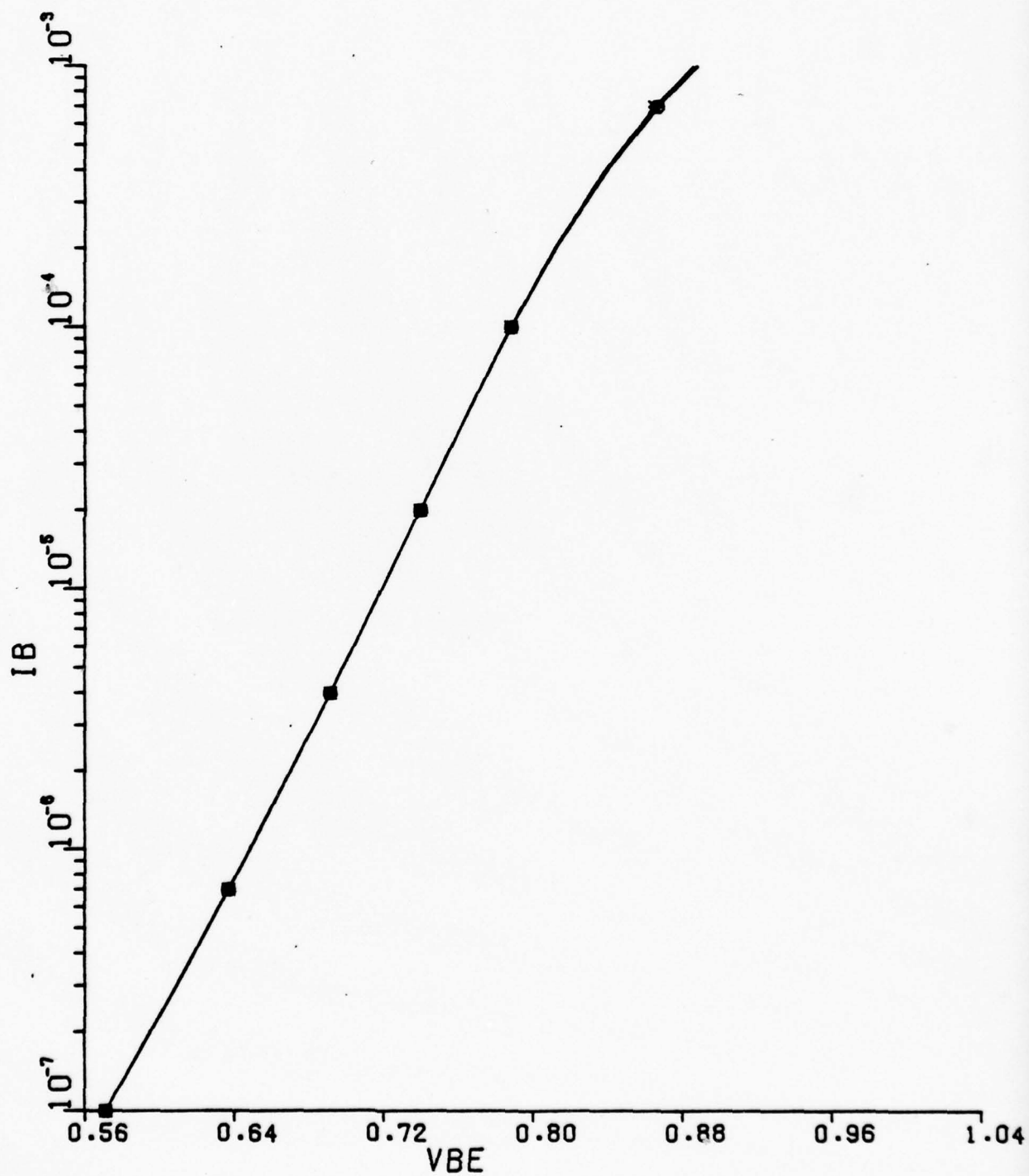
■ --	IER	=	3.000E-16
+ --	IER	=	3.000E-12
0 --	IER	=	3.200E-14



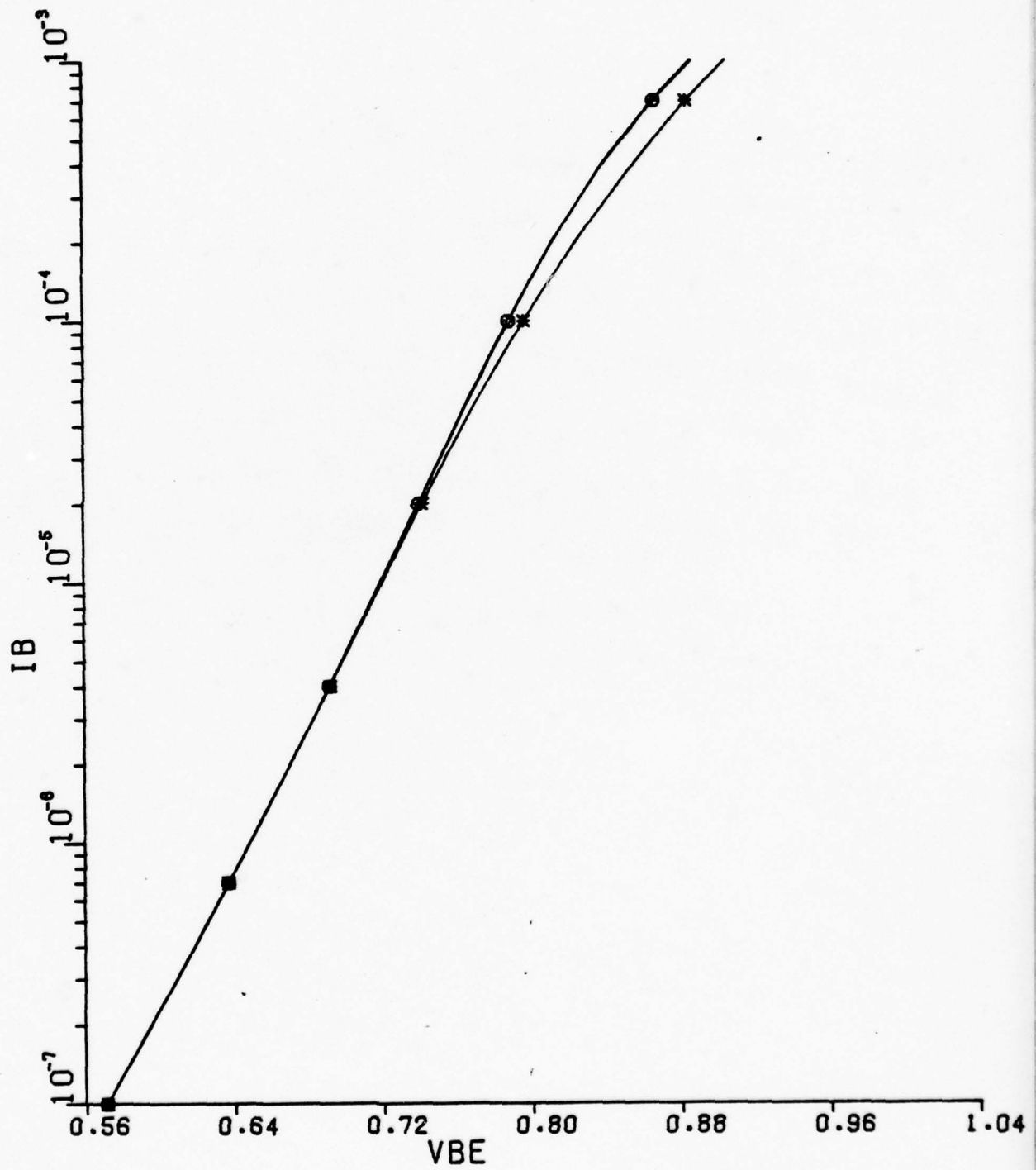
■ --	IBR	=	3.000E-15
+ --	IBR	=	3.000E-11
0 --	IBR	=	3.000E-13



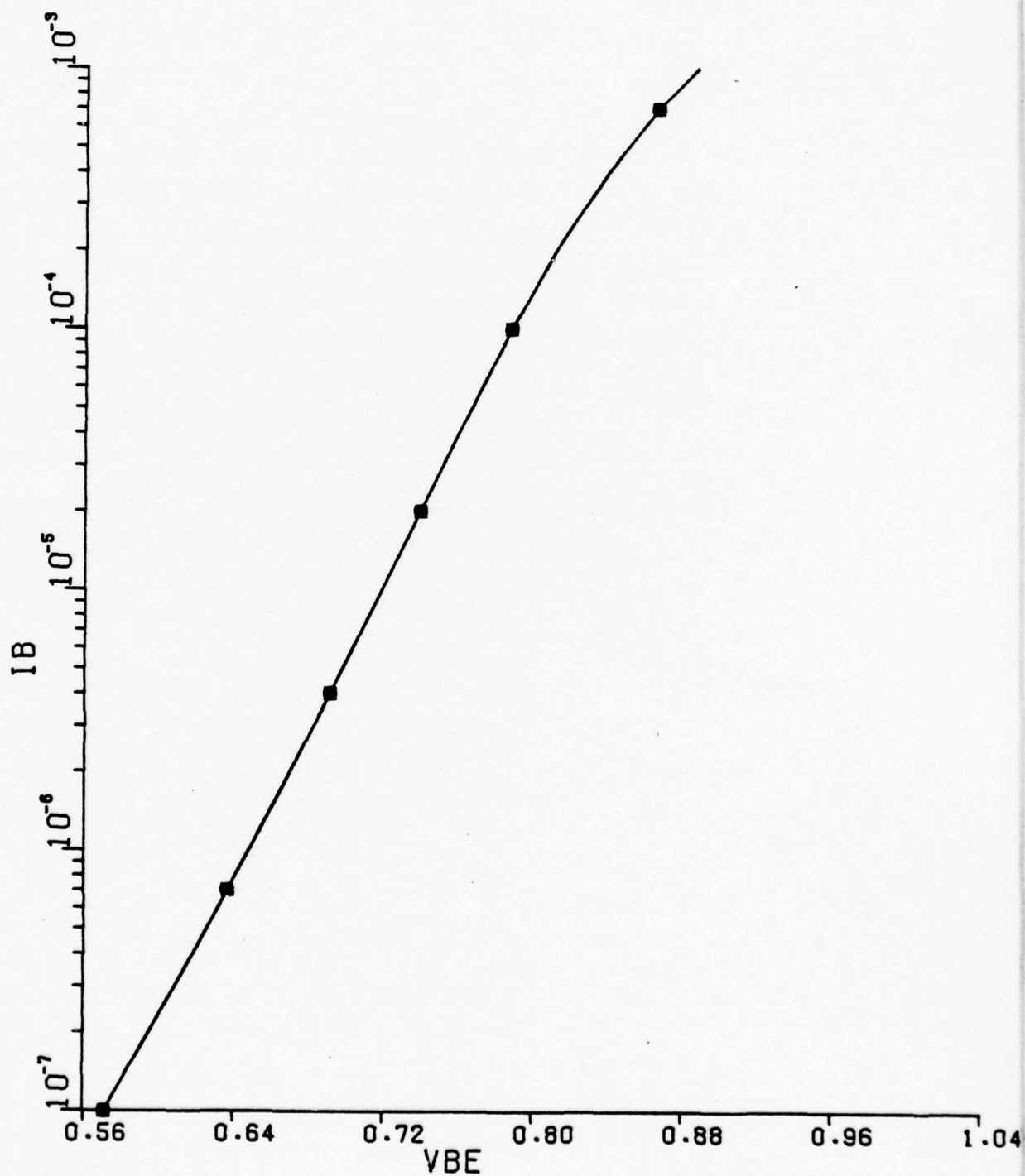
■ --	VER	=	5.000E+00
+ --	VER	=	5.000E+01
0 --	VER	=	2.000E+01



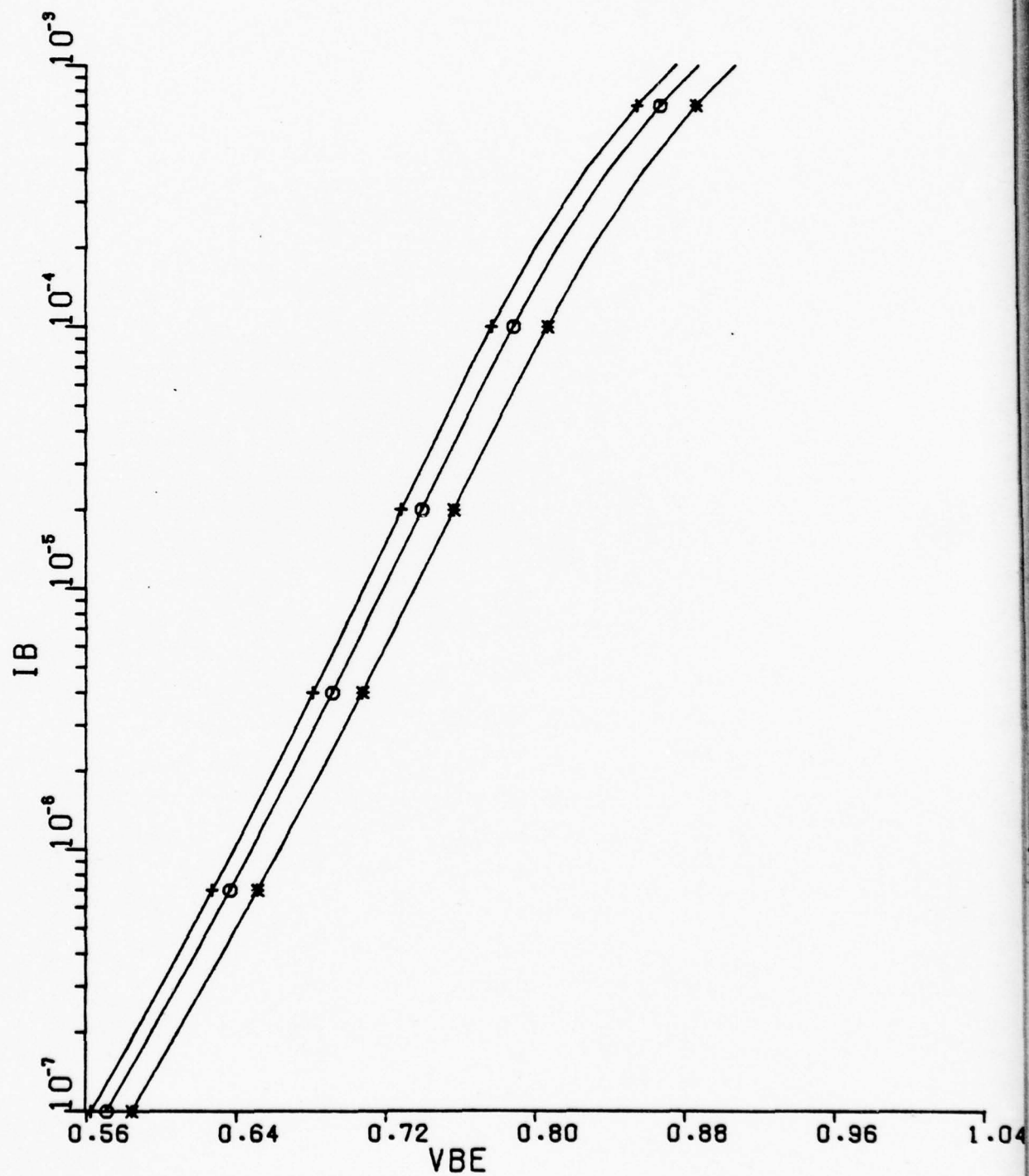
■ --	VCR	=	5.000E+00
+ --	VCR	=	3.000E+02
o --	VCR	=	6.000E+01



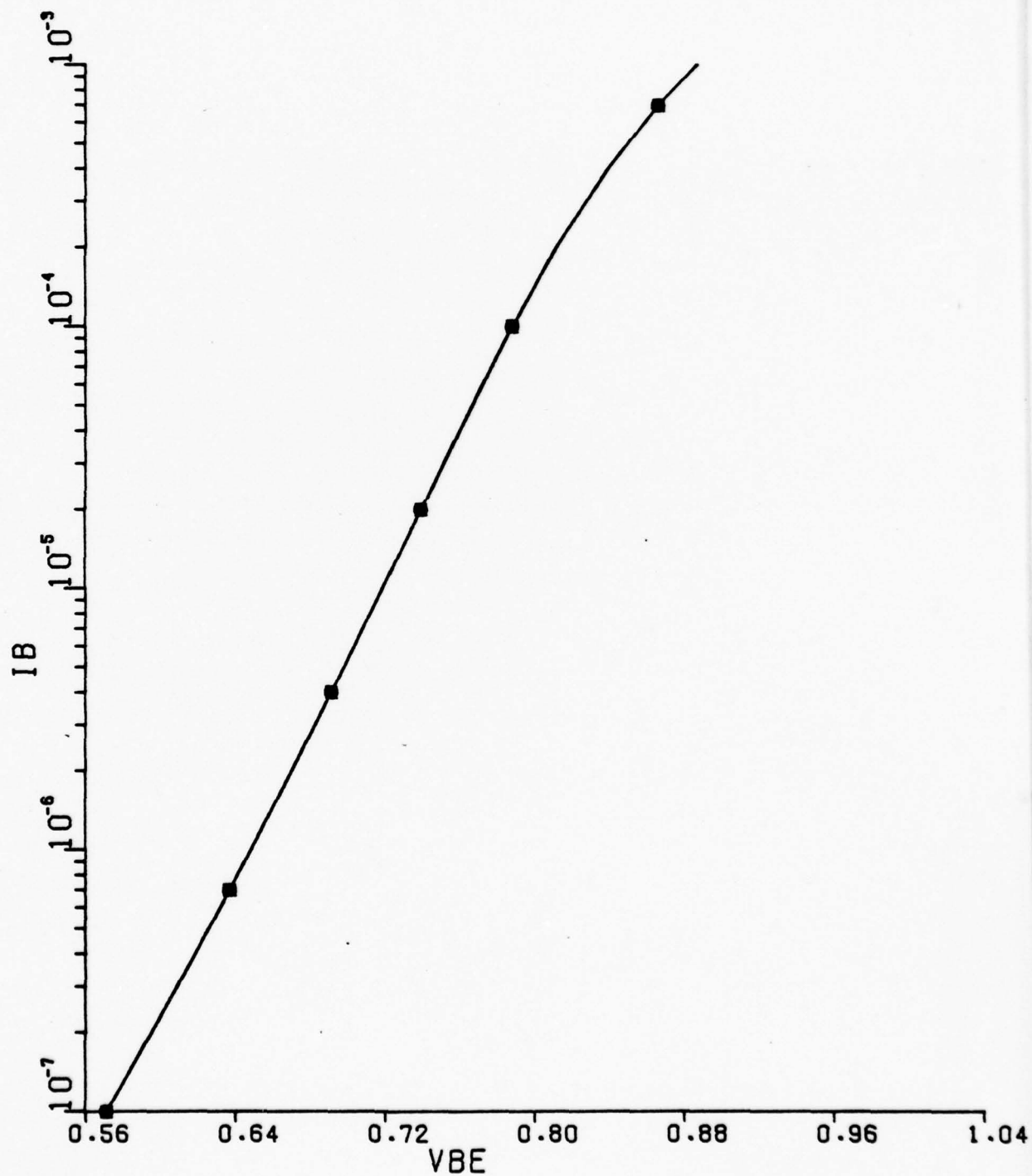
* --	NC	= 8.000E-01
+ --	NC	= 2.300E+00
0 --	NC	= 1.800E+00



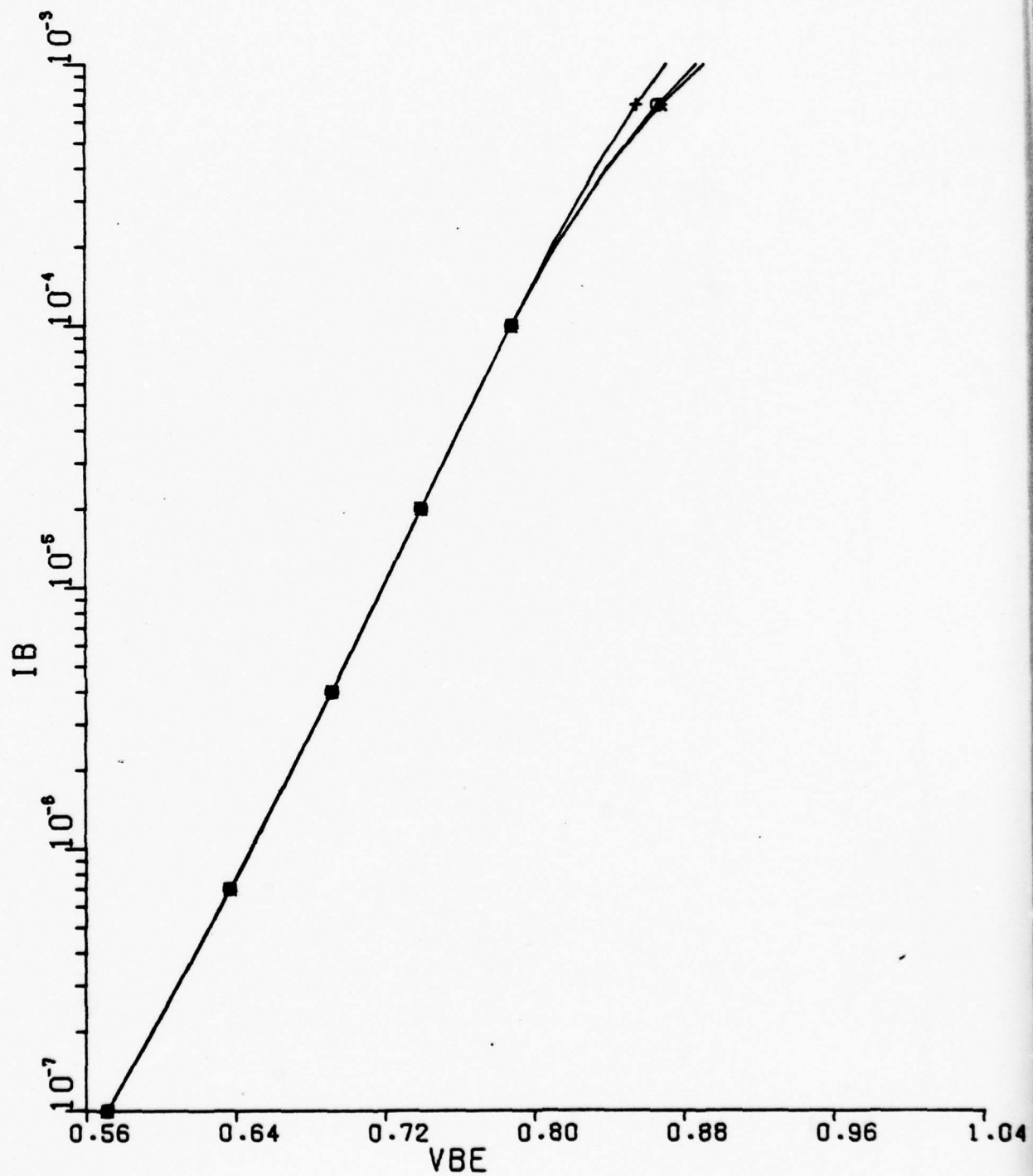
* --	VT	=	2.650E-02
+ --	VT	=	2.550E-02
o --	VT	=	2.590E-02



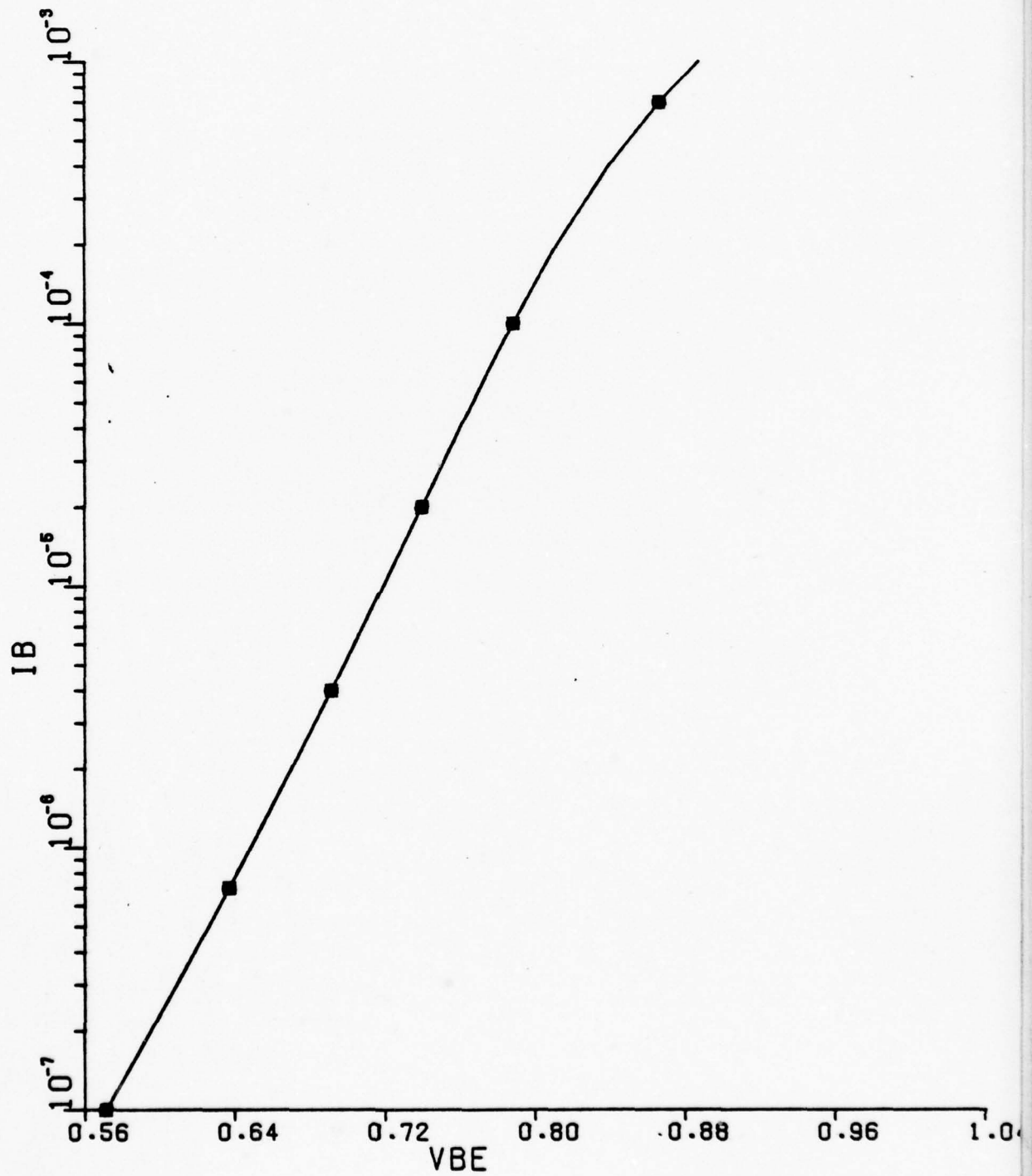
■ --	VTS	=	2.550E-02
+ --	VTS	=	2.650E-02
0 --	VTS	=	2.590E-02



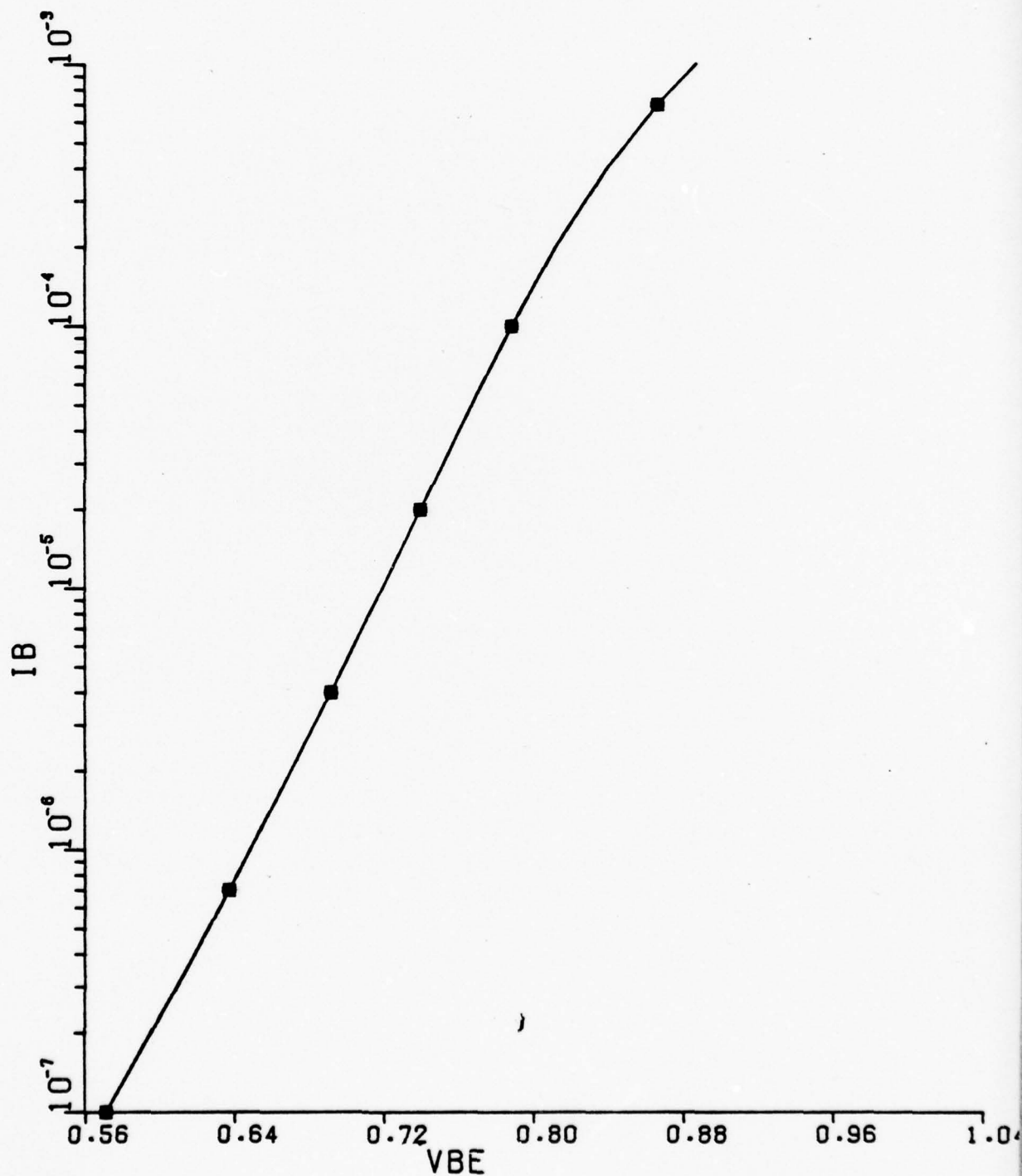
■ --	QFN	=	1.500E-18
+ --	QFN	=	1.500E-14
0 --	QFN	=	1.500E-16



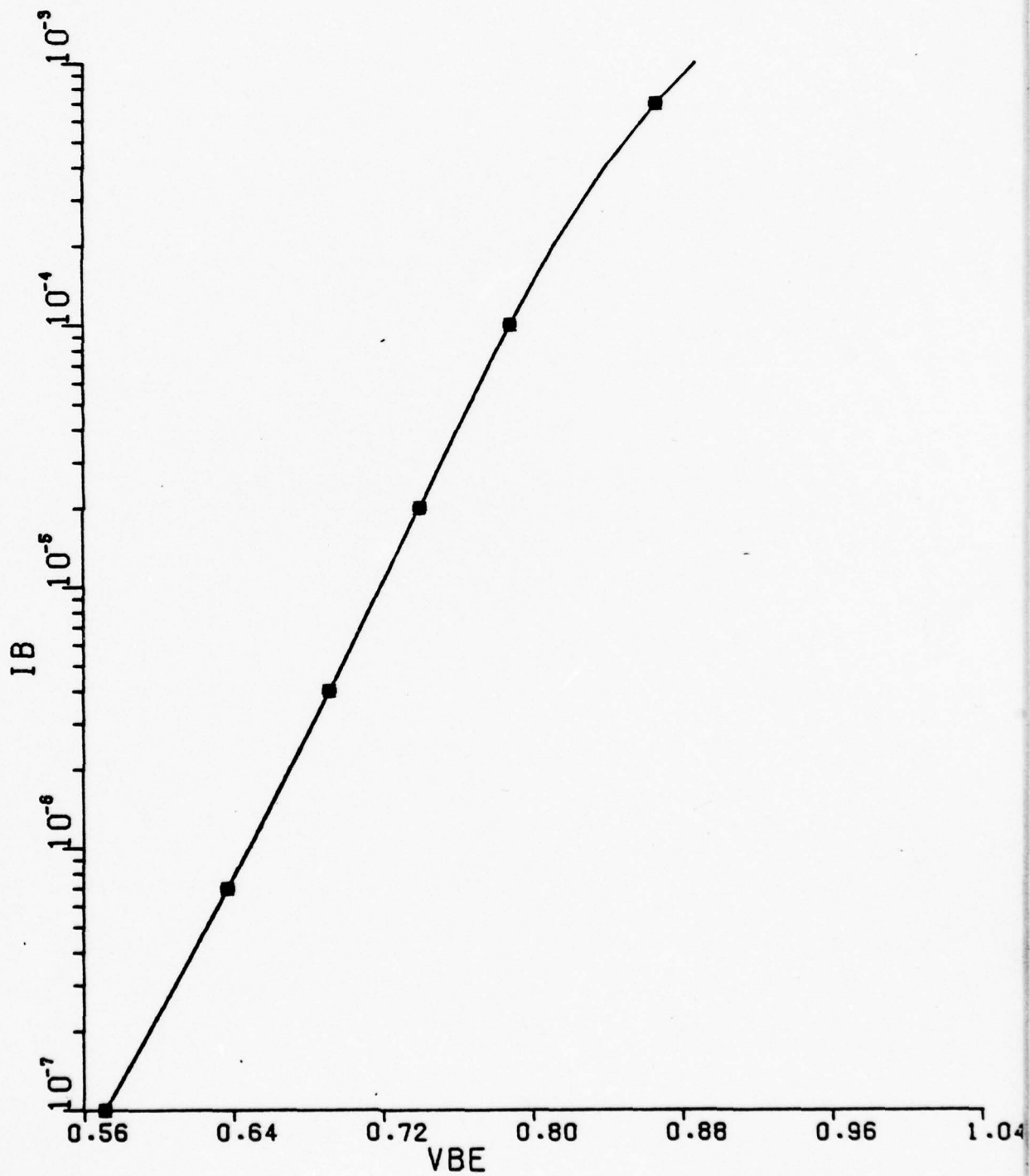
■ --	QRN	=	1.500E-14
+ --	QRN	=	1.500E-10
0 --	QRN	=	1.500E-12



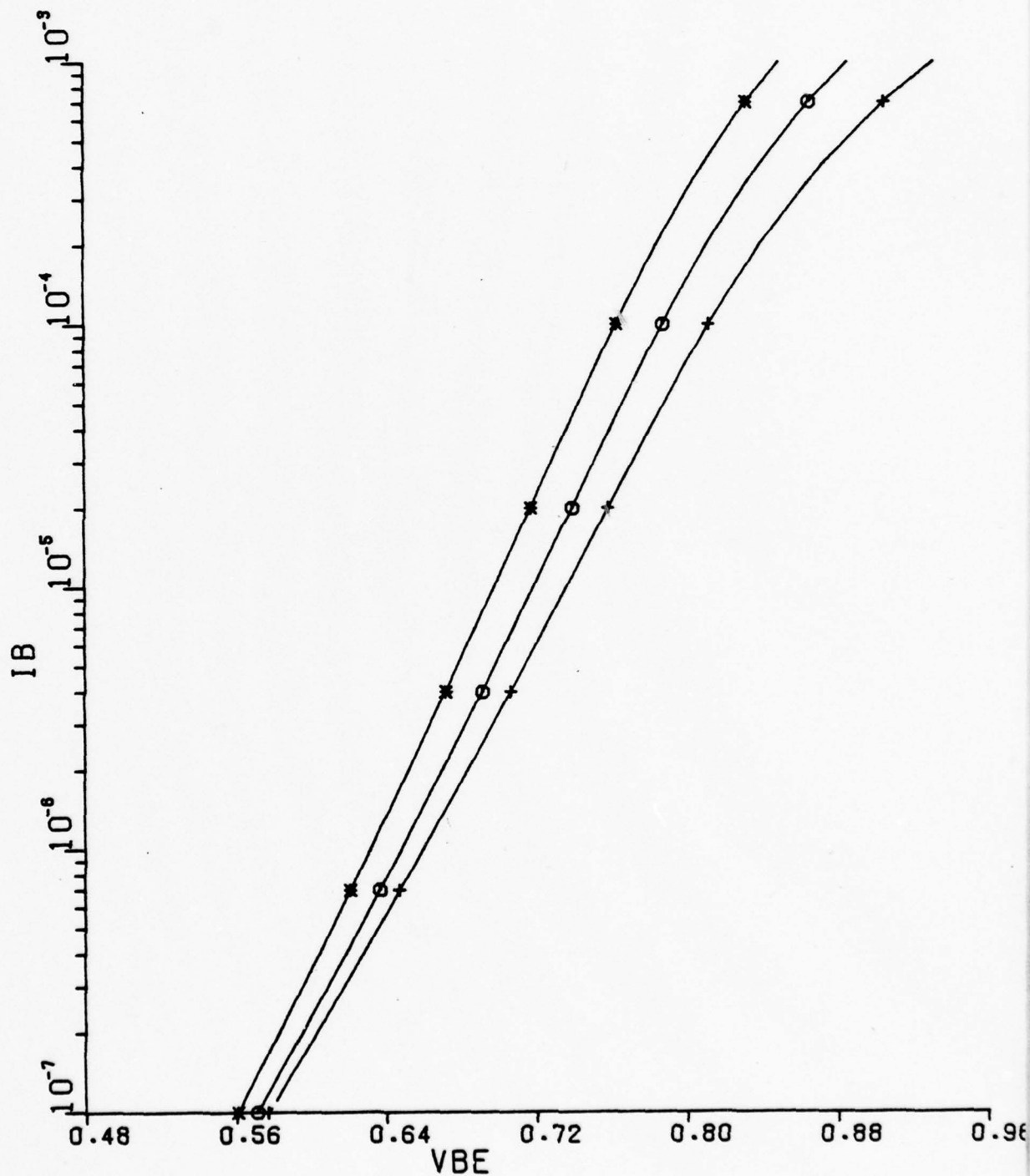
* --	TAUFO	=	1.590E-09
+ --	TAUFO	=	1.590E-08
0 --	TAUFO	=	1.590E-10



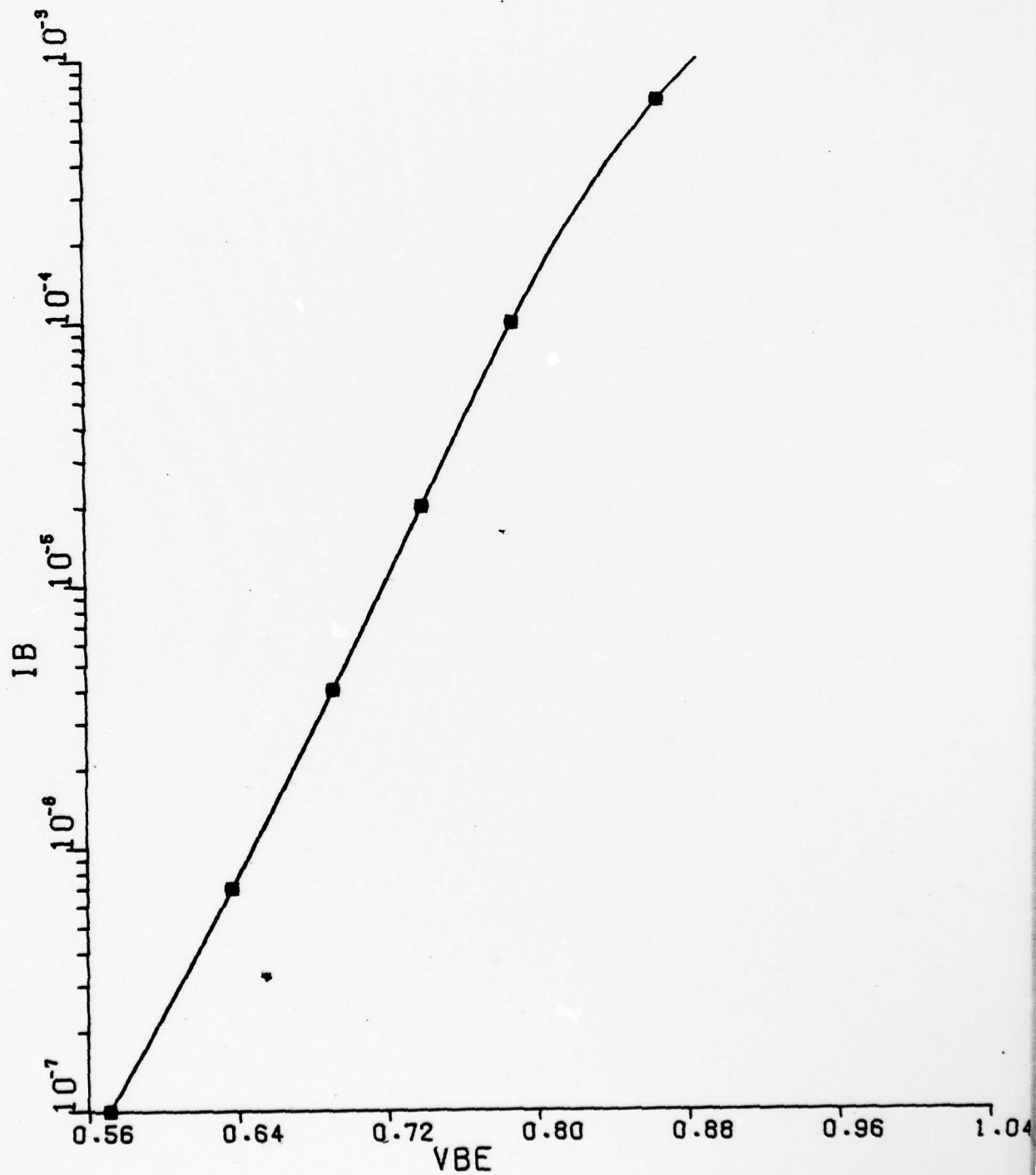
■	--	TASUR	=	1.000E-06
+	--	TASUR	=	1.270E-11
0	--	TASUR	=	1.270E-09



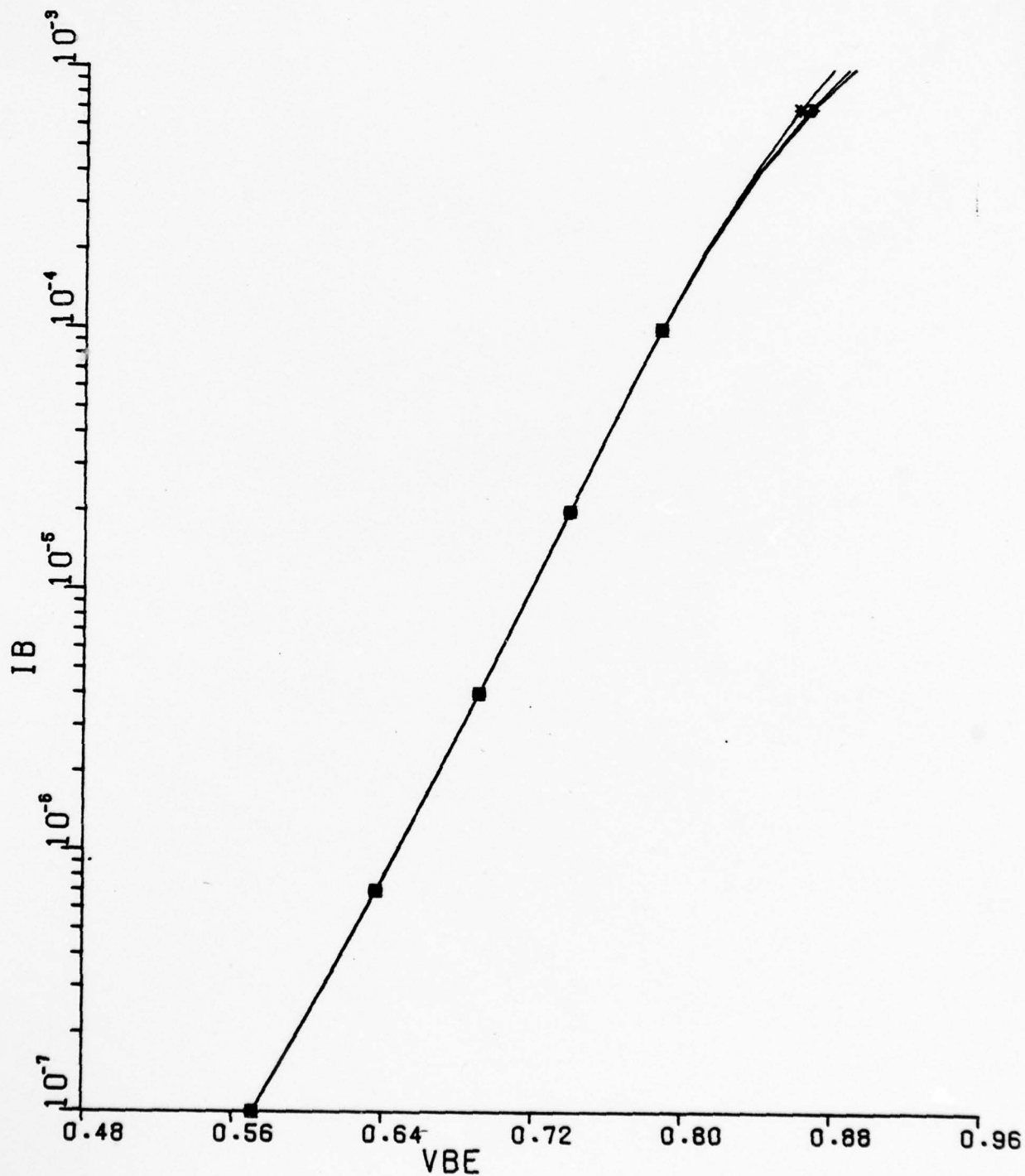
* --	BETAO	=	2.000E+01
+ --	BETAO	=	1.500E+02
o --	BETAO	=	5.500E+01



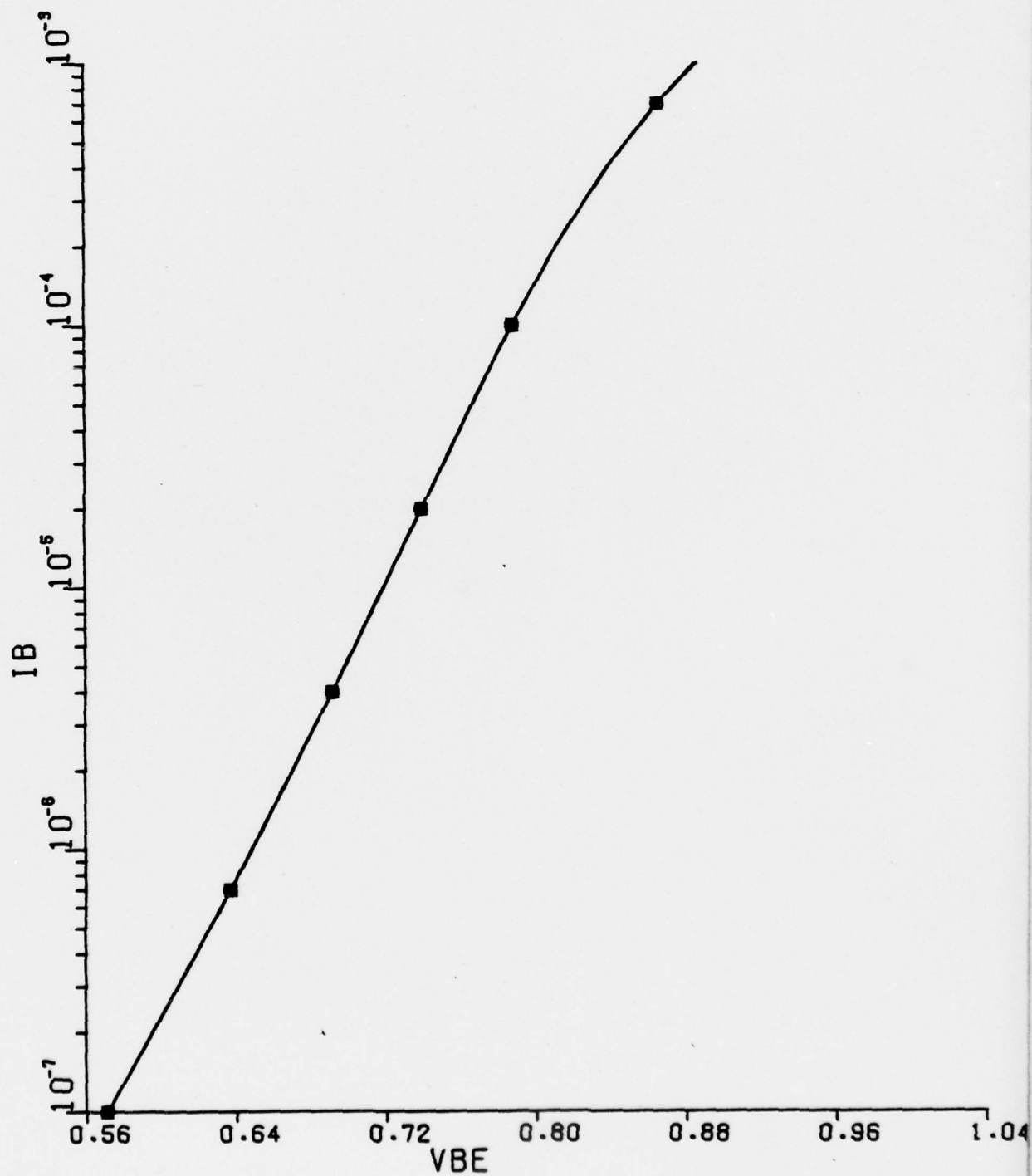
■ --	BETAR	=	6.000E+00
+ --	BETAR	=	1.100E+00
0 --	BETAR	=	1.500E+00



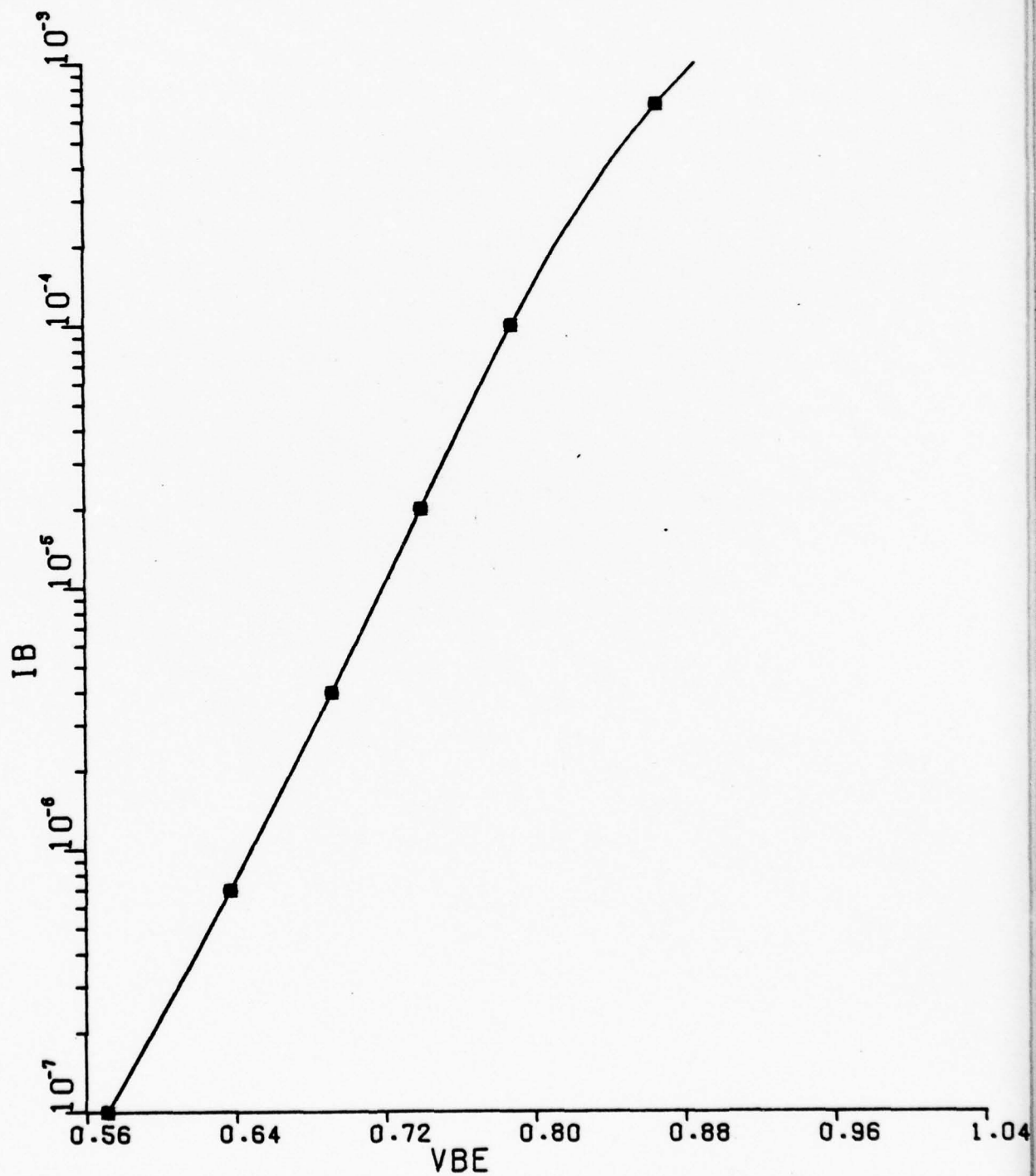
* --	W	=	2.000E-05
+ --	W	=	2.000E-04
0 --	W	=	6.000E-05



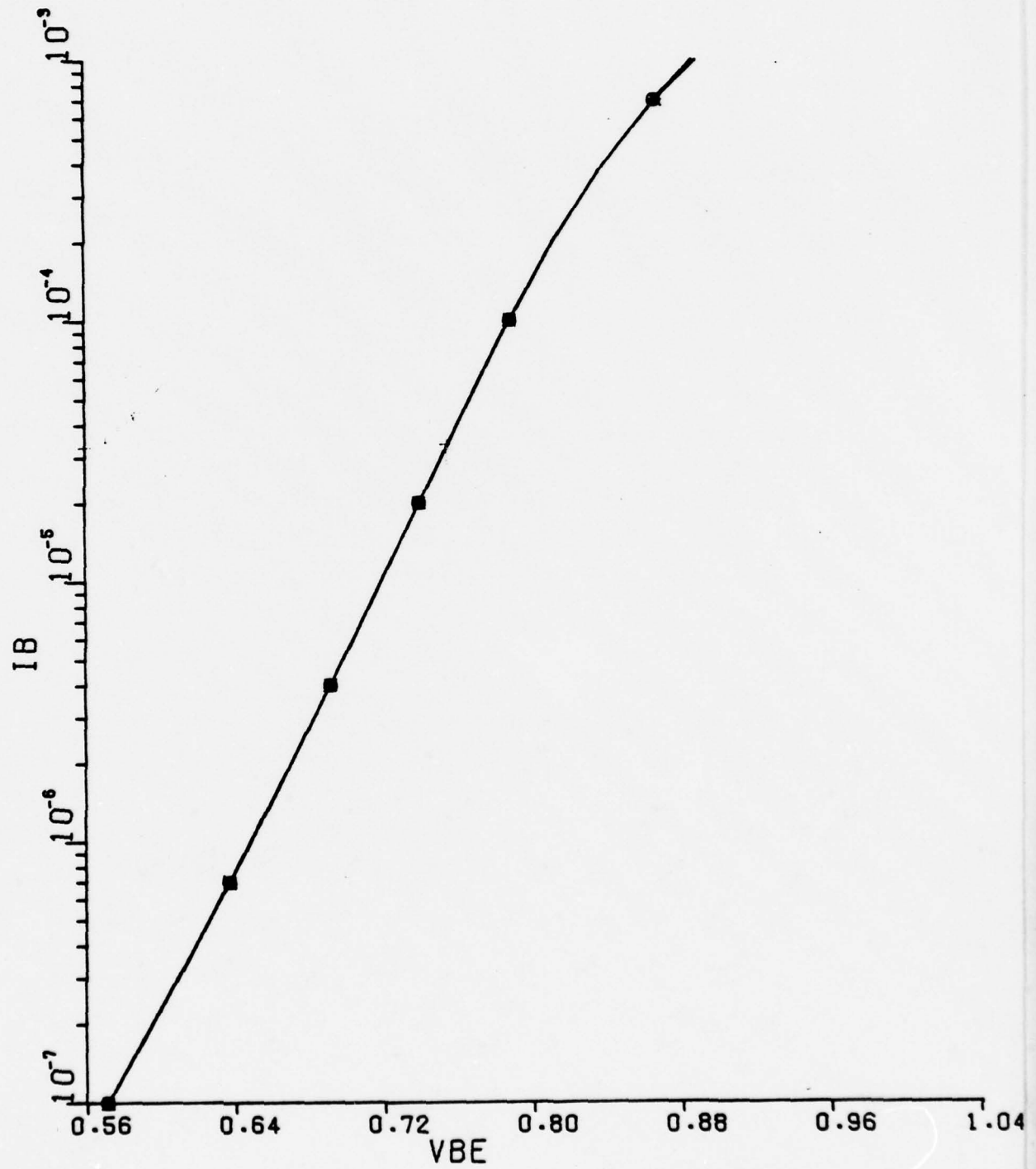
■ --	AE	=	1.000E-08
+ --	AE	=	1.000E-04
0 --	AE	=	9.800E-07



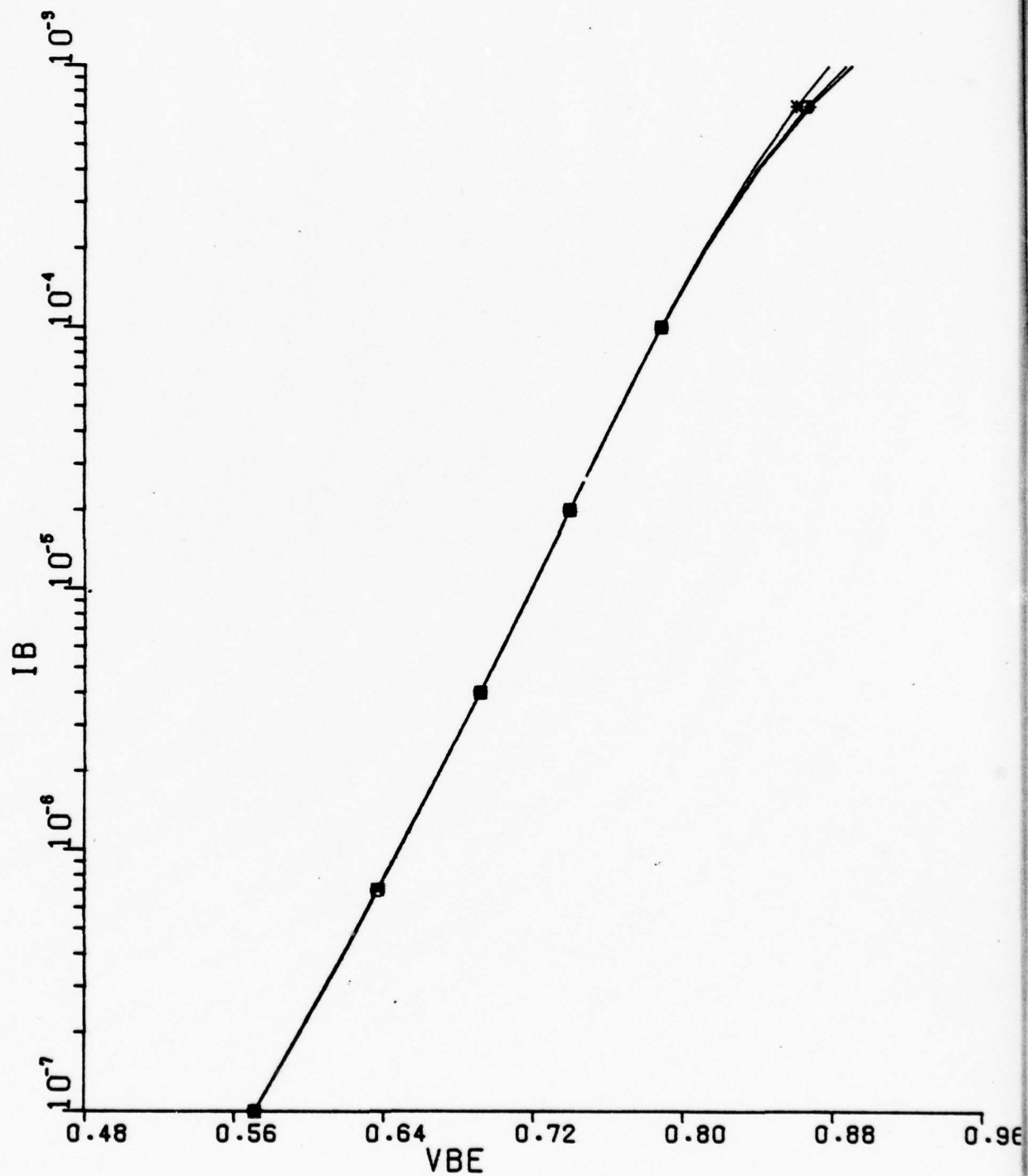
■ --	VLIM	=	1.000E+06
+ --	VLIM	=	1.500E+07
0 --	VLIM	=	6.000E+06



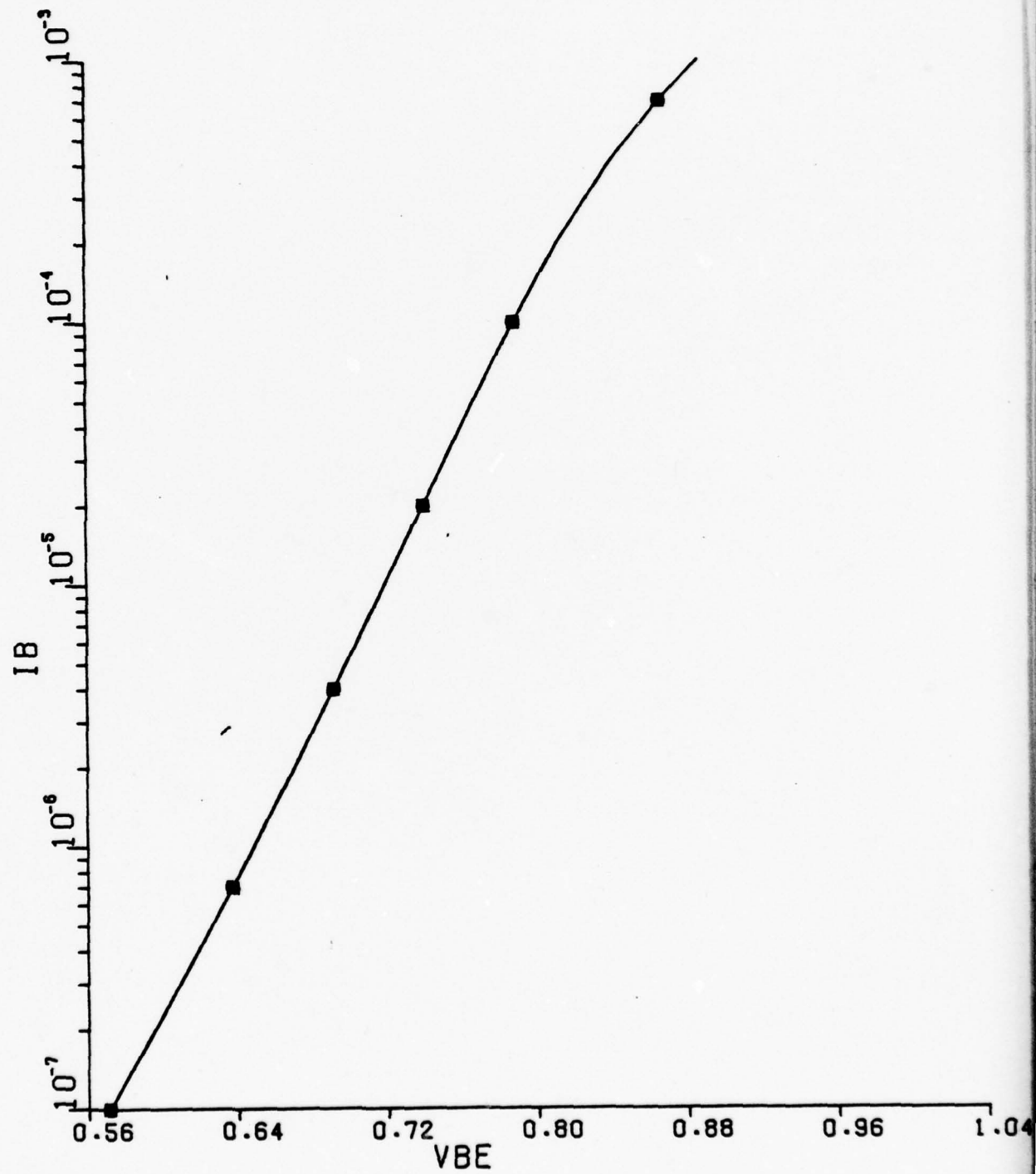
■ --	ONB	=	1.000E+01
+ --	ONB	=	3.000E+01
0 --	ONB	=	2.260E+01



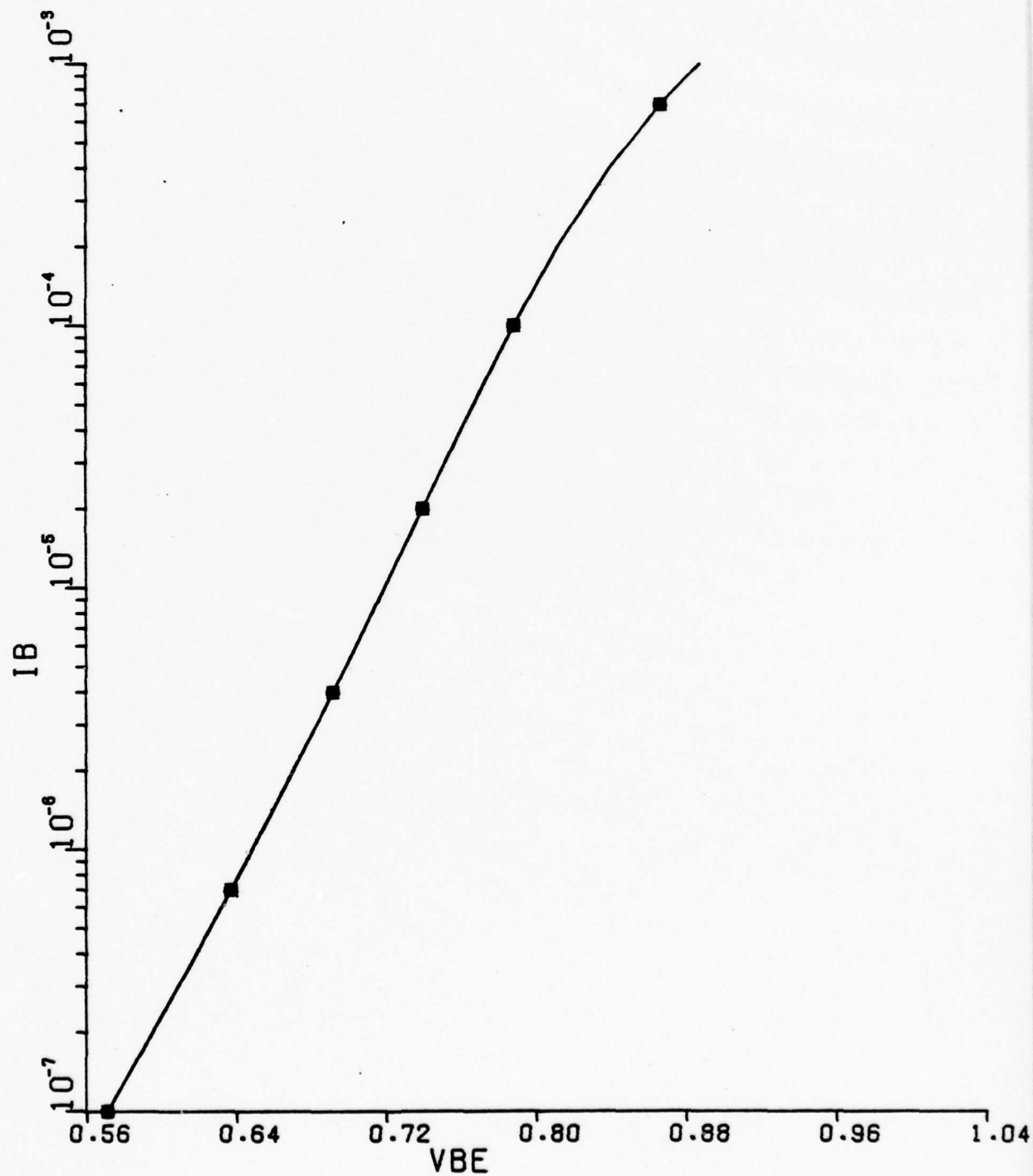
■ --	WCPRIME	=	1.000E-03
+ --	WCPRIME	=	1.000E-04
0 --	WCPRIME	=	3.000E-04



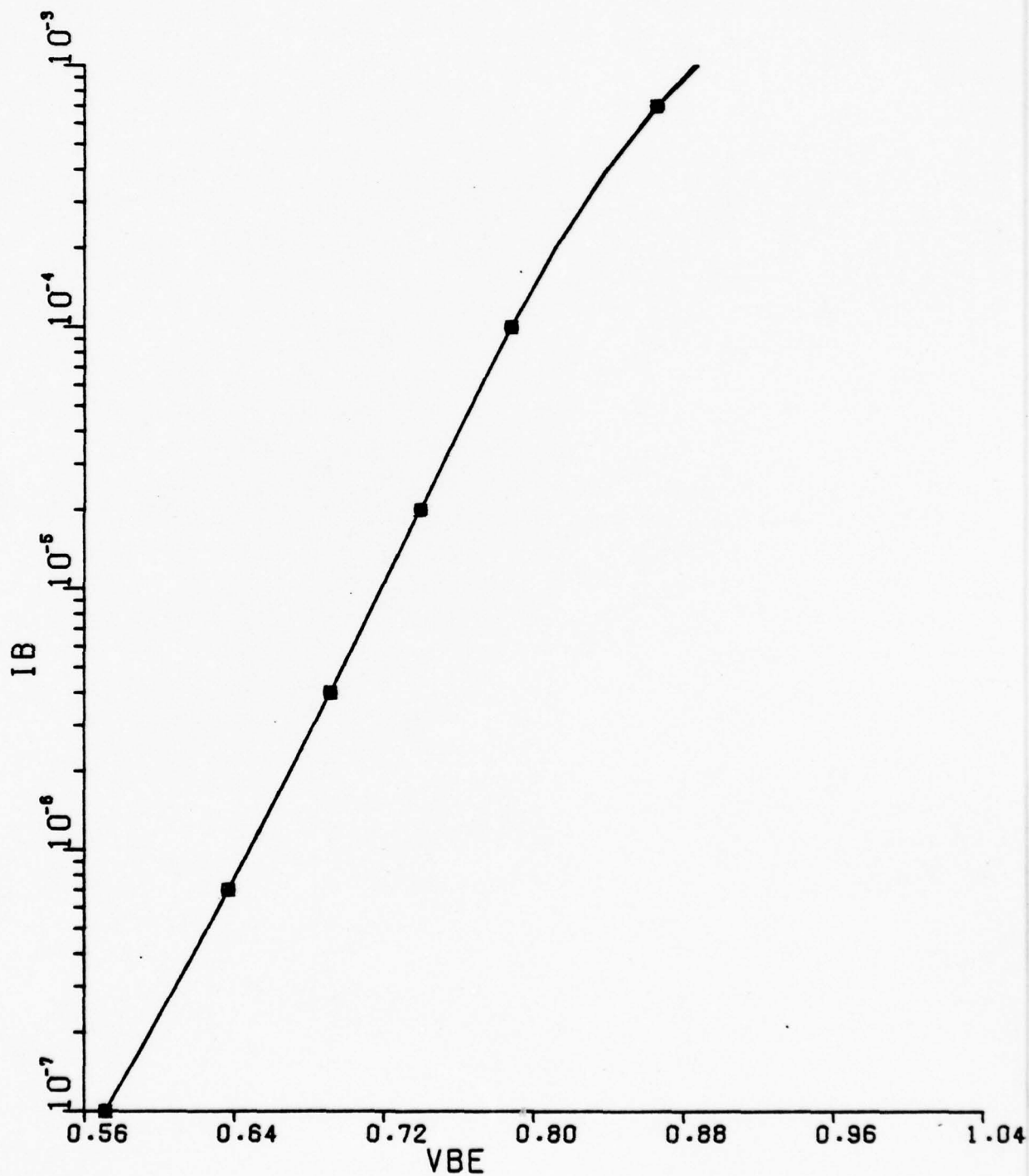
■ --	NOC	=	1.000E+20
+ --	NOC	=	1.000E+13
0 --	NOC	=	1.000E+16



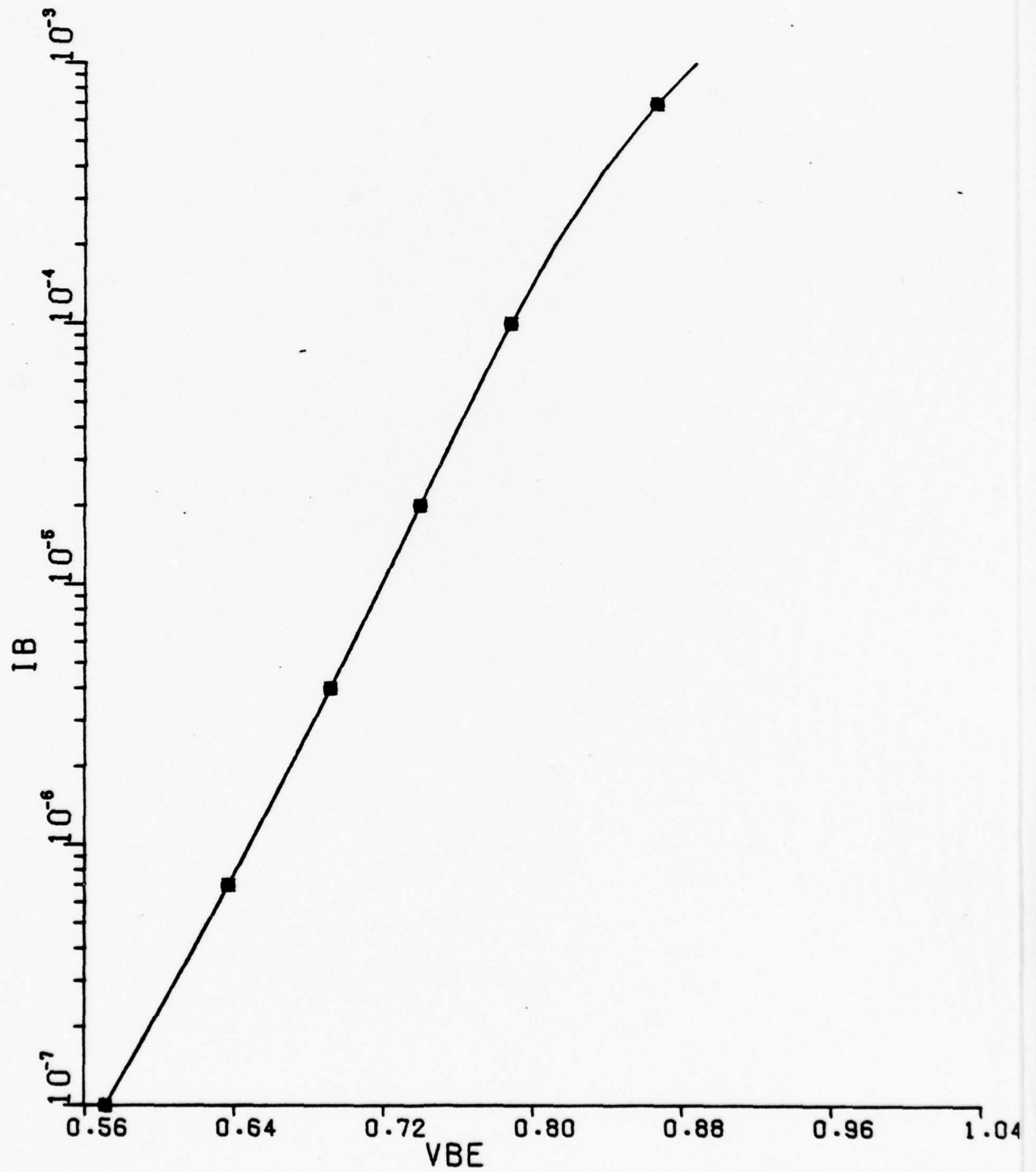
■ --	PHIC	=	4.000E-01
+ --	PHIC	=	1.200E+00
0 --	PHIC	=	7.000E-01



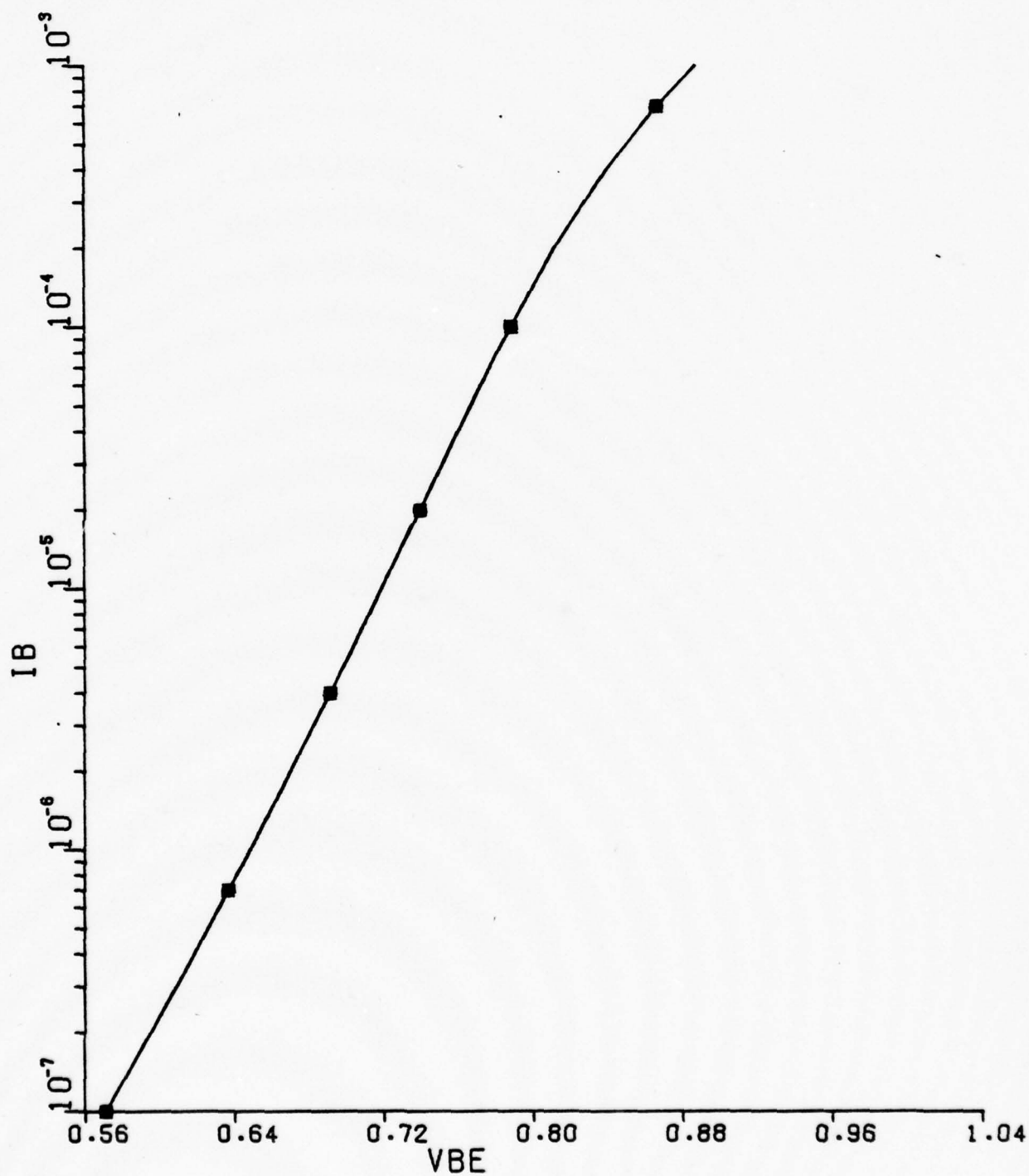
■ --	DNC	=	3.000E+01
+ --	DNC	=	6.000E+01
0 --	DNC	=	4.800E+01



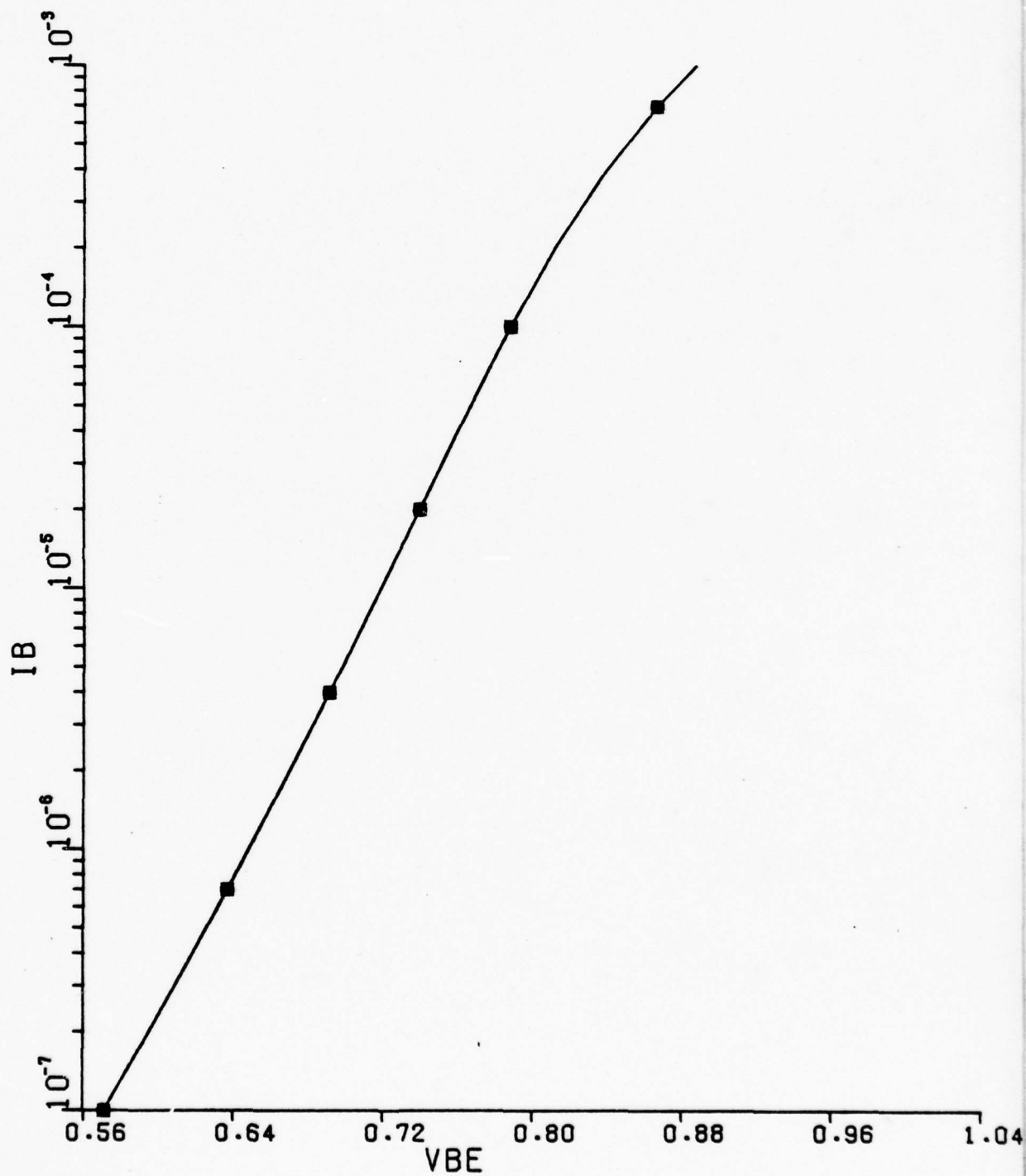
■ --	X0	=	4.000E-05
+ --	X0	=	2.400E-04
0 --	X0	=	1.200E-04



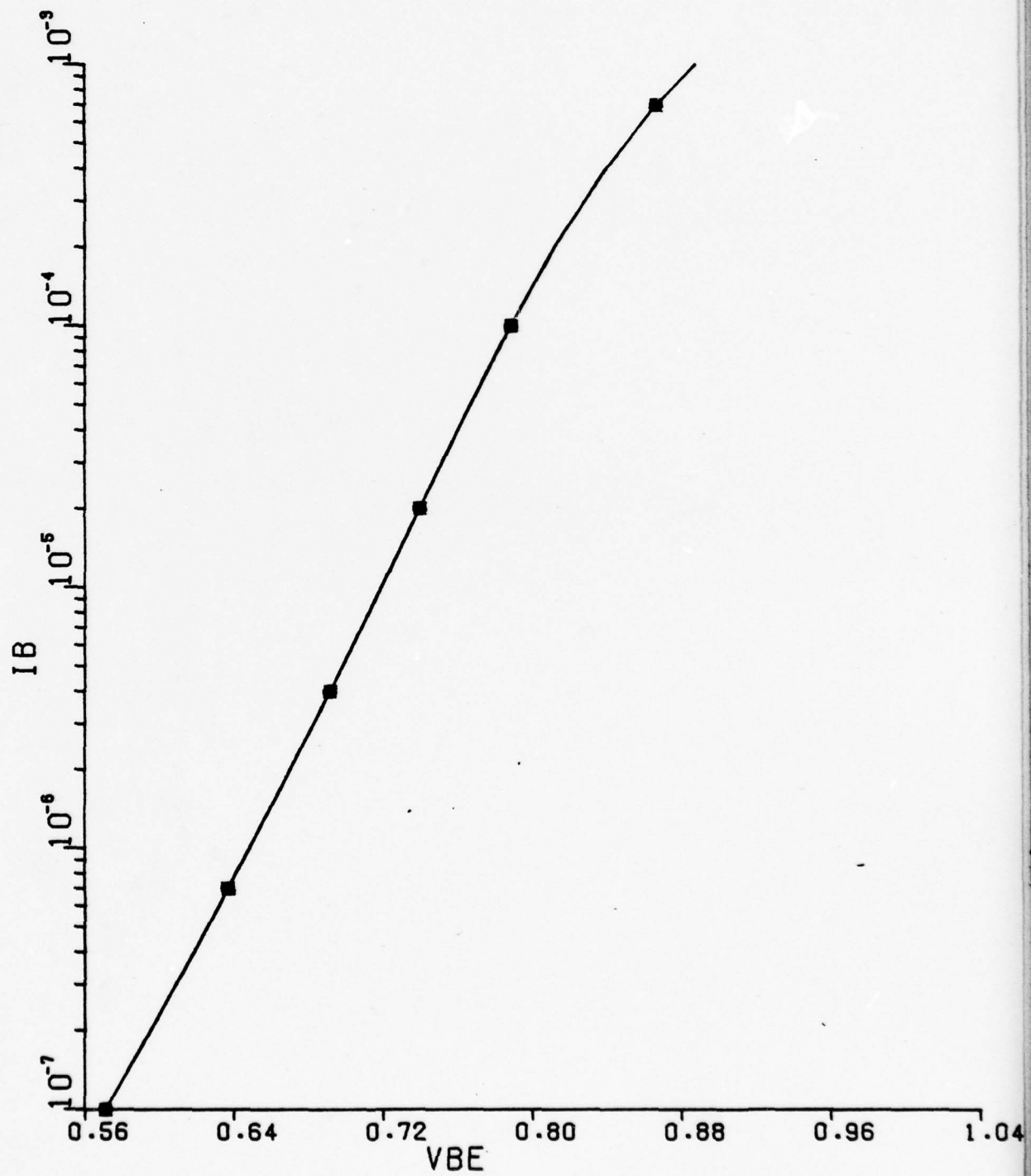
■ --	KR	=	1.000E-01
+ --	KR	=	9.000E-01
0 --	KR	=	4.000E-01



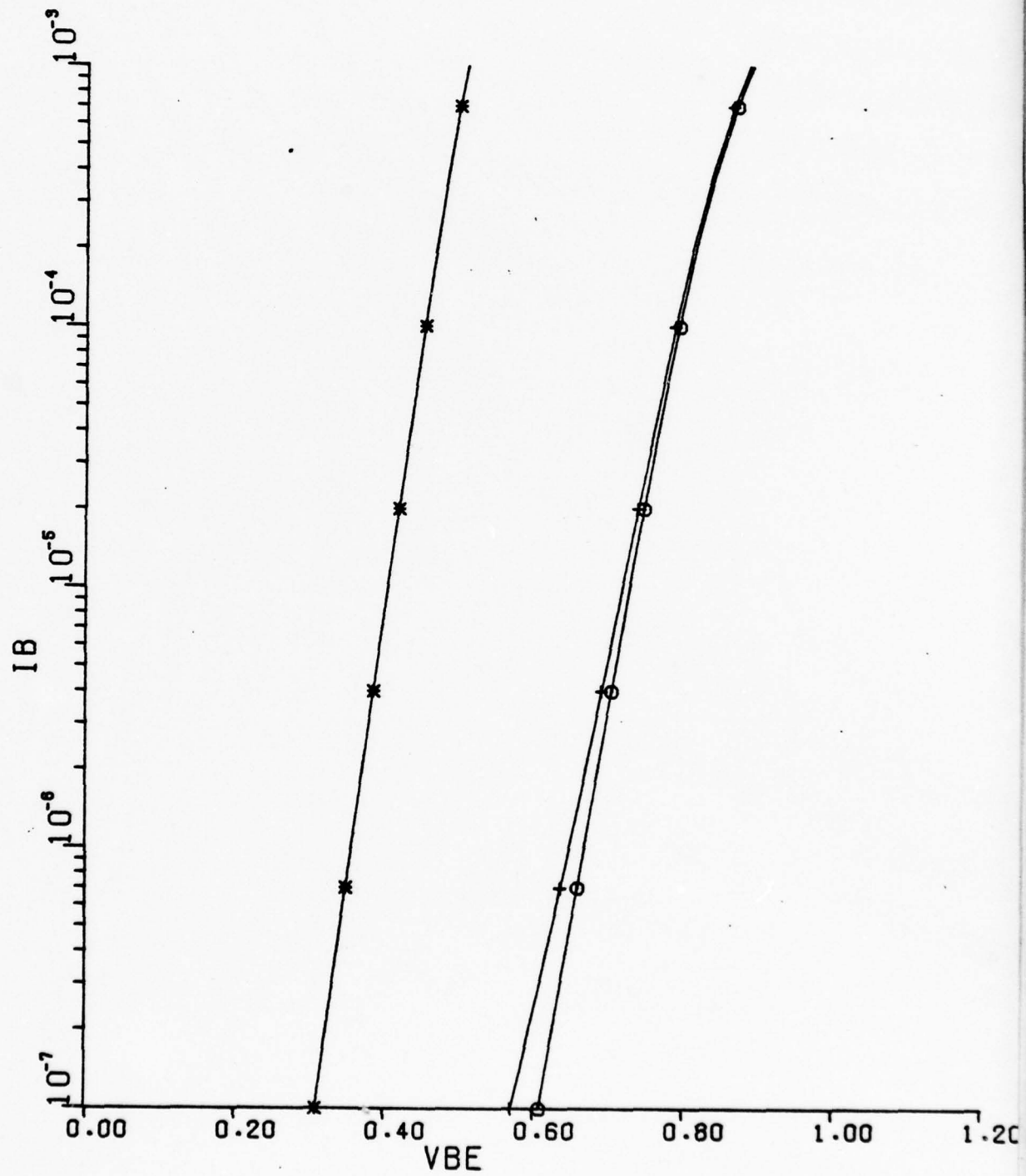
■ --	T0	=	2.000E-12
+ --	T0	=	2.000E-10
0 --	T0	=	2.000E-11



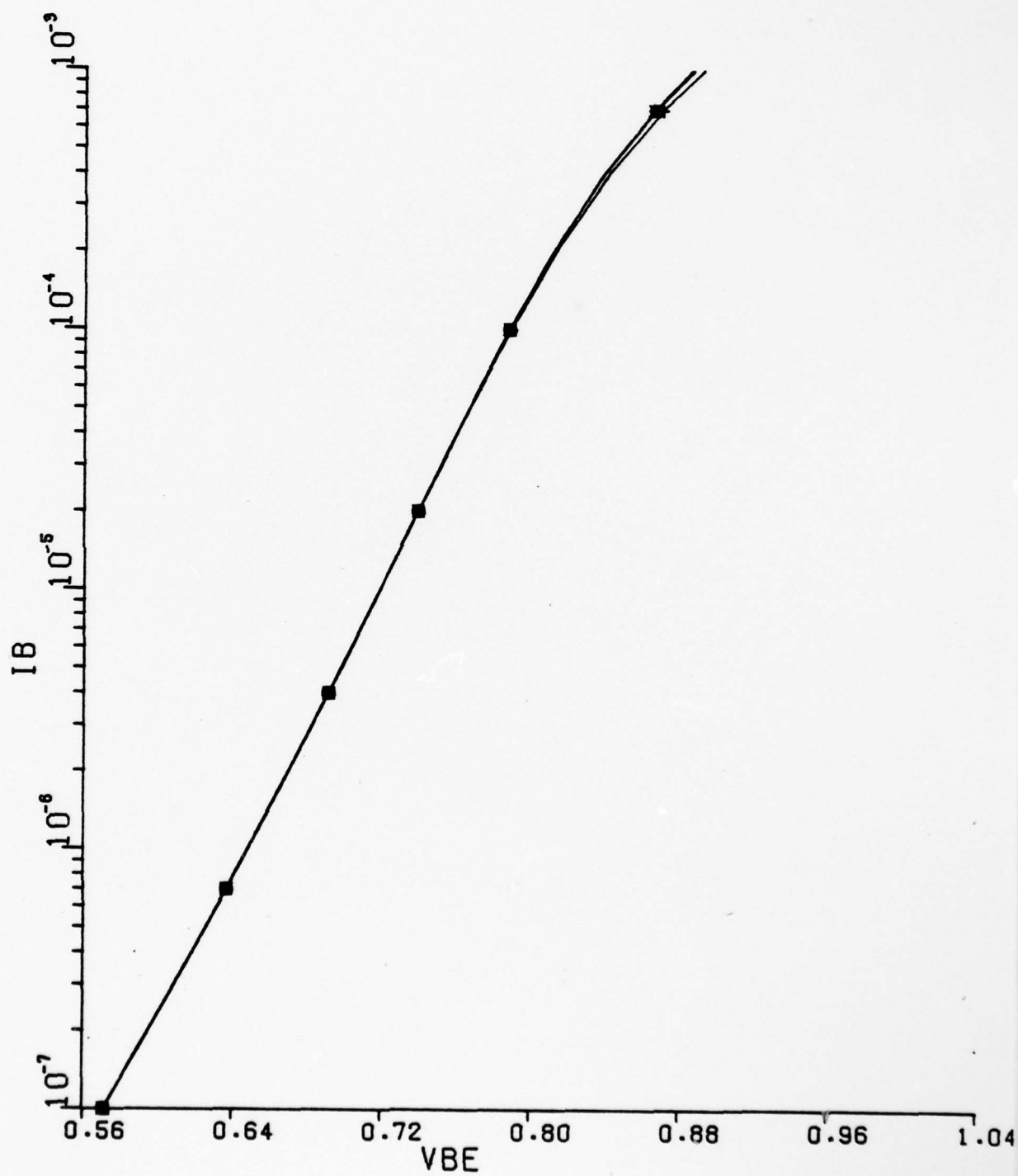
■	--	M	=	1.000E+00
+	--	M	=	1.000E+01
0	--	M	=	2.000E+00



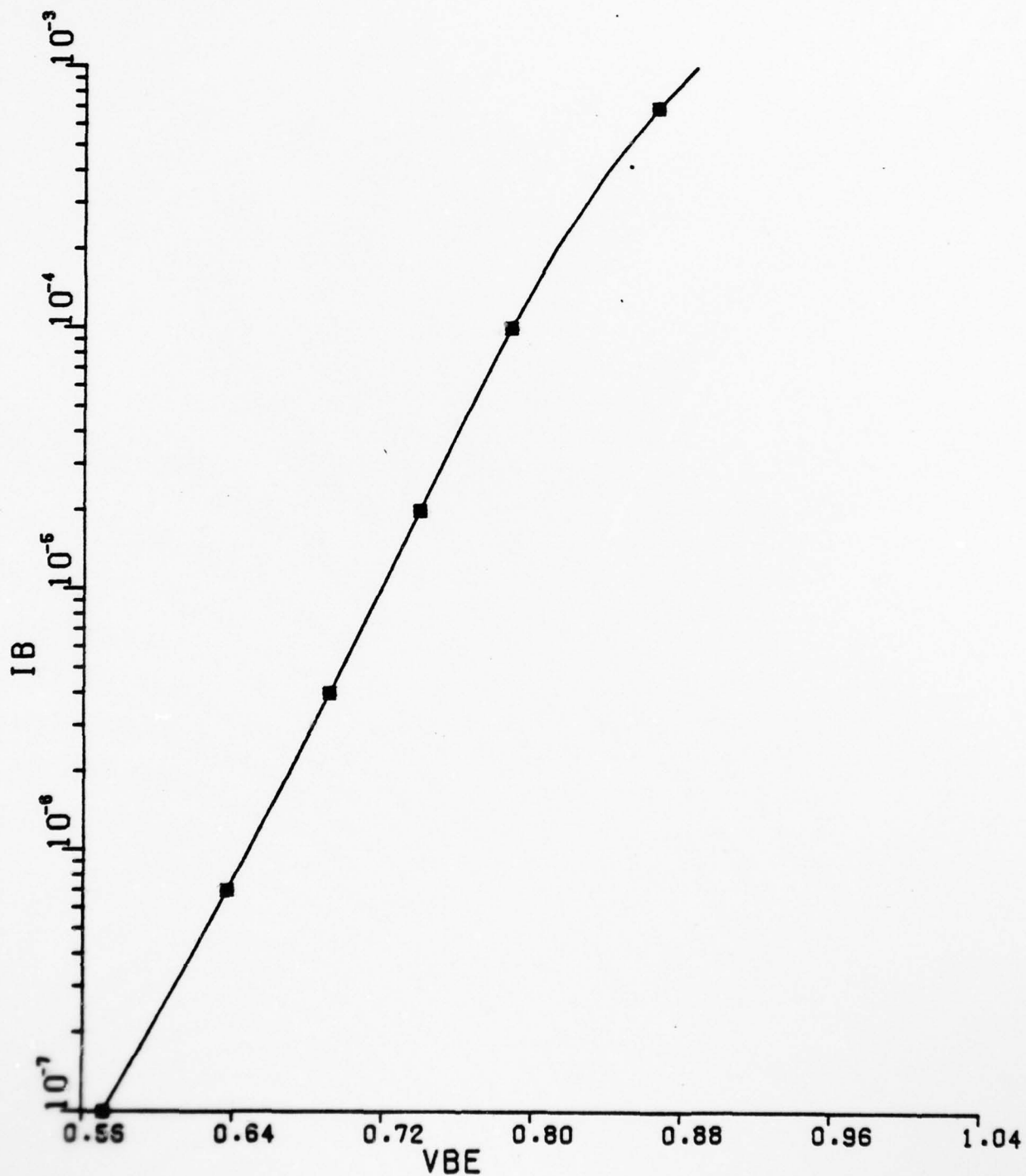
* --	NE	=	8.000E-01
+ --	NE	=	1.500E+00
o --	NE	=	2.300E+00



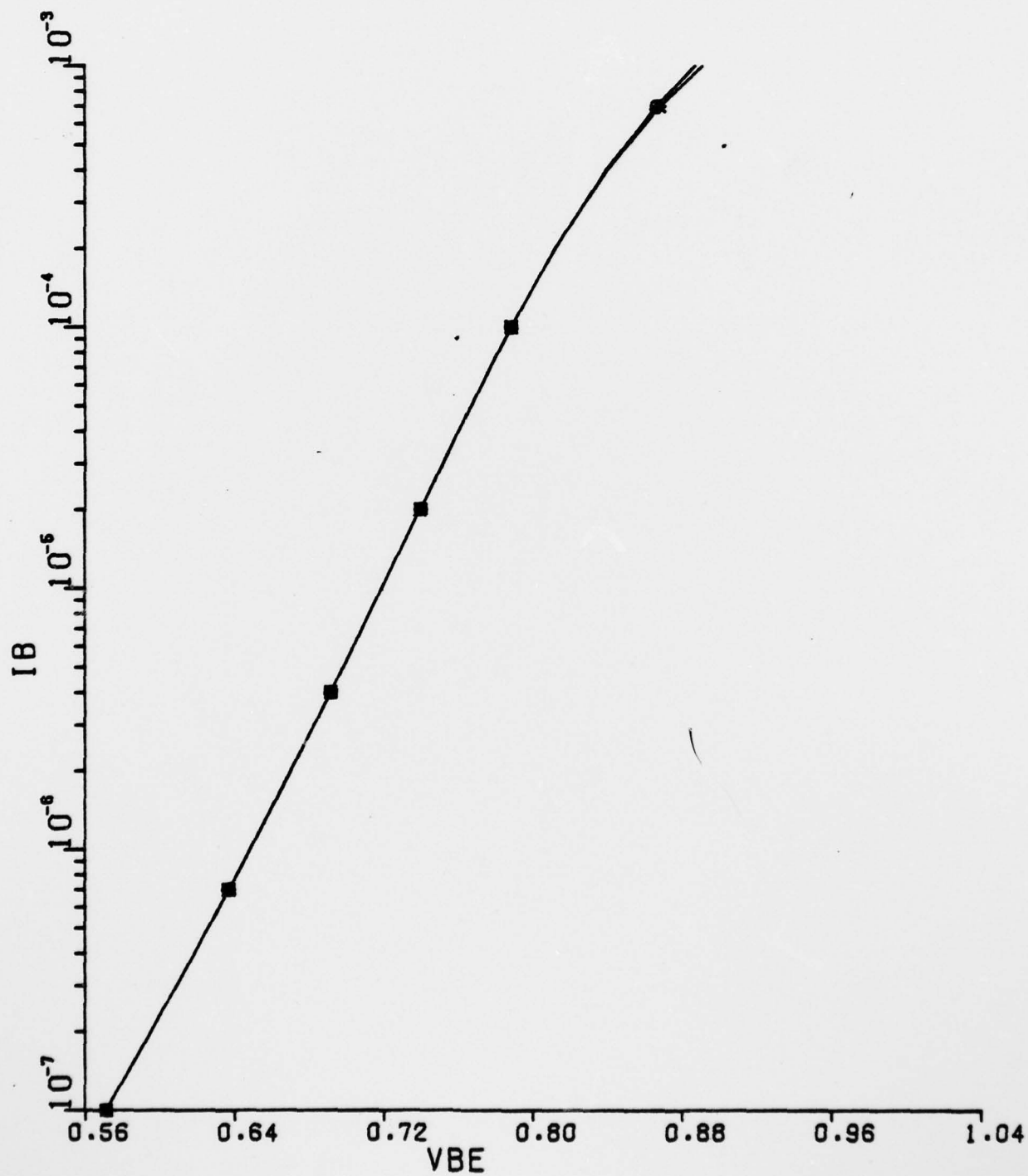
■ --	VCE	=	1.500E+00
+ --	VCE	=	1.500E+01
0 --	VCE	=	5.000E+00



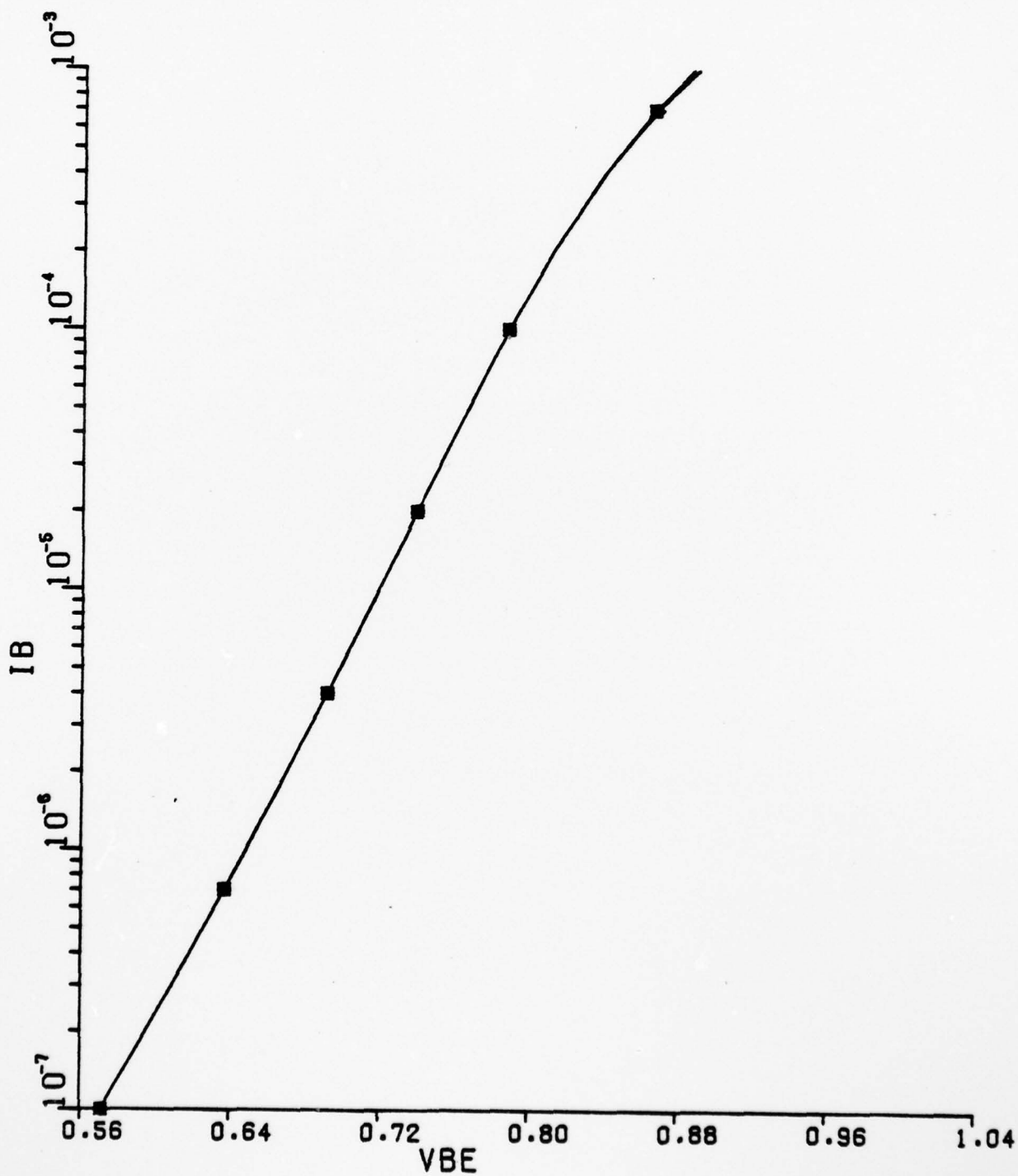
* --	VB	=	1.500E+01
+ --	VB	=	2.000E+01
0 --	VB	=	1.779E+01



* --	VF	=	2.590E-01
+ --	VF	=	2.590E-03
0 --	VF	=	2.590E-02

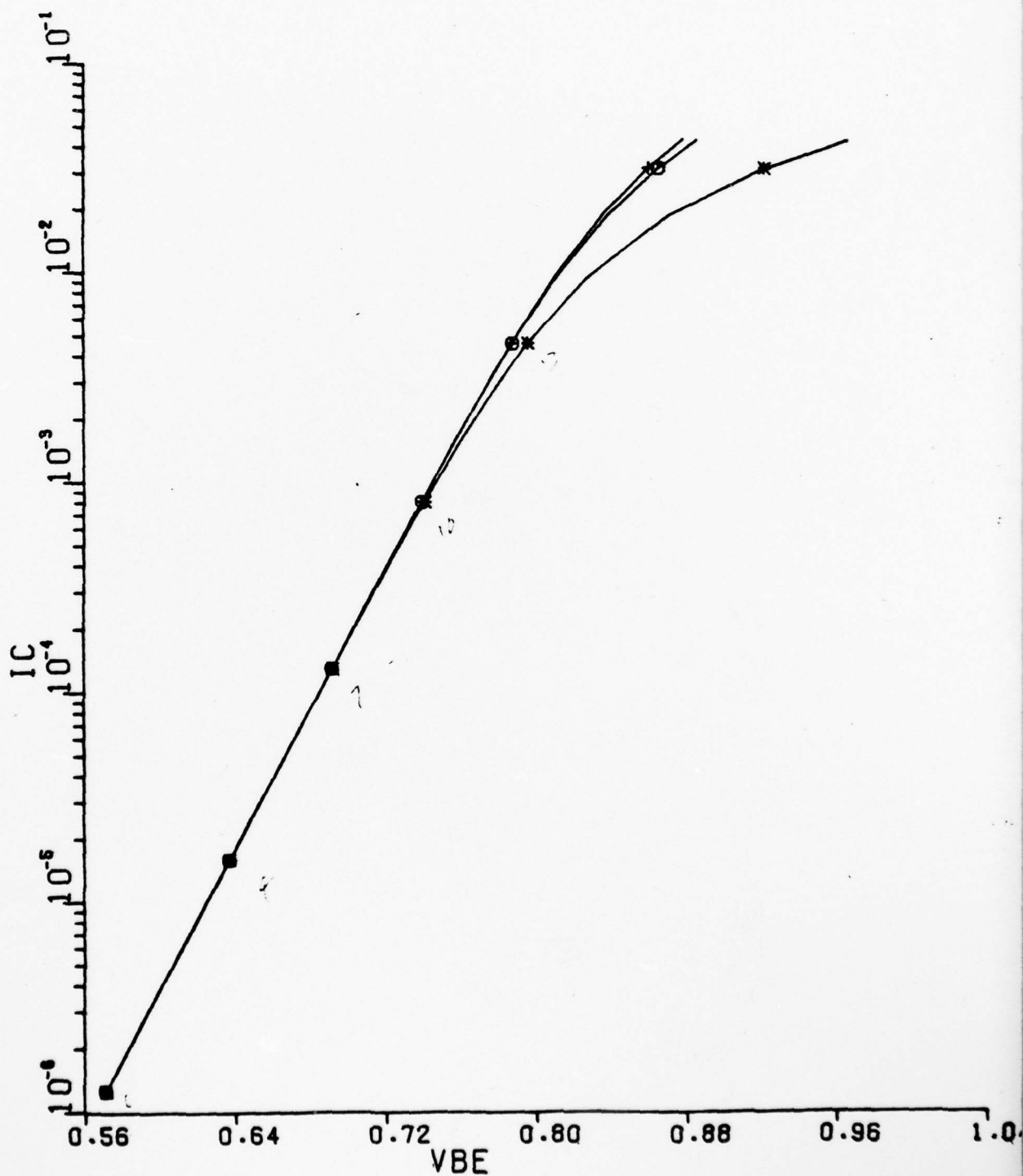


■ --	FF	= 1.336E-13
+ --	FF	= 1.336E-15
0 --	FF	= 1.336E-14

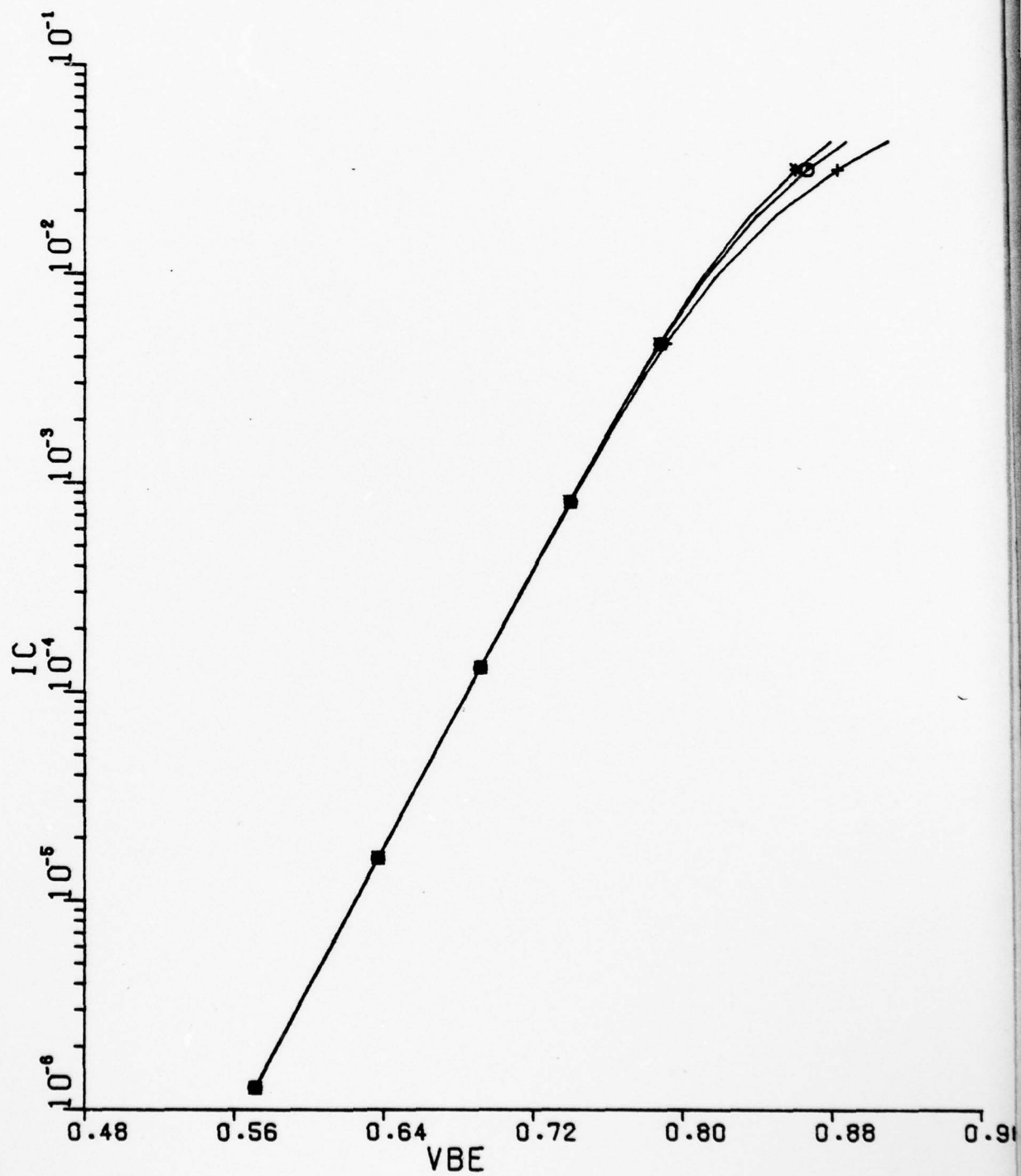


B.2 I_C vs. V_{BE} Curves

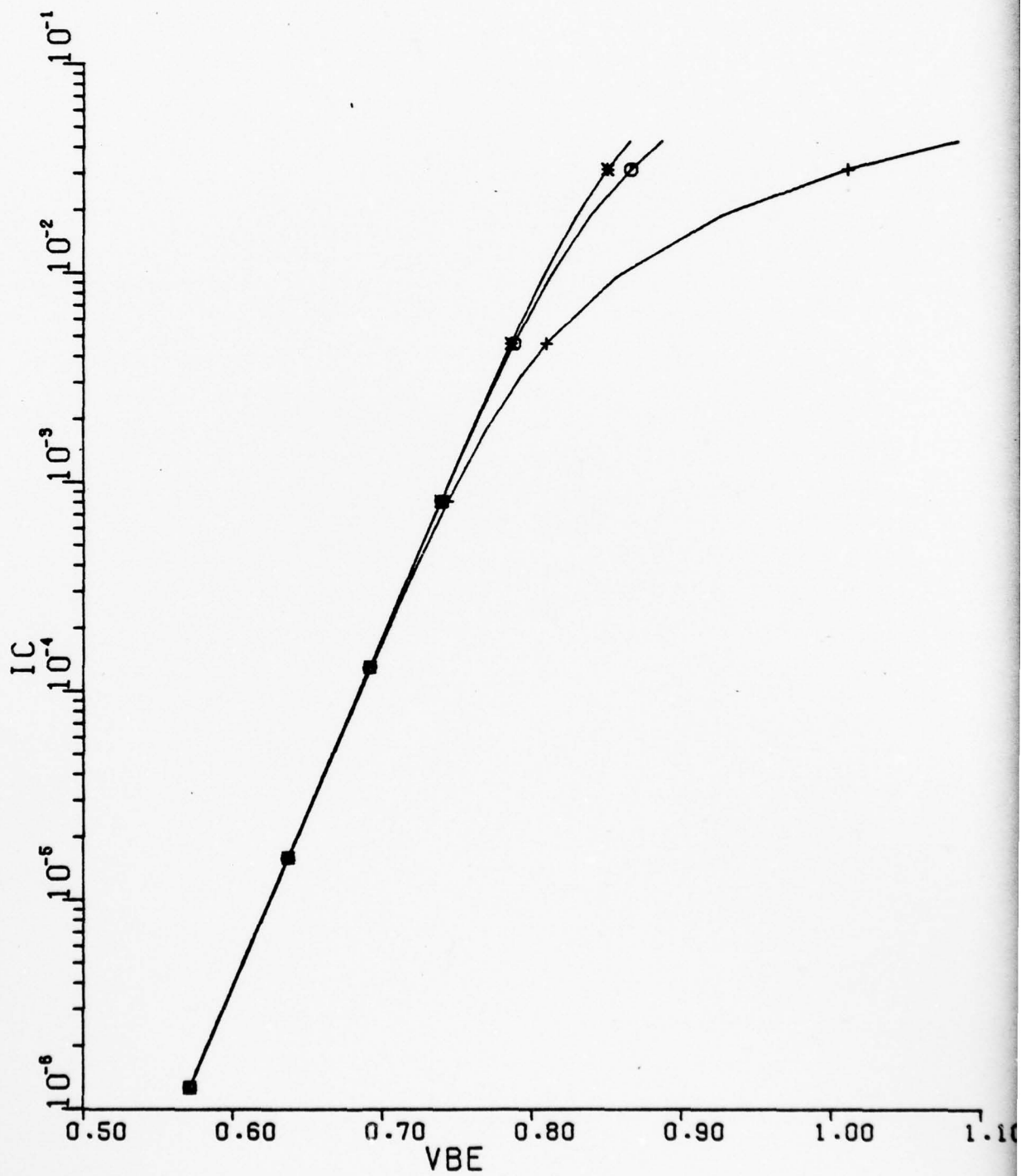
* --	RBO	=	9.000E+01
+ --	RBO	=	9.000E-01
0 --	RBO	=	9.000E+00



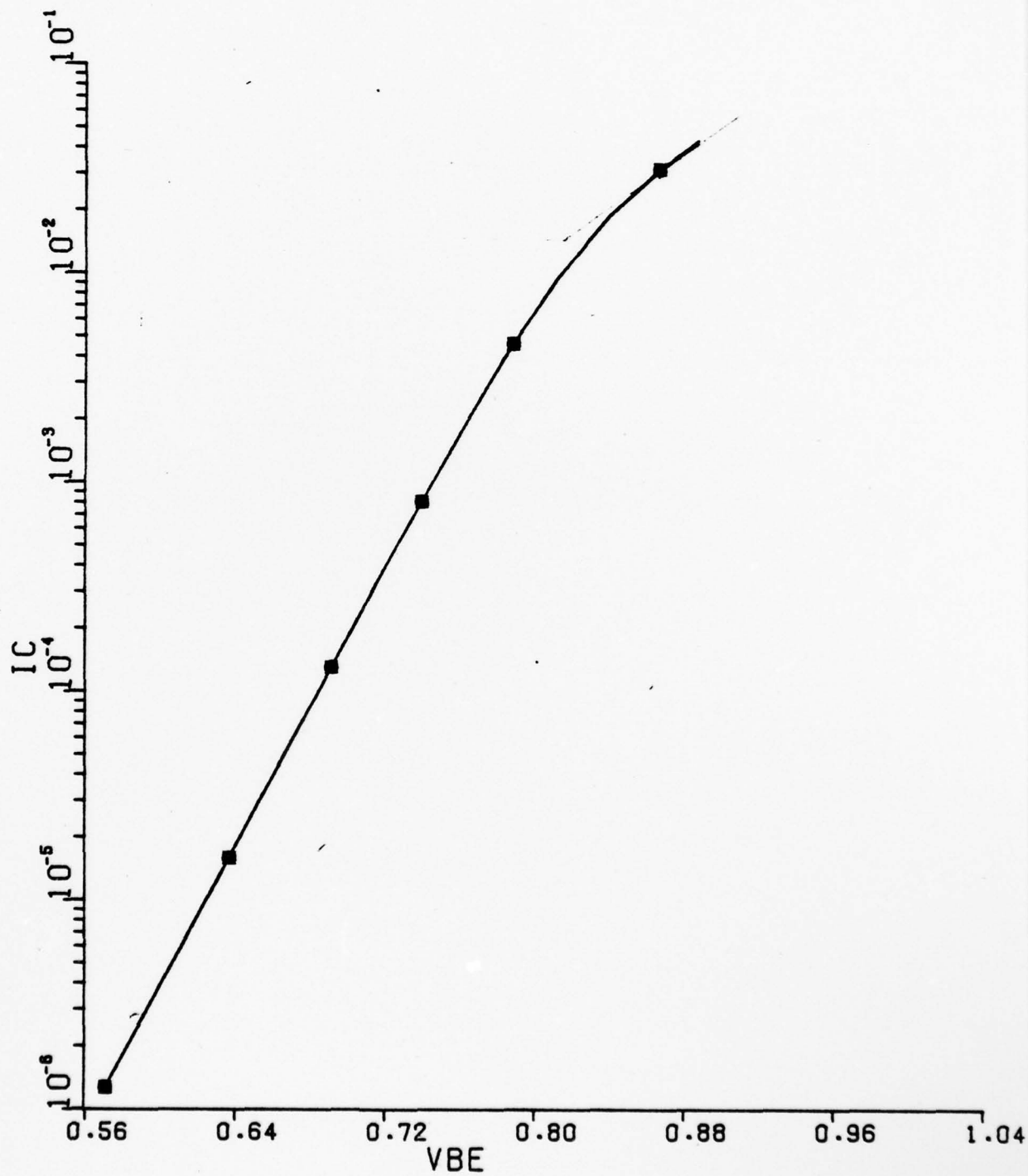
■ --	RBB	=	1.500E+01
+ --	RBB	=	5.000E+02
0 --	RBB	=	1.500E+02



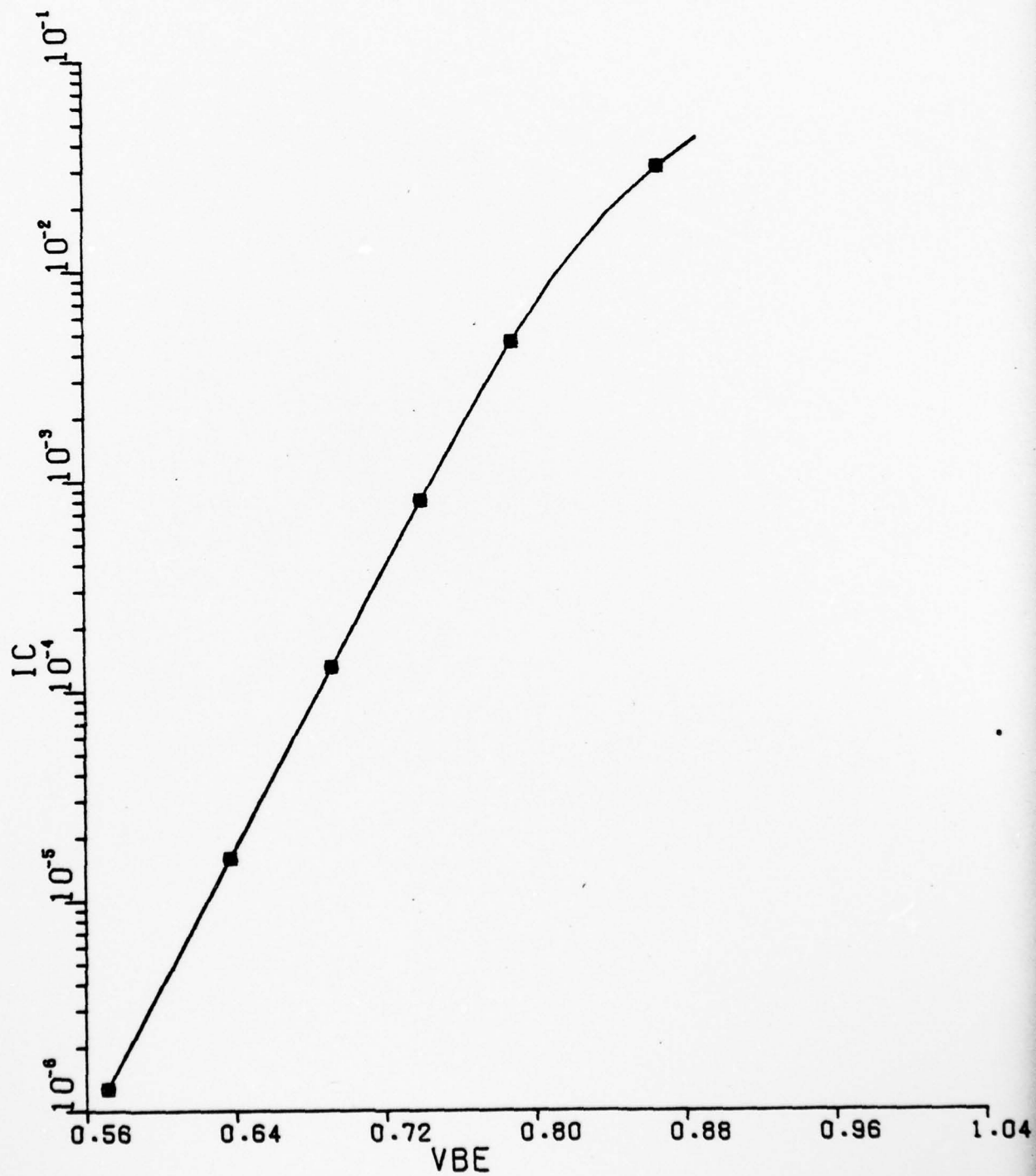
* --	RE	=	1.000E-02
+ --	RE	=	5.000E+00
o --	RE	=	5.000E-01



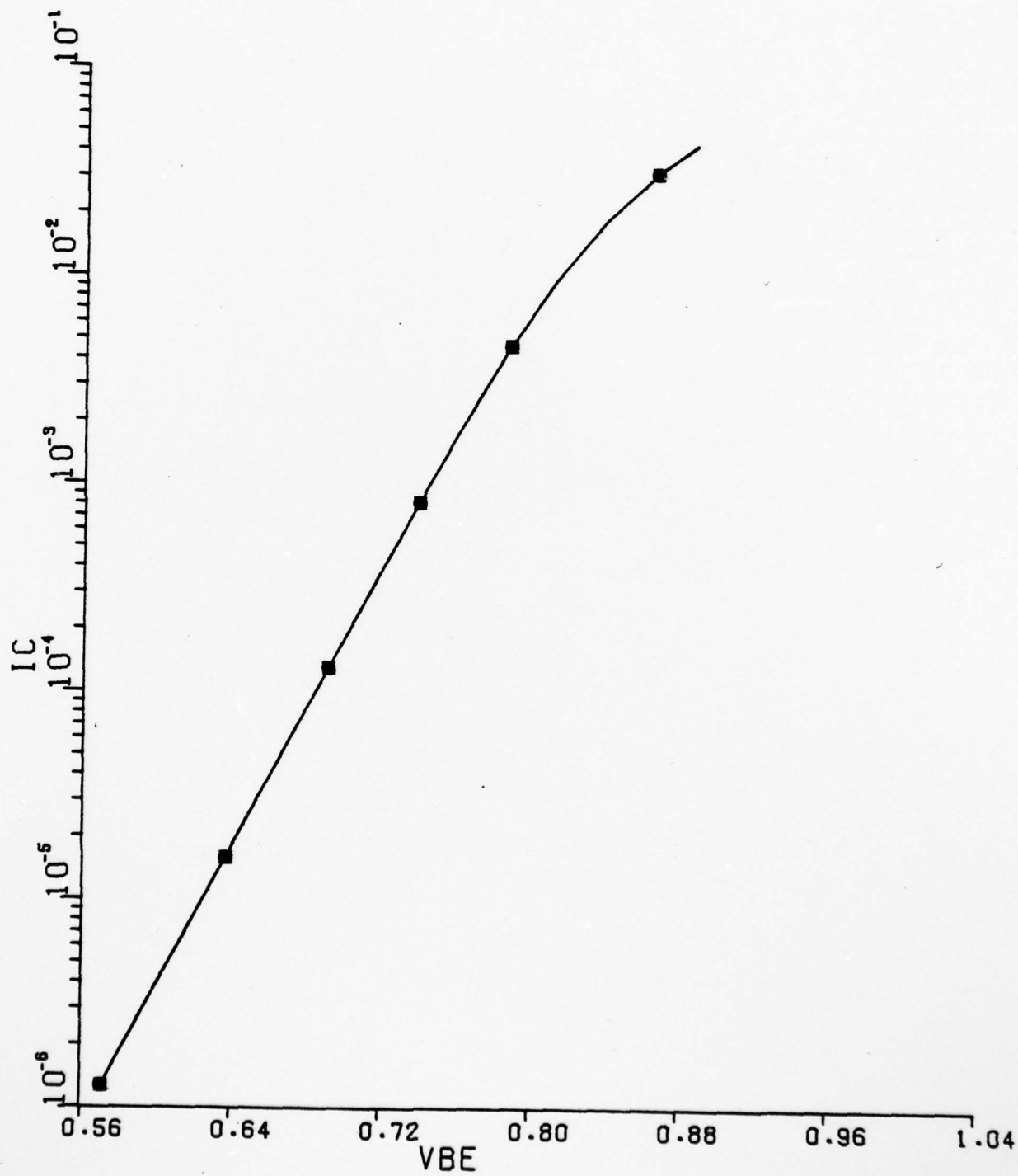
■ --	RCO	=	1.000E+00
+ --	RCO	=	5.000E+01
0 --	RCO	=	5.000E+00



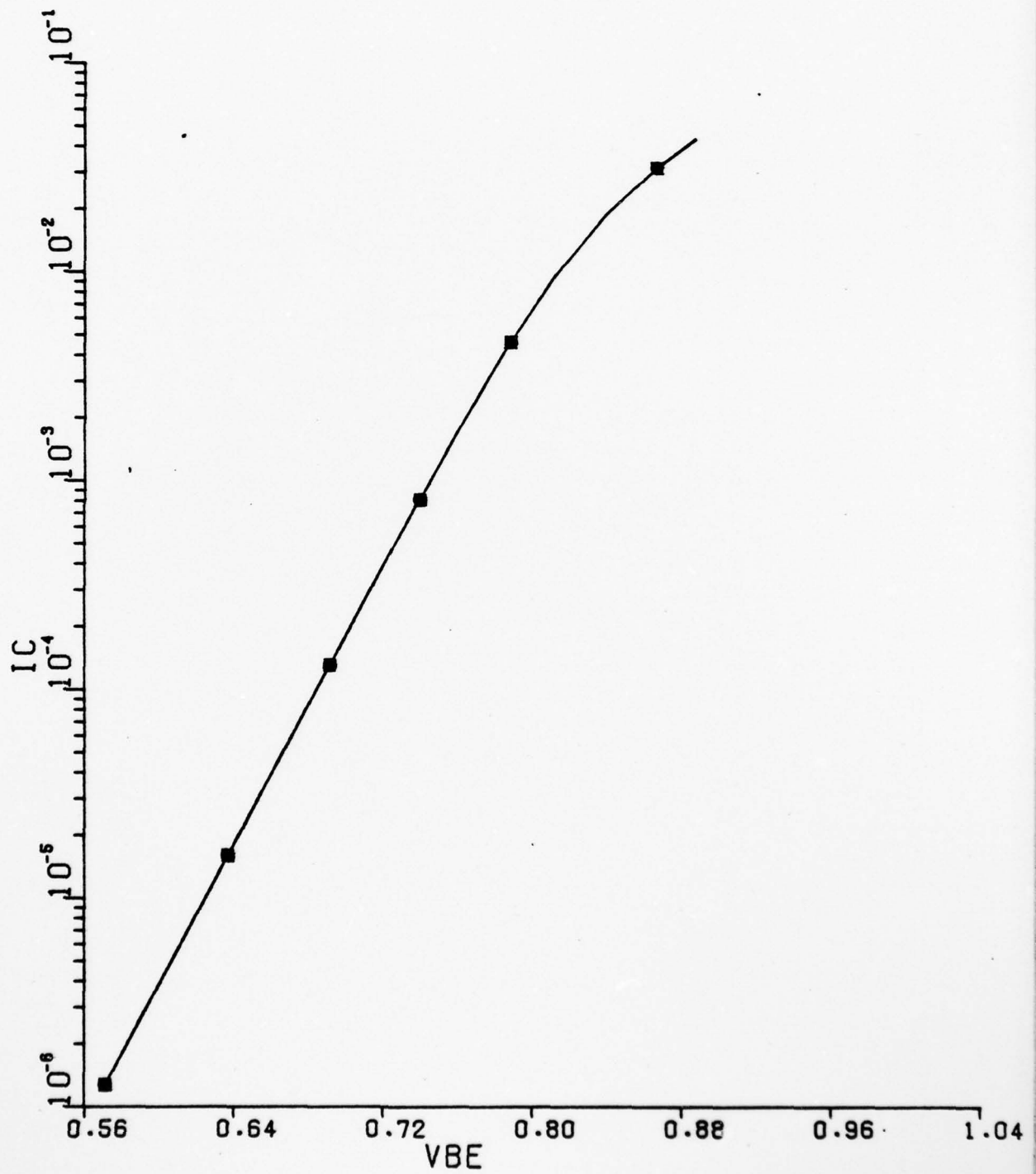
* --	PC	=	6.000E-03
+ --	PC	=	1.000E-03
0 --	PC	=	3.250E-03



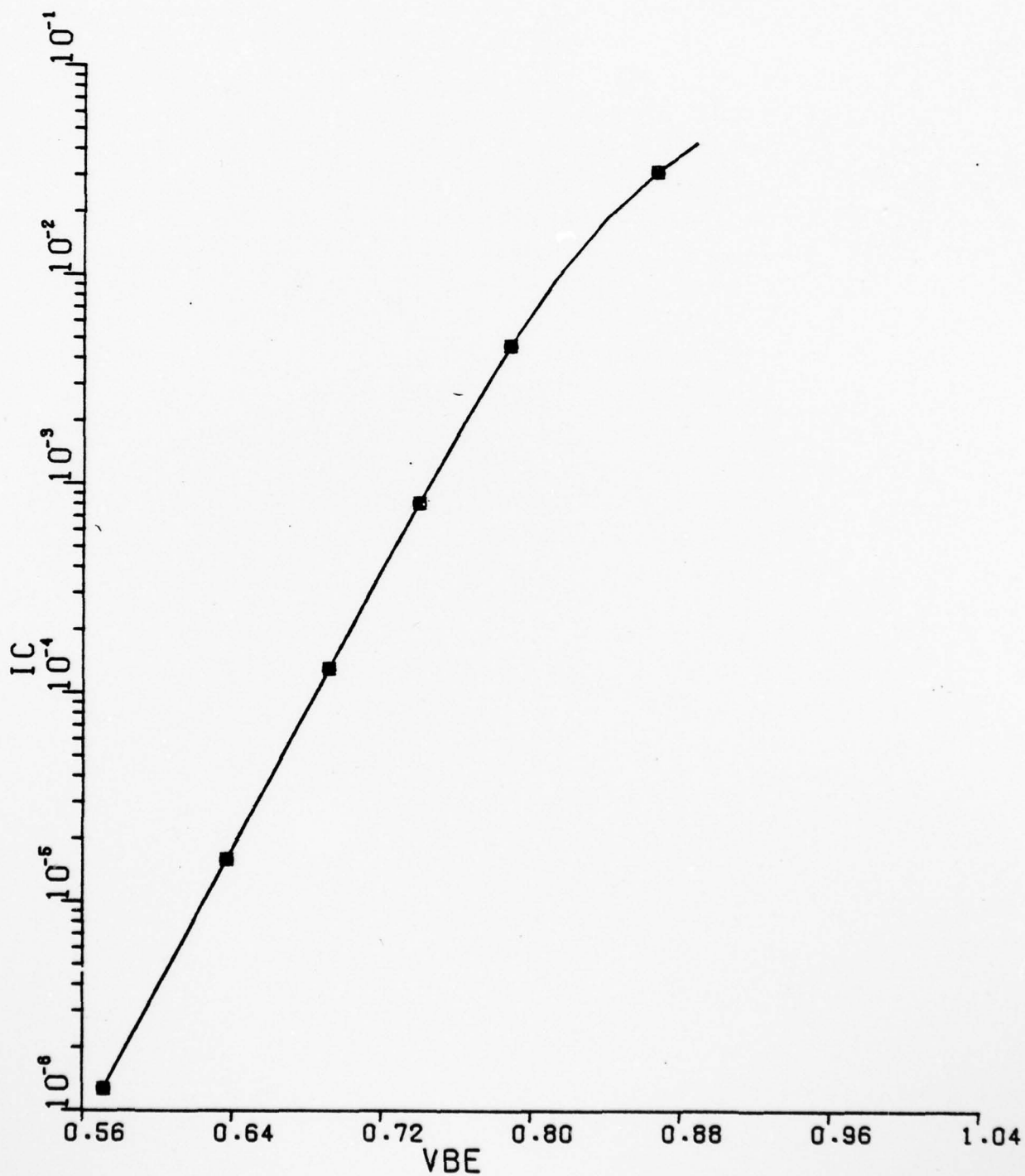
■ --	BS	=	2.500E-01
+ --	BS	=	5.000E-01
0 --	BS	=	3.333E-01



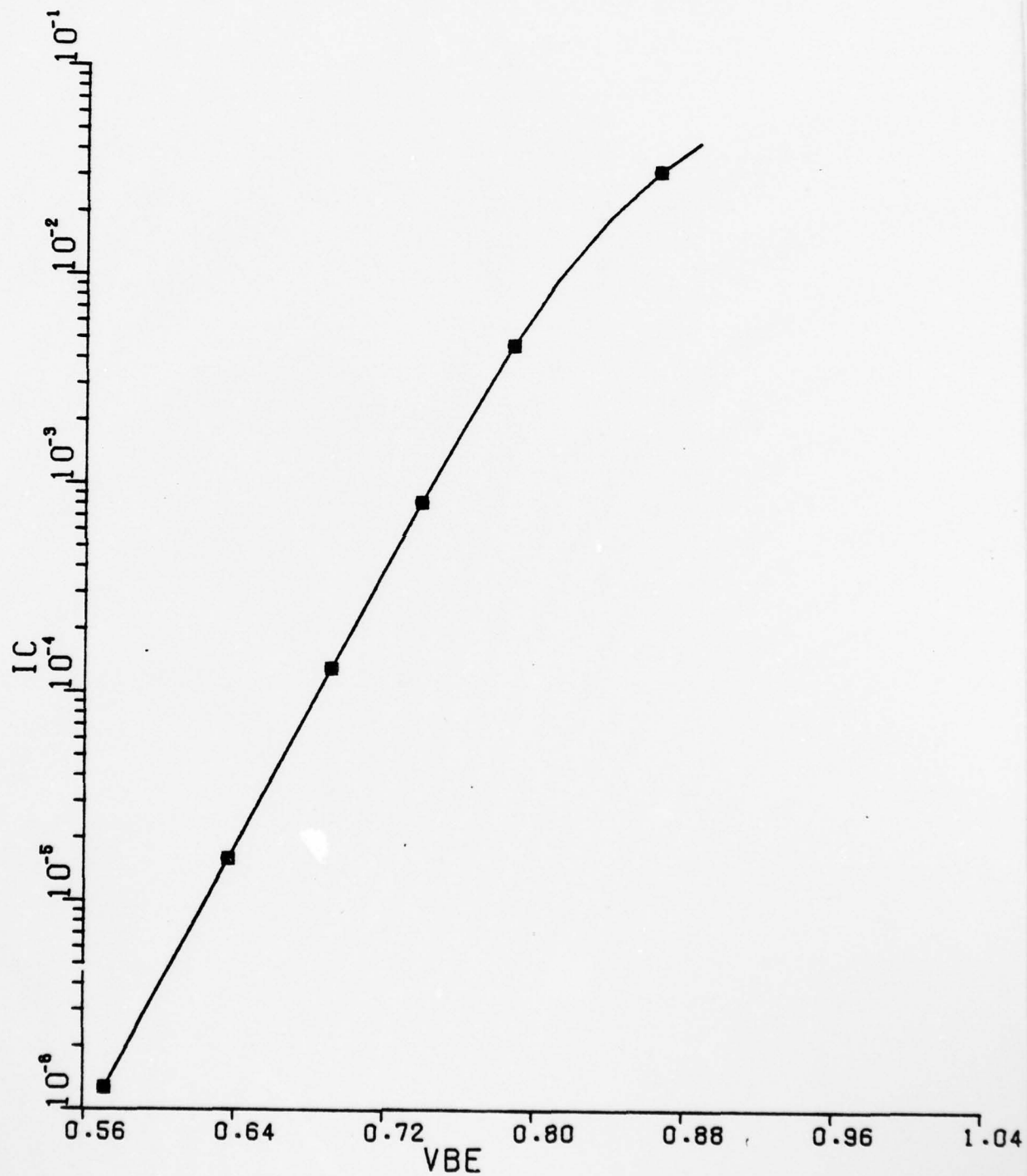
■ --	BC	=	2.500E-01
+ --	BC	=	3.333E-01
0 --	BC	=	5.000E-01



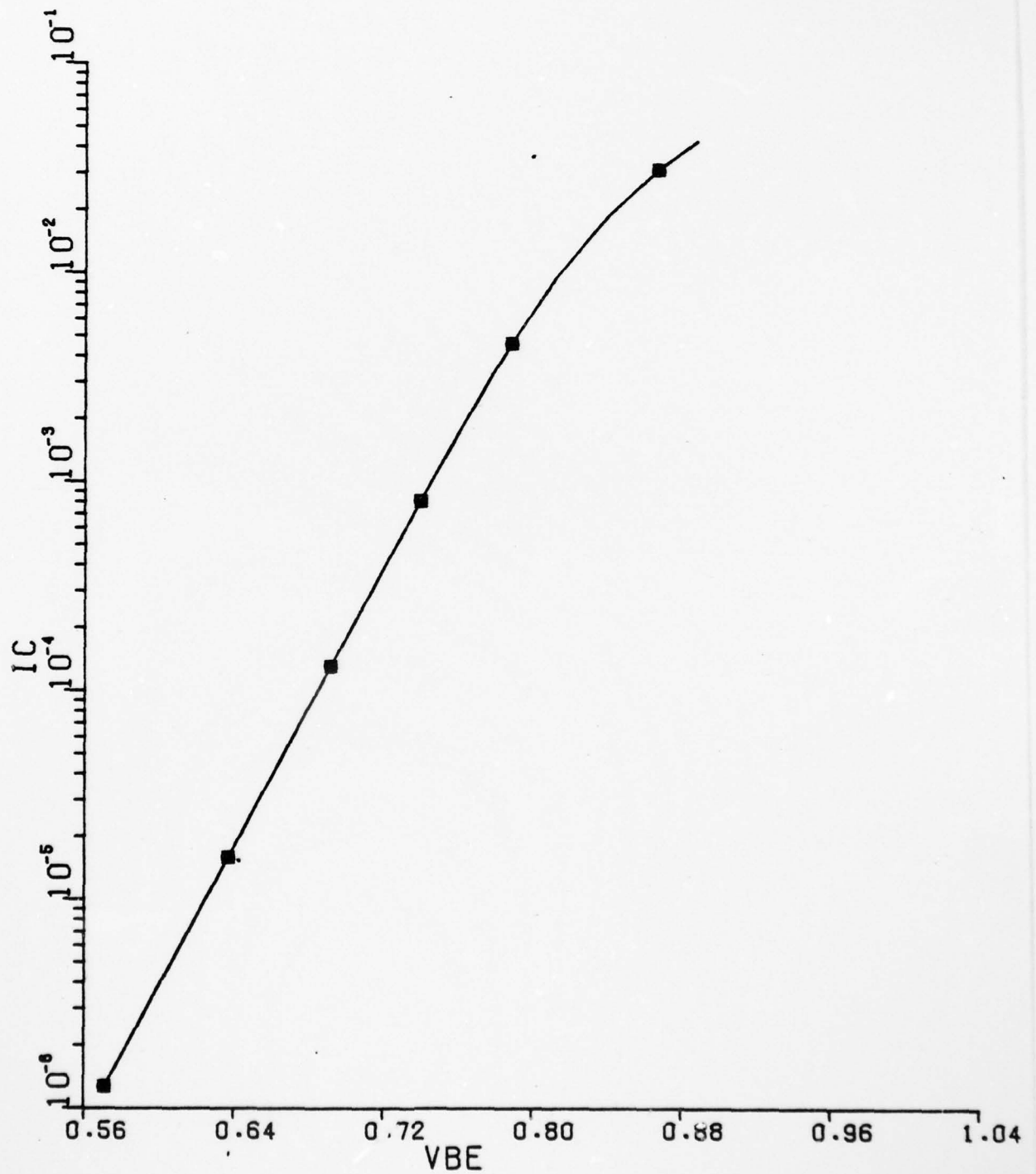
■ --	BE	=	2.500E-01
+ --	BE	=	3.333E-01
0 --	BE	=	5.000E-01



■	--	CS0	=	4.000E-13
+	--	CS0	=	1.000E-11
0	--	CS0	=	2.000E-12



■ --	CEO	=	4.000E-13
+ --	CEO	=	1.000E-11
0 --	CEO	=	9.000E-13



AD-A062 790

TRW DEFENSE AND SPACE SYSTEMS GROUP REDONDO BEACH CALIF F/G 9/1
PROCESS-ORIENTED, HIGH-INJECTION CIRCUIT MODELS FOR INTEGRATED --ETC(U)
JAN 78 J CHOMA

N00014-77-C-0043

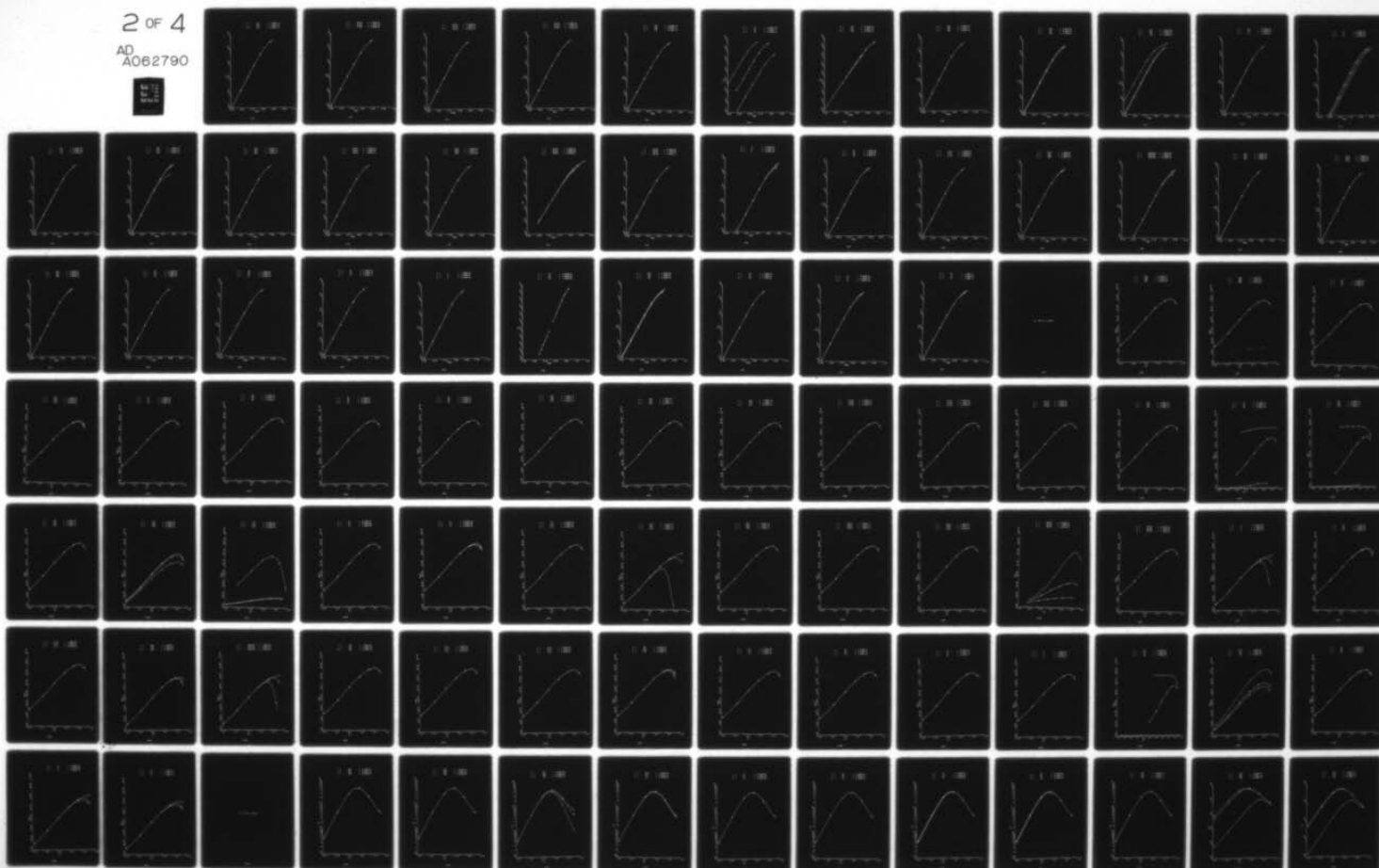
UNCLASSIFIED

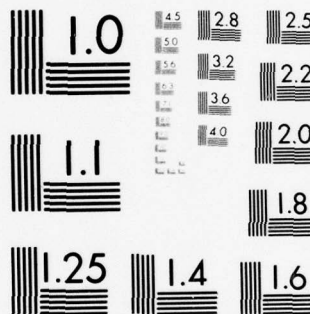
TRW-78.4734.7-023-PT-2-V0

NL

2 OF 4

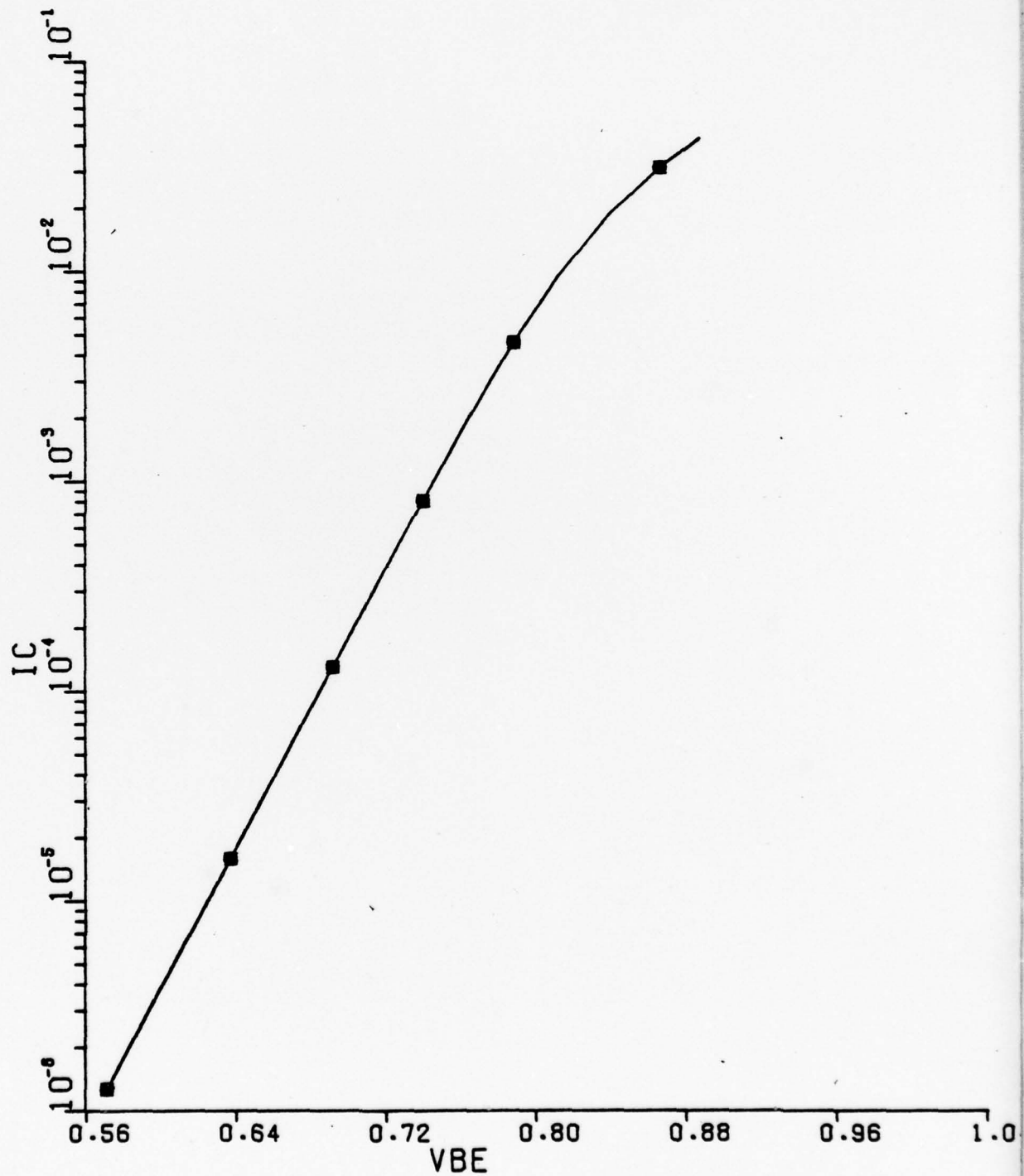
AD
A062790



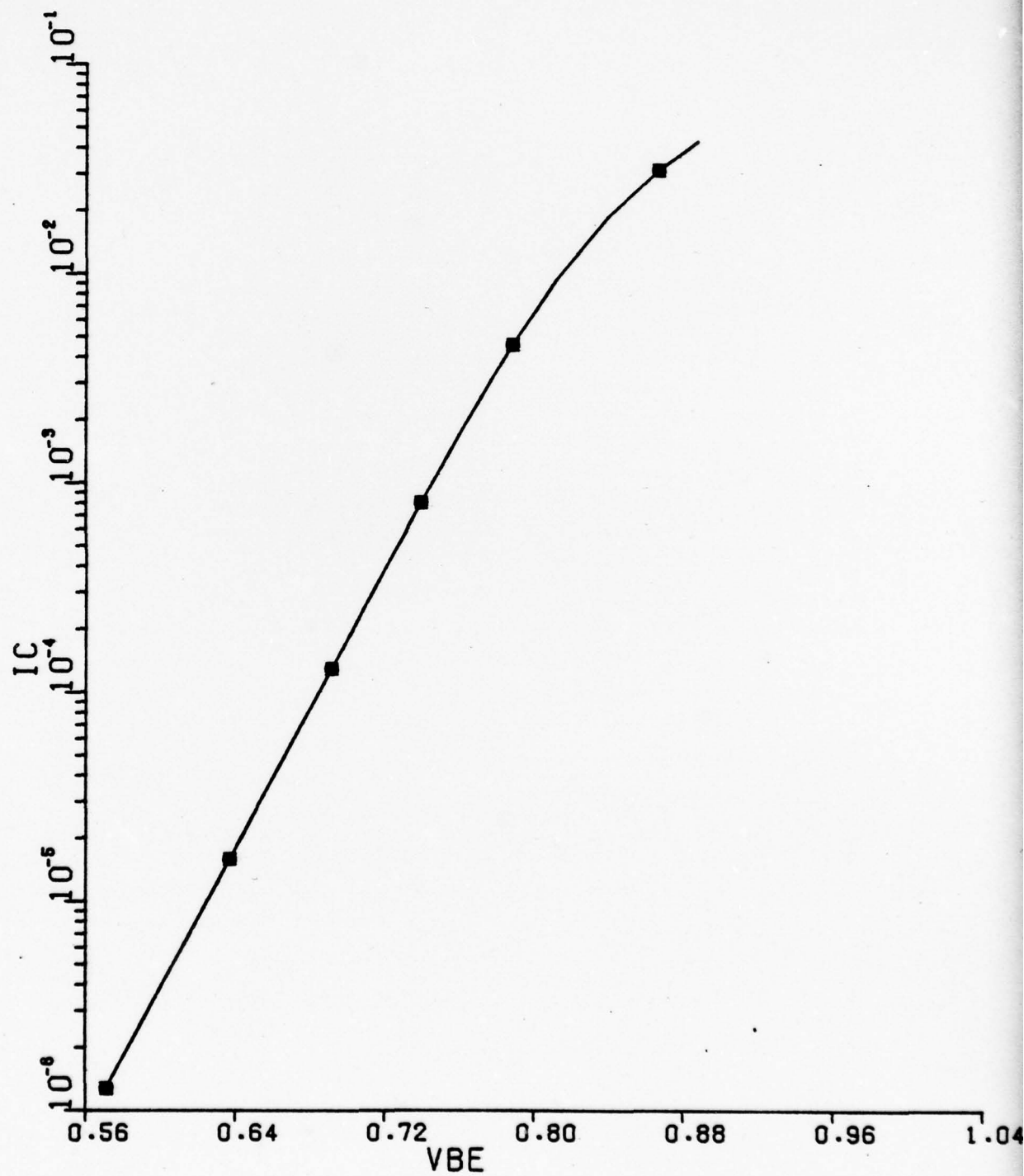


MICROCOPY RESOLUTION TEST CHART
NATIONAL BUREAU OF STANDARDS-1963-A

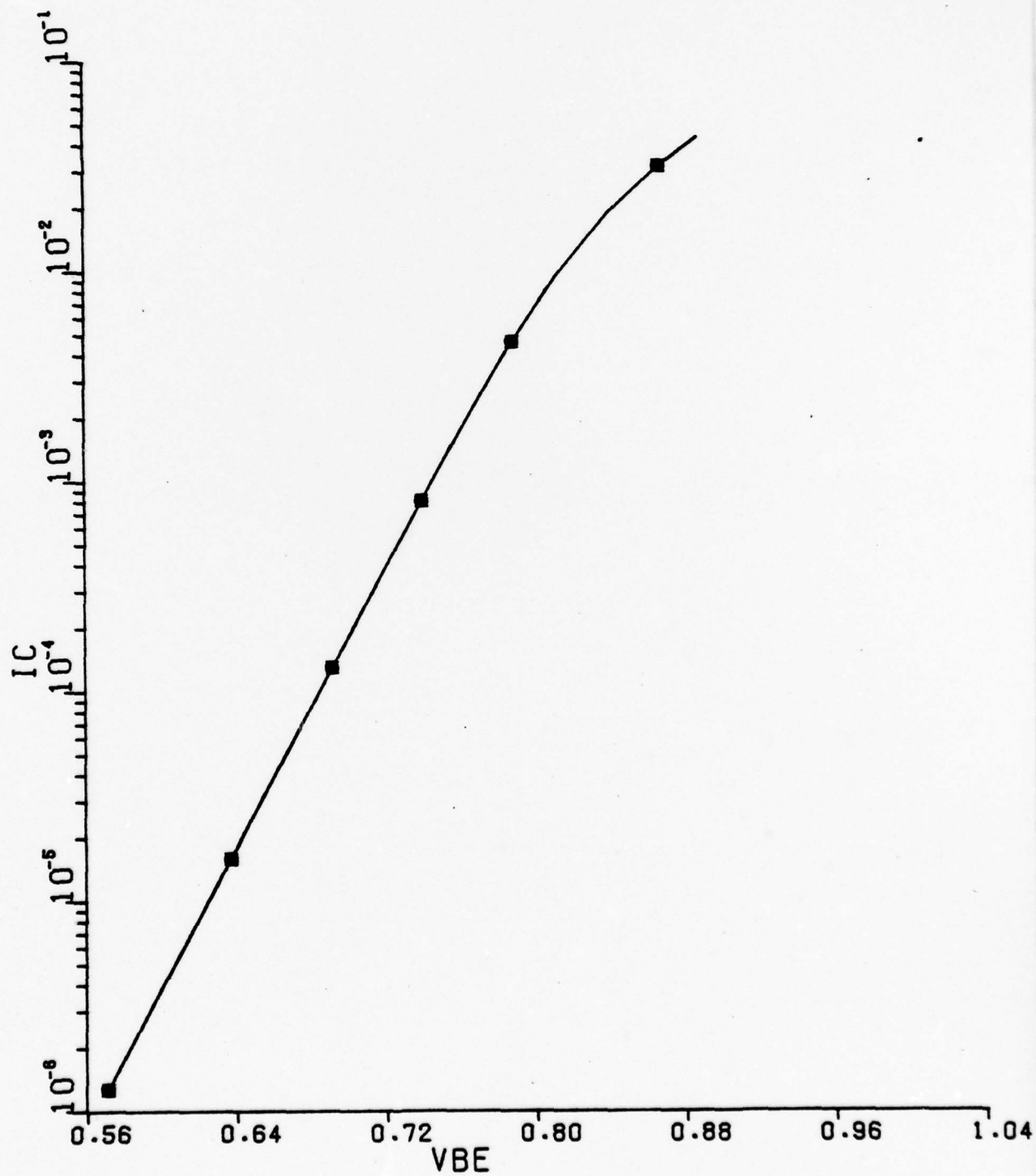
■	--	CC0	=	4.000E-13
+	--	CC0	=	1.000E-10
0	--	CC0	=	8.000E-13



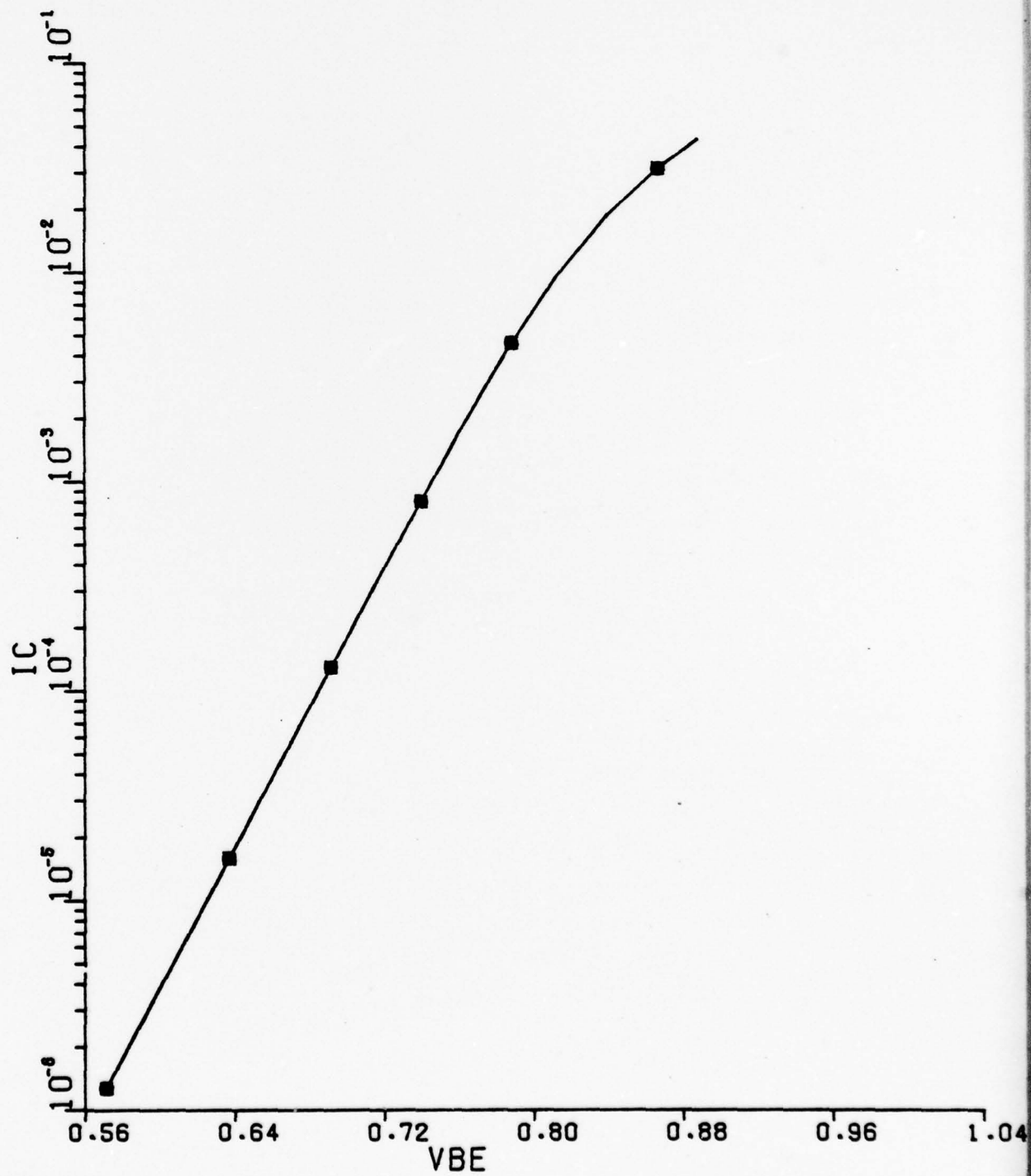
■ --	PHISS	=	5.000E-01
+ --	PHISS	=	1.200E+00
0 --	PHISS	=	9.000E-01



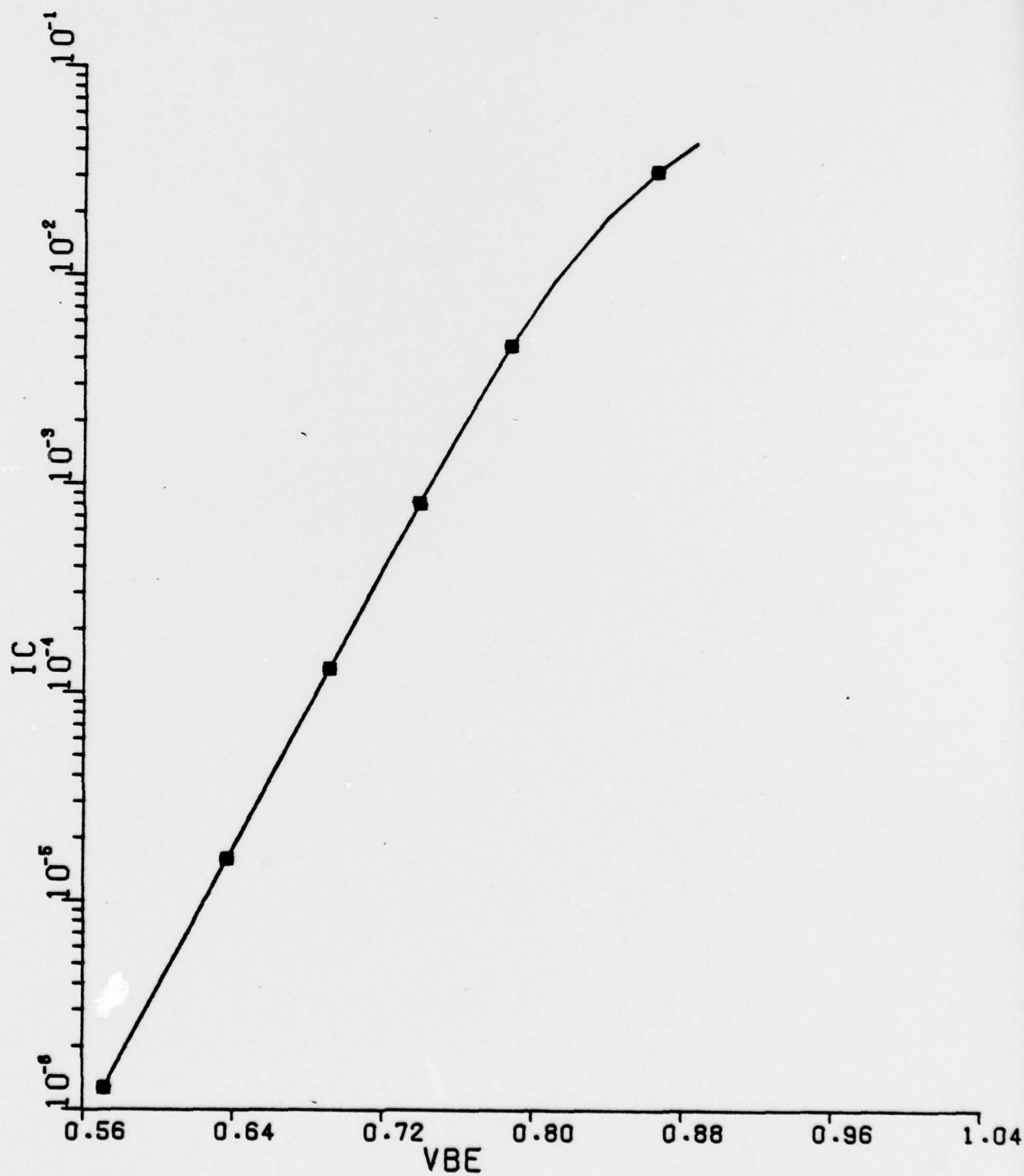
* --	PHICO	=	5.000E-01
+ --	PHICO	=	1.200E+00
0 --	PHICO	=	9.000E-01



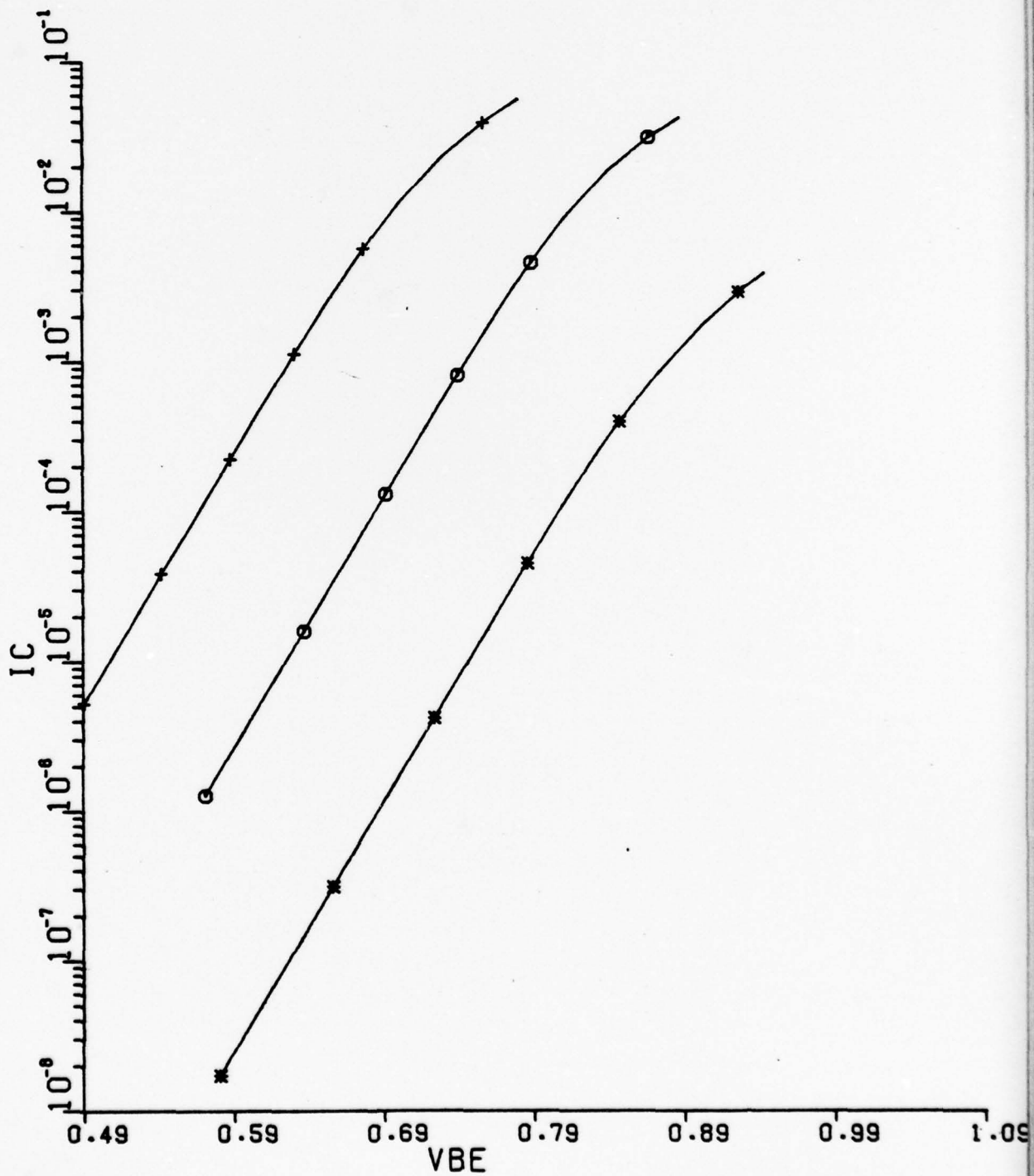
* --	PHIEO	=	5.000E-01
+ --	PHIEO	=	1.500E+00
0 --	PHIEO	=	1.200E+00



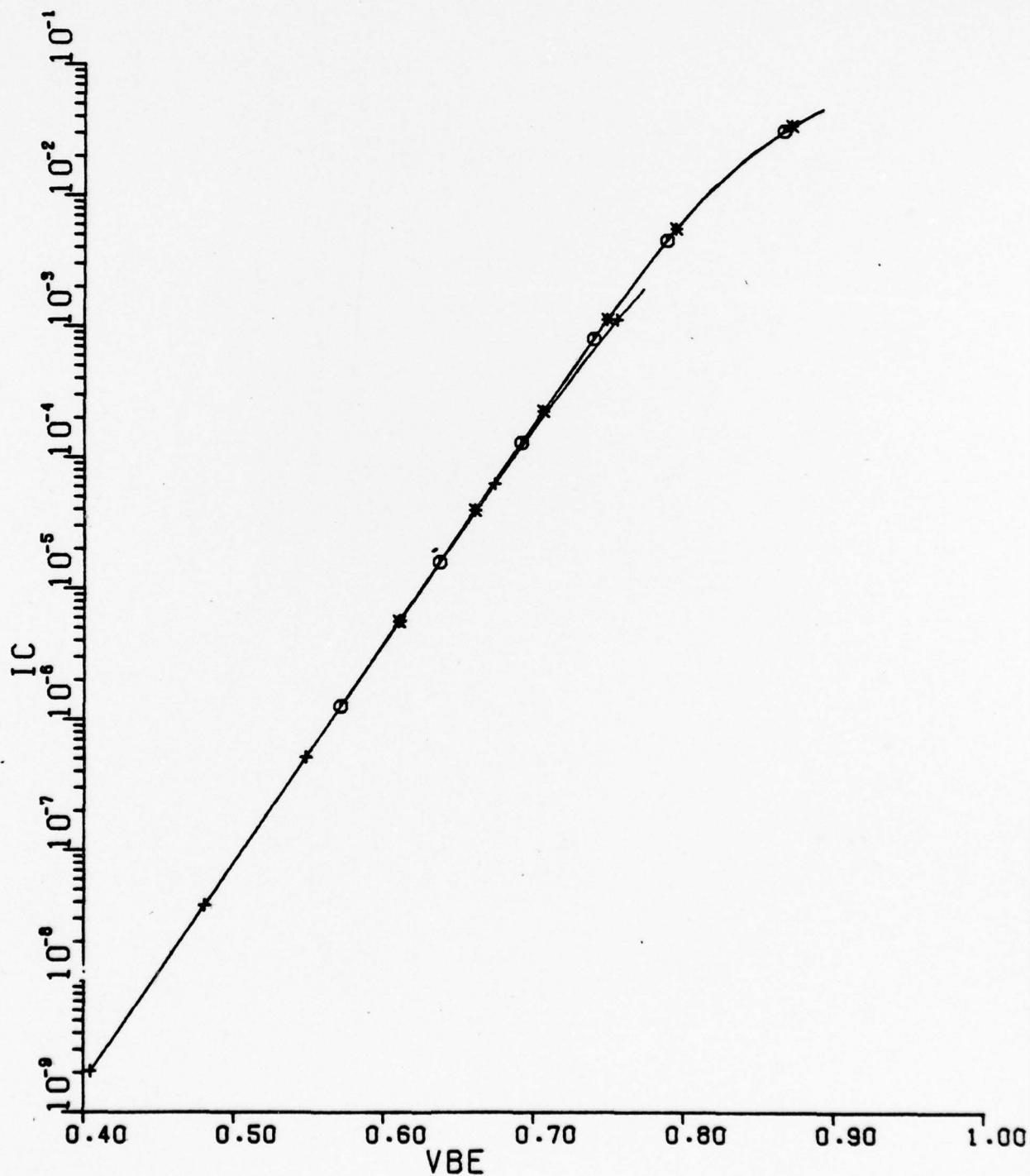
■ --	ISR	=	3.000E-13
+ --	ISR	=	3.000E-11
0 --	ISR	=	3.000E-12



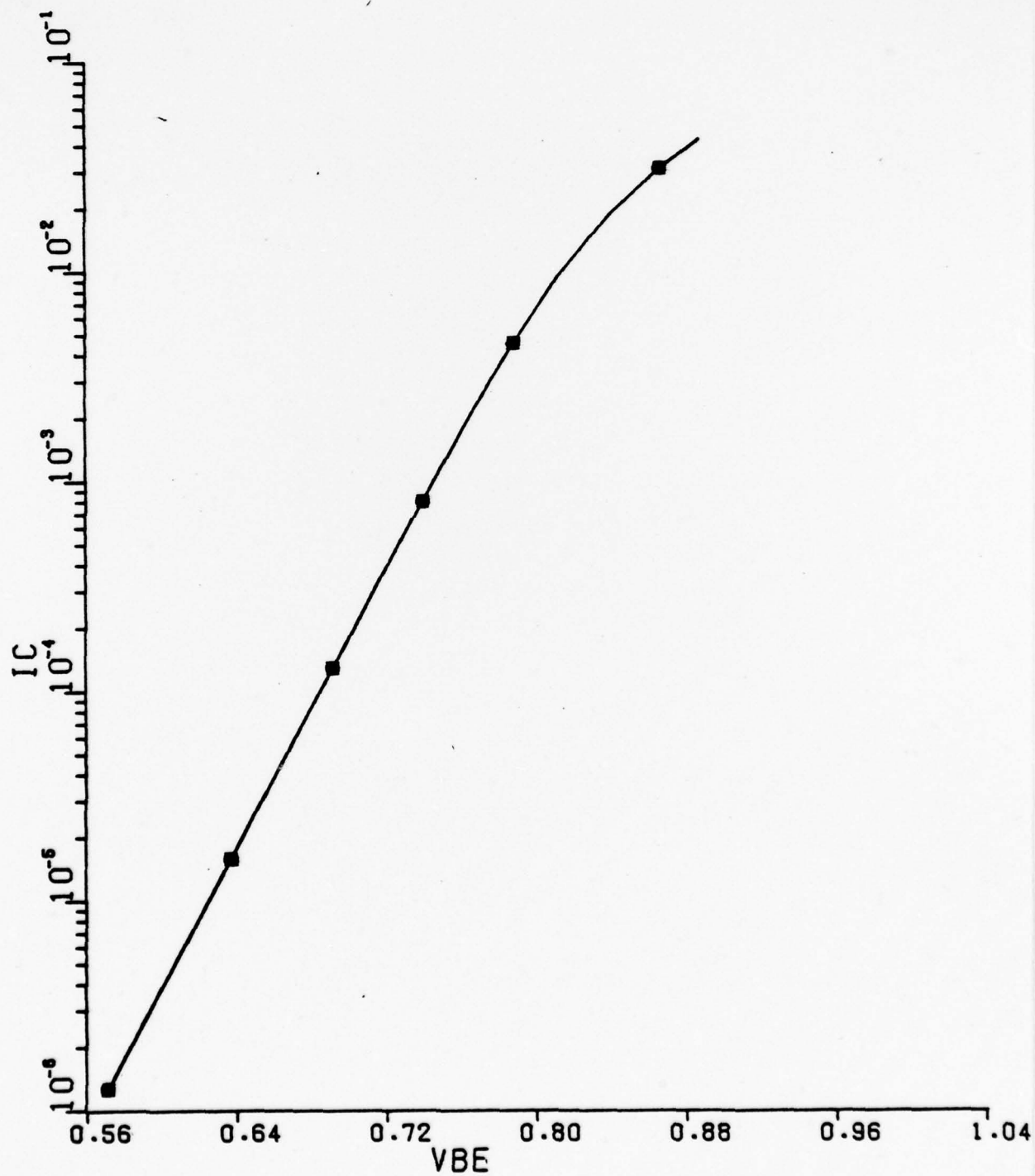
* --	IS	=	3.000E-18
+ --	IS	=	3.000E-14
o --	IS	=	3.200E-16



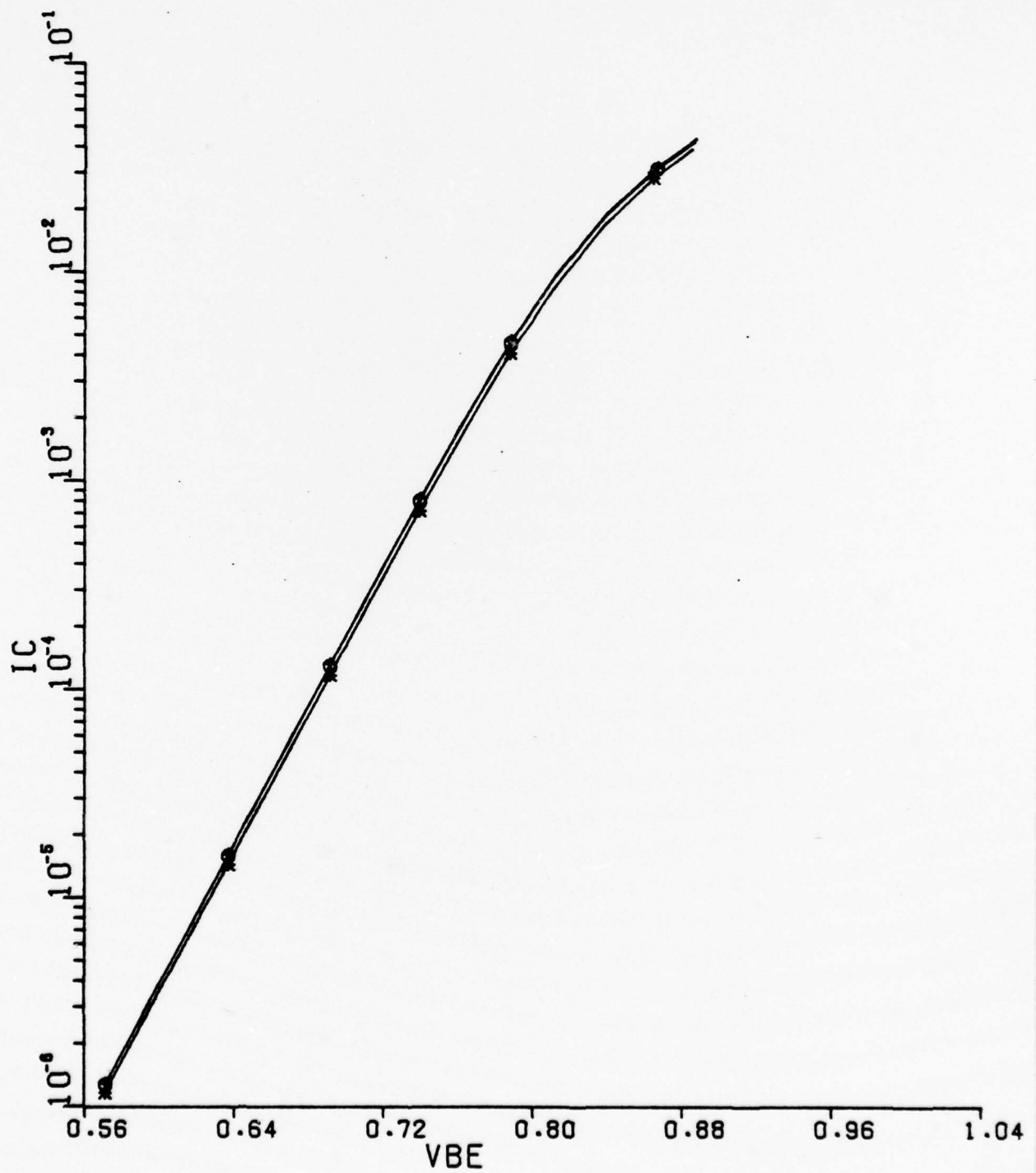
* --	IER	=	3.000E-16
+ --	IER	=	3.000E-12
o --	IER	=	3.200E-14



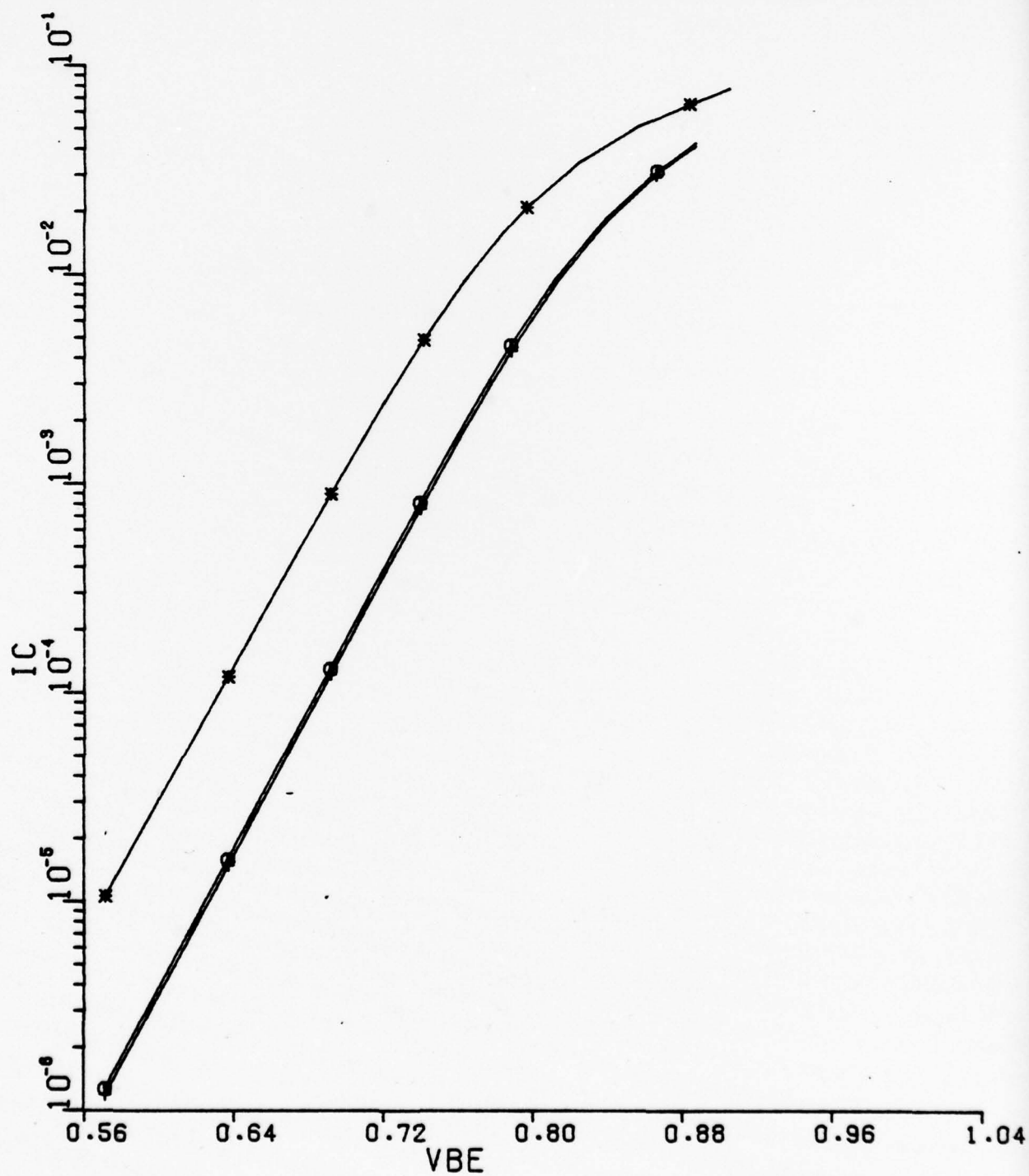
■ --	IBR	=	3.000E-15
+ --	IBR	=	3.000E-11
0 --	IBR	=	3.000E-13



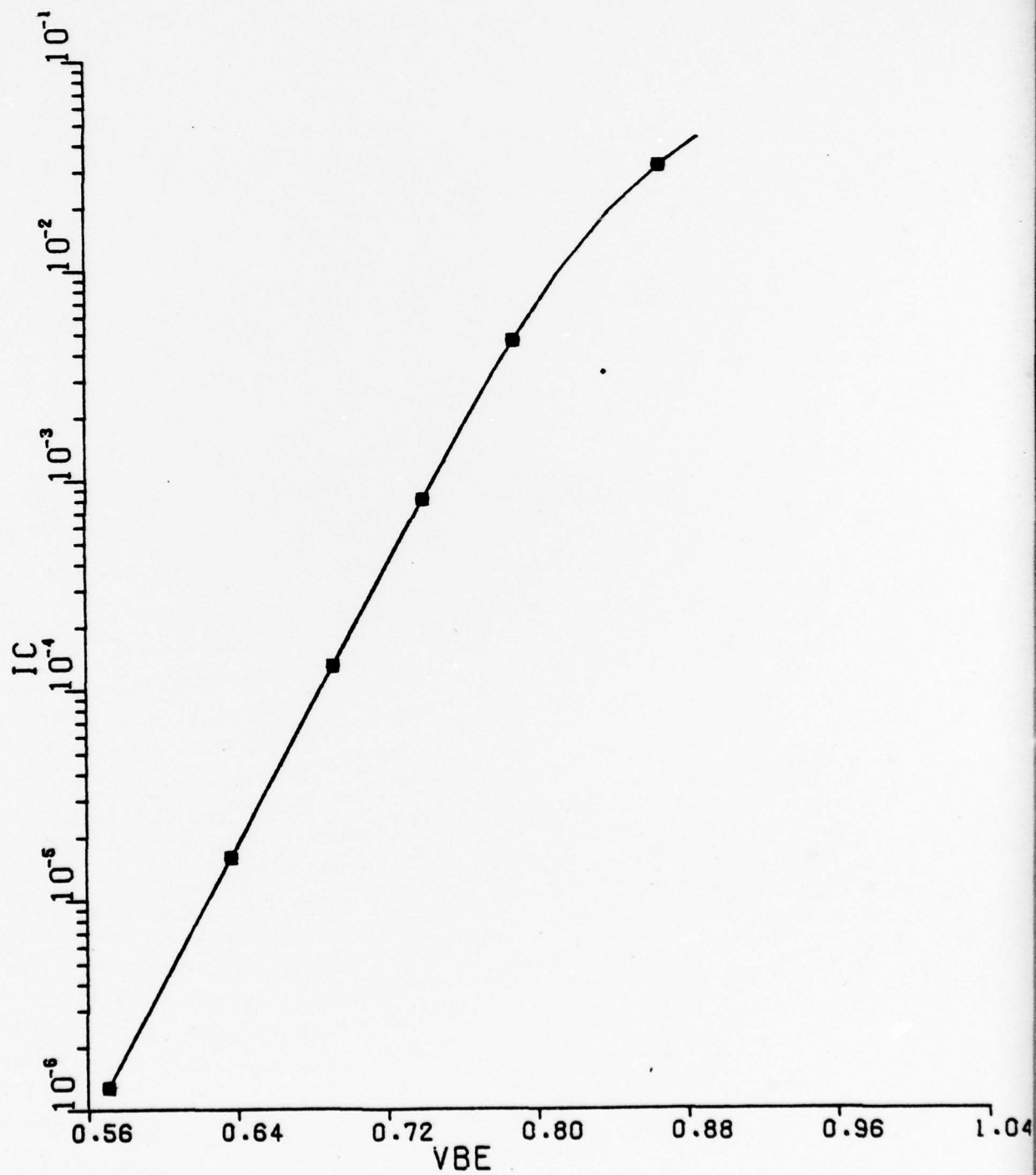
■ --	VER	=	5.000E+00
+ --	VER	=	5.000E+01
0 --	VER	=	2.000E+01



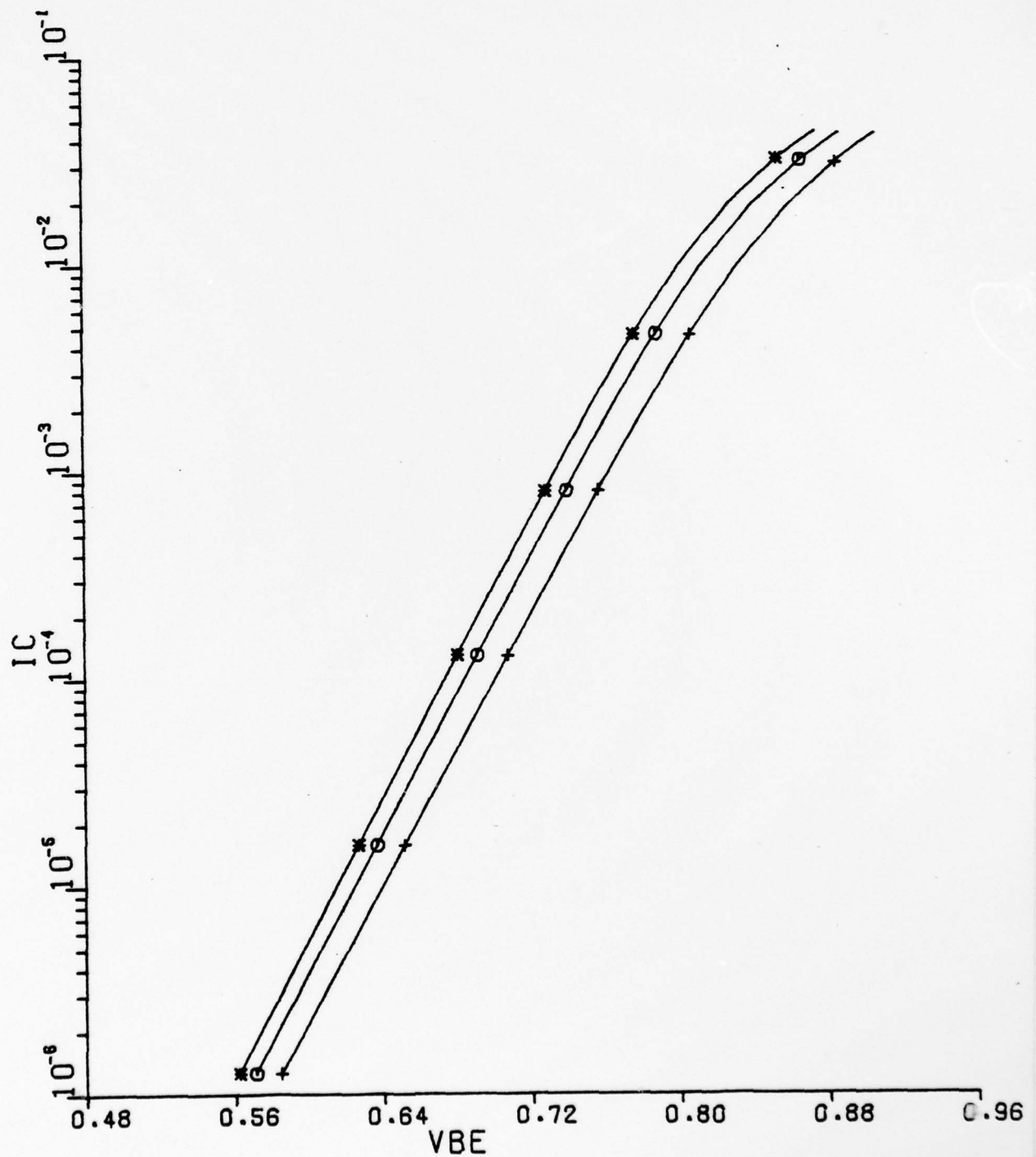
* --	VCR	=	5.000E+00
+ --	VCR	=	3.000E+02
0 --	VCR	=	6.000E+01



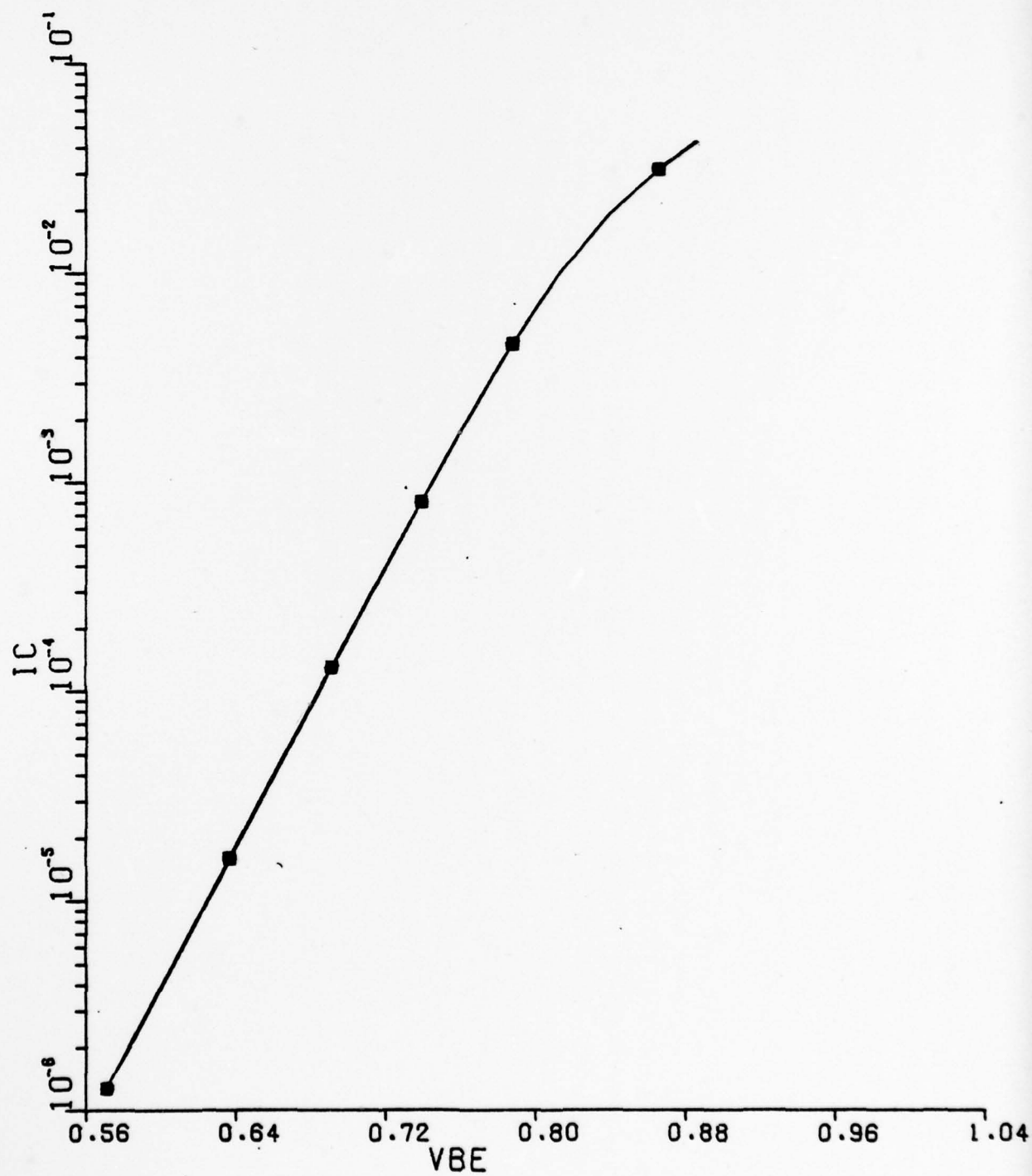
■ ---	NC	=	8.000E-01
+ ---	NC	=	2.300E+00
0 ---	NC	=	1.800E+00



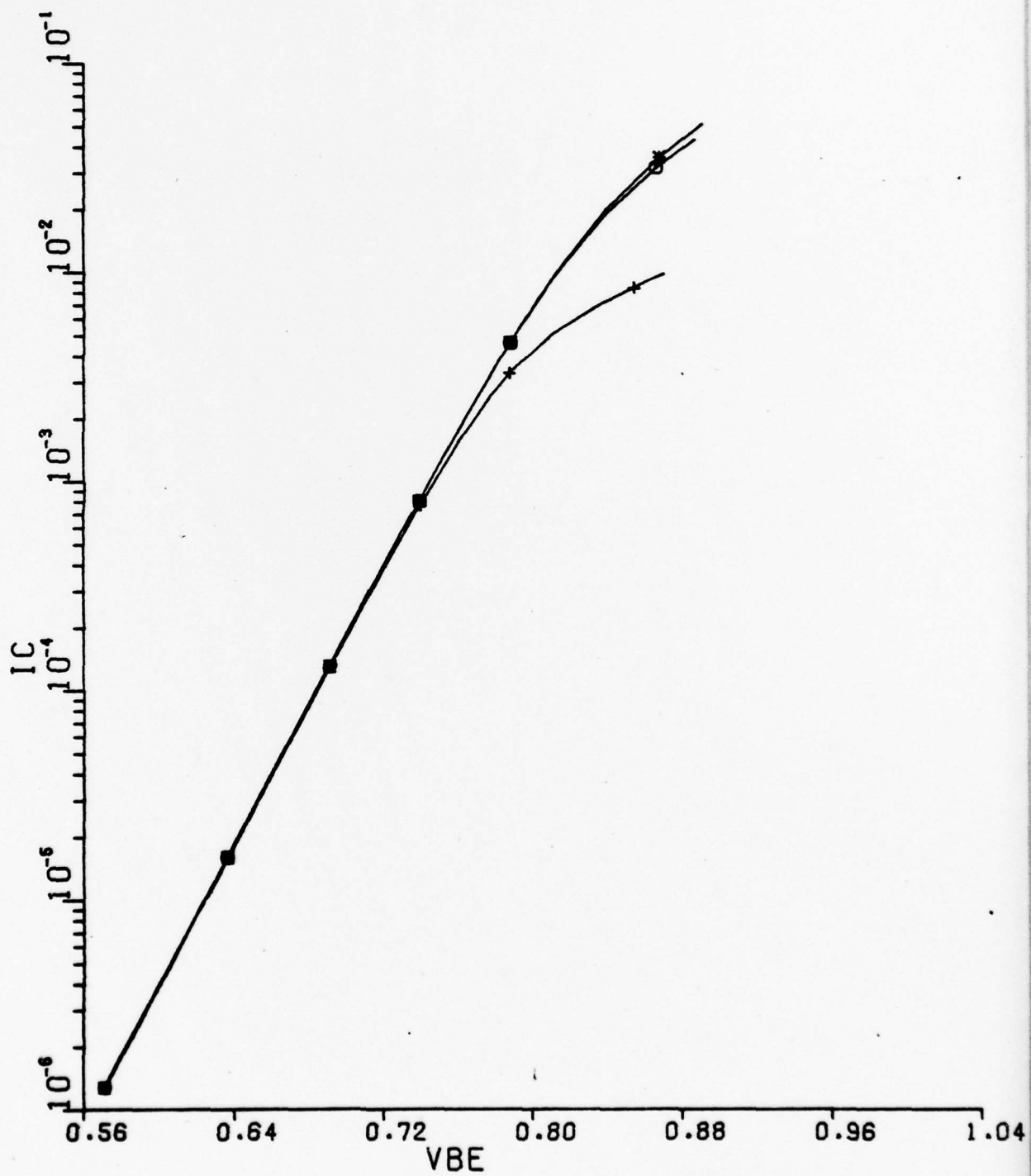
* --	VT	=	2.550E-02
+ --	VT	=	2.650E-02
0 --	VT	=	2.590E-02



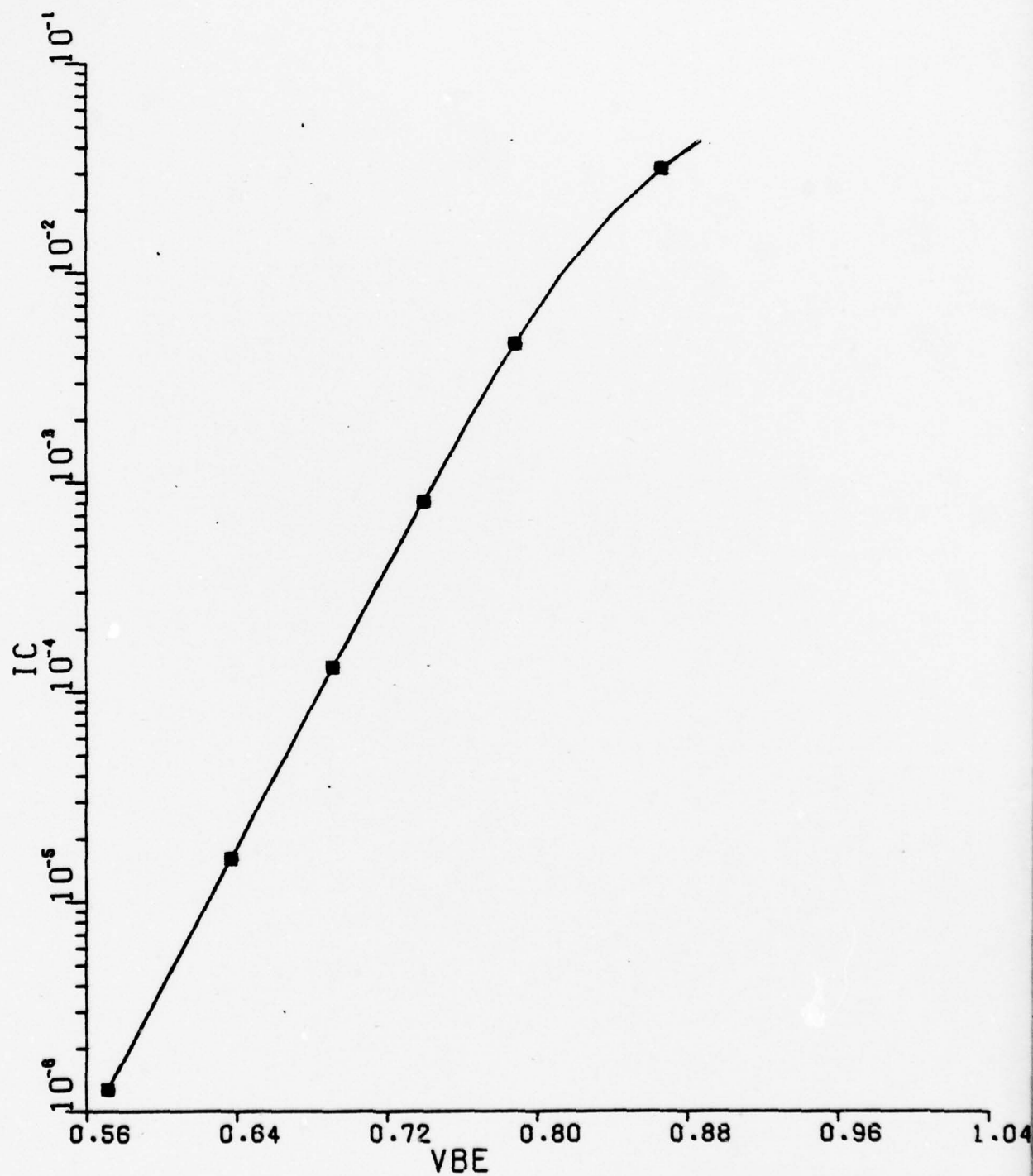
■ --	VTS	=	2.600E-02
+ --	VTS	=	2.500E-02
0 --	VTS	=	2.700E-02



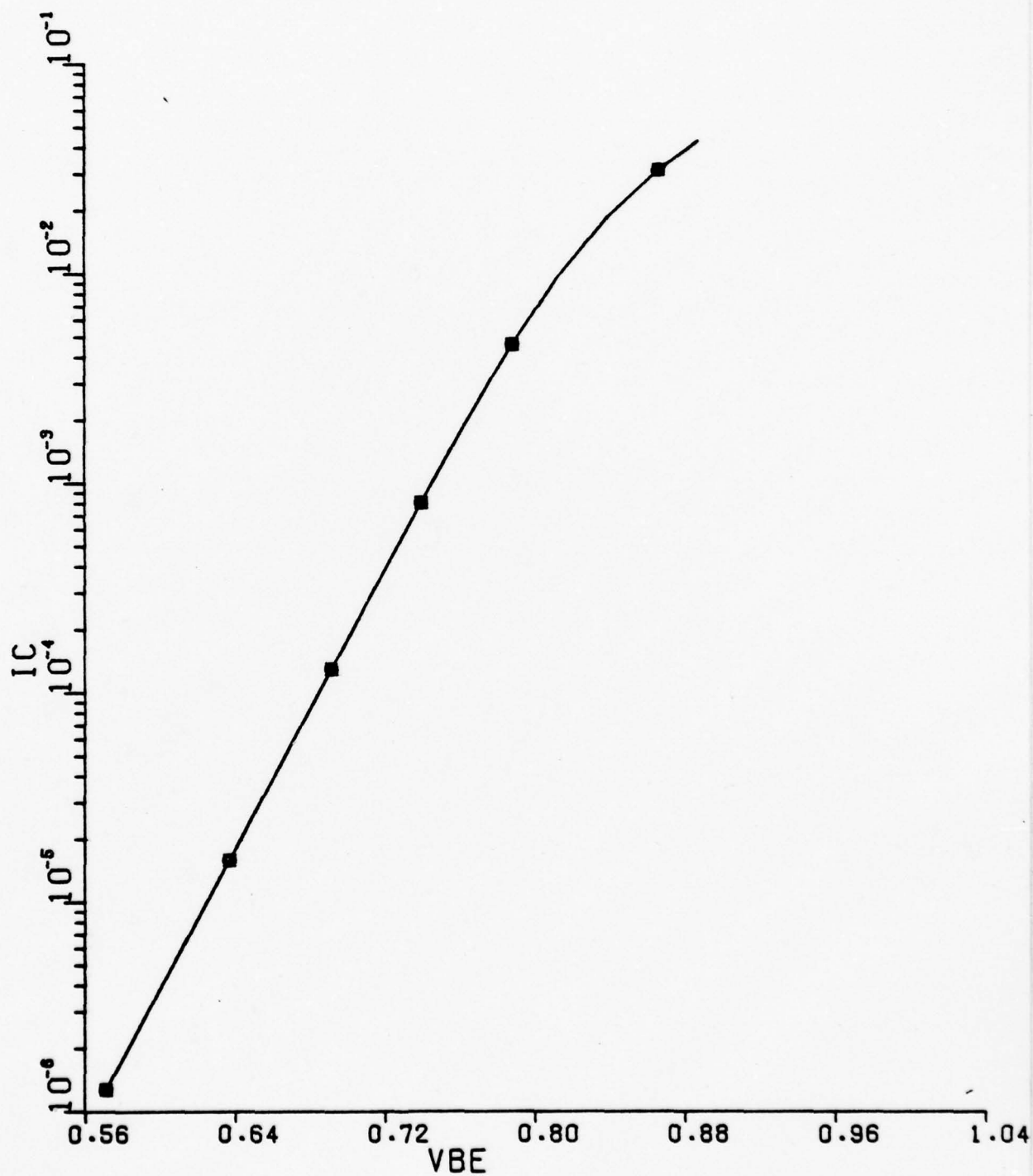
■ --	QFN	=	1.500E-18
+ --	QFN	=	1.500E-14
0 --	QFN	=	1.500E-16



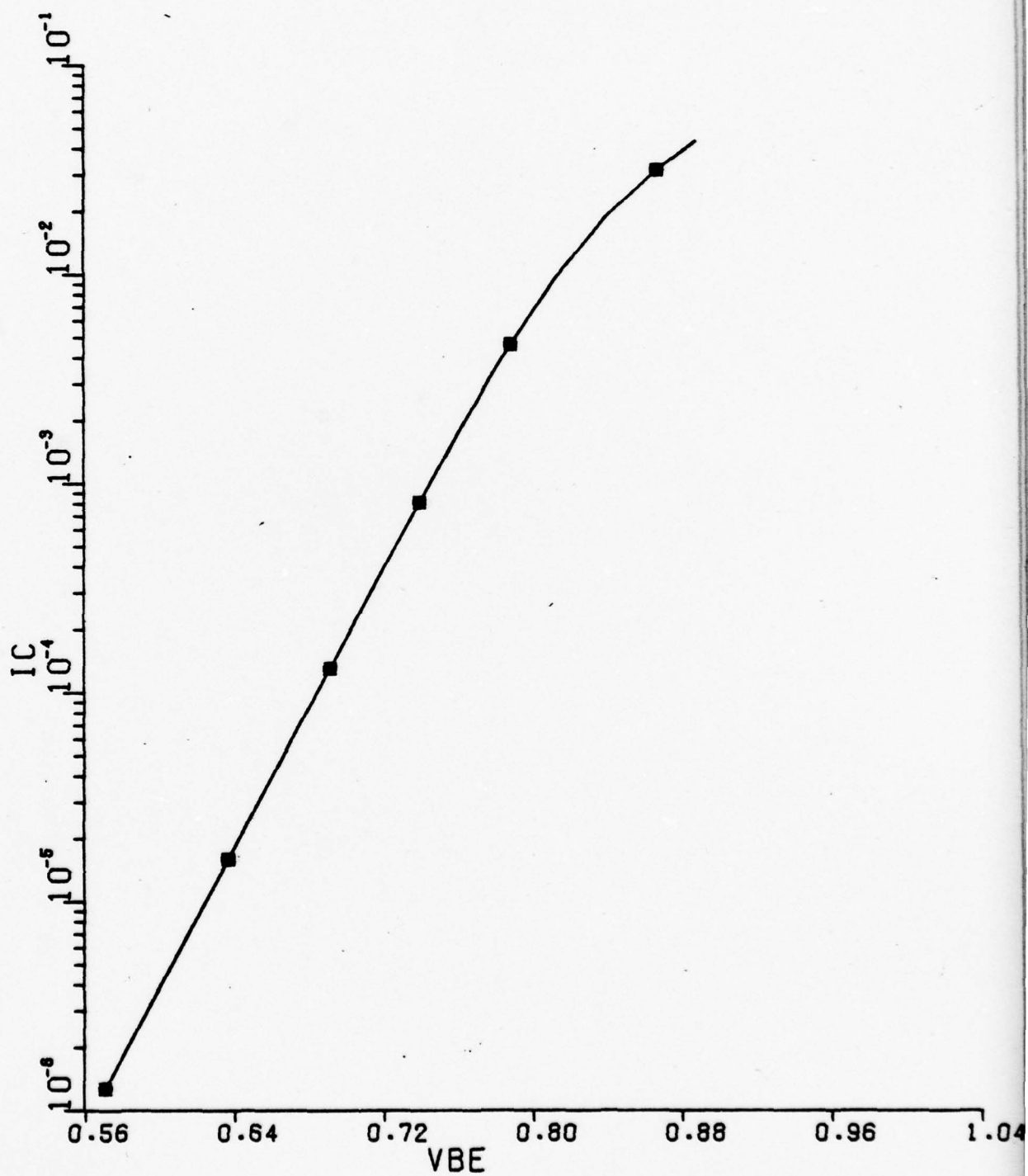
■	--	QRN	=	1.500E-14
+	--	QRN	=	1.500E-10
0	--	QRN	=	1.500E-12



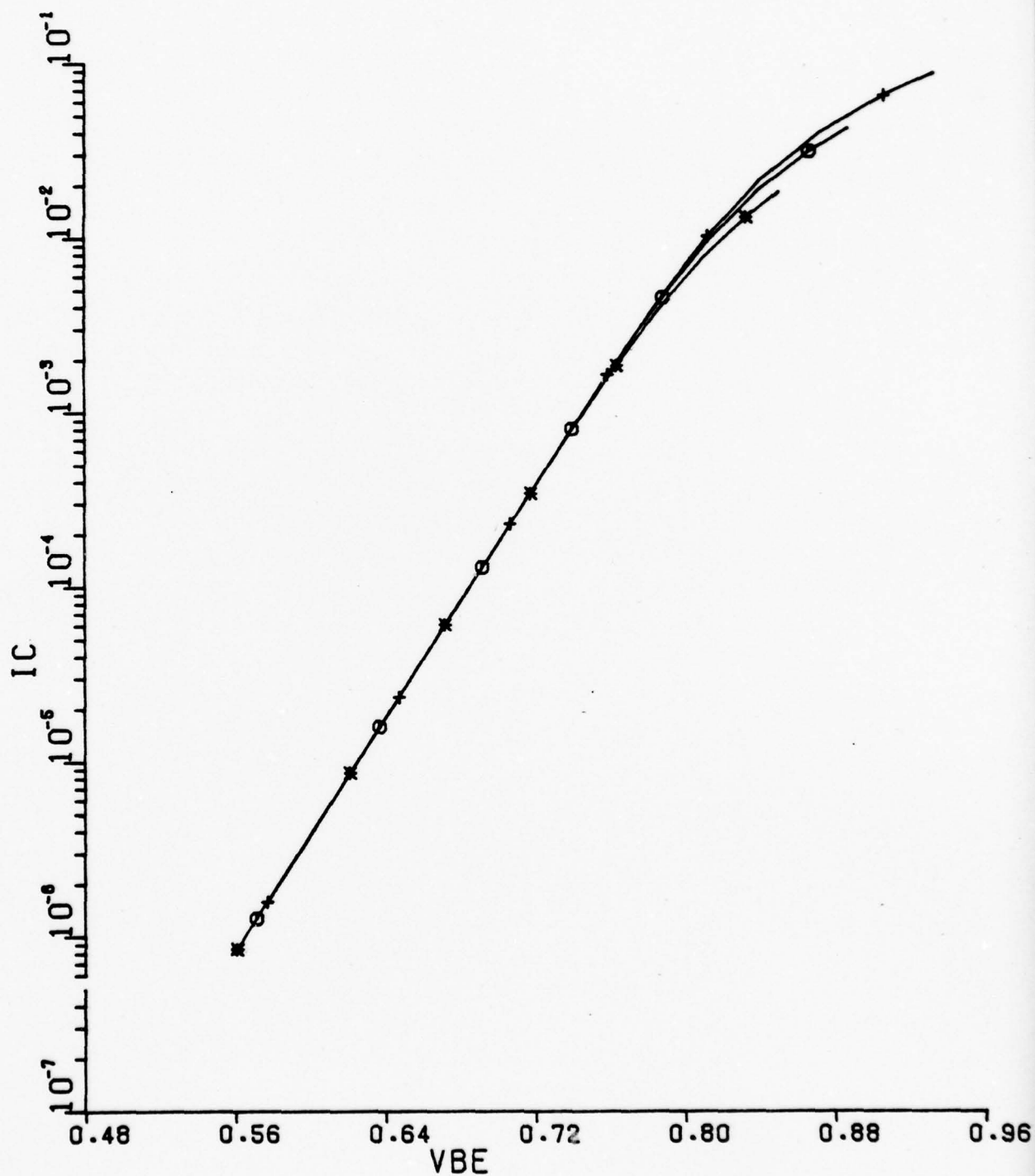
■ --	TAUFO	=	1.590E-09
+ --	TAUFO	=	1.590E-08
0 --	TAUFO	=	1.590E-10



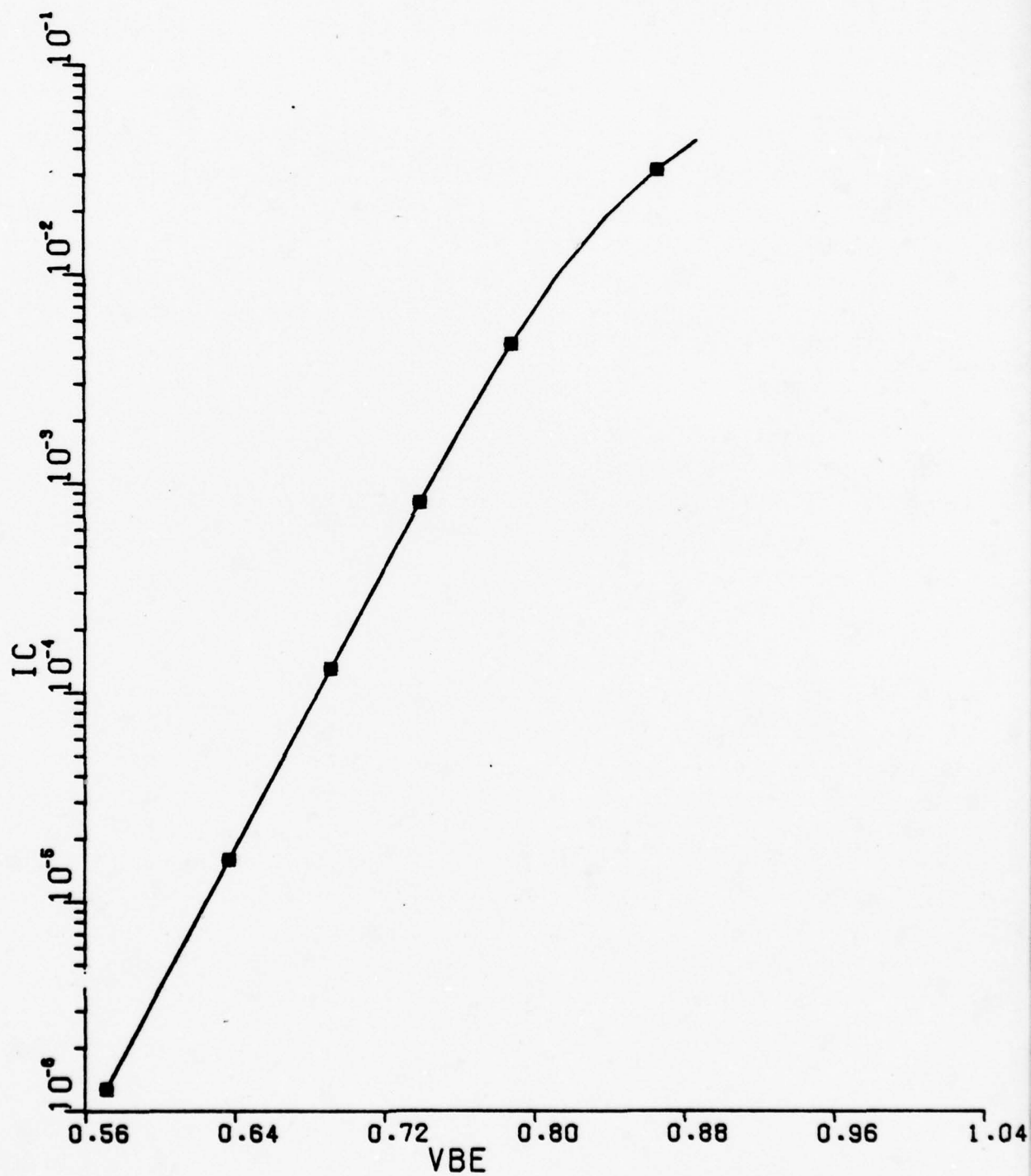
■	--	TAUR	=	1.000E-06
+	--	TAUR	=	1.270E-11
0	--	TAUR	=	1.270E-09



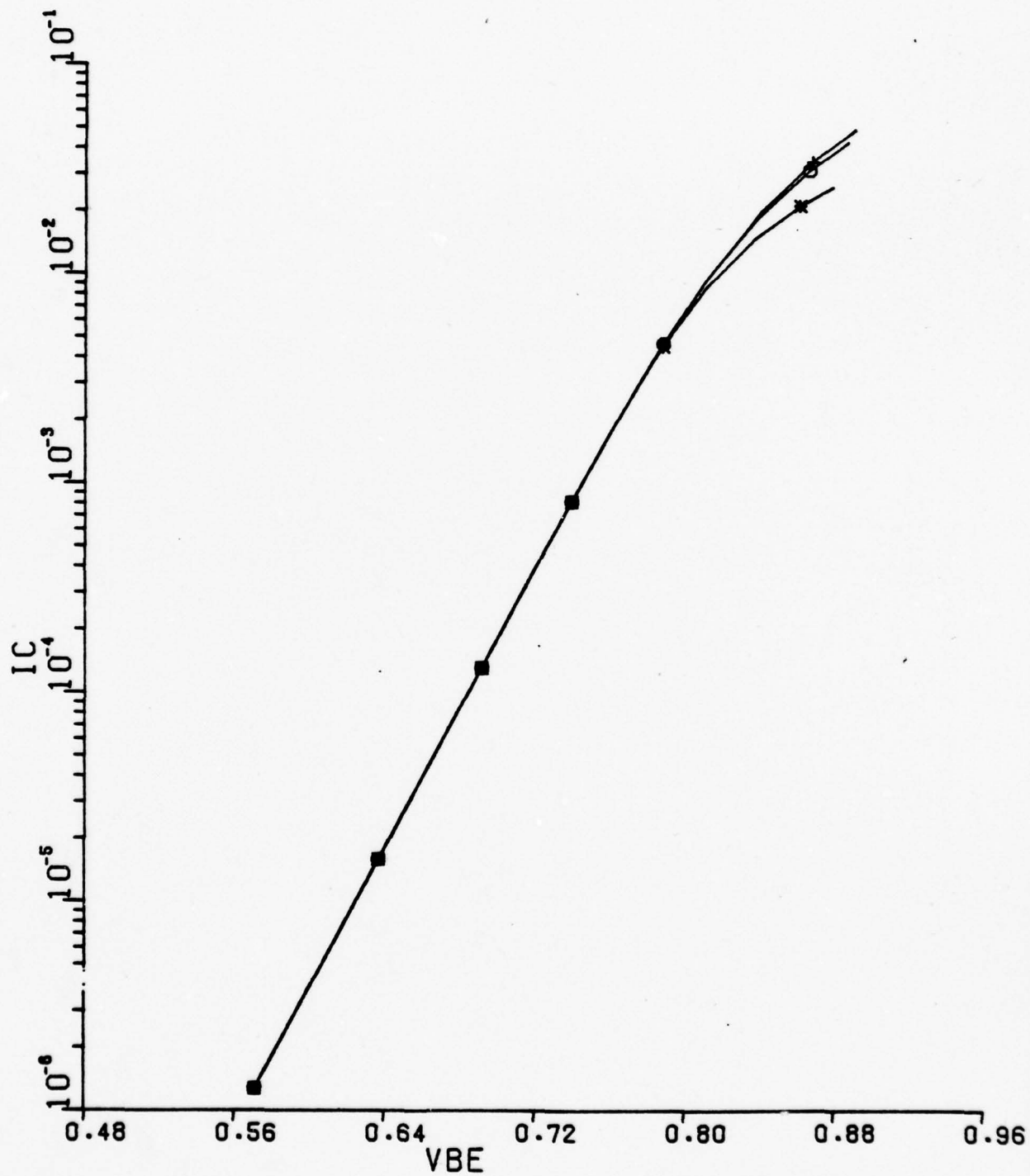
■ --	BETAO	=	2.000E+01
+ --	BETAO	=	1.500E+02
0 --	BETAO	=	5.500E+01



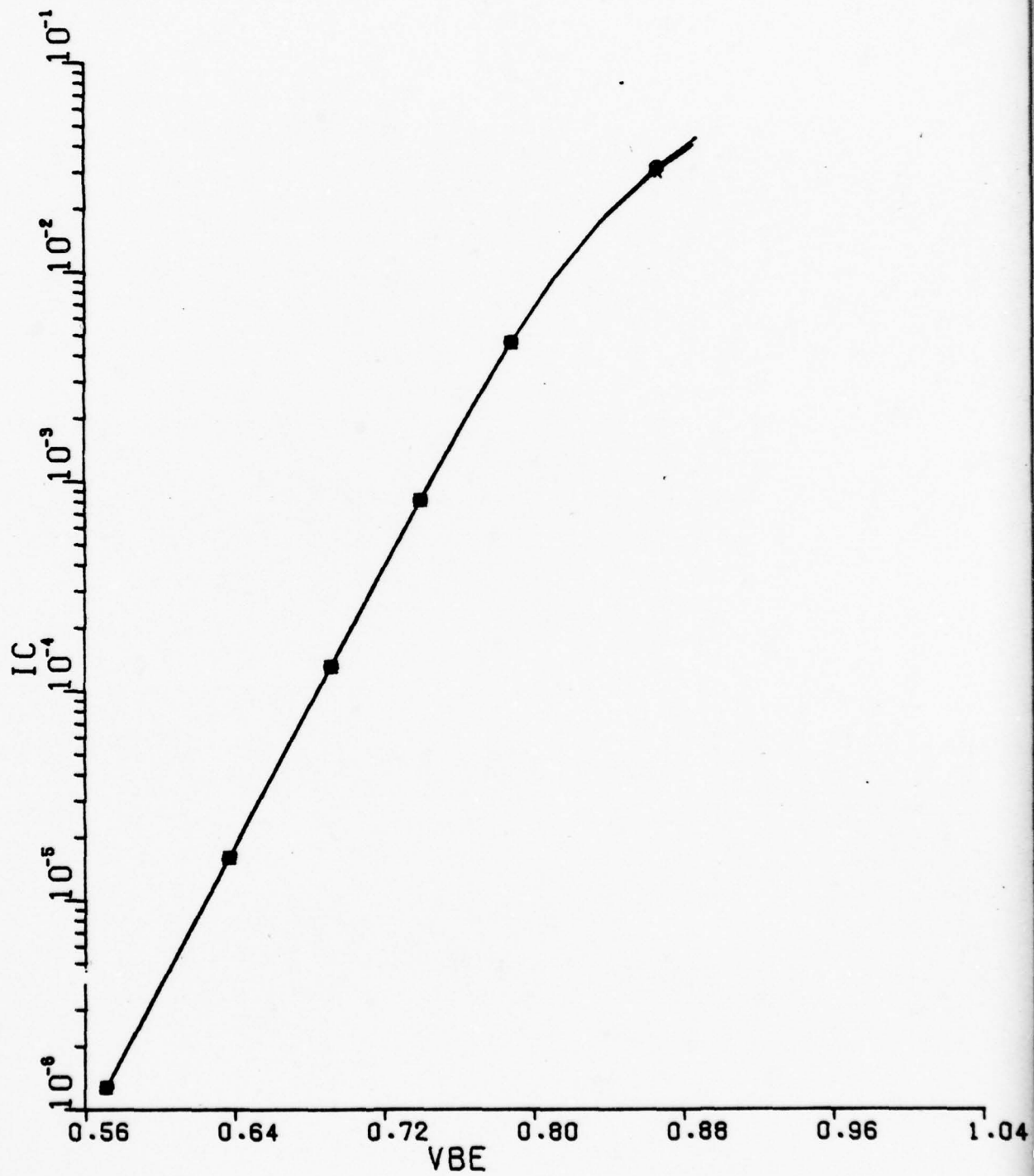
■ --	BETAR	=	6.000E+00
+ --	BETAR	=	1.100E+00
0 --	BETAR	=	1.500E-01



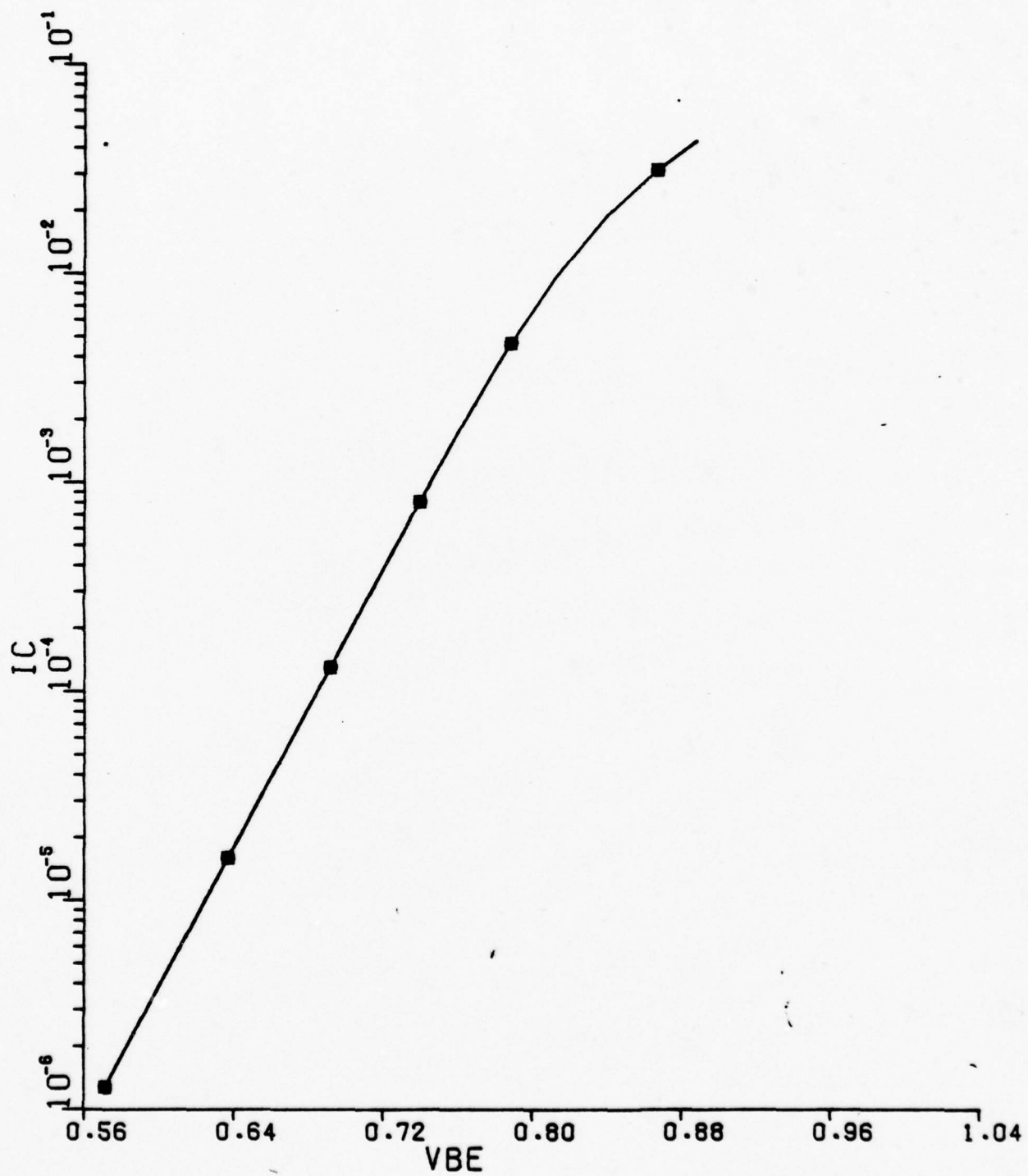
■	--	W	=	2.000E-05
+	--	W	=	2.000E-04
o	--	W	=	6.000E-05



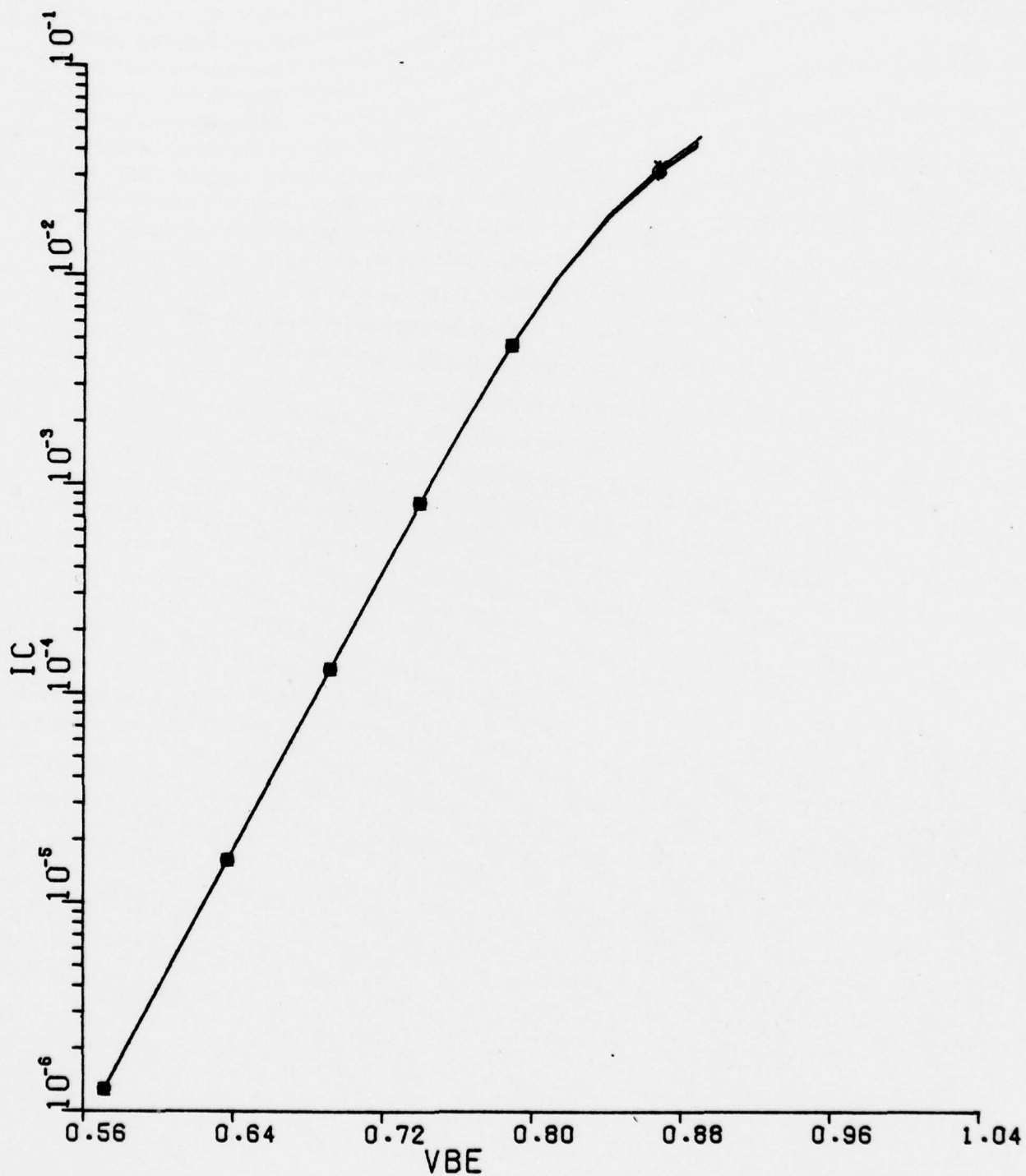
■ ---	AE	=	1.000E-08
+ ---	AE	=	1.000E-04
0 ---	AE	=	9.800E-07



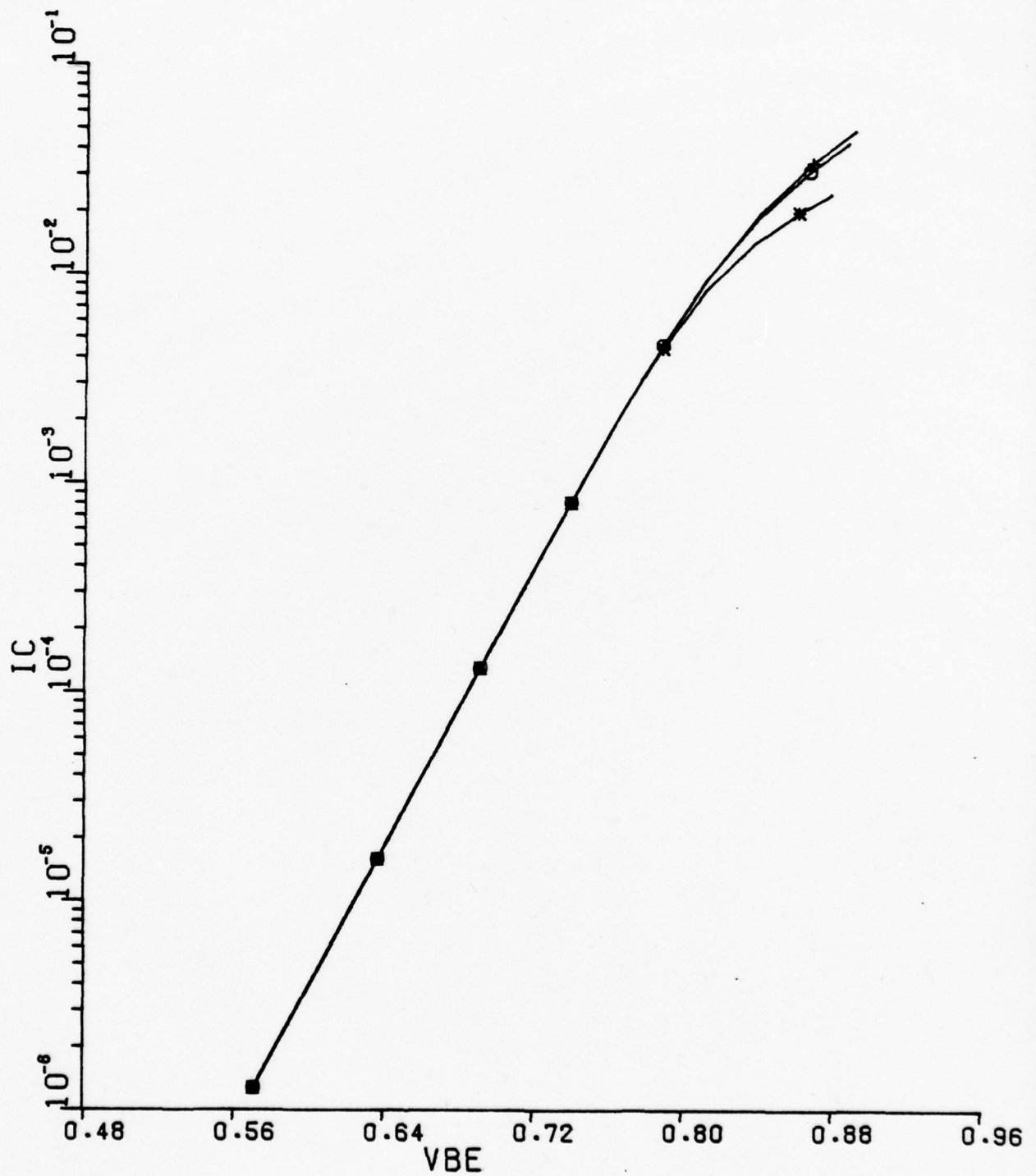
■ --	VLIM	=	1.000E+06
+ --	VLIM	=	1.500E+07
0 --	VLIM	=	6.000E+06



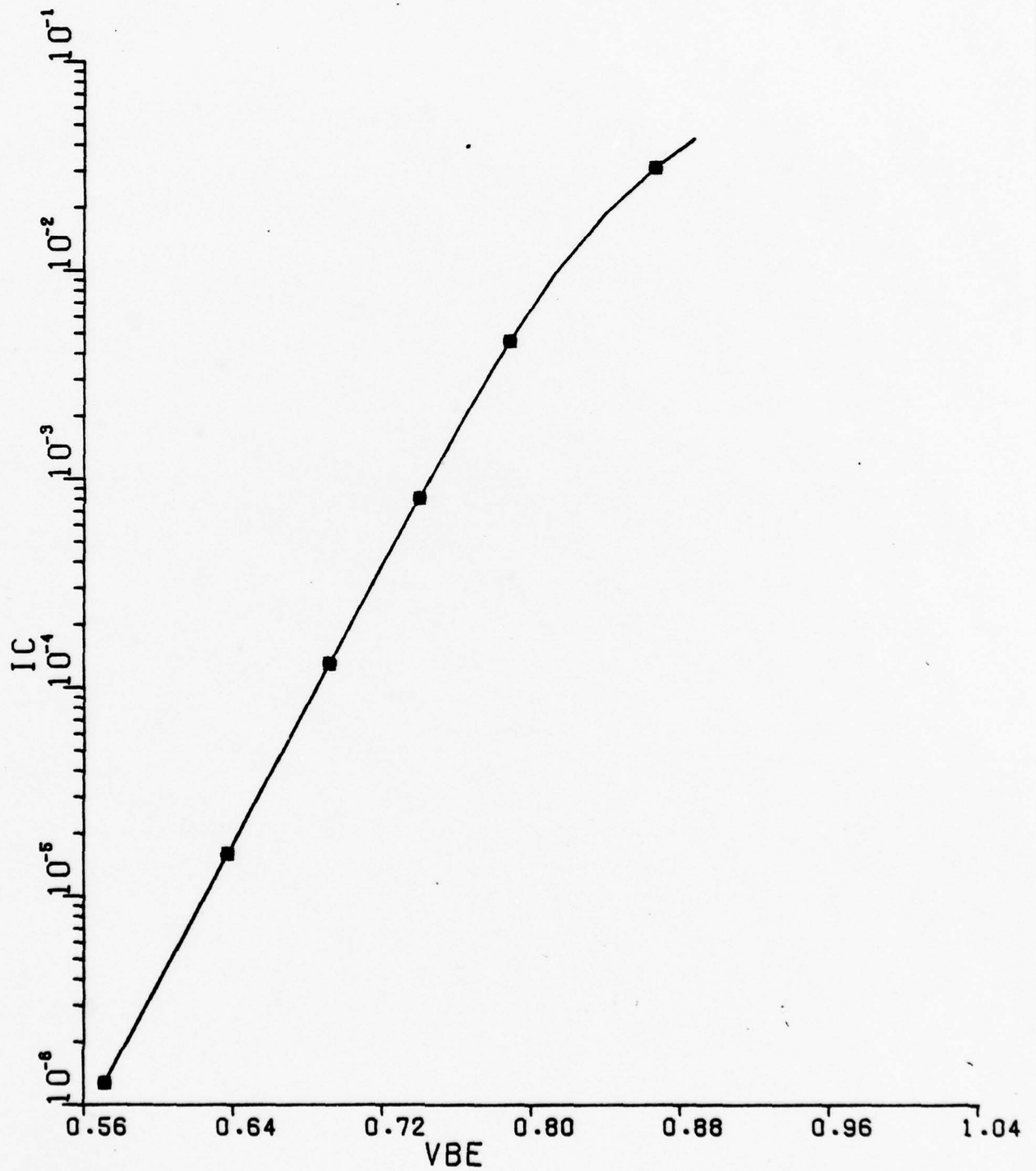
■ --	DNB	=	1.000E+01
+ --	DNB	=	3.000E+01
0 --	DNB	=	2.260E+01



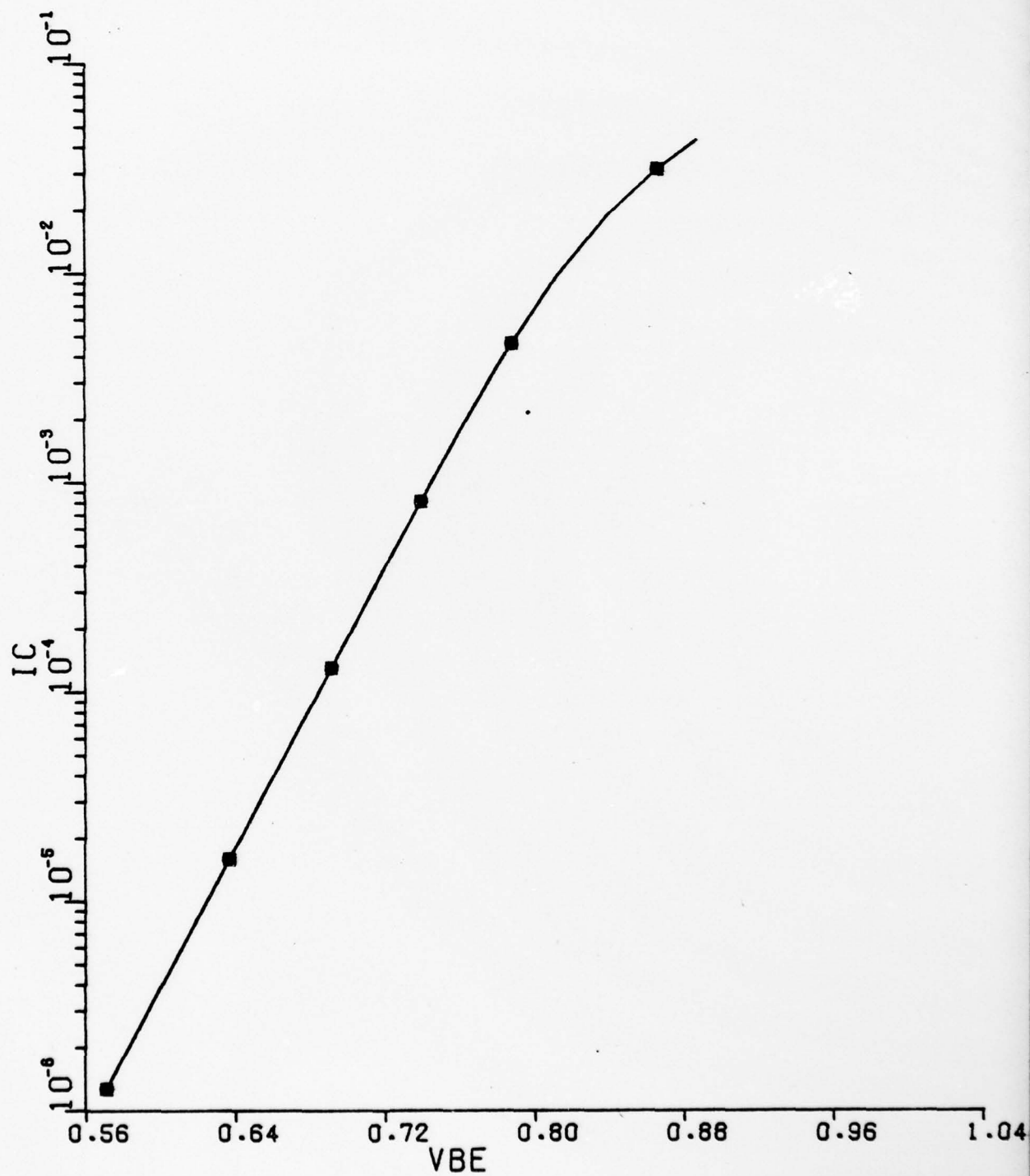
■ --	WCPRIME	=	1.000E-03
+ --	WCPRIME	=	1.000E-04
0 --	WCPRIME	=	3.000E-04



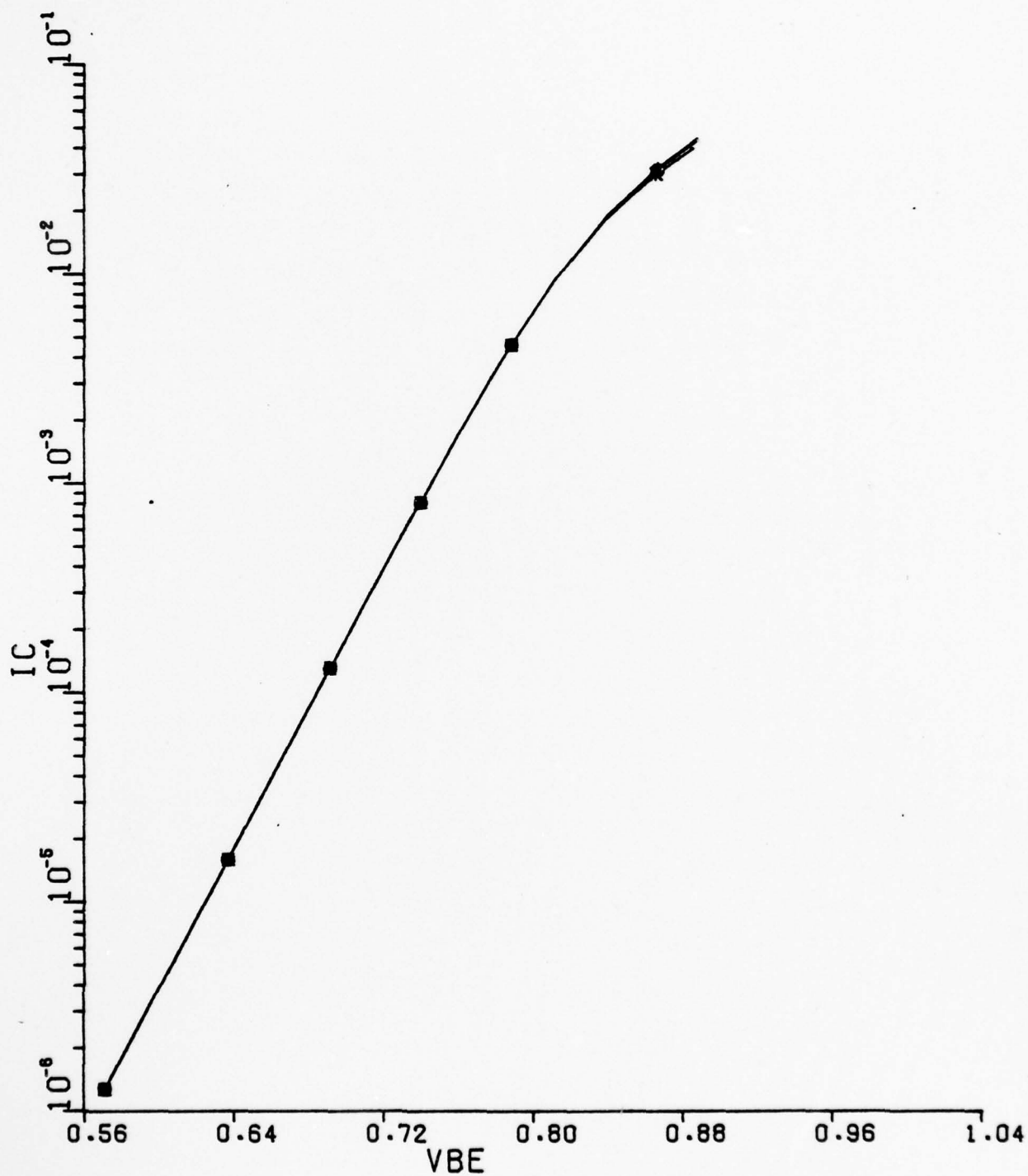
■ --	NDC	=	1.000E+20
+ --	NDC	=	1.000E+13
0 --	NDC	=	1.000E+16



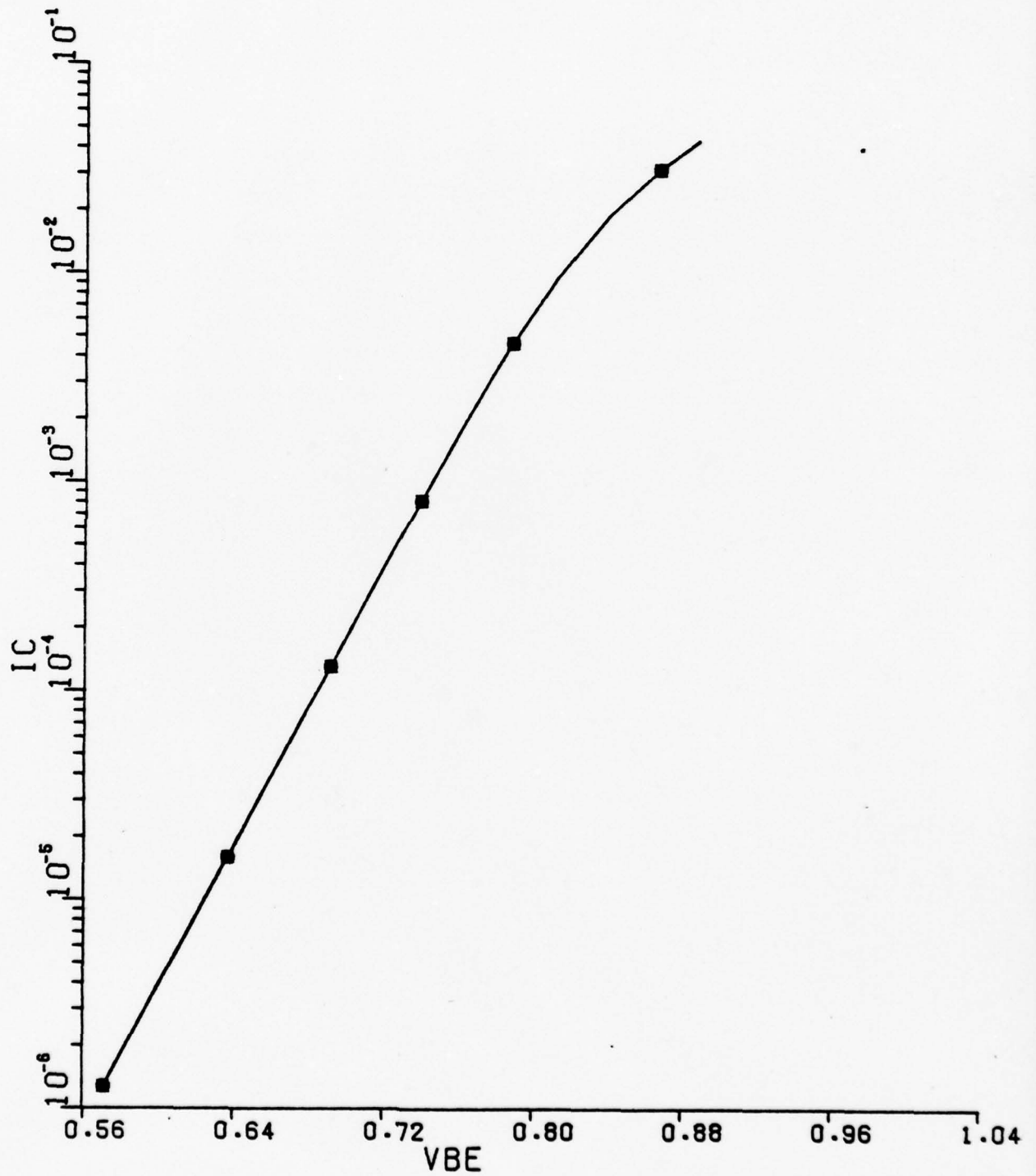
■ --	PHIC	=	4.000E-01
+ --	PHIC	=	1.200E+00
0 --	PHIC	=	7.000E-01



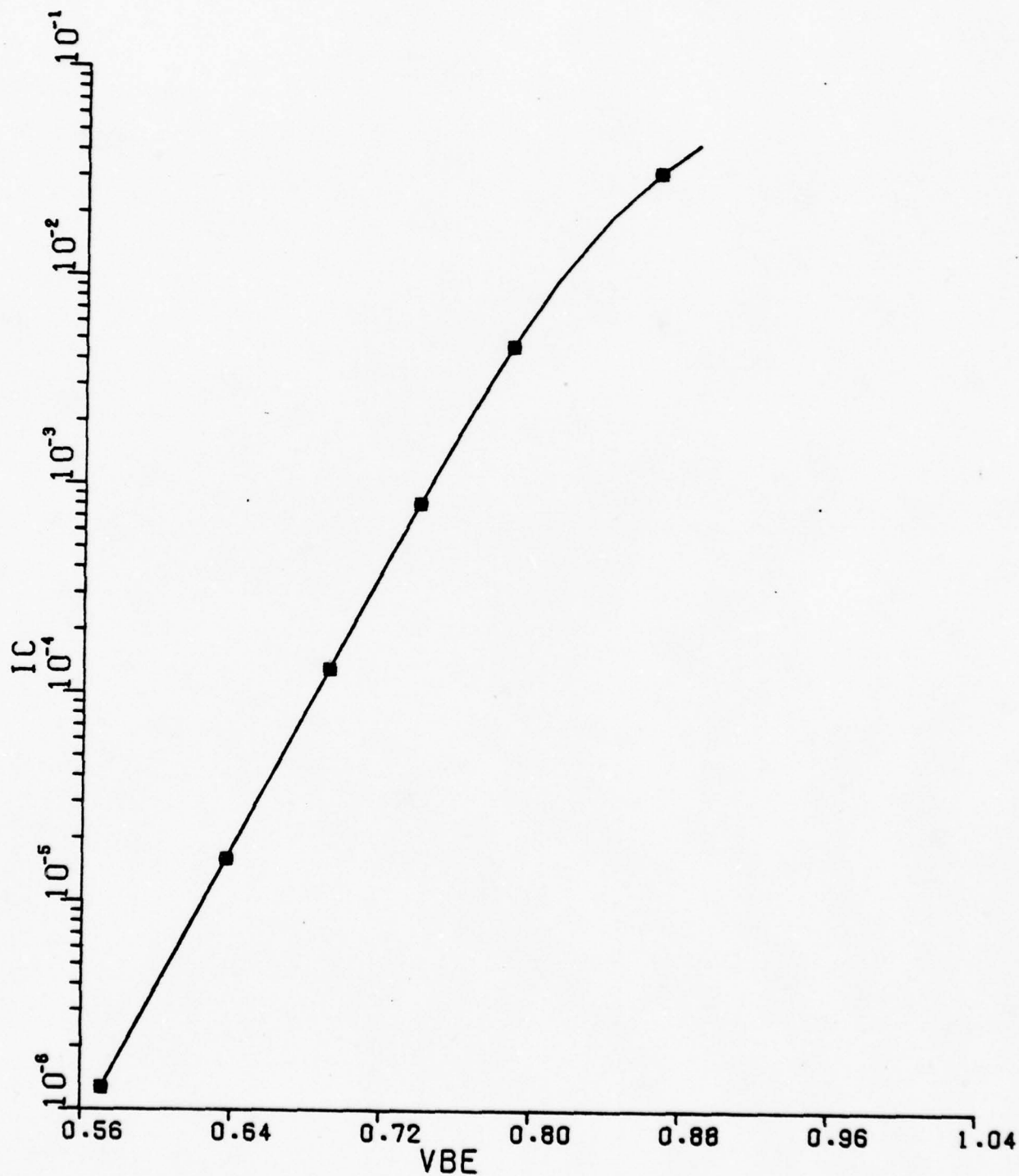
■ --	DNC	=	3.000E+01
+ --	DNC	=	6.000E+01
0 --	DNC	=	4.800E+01



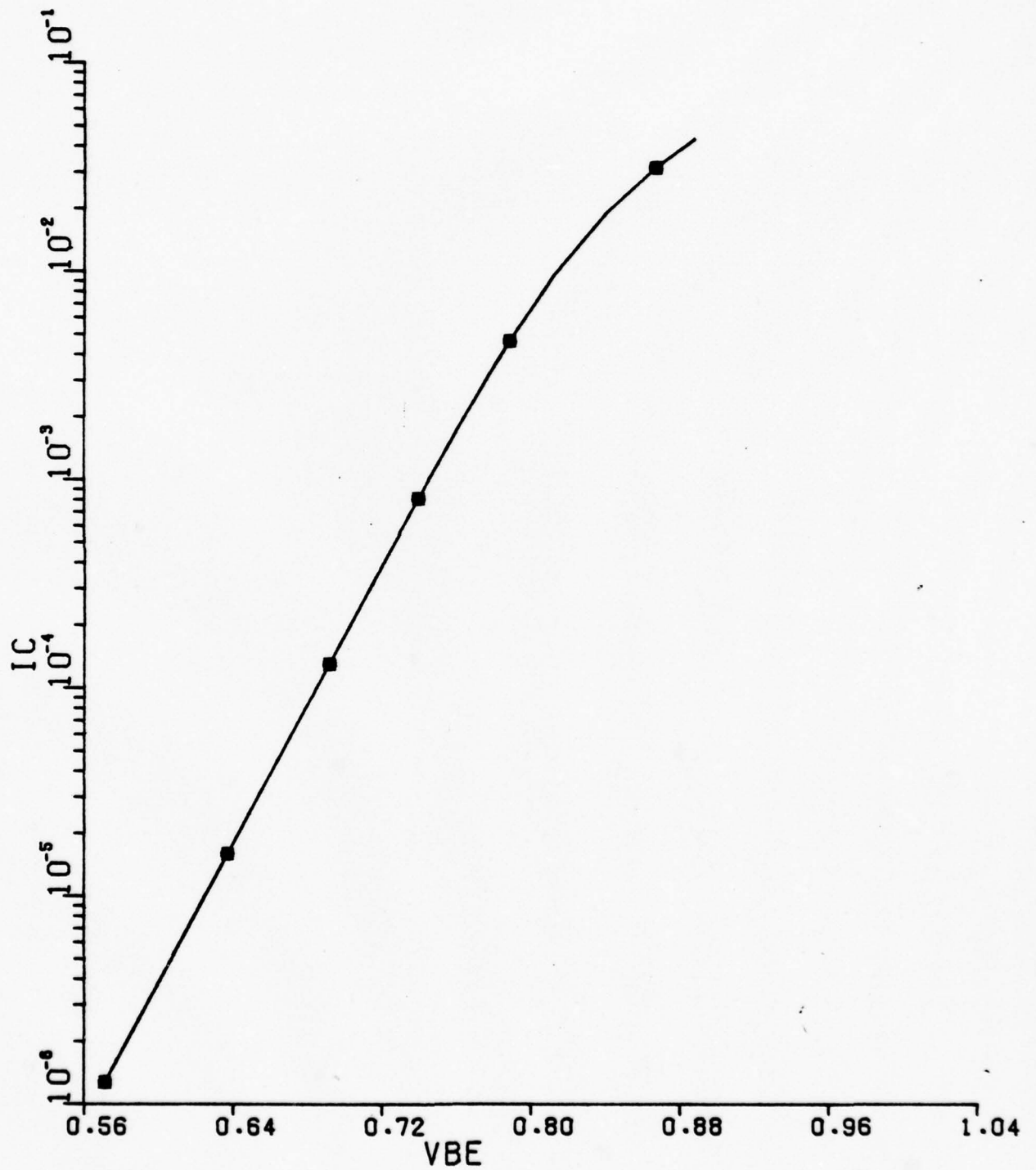
■ --	X0	=	4.000E-05
+ --	X0	=	2.400E-04
0 --	X0.	=	1.200E-04



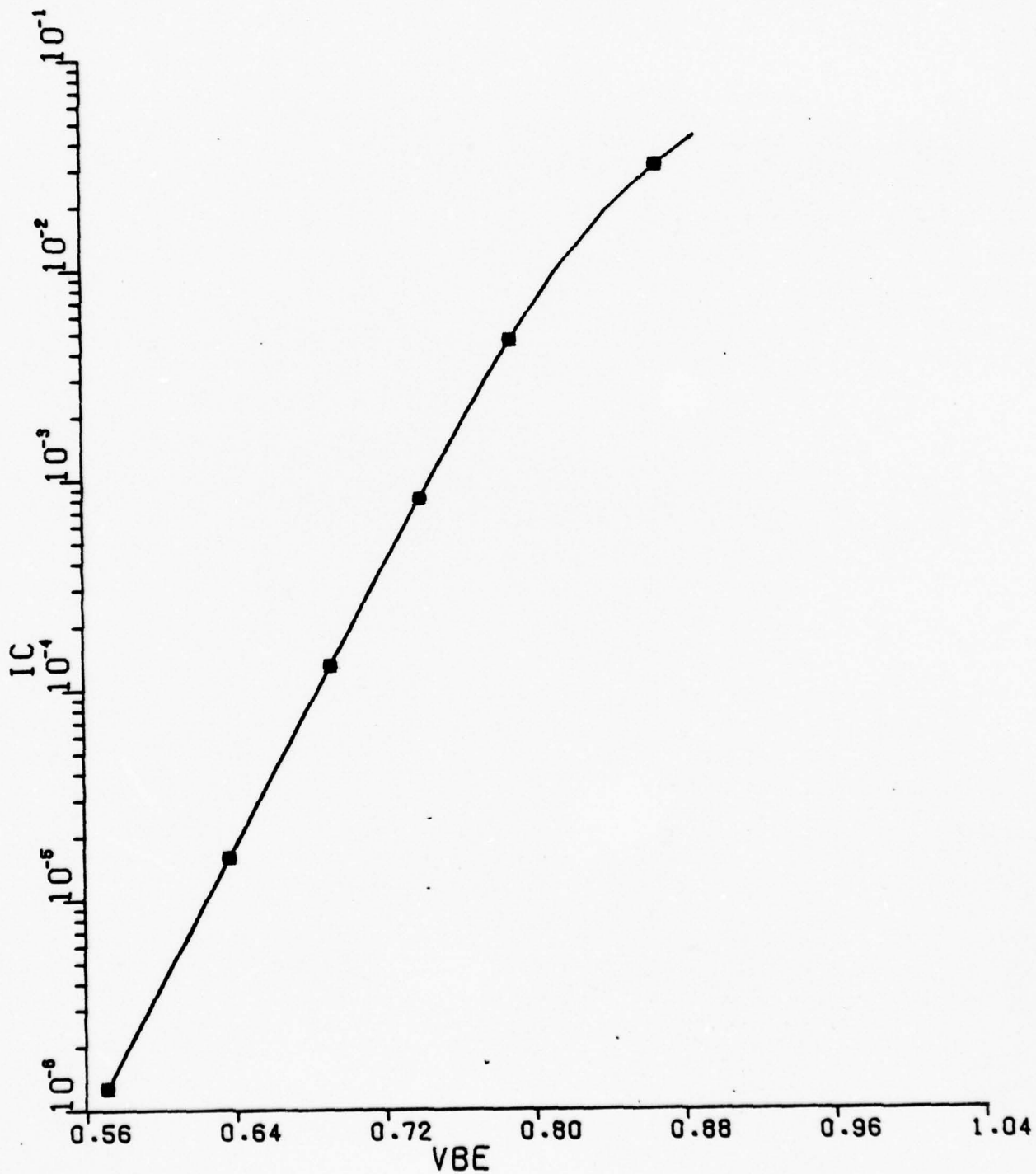
■ --	KR	= 1.000E-01
+ --	KR	= 9.000E-01
0 --	KR	= 4.000E-01



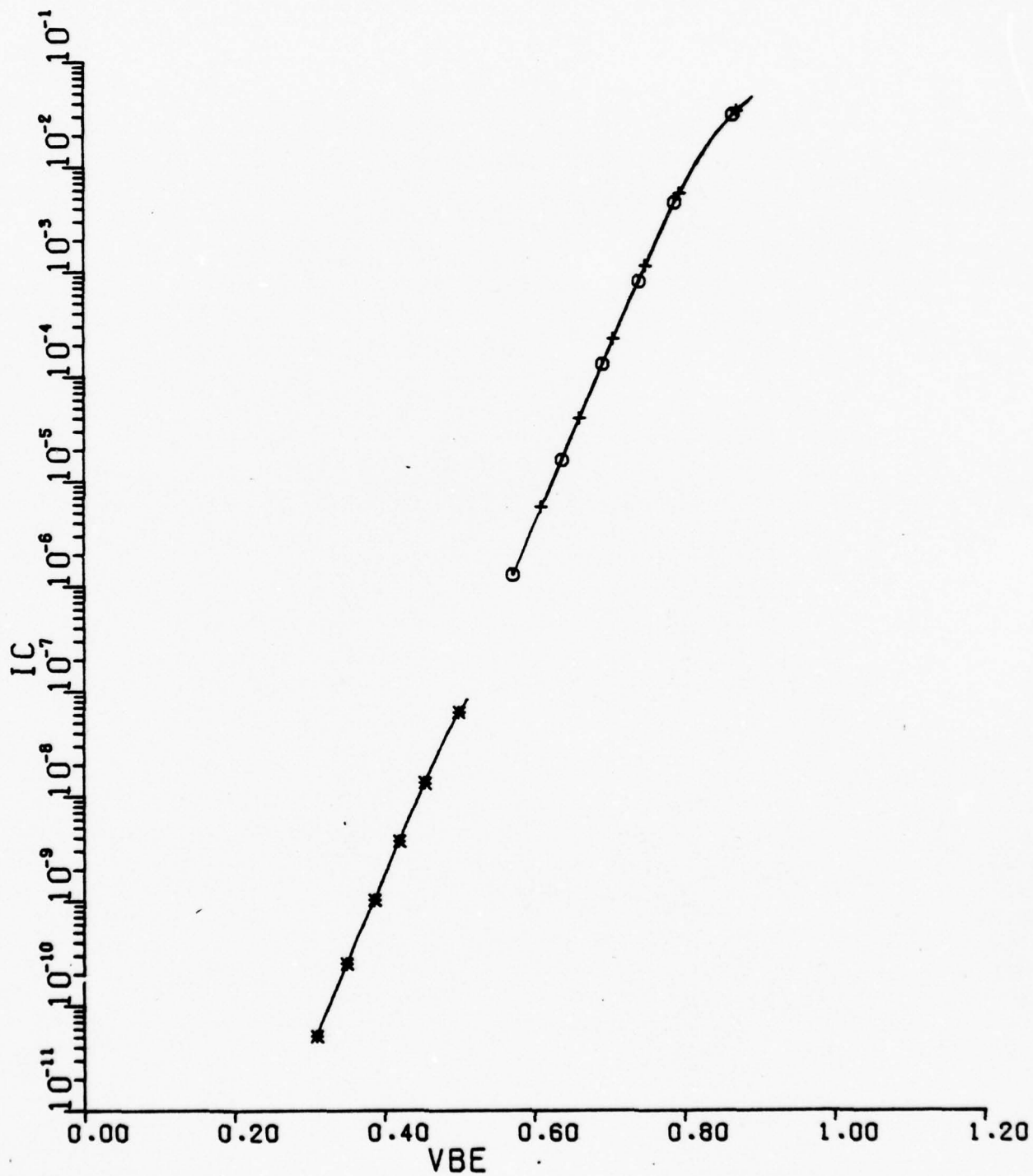
■ --	TO	=	2.000E-12
+ --	TO	=	2.000E-10
0 --	TO	=	2.000E-11



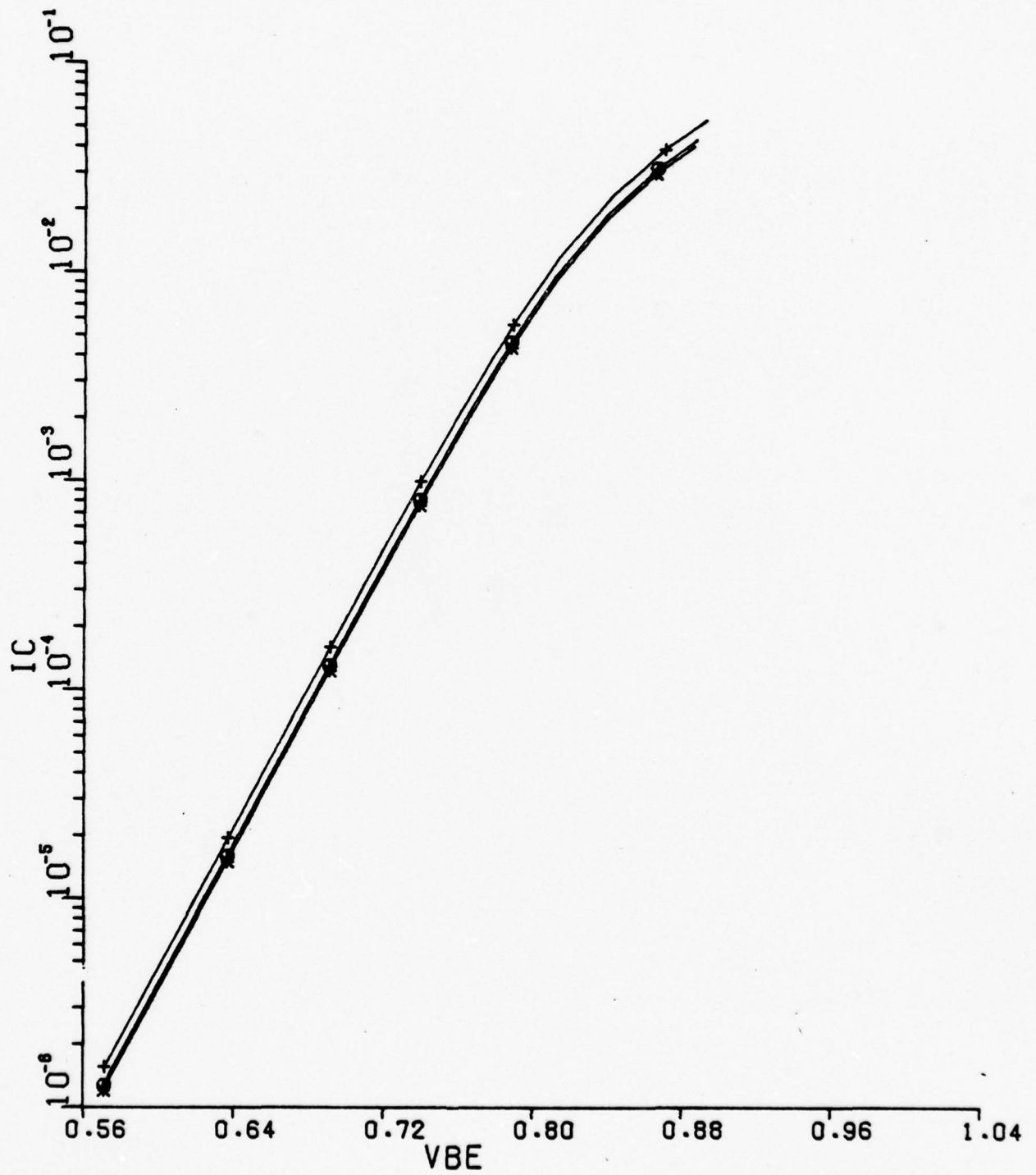
■	--	M	=	1.000E+00
+	--	M	=	1.000E+01
0	--	M	=	2.000E+00



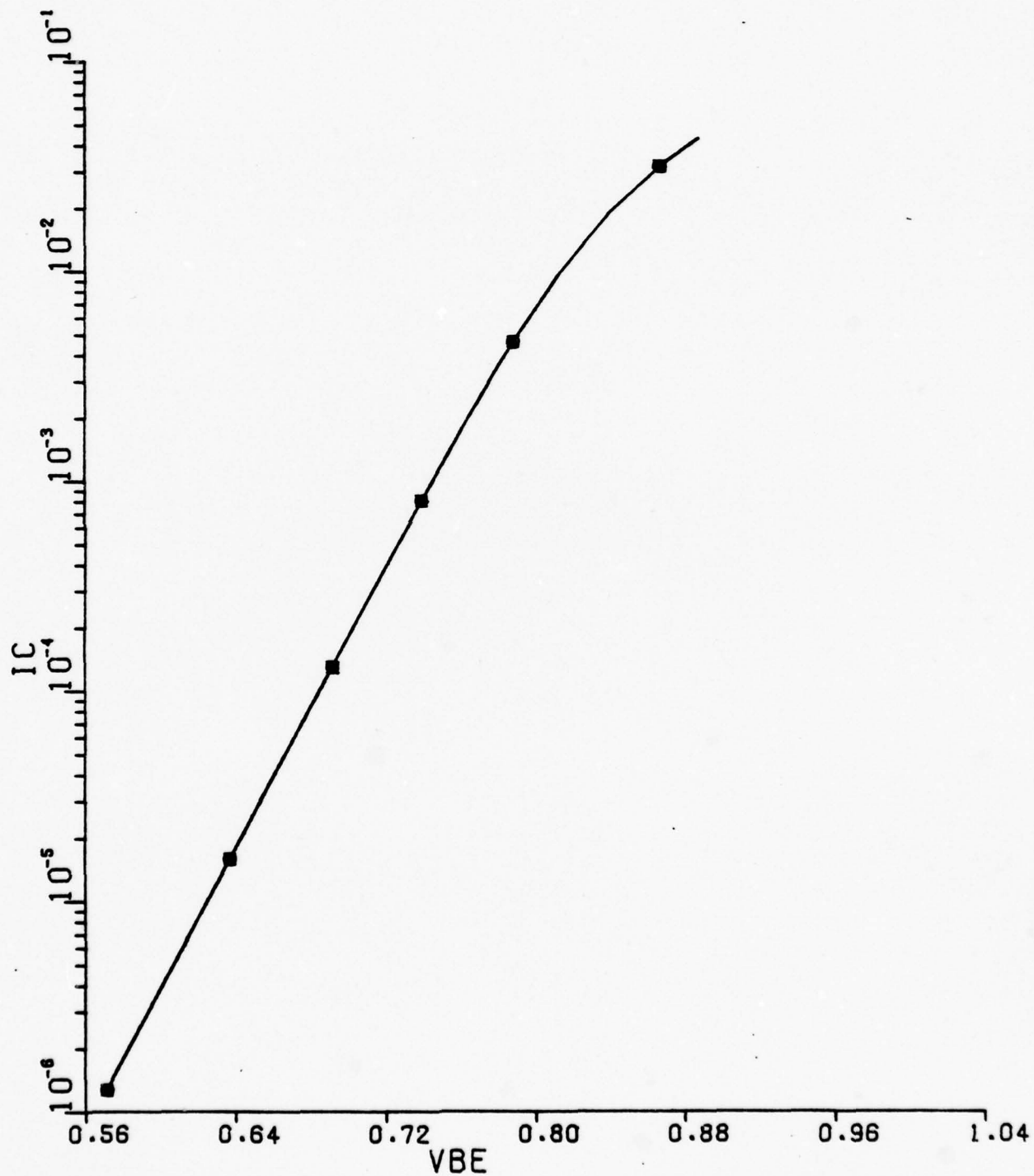
■ --	NE	=	8.000E-01
+ --	NE	=	2.300E+00
o --	NE	=	1.500E+00



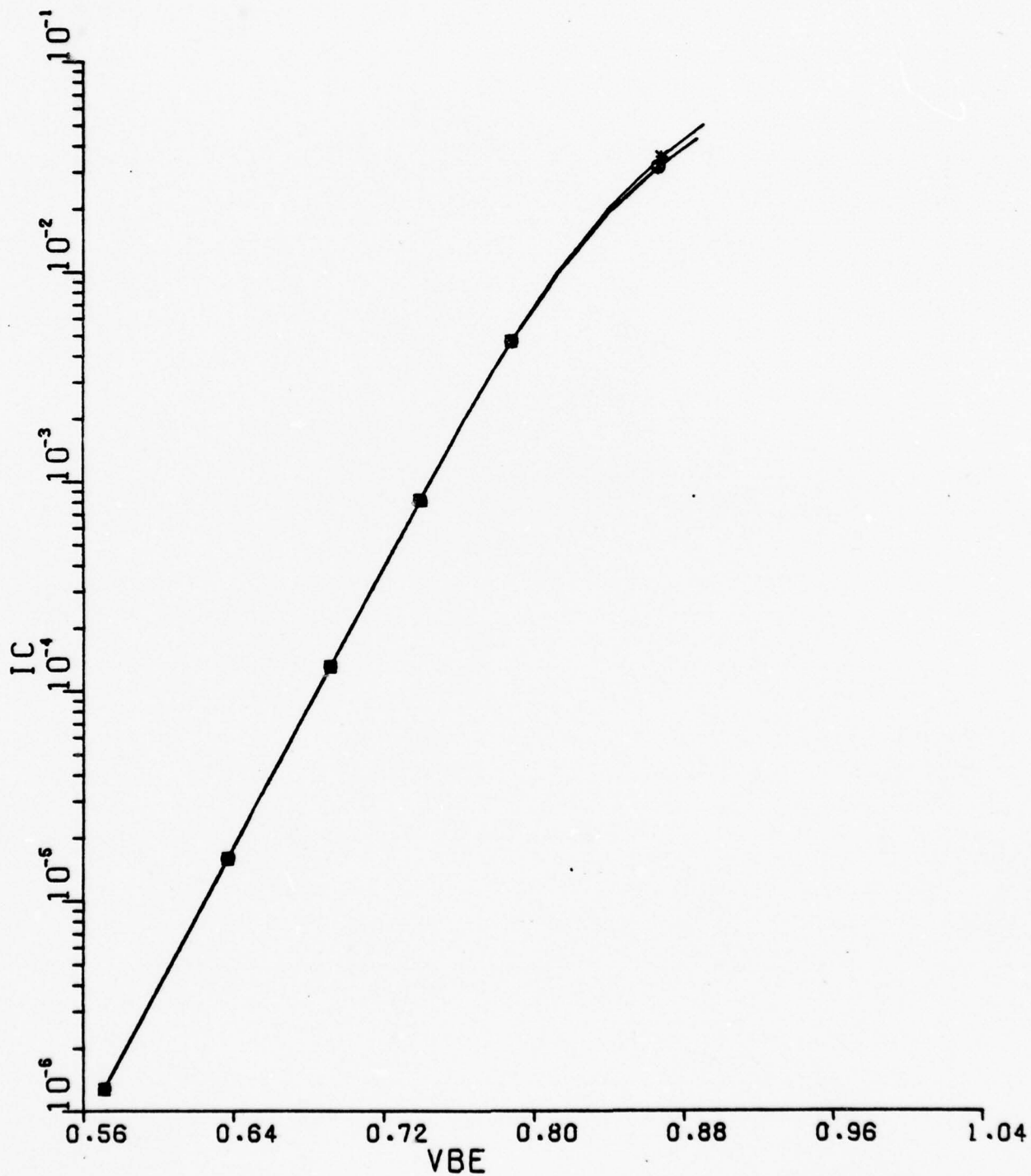
■ --	VCE	=	1.500E+00
+ --	VCE	=	1.500E+01
0 --	VCE	=	5.000E+00



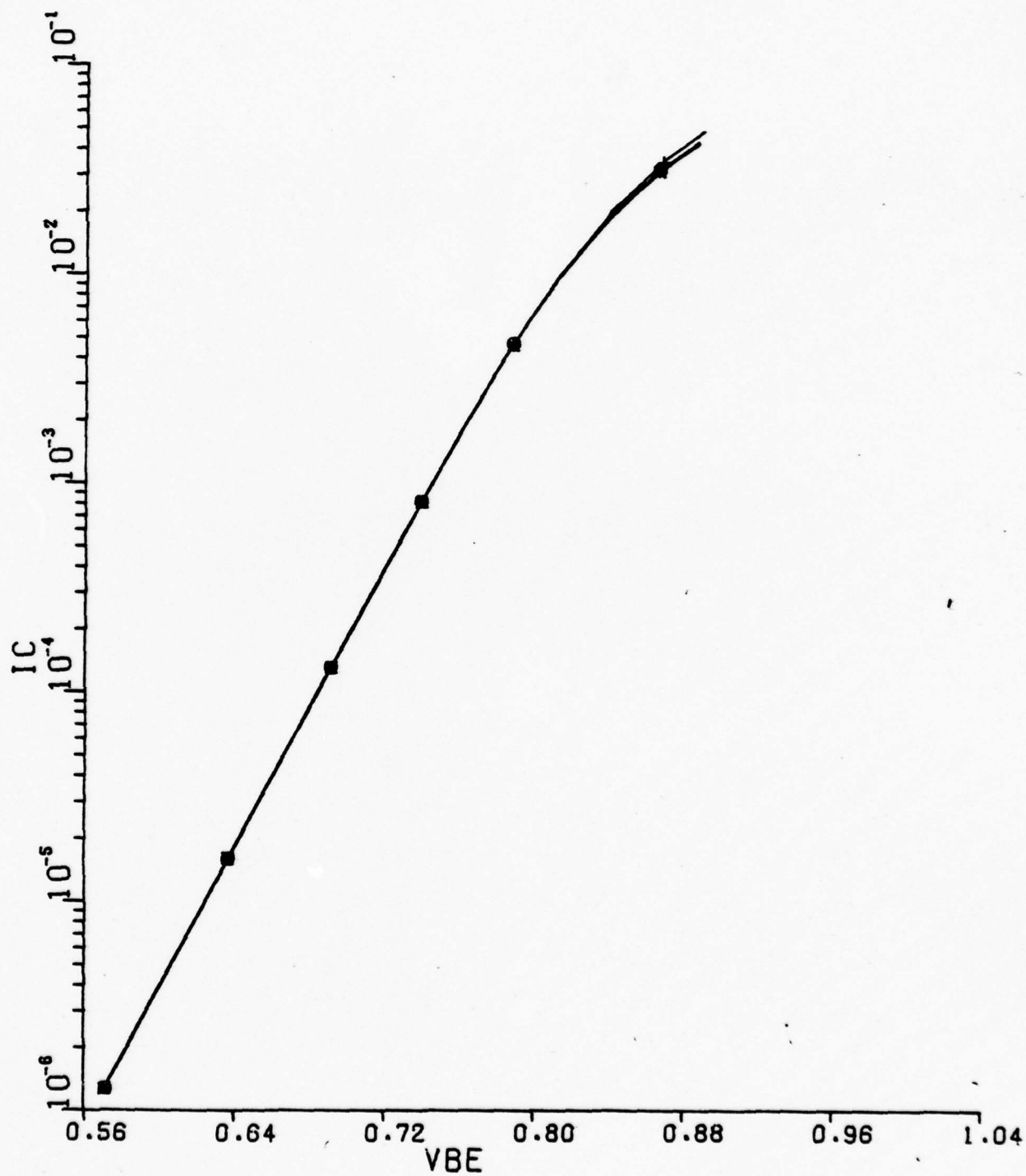
■ --	VB	=	1.500E+01
+ --	VB	=	2.000E+01
0 --	VB	=	1.779E+01



■	--	VF	=	2.590E-01
+	--	VF	=	2.590E-03
0	--	VF	=	2.590E-02

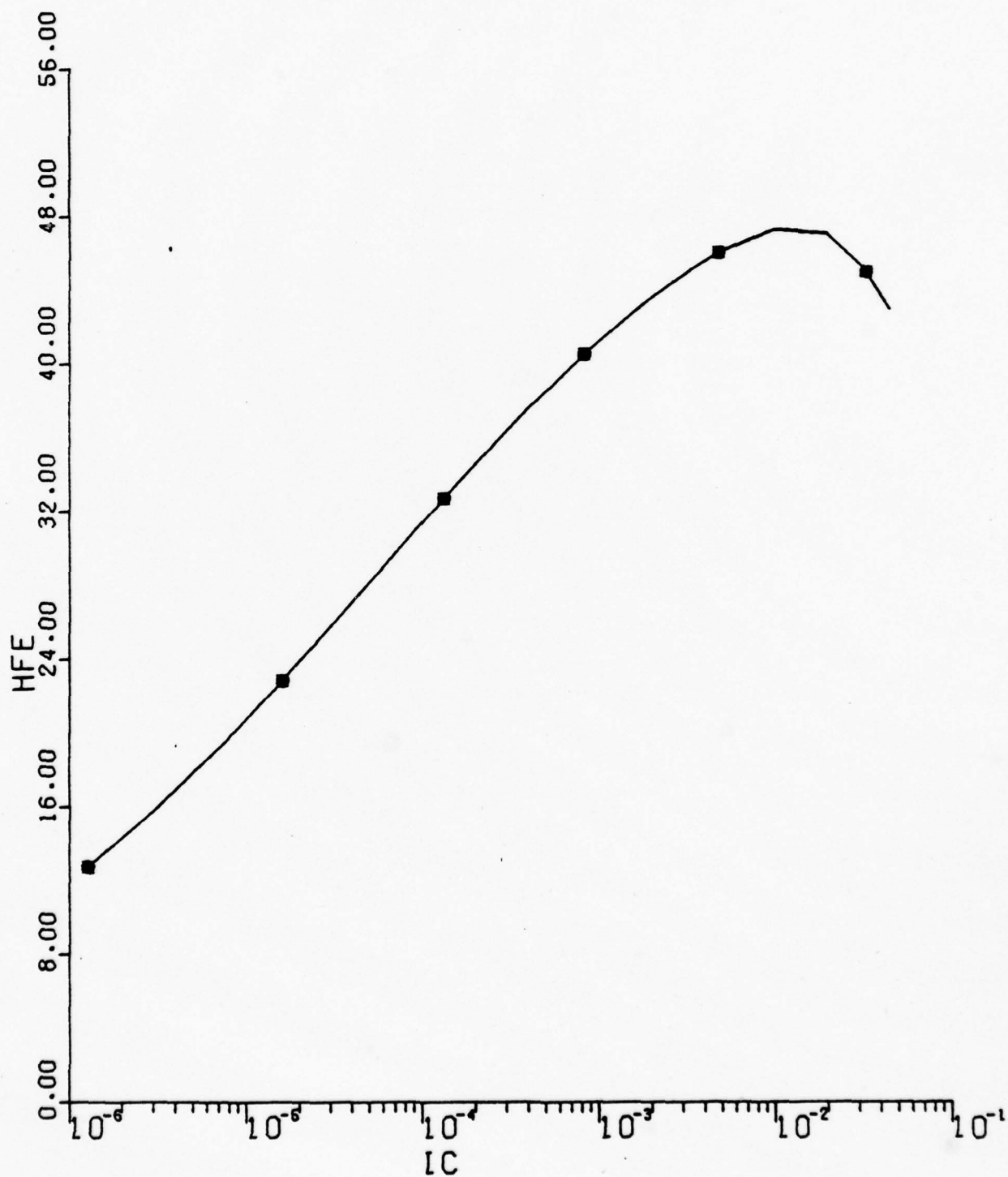


■ --	FF	=	1.336E-13
+ --	FF	=	1.336E-15
○ --	FF	=	1.336E-14

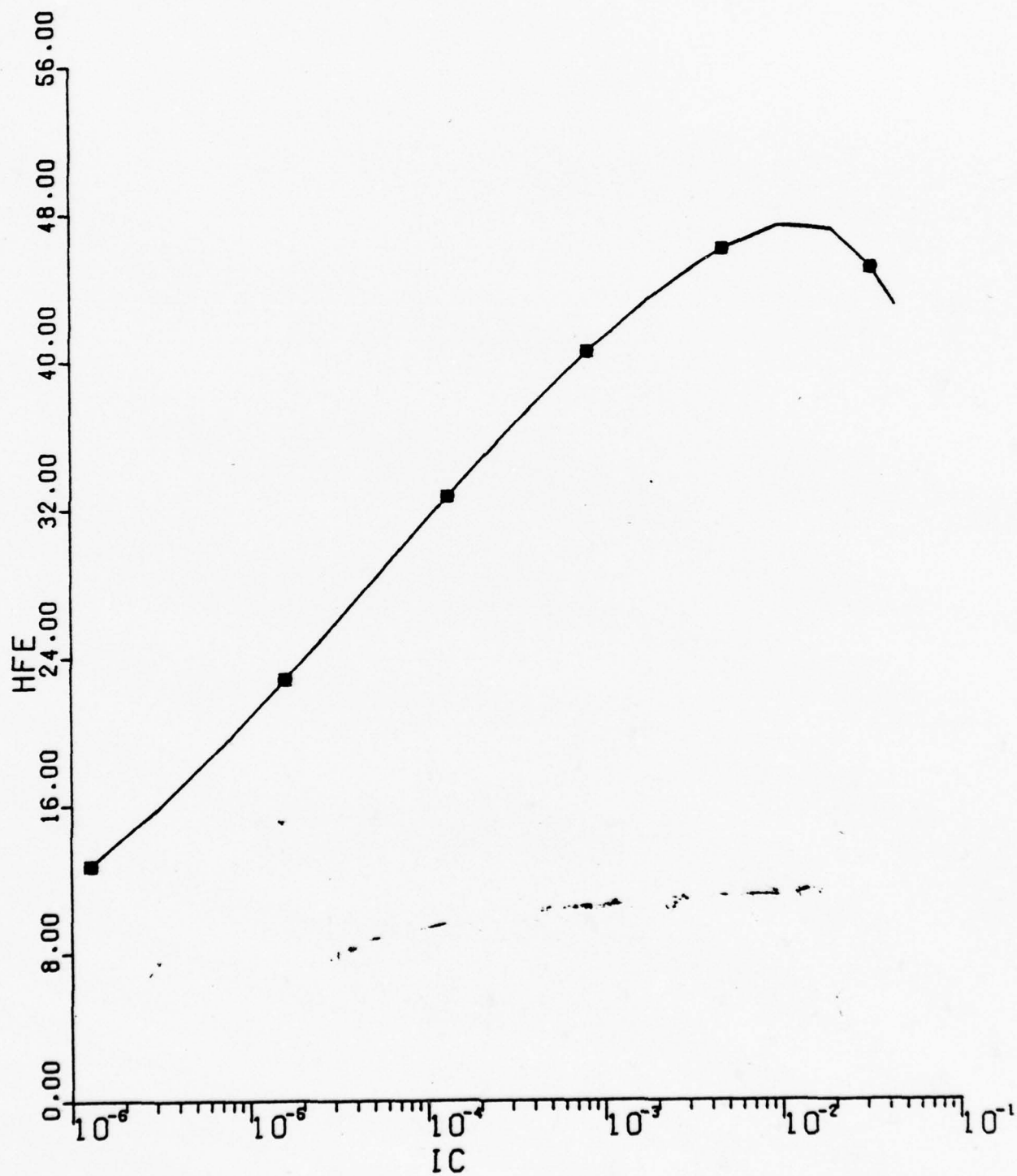


B.3 HFE vs. I_c Curves

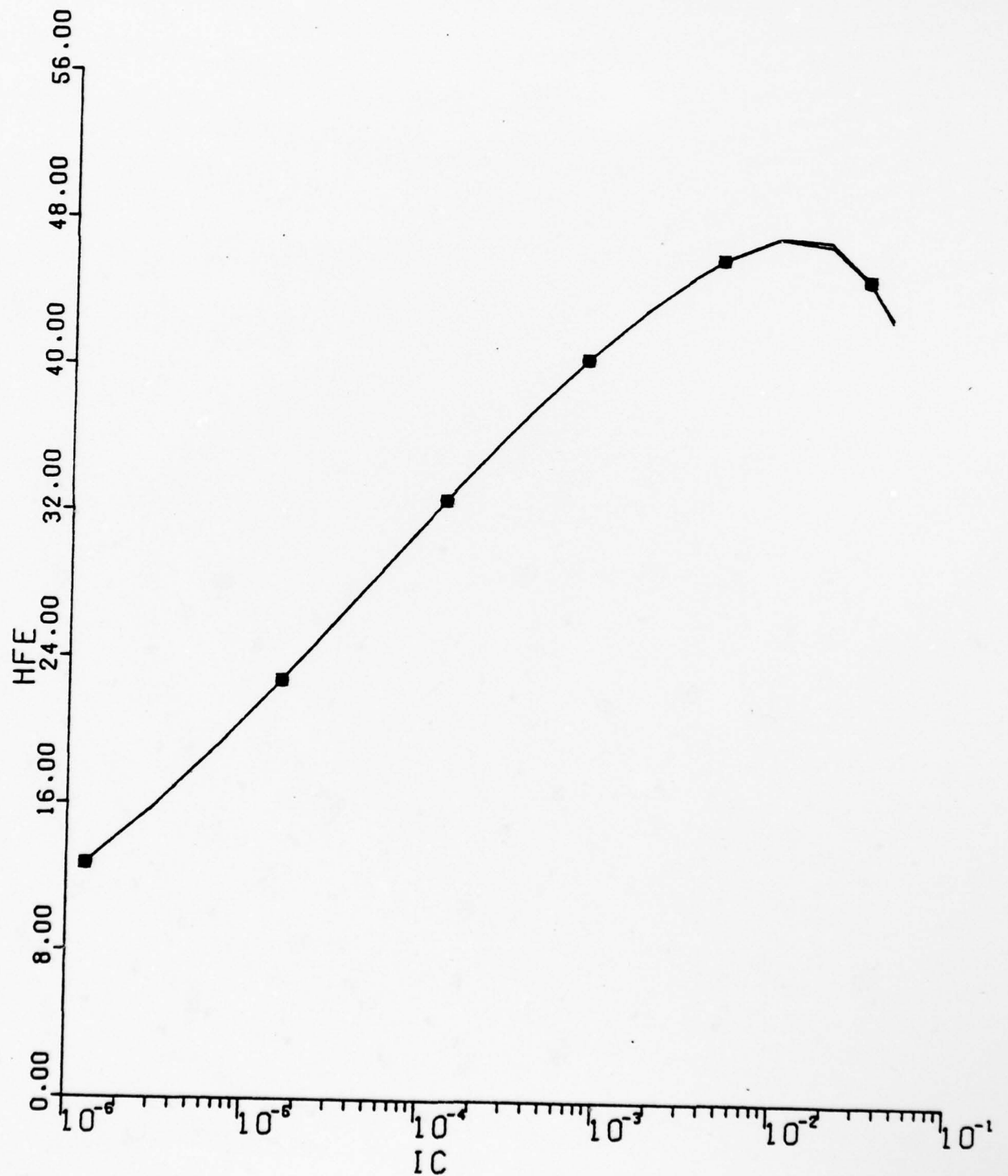
■ --	RB0	=	9.000E+01
+ --	RB0	=	9.000E-01
0 --	RB0	=	9.000E+00



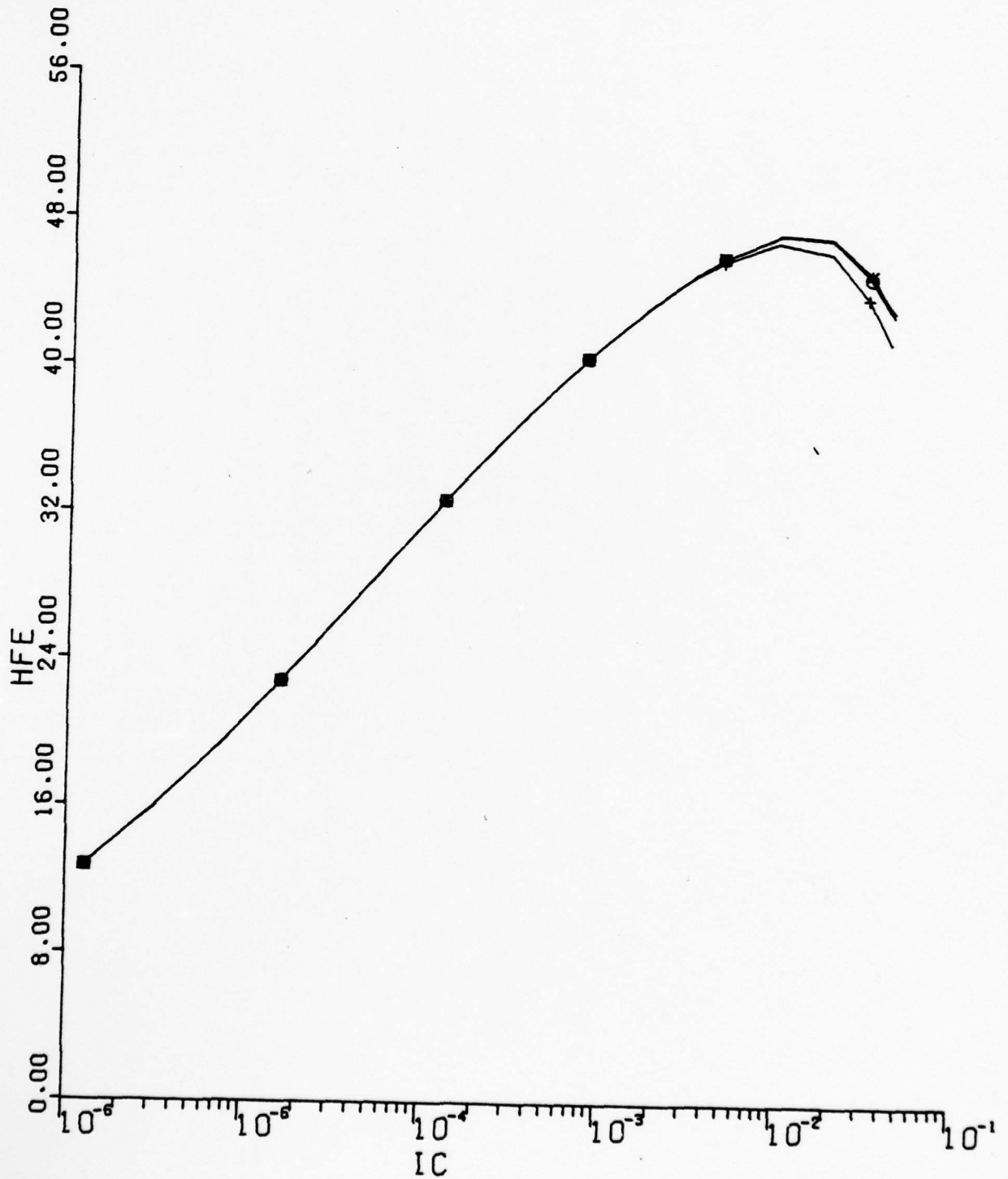
■	--	RBB	=	1.500E+01
+	--	RBB	=	5.000E+02
0	--	RBB	=	1.500E+02



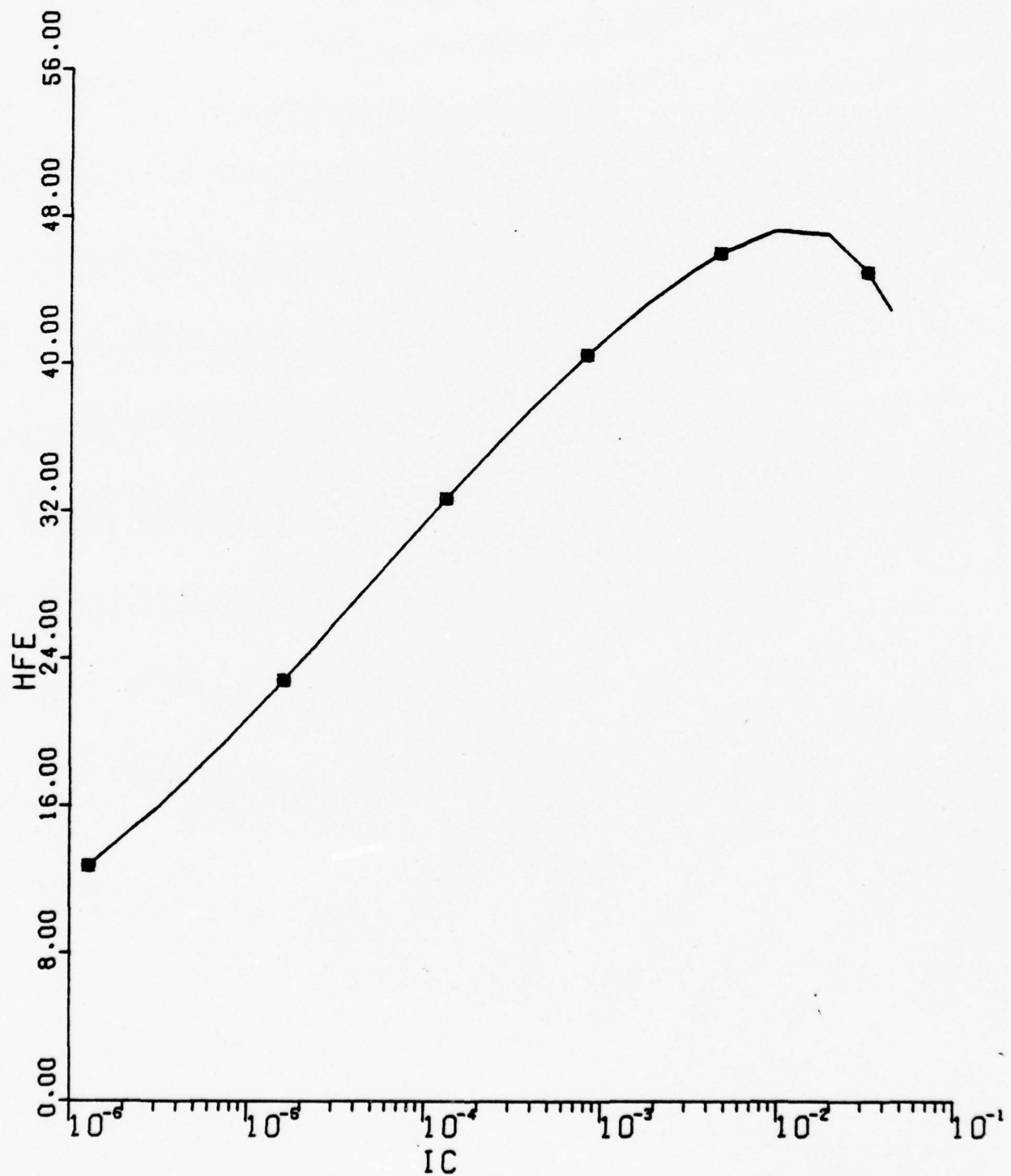
■ --	RE	=	1.000E-02
+ --	RE	=	5.000E+00
0 --	RE	=	5.000E-01



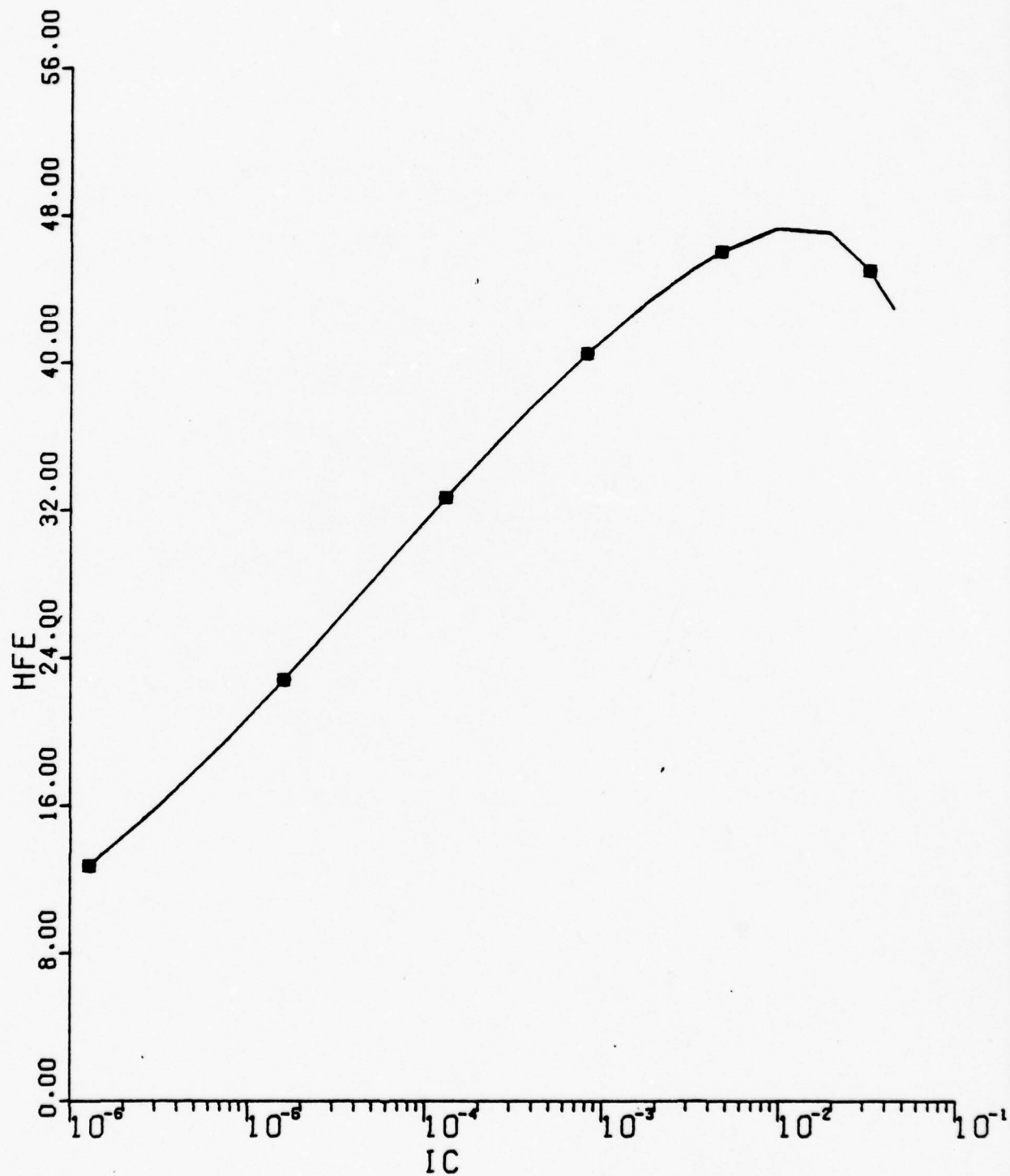
■ --	RC0	=	1.000E+00
+ --	RC0	=	5.000E+01
0 --	RC0	=	5.000E+00



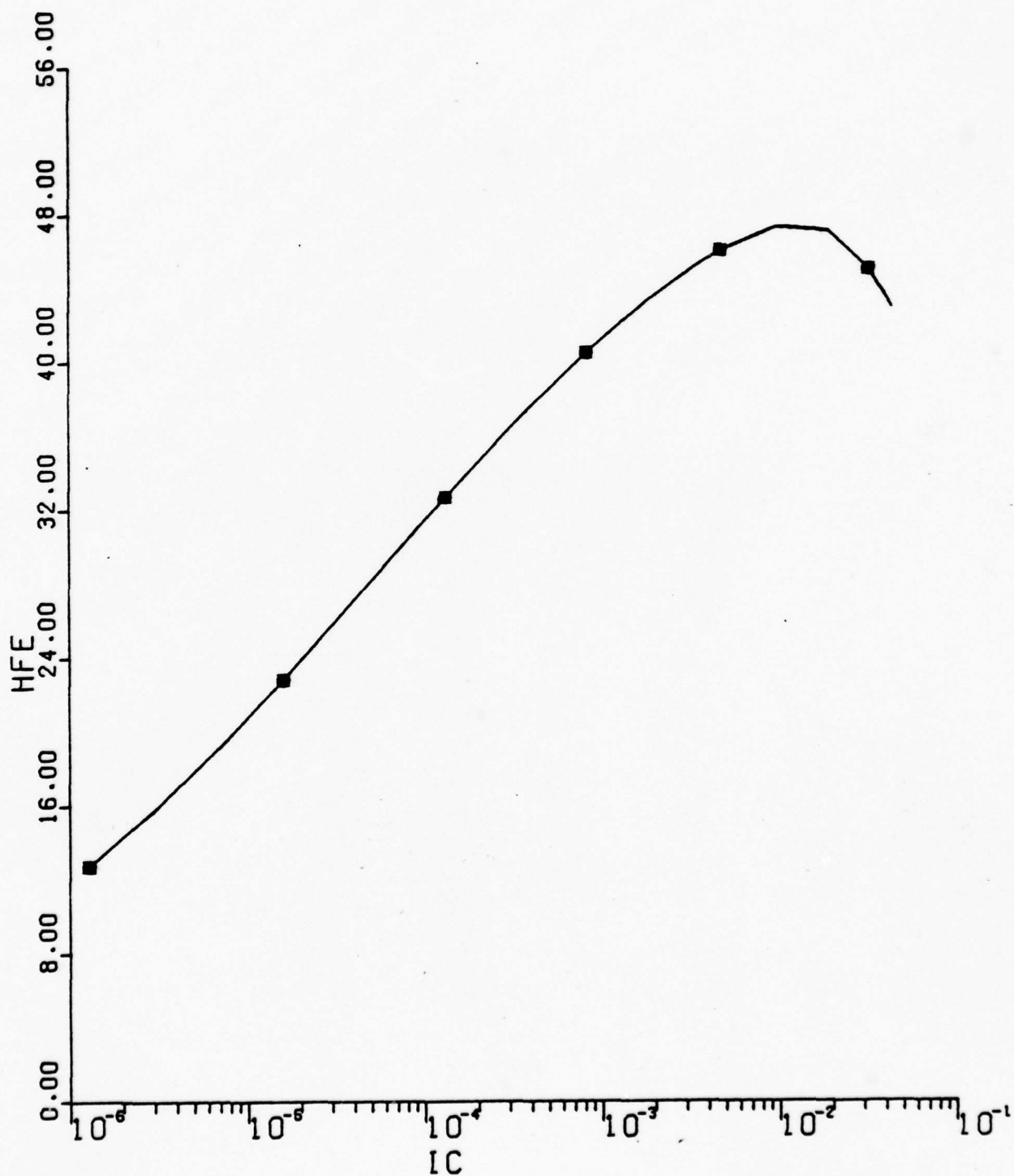
■ --	PC	=	1.000E-04
+ --	PC	=	1.000E-03
0 --	PC	=	3.250E-03



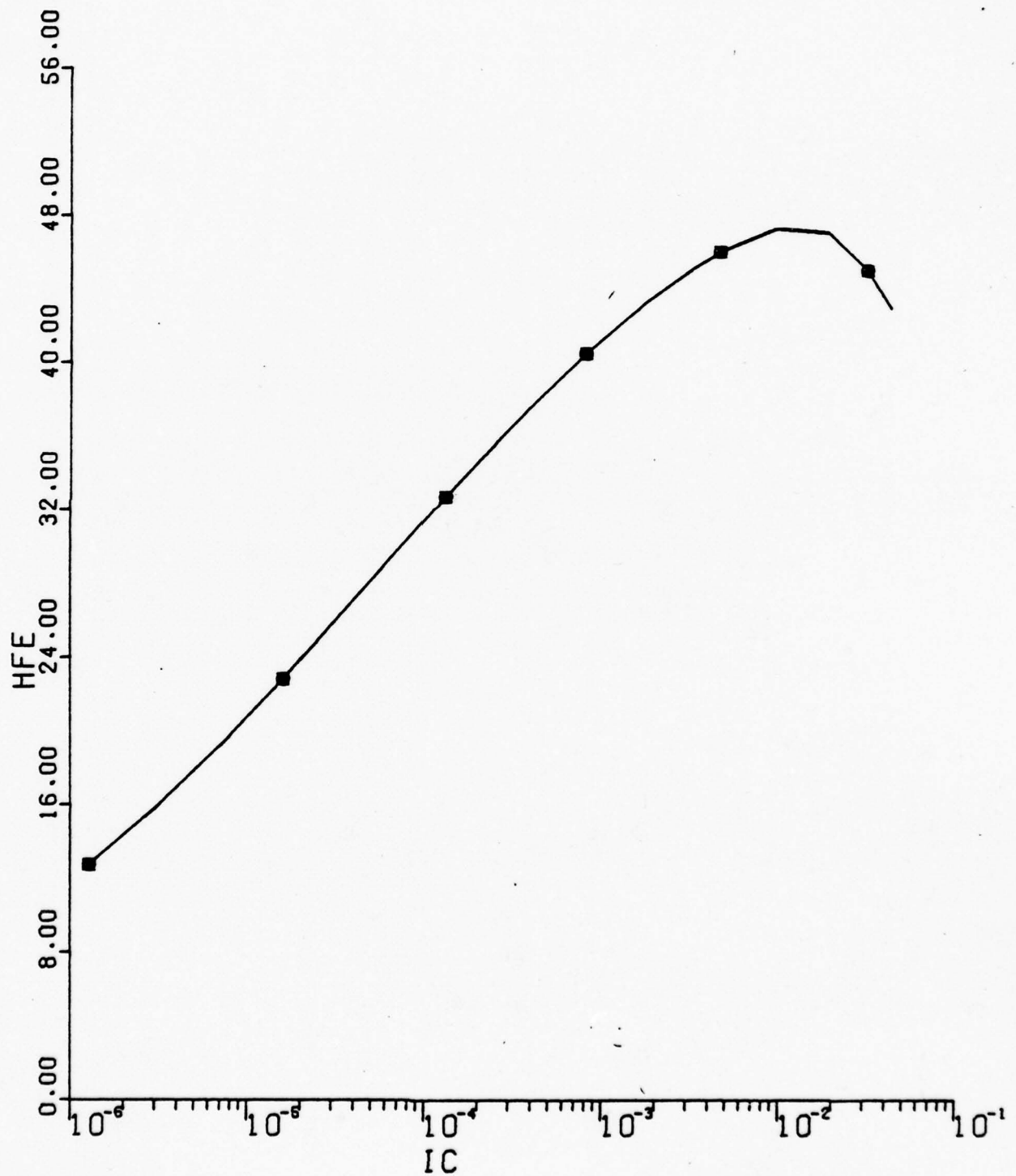
■	--	BS	=	2.500E-01
+	--	BS	=	5.000E-01
0	--	BS	=	3.333E-01



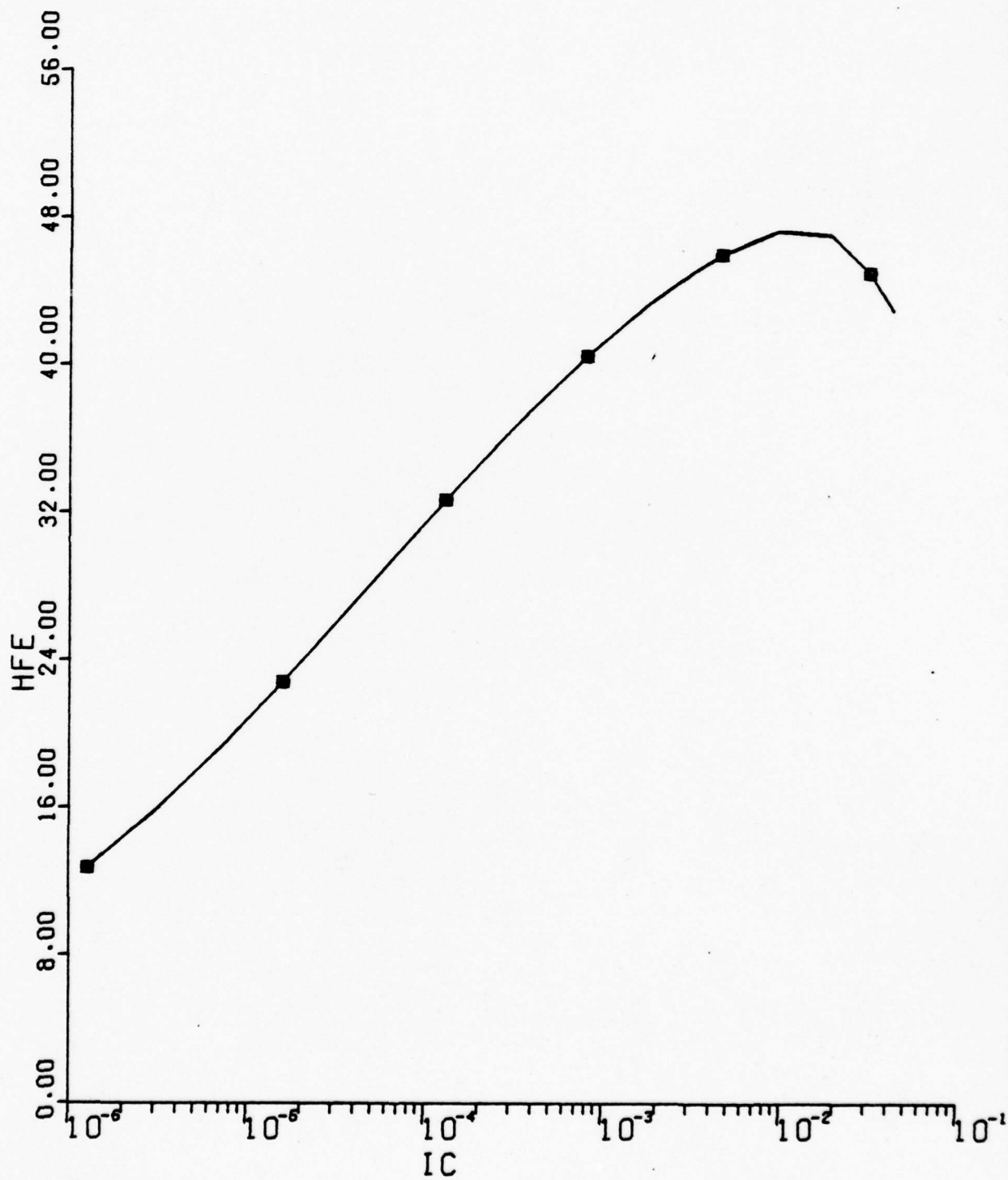
■ --	BC	=	2.500E-01
+ --	BC	=	5.000E-01
0 --	BC	=	3.333E-01



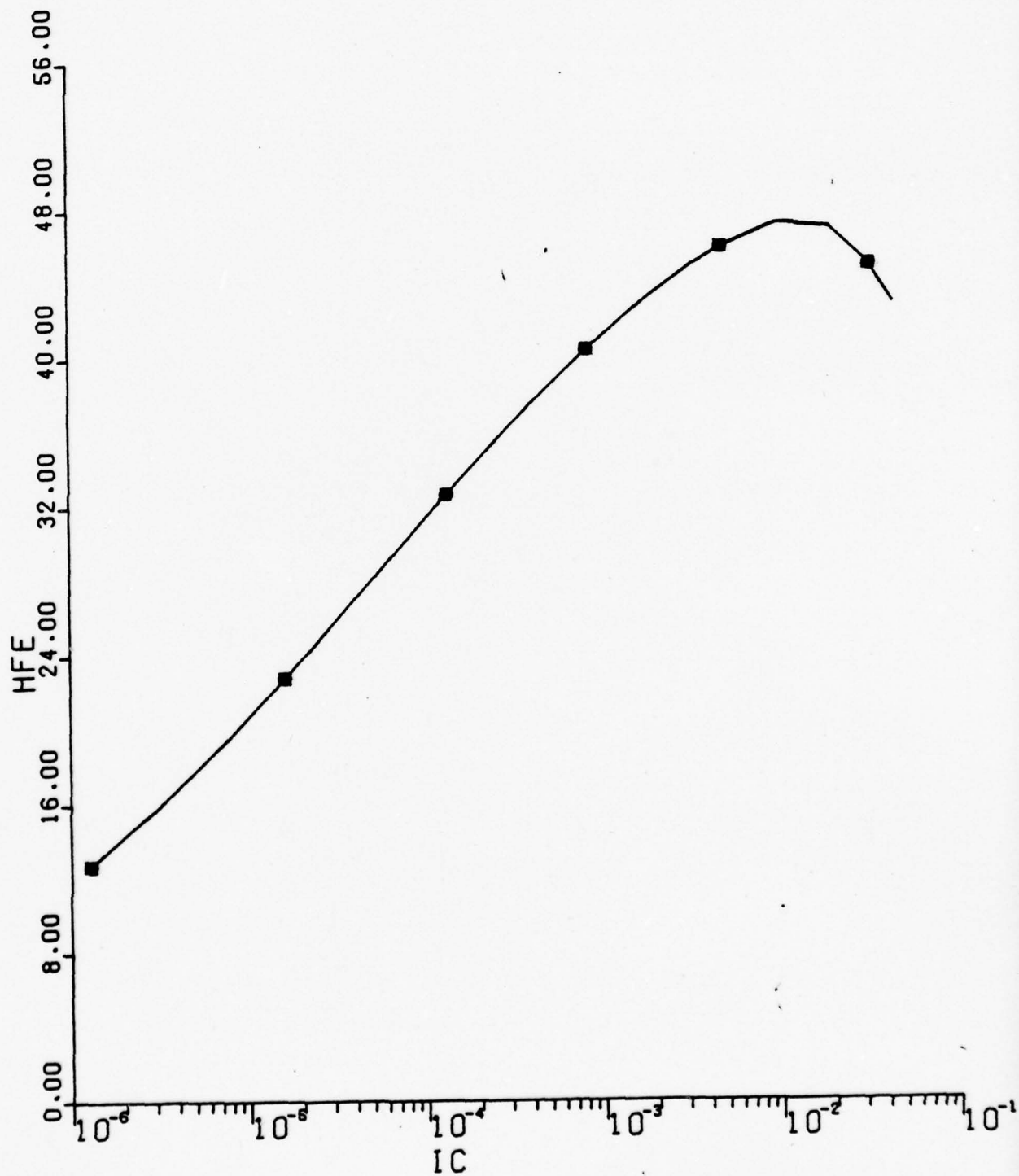
■ --	BE	=	2.500E-01
+ --	BE	=	3.333E-01
0 --	BE	=	5.000E-01



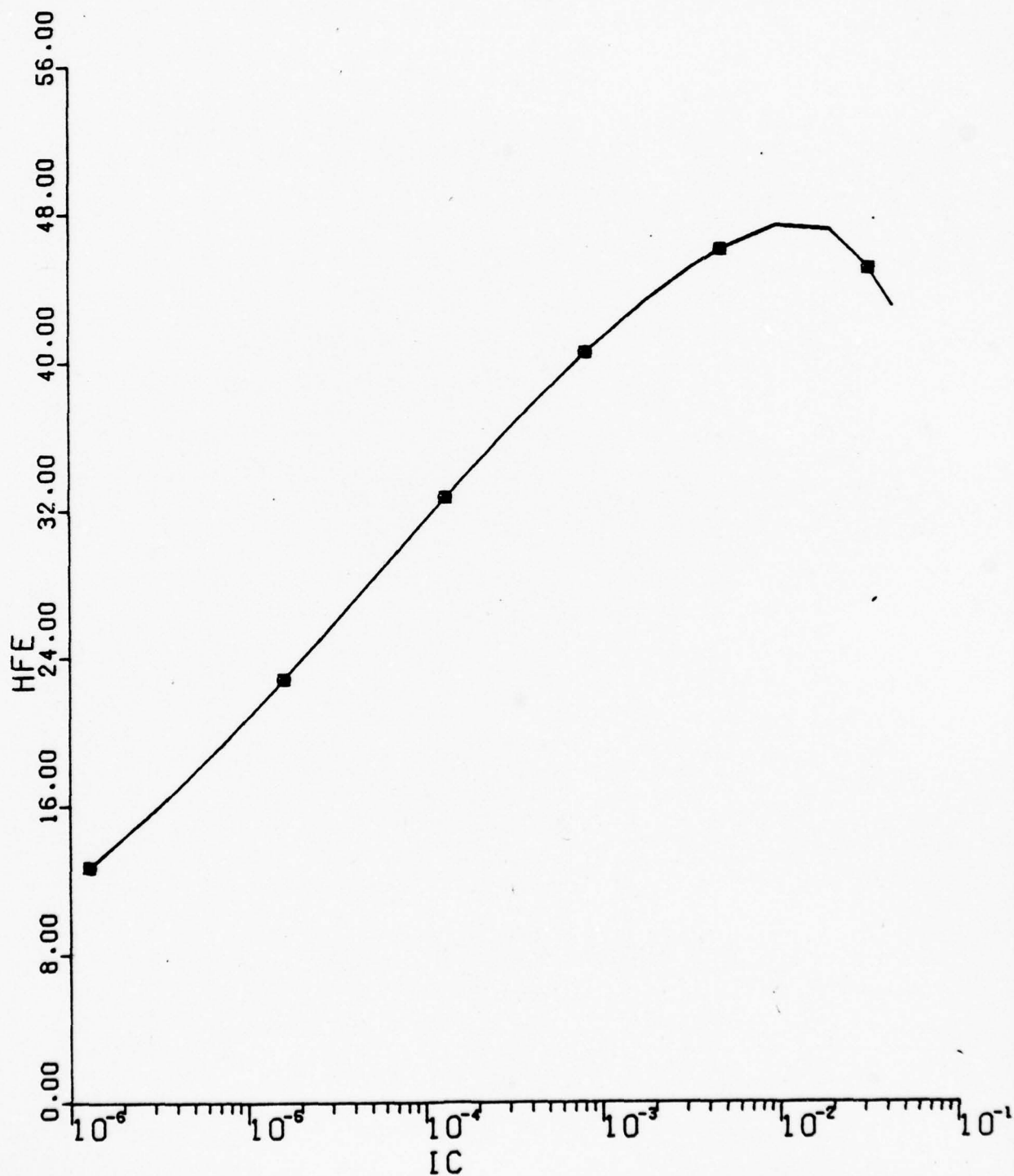
■ --	CS0	=	4.000E-13
+ --	CS0	=	1.000E-11
0 --	CS0	=	2.000E-12



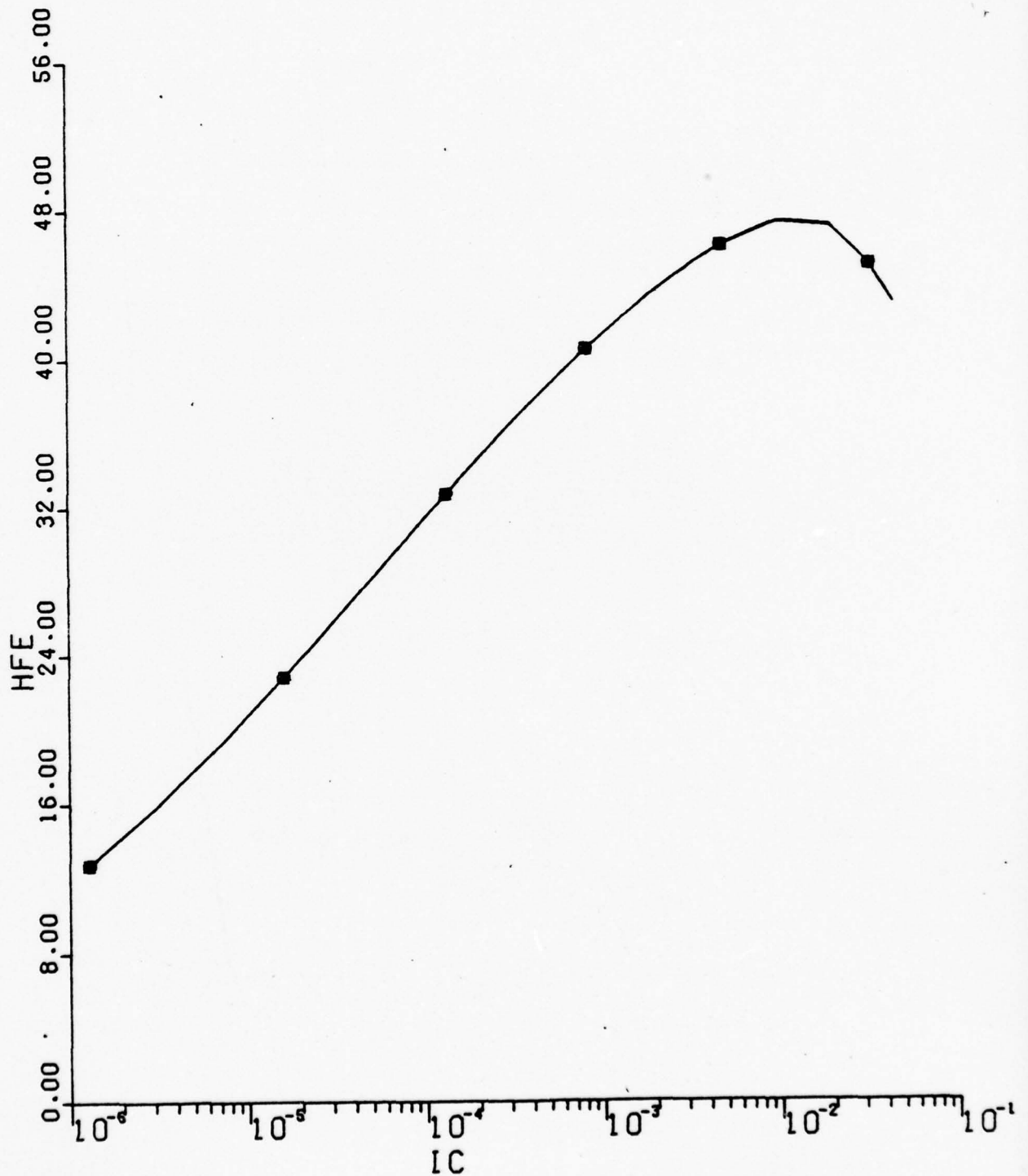
■ --	CEO	=	4.000E-13
+ --	CEO	=	1.000E-11
0 --	CEO	=	9.000E-13



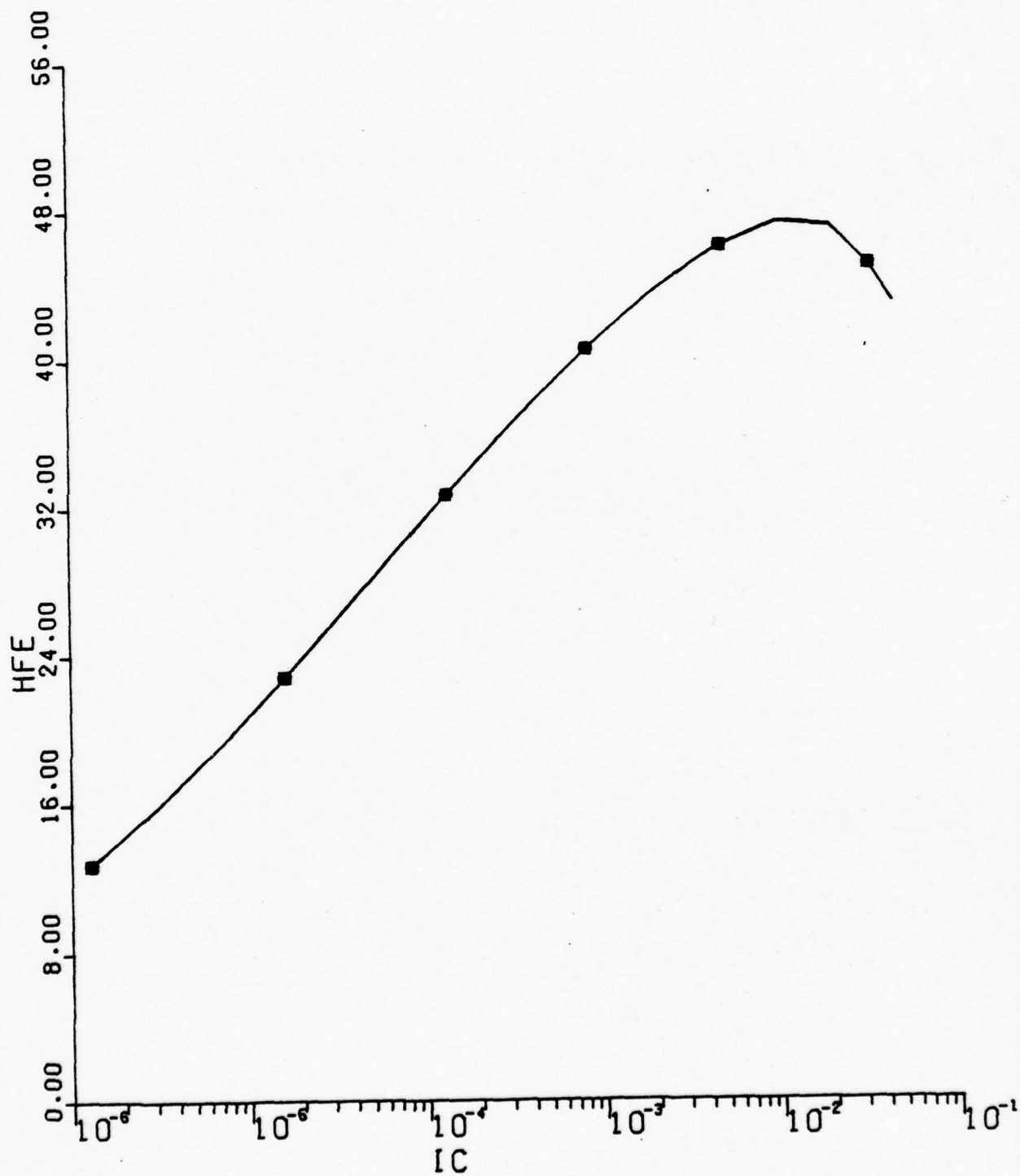
■	--	CC0	=	4.000E-13
+	--	CC0	=	1.000E-10
0	--	CC0	=	8.000E-13



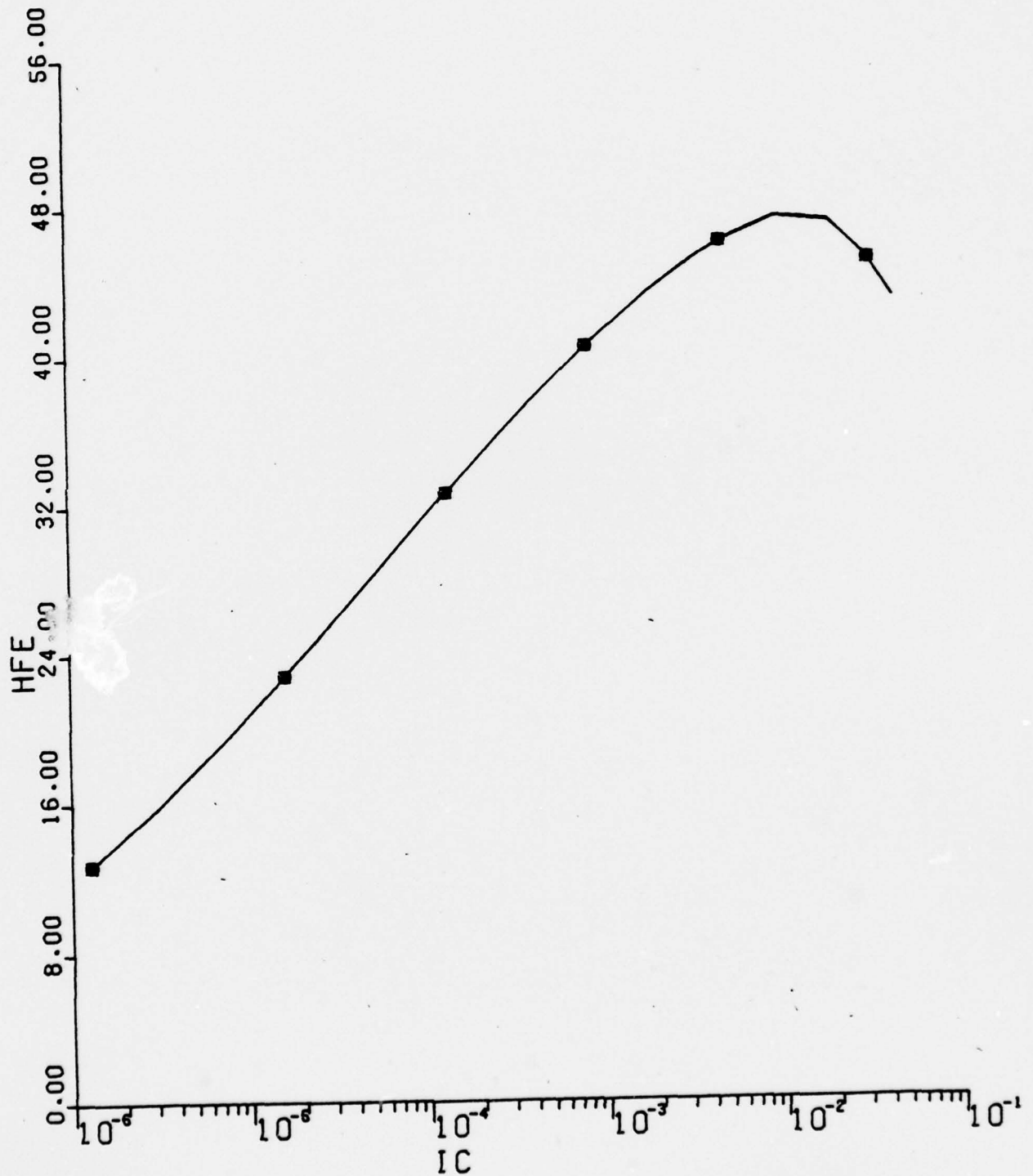
■ --	PHISS	=	5.000E-01
+ --	PHISS	=	1.200E+00
0 --	PHISS	=	9.000E-01



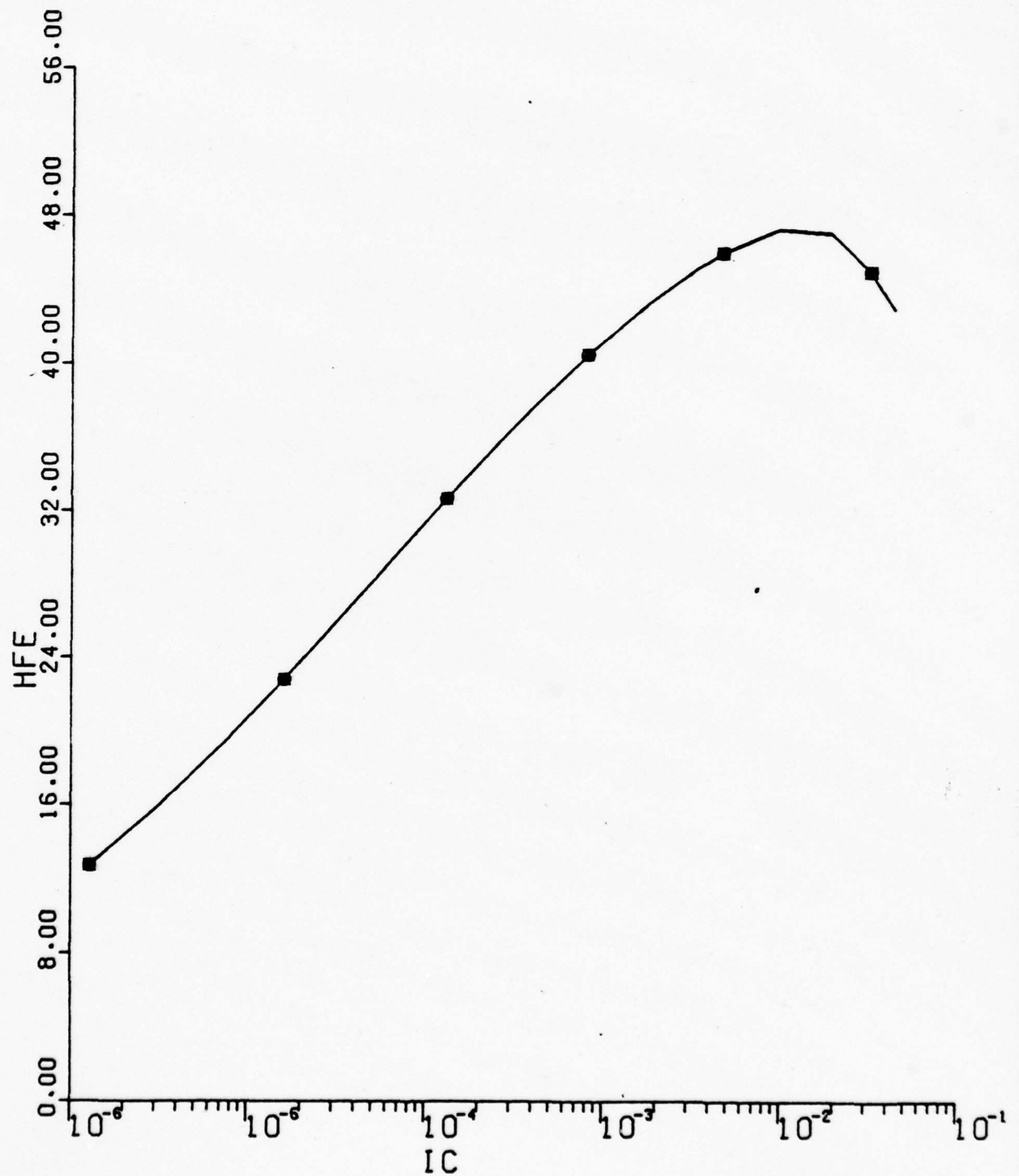
■ --	PHICO	=	5.000E-01
+ --	PHICO	=	1.200E+00
0 --	PHICO	=	9.000E-01



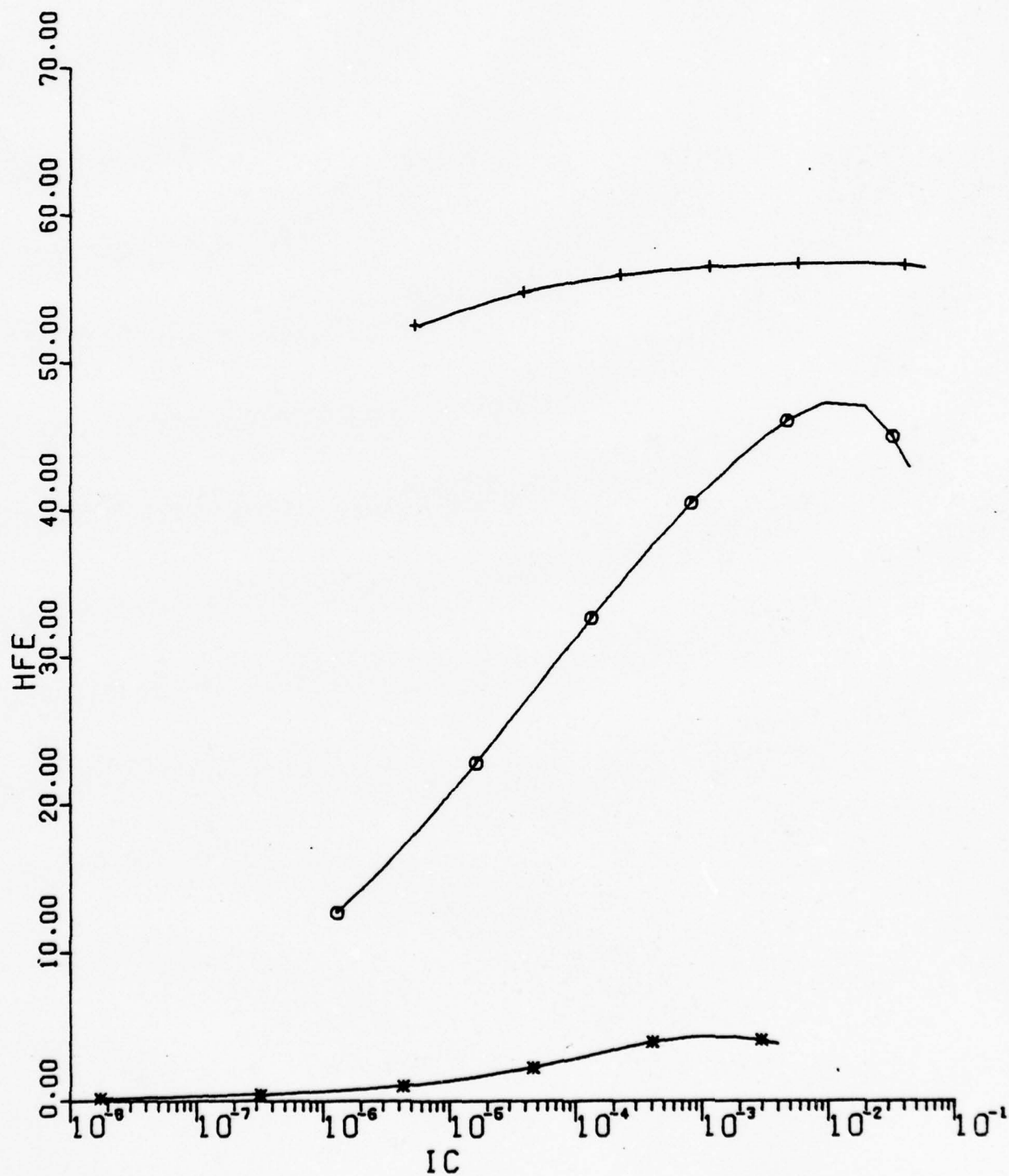
■ --	PHIE0	=	5.000E-01
+ --	PHIE0	=	1.500E+00
0 --	PHIE0	=	1.200E+00



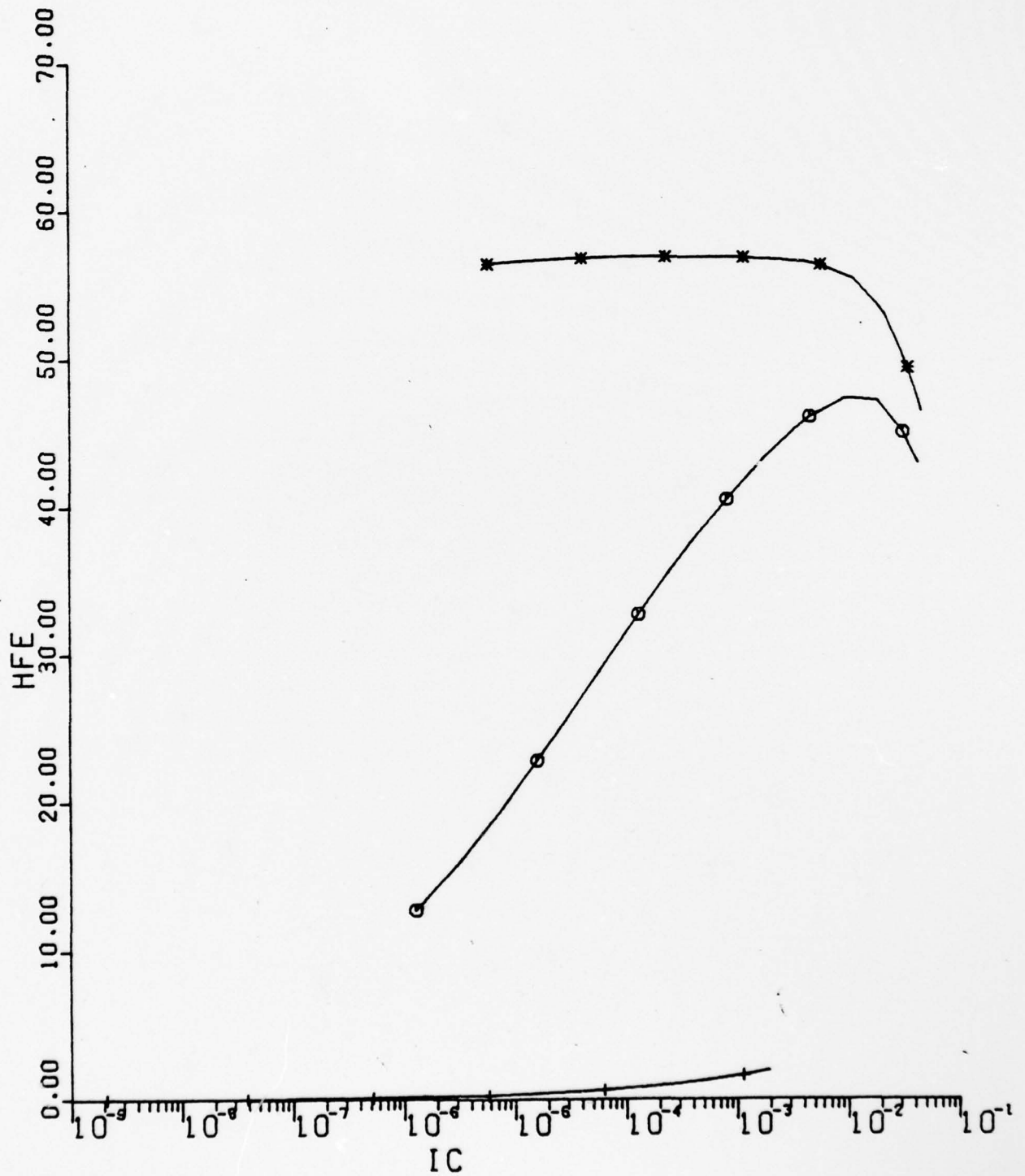
■ --	ISR	=	3.000E-13
+ --	ISR	=	3.000E-11
0 --	ISR	=	3.000E-12



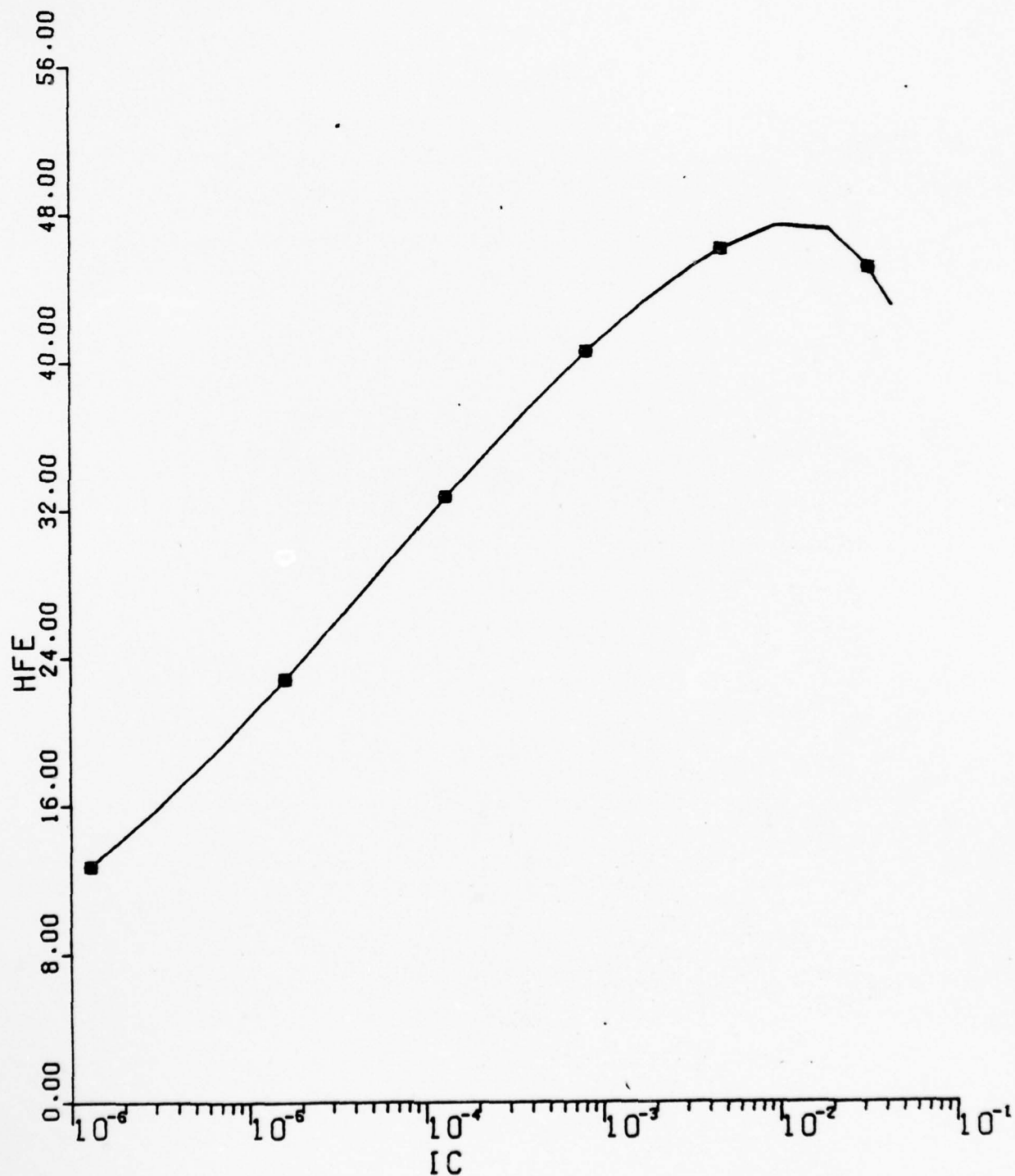
* --	IS	=	3.000E-18
+ --	IS	=	3.000E-14
o --	IS	=	3.200E-16



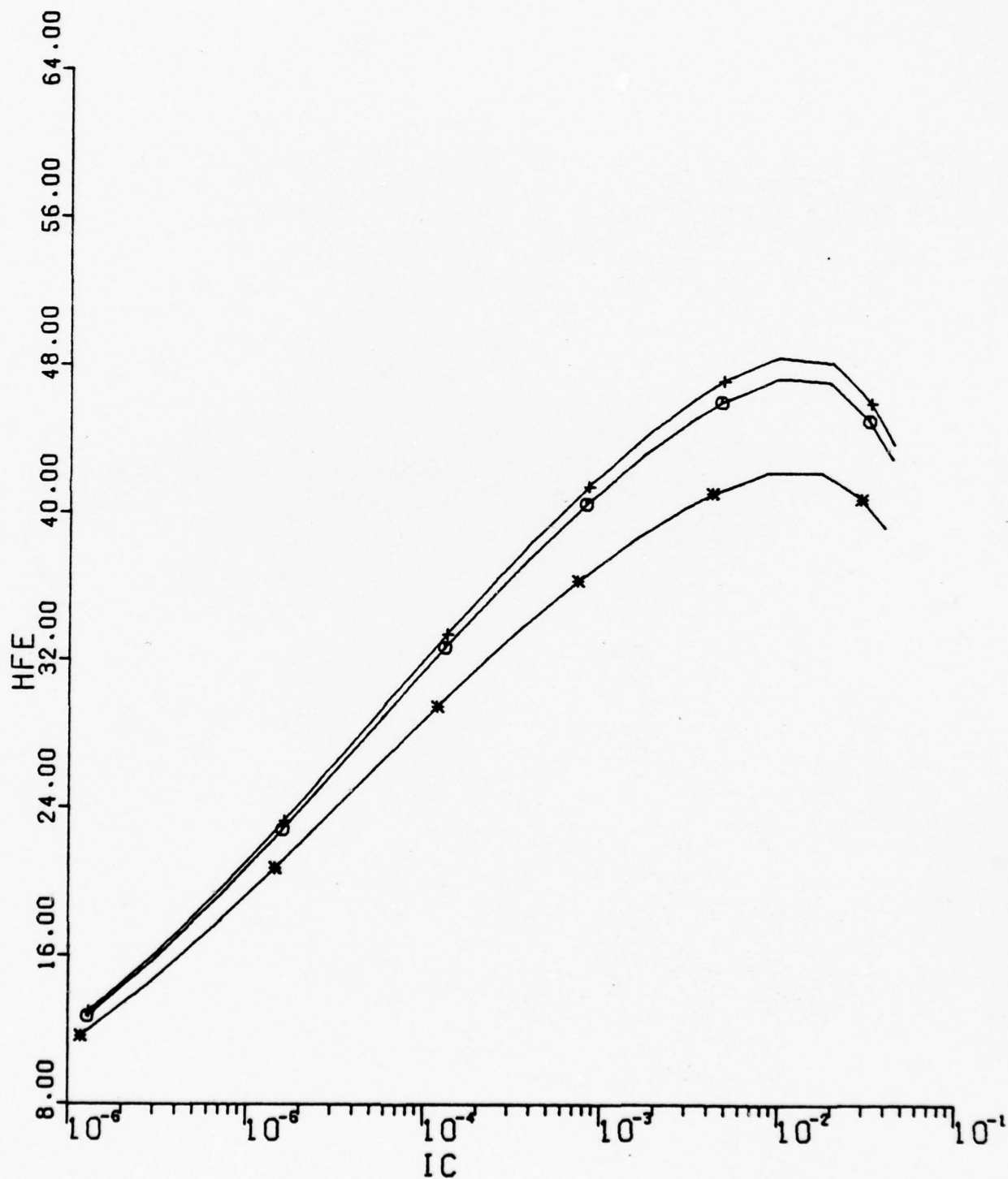
* --	IER	=	3.000E-16
+ --	IER	=	3.000E-12
o --	IER	=	3.200E-14

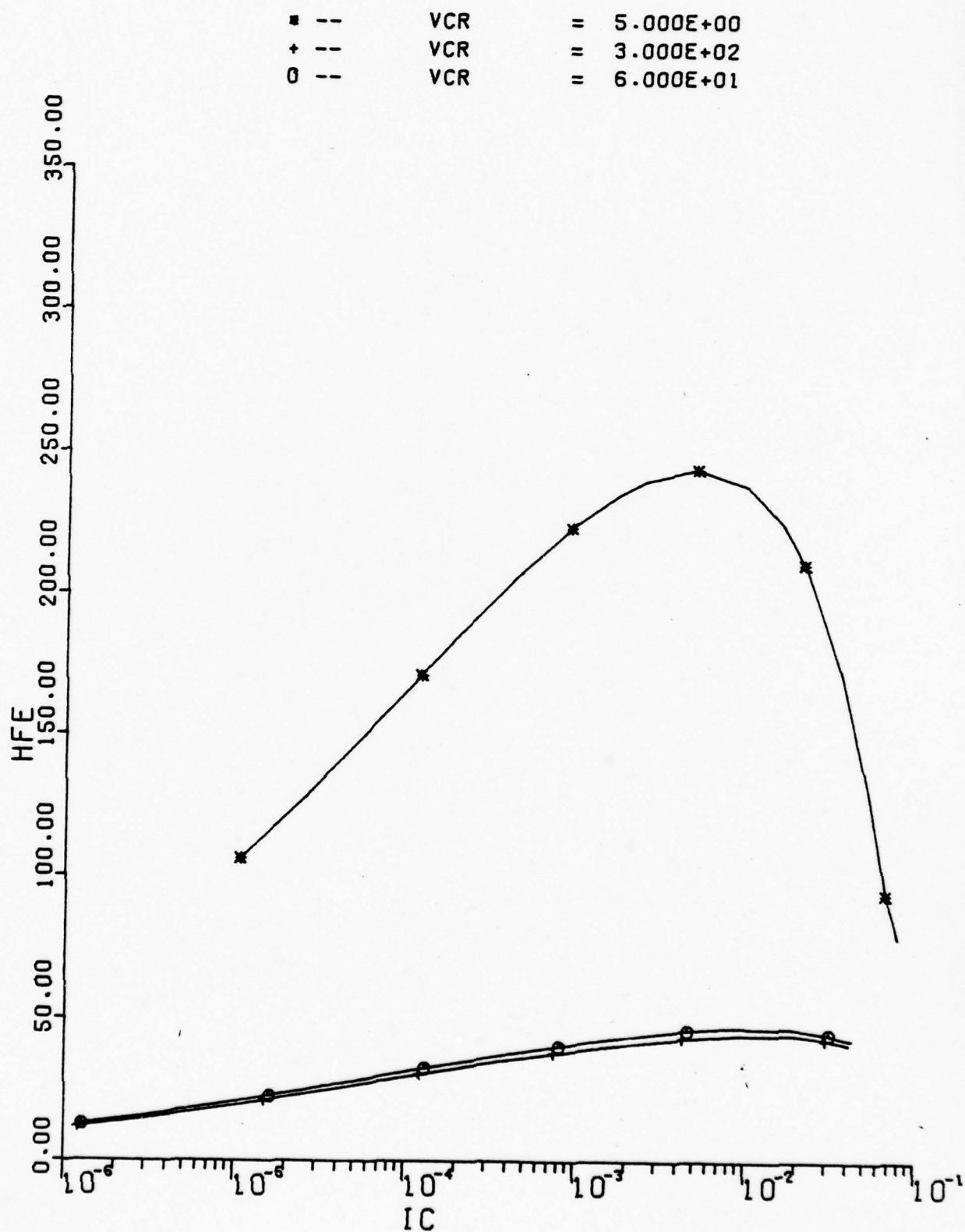


■ --	IBR	=	3.000E-15
+ --	IBR	=	3.000E-11
0 --	IBR	=	3.000E-13

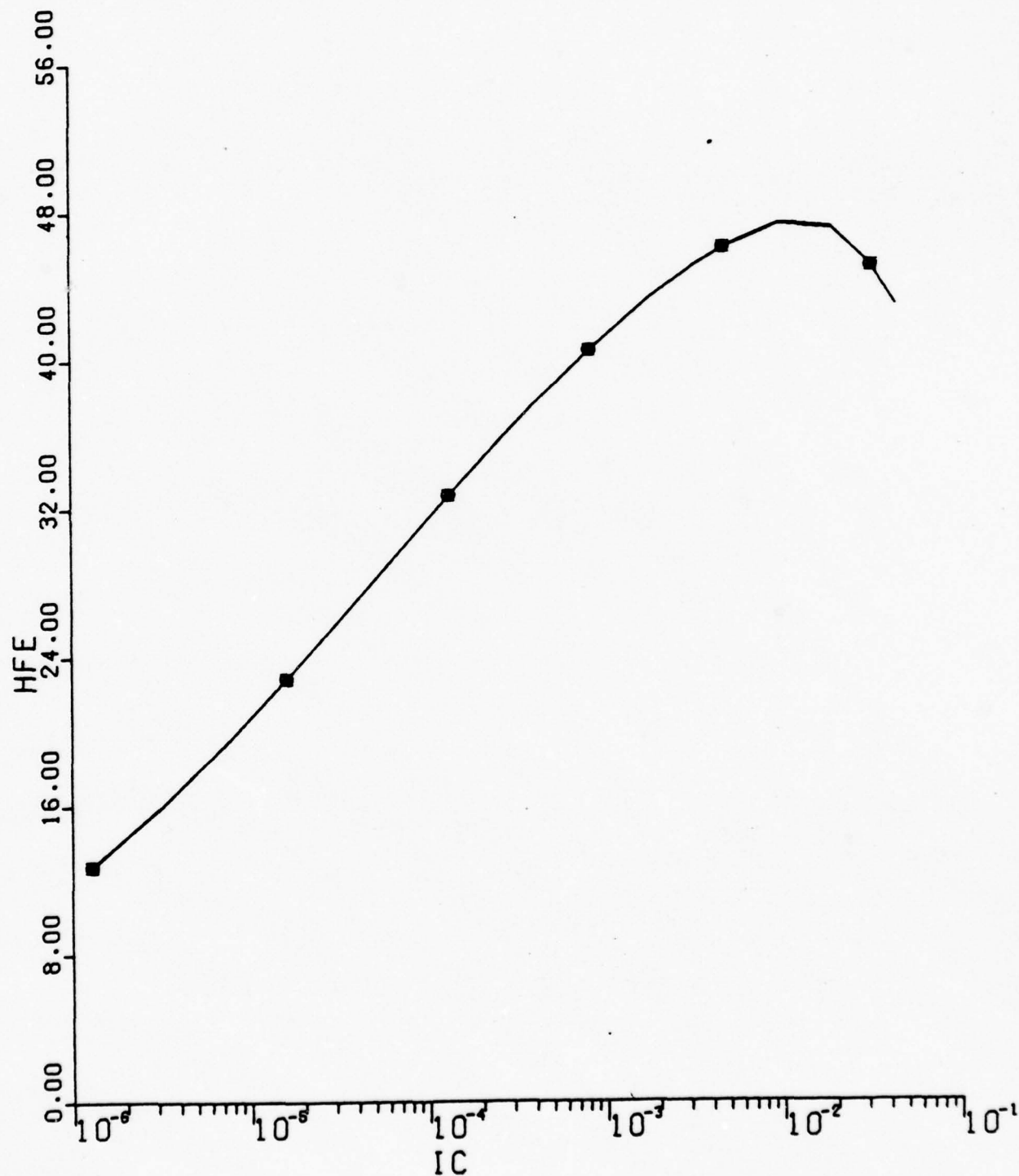


* --	VER	=	5.000E+00
+ --	VER	=	5.000E+01
o --	VER	=	2.000E+01

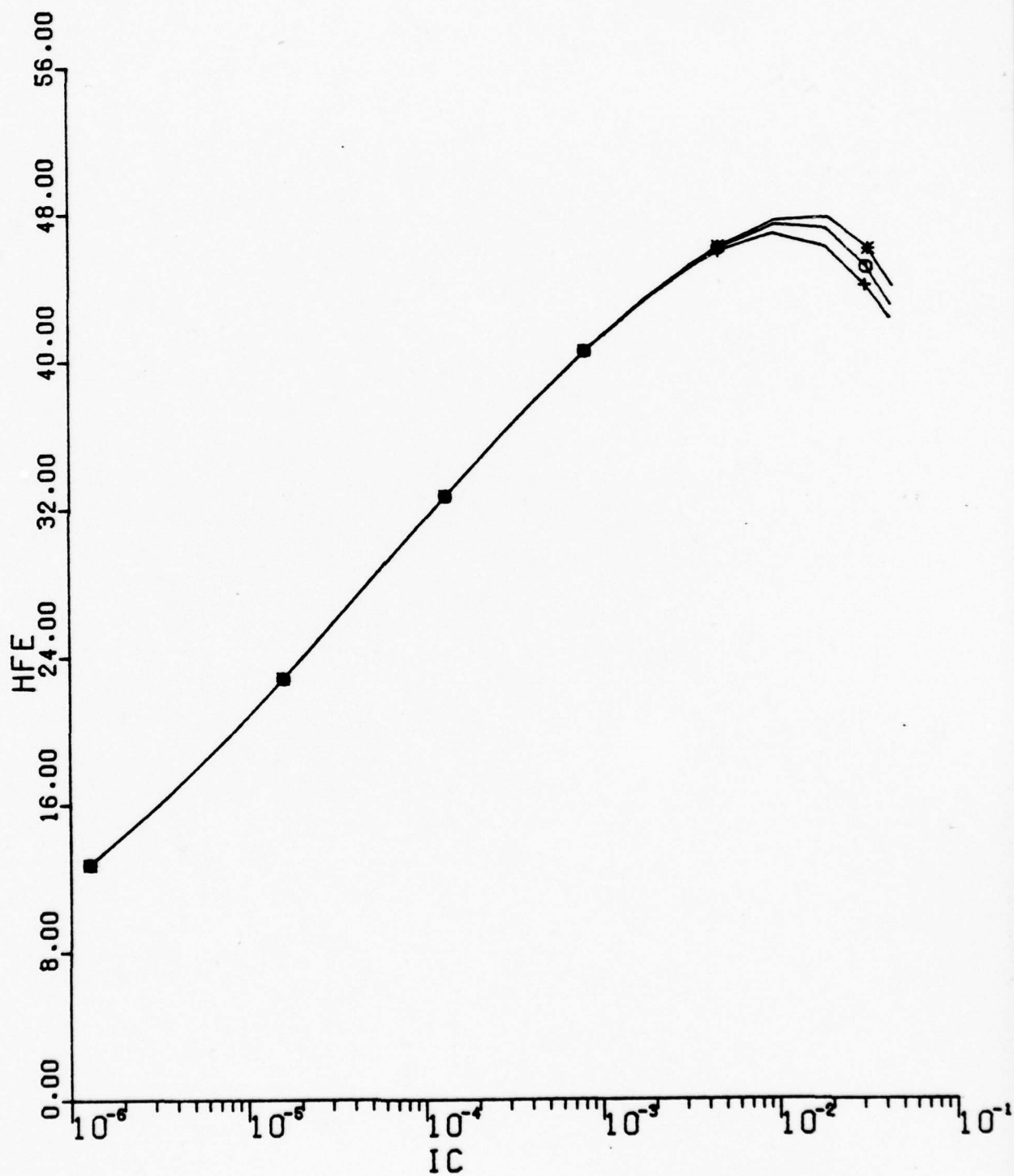




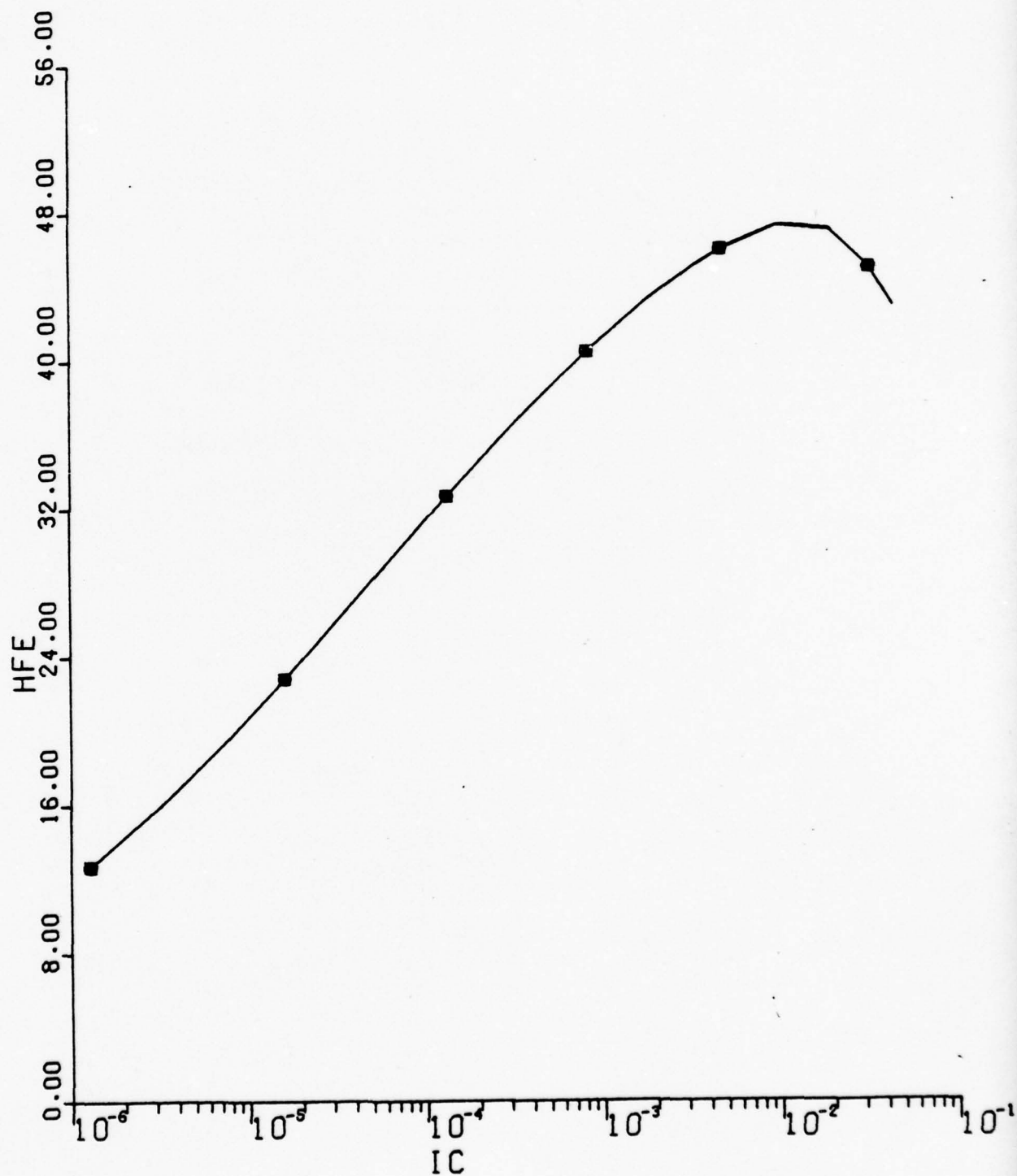
* --	NC	= 8.000E-01
+ --	NC	= 2.300E+00
0 --	NC	= 1.800E+00



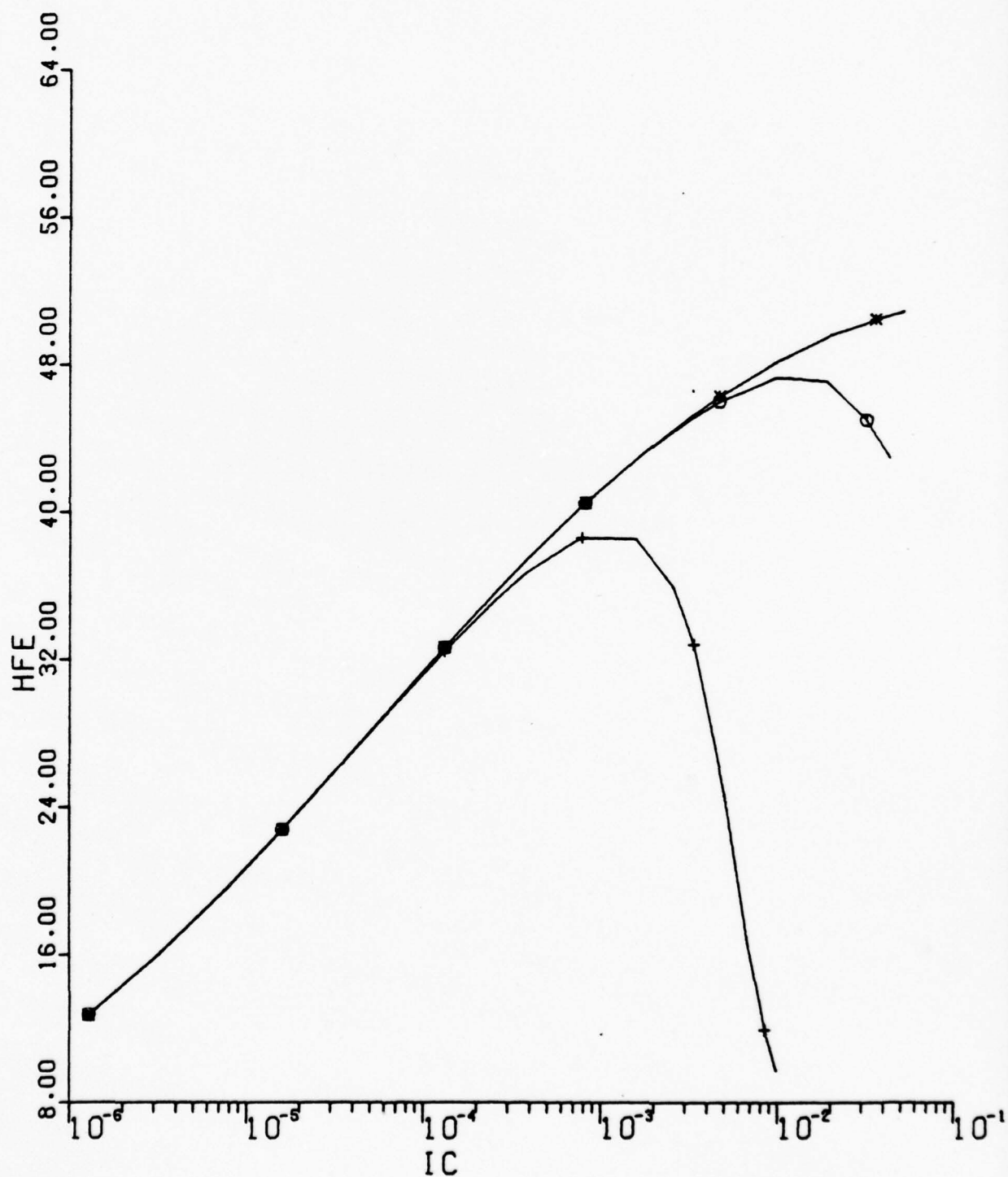
■ --	VT	=	2.550E-02
+ --	VT	=	2.650E-02
0 --	VT	=	2.590E-02



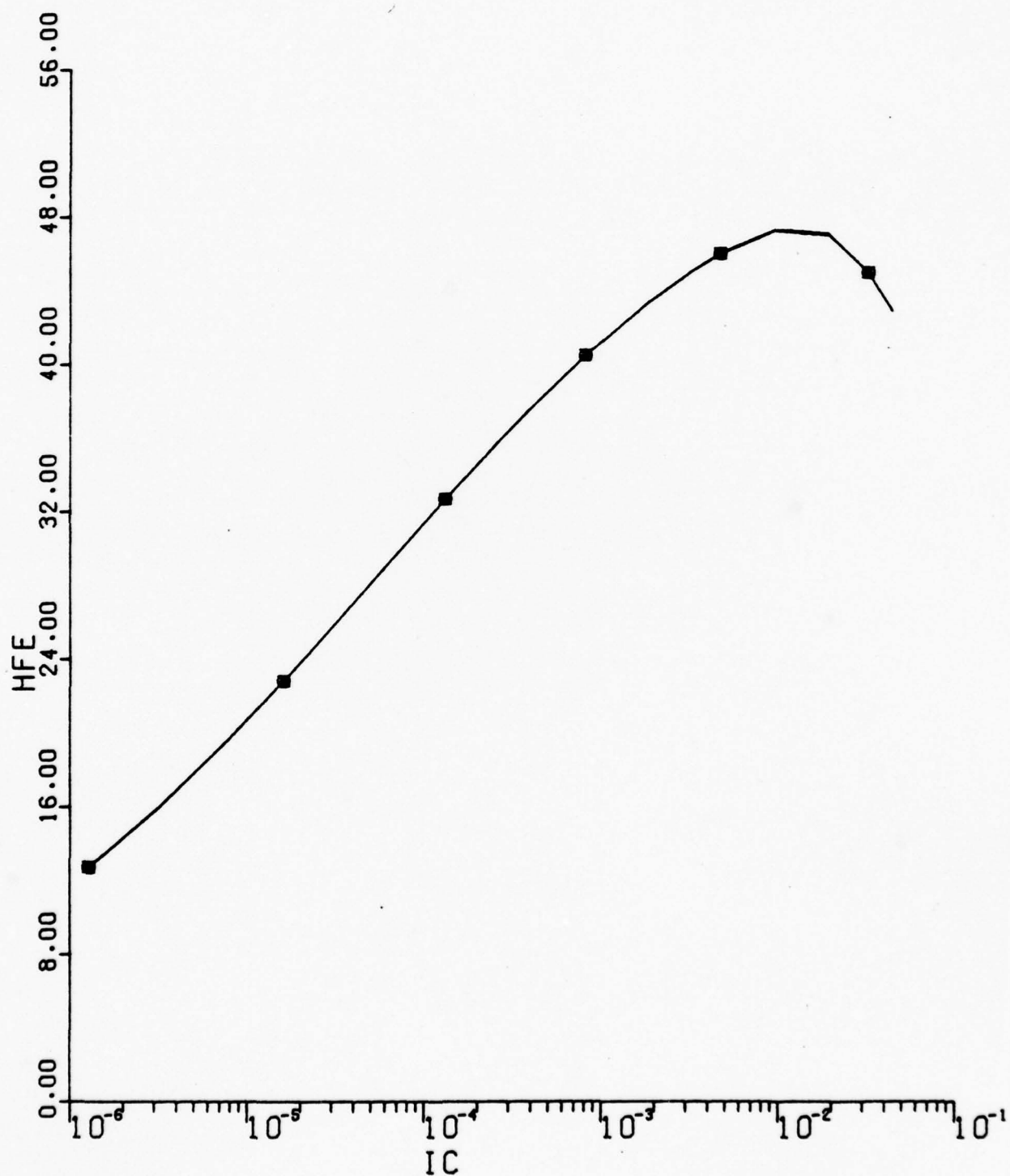
■ --	VTs	=	2.220E-02
+ --	VTs	=	2.590E-02
0 --	VTs	=	3.000E-02



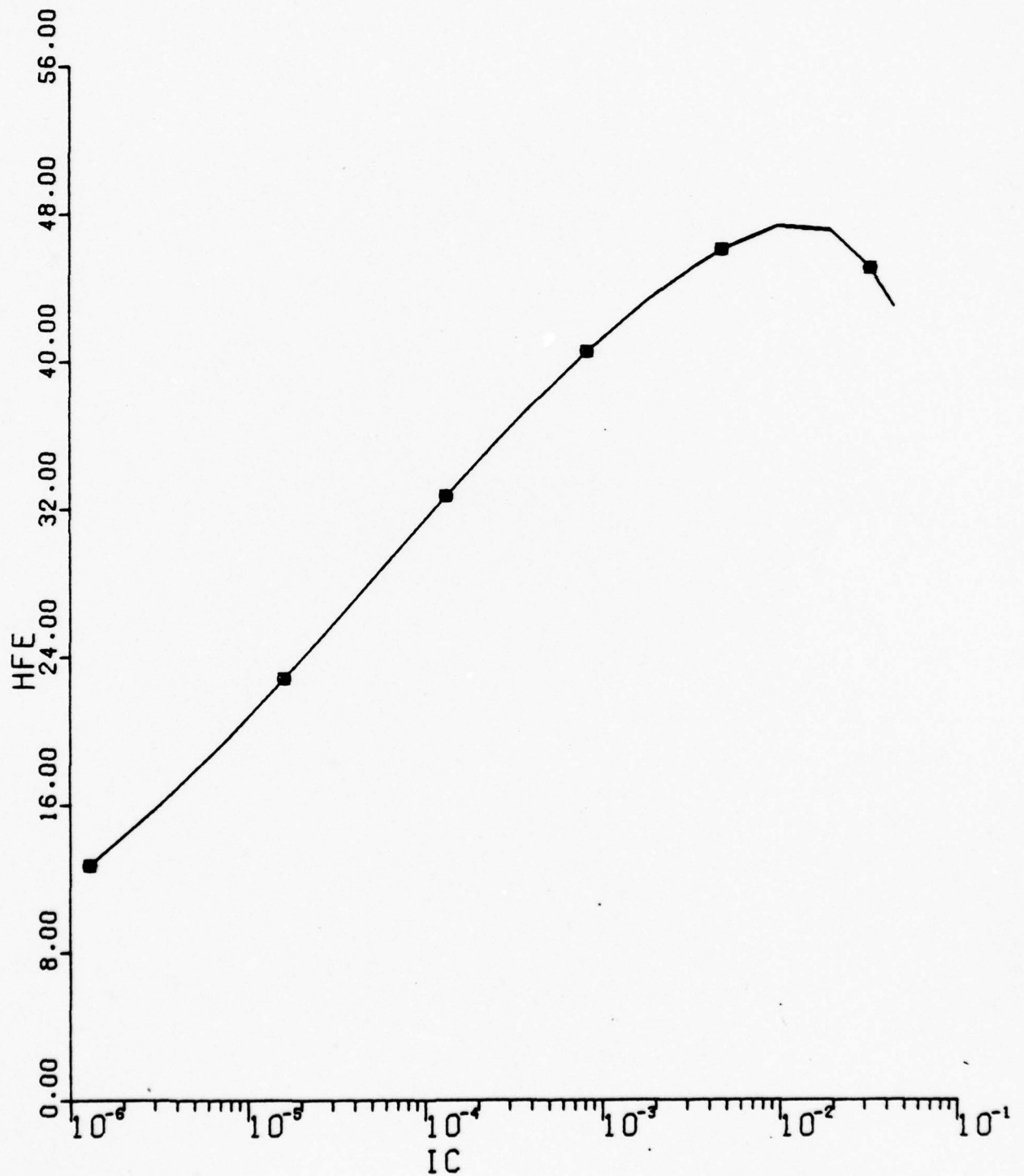
* --	QFN	=	1.500E-18
+ --	QFN	=	1.500E-14
0 --	QFN	=	1.500E-16



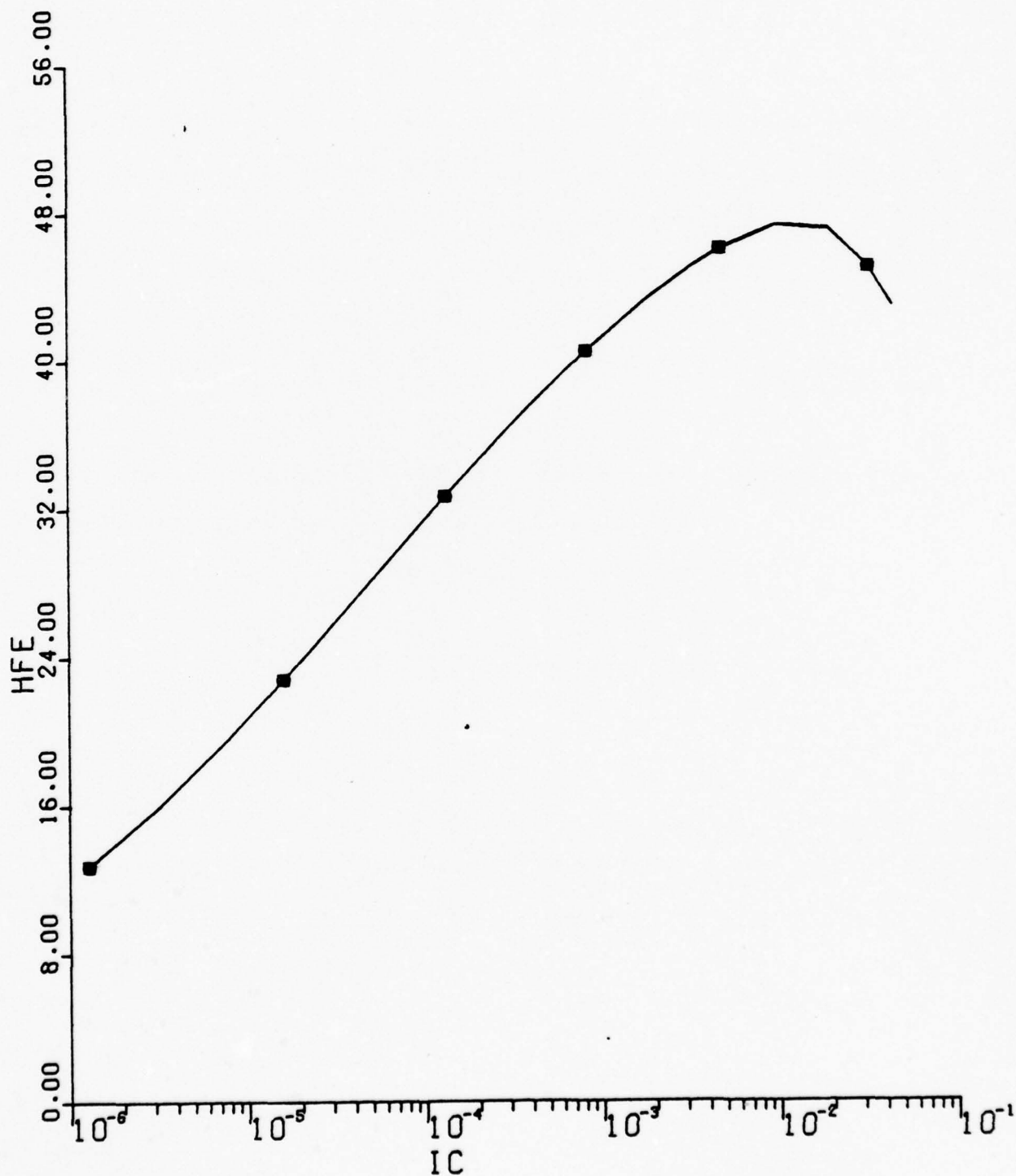
■	--	QRN	=	1.500E-14
+	--	QRN	=	1.500E-10
0	--	QRN	=	1.500E-12



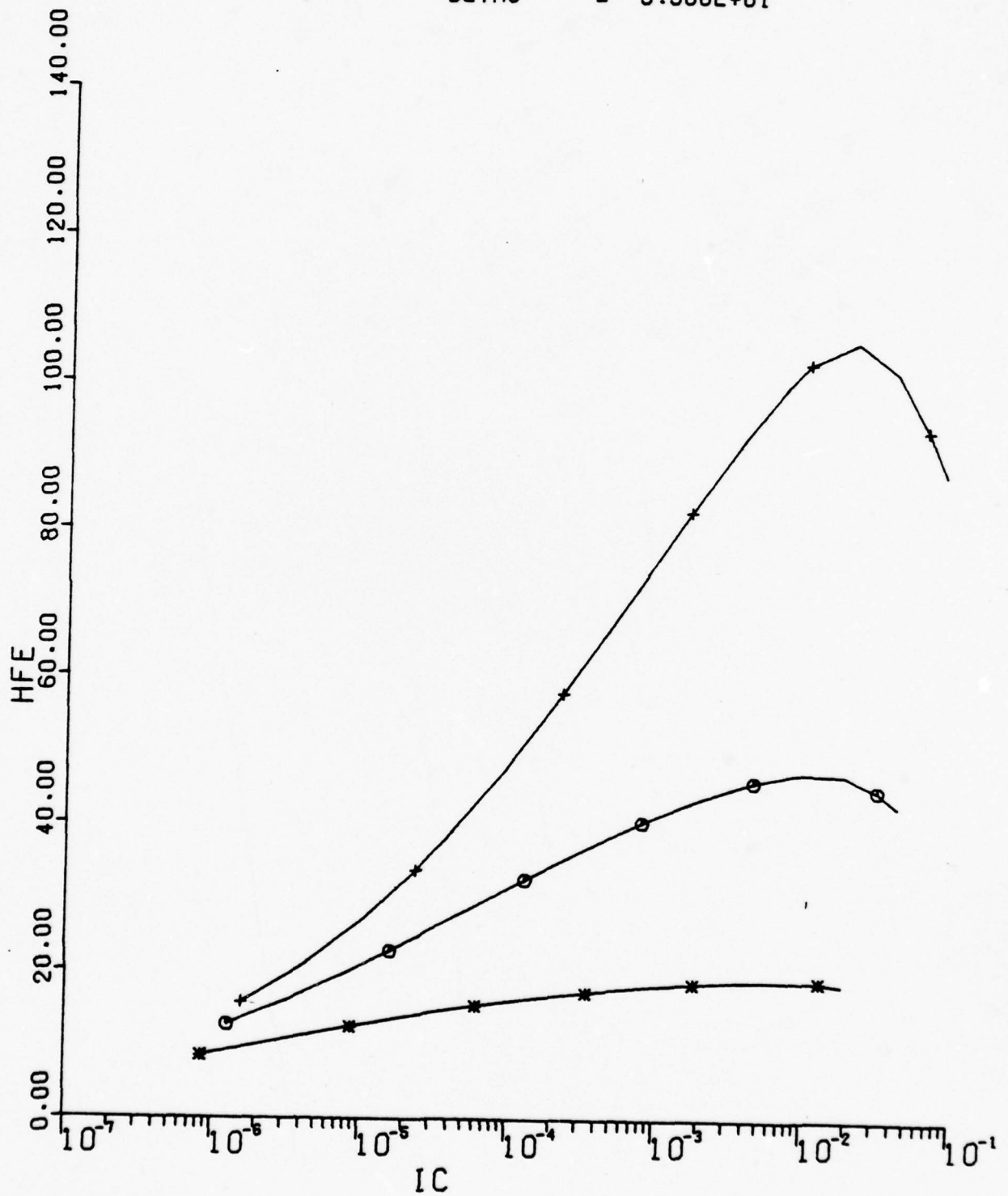
* --	TAUFO	=	1.590E-11
+ --	TAUFO	=	1.500E-12
0 --	TAUFO	=	1.590E-10



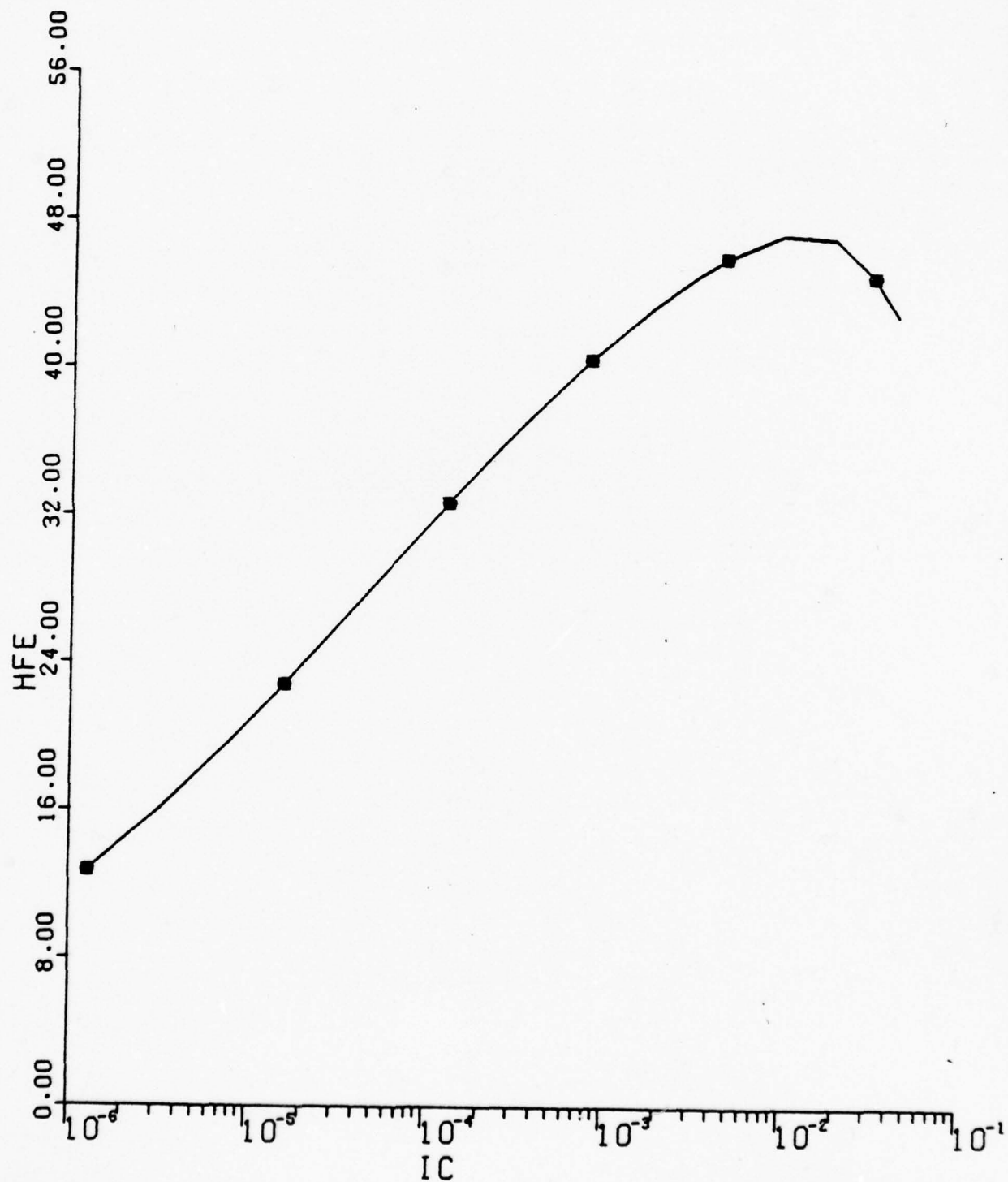
■ --	TAUR	=	1.000E-06
+ --	TAUR	=	1.270E-11
0 --	TAUR	=	1.270E-09

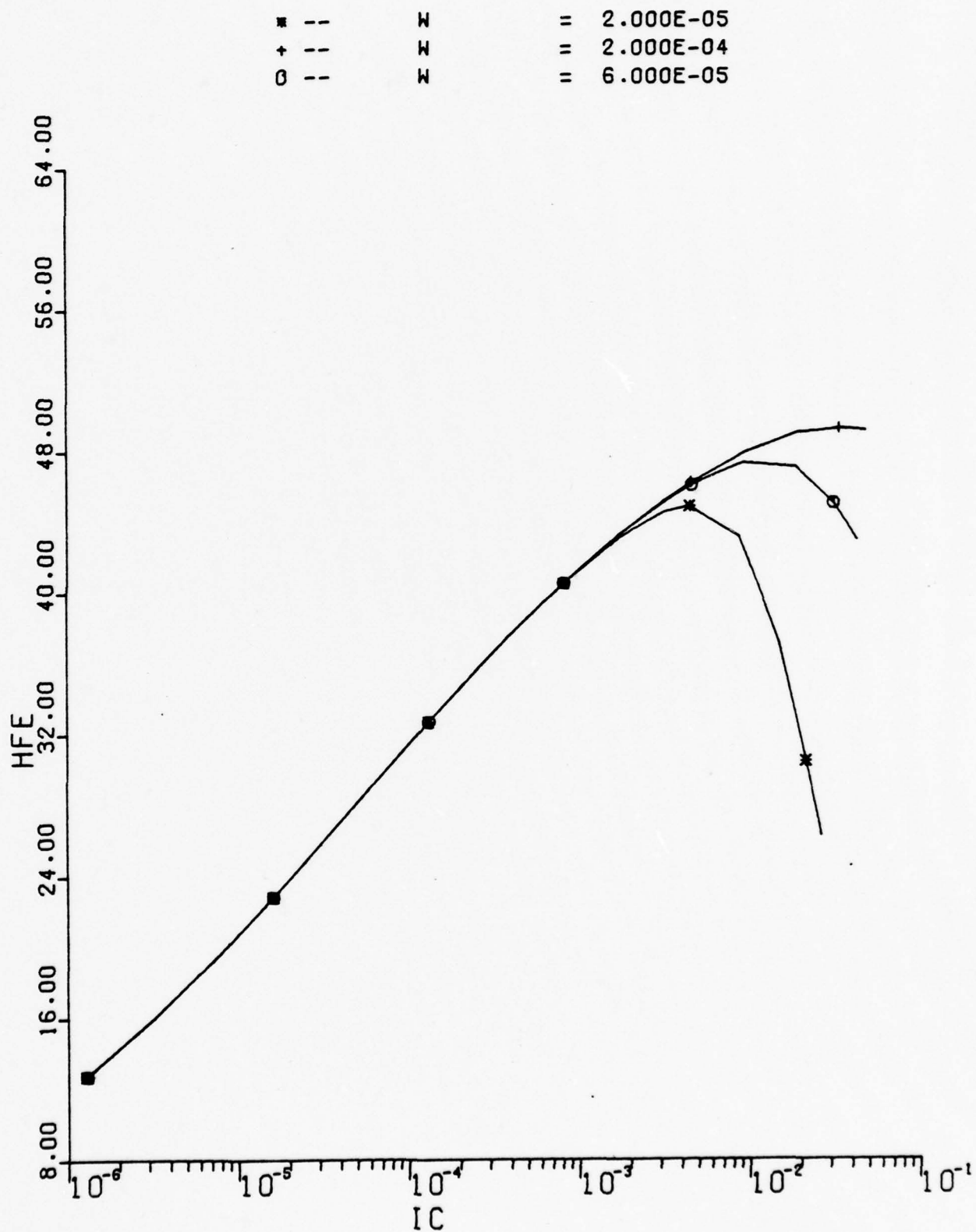


* --	BETA0	=	2.000E+01
+ --	BETA0	=	1.500E+02
0 --	BETA0	=	5.500E+01

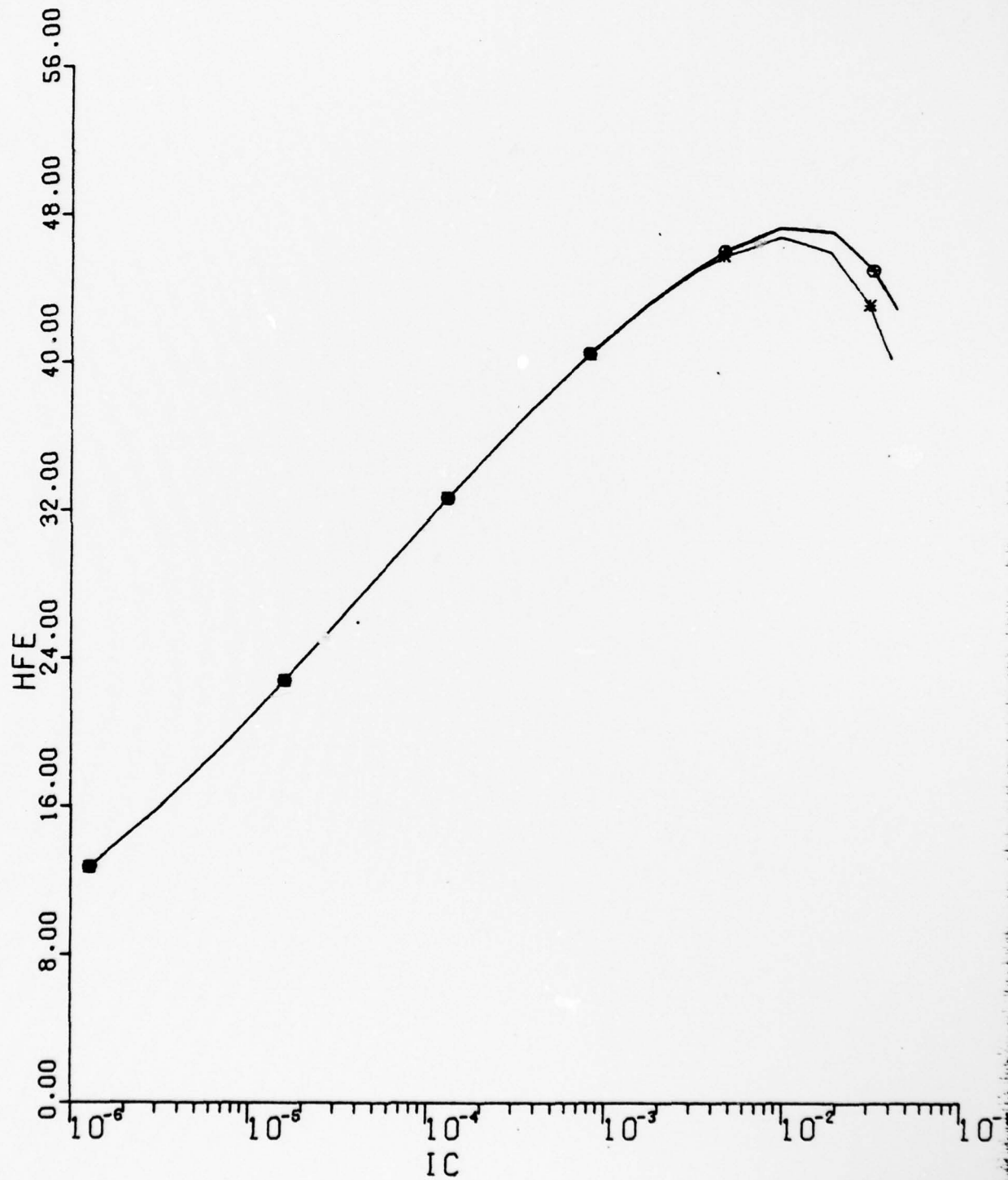


■ --	BETAR	=	6.000E+00
+ --	BETAR	=	1.100E+00
0 --	BETAR	=	1.500E+00

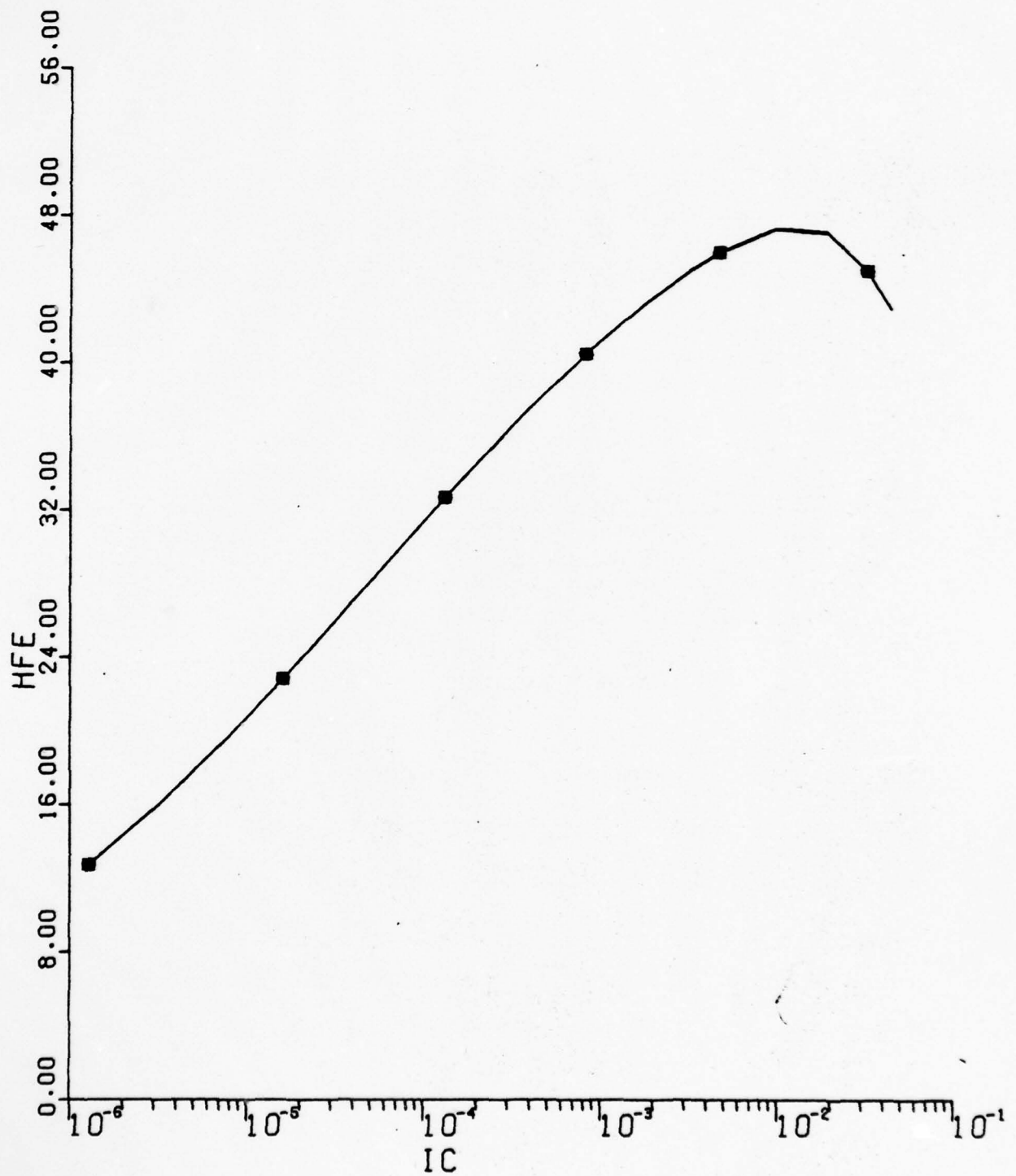




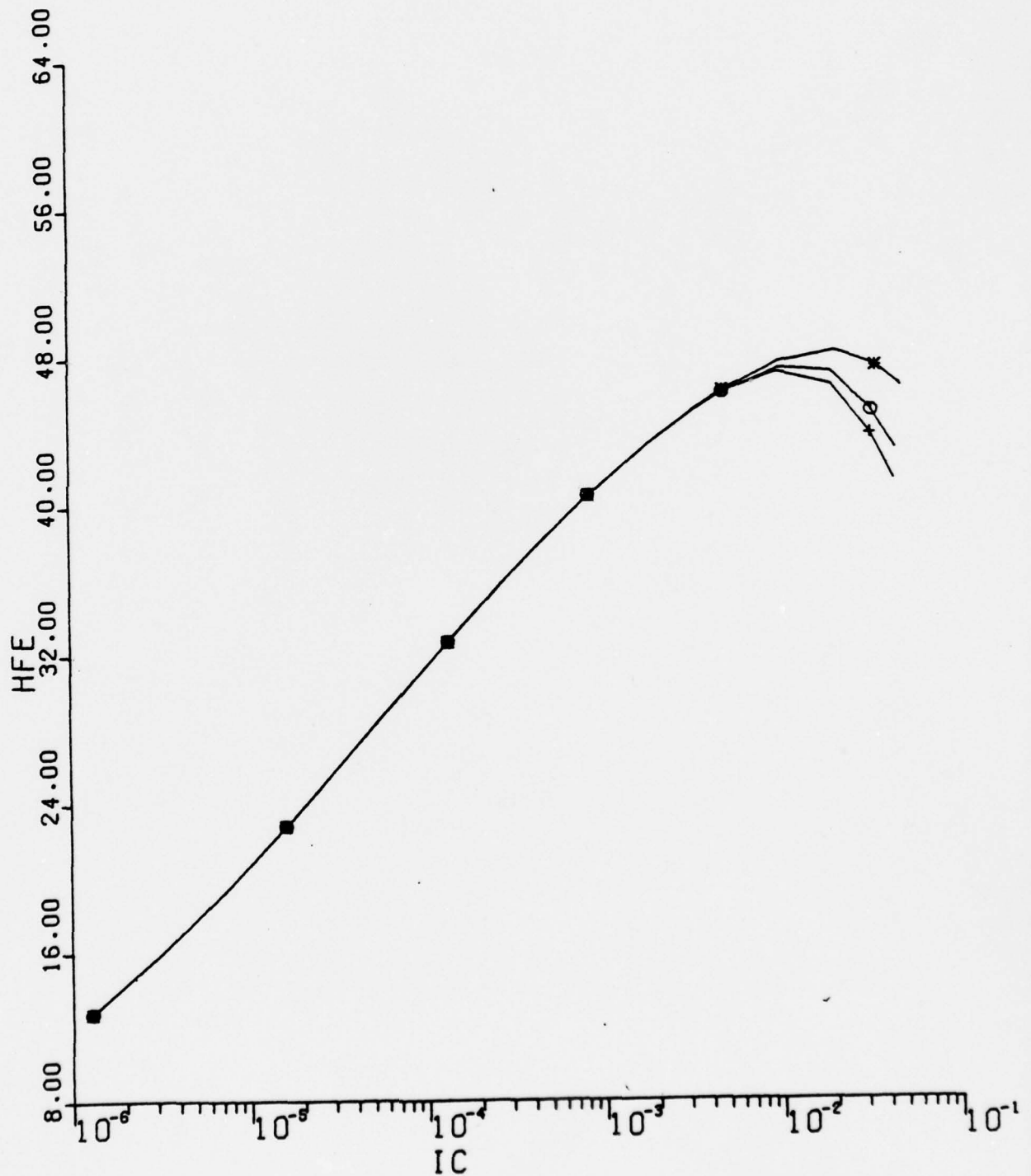
* --	AE	=	1.000E-08
+ --	AE	=	1.000E-04
0 --	AE	=	9.800E-07



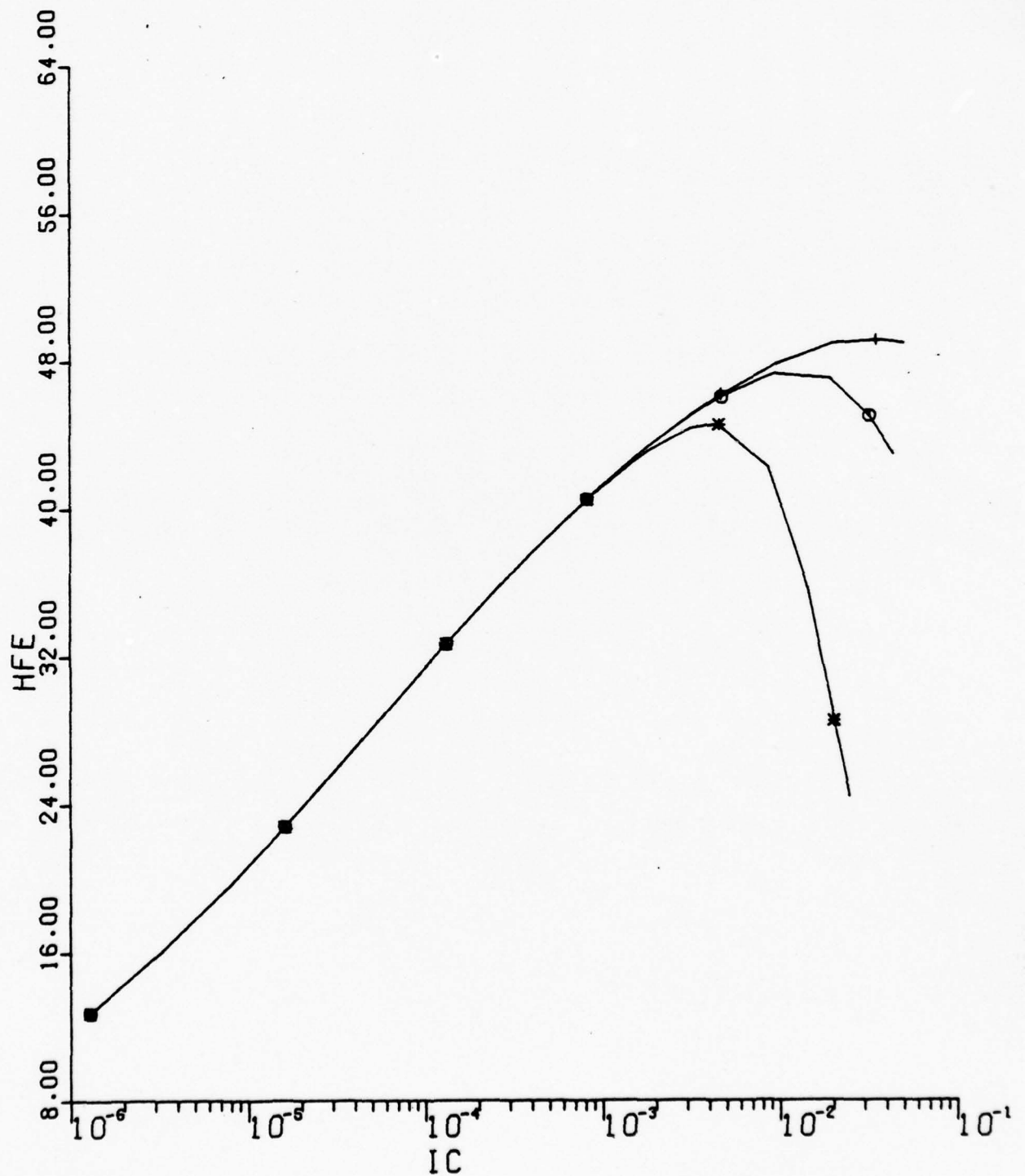
* --	VLIM	=	1.000E+06
+ --	VLIM	=	1.500E+07
0 --	VLIM	=	6.000E+06



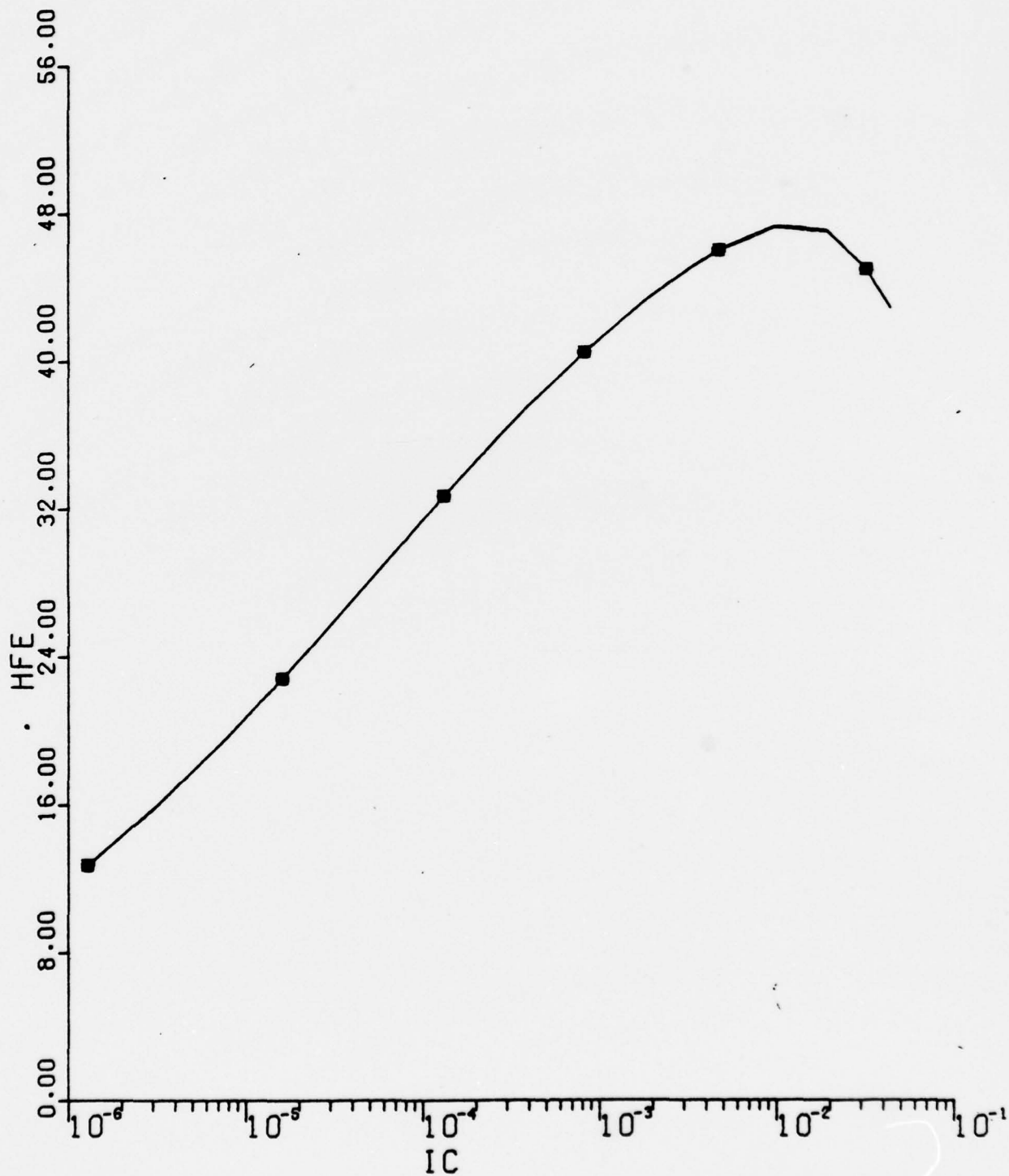
* --	DNB	=	1.000E+01
+ --	DNB	=	3.000E+01
0 --	DNB	=	2.260E+01



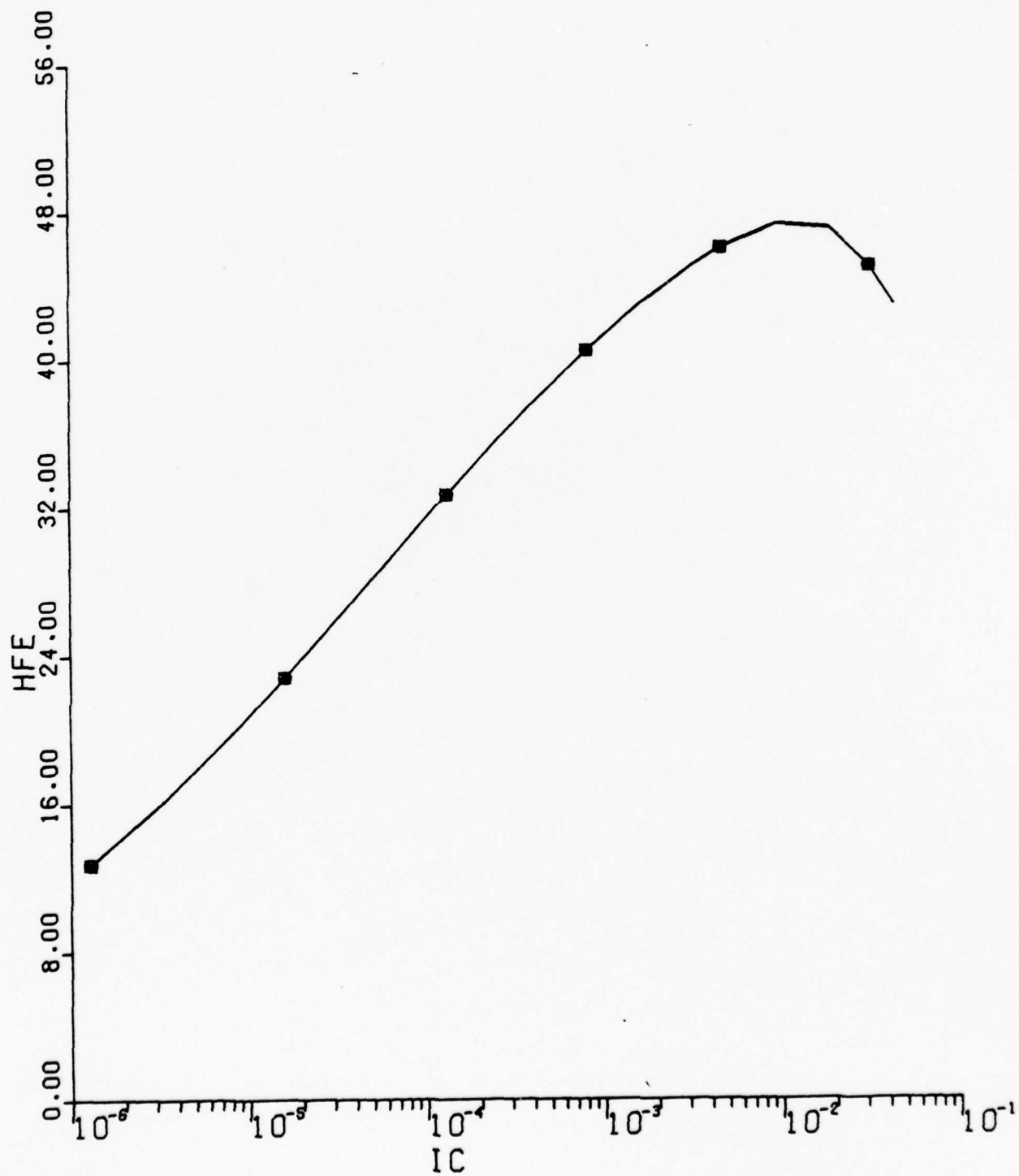
* --	WCPRIME	=	1.000E-03
+ --	WCPRIME	=	1.000E-04
0 --	WCPRIME	=	3.000E-04



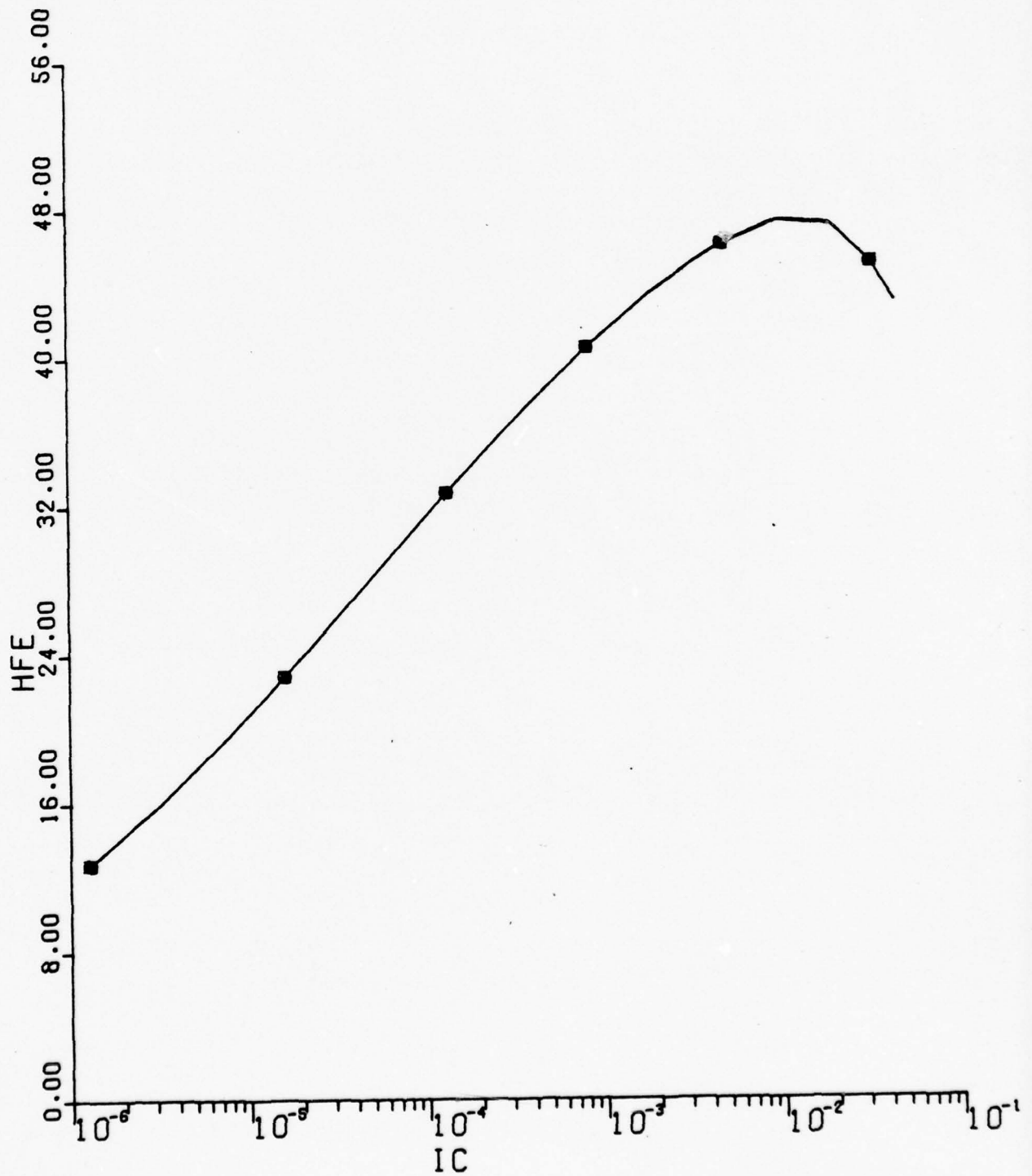
■ --	NDC	=	1.000E+20
+ --	NDC	=	1.000E+13
0 --	NDC	=	1.000E+16

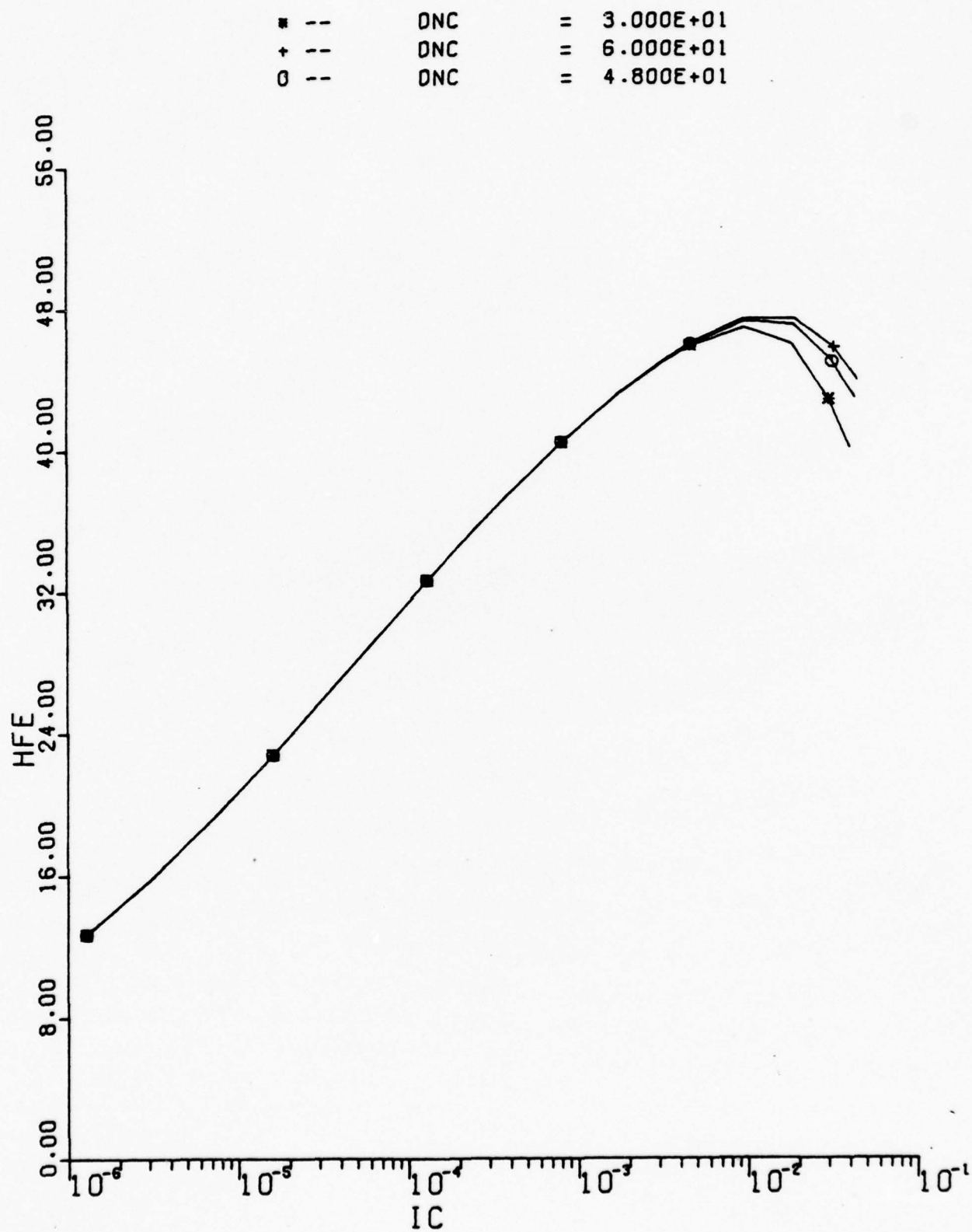


* --	PHIC	=	4.000E-01
+ --	PHIC	=	1.200E+00
0 --	PHIC	=	7.000E-01

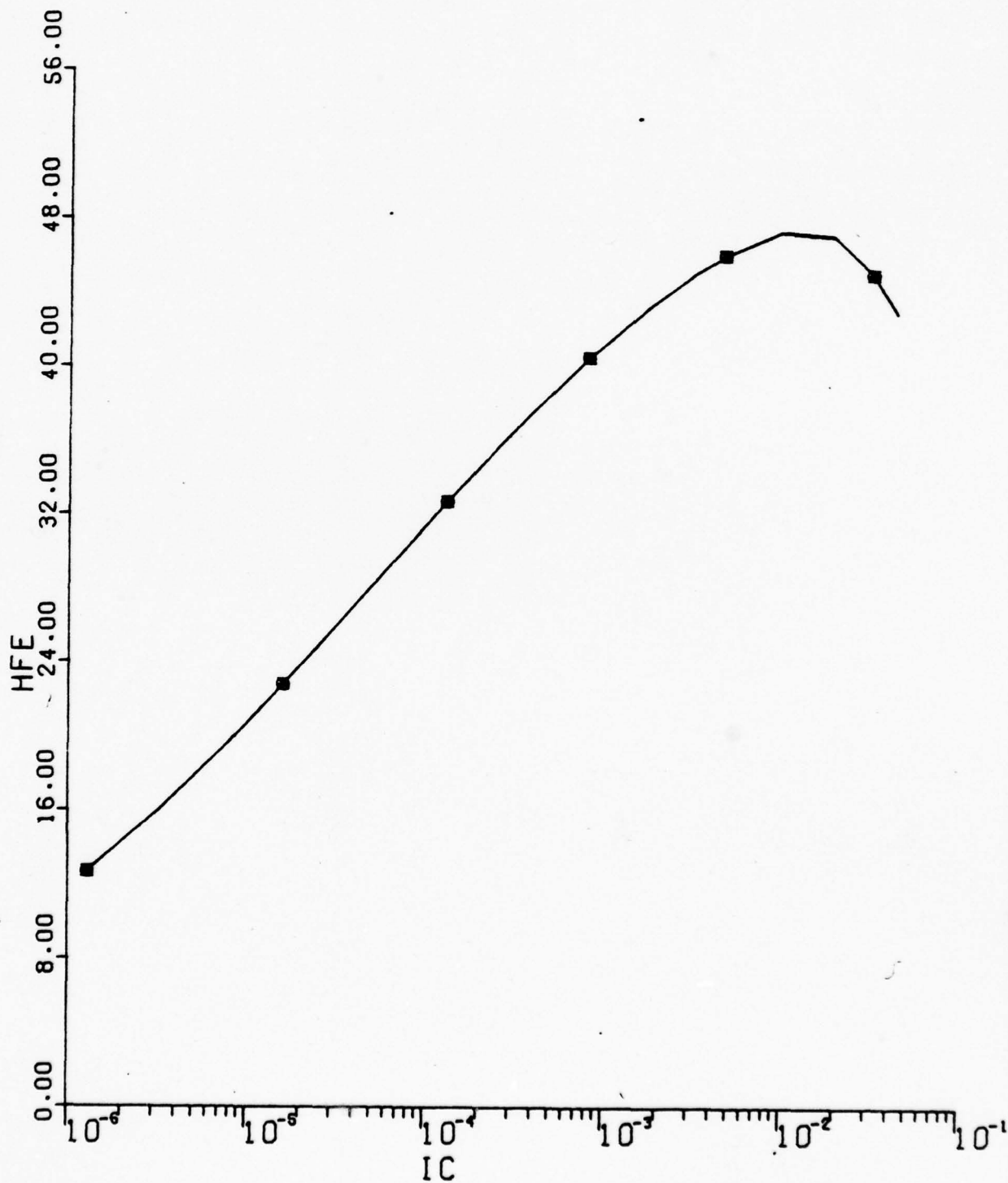


■ --	PHIC	=	4.000E-01
+ --	PHIC	=	1.200E+00
0 --	PHIC	=	7.000E-01

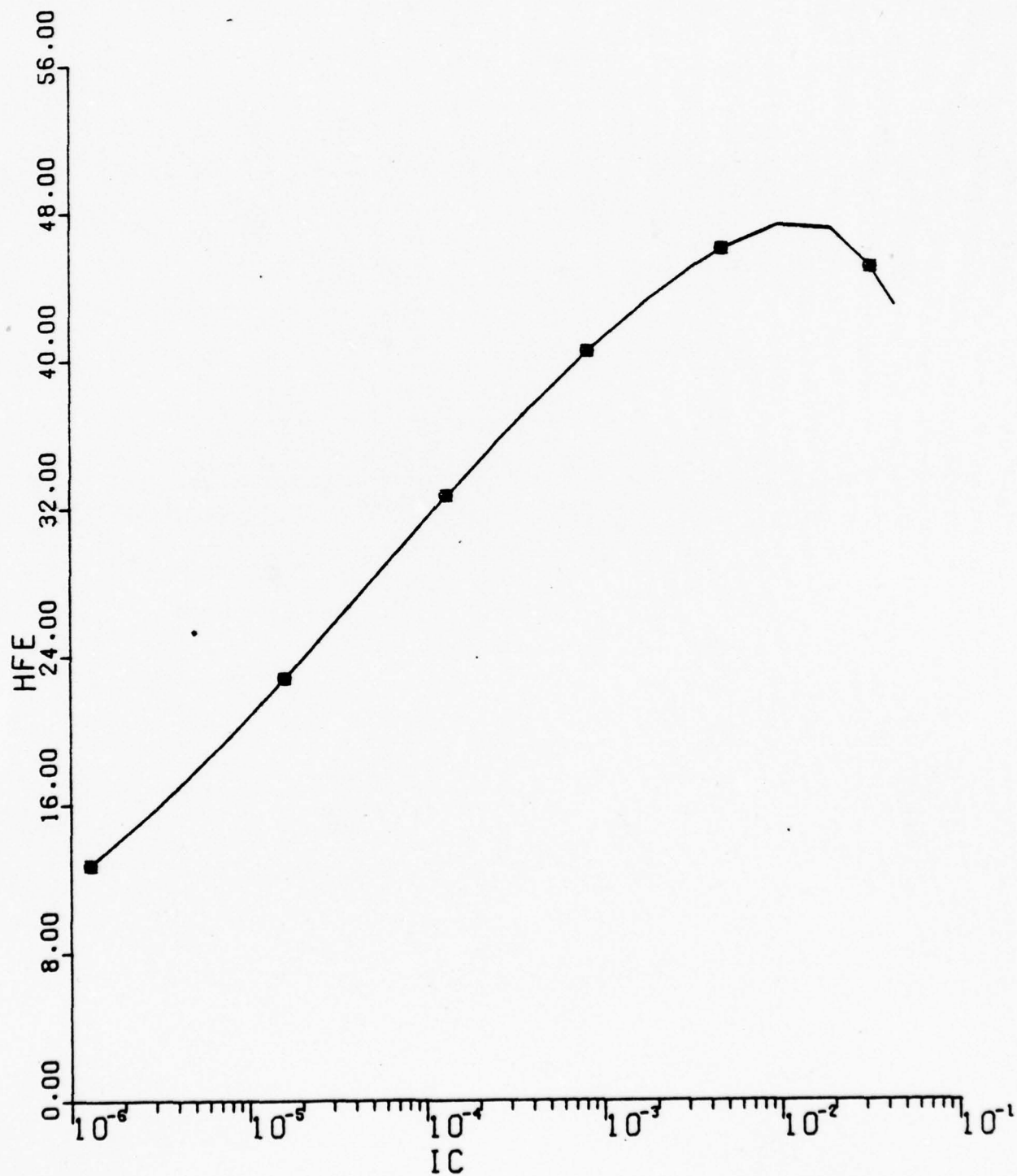




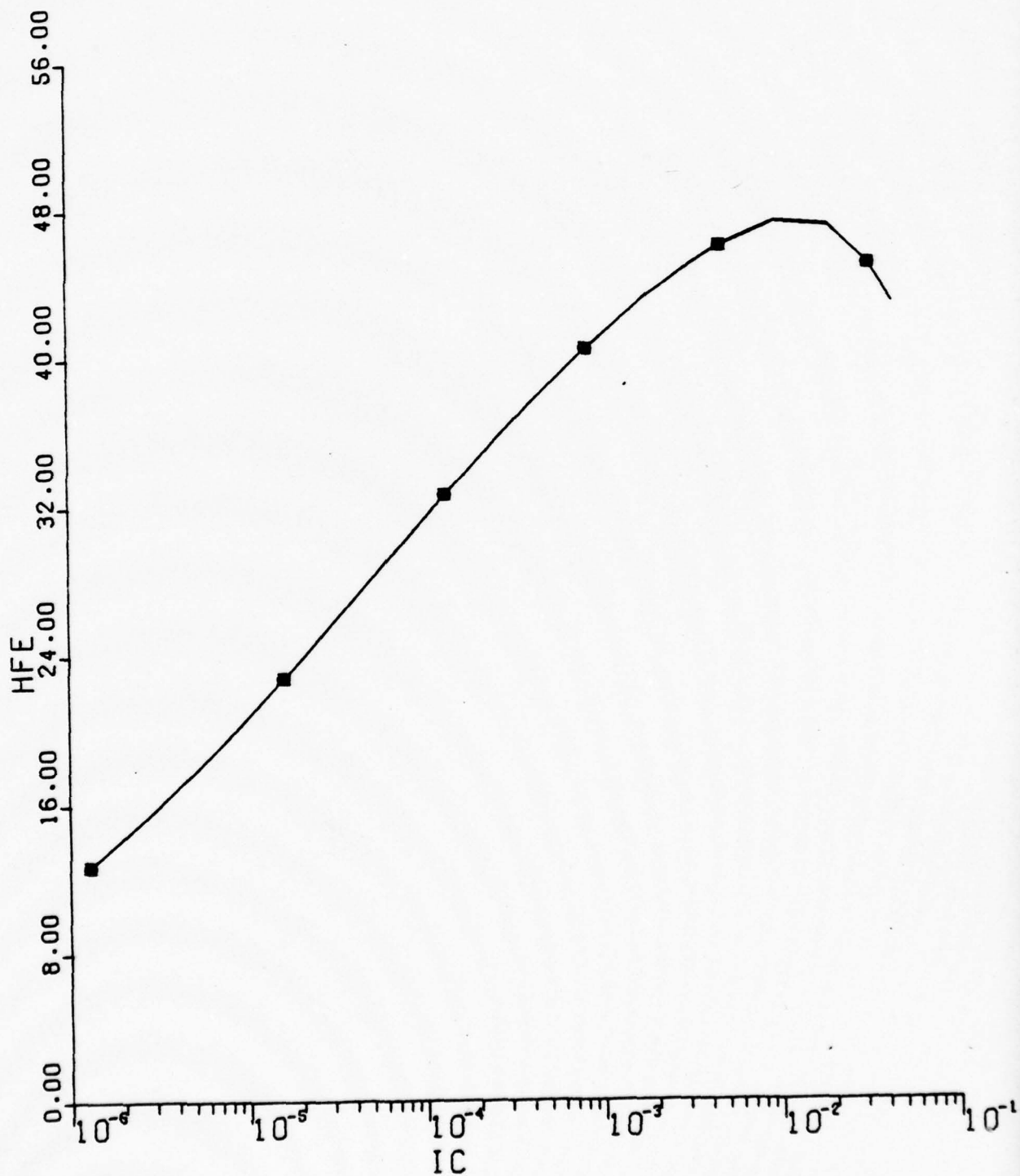
■ --	X0	=	4.000E-05
+ --	X0	=	2.400E-04
0 --	X0	=	1.200E-04



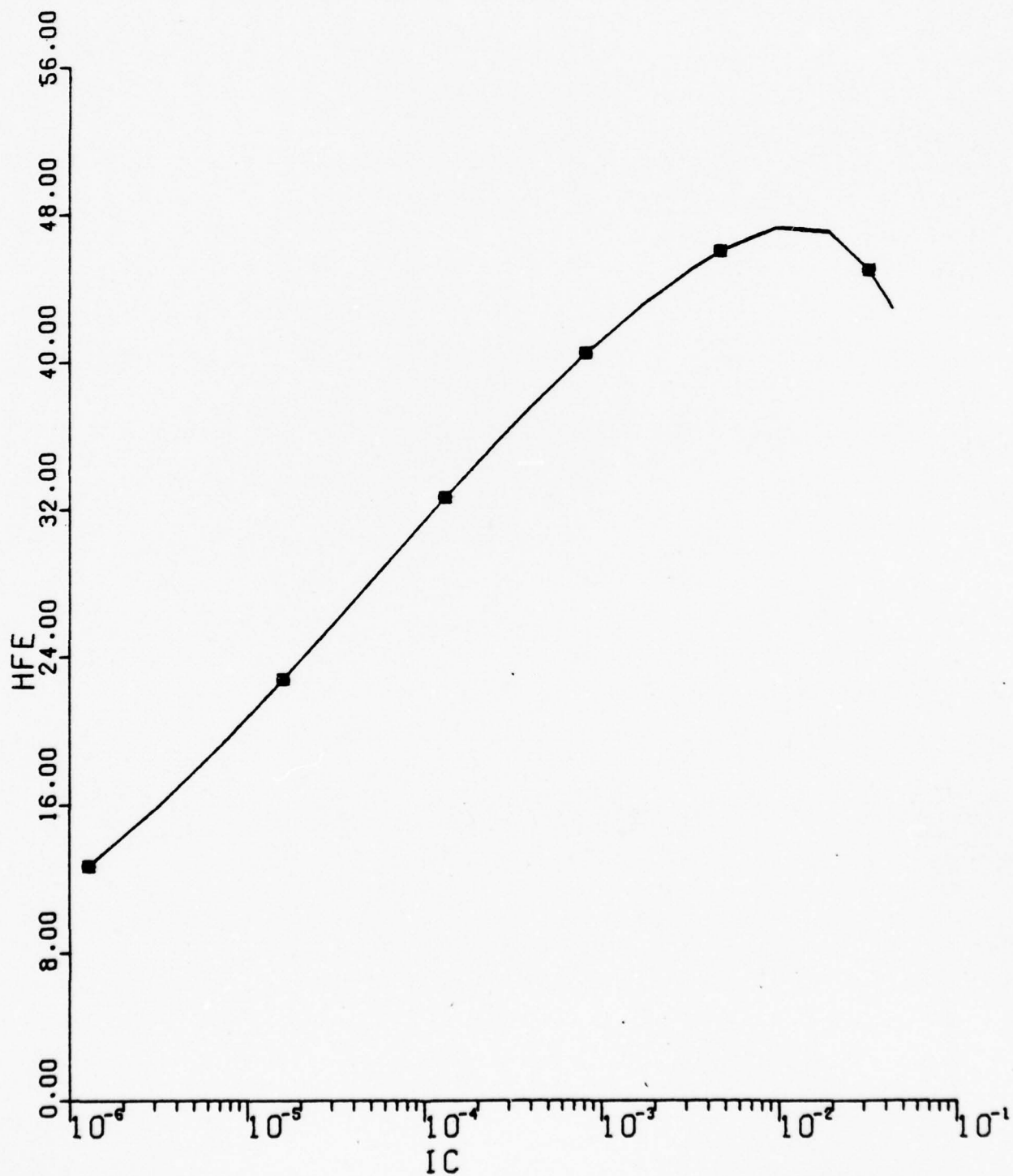
■ --	KR	=	1.000E-01
+ --	KR	=	9.000E-01
0 --	KR	=	4.000E-01



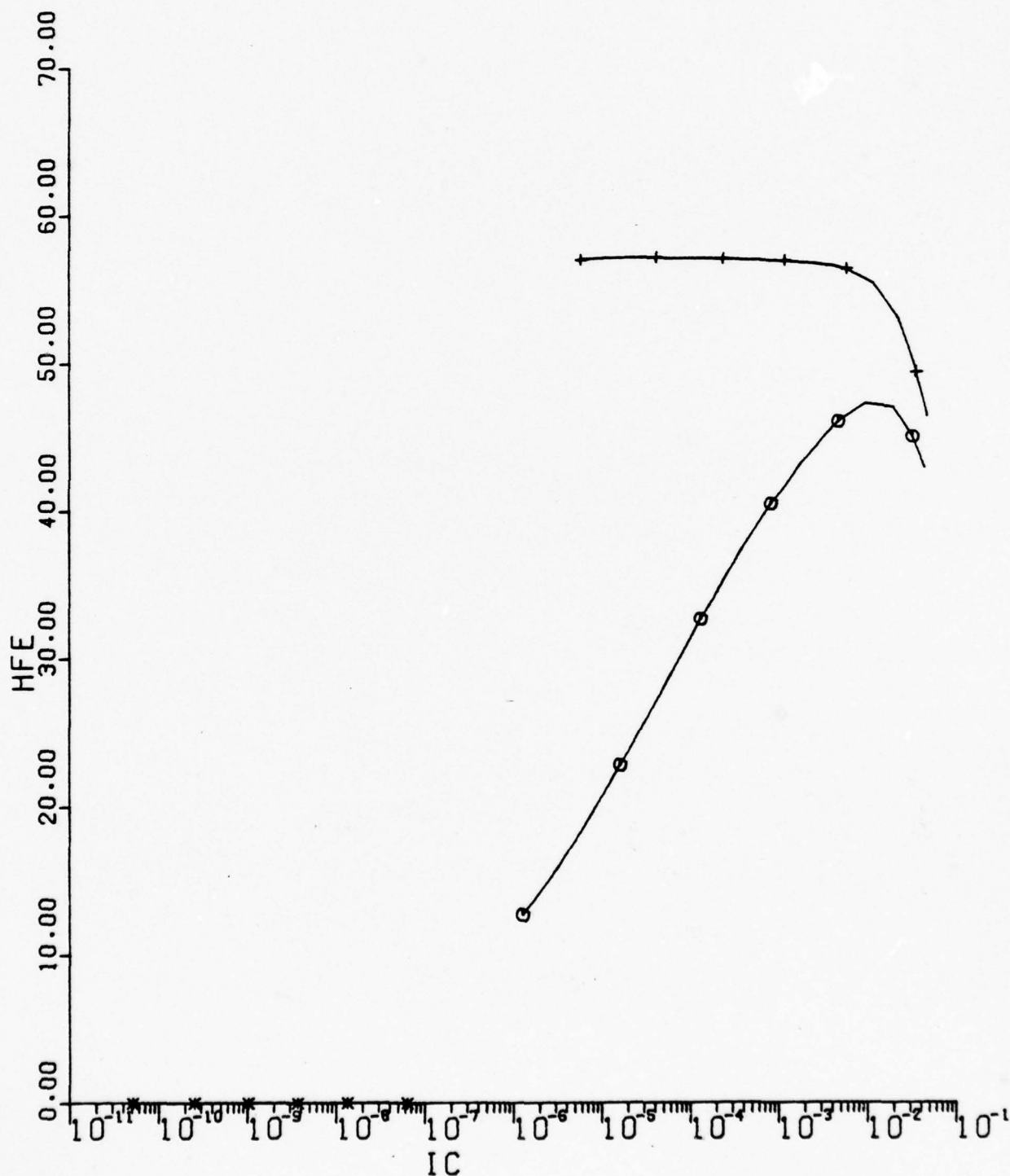
■ --	TD	=	2.000E-12
+ --	TD	=	2.000E-10
0 --	TD	=	2.000E-11



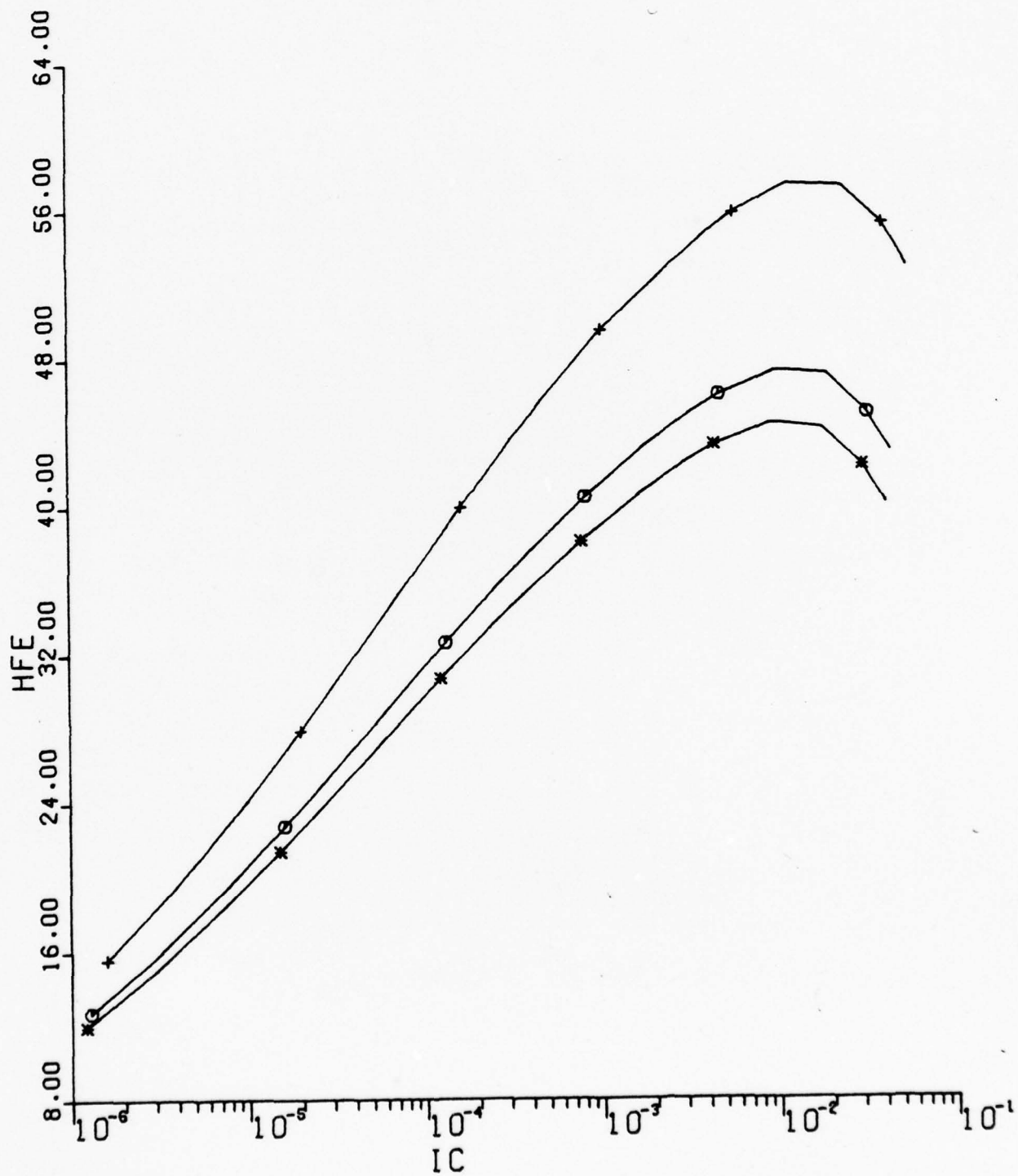
*	--	M	=	1.000E+00
+	--	M	=	1.000E+01
0	--	M	=	2.000E+00



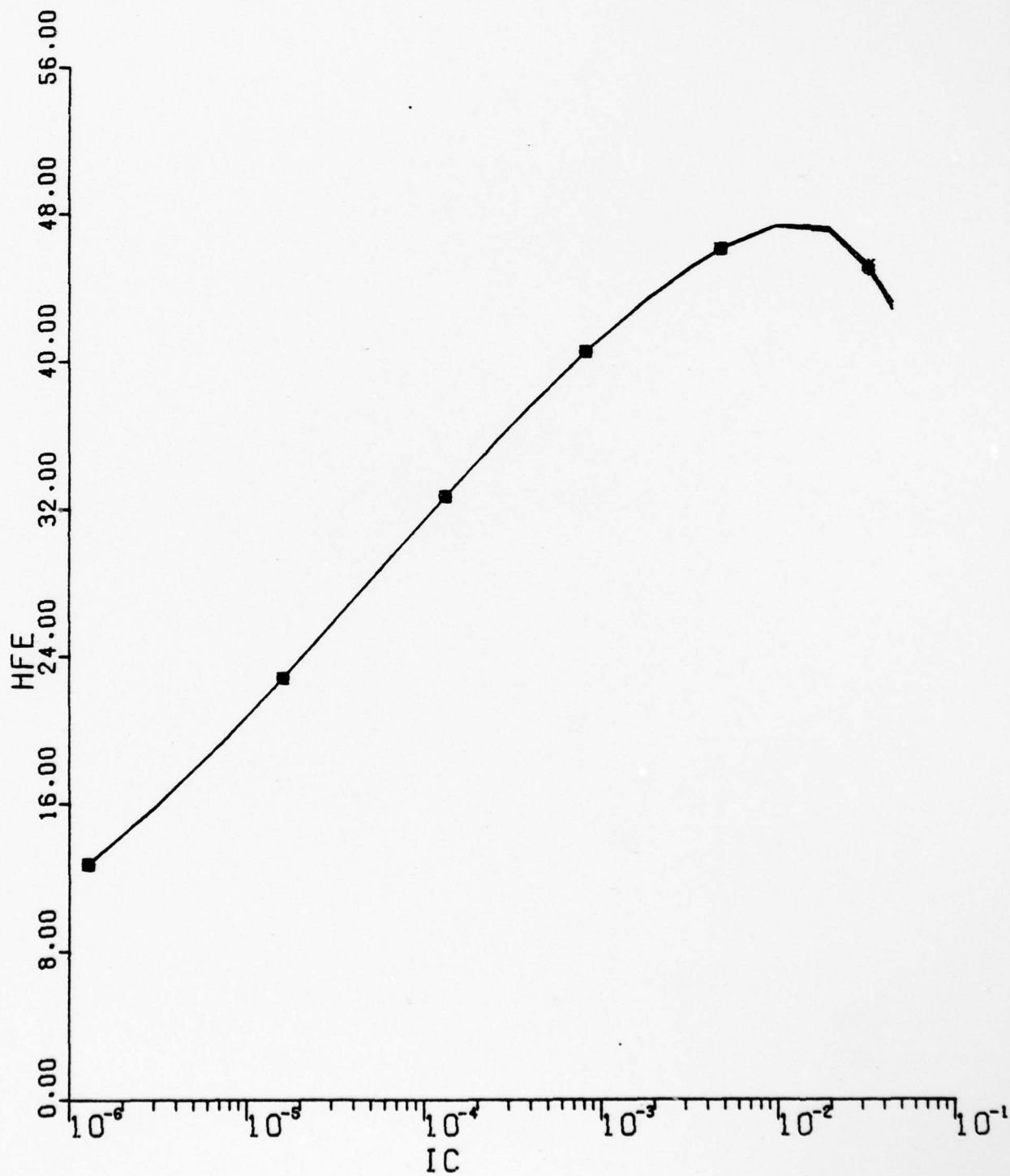
* --	NE	=	8.000E-01
+ --	NE	=	2.300E+00
0 --	NE	=	1.500E+00



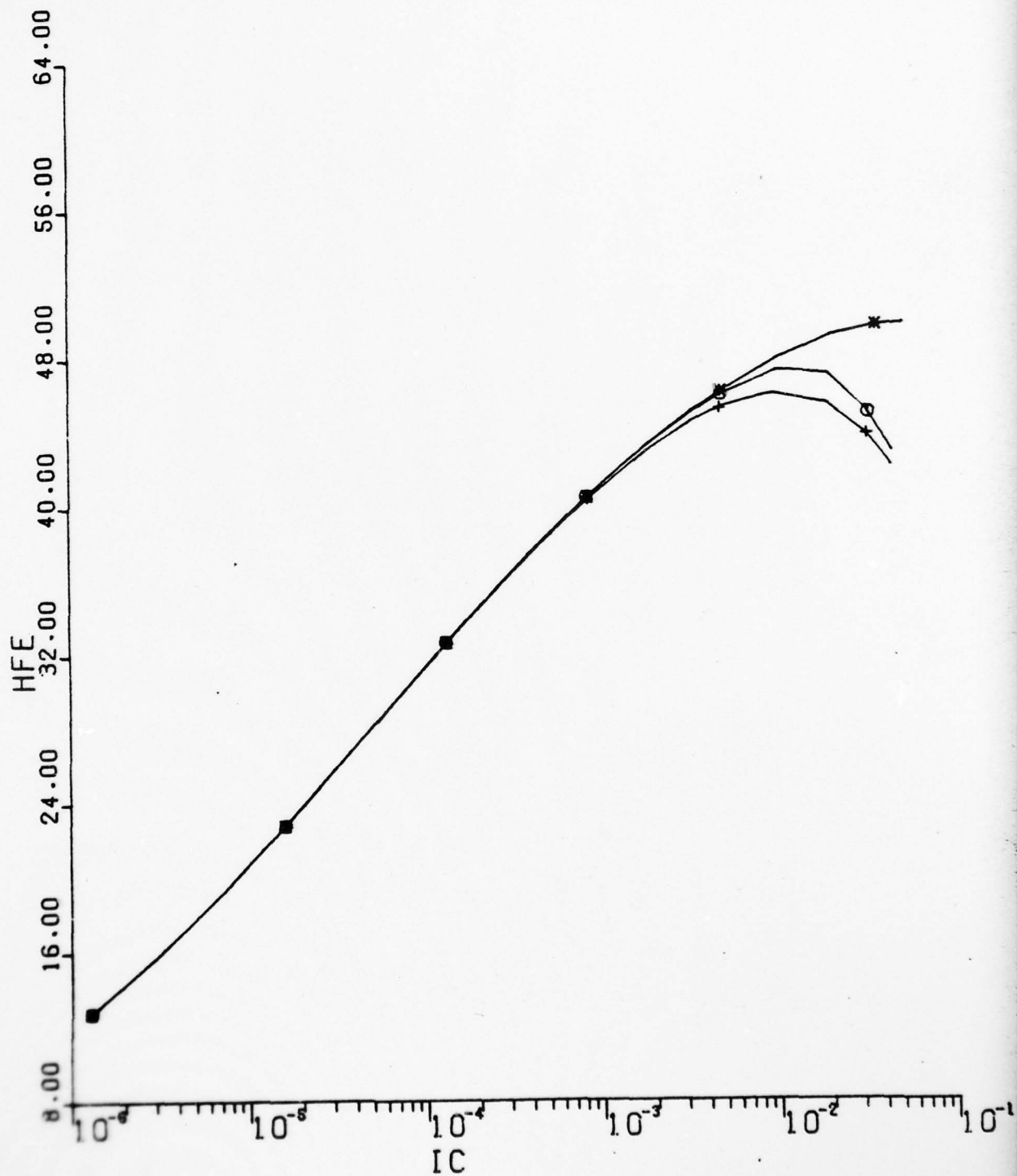
* --	VCE	=	1.500E+00
+ --	VCE	=	1.500E+01
0 --	VCE	=	5.000E+00

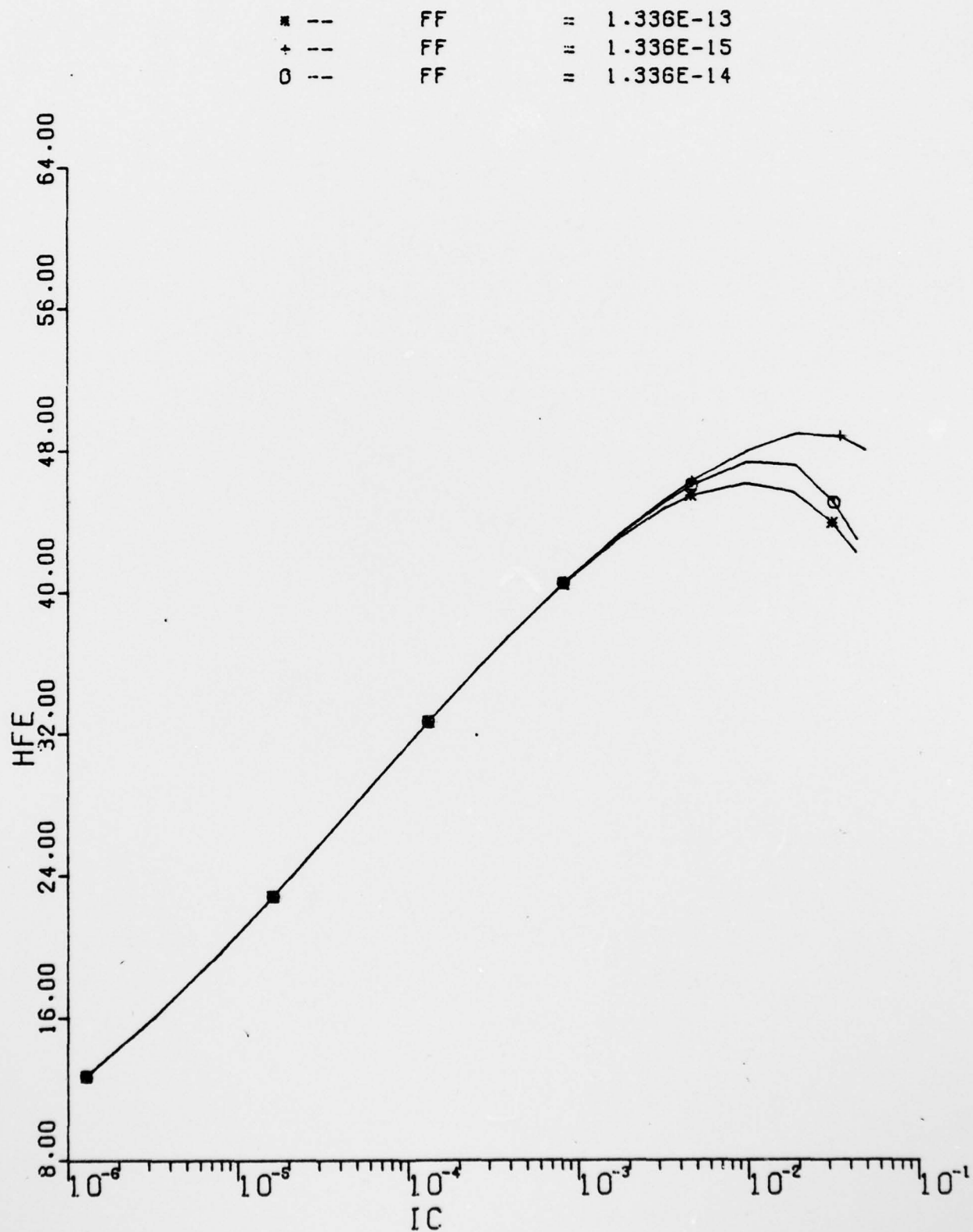


■ --	VB	=	1.500E+01
+ --	VB	=	2.000E+01
0 --	VB	=	1.779E+01



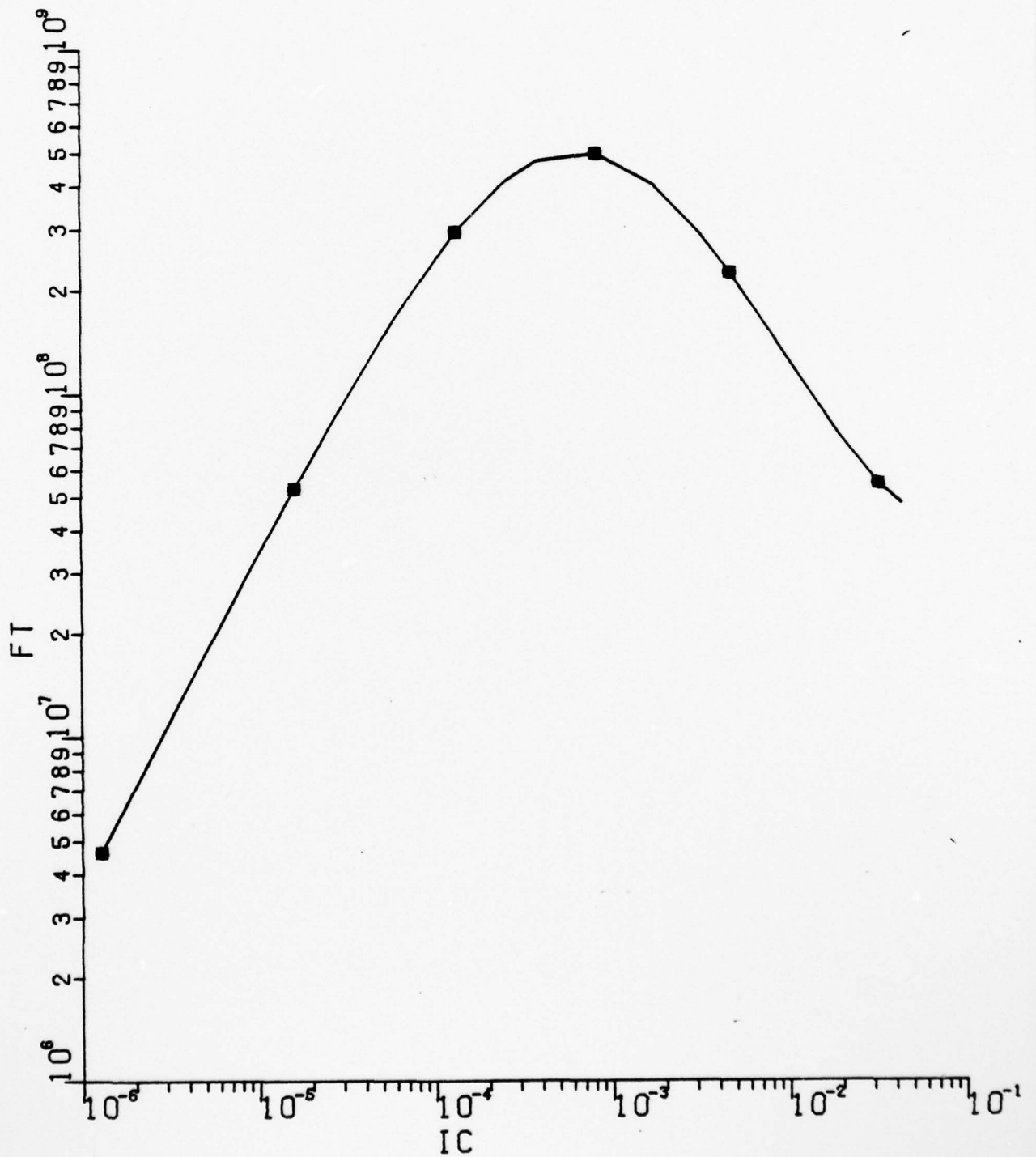
■ --	VF	=	2.590E-01
+ --	VF	=	2.590E-03
0 --	VF	=	2.590E-02



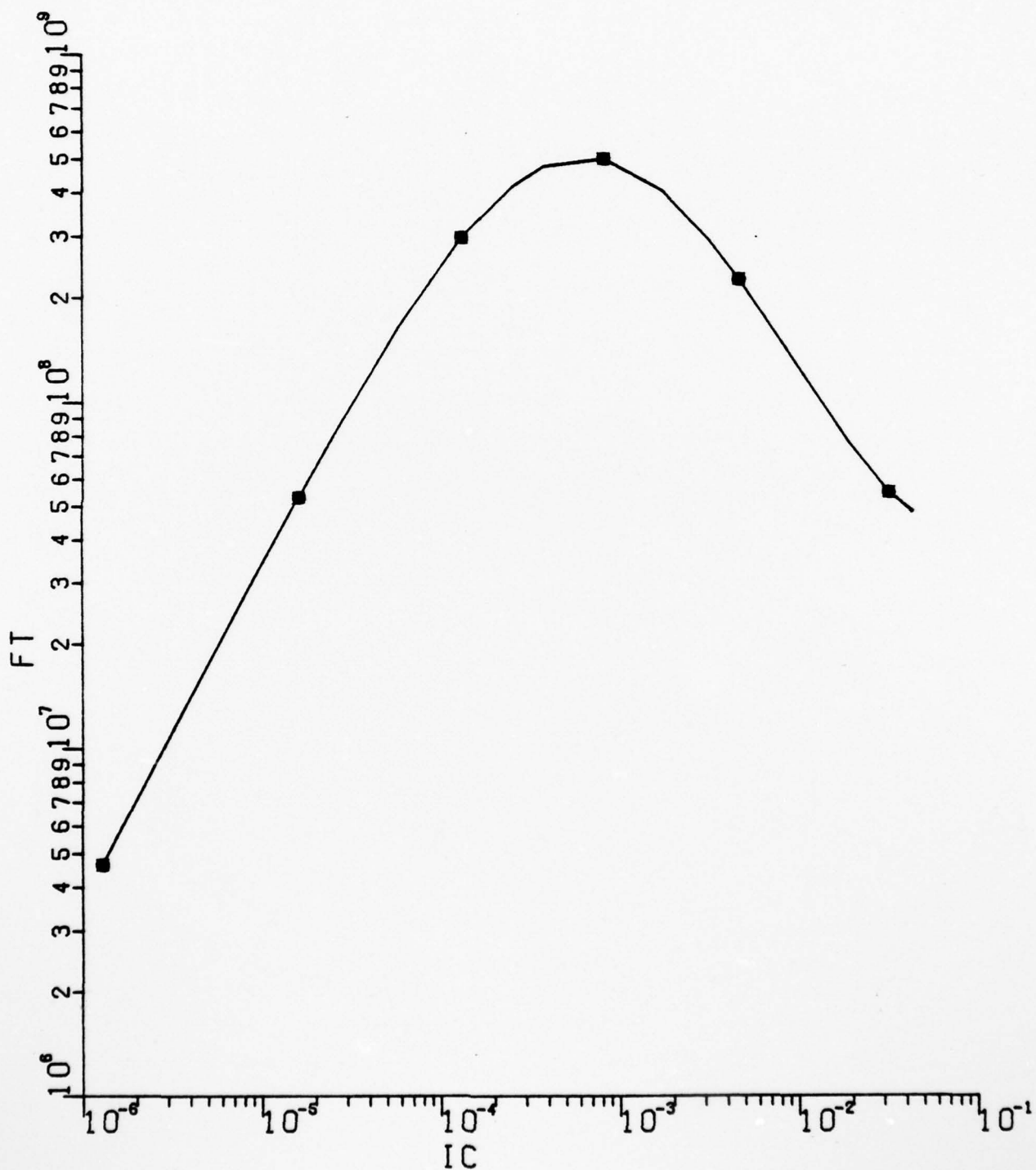


B.4 F_T vs. I_c Curves

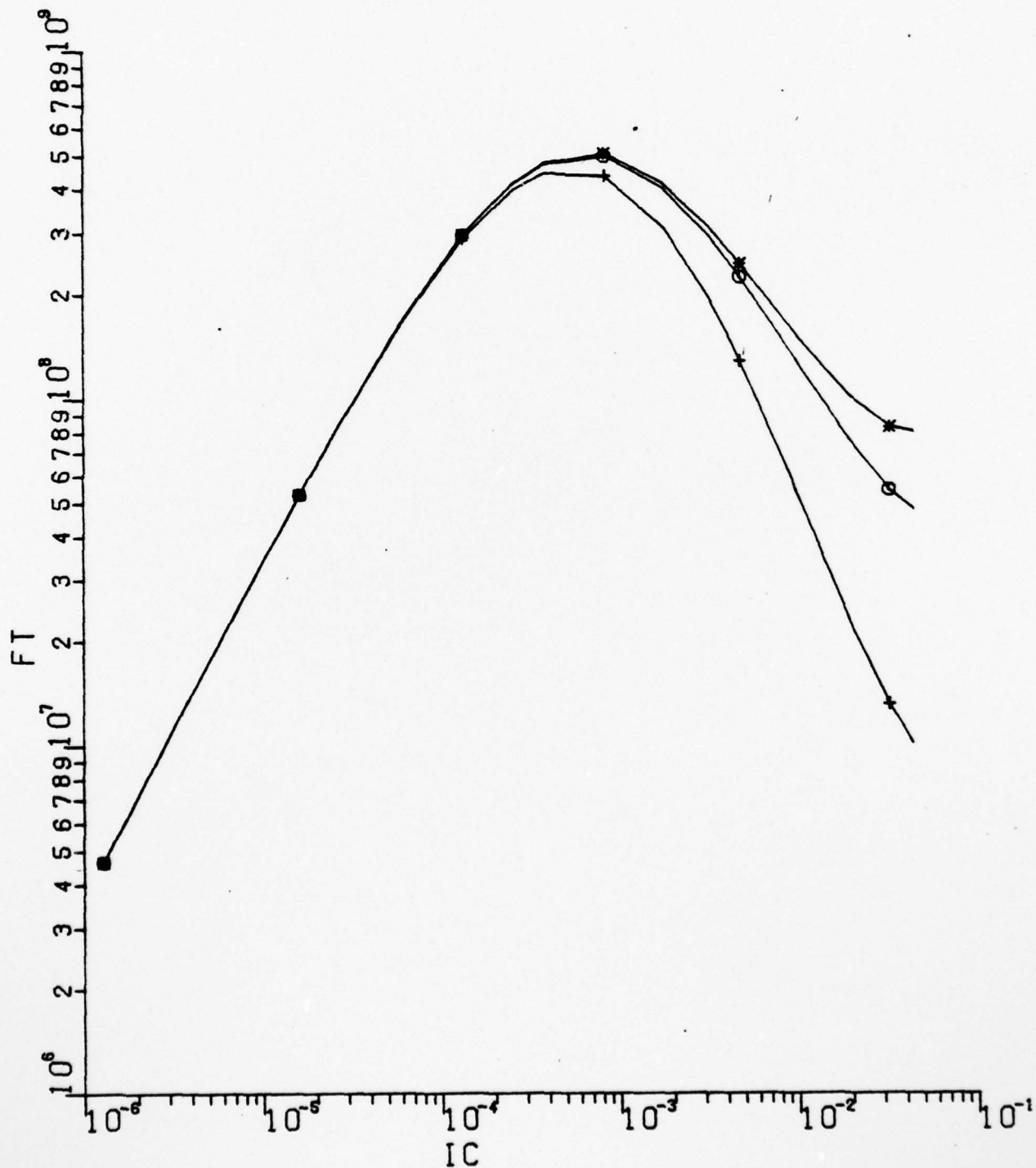
* --	RBO	=	9.000E+01
+ --	RBO	=	9.000E-01
0 --	RBO	=	9.000E+00



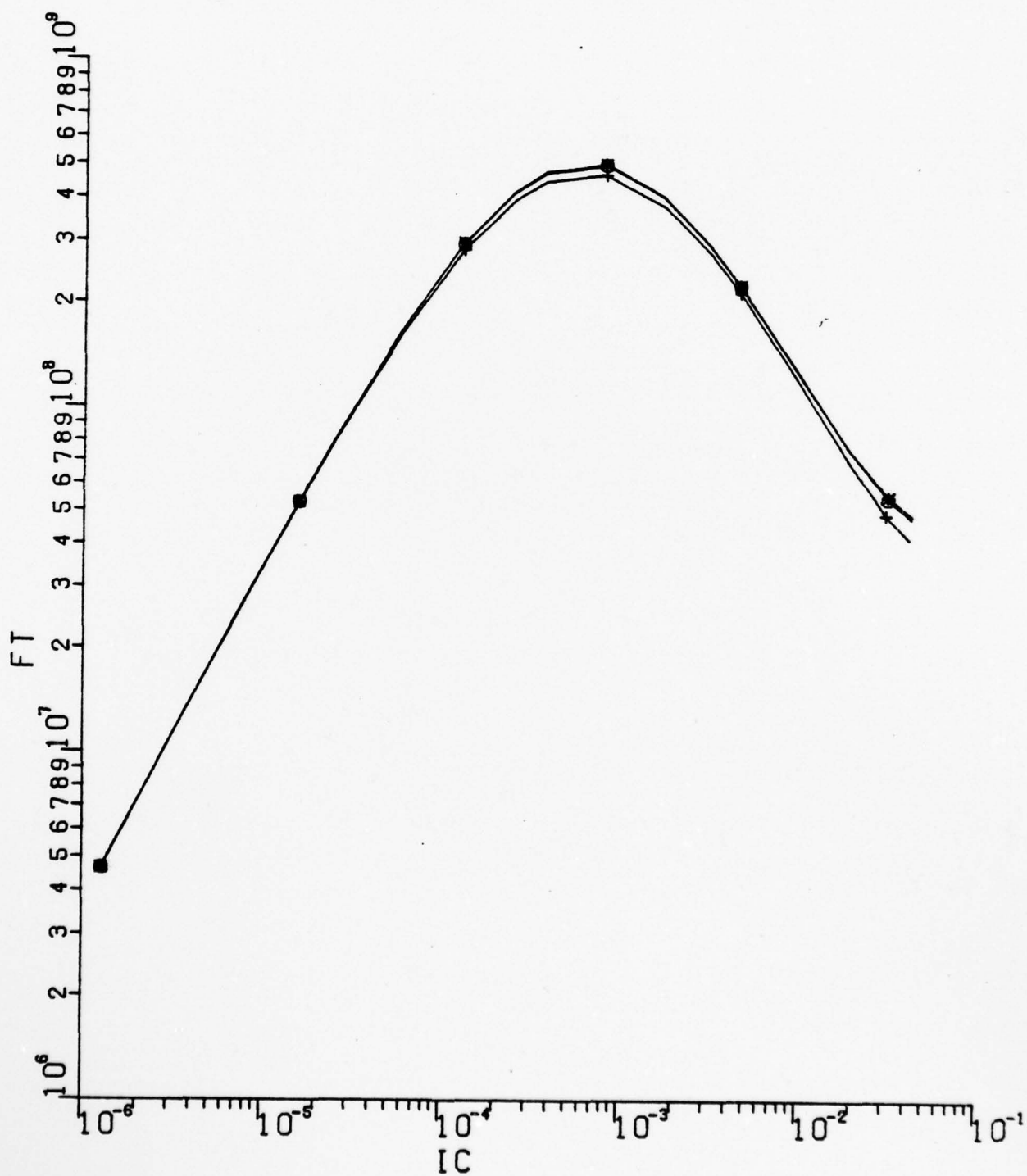
* --	RBB	=	1.500E+01
+ --	RBB	=	5.000E+02
0 --	RBB	=	1.500E+02



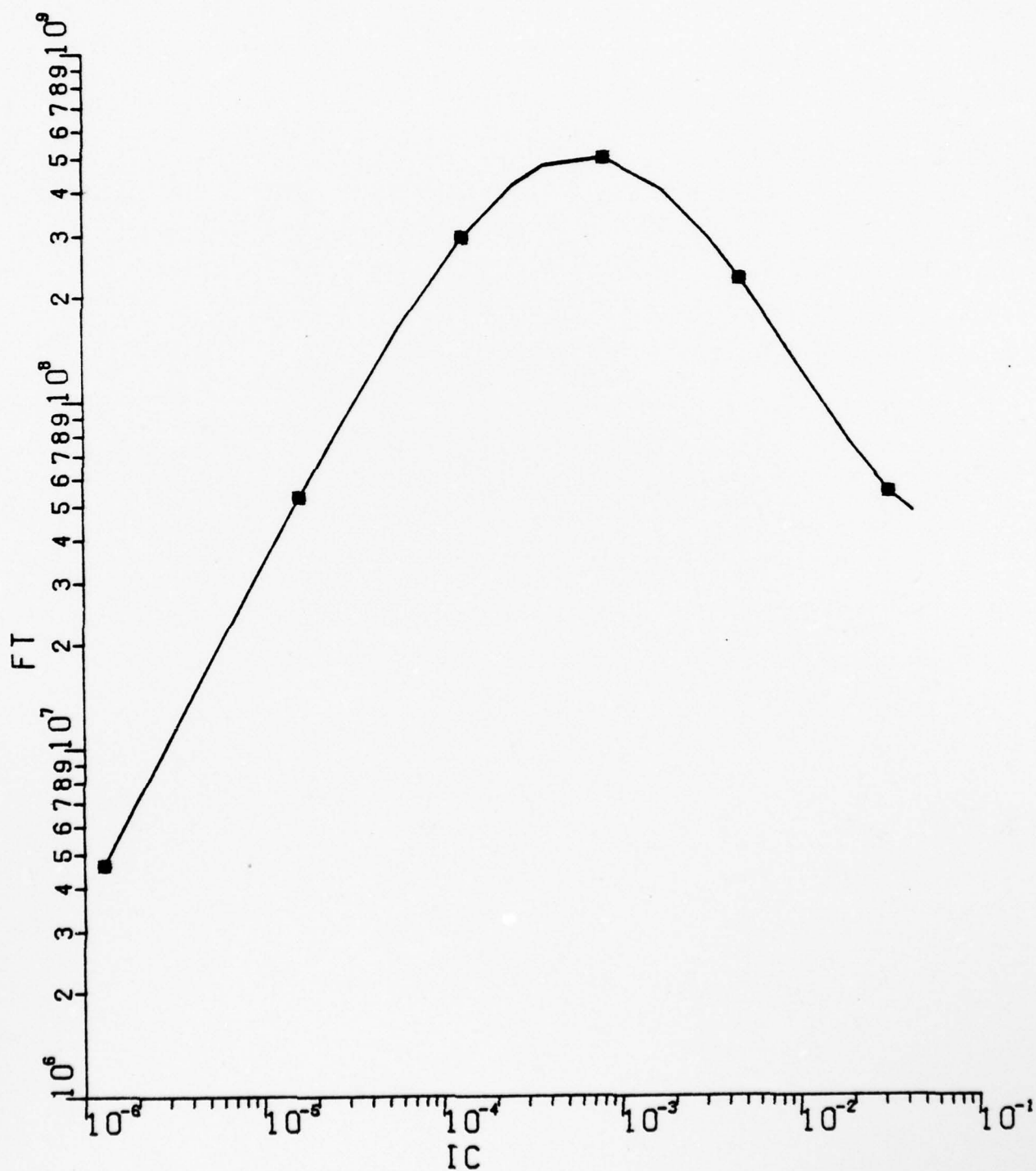
* --	RE*	=	1.000E-02
+ --	RE*	=	5.000E+00
o --	RE*	=	5.000E-01



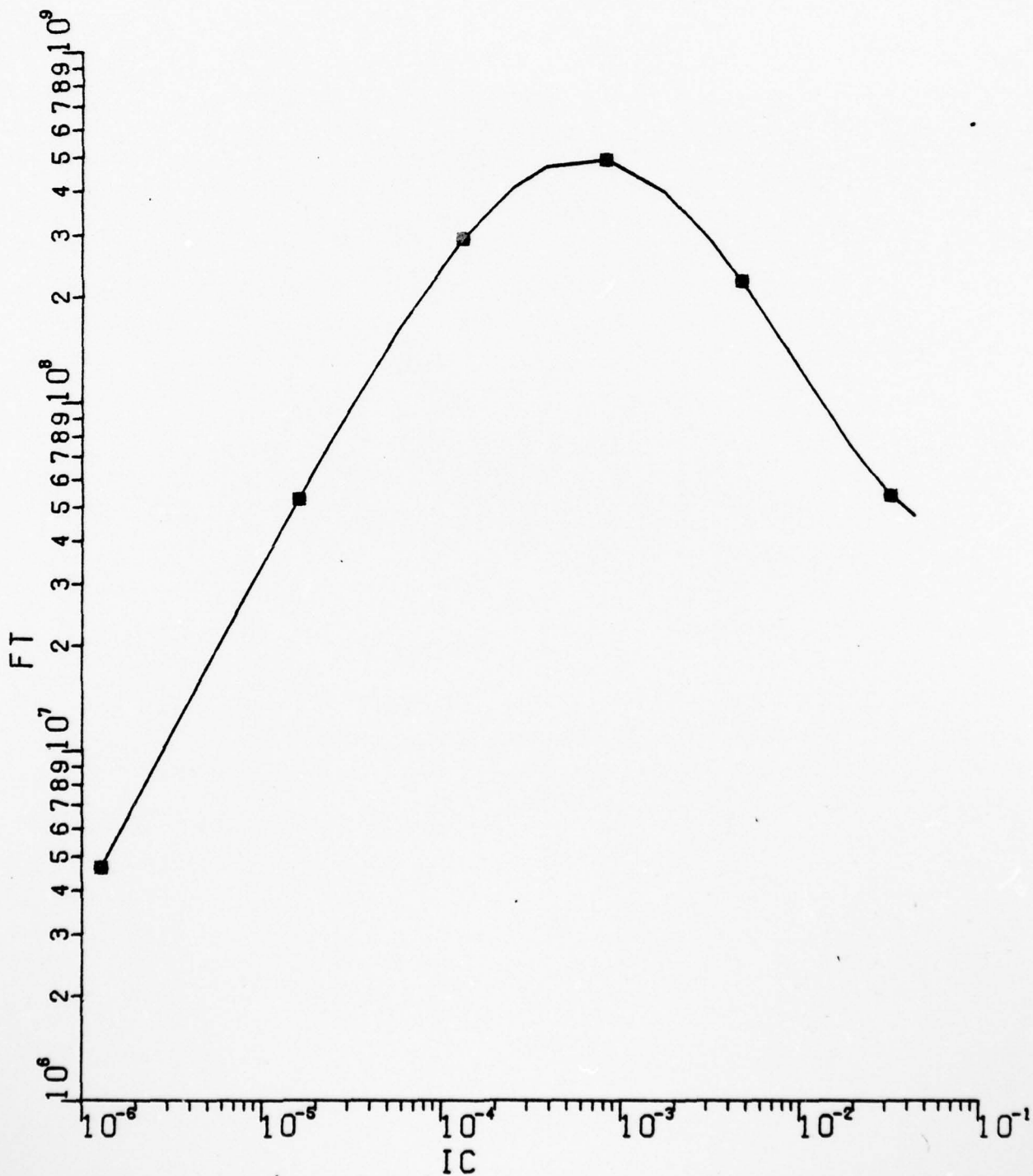
* --	RCO	=	1.000E+00
+ --	RCO	=	5.000E+01
0 --	RCO	=	5.000E+00



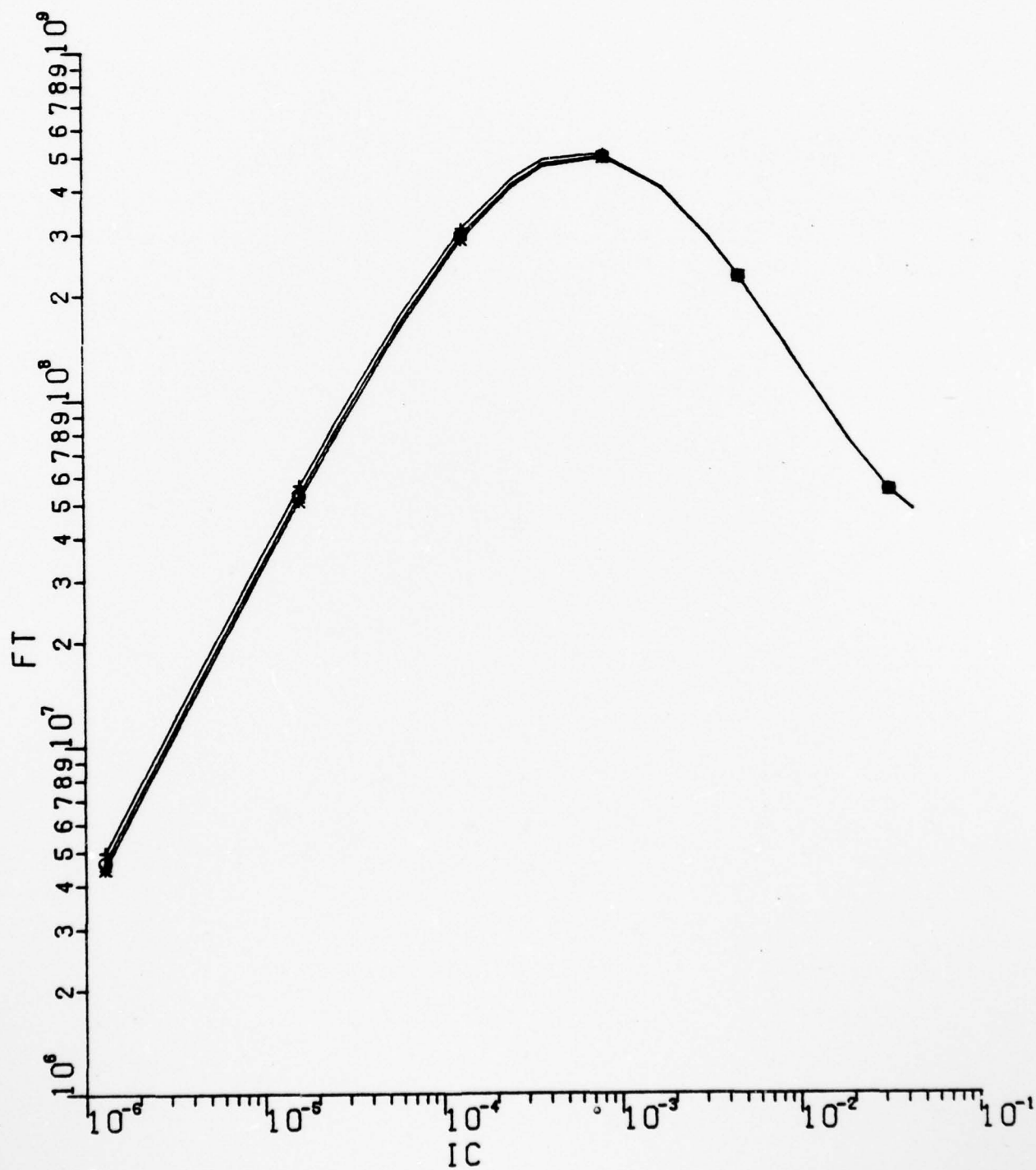
* --	PC	=	6.000E-03
+ --	PC	=	1.000E-03
0 --	PC	=	3.250E-03



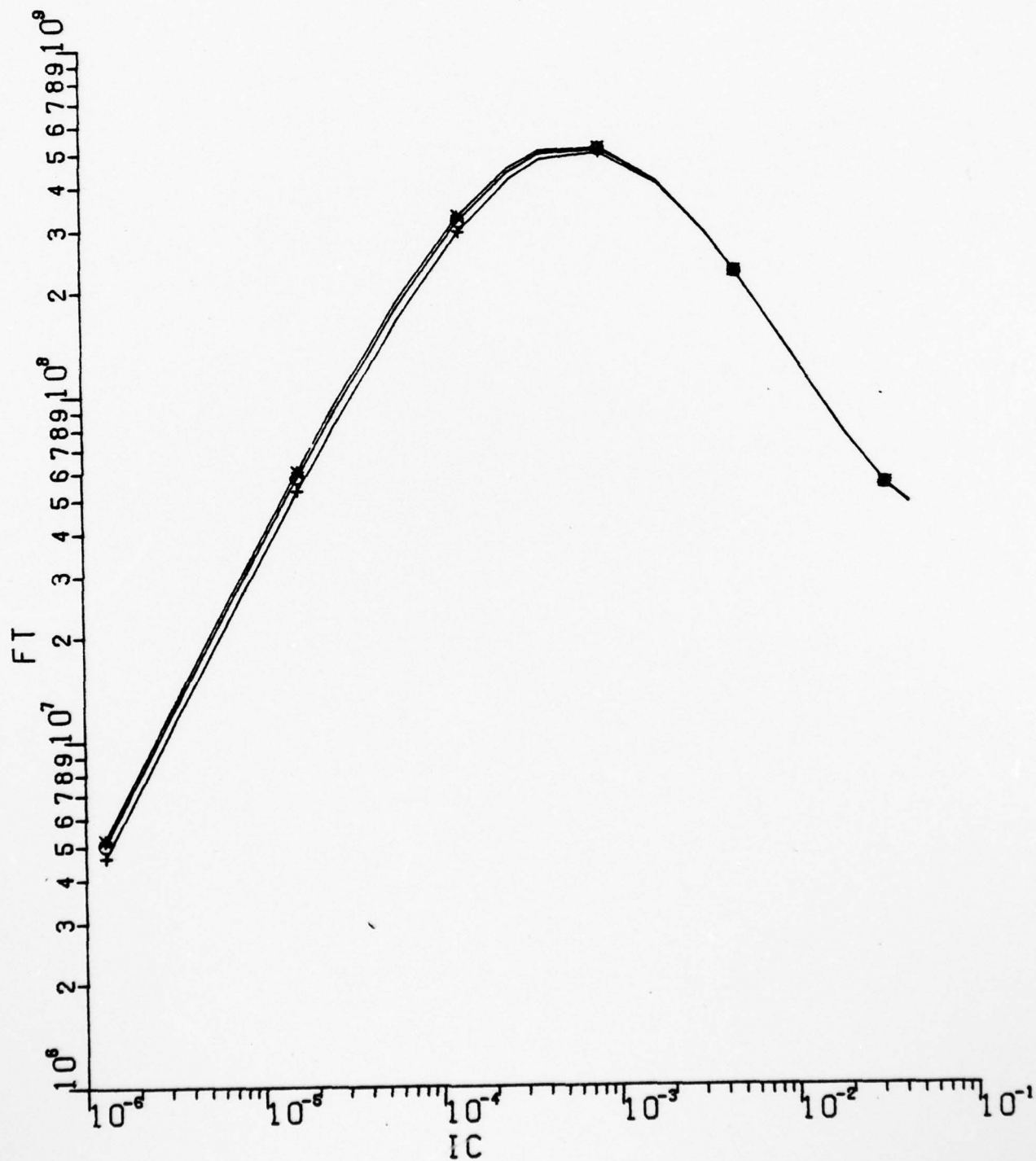
*	--	BS	=	2.500E-01
+	--	BS	=	5.000E-01
0	--	BS	=	3.330E-01



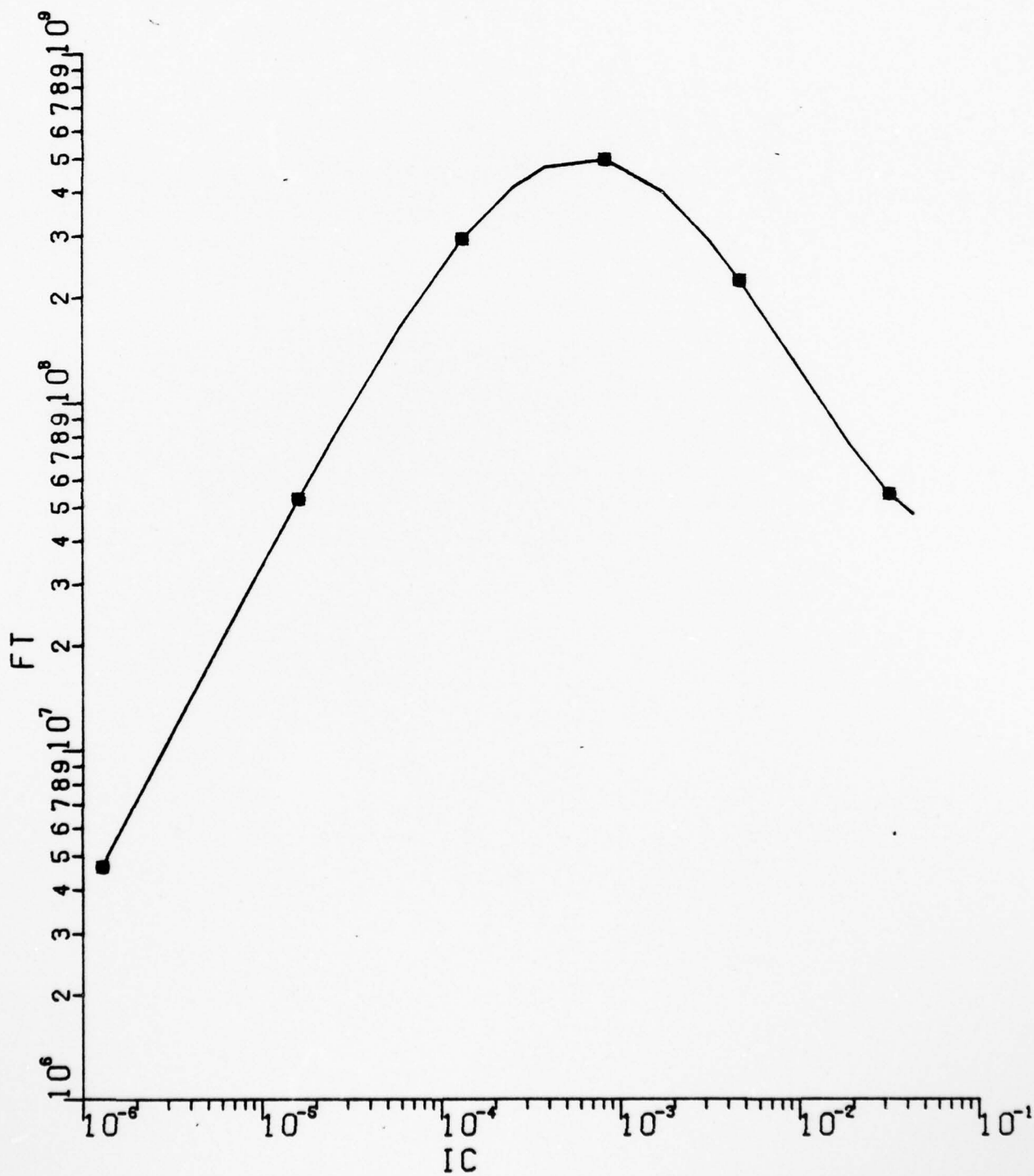
*	--	BC	=	2.500E-01
+	--	BC	=	5.000E-01
0	--	BC	=	3.333E-01



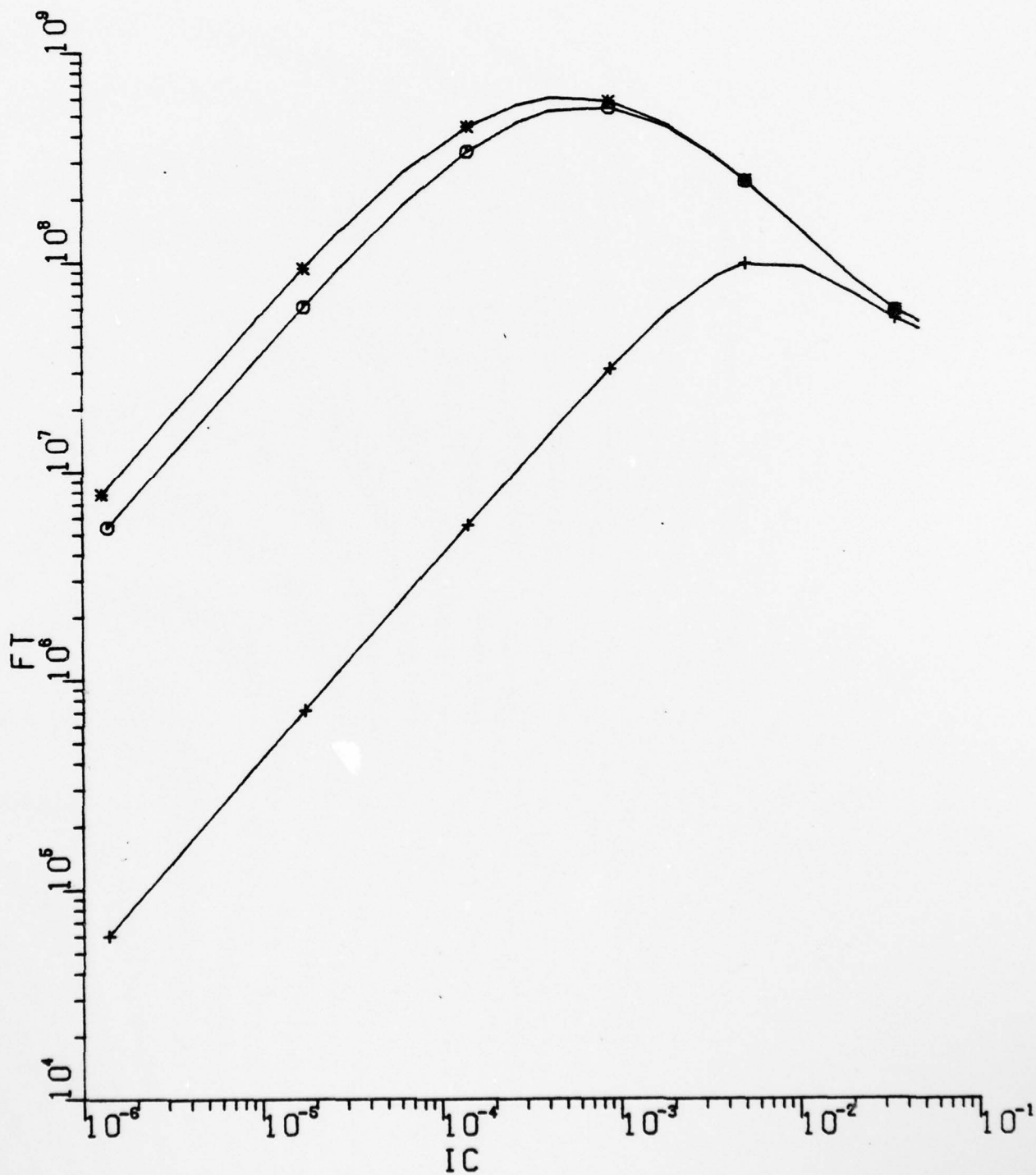
■ --	BE	=	2.500E-01
+ --	BE	=	5.000E-01
0 --	BE	=	3.333E-01



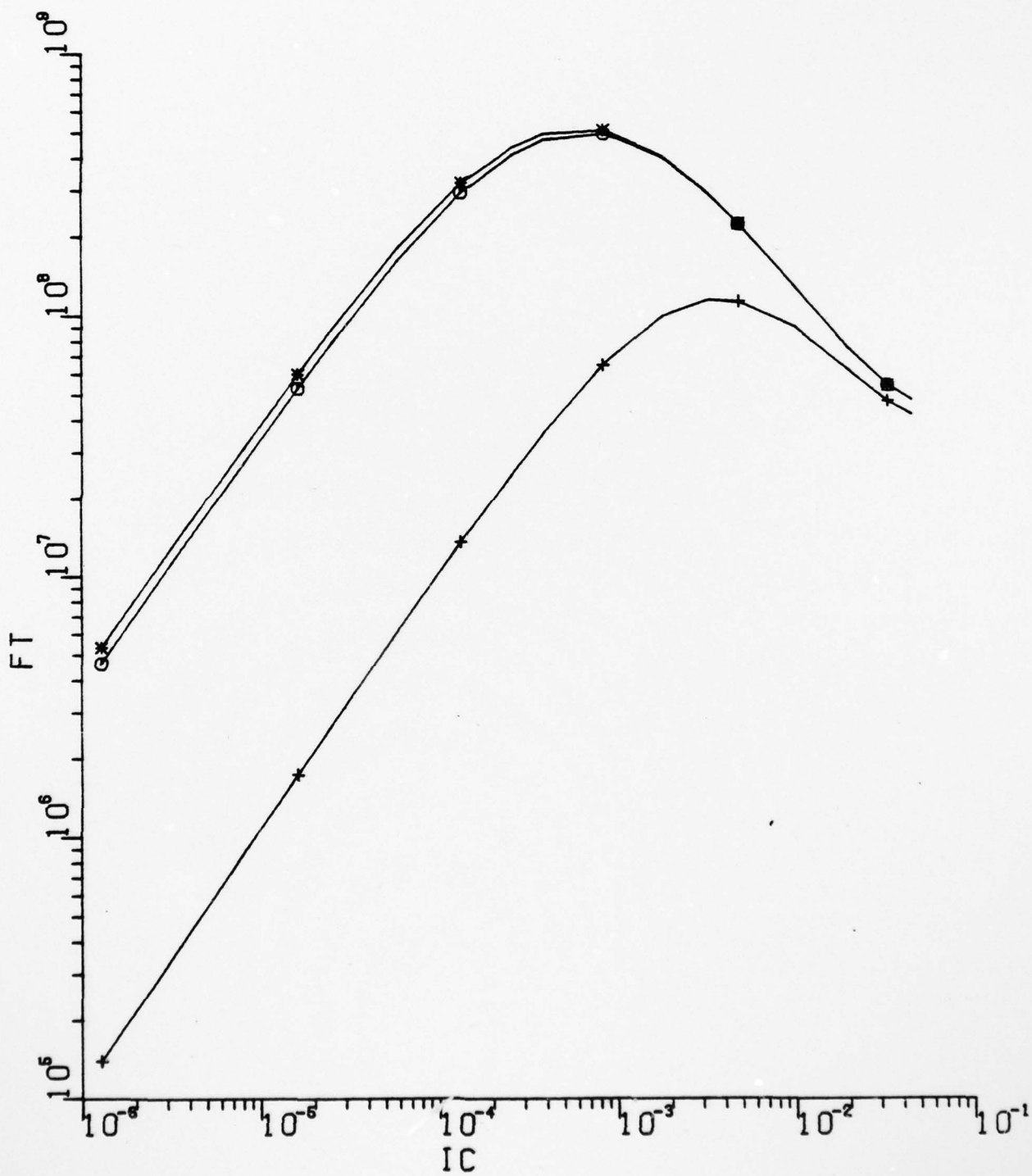
■	--	CS0	=	4.000E-13
+	--	CS0	=	1.000E-11
0	--	CS0	=	2.000E-12



* --	CE0	=	4.000E-13
+ --	CE0	=	1.000E-10
0 --	CE0	=	8.000E-13



* --	CC0	=	4.000E-13
+ --	CC0	=	1.000E-10
o --	CC0	=	8.000E-13



AD-A062 790

TRW DEFENSE AND SPACE SYSTEMS GROUP REDONDO BEACH CALIF F/G 9/1
PROCESS-ORIENTED, HIGH-INJECTION CIRCUIT MODELS FOR INTEGRATED --ETC(U)
JAN 78 J CHOMA

N00014-77-C-0043

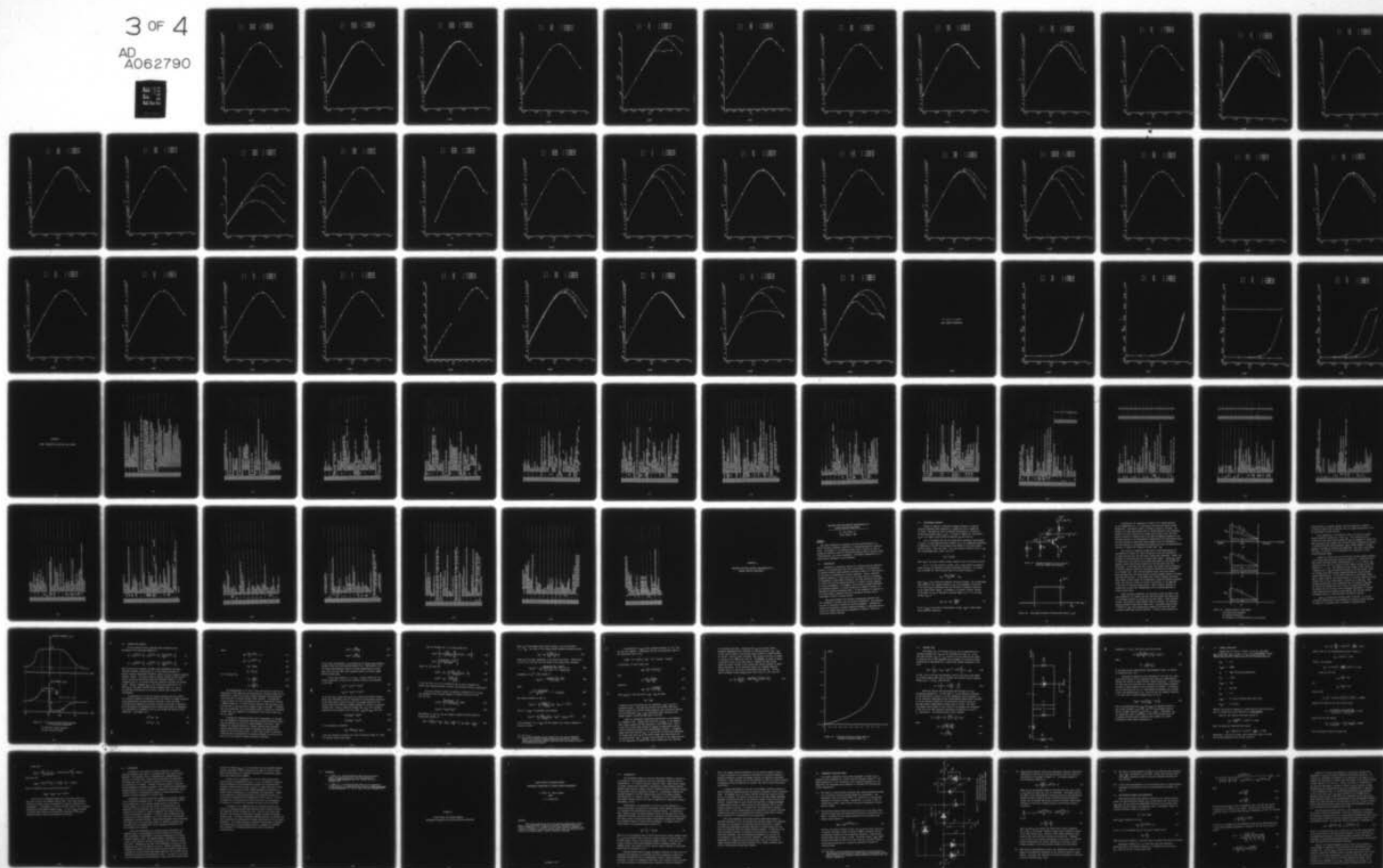
UNCLASSIFIED

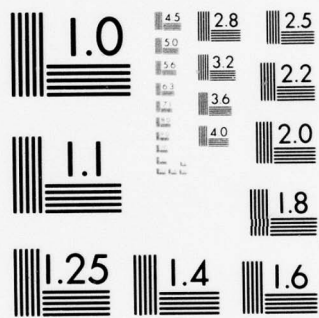
TRW-78.4734.7-023-PT-2-V0

NL

3 OF 4

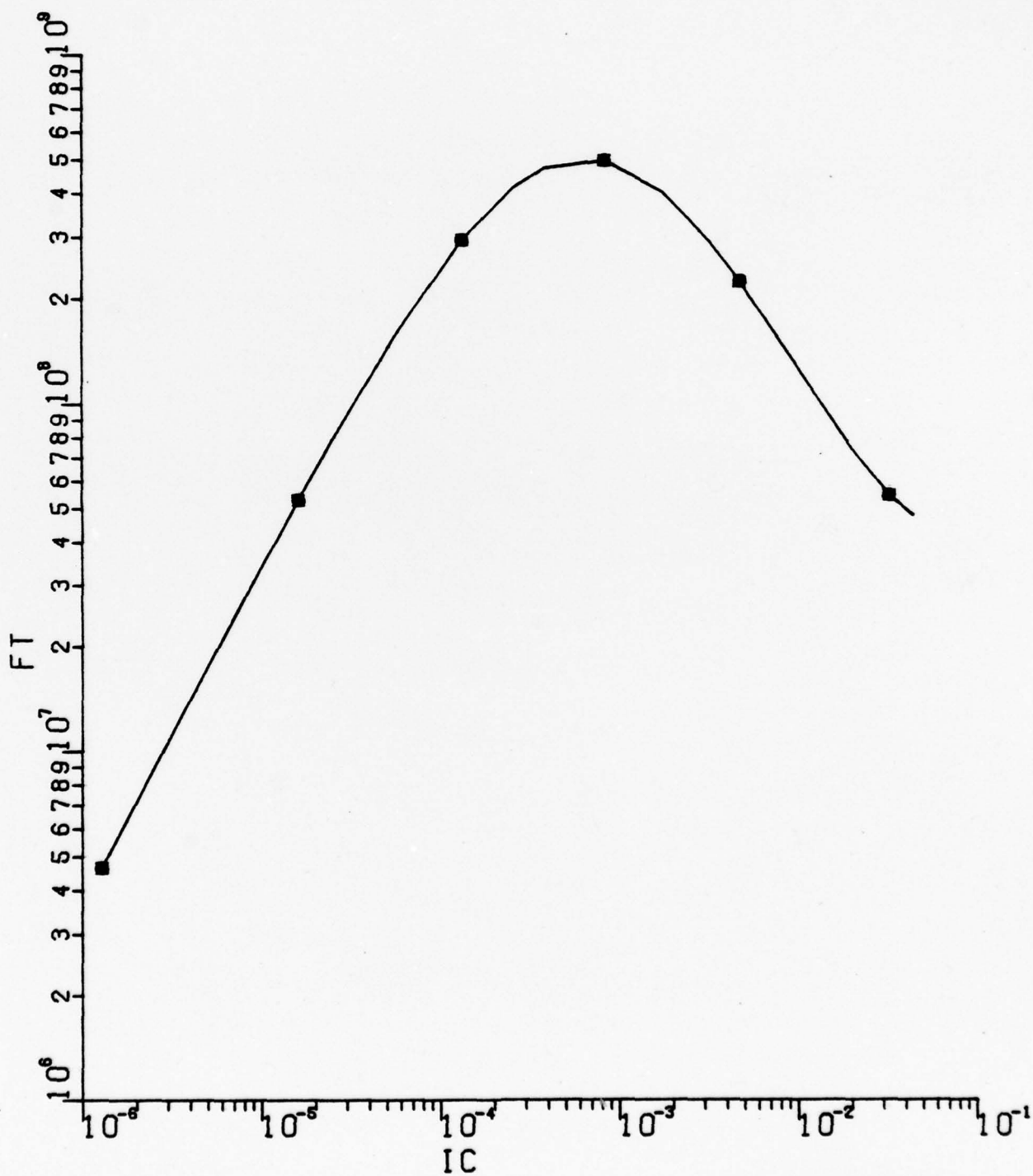
AD
A062790



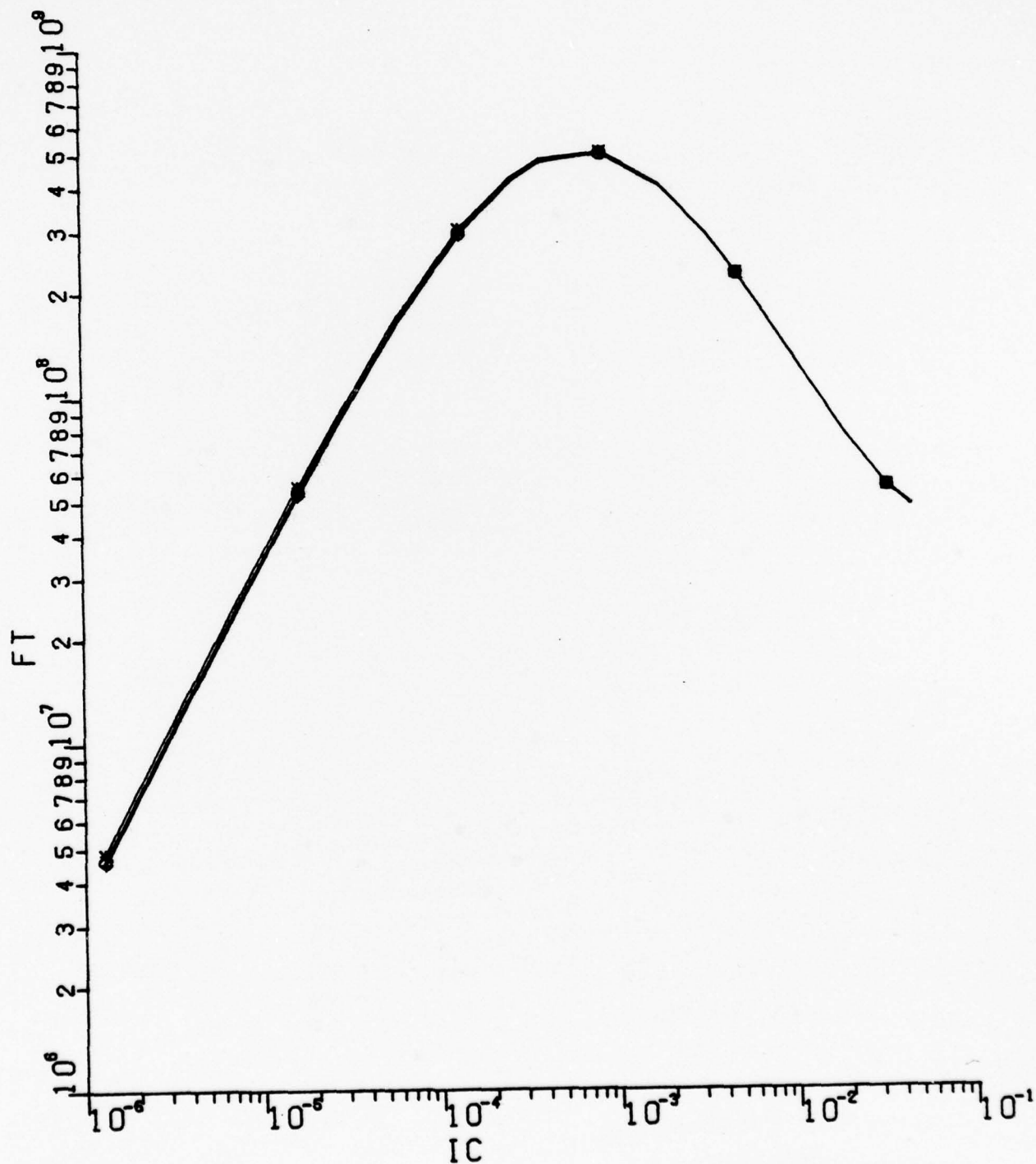


MICROCOPY RESOLUTION TEST CHART
NATIONAL BUREAU OF STANDARDS-1963-A

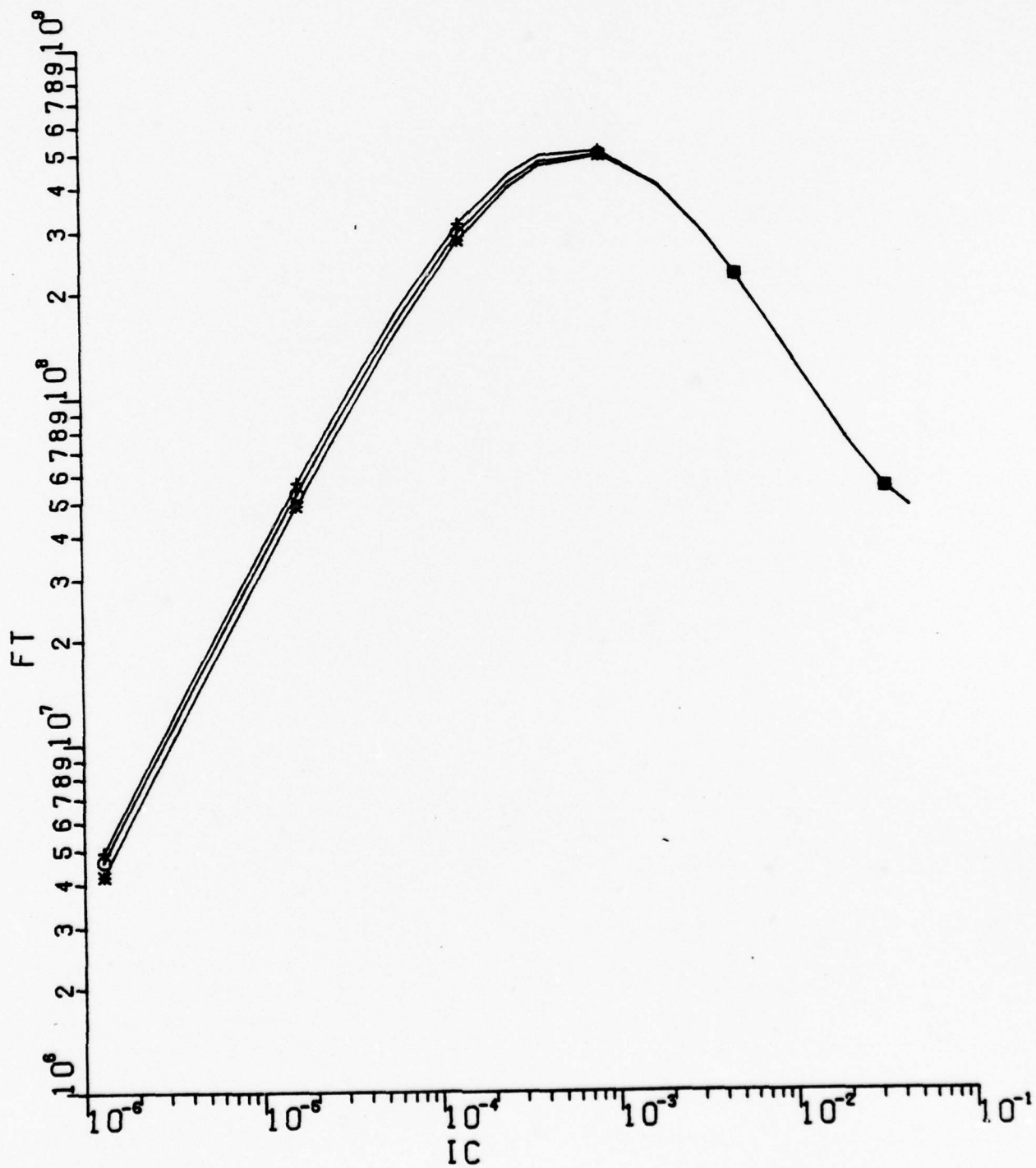
* --	PHISS	=	5.000E-01
+ --	PHISS	=	1.200E+00
0 --	PHISS	=	9.000E-01



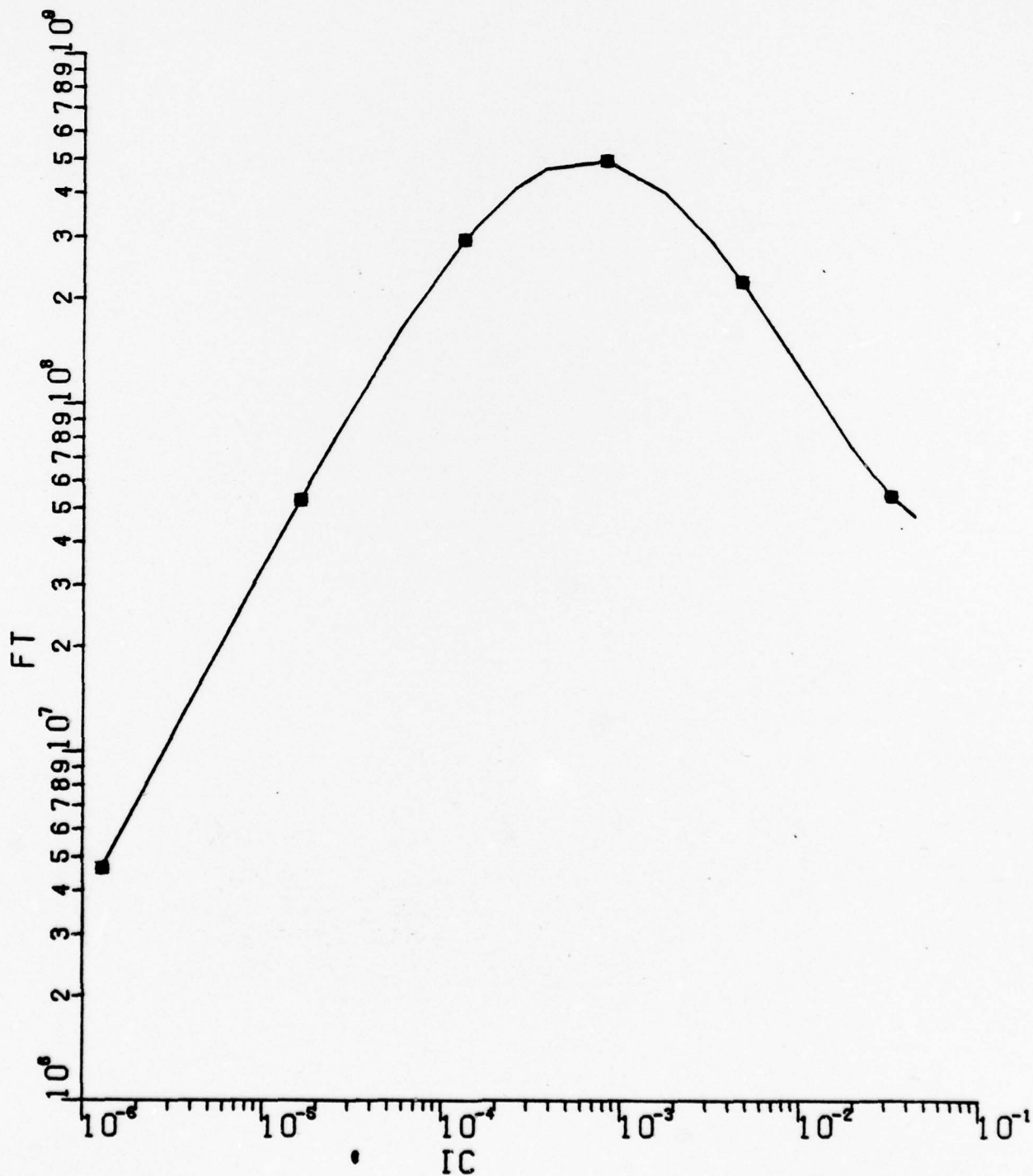
■ --	PHICO	=	5.000E-01
+ --	PHICO	=	1.200E+00
0 --	PHICO	=	9.000E-01



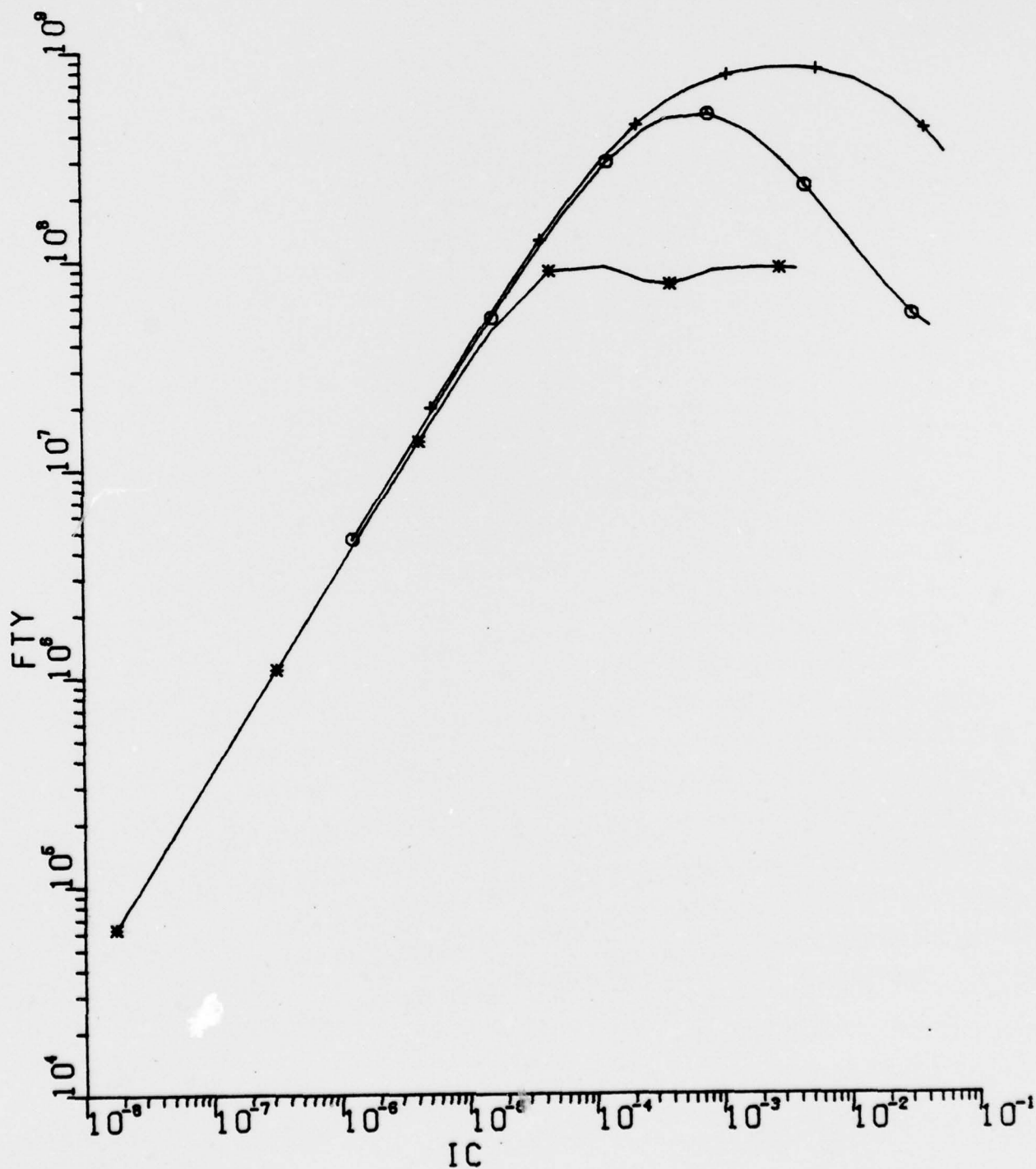
* --	PHIE0	=	5.000E-01
+ --	PHIE0	=	1.500E+00
0 --	PHIE0	=	1.200E+00



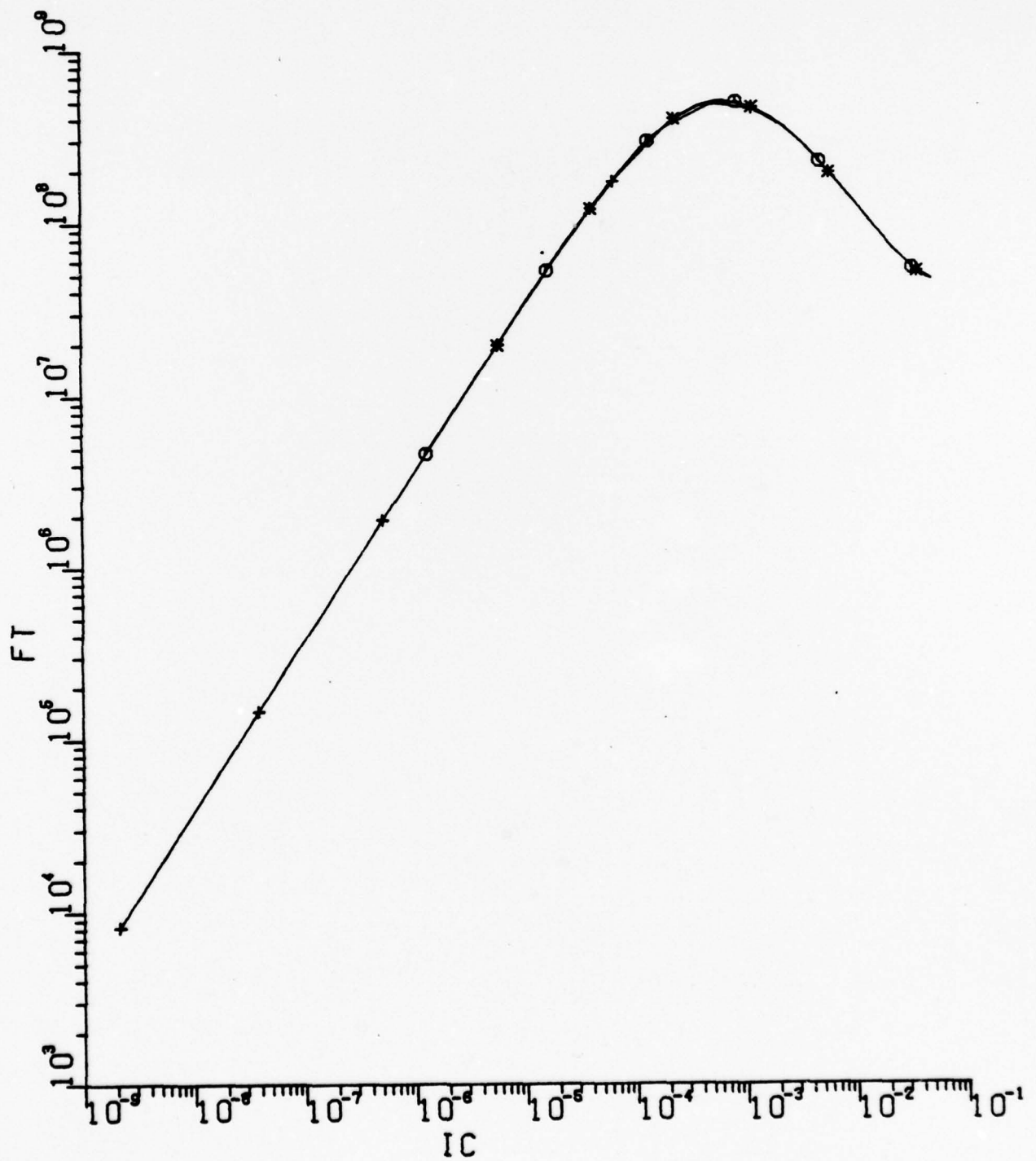
* --	ISR	=	3.000E-13
+ --	ISR	=	3.000E-11
0 --	ISR	=	3.000E-12



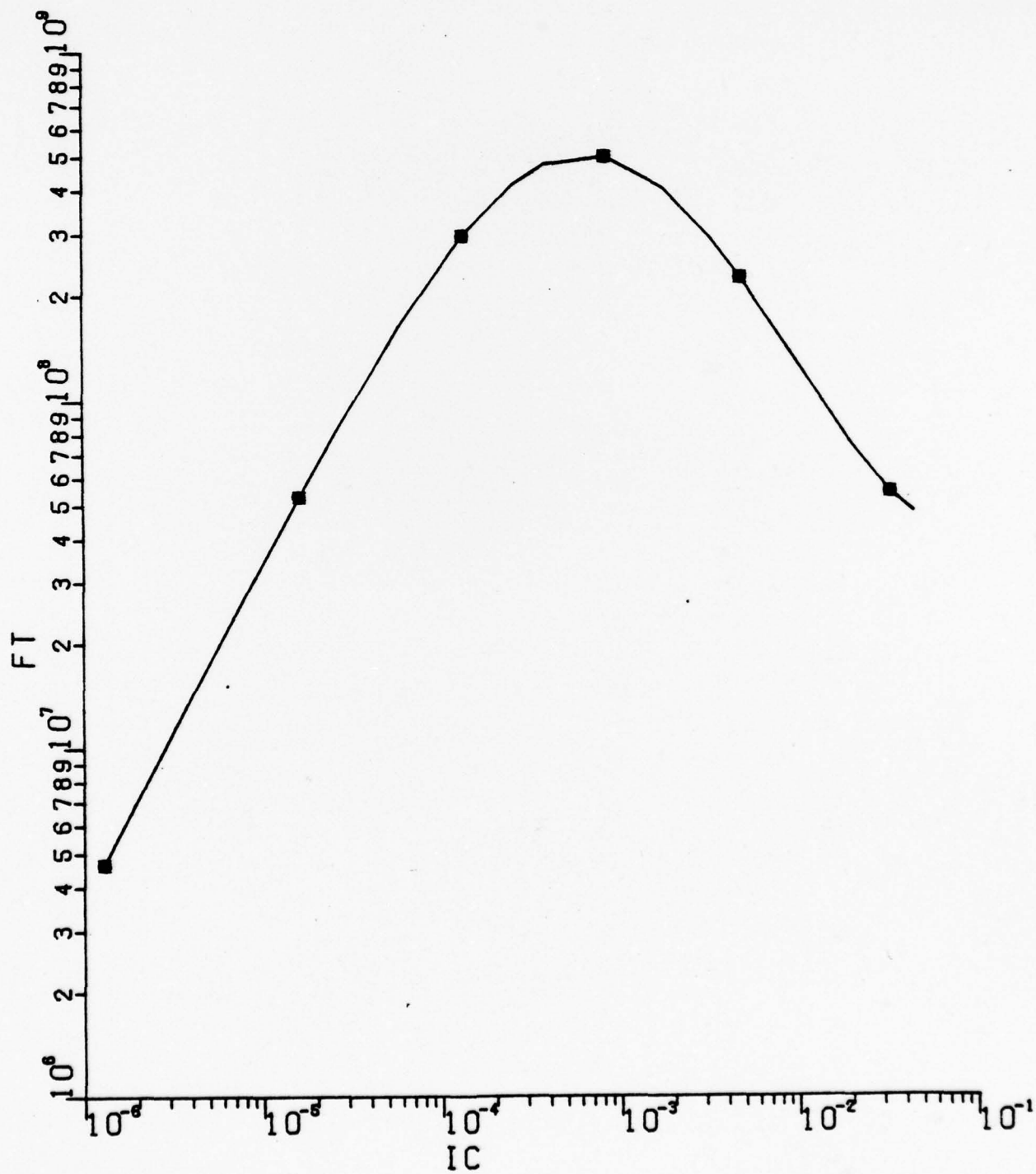
* --	IS	=	3.000E-18
+ --	IS	=	3.000E-14
0 --	IS	=	3.200E-16



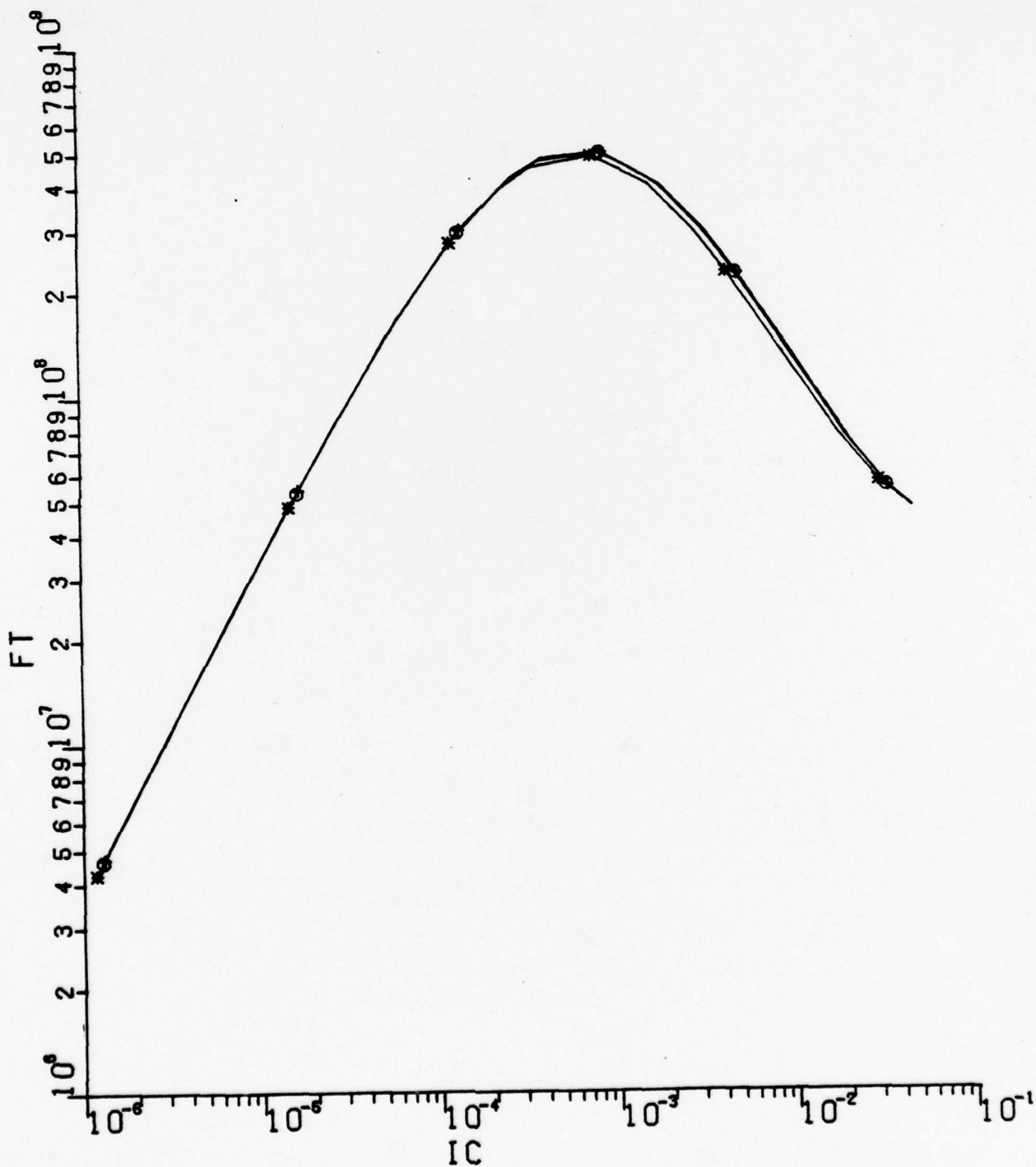
■ --	IER	=	3.000E-16
+ --	IER	=	3.000E-12
o --	IER	=	3.200E-14

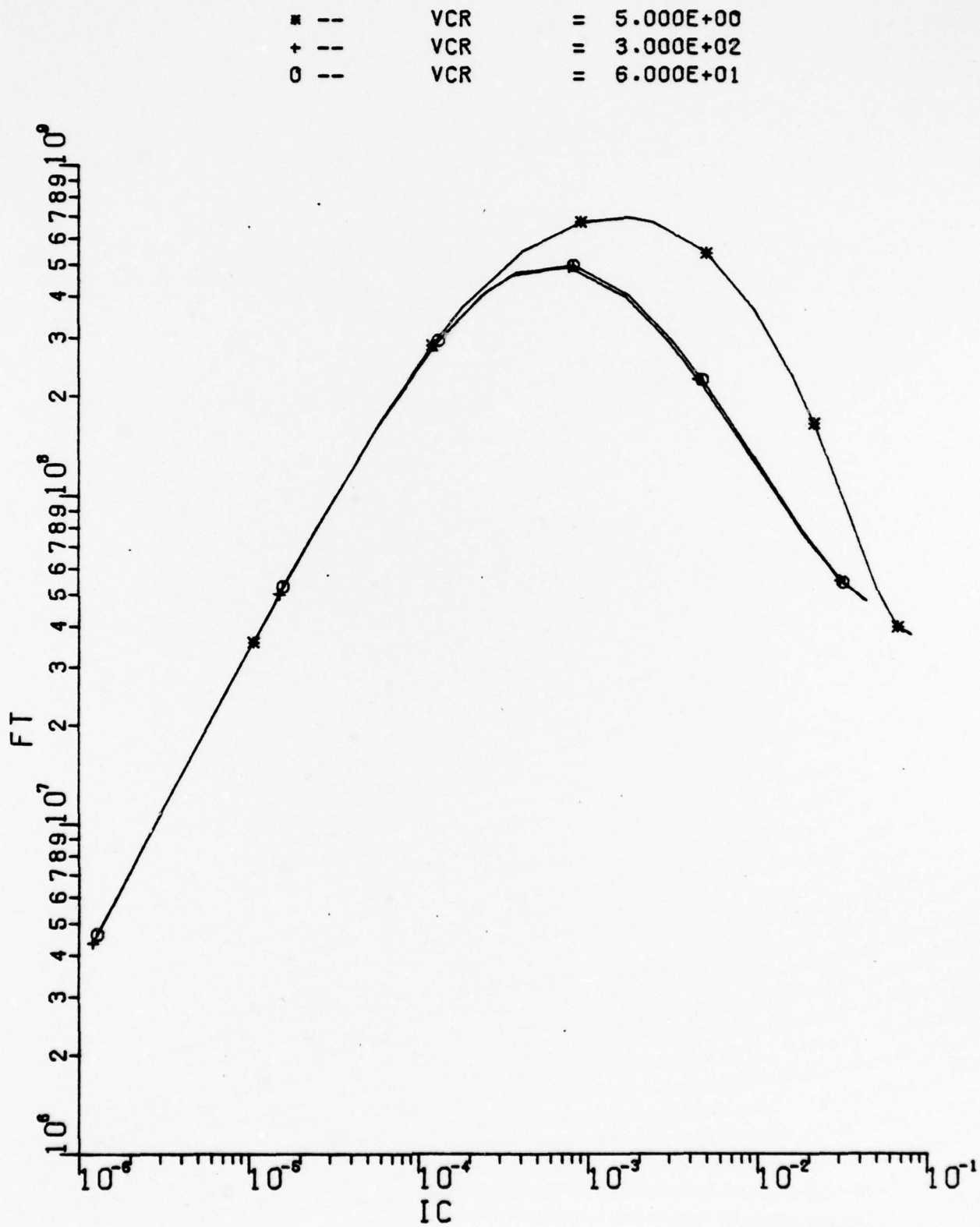


* --	IBR	=	3.000E-15
+ --	IBR	=	3.000E-11
0 --	IBR	=	3.000E-13

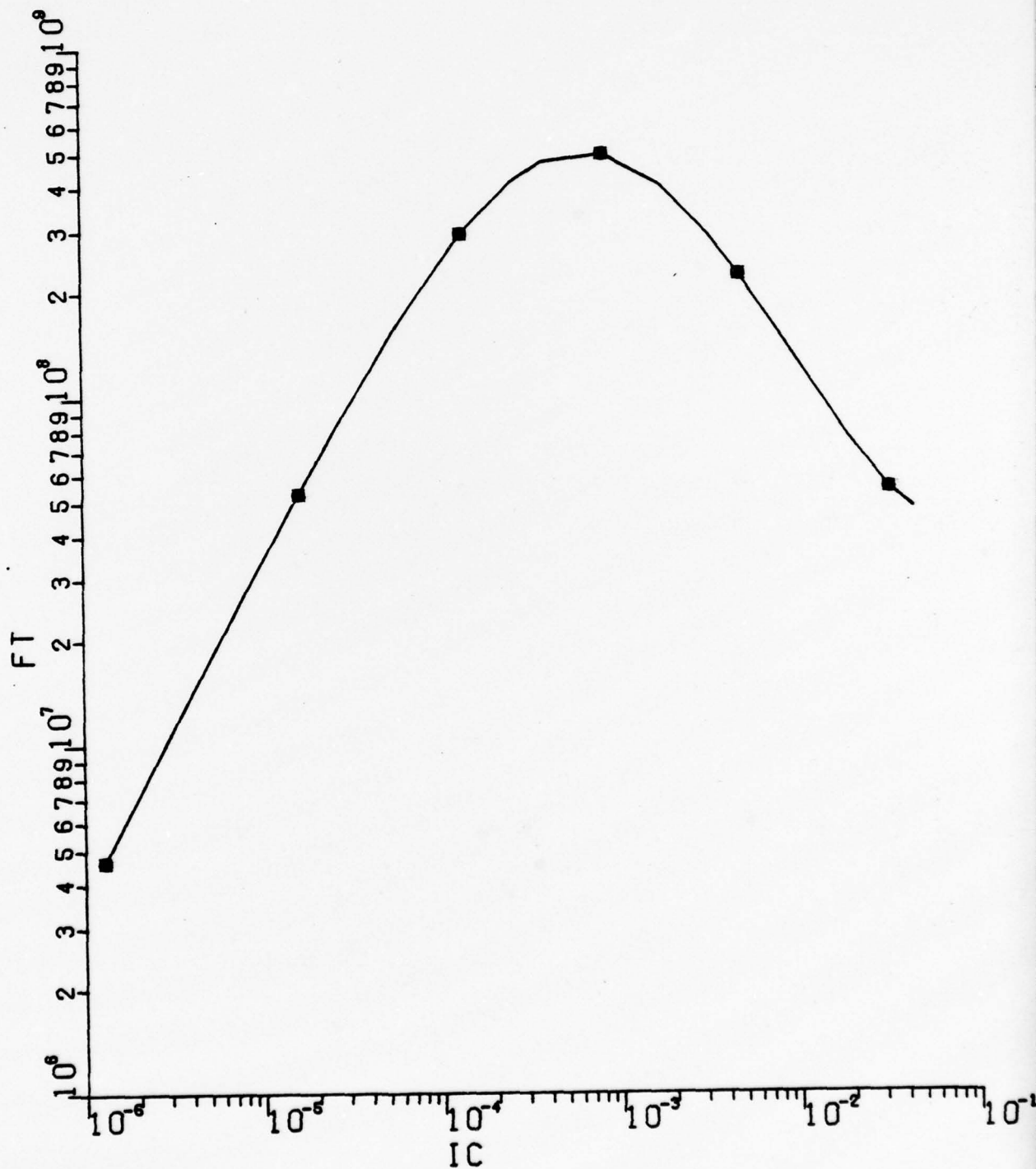


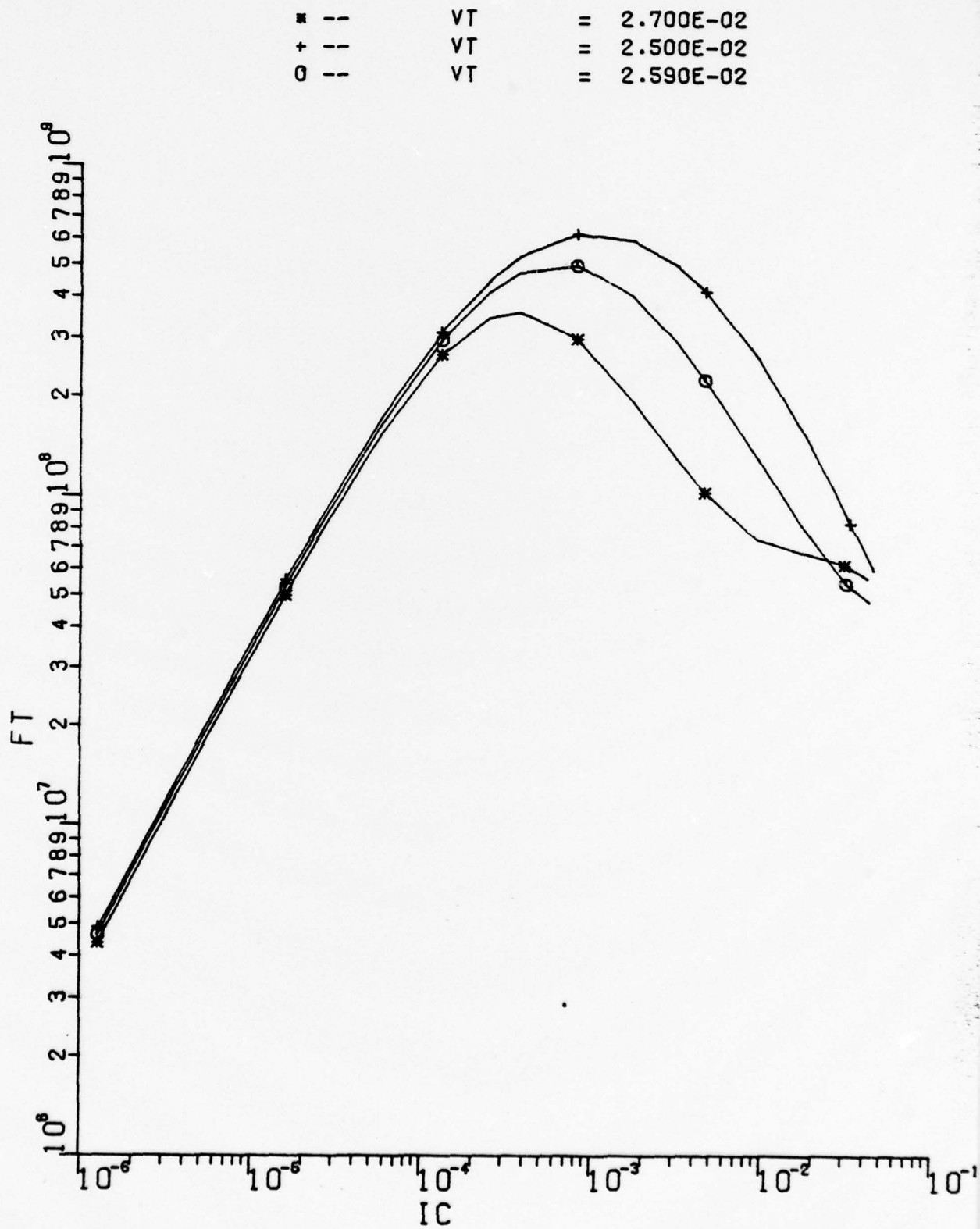
*	--	VER	=	5.000E+00
+	--	VER	=	5.000E+01
0	--	VER	=	2.000E+01



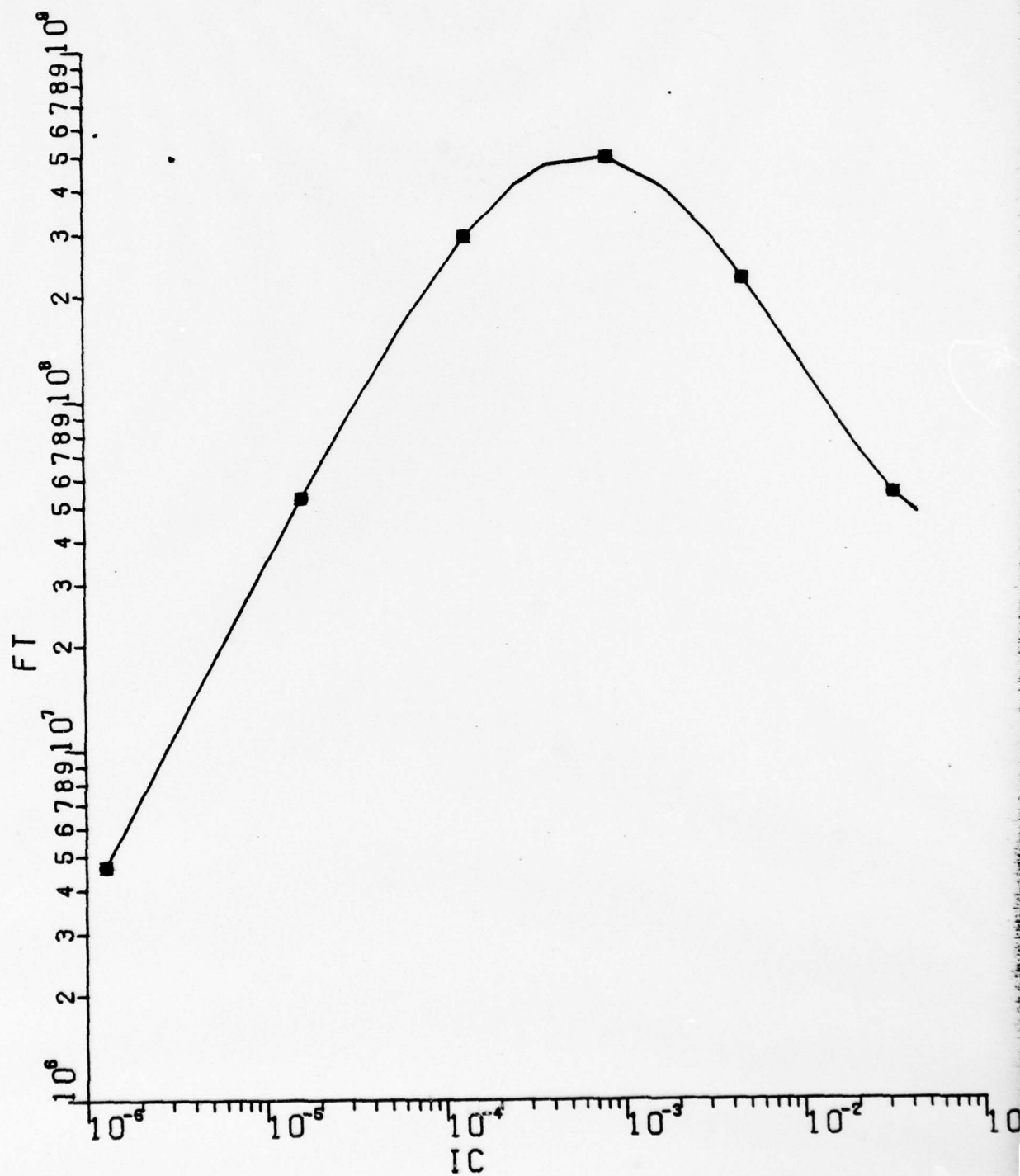


*	--	NC	=	8.000E-01
+	--	NC	=	2.300E+00
0	--	NC	=	1.800E+00

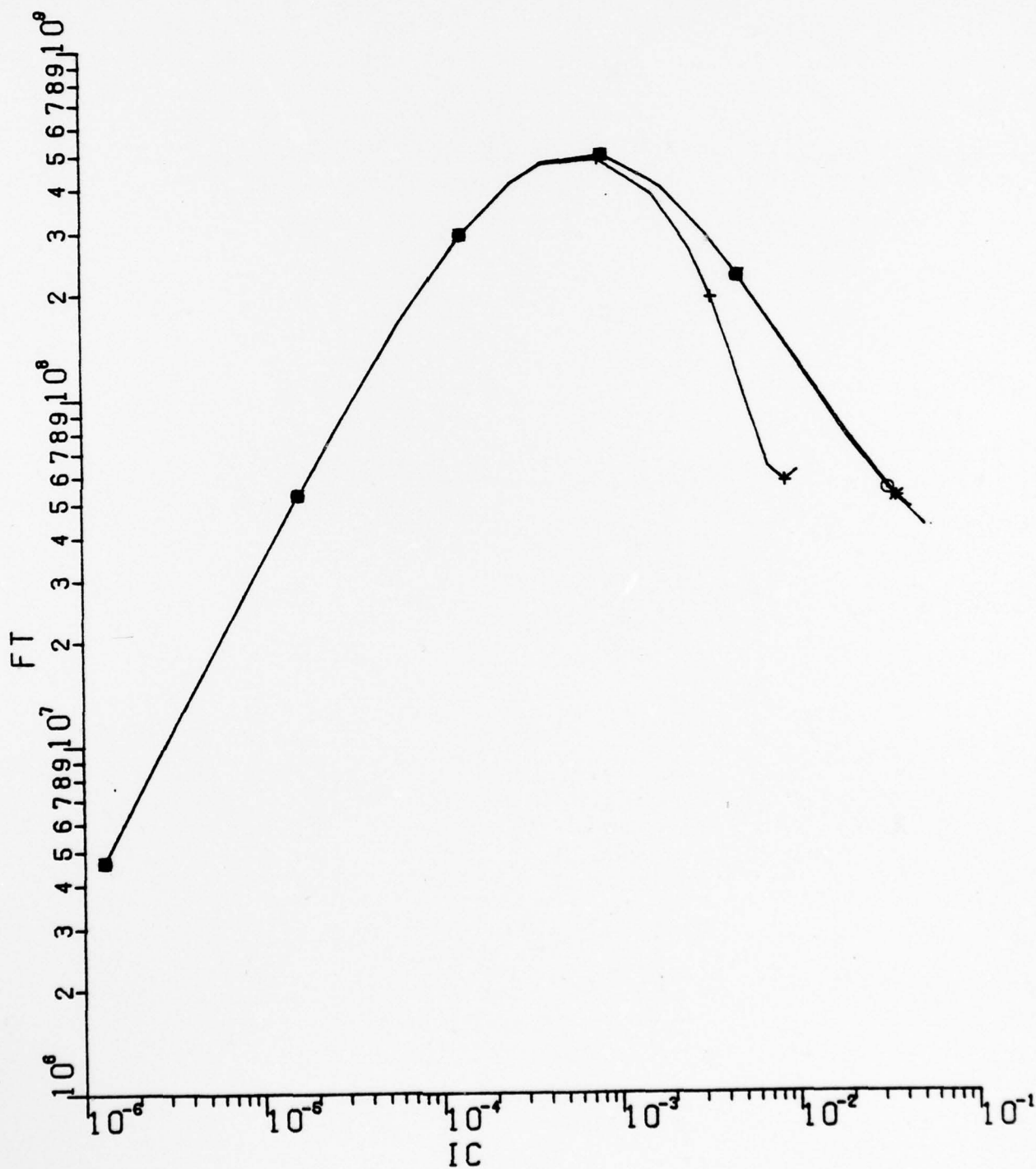




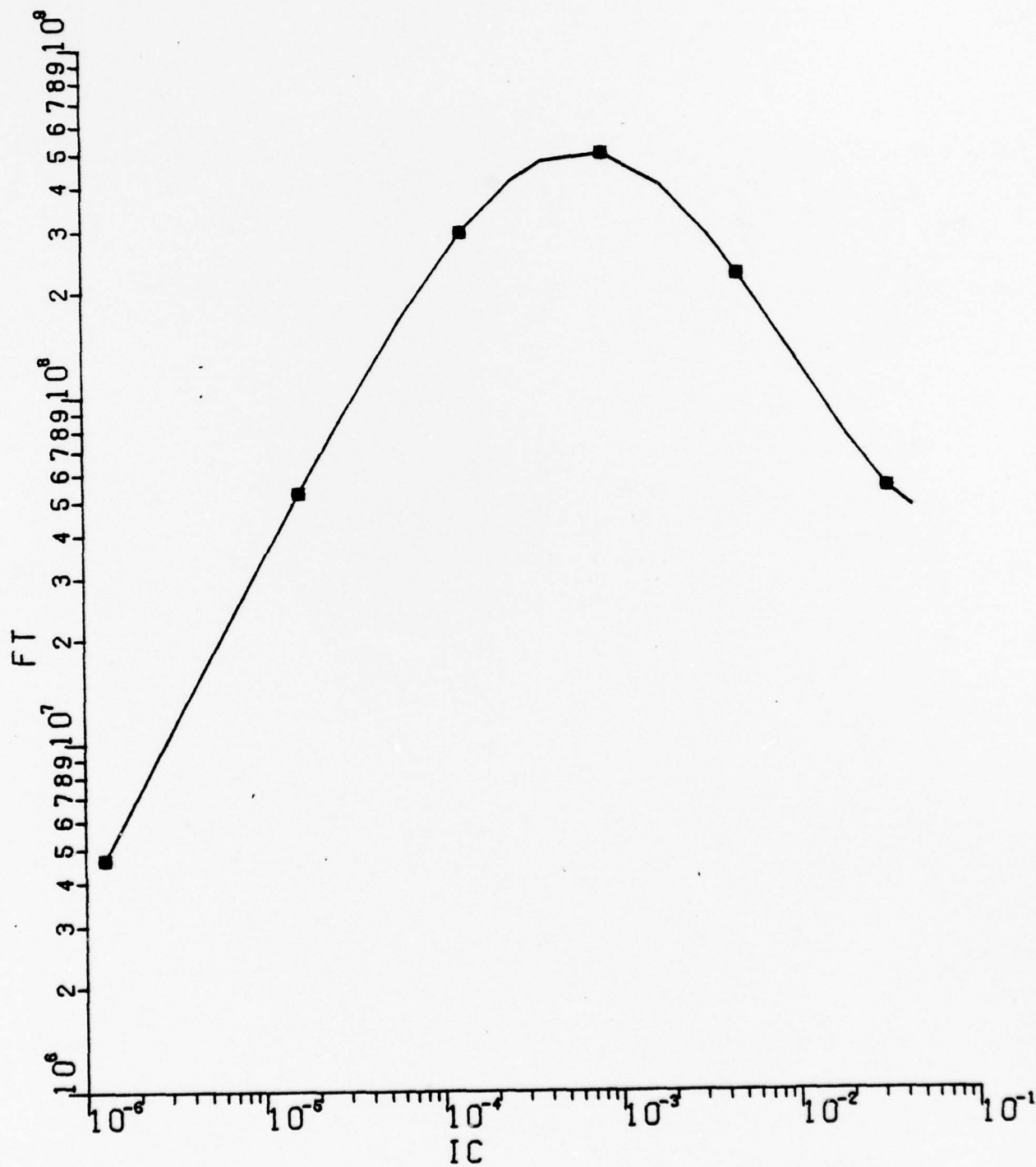
* --	VTS	=	2.500E-02
+ --	VTS	=	2.700E-02
0 --	VTS	=	2.590E-02



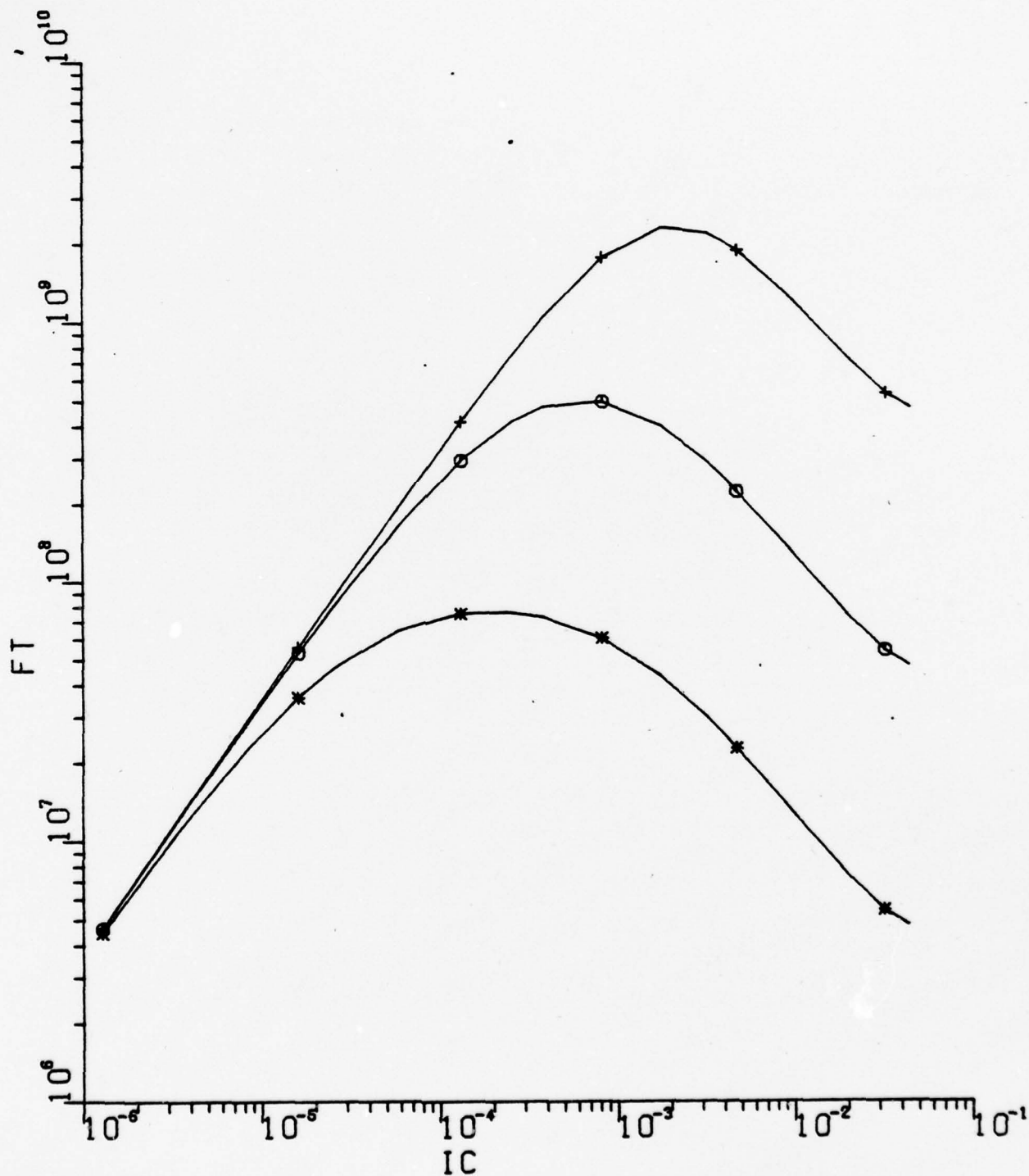
* --	QFN	=	1.500E-18
+ --	QFN	=	1.500E-14
o --	QFN	=	1.500E-16



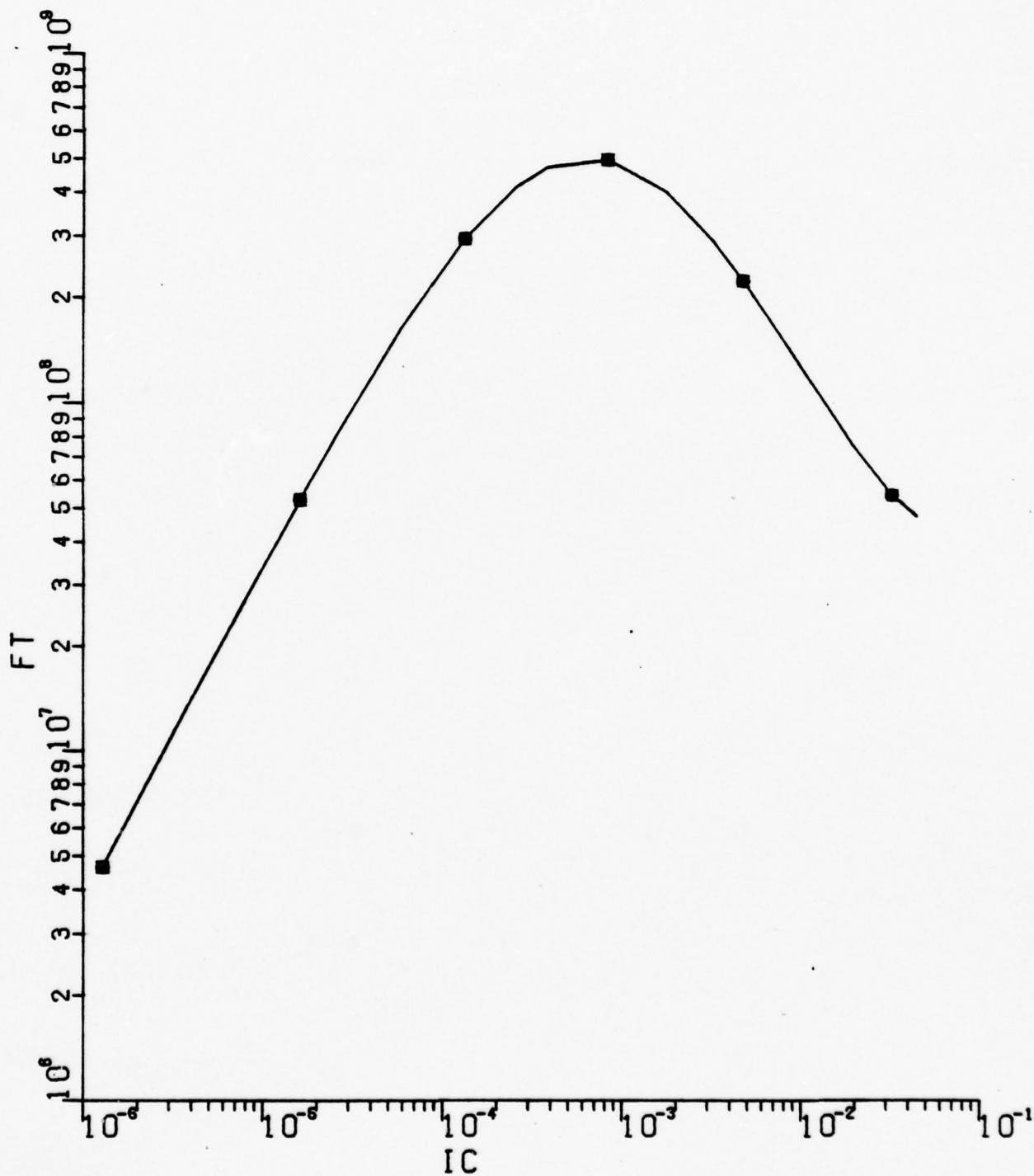
*	--	QRN	=	1.500E-14
+	--	QRN	=	1.500E-10
0	--	QRN	=	1.500E-12



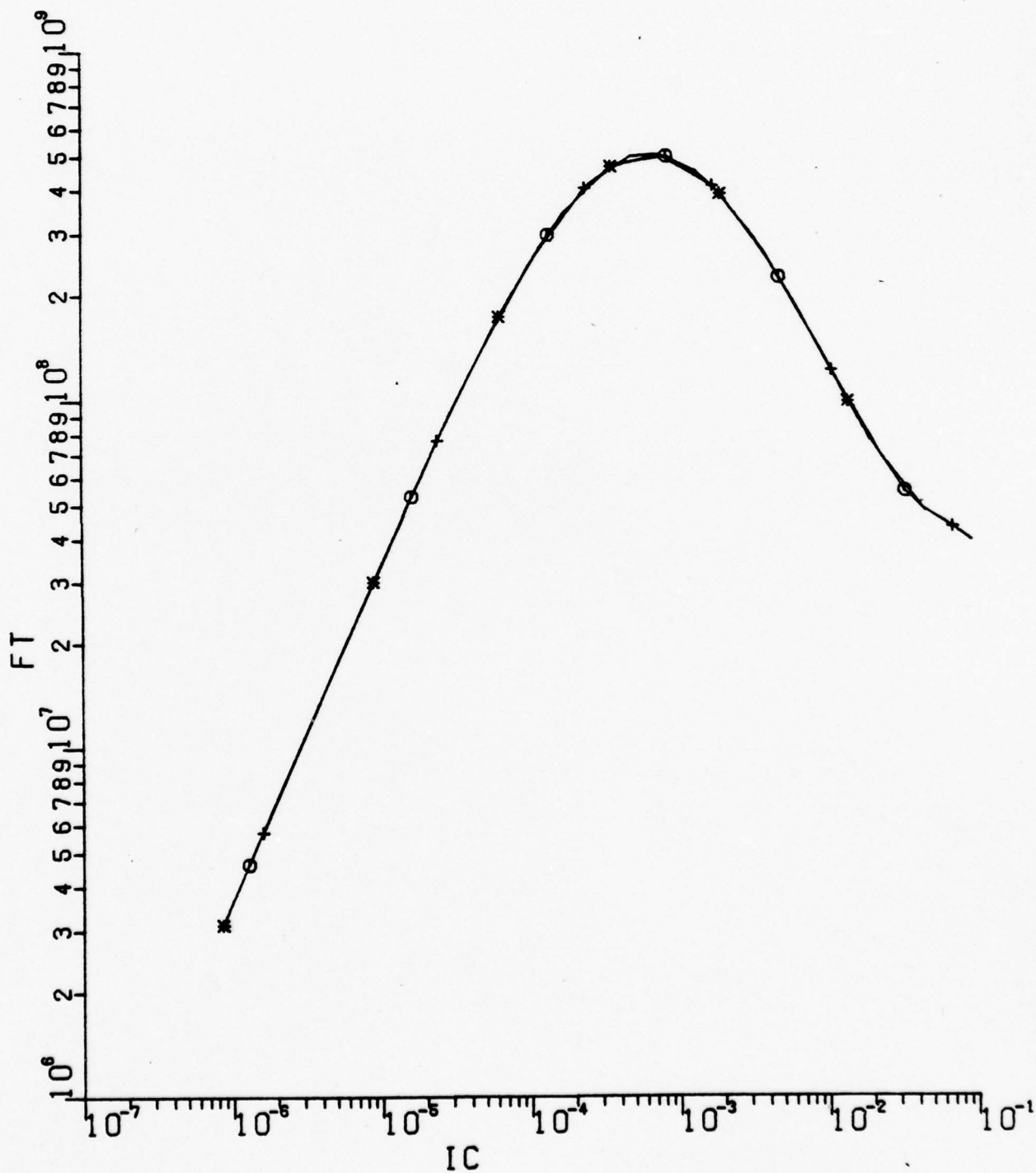
* --	TAUFO	=	1.590E-09
+ --	TAUFO	=	1.590E-11
0 --	TAUFO	=	1.590E-10



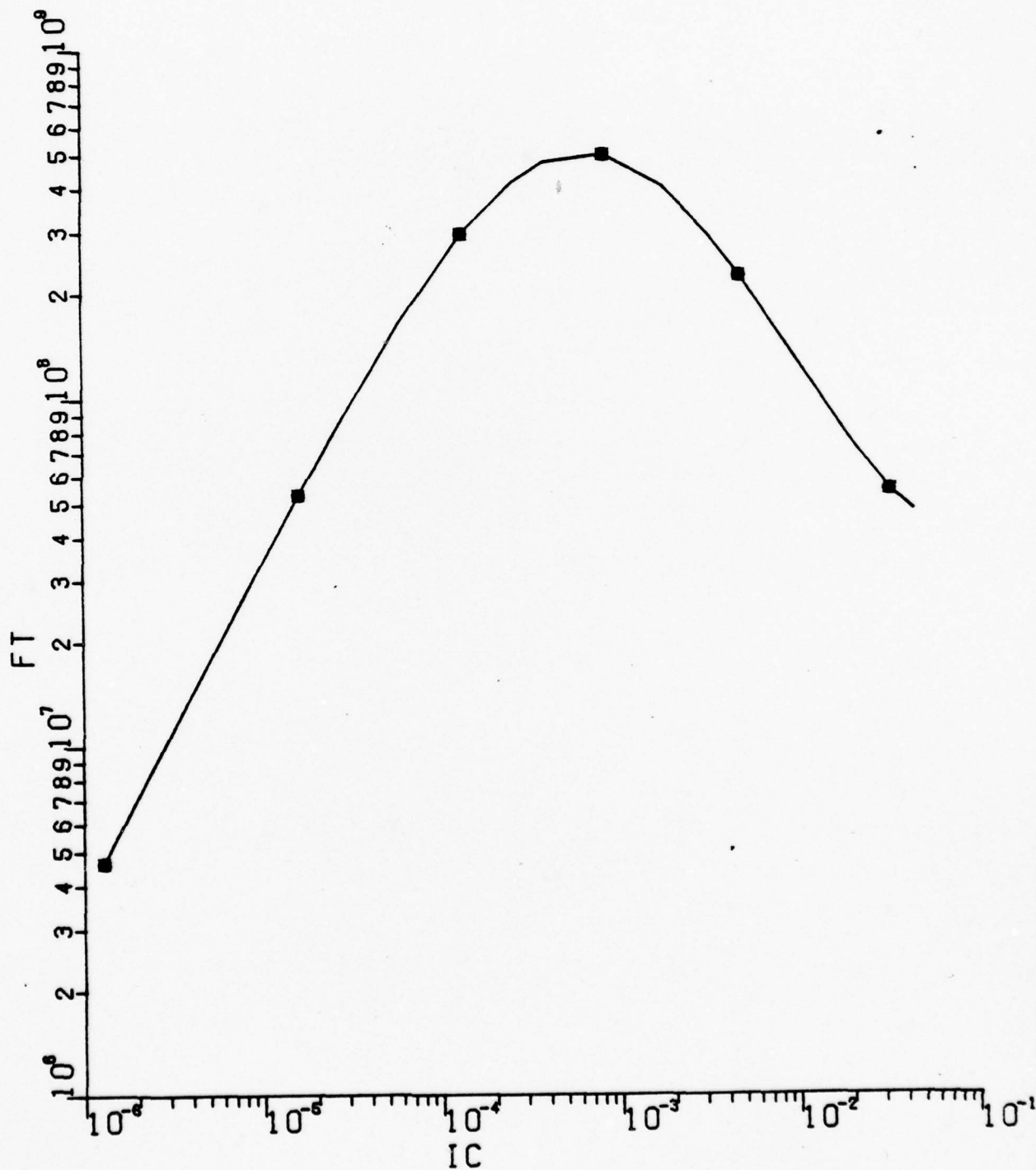
■ --	TAUR	=	1.000E-06
+ --	TAUR	=	1.270E-11
0 --	TAUR	=	1.270E-09

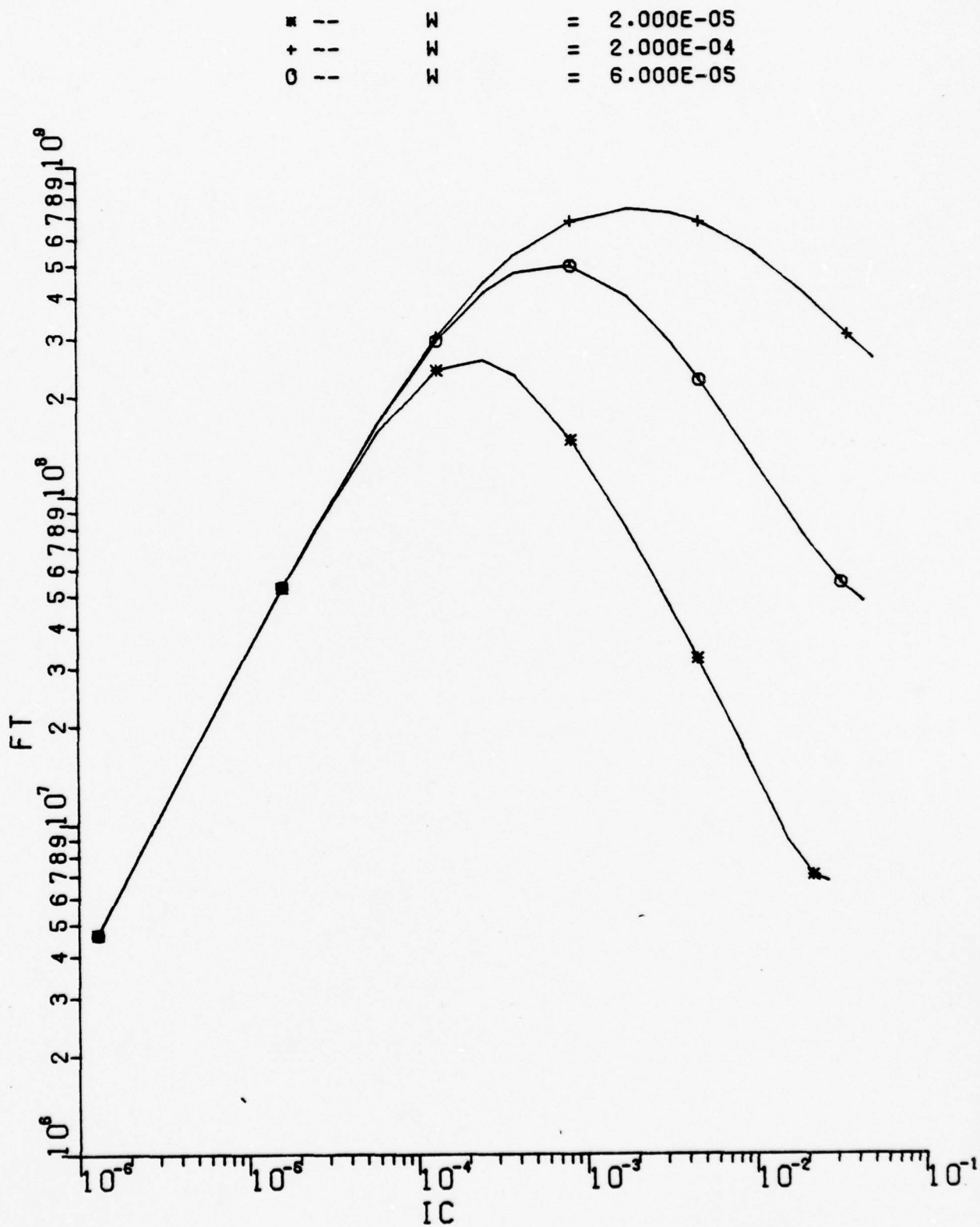


*	--	BETAO	=	2.000E+01
+	--	BETAO	=	1.500E+02
o	--	BETAO	=	5.500E+01

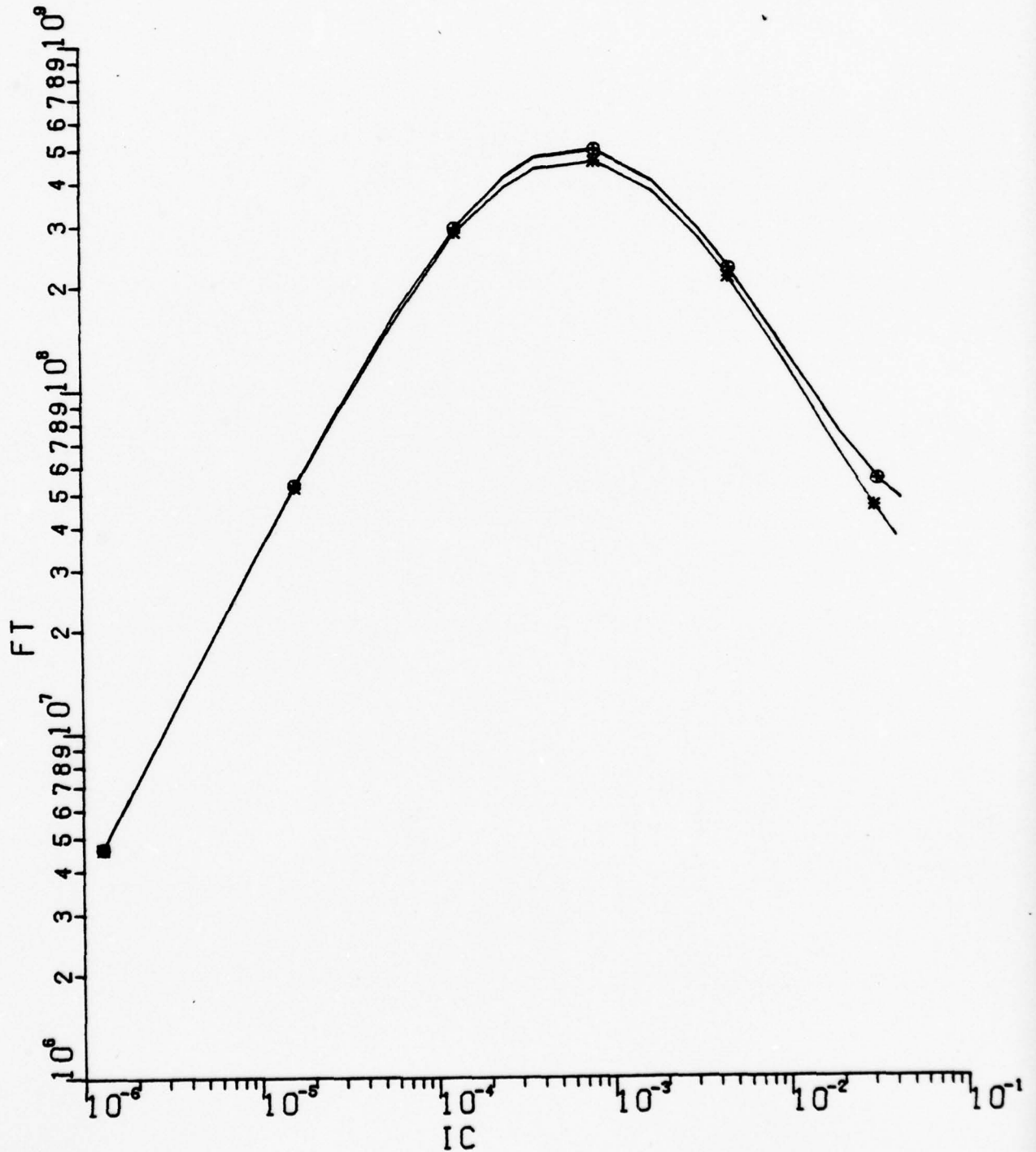


* --	BETAR	=	6.000E+00
+ --	BETAR	=	1.100E+00
0 --	BETAR	=	1.500E+00

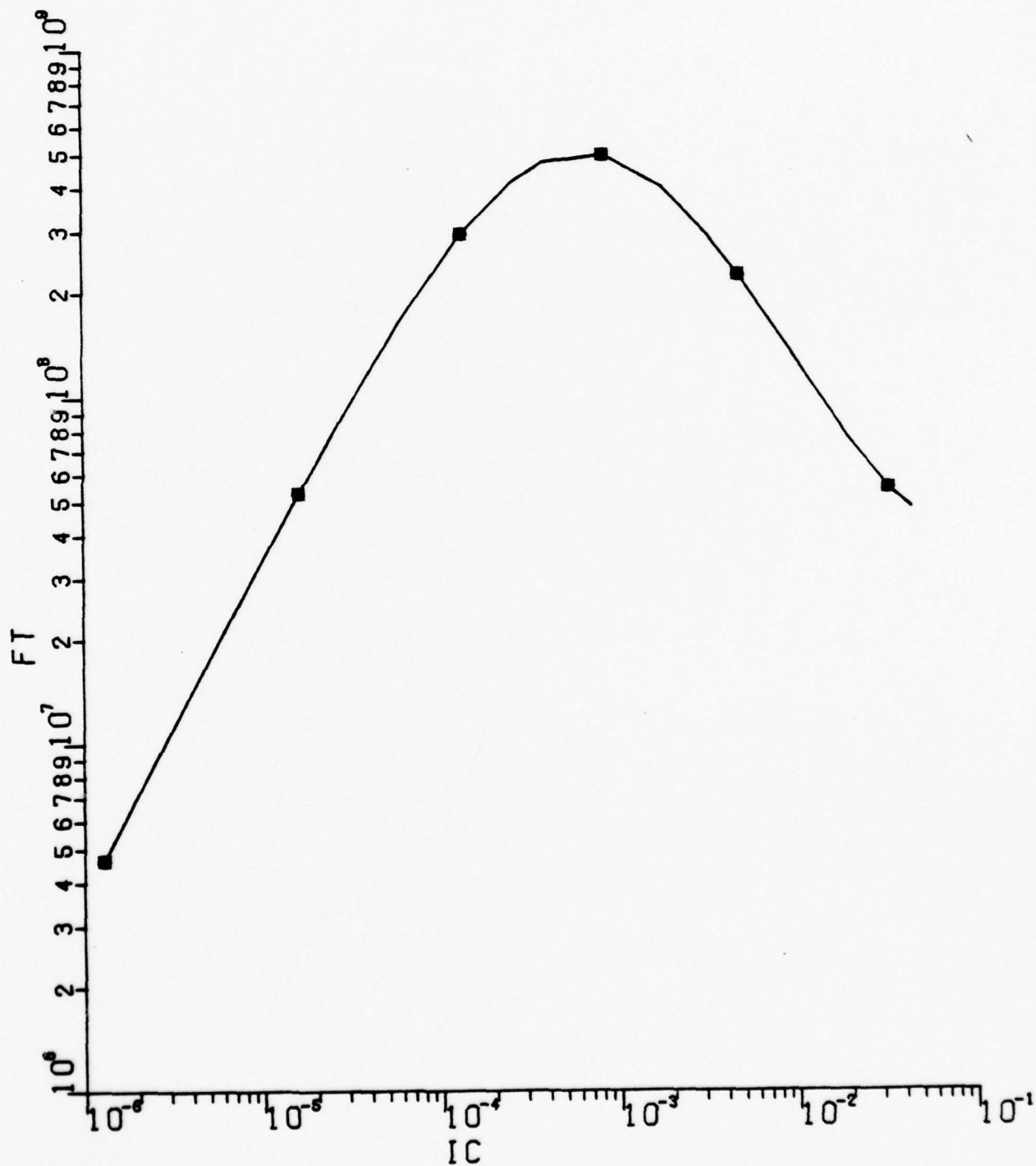




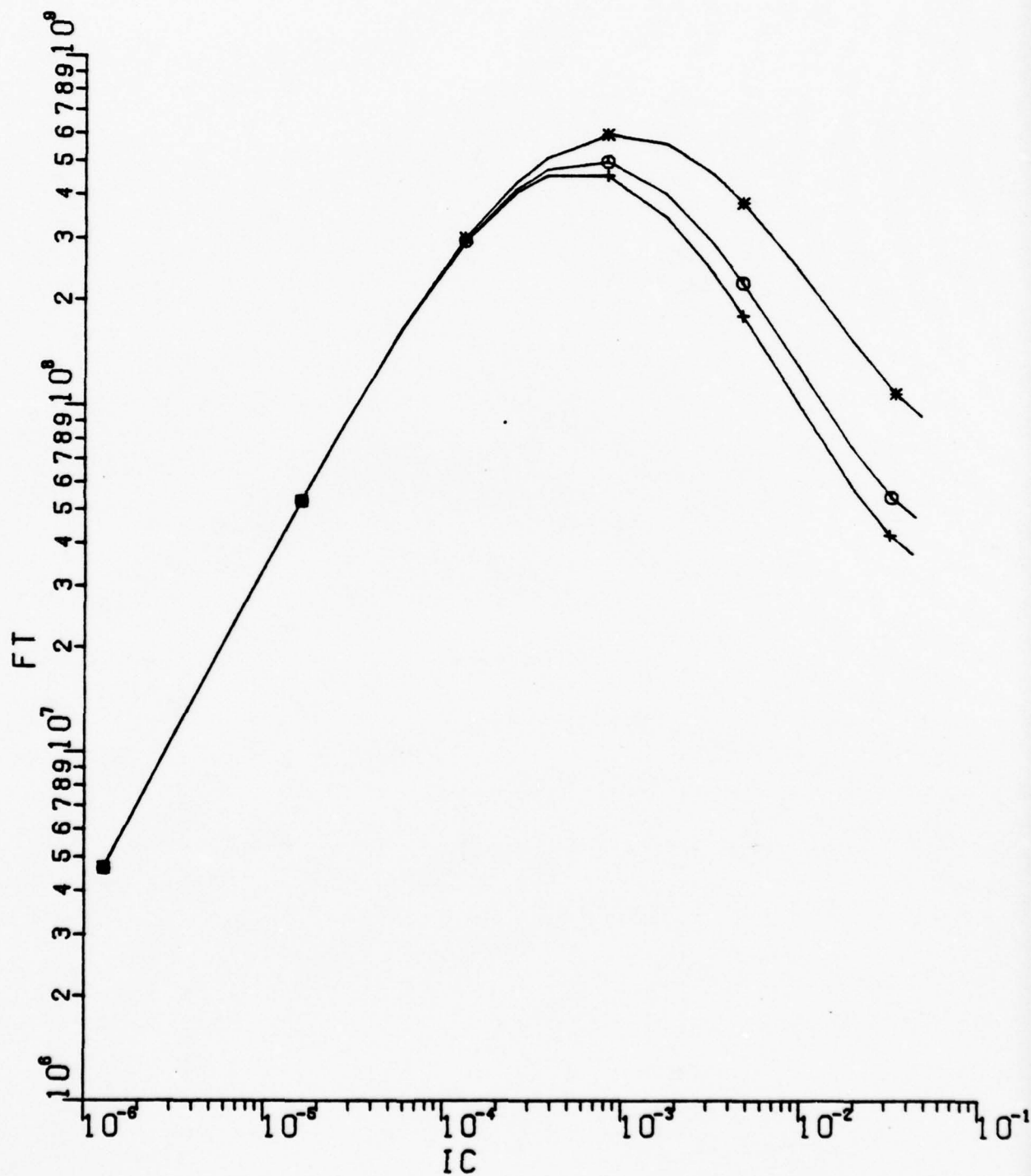
* --	AE	=	1.000E-08
+ --	AE	=	1.000E-04
0 --	AE	=	9.800E-07



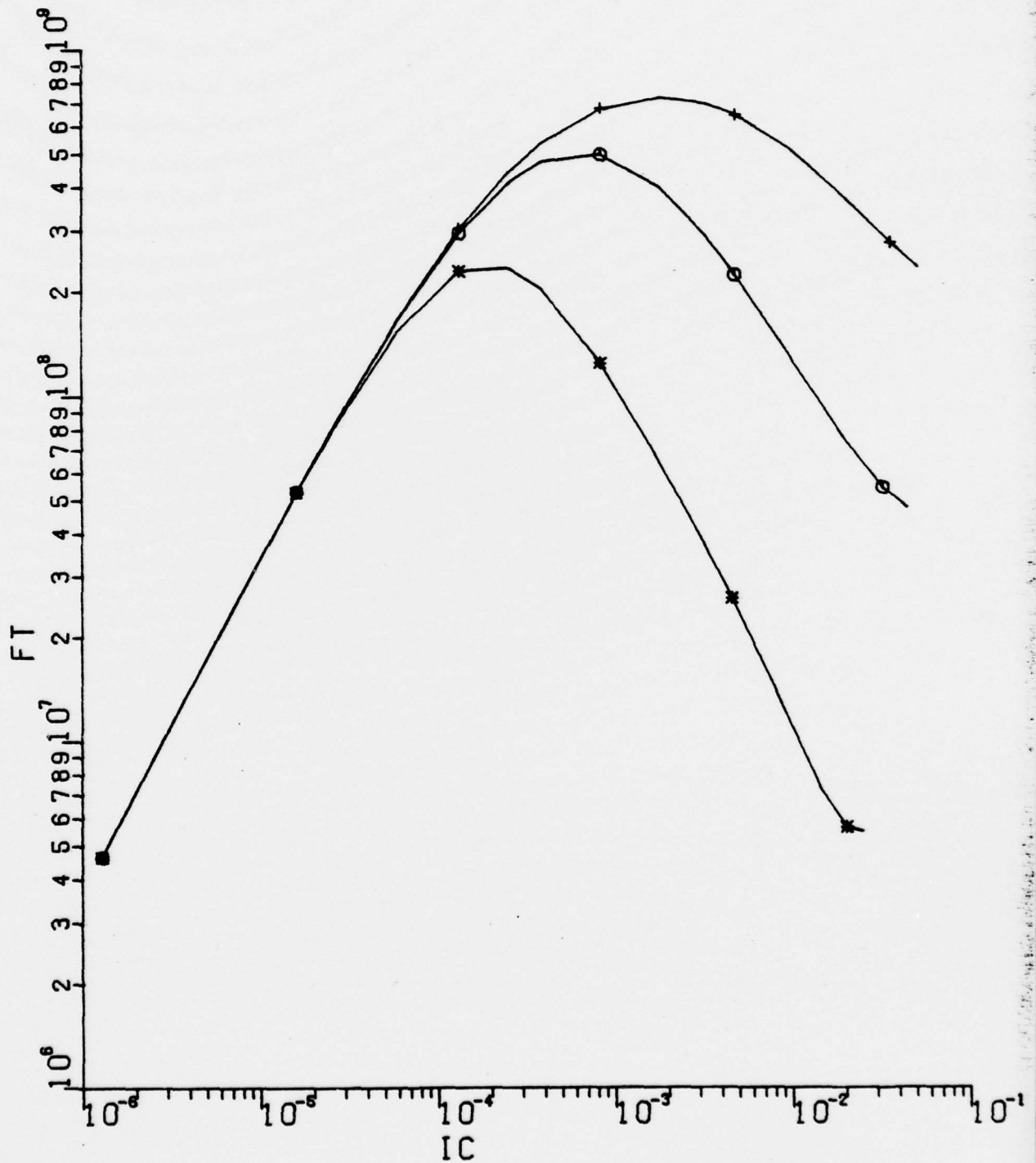
* --	VLIM	=	1.000E+06
+ --	VLIM	=	1.500E+07
0 --	VLIM	=	6.000E+06



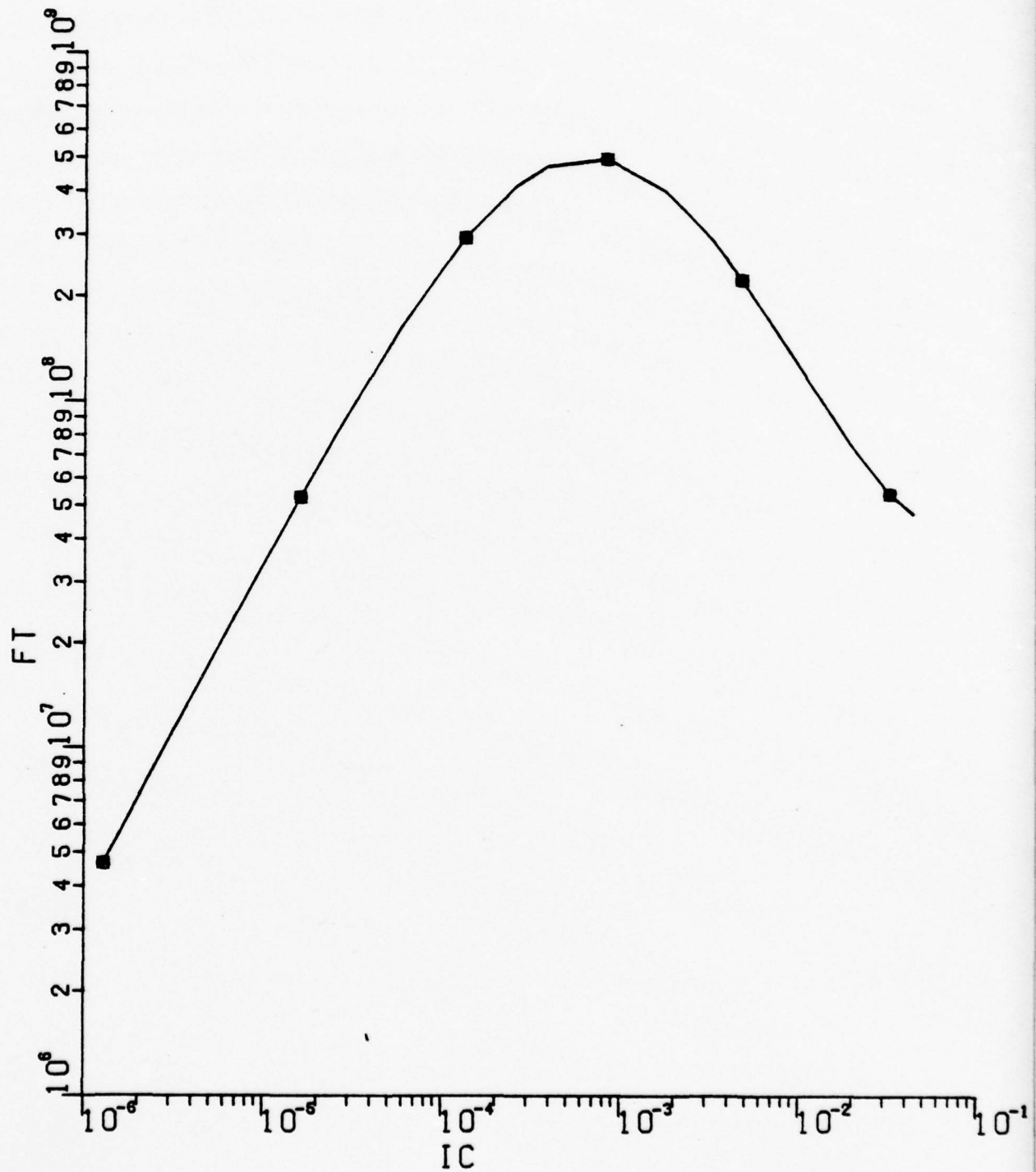
* --	DNB	=	1.000E+01
+ --	DNB	=	3.000E+01
0 --	DNB	=	2.260E+01



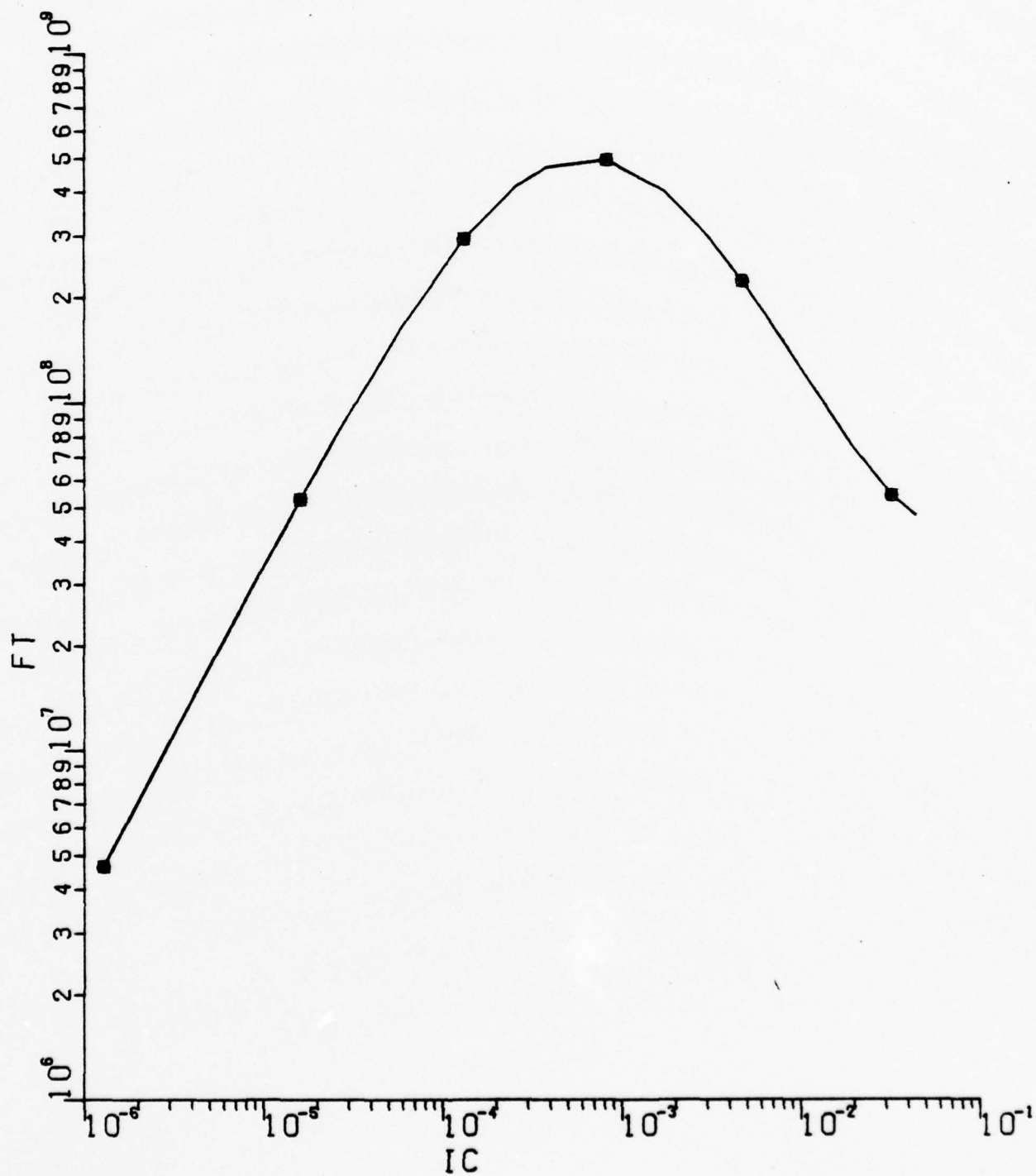
* --	WCPRIME	=	1.000E-03
+ --	WCPRIME	=	1.000E-04
o --	WCPRIME	=	3.000E-04



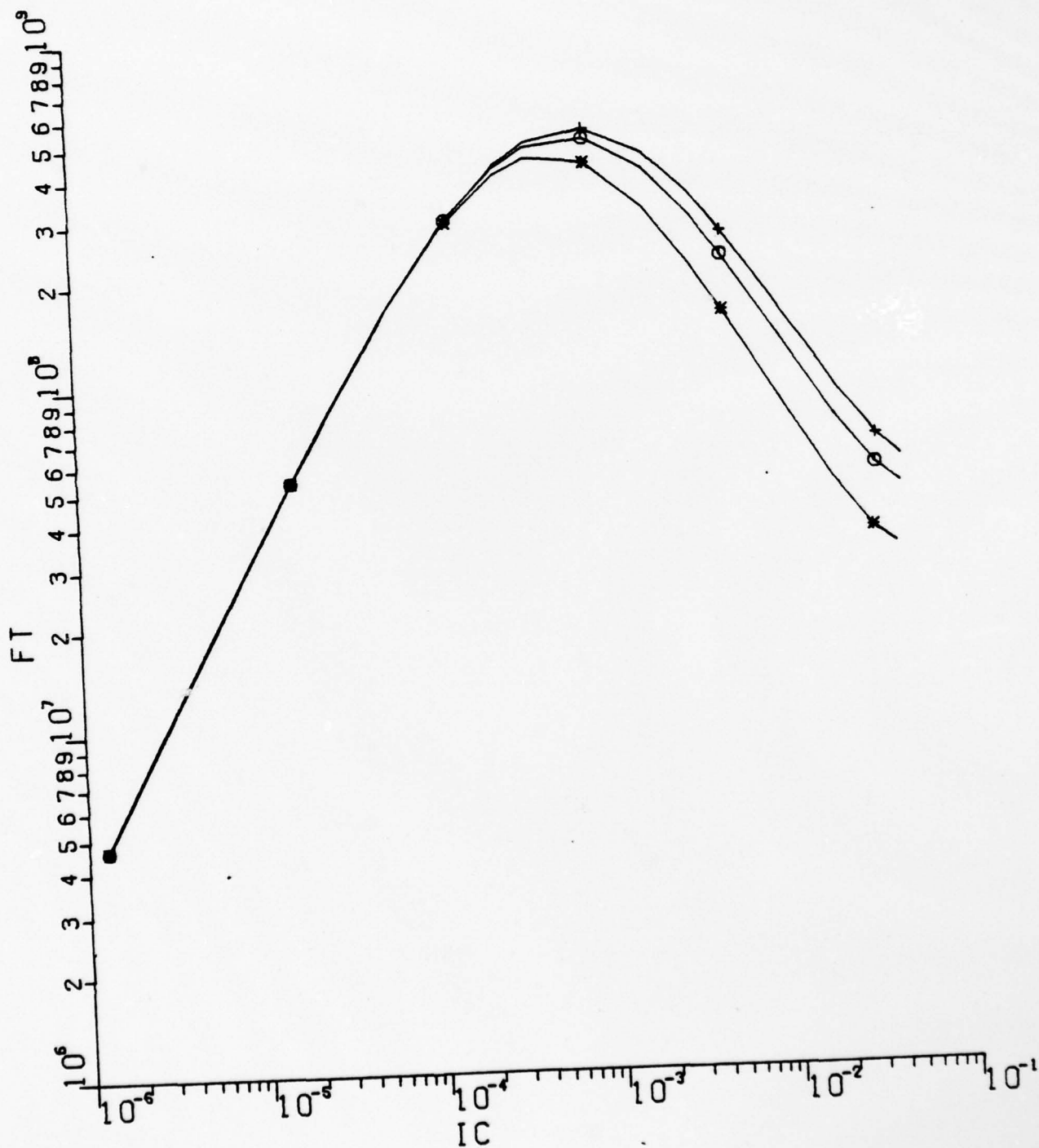
* --	NDC	=	1.000E+20
+ --	NDC	=	1.000E+13
0 --	NDC	=	1.000E+16



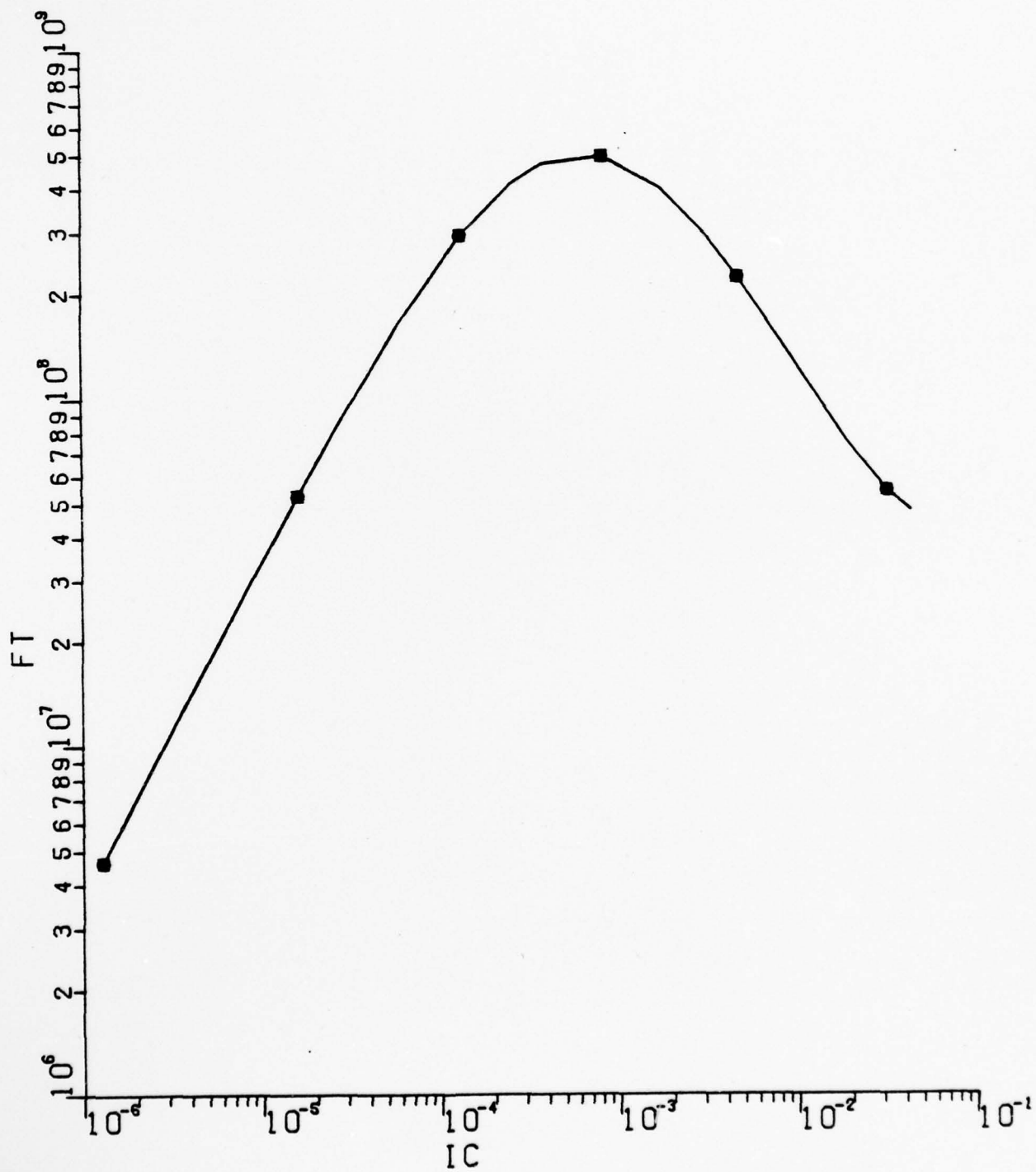
x --	PHIC	=	4.000E-01
+ --	PHIC	=	1.200E+00
o --	PHIC	=	7.000E-01



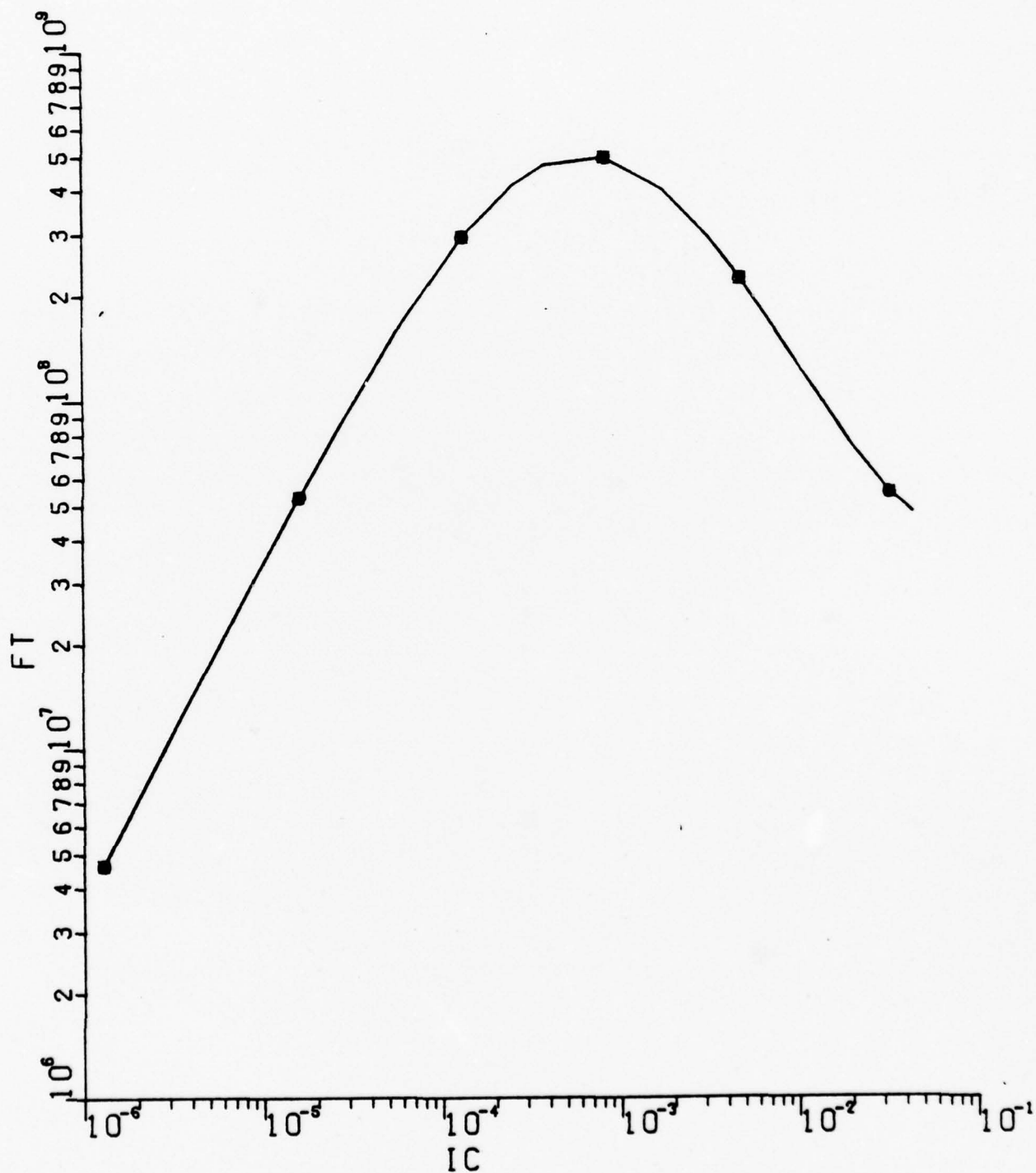
■	--	DNC	=	3.000E+01
+	--	DNC	=	6.000E+01
0	--	DNC	=	4.800E+01



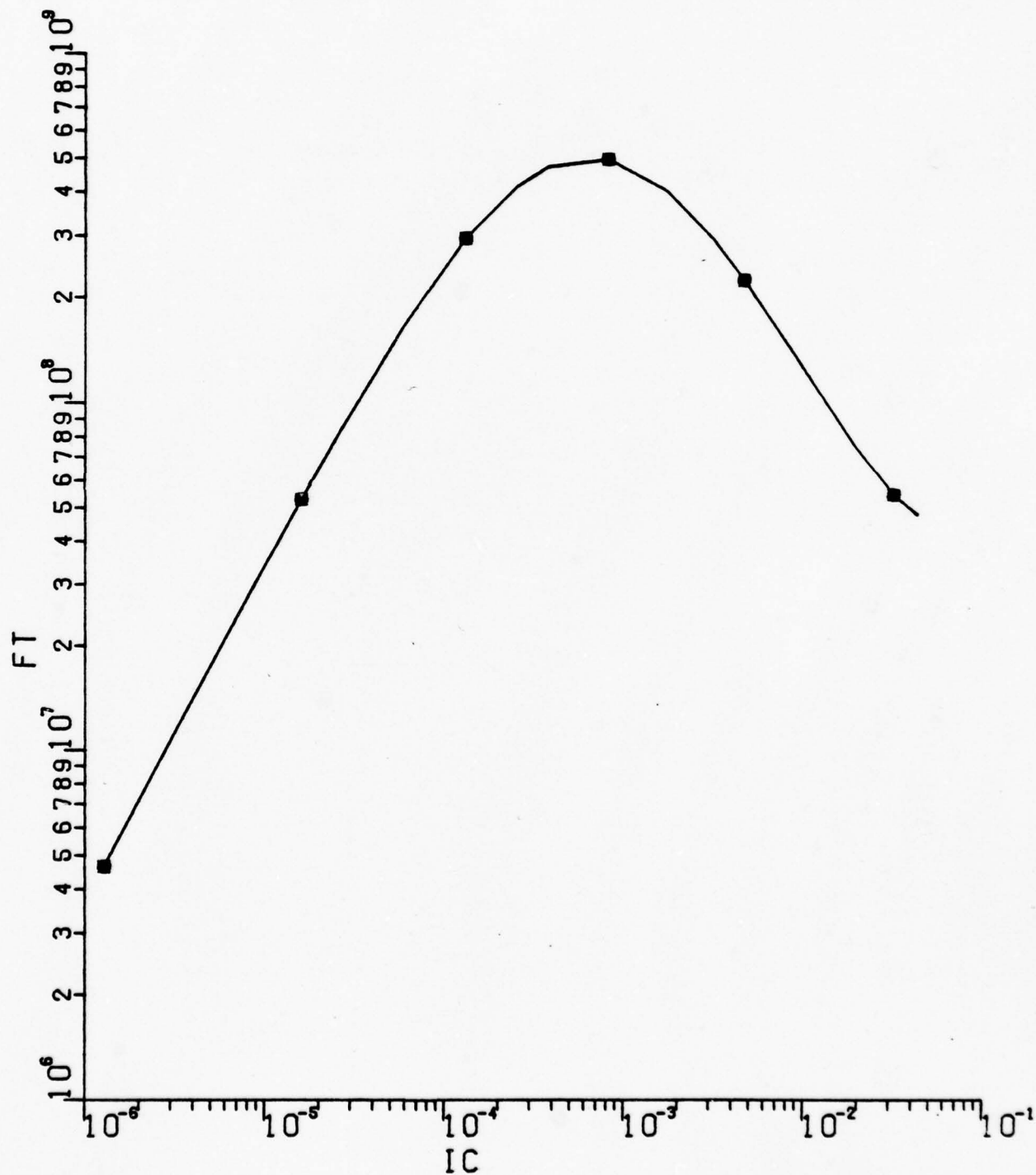
■ --	X0	=	4.000E-05
+ --	X0	=	2.400E-04
0 --	X0	=	1.200E-04



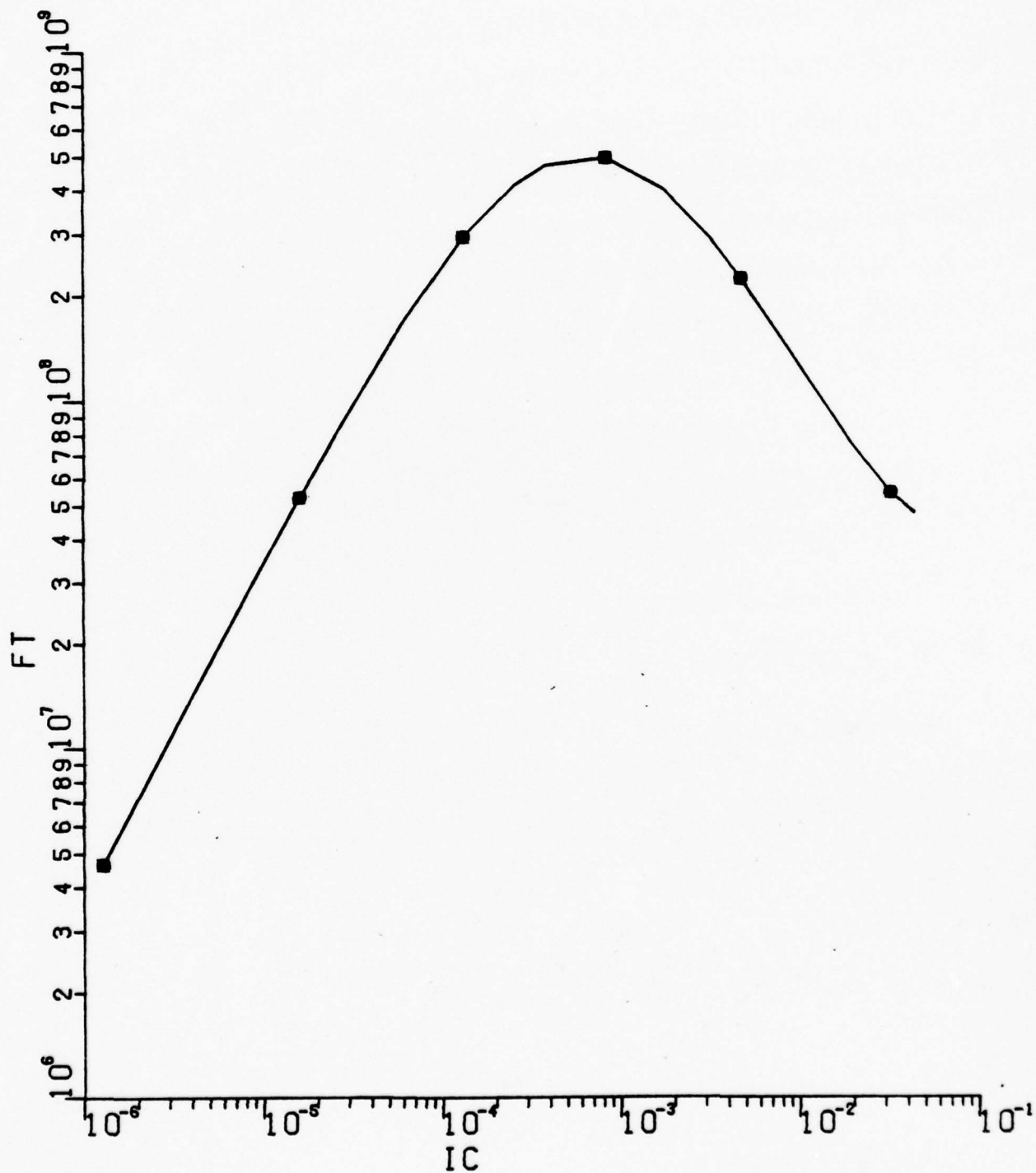
* --	KR	=	1.000E-01
+ --	KR	=	9.000E-01
0 --	KR	=	4.000E-01



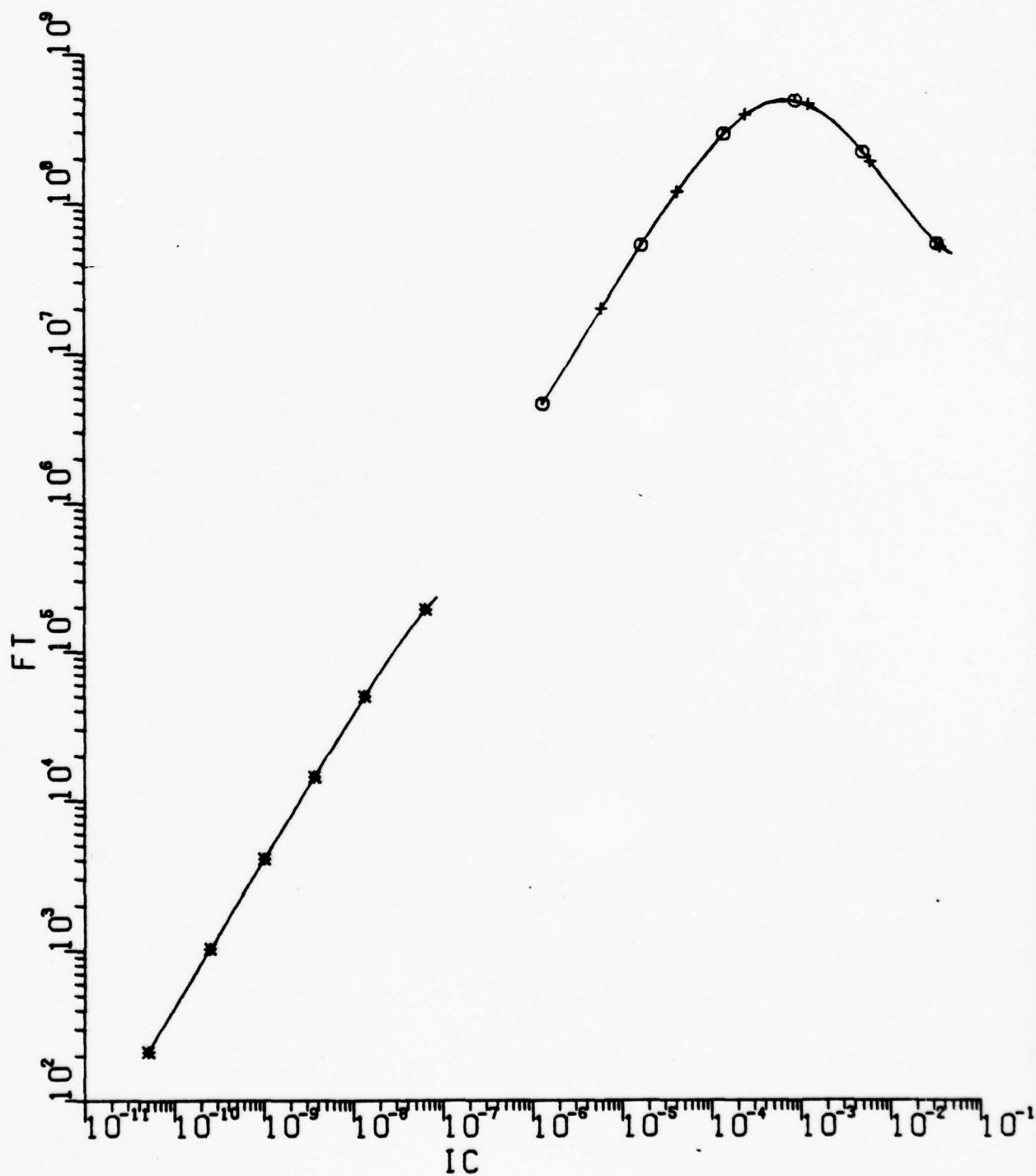
■ --	TD	=	2.000E-12
+ --	TD	=	2.000E-10
0 --	TD	=	2.000E-11



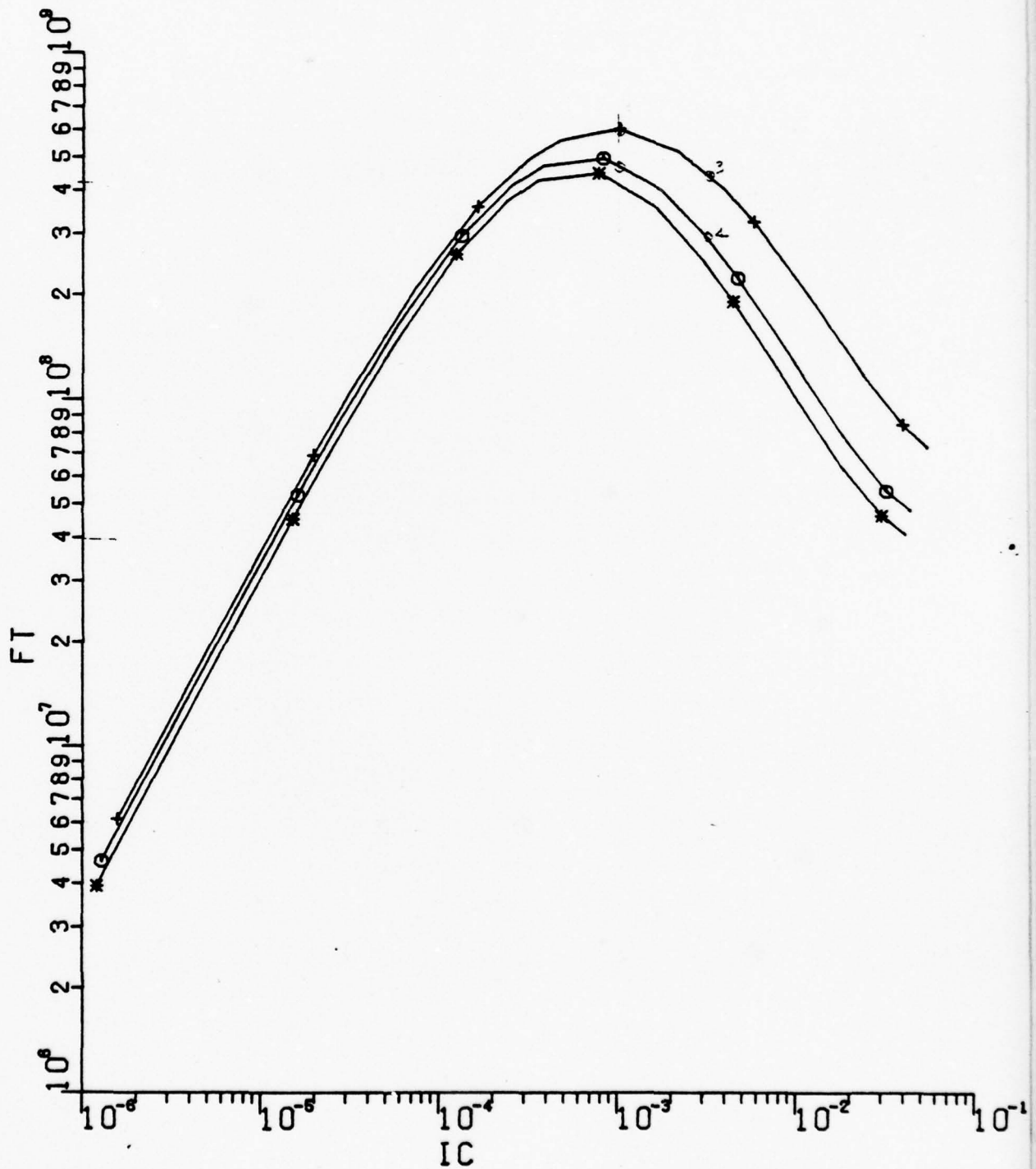
■	--	M	=	1.000E+00
+	--	M	=	1.000E+01
0	--	M	=	2.000E+00



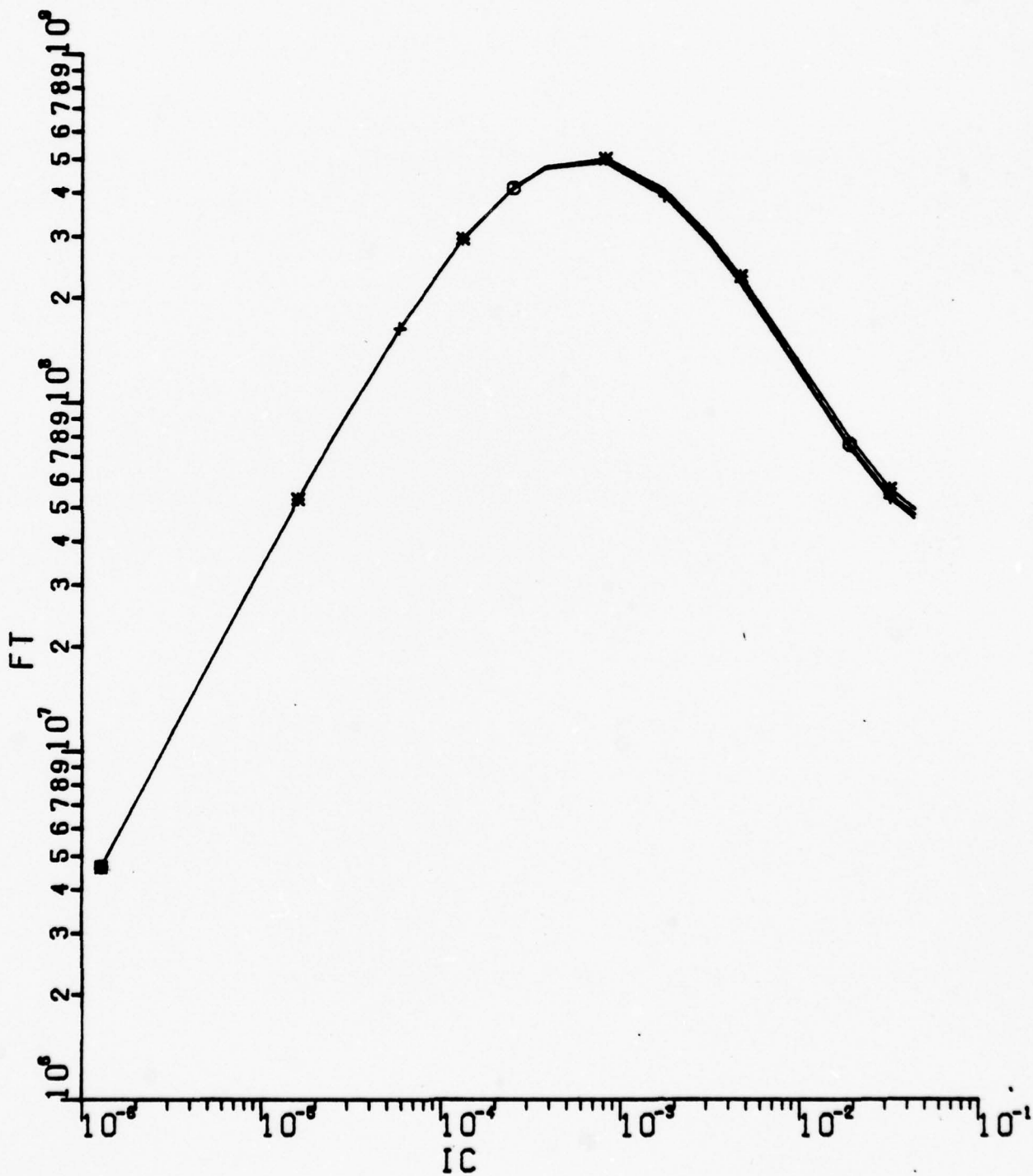
■ --	NE	=	8.000E-01
+ --	NE	=	2.300E+00
o --	NE	=	1.500E+00

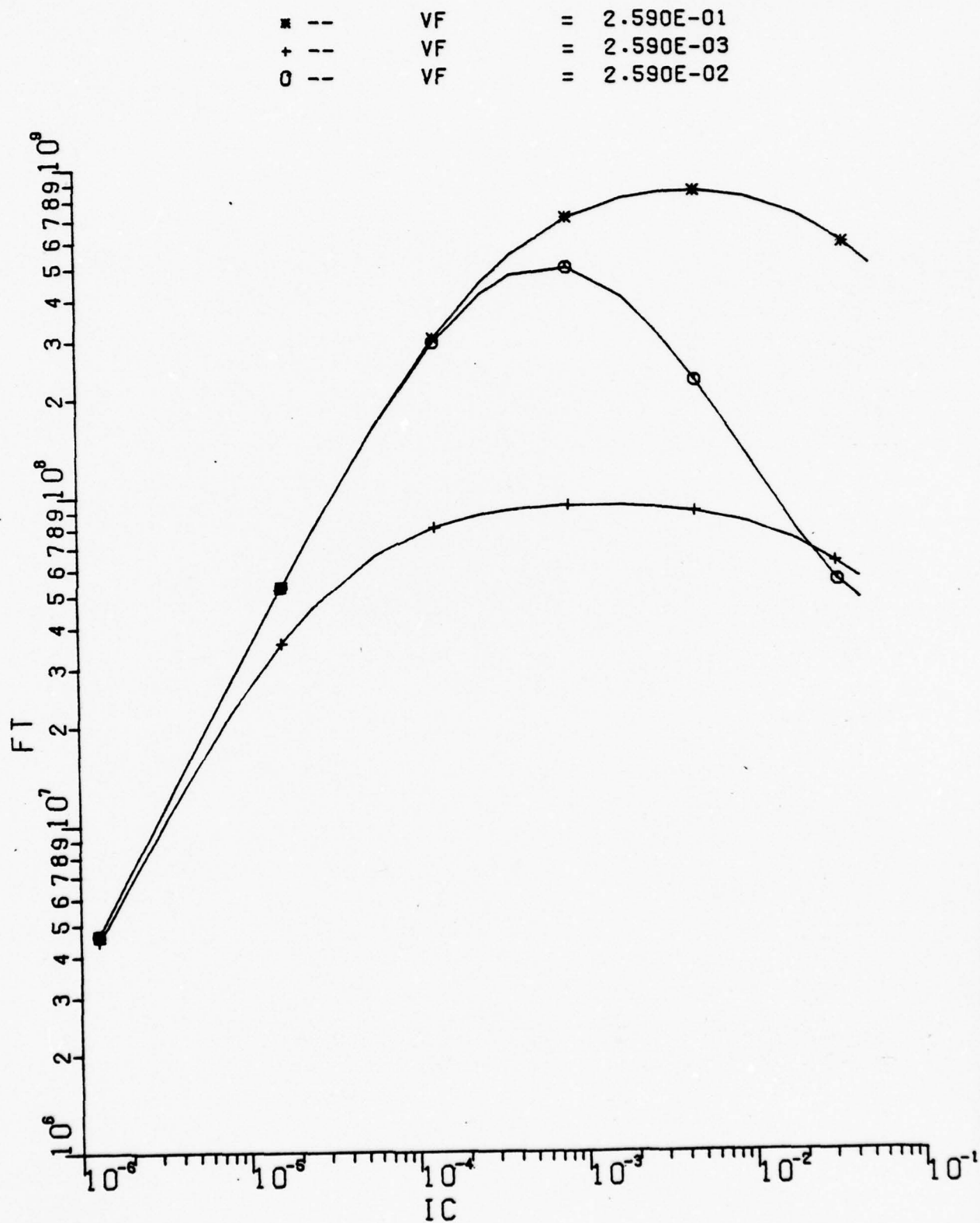


* --	VCE	=	1.500E+00
+ --	VCE	=	1.500E+01
o --	VCE	=	5.000E+00

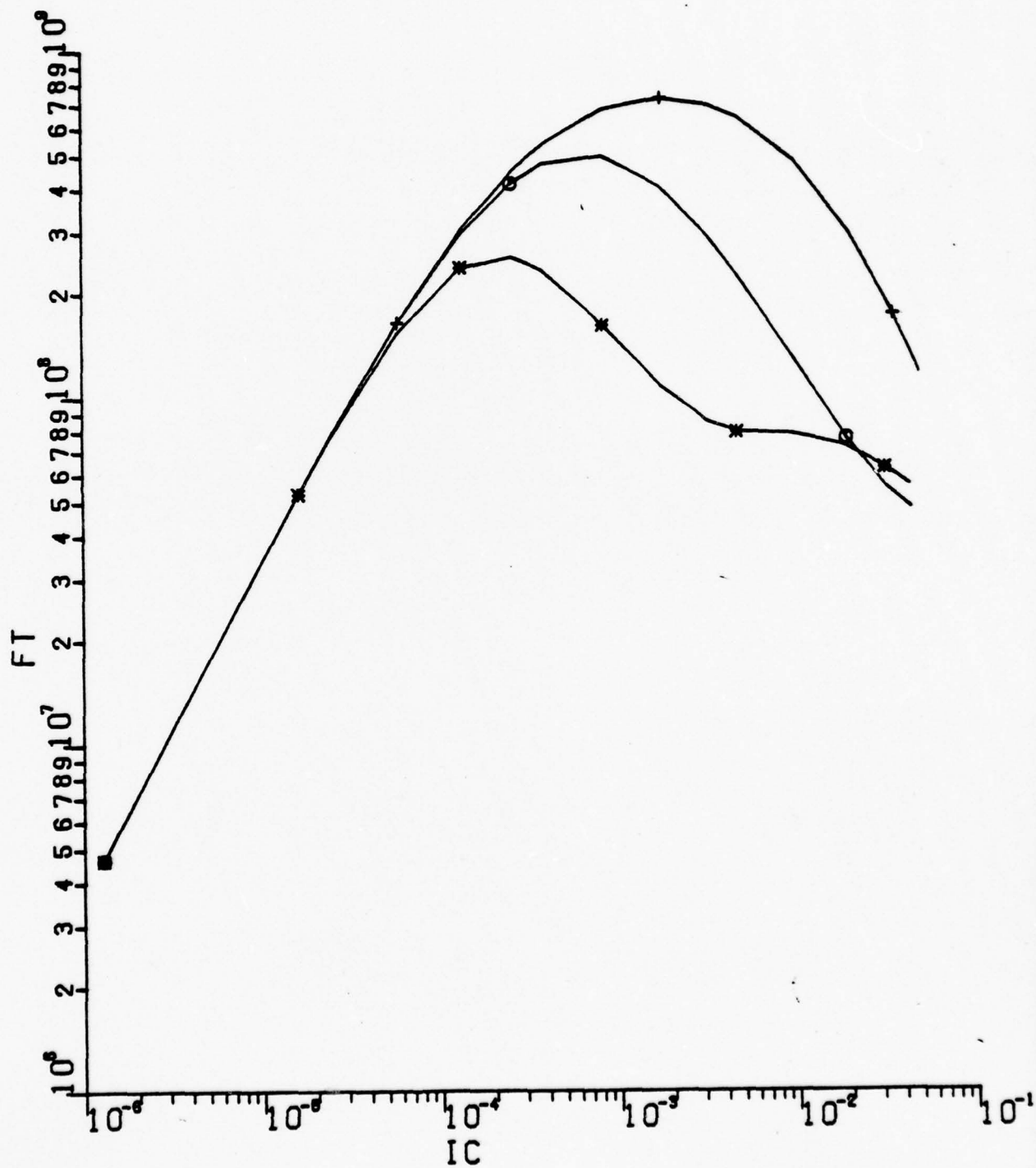


x	--	VB	=	1.500E+01
+	--	VB	=	2.000E+01
o	--	VB	=	1.779E+01



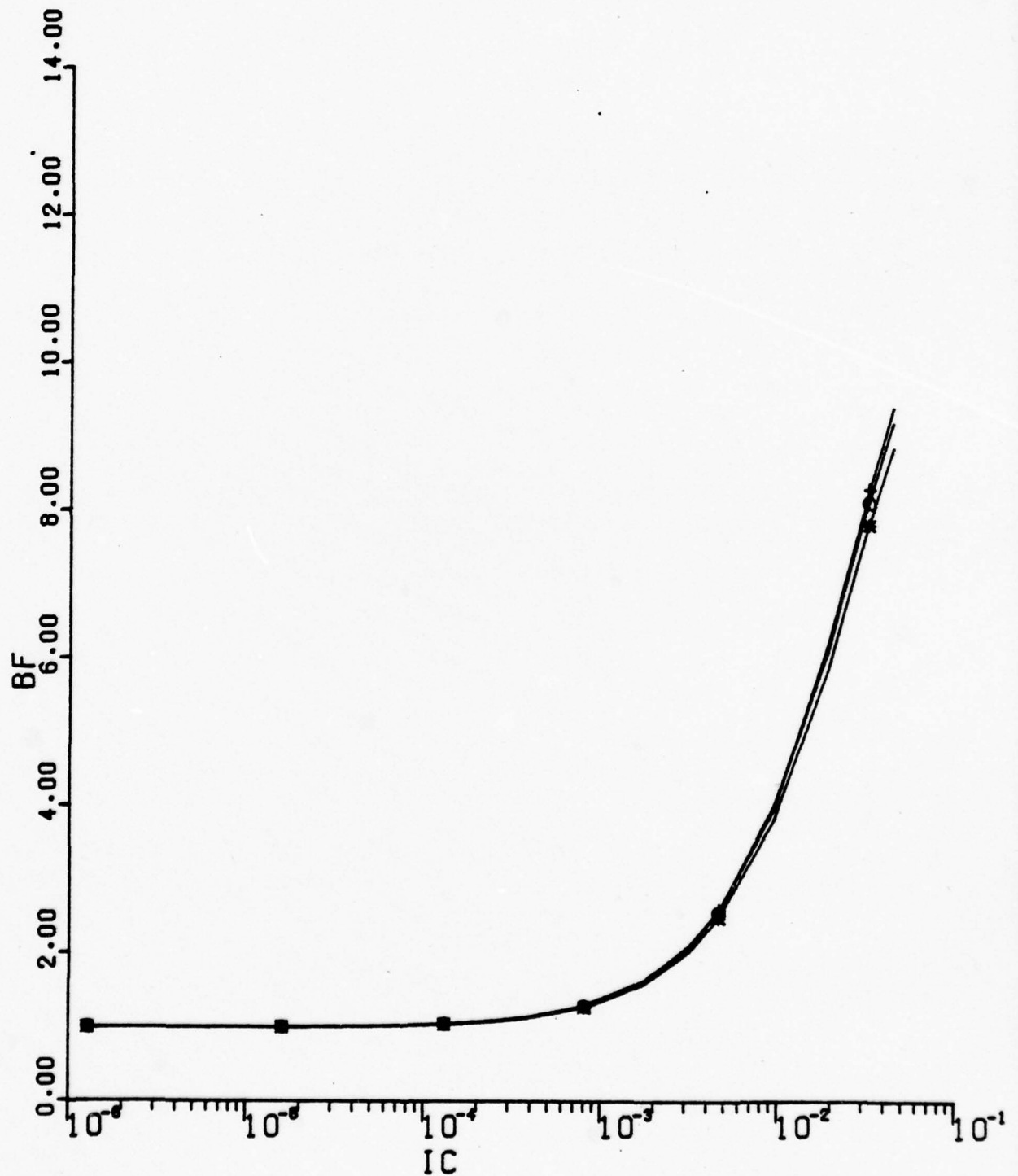


* --	FF	=	1.336E-13
+ --	FF	=	1.336E-15
0 --	FF	=	1.336E-14

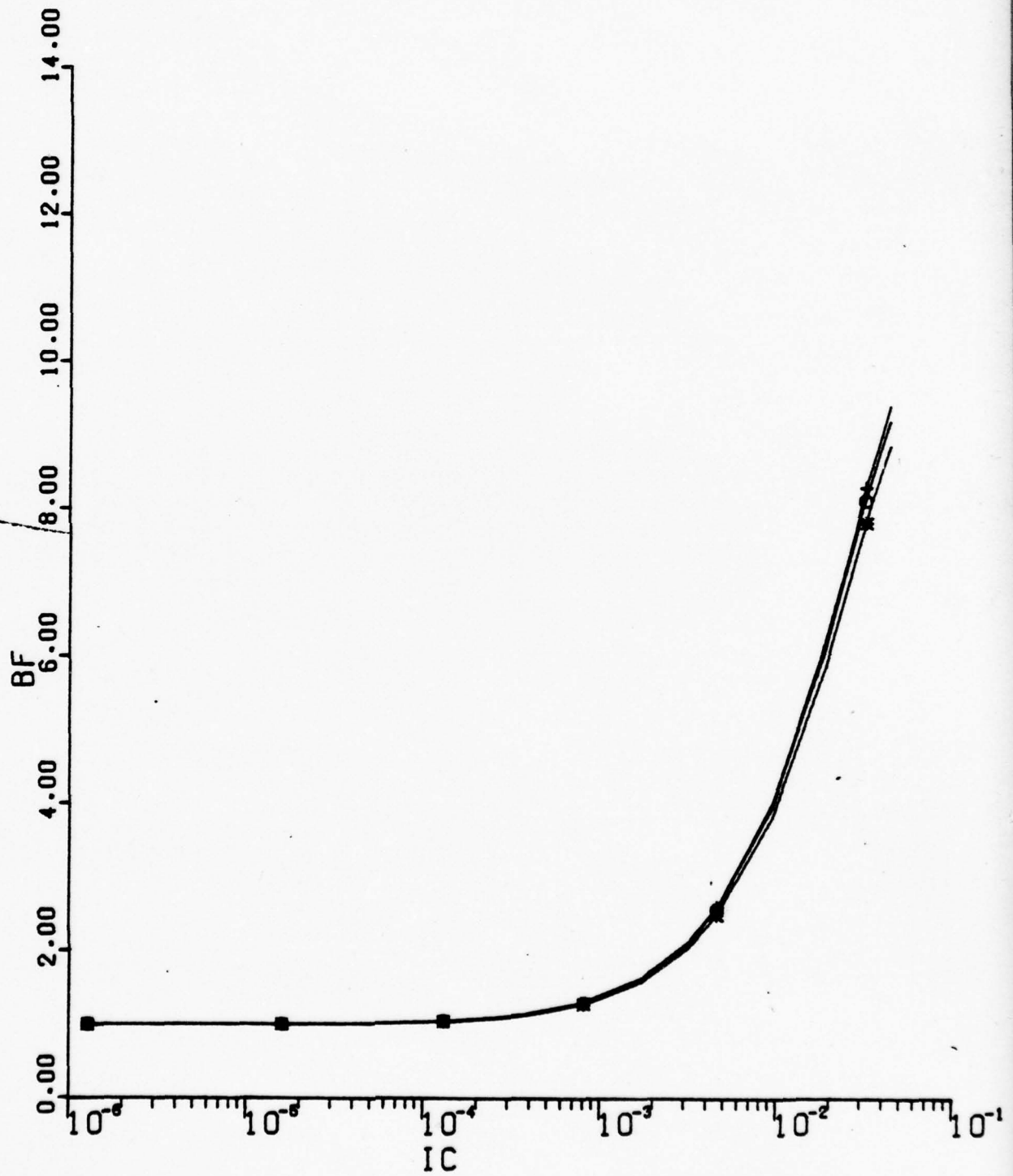


B.5 B_F vs. I_c Curves
(BASE PUSHOUT PARAMETERS)

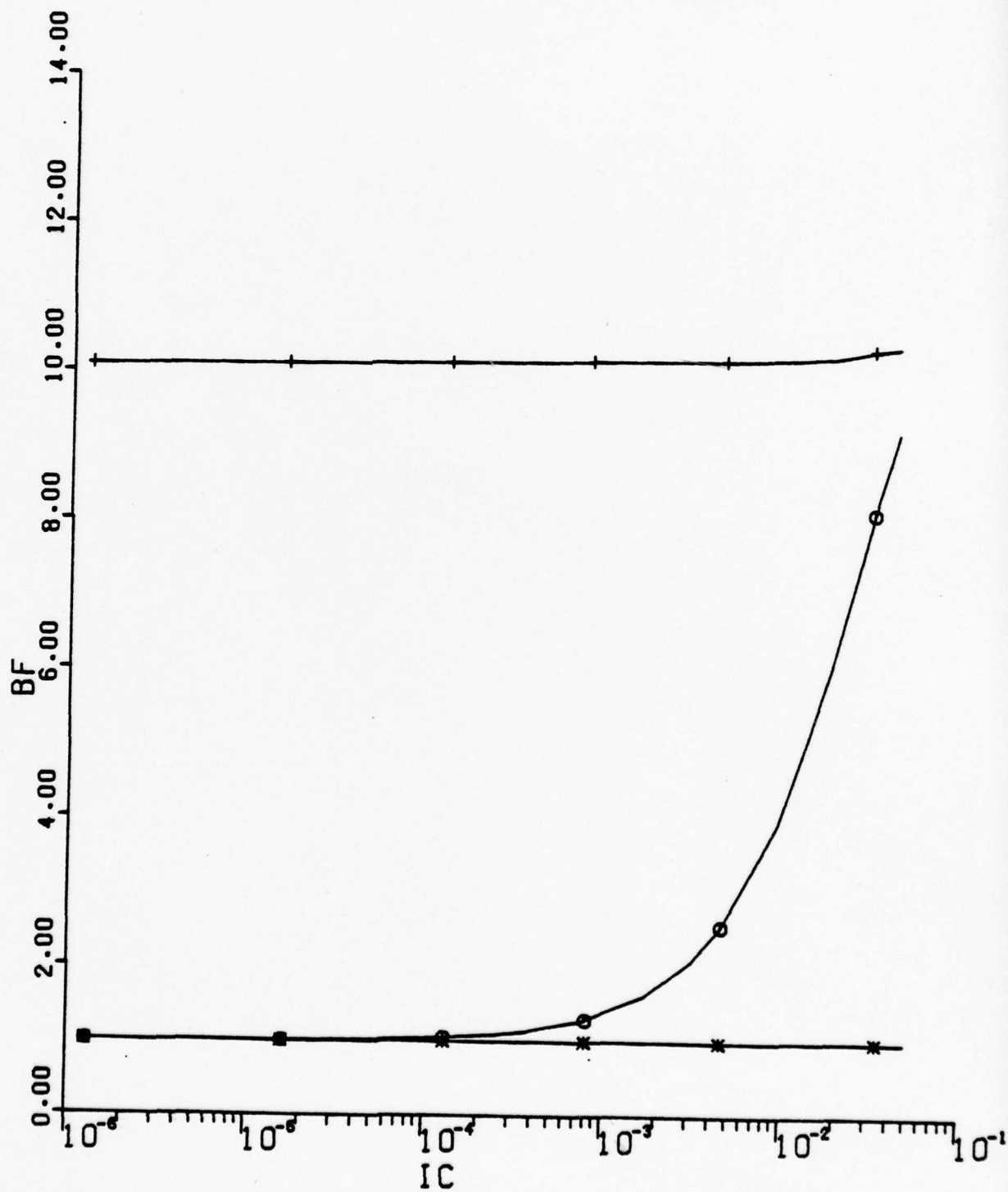
x --	VB	=	1.500E+01
+ --	VB	=	2.000E+01
o --	VB	=	1.779E+01



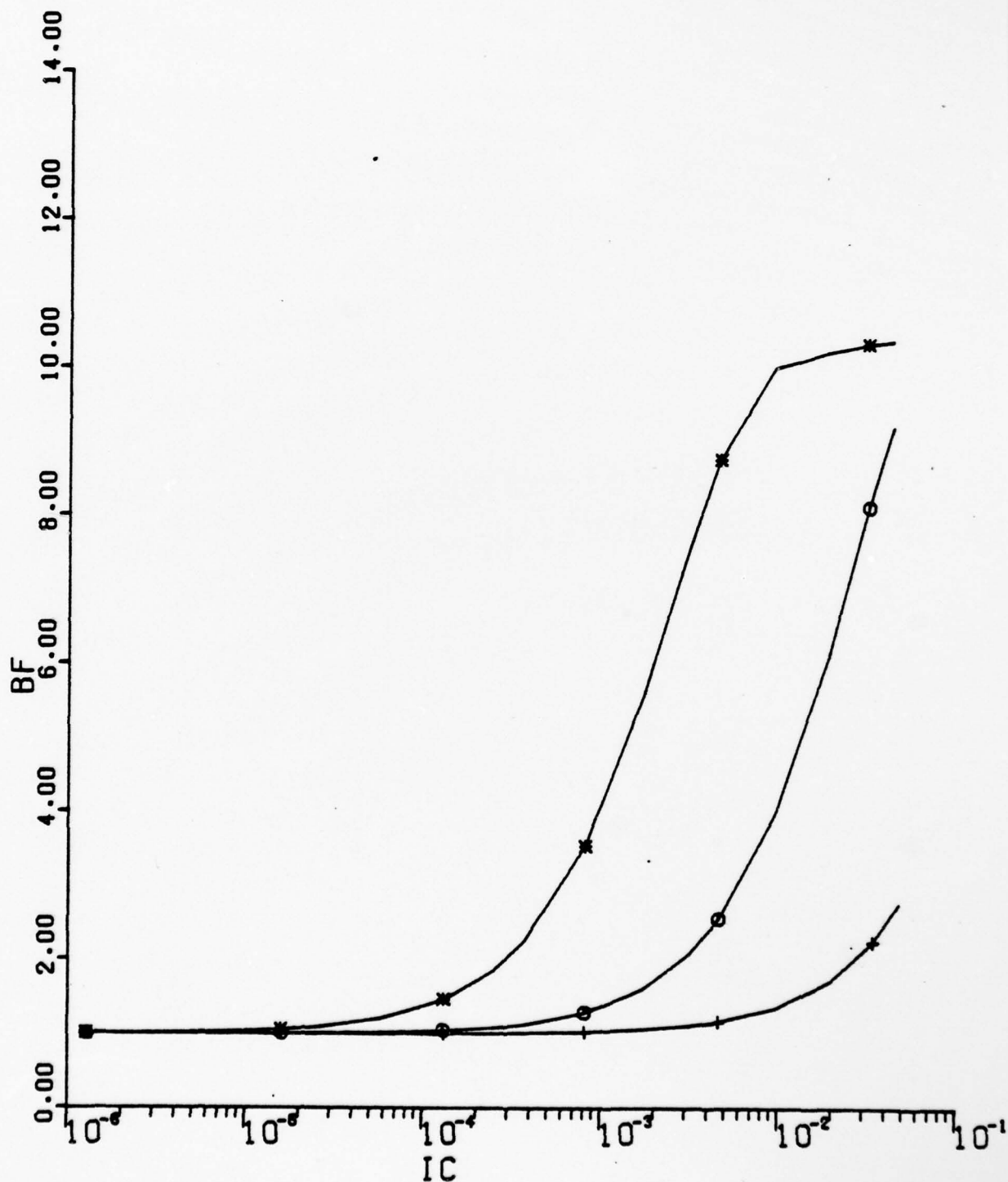
■ --	VB	=	1.500E+01
+ --	VB	=	2.000E+01
○ --	VB	=	1.779E+01



■ --	VF	=	2.590E-01
+ --	VF	=	2.590E-03
o --	VF	=	2.590E-02



x --	FF	=	1.336E-13
+ --	FF	=	1.336E-15
o --	FF	=	1.336E-14



APPENDIX C

PAREV (PARAMETER EVALUATION) CODE LISTING

```

00100 PROGRAM PAREV(INPUT,OUTPUT,TAPE3=INPUT,TAPE6,TAPE1,TAPE2)
00110 DIMENSION AIB(20),AIC(20),VBE(20),SCR(100),P(3)
00120 DIMENSION Y(2,20),Z(3,20),PI(3),PO(3)
00130 COMMON/PARAM/VT,IER,NE,IS,BETAD,RBO,RBB,IBB,RE,RCC,BE,Z
00140 + V8,FF,VER,VCR
00150 COMMON/DPPT/XIB,XIC,XVBE
00160 COMMON/TEMP/THETA
00170 EXTERNAL ZFIND,FUNCF,FUNEJ,FUNCF,FUNIBE
00180 DIMENSION AIBR(20),AICR(20),VBER(20)
00190 REAL IER,IBR,IS,ISR,NE,NC,NS,IBB,L,KR
00200 C#####
00210 C
00220 C++++PARAMETER EVALUATION CODE FOR CHOMA BIPOLAR TRANSISTOR MODEL+++
00230 C
00240 C THIS CODE IS AN INTERACTIVE CODE WHICH ACCEPTS ELECTRICAL AND
00250 C GEOMETRY DATA AND GENERATES PARAMETERS FOR THE CHOMA BJT MODEL.
00260 C THE PARAMETERS ARE USED FOR SIMULATION IN GENERAL CAD PROGRAMS
00270 C OR IN THE COMPANION CODE(ESOLVE) GENERATED SPECIFICALLY FOR
00280 C THE SIMULATION OF THE CHOMA MODEL.
00290 C SEVERAL MODULES IN THE CODE MAY BE BYPASSED VIA DEFAULT OR
00300 C USER OVERRIDE. HOWEVER,SOME MODULES ARE VITAL TO SUBSEQUENT
00310 C MODULE EXECUTION,CONSULT DOCUMENTATION FOR DETAILS.
00320 C
00330 C E. MOCK TRW SYSTEMS/DSSG SEPT. 1977
00340 C#####
00350 C NAMELIST/INDATA/RHOB,TE,AB,RBO,L,H,W,RBB,RE,RHOC,WCPRIME,XO,
00360 + AE,RCC,RCO,I,VTS,ISR,CSD,PHISS,CEO,PHIEO,CCO,PHICO,
00370 + TER,NE,IS,BETAD,IBR,NC,BETAR,VER,VCR,QFN,QRN,
00380 + TAUFN,TAUR,KR
00390 NAMELIST/TRANS/RBO,RBB,RE,RCO,BS,BC,BE,CSD,CEO,CCO,
00400 + PHISS,PHICO,PHIEO,ISR,IS,IER,IBR,VER,VCR,
00410 + NC,VT,VTS,QFN,QRN,TAUFN,TAUR,BETAD,BETAR,
00420 + AE,XO,WCPRIME,NE,KR,BF2,V8,VF,FF,VCE,IBB,PC
00430 DATA RHOB,TE,AB,RBO,L,H,W,RBB,RE,PHOC,WCPRIME,XO,AE,RCC,RCO/
00440 + 9E-3,1E-4,5E-7,0.,6E-5,6E-5,0.,5,3.25E-3,3E-4,
00450 + 2.7E-4,9.8E-7,0./
00460 DATA T,ISR,IER,NE,IS,BETAD,IBR,NC,BETAR/
00470 + 27.,3E-12,3.2E-14,1.5,3.2E-16,55.,3E-13,1.8,1.5/
00480 DATA VER,VCR,GOF,QFN,QRN,TAUFN,TAUR,KR/
00490 + 20.,60.,0.,0.,1.5E-16,1.5E-12,1.59E-10,1.27E-9,.5/
00500 DATA CSD,CEO,CCO,PHISS,PHICO,PHIEO/
00510 + 2.E-15,9.E-13,8.E-13,.9,.9,1.2/

```



```

00520 DATA VT,VIS,BE2,VB,VF,EF,VCE,IBB/
00530 +.0259,.03,13.64,17.79,.0259,1.336E-14,5.1.38E-4/
00540 C*****
00550 C
00560 C READ IN THE NAMELIST DATA
00570 C
00580 C*****
00590 REWIND 1
00600 READ(1,INDATA)
00610 C*****
00620 C
00630 C PERFORM THE DEFAULT CALCULATIONS
00640 C
00650 C*****
00660 IF(RHO.EQ.0.) RBO=RHO8*TE/AB
00670 IF(RBO.EQ.0.) RBB=RHO8*L/(W*H)
00680 IF(RCC.EQ.0.) RCC=RHO8*WCPRIME/AE
00690 IF(KR.NE..5) KR=(1.-AE/(AE*AB))
00700 C*****
00710 C
00720 C ENTER THE ITERATIVE LOOP
00730 C
00740 C*****
00750 50 DISPLAY +----INPUT INDEX-----+
00760 ACCEPT MASTER
00770 GO TO (50,100,200,300,400,500,600,700,800,900,1000,1100) MASTER
00780 C*****
00790 C
00800 C-CODE FOR JUNCTION CAPACITANCES PARAMETER, FITTING
00810 C
00820 C ASSIGN ESTIMATE AND BOUNDS
00830 C P(1)=CXD P(2)=PHIXO P(3)=PARASITIC CAP.
00840 100 P(1)=2.E-12
00850 P(1)=1.E-14
00860 P(1)=1E-10
00870 P(2)=.9
00880 P(2)=.4
00890 P(2)=1.5
00900 P(3)=1.E-12
00910 P(3)=0.
00920 P(3)=1E-11
00930 NV=2

```



```

00940 NP1=4
00950 TOL=EPS=1E-5
00960 ND=1
00970 MXIT=80
00980 LLK=1
00990 IM=0
01000 C
01010 C-READ IN THE EMITTER CAPAC. CURVE VALUES
01020 C Y(1,I)=CJE Y(2,I)=VJE
01030 C
01040 ACCEPT(1) NPT
01050 DO 5 I=1,NPT
01060 ACCEPT(1) Y(1,I),Y(2,I)
01070 5 CONTINUE
01080 DISPLAY *EMITTER JUNCTION CAPACITANCE FIT*
01090 CALL MINIZ(Y,SCR,P,NV,NPT,NP1,TOL,EPS,EE,ND,
01100 * MXIT,LLK,PO,PL,IM,FUNCJ)
01110 DISPLAY *CED EST. PHIED EST. PARASIT. EST. MSE*
01120 DISPLAY P(1),P(2),P(3),EE
01130 CED=P(1)
01140 PHIED=P(2)
01150 GO TO 50
01160 C*****
01170 C-READ IN THE COLLECTOR CAPAC. CURVE VALUES
01180 C Y(1,I)=CJC Y(2,I)=VJC
01190 C*****
01200 200 ACCEPT(1) NPT
01210 DO 7 I=1,NPT
01220 ACCEPT(1) Y(1,I),Y(2,I)
01230 7 CONTINUE
01240 DISPLAY *COLLECTOR JUNCTION CAPACITANCE FIT*
01250 DISPLAY *CO EST. PHICO EST. PARASIT. EST. MSE*
01260 CALL MINIZ(Y,SCR,P,NV,NPT,NP1,TOL,EPS,EE,ND,
01270 * MXIT,LLK,PO,PL,IM,FUNCJ)
01280 DISPLAY P(1),P(2),P(3),EE
01290 CCO=P(1)
01300 PHICO=P(2)
01310 GO TO 50
01320 C*****
01330 C
01340 C READ IN THE SUBSTRATE CAPAC. CURVE VALUES
01350 C Y(1,I)=CJS Y(2,I)=VJS

```

```

01360 C *****
01370 C *****
01380 300 ACCEPT(1) NPT
01390 DO 8 I=1,NPT
01400 ACCEPT(1) Y(1,I),Y(2,I)
01410 8 CONTINUE
01420 DISPLAY *SUBSTRATE JUNCTION CAPACITANCE FIT*
01430 DISPLAY *CSD EST. PHISS EST. PARASIT. EST MSE*
01440 CALL MINIZ(Y,SCR,P,NV,NPT,NP1,TOL,EPS,EE,ND,
01450 *INITIAL,K,P0,P1,IM,FUNC,J)
01460 DISPLAY P(1),P(2),P(3),EE
01470 CSD=P(1)
01480 PHISS=P(2)
01490 GO TO 50
01500 C *****
01510 C
01520 C VER AND VCR EVALUATION CODE
01530 C
01540 C *****
01550 400 DISPLAY *INPUT GOF,GOR,VBE,VBC,ICO,IEO*
01560 ACCEPT GOF,GOR,VBEX,VBCX,R11,R12
01570 XNUM=R11*P12-GOF*GOR*VBEX*VBCX
01580 VCR=XNUM/(GOF*(R12+GOR*VBEX))
01590 VER=XNUM/(GOR*(R11+GOF*VBCX))
01600 DISPLAY *VER=*,VER,*VCR=*,VCR
01610 GO TO 50
01620 C *****
01630 C-RELABLE THE INPUT FOR IB-VBE FIT FOR IS/BETA0,IER,NE
01640 C *****
01650 C *****
01660 500 ACCEPT (1) NCTF,VCEX
01670 DO 10 I=1,NCTF
01680 ACCEPT(1) AIB(I),AIC(I),VBE(I)
01690 10 CONTINUE
01700 DO 12 I=1,NCTF
01710 Y(1,I)=AIB(I)
01720 Y(2,I)=VBE(I)
01730 12 CONTINUE
01740 C---SET UP GUESSES AND OTHER CONSTANTS
01750 C
01760 P(1)=1E-14
01770 P(2)=27

```

```

01780 P(3)=1F-12
01790 P(1)=P(3)=0.
01800 P(2)=20
01810 P(1)=P(12)=1.
01820 P(2)=40
01830 NV=2
01840 NP=3
01850 NP1=4
01860 TOL=EPS=1E-5
01870 ND=1
01880 MXIT=90
01890 LLK=1
01900 TW=0
01910 C-----CALCULATE TEMPERATURE ESTIMATE FROM IC DATA
01920 NCTM1=NCTF-1
01930 DISPLAY *POINT TO POINT TEMPERATURE (DEG. C)*
01940 DO 20 I=1,NCTM1
01950 J=I+1
01960 T=-273+11594.2*(Y(2,J)-Y(2,I))/(ALOG(AIC(J)/AIC(I)))
01970 THI=11594.2*(Y(2,J)-Y(2,I))/(T+273.)
01980 20 DISPLAY I,J,T
01990 DISPLAY * INPUT TEMP. ESTIMATE (DEG. C)*
02000 ACCEPT(5) T
02010 THETA=11594.2/(T+273)
02020 VT=1./THETA
02030 C**
02040 C OUTPUT THE CALCULATED VALUES OF IS BASED ON AN INPUT
02050 C VALUE OF TEMPERATURE
02060 C**
02070 DISPLAY *POINT IS*
02080 DO 25 I=1,NCTF
02090 IS=AIC(I)/EXP(VBE(I)/VT)
02100 DISPLAY I,IS
02110 25 CONTINUE
02120 C---ACCEPT THE IS ESTIMATE
02130 DISPLAY *ENTER THE IS ESTIMATE*
02140 ACCEPT IS
02150 C*****
02160 C---START THE 3-PARAMETER MOVING FIT
02170 C---START WITH 4 POINTS AND INCREASE NO. OF POINTS IN FIT
02180 DISPLAY *NPTS IER NE IS/BO
02190 * * *

```

```

02300 DO 30 NNC=4,NCTE
02310 CALL MINIZ(V,SCR,P,NV,NNC,NP1,TOL,EPS,
02320 + EE,ND,MXIT,LLK,PO,P1,IM,FUNIBE)
02330 RME=EE/ELQAT(NNC)
02340 NE=THETA/P(2)
02350 30 DISPLAY NNC,P(1),NE,P(3),EE
02360 DISPLAY *INPUT IER,NE,BETAD,ESTIMATE*
02370 ACCEPT IER,NE,BETAD
02380 GO TO 50
02390 C*****
02400 C
02410 C EVALUATE THE REVERSE DIODE CHARACTERISTICS:IBR,NC,IS/BETAR
02420 C
02430 C*****
02440 600 ACCEPT(1) NCT,XX
02450 DO 71 J=1,NCT
02460 ACCEPT(1) Y(1,I),XX,Y(2,I)
02470 71 CONTINUE
02480 C--START THE 3 PARAMETER MOVING FIT
02490 C--START WITH 4 POINTS AND INCREASE NO. OF POINTS
02500 DISPLAY *NPTS IBR NC
02510 + *
02520 DO 81 NNC=4,NCT
02530 CALL MINIZ(V,SCR,P,NV,NNC,NP1,TOL,EPS,
02540 + EE,ND,MXIT,LLK,PO,P1,IM,FUNIBE)
02550 RME=EE/FLOAT(NNC)
02560 NC=THETA/P(2)
02570 DISPLAY NNC,P(1),NC,P(3),EE
02580 81 CONTINUE
02590 DISPLAY *INPUT IBR,NC,BETAR ESTIMATES*
02600 ACCEPT IBR,NC,BETAR
02610 GO TO 50
02620 C*****
02630 C
02640 C-EVALUATE THE BASE PUSHOUT PARAMETERS-BF2,V8,FF
02650 C*****
02660 700 DISPLAY *INPUT 1 FOR SINGLE STRIPE,2 FOR DOUBLE*
02670 ACCEPT NST
02680 RMST=FLOAT(NST)
02690 IRB=RMST*RMST*2.*VT/R88
02700 DISPLAY *INPUT 4-POINT BASE PUSHOUT DATA*
02710 DISPLAY *INPUT FT1,FT2,FT3,FT4,IC1,IC3,VCE1,VCE4*

```



```

02620 ACCEPT F1,F2,F3,F4,R1C1,R1C2,R1C3,VCE1,VCE4
02630 C--CALCULATE OF(SMALL) FROM POINTS 1-2
02640 F2=F1/F2-1.
02650 C-CALCULATE VB FROM POINTS 3-4
02660 C-----CALC VE VC (INTERNAL) AT 3-4
02670 99 XBF3=F1/F3
02680 CALL VINT(XBF3,R1C2,VCE1,VE3,VC3,AIB,AIC,VBE,NCT)
02690 XBF4=F1/F4
02700 CALL VINT(XBF4,R1C3,VCE4,VE4,VC4,AIB,AIC,VBE,NCT)
02710 VB=(VC3-VC4)/(ALOG(XBF3-1.))-ALOG(XBF4-1.)
02720 C--CALCULATE FF FROM POINT 4
02730 FF=-ALOG(1.-(XBF4-1.)/(BF2*EXP(VC4/VB)))/(EXP(VBE/VT)-1.)
02740 DISPLAY #BF2,#BF3,#VB,#FF,#FF
02745 GO TO 50
02750 C
02760 C*****
02770 C---QFN EVALUATION CODE-----
02780 C*****
02790 C REORDER THE INPUT ARRAYS FOR QFN CALCULATIONS
02800 800 DO 51 I=1,NCTF
02810 N8=NCTF-I+1
02820 Z(1,I)=AIC(N8)
02830 XIB=AIB(N8)
02840 C-CALL GRTH TO EVALUATE Z FOR THE DATA POINT
02850 CALL GRTH(1,VALU,1,50,ZFIND,0,1,5,-6)
02860 Z2=VALU
02870 C Z(2,I)=VEPRIME FOR DATA POINT
02880 N8=R8*(TAN(Z2)-Z2)/(4.*Z2*(TAN(Z2)+2))
02890 Z(2,I)=VBE(N8)-XIB*(R8+R8)+R8*IER*EXP((VBE(N8)-XIB*R8)/(NE+VT))
02900 Z(2,I)=Z(2,I)-RE*(XIB+Z(1,I))
02910 C APPROXIMATE PC BY .5*VCC(LOW CURRENT VALUE) FOR VCPRIME EVALUATION
02920 C Z(3,I)=VCPRIME
02930 Z(3,I)=Z(2,I)+(XIB+Z(1,I))*RE+Z(1,I)*.5*VCC-VCEX
02940 51 CONTINUE
02950 C
02960 C--PERFORM NONLINEAR LEAST SQUARES FIT FOR QFN USING THE IC EON.
02970 C--FITTED TO VARIABLES VEPRIME AND VCPRIME
02980 C
02990 C
03000 C START WITH TWO HIGHEST INJECTION POINTS AND INCREASE
03010 P(1)=1E-15 ASSIGN ESTIMATE AND BOUNDS FOR QFN
03020 P(1)=0.

```

```

03030 P111=1,
03040 NV=3
03050 NP1=2
03060 TOL=EPS=1E-5
03070 ND=1
03080 MXIT=80
03090 LK=1
03100 IV=0
03110 DISPLAY *QFN FIT*
03120 DISPLAY *NPTS*, * QFN EST., * MEAN SQ. ERROR*, * MSE/NPTS*
03130 DO 70 NNC=2, NCTF
03140 CALL MINIZ(2, SCR, P, NV, NNC, NP1, TOL, EPS,
03150 * EE, ND, MXIT, LK, PO, P1, IV, FUNGFM)
03160 RMEP=EE/FLOAT(NNC)
03170 DISPLAY NNC, P11, EE, RMEP
03180 70 CONTINUE
03190 DISPLAY *INPUT QFN ESTIMATE*
03200 ACCEPT QFN
03210 GO TO 50
03220 C*****
03230 C
03240 C CALCULATE TAUF0 FROM MAXIMUM FT DATA POINT
03250 C
03260 C*****
03270 900 CJE=CCD/(1.-.7/PHIED)**.5
03280 CJC=CCD/(1.-.7-VCE1)/PHICO)**.33333
03290 TAUF0=(.15915/FT1-(CJE+CJC*(1.+RIC1*CC/VT)))*VT/RIC1)*
03300 * (1.-.7-VCE1)/VCR)**.2
03310 DISPLAY *TAUF0=*, TAUF0
03320 GO TO 50
03330 C*****
03340 C
03350 C TAUR CALCULATION FROM SATURATION TIME DATA
03360 C
03370 C*****
03380 1000 DISPLAY *INPUT IBF, IBR, ICF, TS*
03390 ACCEPT RB1, RB2, RCL, RTS
03400 TSAT=RTS/ALOG((RB1+RB2)/(RCL/BETAD+RB2))
03410 TAUR=TSAT*(1.+1./BETAR-BETAD/(BETAD+1.))-
03420 * (BETAD*(BETAR+1.))/(BETAR*(BETAD+1.))*TAUF0
03430 QRN=QFN*TAUR/TAUF0
03440 DISPLAY *TSAT=*, TSAT, *TAUR=*, TAUR, *QRN=*, QRN

```



```

03450      60 IQ 90
03460 C*****
03470 C
03480 C  OUTPUT THE VALUES OF MODEL PARAMETERS TO UNIT (2)
03490 C
03500 C*****
03510      1100 CONTINUE
03520      VF=VT
03530      BS=BC-1./3.
03540      BF=0.5
03550      PC=RHOC
03560      WRITE(2,TRANS)
03570      END
03580      SUBROUTINE ZFIND(Z,FZ)
03590 C--ZFIND CALCULATES Z GIVEN IB,IBB IN CONJ. WITH GRM ROOTFINDER
03600      COMMON/PARAM/SKIP(7),IBB,SKIP2(7)
03610      COMMON/OPPT/IB,SKIP3(2)
03620      REAL IBB,IB
03630      FZ=Z*TAN(Z)-(IB/IBB)
03640      RETURN
03650      END
03660      SUBROUTINE VINT(XBF,RCIN,VCEIN,VEOT,VCEI,AIC,VBE,NCT)
03670 C-----SUBR. CALCULATES INTERNAL EMITTER AND COLLECTOR VOLTAGES GIVEN
03680 C-----ICIN=COLLECTOR CURRENT
03690 C-----VCEIN=COLLECTOR - EMITTER VOLTAGE
03700 C-----REMAINING DATA IS FROM THE PREVIOUSLY INPUT
03710 C-----IC,IB,VBE TABLES AND MODEL PARAMETERS
03720      COMMON/PARAM/VI,IER,NE,IS,BETA0,RB0,RBB,IBB,RE,RCC,BF2,
03730      + VB,FFAVER,VCR
03740      COMMON/OPPT/XIB,XIC,XVBE
03750      EXTERNAL ZFIND
03760      REAL IFR,NE,IS,IBB
03770 C-FIND IB BY INTERPOLATION OF IC
03780      CALL INTERP(AIC,IB,NCT,RCIN,XIB)
03790 C-FIND VBE BY INTERPOLATION
03800      CALL INTERP(AIC,VBE,NCT,RCIN,XVBE)
03810 C-FIND RB VIA ROOT FINDER ROUTINE
03820      CALL GRTH(1,VALU,1.50,ZFIND,0,1.E-6)
03830      Z=VALU
03840      RB=RBB+(TAN(Z)-2)/((4.*2*(TAN(Z)+2)))
03850      VEOT=XVBE-XIB*(RB0+RB)+RB*IER*EXP(((XVBE-XIB+RB0)/(NE*VT)))
03860      VEOT=VEOT-RE*(XIB+RCIN)

```

```

03870 C-FIND PC BY BASE PUSHOUT EVALUATION
03880 RC=AMAX(0, RCC*(1-SQRT(1-RC*RC-1.)))/(BF2))
03890 90 VCOY=VEDT+(XIB+RICIN)*RC*RCIN+RC-VCEIN
03900 RETURN
03910 END
03920 SUBROUTINE INTERP(X,Y,N,VAL,OUTP)
03930 C-LINEAR INTERPOLATION ROUTINE
03940 DIMENSION X(1),Y(1)
03950 IF(VAL.LT.X(1))WRITE(6,100) VAL,X(1)
03960 IF(VAL.GT.X(N))WRITE(6,110) VAL,X(N)
03970 I=0
03980 10 I=I+1
03990 XT=X(I)
04000 IF(XT-VAL) 10,20,30
04010 C-EXACT VALUE IN TABLES
04020 20 OUTP=Y(I)
04030 RETURN
04040 C-INTERPOLATION REQUIRED
04050 30 OUTP=Y(I-1)+(VAL-X(I-1))*(Y(I)-Y(I-1))/(X(I)-X(I-1))
04060 RETURN
04070 100 FORMAT(*INTERP ROUTINE IS OFF THE LOW END FOR INPUT=*,E10.4,
04080 + *AND MIN TABLE VALUE=*,E10.4)
04090 110 FORMAT(*INTERP ROUTINE IS OFF THE HIGH END FOR INPUT=*,E10.4,
04100 + *AND MAX TABLE VALUE=*,E10.4)
04110 END
04120 SUBROUTINE GRTH(IN,C,IN,MAXI1,AUX,KNN,EPS)
04130 DIMENSION C(1),T(3),X(3)
04140 EPS1=ABS(EPS)
04150 IF(EPS1.EQ.0.) EPS1=1.0E-6
04160 L1=KNN+1
04170 L2=KNN+M
04180 IOUT=IN
04190 C
04200 C BEGIN LOOP TO FIND N ROOTS
04210 C
04220 DO 170 L=L1,L2
04230 T(1)=C(L)
04240 H=-1.0
04250 IF(T(1).NE.0.) H=-T(1)/10.
04260 D=-.5
04270 J1=MAXIT
04280 100 MAXJ=J1

```

1	GRTH
2	GRTH
3	GRTH
4	GRTH
5	GRTH
6	GRTH
7	GRTH
8	GRTH
9	GRTH
10	GRTH
11	GRTH
12	GRTH
13	GRTH
14	GRTH
15	GRTH
16	GRTH
17	GRTH

04290	RT=T(1)		GRIM	18
04300	IF(MAXJ.EQ.0) GO TO 155		GRIM	19
04310	T(2)=T(1)-H		GRIM	20
04320	T(3)=T(1)+H		GRIM	21
04330 C			GRIM	22
04340 C	BEGIN ITERATIONS TO FIND ONE ROOT		GRIM	23
04350 C			GRIM	24
04360	DO 150 J=1,MAXJ		GRIM	25
04370	CALL AUX(RT,FPRT)		GRIM	26
04380	FPRT=FPRT		GRIM	27
04390	IF(L.EQ.1) GO TO 110		GRIM	28
04400 C			GRIM	29
04410 C	EVALUATE FPRT		GRIM	30
04420 C			GRIM	31
04430	DO 105 I=2,L		GRIM	32
04440	DEN=RT-C(I-1)		GRIM	33
04450	IF(J.GT.3) GO TO 105		GRIM	34
04460	J1=J1-1		GRIM	35
04470	IF(ABS(DEN).GE.1.E-20) GO TO 105		GRIM	36
04480 C			GRIM	37
04490 C	RESTART ITERATION WHEN ANY OF THE THREE STARTING		GRIM	38
04500 C	VALUES ARE TOO CLOSE TO A PREVIOUS ROOT		GRIM	39
04510 C			GRIM	40
04520	IF(OUT.EQ.0) WRITE(6,500) L		GRIM	41
04530	T(1)=T(1)+.001		GRIM	42
04540	GO TO 100		GRIM	43
04550 105	FPRT=FPRT/DEN		GRIM	44
04560 110	IF(OUT.EQ.0) WRITE(6,500) L,RT,FPRT		GRIM	45
04570 C			GRIM	46
04580 C	RT IS A ROOT IF F(RT) AND FP(RT) ARE BOTH SMALL		GRIM	47
04590 C			GRIM	48
04600	IF(ABS(FRT).LT.1.E-20).AND.(ABS(FPRT).LT.1.E-20)) GO TO 160		GRIM	49
04610	IF(J.GT.3) GO TO 115		GRIM	50
04620	X(J)=FPRT		GRIM	51
04630	IF(J.EQ.3) GO TO 114		GRIM	52
04640	RT=T(J+1)		GRIM	53
04650	GO TO 150		GRIM	54
04660 114	RT=T(1)		GRIM	55
04670	GO TO 125		GRIM	56
04680 115	IF(ABS(FPRT).LT.ABS(X(1)+10.)) GO TO 120		GRIM	57
04690 C			GRIM	58
04700 C	FPRT IS TOO LARGE---REDUCE H AND TRY AGAIN		GRIM	59

04710 C				GRIM	60
04720	DI=DI+.5			GRIM	61
04730	H=H+.5			GRIM	62
04740	RT=RT-H			GRIM	63
04750	GO TO 150			GRIM	64
04760 C				GRIM	65
04770 C	MOVE DATA			GRIM	66
04780 C				GRIM	67
04790 120	X(3)=X(2)			GRIM	68
04800	X(2)=X(1)			GRIM	69
04810	X(1)=FPRT			GRIM	70
04820	D=DI			GRIM	71
04830 C				GRIM	72
04840 C	CALCULATE NEXT APPROXIMATION			GRIM	73
04850 C				GRIM	74
04860 125	A=1.0+D			GRIM	75
04870	B=X(3)+0+D-X(2)+A+X(1)+(A+D)			GRIM	76
04880	DEN=B+8-(4.0+X(1)+D+A)+(X(3)+D-X(2)+A+X(1))			GRIM	77
04890	DI=-2.0+X(1)+A			GRIM	78
04900	IF(DEN.LE.0.) GO TO 130			GRIM	79
04910	DEN=SQRT(DEN)			GRIM	80
04920	IF(B.NF.0.) DEN=B+SIGN(DEN,B)			GRIM	81
04930	GO TO 135			GRIM	82
04940 130	IF(OUT.EQ.0) WRITE(6,500) L,DEN			GRIM	83
04950	IF(B.EQ.0.) GO TO 140			GRIM	84
04960	DFN=B			GRIM	85
04970 135	DT=DI/DFN			GRIM	86
04980 140	H=DI+H			GRIM	87
04990	RT=RT+H			GRIM	88
05000	IF (ABS(H).LE.EPS1+ABS(RT)) GO TO 155			GRIM+1	1
05010 150	CONTINUE			GRIM	90
05020 155	CALL AUX(RT,FRT)			GRIM	91
05030 160	C(L)=RT			GRIM	92
05040	IF(OUT.EQ.0) WRITE(6,501) L,RT,FRT			GRIM	93
05050 170	CONTINUE			GRIM	94
05060	IF(OUT.EQ.0) WRITE(6,502)			GRIM	95
05070	RETURN			GRIM	96
05080 500	FORMAT(I3,3E20.8)			GRIM	97
05090 501	FORMAT(I3,2E20.8/1H)			GRIM	98
05100 502	FORMAT(1H1)			GRIM	99
05110	END			GRIM	100
05120	SUBROUTINE MINIZ(X,A,P,NV,NC,NP1,TOL,EPS,				


```

05130      + EE,ND,MXIT,LLK,PO,P1,IW,FUN)
05140 C      SUBROUTINE MINIZ FOR BND07R      APRIL 4, 1966
05150      DIMENSION A(NP1,NP1),X(NV,NC),P(100),FP(100),D(100),PO(100),P1(100
05160      1,2,B(10)
05170 C      DIMENSION PPO(100)
05180
05190 C
05200 C
05210 C
05220      IF(IW,FO,0)C=1.0
05230      NP=NP1-1
05240      MMAIL = 10
05250      MAIL = 0
05260      DO 557 I=1,NP
05270 557 PPO(I)=P(I)
05280 C
05290      EPS1=5.*EPS+1.
05300      WRITE(6,23)(PO(I),I=1,NP)
05310 23 FORMAT(11MINIMA,15X,1P9E12.4/(22X,1P9E12.4))
05320      WRITE(6,22)(P1(I),I=1,NP)
05330 22 FORMAT(10MAXIMA,15X,1P9E12.4/(22X,1P9E12.4))
05340      WRITE(6,195)
05350 195 FORMAT(10ITERATION      ERROR      PARAMETERS/14X,+MEAN*/14X,+SQUARE
05360 1*)
05370 194 LLL=5
05380      LIT=0
05390      HU=NC
05400      H=0.
05410      LLL=5
05420      EO=7.2E75
05430      DO 556 I=1,NP
05440 556 P(I)=PPO(I)
05450      FNC=NC-NP
05460 29 DO 85 I=1,NP1
05470      DN 85 J=1,I
05480      A(I,J)=0.
05490      DN 2 L=1,NC
05500 C      CALL FUN(F(I),FP,X(1,L),P,LLK)
05510      CALL FUN(Q,FP,P,X(1,L))
05520      FP(NP1)=X(ND,L)-Q
05530      IF(IW,NE,0)C=X(IW,L)
05540      IF(C.LY.(1.E-20)) GO TO 2

```

```

05550      DO 1 I=1,NP1
05560      FPIC=FP(I)+C
05570      DO 1 J=1,I
05580          1 A(I,J)=A(I,J)+FPIC*FP(I)
05590          2 CONTINUE
05600      EE=A(NP1,NP1)/FNC
05610          6 IF(EE.LE.FO) GO TO 871
05620      NAIL=NAIL+1
05630      IF(NAIL.GT.MNAIL) GO TO 871
05640      DO 872 I=1,NP
05650          P(I)=PP(I)+D(I)/2.
05660      872 D(I)=D(I)/2.
05670      GO TO 29
05680      C
05690      C
05700      871 WRITE(6,199) LIT, NAIL, EE, (P(I), I=1, NP)
05710      199 FORMAT(16,1X,I2,1X,1P10E12.4,/(22X,1P9E12.4))
05720      NAIL=0
05730      8191 LIT=LIT+1
05740      CALL STEP(A,D,P,FO,P1,NP1,TOL)
05750      IF(LIT.GT.MXIT) GO TO 200
05760      IF(EE.FO.O.) GO TO 470
05770      PC=1.
05780      IF(EO.NE.7.2E75) PC=ABS((EO-EE)/EE)
05790      EO=EE
05800      IF(PC.LT.EPS) GO TO 100
05810      LLL=LLL
05820      121 DO 28 I=1,NP
05830          PP(I)=P(I)
05840      28 P(I)=P(I)+O(I)
05850      GO TO 29
05860      200 WRITE(6,201)
05870      201 FORMAT(30H) THE PROCESS IS NOT CONVERGING)
05880      GO TO 470
05890      100 LLL=LLL-1
05900      IF(LLL.NE.0) GO TO 121
05910      470 DO 778 I=1,NP
05920          778 FP(I)=SQRT(ABS(A(I,I)+EE))
05930      WRITE(6,779) (FP(I), I=1, NP)
05940      779 FORMAT(40ASYMPTOTIC STANDARD DEVIATIONS OF THE PARAMETERS+//
05950          X(10X,1P10E12.4))
05960      DO 841 I=1,NP

```



```

05970      FP(I)=SQRT(ABS(A(I,I)))
05980      DO 841 J=1,I
05990      841 A(J,I)=A(I,J)
06000      WRITE(6,774)
06010      774 FORMAT(40ASYMPTOTIC CORRELATION MATRIX OF THE PARAMETERS*)
06020      L1=0
06030      371 L0=L1+1
06040      L1=MIN0(NP,L1+10)
06050      WRITE(6,372)(LJ=L0,L1)
06060      372 FORMAT(40,10I12)
06070      DO 842 I=1,NP
06080      K=0
06090      DO 373 J=L0,L1
06100      K=K+1
06110      IF(FP(I).EQ.0.0.OR.FP(J).EQ.0.0.OR.A(I,J).EQ.0.0)GO TO 843
06120      8(KI=A(I,J))/(FP(I)*FP(J))
06130      GO TO 373
06140      843 8(K)=0.0
06150      373 CONTINUE
06160      842 WRITE(6,374)I,(8(J),J=1,K)
06170      374 FORMAT(14,2X,10F12.5)
06180      IF(L1.NE.NP)GO TO 371
06190      1515 WRITE(6,553)
06200      553 FORMAT(1CASE
06210      1,1/30X,1DEVIATION,1/30X,1OF ESTIMATE*)
06220      DO 551 L=1,NC
06230      SDEST=0.0
06240      CALL FUN(Q,FP,P,X(1,L))
06250      DO 24 J=1,NP
06260      DO 24 J=1,NP
06270      24 SDEST=SDEST+FP(I)*FP(J)*A(I,J)
06280      SDEST=SQRT(SDEST*EE)
06290      TT=X(ND,L)-Q
06300      551 WRITE(6,552)L,Q,TT,SDEST,(X(I,L),I=1,NV)
06310      552 FORMAT(1X,14,10F12.5/141X,7F12.5)
06320      RETURN
06330      END
06340      SURROUTINE STEP(A,D,P,P0,P1,NP1,TOL)
06350      C      SUBROUTINE STEP FOR BMD07R
06360      C      DIMENSION A(NP1,NP1),V(100),D(100),IN(100),P0(100),P1(100),P(100)
06370      C
06380      NP=NP1-1

```

APRIL 4, 1966

```

06390 DO 20 I=1,NP1
06400 V(I)=SORT(A(I,I))
06410 DO 20 J=1,I
06420 IF (V(I)+V(J)).EQ.0.1 GO TO 212
06430 A(I,J)=A(I,J)/(V(I)+V(J))
06440 GO TO 20
06450 212 A(I,J)=0.
06460 20 CONTINUE
06470 DO 2 I=1,NP
06480 2 IN(I)=0
06490 8 K=0
06500 R=0.
06510 DO 1 I=1,NP
06520 IF(IN(I).NE.0 .OR. A(I,I).LE.TOL) GO TO 1
06530 Q=A(NP1,I)+A(NP1,I)/A(I,I)
06540 IF(Q.LT.R) GO TO 1
06550 K=I
06560 R=Q
06570 1 CONTINUE
06580 IFIX.EQ.0) GO TO 3
06590 C=-1.
06600 4 DO 5 I=1,K
06610 D(I)=A(K,I)
06620 5 A(K,I)=0.
06630 PP=D(K)
06640 DO 6 I=K,NP1
06650 D(I)=A(I,K)
06660 6 A(I,K)=0.
06670 D(K)=C
06680 IN(K)=IN(K)+1
06690 DO 7 I=1,NP1
06700 IF (PP.EQ.0..OR.D(I).EQ.0.) GO TO 24
06710 Y=D(I)/PP
06720 GO TO 25
06730 24 Y=0.
06740 25 CONTINUE
06750 DO 7 J=1,I
06760 7 A(I,J)=A(I,J)-D(J)*Y
06770 GO TO 6
06780 3 R=1.
06790 DO 9 I=1,NP
06800 IF(IN(I).NE.1) GO TO 9

```

```

06810 IF (V(I),EQ,0.1) GO TO 12
06820 D(I)=A(NP1,I)+V(NP1)/V(I)
06830 C
06840 C
06850 C
06860 C
06870 16 IF (D(I),EQ,0.1) GO TO 17
06880 H=AMAX1((P(I)-P(I))/D(I)),(P(I)-P(I))/D(I))
06890 GO TO 18
06900 15 D(I)=0.0
06910 17 H=1.
06920 18 CONTINUE
06930 IF (H,GE,R) GO TO 9
06940 R=H
06950 K=1
06960 9 CONTINUE
06970 C=1.
06980 IF (R,LE,TOL) GO TO 4
06990 DO 10 I=1,NP
07000 IF (IM(I),NE,1) GO TO 11
07010 D(I)=D(I)+R
07020 DO 21 J=1,I
07030 IF ((V(I)+V(J)),EQ,0.0) GO TO 30
07040 A(I,J)=A(I,J)/(V(I)+V(J))
07050 GO TO 21
07060 30 A(I,J)=0.
07070 A(J,I)=A(I,J)
07080 GO TO 10
07090 D(I)=0.
07100 DO 22 J=1,NP
07110 A(I,J)=0.
07120 22 A(J,I)=0.
07130 10 CONTINUE
07140 RETURN
07150 END
07160 SUBROUTINE FUNIBE(F,D,P,X)
07170 C
07180 C-THIS ROUTINE PROVIDES FUNCTION AND DERIVATIVE VALUES FOR
07190 C- THE EVALUATION OF IER,NE,IS/80 USING 18-VBE VALUES
07200 C E. MOCK TRW SYSTEMS SEPT 1977
07210 COMMON/TEMP/THETA
07220 DIMENSION X(1),D(1),P(1)

```

```

07230 F=P(1)*(EXP(P(2)*X(2))-1.0)+P(3)*(EXP(THETA*X(2))-1.0)
07240 D(1)=EXP(P(2)*X(2))-1.0
07250 D(2)=P(1)*X(2)+EXP(P(2)*X(2))
07260 D(3)=EXP(THETA*X(2))-1.0
07270 RETURN
07280 END
07290 SUBROUTINE FUNEJ(F,D,P,X)
07300 C
07310 C-THIS ROUTINE PROVIDES FUNCTION AND DERIVATIVES FOR EVALUATION
07320 C OF CJEO AND PHICD VIA CJE FIT, E. MOCK TRW SYSTEMS AUG. 1977
07330 C
07340 C NOTE: BE=1/2 PERMANENT ASSIGNMENT
07350 C
07360 DIMENSION D(1),X(1),P(1)
07370 F=P(1)/(1.-X(2)/P(2))+.5)+P(3)
07380 D(1)=F/P(1)
07390 D(2)=-P(1)+.5+X(2)/(P(2)+P(2)*X(2)+1.-X(2)/P(2))+1.5)
07400 D(3)=1.
07410 RETURN
07420 END
07430 SUBROUTINE FUNCJ(F,D,P,X)
07440 C
07450 C-THIS ROUTINE PROVIDES FUNCTION AND DERIVATIVES FOR EVALUATION
07460 C OF CJCO AND PHICO VIA CJC FIT, E. MOCK TRW SYSTEMS AUG. 1977
07470 C
07480 C NOTE: BC=1/3 PERMANENT ASSIGNMENT
07490 C
07500 DIMENSION D(1),X(1),P(1)
07510 F=P(1)/(1.-X(2)/P(2))+.333333)+P(3)
07520 D(1)=F/P(1)
07530 D(2)=-P(1)+.333333+X(2)/(P(2)+P(2)*X(2)+1.-X(2)/P(2))+1.333333)
07540 D(3)=1.
07550 RETURN
07560 END
07570 SUBROUTINE FUNGF(F,D,P,X)
07580 COMMON/PARAM/VT,IER,NE,IS,BETAD,RBO,RBB,I0B,RE,RCC,BF2,V8,
07590 +FF,VER,VCR
07600 C THIS SUBROUTINE PROVIDES FUNCTION AND DERIVATIVES FOR
07610 C EVALUATION OF QFN FOR COLLECTOR CURRENT FIT BY ROUTINE
07620 C MINIZ E. MOCK TRW SYSTEMS AUG. 1977
07630 C-----
07640 DIMENSION D(1),P(1),X(1)

```

```

07650      REAL IER,NE,IS,IBB,LMB2
07660      FFX=FF*(EXP(X(2)/VT)-1.)
07670      LMB2=(1.+X(2)/VER+X(3)/VCR)/2.
07680      RF=1.+BF2*EXP(X(3)/VB)*I1.-EXP(FFX)
07690      XSQR=SQRT(LMB2*LMB2+BF*P(1)+EXP(X(2)/VT))
07700      RK1=IS*EXP(X(2)/VT)
07710      F=RK1/(LMB2+XSQR)
07720      D(1)=(-RK1+BF*EXP(X(2)/VT))/(2.*(LMB2+XSQR)+XSQR)
07730      RETURN
07740      END
07750      SUBROUTINE ATQF(A,N,F)
07760      DIMENSION A(1)
07770      LOGICAL BLANK
07780      BLANK=.TRUE.
07790      S=1.0
07800      NUMB=0
07810      TEN=1.0
07820      DIV=1.0
07830      DO 10 I=1,N
07840      L=INTCHR(A,I)
07850      IF(L.EQ.36) GO TO 10
07860      BLANK=.FALSE.
07870      IF(L.NE.36) GO TO 2
07880      S=-1.0
07890      GO TO 10
07900      2 IF(L.NE.44) GO TO 4
07910      TEN=10.0
07920      GO TO 10
07930      4 IF(L.GT.9) GO TO 9
07940      NUMB=NUMB+10+L
07950      DIV=DIV*TEN
07960      9 CONTINUE
07970      10 CONTINUE
07980      IF(BLANK)RETURN
07990      F=S*FLOAT(NUMB)/DIV
08000      RETURN
08010      END
08020      FUNCTION INTCHR(STRING,N)
08030      DIMENSION SEQ(50),STRING(1),EBCD(5)
08040      DATA SEQ/1H0,1H1,1H2,1H3,1H4,1H5,1H6,1H7,1H8,1H9,
08050      1HA,1HB,1HC,1HD,1HE,1HF,1HG,1HH,1HI,1HJ,
08060      1HK,1HL,1HM,1HN,1HO,1HP,1HQ,1HR,1HS,1HT,

```



```

08070      X      1MU,1HV,1HW,1HX,1HY,1H2,1H,1H*,1H-,1H,1H /
08080      X      1H/,1H(,1H),1H(,1H),1H*,1H-,1H*,1H,1H /
08090      DATA EBCD(1H,1H(,1H),1H*,1H-,1H*,1H,1H /
08100      CALL GETCHR(STRING,N,CHR)
08110      IF (CHR.NE.SEQ(37)) GO TO 2
08120      INTCHR = 36
08130      GO TO 10
08140      2 DD 1 I=1,48
08150      IF(SEQ(I).EQ.CHR) GO TO 9
08160      1 CONTINUE
08170      I=51
08180      IF(EBCD(1).EQ.CHR) I=38
08190      IF(EBCD(2).EQ.CHR) I=52
08200      IF(EBCD(3).EQ.CHR) I=43
08210      IF(EBCD(4).EQ.CHR) I=46
08220      IF(EBCD(5).EQ.CHR) I=47
08230      9 INTCHR=I-1
08240      10 RETURN
08250      END
08260      SUBROUTINE GETCHR(A,N,C)
08270      DIMENSION A(N)
08280      DIMENSION FMAT(6)
08290      DATA FMAT/4H(A1),7H(1X,A1),7H(2X,A1),7H(3X,A1),7H(4X,A1),
08300      + 7H(5X,A1)/
08310      DECODE(10,FMAT(N),A1C
08320      RETURN
08330      END

```


APPENDIX D

TRANSIENT RADIATION RECOVERY CHARACTERISTICS OF
BIPOLAR JUNCTION TRANSISTORS

TRANSIENT RADIATION RECOVERY CHARACTERISTICS OF BIPOLAR JUNCTION TRANSISTORS

Dr. John Choma, Jr.
Senior Member, IEEE

ABSTRACT

This paper addresses the transient recovery characteristics of a bipolar junction transistor subjected to a saturating dose-rate radiation event. An estimate of the maximum recovery time is derived in terms of parameters typically listed on device specification sheets, physical device characteristics, and circuit parameters. Performance degradation due to high-injection phenomena is also addressed.

1.0 INTRODUCTION

Saturation is invariably incurred by a bipolar junction transistor exposed to an ionizing dose rate event, particularly if the transistor in question conducts large quiescent collector current or if the collector of the device is terminated in a large resistance. Since a saturated transistor behaves as a short-circuit in the sense that it is incapable of responding to input signal excitation, the time required by the device to recover from the saturating excitation is clearly a critical measure of circuit performance. For example, this recovery certainly influences the frequency response of a linear system and in digital circuitry, it degrades the nominal propagation delay. If the transistor in question is in a power supply, excessive recovery requirements may well lead to catastrophic circuit or system failure.

This paper addresses the problem of generating realistic worst case estimates of recovery time in saturated transistors. The equations are cast as functions of device and circuit parameters. Although the results are predicated on simple modeling techniques, a semi-quantitative account of complex high-injection phenomena is offered to refine the first-order results obtained.

2.0 PHOTOCURRENT RESPONSE

Figure (1) depicts a simplified schematic diagram of a bipolar junction transistor (BJT) subjected to a gamma dose rate or gamma dot ($\dot{\gamma}$) event. The gamma dot event is modeled electrically by a collector-to-base photocurrent source, $i_{pp}(t)$. As shown in Figure (2), photocurrent $i_{pp}(t)$ is a simple current pulse of amplitude I_{pp} and width T_p .

Let it be assumed that for all steady-state conditions corresponding to $i_{pp}(t) = 0$, the effective source current, I_S , is of a magnitude appropriate to operation of the BJT in the linear active region of its static characteristic curves. Thus, for time $t < -T_p$, the collector current is $i_c(t) = I_{CA}$. The corresponding base current, $i_b(t)$, is

$$I_{BA} = I_{CA}/h_{FE}, \quad (1)$$

where h_{FE} is the static forward current transfer ratio of the bipolar device.

At $t = -T_p$, the collector current, $i_c(t)$, rises toward its saturated value, say I_{CS} , in response to abrupt photocurrent excitation. By inspection of Figure (1), this saturated value of collector current is

$$I_{CS} = \frac{V_{CC} - V_{CSAT}}{R_C} - I_{PP}, \quad (2)$$

where V_{CSAT} is the collector-to-emitter saturation voltage. The corresponding base current is not linearly related to I_{CS} by an expression of the form of (1) since h_{FE} is defineable only for the case of transistor operation in its linear active region. Accordingly, if constant collector current in the amount of I_{CS} is achieved in the time frame, $-T_p < t < 0$, the base current, I_{BS} , is

$$I_{BS} = I_S + I_{PP} - \frac{V_{BSAT}}{R_{BB}}. \quad (3)$$

In (3), V_{BSAT} is the value of base-emitter voltage, $v_{BE}(t)$, under steady-state saturated conditions.

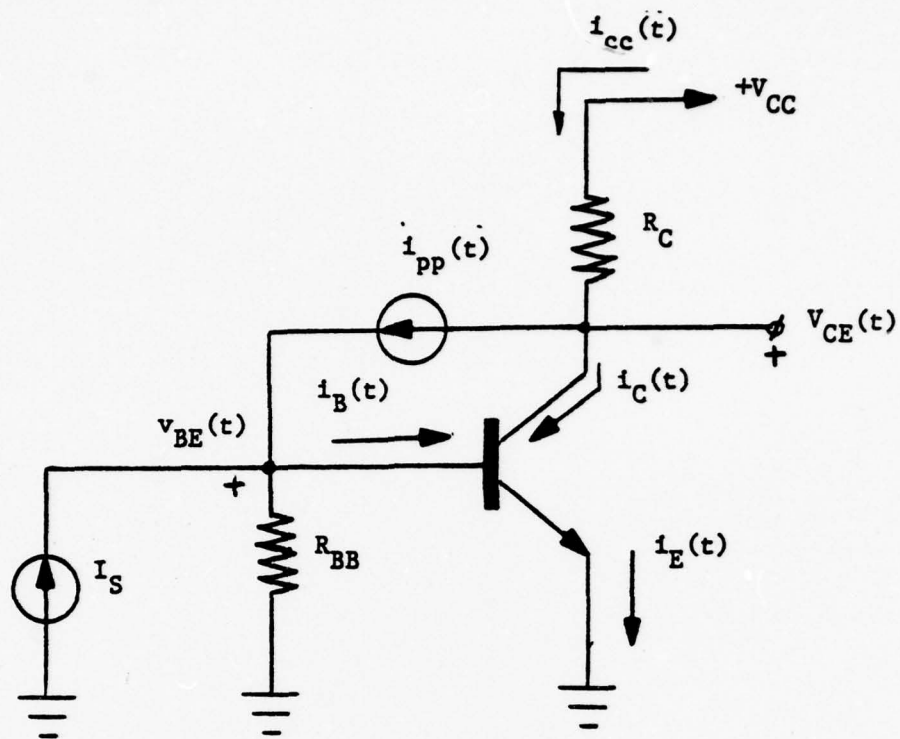


Figure (1). Schematic Diagram of Circuit Used For Radiation Storage Time Analysis

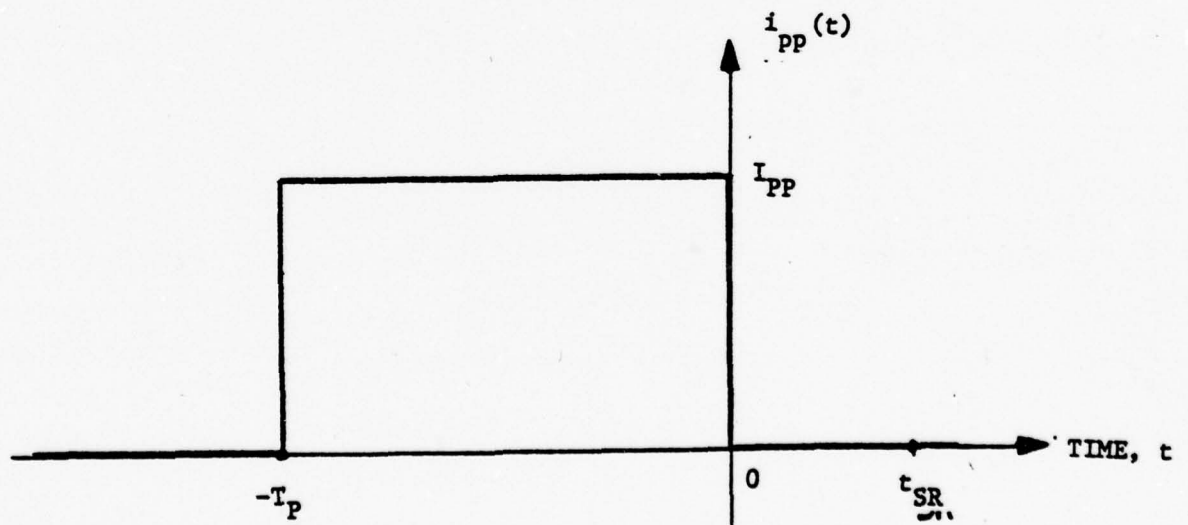


Figure (2). Time Domain Variation of Photocurrent Source, $i_{pp}(t)$

Assuming that the transistor in Figure (1) is indeed saturated in the neighborhood of $t < 0$, both device junctions are forward biased. Resultantly, a substantial amount of charge is stored in the base. The presence of excess base charge, which is viewed herewith as the difference between total base charge and the charge that accrues if only the base-emitter junction is forward biased, precludes an immediate response of the collector current to the instantaneous termination of the photocurrent pulse. The time required to reduce the excess charge to zero or equivalently, the time required to re-establish non-forward bias across the base-collector junction, is termed the "radiation storage time," t_{SR} .

The concept of radiation storage time is best appreciated by an investigation of Figure (3), which conceptually plots the distribution of charge injected into the base under varying bias conditions. Figure (3a) pertains to a BJT operating in its linear active region. Charge Q_{B0} , which is symbolized by the area of the cross-hatched region, is the equilibrium minority carrier distribution evidenced in the base under zero bias conditions. If the base width (W) is small, the charge profile arising out of forward injection across the base-emitter junction can be approximated by a straight line. This line has negative slope, since the reverse bias existing across the base-collector junction promotes removal of charges from base-to-collector. To the extent that carrier transport resulting from removal of base charge can be explained in terms of diffusion mechanics alone, the collector current is directly proportional to the magnitude of the slope of injected charge profile. Thus, collector current increases are in one-to-one correspondence with increasing magnitude of charge profile slope.

Under saturated conditions, the collector current is fixed at the level defined by (2), despite the fact that photocurrent flow gives rise to continuing injection of charge into the base region. Since collector current, and therefore charge profile slope, is constant, the resultant charge distribution must mirror Figure (3b). The excess charge alluded to earlier is Q_{BS} , which materializes primarily from injection across a forward biased base-collector junction. In short, both junctions are

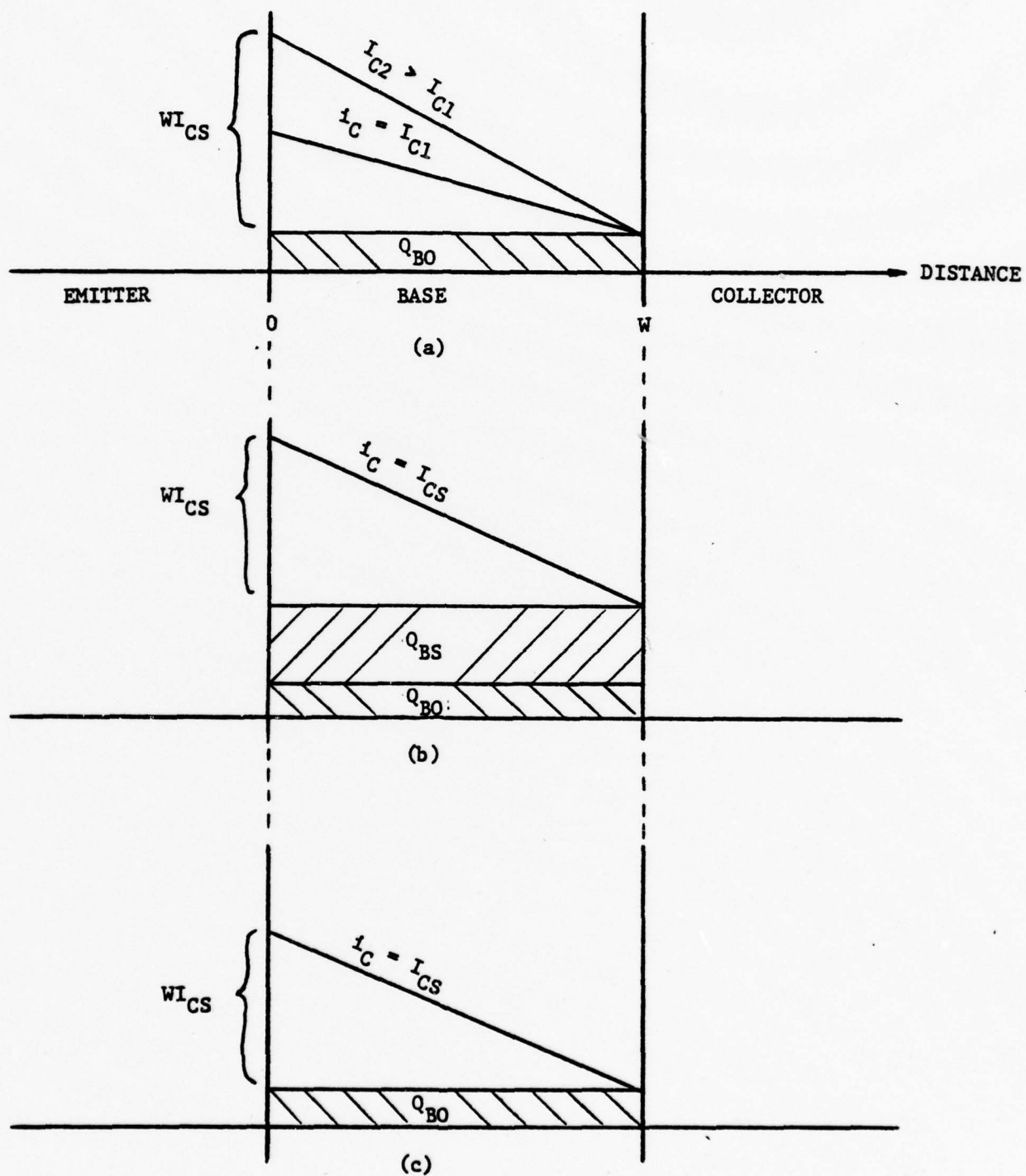


Figure (3). Charge Profiles In Base Region

(a) Normal Active Operation

(b) Saturated Conditions

(c) Threshold of Saturated-Normal Active Operation

forward biased in saturated regimes, and this condition is properly reflected in Figure (3b) by the fact that the charge distribution is not in equilibrium at either junction.

Upon termination of the radiation event, the collector current remains nominally constant for a time, t_{SR} . This situation can be visualized as spacially uniform removal of Q_{BS} , as suggested in Figure (3c). When t_{SR} seconds have elapsed, the collector current commences its response to photocurrent pulse discontinuation, since further removal of charge mandates a decrease in profile slope magnitude. Note that at the instant when $Q_{BS} = 0$, the BJT is at the threshold of re-entering its linear active operating regime.

Figure (4) offers plots of the collector and base current responses to the photocurrent excitation defined in Figure (2). Observe that the base current decreases almost instantaneously at $t = 0$ to a level, I_{BO} , despite the fact that the collector current remains constant in the time interval, $0 < t < t_{SR}$. The magnitude of this change in base current is a function only of I_{PP} and resistive loading in the base circuit, since the voltage across the strongly charged base-emitter junction cannot change instantaneously. To the extent that most of the excess charge, Q_{BS} , is swept primarily into either emitter or collector regions, the base current level of I_{BO} is essentially a constant up to time t_{SR} . This statement reflects the tacit assumptions that (1) removal of Q_{BS} does not perturb the charge stored as a result of forward injection from the emitter and (2) the base current component attributed to a forward biased base-collector junction is much smaller than the base current attributed solely to a forward-biased base-emitter junction.

Time t_R is termed the "recovery time" of the BJT. It is conventionally defined as the time required for collector current decrease to within 5% of quiescent value, following a saturating event.

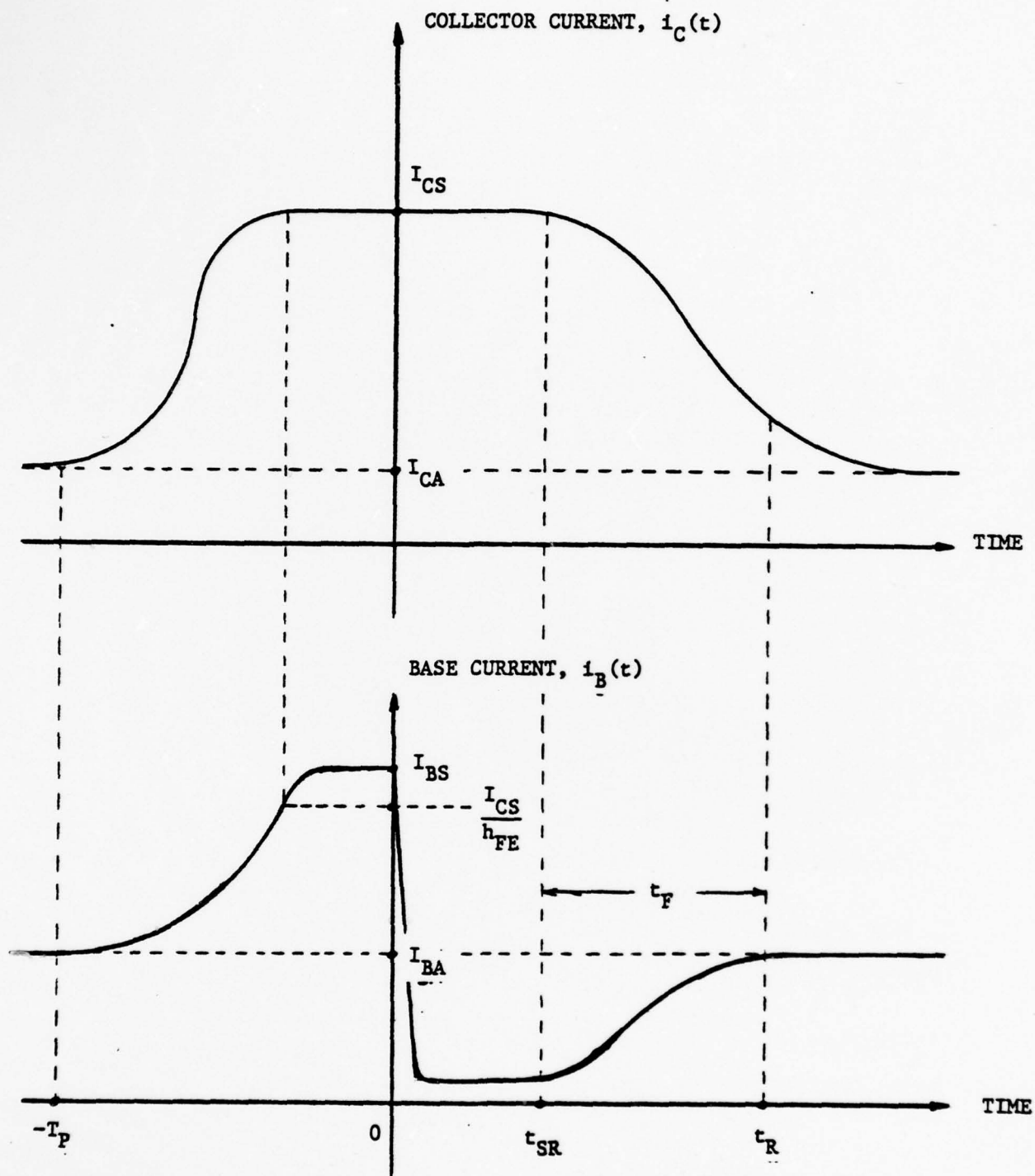


Figure (4). Collector And Base Current Responses To Photocurrent Excitation

(a) Collector Current Waveform

(b) Base Current Waveform

3.0 STORAGE TIME ANALYSIS

The low injection static equations which characterize BJT performance in all operating regimes are

$$I_E = I_S \left[e^{V_E'/V_T} - 1 \right] - I_S \left[e^{V_C'/V_T} - 1 \right] + \frac{I_S}{h_{FE}} \left[e^{V_E'/V_T} - 1 \right] \quad (3)$$

$$I_C = I_S \left[e^{V_E'/V_T} - 1 \right] - I_S \left[e^{V_C'/V_T} - 1 \right] - \frac{I_S}{h_{FR}} \left[e^{V_C'/V_T} - 1 \right], \quad (4)$$

where V_E' and V_C' are intrinsic voltages across base-emitter and base-collector junctions, respectively, V_T is the voltage equivalent of absolute junction temperature (25.9mV at 300°K), and I_S is termed a reference transport current. The static values of emitter current I_E and collector current I_C flow in the polarity directions defined in Figure (1), and voltages V_E' and V_C' are positive when the respective junctions are forward biased. Finally, parameter h_{FE} is the forward gain exploited in (1), while h_{FR} is the static reverse current transfer ratio; i.e., h_{FR} is the gain that materializes if the roles of emitter and collector are interchanged.

An inspection of (3) and (4) readily indicates that both emitter and collector currents are superpositions of the effects of charge injection across base-emitter and base-collector junctions. Since the terms involving V_E' are dominant for forward or linear active modes of operation, while the terms in V_C' predominate under inverted operational circumstances, it is reasonable to decompose I_E and I_C into forward and inverse current components. Accordingly, let

$$I_E \stackrel{\Delta}{=} I_{EF} - I_{EI} \quad (5)$$

$$I_C \stackrel{\Delta}{=} I_{CF} - I_{CI}, \quad (6)$$

where

$$I_{EF} = \frac{I_S}{\alpha_F} (\epsilon^{V'_E/V_T} - 1), \quad (7)$$

$$I_{EI} = I_S (\epsilon^{V'_C/V_T} - 1), \quad (8)$$

$$I_{CF} = \alpha_F I_{EF}, \quad (9)$$

$$I_{CI} = I_{EI} / \alpha_R. \quad (10)$$

In (7) through (10),

$$\alpha_F = \frac{h_{FE}}{h_{FE} + 1} \quad (11)$$

$$\alpha_R = \frac{h_{FR}}{h_{FR} + 1} \quad (12)$$

The decomposition of (3) and (4) into the form of (5) and (6) is significant in the sense that the constituents of the BJT current can be identified in terms of the charge storage components which materialize in the base due to injection across either junction. In particular, if Q_{BS} in Figure (3) can be attributed solely to charges which traverse a forward-biased ($V'_C > 0$) base-collector junction, both I_{EI} and I_{CI} are non-zero only if the time rate of change of Q_{BS} is non-zero. It follows that upon termination of the photocurrent pulse, a solution for radiation storage time, t_{SR} , embodies an investigation of the time at which I_{EI} and I_{CI} vanish.

Although the foregoing solution tact is meaningful, (5) through (10) are incapable of delivering time-domain response information unless they are modified to account for charge dynamics in the base. These dynamics are typically modeled by currents flowing across nonlinear junction capacitances which charge or discharge upon application or removal of the photocurrent pulse. A first order account of dynamical charge effects is accomplished by replacing constants α_F and α_R in (11) and (12) by the respective complex frequency transforms,

$$\alpha_F(s) = \frac{\alpha_{FO}}{1 + s/\omega_F} \quad (13)$$

$$\alpha_R(s) = \frac{\alpha_{RO}}{1 + s/\omega_F} \quad (14)$$

In the above relationships, ω_F is defined as the forward gain-bandwidth product, while ω_R is the inverted analog of ω_F . Specifically, ω_F is the radial gain bandwidth product of forward common-emitter current gain, and ω_R is the radial gain bandwidth product of inverse common-emitter current gain.

In the time interval, $0 \leq t \leq t_{SR}$, it may be argued that the inverse components of emitter and collector currents are expressible in the form,

$$i_{EI}(t) = i_{EI}(0) + \Delta i_{EI}(t) \quad (15)$$

$$i_{CI}(t) = i_{CI}(0) + \Delta i_{CI}(t) \quad (16)$$

In (15) and (16), $i_{EI}(0)$ and $i_{CI}(0)$ are steady-state inverse currents which exist immediately prior to termination of photocurrent excitation. On the other hand, $\Delta i_{EI}(t)$ and $\Delta i_{CI}(t)$ are changes incurred in the inverse emitter and collector currents during the interval of radiation storage time. Clearly, radiation storage time, t_{SR} , can be defined implicitly as the largest of the two times, t_{SRE} and t_{SRC} , such that

$$\Delta i_{EI}(t_{SRE}) = i_{EI}(0). \quad (17)$$

$$\Delta i_{CI}(t_{SRC}) = i_{CI}(0). \quad (18)$$

It is necessary to stipulate

$$t_{SR} = \text{MAX}(t_{SRE}, t_{SRC}), \quad (19)$$

since the transistor re-enters its active operational region only when all inverse current flow ceases.

From (5) through (10), it is easily shown that

$$I_{EI}(s) = \left[\frac{\alpha_R(s)}{1 - \alpha_F(s)\alpha_R(s)} \right] \left[\alpha_F(s)I_E(s) - I_C(s) \right] \quad (20)$$

$$I_{CI}(s) = \left[\frac{\alpha_F(s)I_E(s) - I_C(s)}{1 - \alpha_F(s)\alpha_R(s)} \right] \quad (21)$$

whence, by (13) and (14)

$$i_{EI}(0) \equiv I_{EI} = \left(\frac{\alpha_{RO}}{1 - \alpha_{FO}\alpha_{RO}} \right) (\alpha_{FO}I_E - I_C) \quad (22)$$

$$i_{CI}(0) \equiv I_{CI} = \frac{\alpha_{FO}I_E - I_C}{1 - \alpha_{FO}\alpha_{RO}} \quad (23)$$

In (22) and (23), it is to be understood that I_E and I_C represent the steady state irradiated values of emitter and collector current, respectively.

Since the collector current is nominally constant for $0 \leq t \leq t_{SR}$, the transforms of the incurred changes in inverse currents are, from (20) and (21),

$$\Delta I_{EI}(s) = \left[\frac{\alpha_F(s)\alpha_R(s)}{1 - \alpha_F(s)\alpha_R(s)} \right] \Delta I_E(s) \quad (24)$$

$$\Delta I_{CI}(s) = \Delta I_{EI}(s)/\alpha_R(s). \quad (25)$$

From Figures (1) and (5), the net change in emitter current during the storage time interval is

$$I_E(s) = \frac{1}{s} \left[(I_{BO} + I_{CS}) - (I_{BS} + I_{CS}) \right] = -\frac{1}{s} I_{BS} - (I_{BS} - I_{BO}) \quad (26)$$

where I_{BO} is the nominal base current flowing in the time interval, $0 < t < t_{SR}$. By virtue of the charge storage arguments presented earlier,

$$I_{BO} = I_{BS} - \left(\frac{R_{BB}}{R_{BB} + R_B} \right) I_{PP}, \quad (27)$$

where R_B is the ohmic resistance of the active base region. Substitution of (13), (14), and (26) into (24) leads to the second-order transform,

$$\Delta I_{EI}(s) = - \frac{\alpha_{FO} \alpha_{RO} \omega_F \omega_R (I_{BS} - I_{BO})/s}{s^2 + (\omega_F + \omega_R)s + (1 - \alpha_{FO} \alpha_{RO}) \omega_F \omega_R}. \quad (28)$$

Assuming $\omega_F \gg \omega_R^{(1)}$, (28) reduces to

$$\Delta I_{EI}(s) \approx - \frac{\alpha_{FO} \alpha_{RO} \omega_R (I_{BS} - I_{BO})}{s(s + s_0)}, \quad (29)$$

where

$$s_0 = \frac{(1 - \alpha_{FO} \alpha_{RO}) \omega_R \omega_F}{\omega_R + \omega_F} \approx (1 - \alpha_{FO} \alpha_{RO}) \omega_R. \quad (30)$$

The inverse transform of (29) is

$$\Delta i_{EI}(t) = - \left(\frac{\alpha_{FO} \alpha_{RO}}{1 - \alpha_{FO} \alpha_{RO}} \right) (I_{BS} - I_{BO}) (1 - e^{-s_0 t}), \quad (31)$$

for $0 \leq t \leq t_{SRE}$. An analogous tact produces

$$\Delta i_{CI}(t) = - \left(\frac{\alpha_{FO}}{1 - \alpha_{FO} \alpha_{RO}} \right) (I_{BS} - I_{BO}) (1 - \alpha_{FO} \alpha_{RO} e^{-s_0 t}) \quad (32)$$

in the interval, $0 \leq t \leq t_{SRC}$, for the change in the inverse component of collector current.

(1) The inverse bandwidth is much smaller than the forward bandwidth owing to the reduced transport efficiency incurred as a result of charge injection from a lightly doped collector and charge collection by a heavily doped emitter.

An expression for t_{SRE} evolves straight-forwardly if (17), (22), and (31) are combined. A satisfying form for this expression rests on the observation that in (22),

$$\alpha_{FO} I_E - I_C = \alpha_{FO} (I_{CS} + I_{BS}) - I_{CS} = \alpha_{FO} (I_{BS} - I_{CS}/h_{FE}).$$

In particular, it can be shown that

$$t_{SRE} = \frac{1}{S_0} \ln \left(\frac{1}{1 - N_0} \right), \quad (33)$$

with

$$N_0 \triangleq \frac{I_{BS} - I_{CS}/h_{FE}}{I_{BS} - I_{BO}}. \quad (34)$$

Similarly,

$$t_{SRC} = \frac{1}{S_0} \ln \left(\frac{\alpha_{FO} \alpha_{RO}}{1 - N_0} \right). \quad (35)$$

Since $\alpha_{FO} \alpha_{RO}$ is less than unity, $t_{SRE} > t_{SRC}$ and thus,

$$t_{SR} \approx t_{SRE}. \quad (36)$$

It might be noted in passing that the inequality, $t_{SRE} > t_{SRC}$ is a reasonable result. This assertion follows from the fact that since inverse current flow reflects charge transport from collector-to-emitter, the time difference, $t_{SRE} - t_{SRC}$, represents delays associated with charge transport across the base layer of the BJT.

There is considerable engineering significance to the parameter, N_0 , defined by (34). Observe that the ratio, I_{CS}/h_{FE} , is the minimum base current required for BJT saturation in the steady state. This is to say that a static base current of I_{CS}/h_{FE} is commensurate with the onset of inverse injection across base-collector junction. A slightly larger base drive delivers $Q_{BS} > 0$, and the BJT is forced into saturation. It follows that since I_{BS} is the actual steady state base current for the saturated BJT, $(I_{BS} - I_{CS}/h_{FE})$ in the numerator on the right hand side of (34) represents the excess base current commensurate with assurance

of a saturated condition. Recalling that I_{BO} is the base current evidenced immediately after cessation of the photocurrent, $(I_{BS} - I_{BO})$ in (34) can be viewed as the driving current serving to effect recovery of the BJT. Since I_{BO} must be smaller than I_{CS}/h_{FE} if the BJT is indeed to recover, N_o is always less than one. Accordingly, N_o might be termed a "recovery" factor in the sense that it compares the base current needed for device recovery to the excess base current required to ensure device saturation. As is inferred by Figure (5), minimal radiation storage time is in one-to-one correspondence with small N_o . In turn, small N_o demands a small R_B/R_{BB} ratio, since from (3), (27), and (34),

$$N_o = \left(1 + \frac{R_B}{R_{BB}}\right) \left(1 - \frac{V_{BSAT}/R_{BB} + I_{CS}/h_{FE} - I_S}{I_{PP}}\right). \quad (37)$$

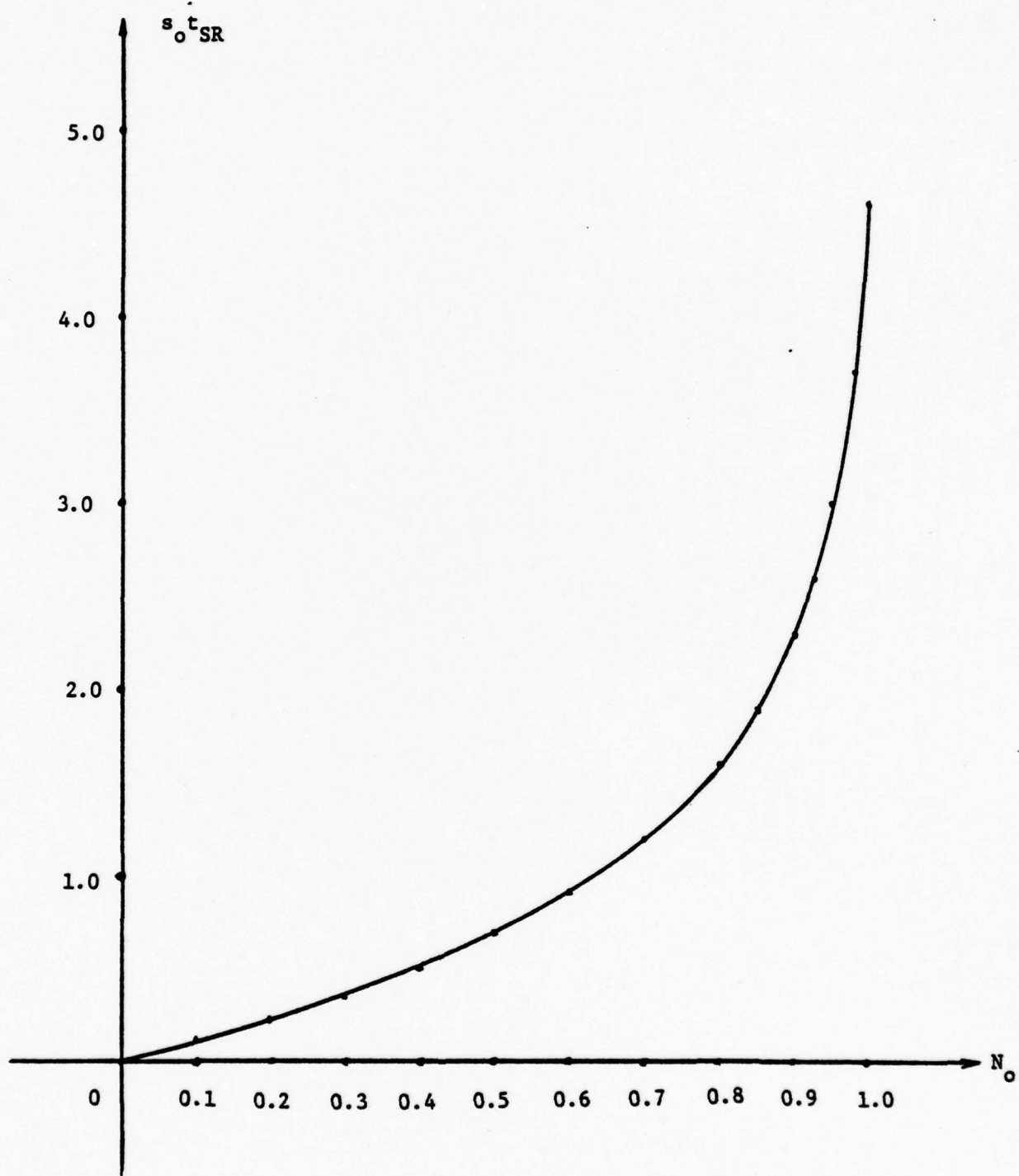


Figure (5). Normalized Radiation Storage Time As A Function of Recovery Factor, N_o

4.0 RECOVERY TIME

From Figure (4), the recovery time, t_R , is the superposition of radiation storage time, t_{SR} , and the so-called fall time, t_F . In the fall-time interval, $t_{SR} < t < t_R$, the BJT is in its linear active region of operation and if pole dominance can be assumed, the collector current waveform may be approximated by a single time constant expression of the form,

$$i_C(t) = \left[I_{CA} - (I_{CA} - I_{CS}) e^{-(t - t_{SR})/T_P} \right] \mu(t - t_{SR}). \quad (38)$$

In (38), $\mu(t)$ is the unit step function, and T_P is the first time moment of the small-signal model used to simulate the collector current response. Taking $i_C(t_R) = 1.05I_{CA}$, (38) delivers,

$$t_F = T_P \left[3.0 + \ln \left(\frac{I_{CS}}{I_{CA}} - 1 \right) \right]. \quad (39)$$

Figure (6) depicts the small-signal model alluded to in the preceeding paragraph [1]. In this model, r_π is the diffusion resistance of the base-emitter junction, r_o is the incremental output resistance, C_μ is the transition capacitance of the reverse-biased base-collector junction, C_π is the diffusion capacity of the base-emitter junction, and β_o is the small-signal common-emitter current gain of the BJT. The first time moment, which equates to the inverse of the dominant pole frequency, is the sum of the time constants individually attributed to C_π and to C_μ , respectively. By straight-forward circuit analysis,

$$T_P = R_1 \left[C_\pi + \left(1 + \frac{\beta_o R_L}{r_\pi} \right) C_\mu \right] + R_L C_\mu, \quad (40)$$

where

$$R_1 = \frac{r_\pi (R_B + R_{BB})}{r_\pi + R_B + R_{BB}}, \quad (41)$$

$$R_L = \frac{r_o R_C}{r_o + R_C}. \quad (42)$$

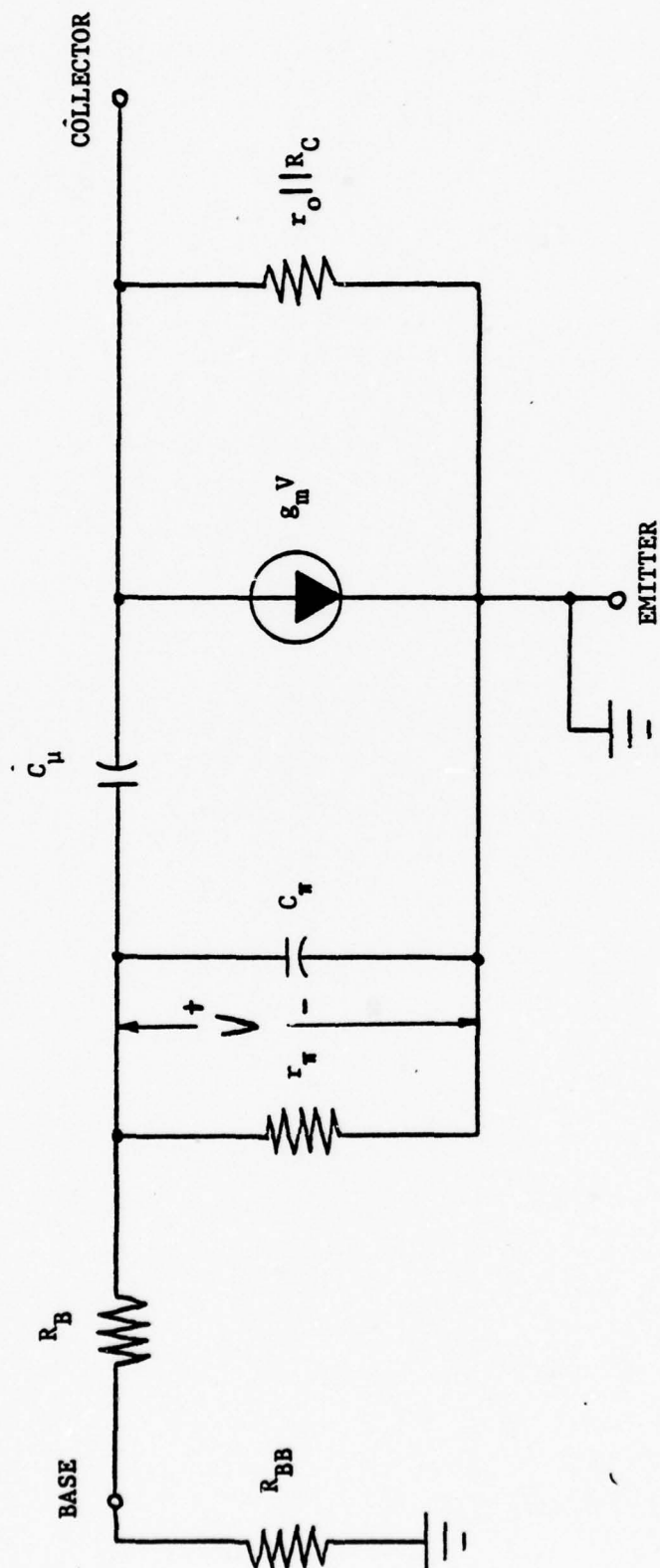


Figure (6). Small-Signal Bipolar Transistor Model Used in the Computation of Fall Time

Assuming $\beta_o \gg r_\pi/R_L$, (40) can be cast into the form

$$T_P = \left(\frac{R_B + R_{BB}}{R_B + R_{BB} + r_\pi} \right) \left(\frac{1}{\omega_F} + R_L C_\mu \right) \beta_o, \quad (43)$$

where

$$\omega_F = \frac{\beta_o}{r_\pi (C_\pi + C_\mu)} \quad (44)$$

is the short-circuit common-emitter gain-bandwidth product, as defined in conjunction with (13).

Care must be exercised in the utilization of (43) and (44), since these results derive from a linearized model which may inappropriately simulate the effects of large collector current excursions. In particular, the model does not incorporate the variations in small-signal parameters incurred by large changes in device currents and voltages. Accordingly, one can rationalize the tact of conservatively estimating t_F by choosing a worst case maximum value of T_P . From (43) and its companion equations, it is clear that a realistic maximum value for T_P is

$$T_{P\text{MAX}} = \beta_{o\text{MAX}} \left[\frac{1}{\omega_{F\text{MIN}}} + R_C C_{ob} \right], \quad (45)$$

with the understanding that $\beta_{o\text{MAX}}$ and $\omega_{F\text{MIN}}$ are extrema pertinent to the current excursion, I_{CS} -to- I_{CA} , and the corresponding collector-emitter voltage variation, V_{CSAT} -to- $(V_{CC} - I_{CA} R_C)$. Furthermore, C_{ob} , the common-base output capacitance for zero collector-base bias, is a commonly specified device parameter which exceeds, but closely approximates, small-signal capacitance C_μ .

5.0 EXAMPLE CALCULATION

Assume that the circuit of Figure (1) has $R_C = 500$ ohms, $R_{BB} = 5,000$ ohms, $V_{CC} = 5$ volts, and $I_S = 200$ micro-amperes. Assume further that the BJT is characterized by the following parameters:

$$h_{FE} = 50;$$

$$f_{TMIN} = 80\text{MHz}$$

$$f_R = 3\text{MHz (inverse gain-bandwidth);}$$

$$C_{ob} = 2.5\text{pF;}$$

$$\beta_{oMAX} = 150;$$

$$R_B = 800 \text{ ohms}$$

$$h_{FR} = 0.4;$$

$$V_{BSAT} = 2.3 \text{ volts (includes ohmic drop in } R_B);$$

$$V_{CSAT} = 0.55 \text{ volts.}$$

Finally, let the BJT be exposed to a gamma dose-rate event which gives rise to a photocurrent pulse amplitude of 2 milli-amperes.

From (2), the collector saturation current is

$$I_{CS} = \frac{5 - 0.55}{500} - (2)(10^{-3}) = 6.9\text{mA},$$

while (3) yields for saturated base current,

$$I_{BS} = (200)(10^{-6}) + (2)(10^{-3}) - \frac{2.3}{5000} = 1.74\text{mA}.$$

Taking $V_{BE} = 0.78$ volt for linear active operation, Figure (1) shows that the pre-irradiated value of base current is

$$I_{BA} = I_S - \frac{V_{BE}}{R_{BB}} = (200)(10^{-6}) - \frac{0.78}{5000} = 44\mu A;$$

hence, from (1), the corresponding collector current is

$$I_{CA} = (50)(44) = 2.2mA.$$

Finally, (27) produces

$$I_{BO} = (1.74)(10^{-3}) - \left(\frac{5000}{5800}\right)(2)(10^{-3}) = 15.9\mu A.$$

Using (11) and (12),

$$\alpha_{FO} = \frac{50}{51} = 0.98$$

and

$$\alpha_{RO} = \frac{0.4}{1.4} = 0.29.$$

Then by (30),

$$s_o = \left[1 - (0.98)(0.29) \right] \left[2\pi(3)(10^6) \right] = 13.5MRPS.$$

Equation (34) gives for the the recovery factor,

$$N_o = \frac{(1.74)(10^{-3}) - (6.9)(10^{-3})/50}{(1.74)(10^{-3}) - (15.9)(10^{-6})} = 0.929,$$

whence (33) and (36) deliver

$$t_{SR} = \frac{1}{(13.5)(10^6)} \ln \left[\frac{1}{1 - 0.929} \right] = 196nsec$$

for the estimated radiation storage time.

Using (21),

$$T_{\text{PMAX}} = 150 \left[\frac{1}{2\pi(80)(10^6)} + (500)(2.5)(10^{-12}) \right] = 486 \text{ nsec.}$$

Then from (39),

$$t_{\text{FMAX}} = (486)(10^{-9}) \left[3.0 + \ln \frac{6.9}{2.2} - 1 \right] = 1.83 \mu\text{sec.}$$

Thus, the estimated worst case BJT recovery time is

$$t_{\text{RMAX}} = t_{\text{FMAX}} + t_{\text{SR}} = 2.0 \mu\text{sec.}$$

Observe in the foregoing example that the storage time is in the order of 10% of the maximum recovery time. This result generally reflects situations actually encountered in realistic radiation test environments. Accordingly, it follows that BJT recovery time is largely determined by time moment parameter T_{PMAX} . In turn, T_{PMAX} is minimal for devices which exude low collector-base capacitance, large gain bandwidth product, and low small-signal current gain.

6.0 CONCLUSIONS

An analysis of the radiation recovery transient in a bipolar junction transistor subjected to a saturating dose rate event has been developed. The analysis, which is supplemented by exemplifying calculations of recovery time, reveals device parameters and performance attributes that must be critically scrutinized if recovery time is to be constrained to a minimum. Although the general nature of sensitive device parameters is properly uncovered, it is crucial that approximations invoked during the course of analysis be understood, particularly if the primary objective of utilizing the analysis in a given application is realistic absolute estimation of recovery time.

Undoubtedly, the most significant assumption is that BJT currents flow by diffusion mechanisms alone. In simplified terminology, it has been presumed that (1) the injected charge profile in the base is linearly graded, (2) the collector current is proportional to the magnitude of profile gradient, and (3) the excess stored charge is removed prior to removal of charge accumulated from forward injection across the base-emitter junction. In reality, drift components of BJT currents are at least comparable to, if not larger than, the diffusion components in saturated devices. These drift components loom increasingly more important if the actual base current is allowed to increase significantly over the minimum base current (I_{CS}/h_{FE}) commensurate with the threshold of saturation.

Aside from compromising the foregoing three presumptions, the immediate effect of non-negligible current transport via high-field drift mechanisms is high-current, low-voltage degradation in the gain-bandwidth product, ω_F [2]. The maximum amount of degradation is proportional to the square of the ratio of epitaxial layer length-to-neutral base width. Depending on the type of BJT addressed, the extent of this degradation can be in the range of 15-to-20. Similar attenuations are evidenced with respect to both the static and small-signal current gains, although the factor by which these gains degrade is not as severe as the degradations quoted for gain-bandwidth product. The upshot of the matter is that if manufacturer's gain-bandwidth product and gain specifications

are used to compute T_{PMAX} , it is conceivable that the estimated maximum recovery time might be low by factors in the range of 5-to-10, since device specifications are invariably applicable to operational regions other than high-injection regimes.

It must also be remembered that (38) and (39) presume device linearity and pole dominance for $t_{SR} < t < t_R$. The effects of inherent device nonlinearities are especially pronounced if the saturated-to-quiescent collector current ratio, I_{CS}/I_{CA} , is larger than four or five. Ringing in the collector and base current responses is indicative of either circuit nonlinearity or a non-dominant pole population. Indeed, if non-linearity is particularly severe, the analytical concept of a pole cannot be exploited in the computation of fall time t_F . It can be envisaged that the impropriety of either linearity or pole dominance is conducive to recovery time estimates that are low by 20%-to-40%.

In summary, it is suggested that the foregoing equations are useful in ascertaining device characteristics which strongly influence the radiation recovery response of a BJT. They are also useful when applied to the problem of bracketing a realistic estimate of maximum recovery time. The lowest anticipated maximum recovery time derives from direct employment of manufacturer's nominal specifications for key device parameters. The largest estimate for maximal recovery time is obtained by allowing gain and gain-bandwidth product to degrade in accordance with specified, or estimated high-injection device performance characteristics.

7.0 REFERENCES

1. J. Choma, Jr., "Process-Oriented, High Injection Circuit Models for Integrated Bipolar Junction Transistors," Office of Naval Research, Report No. N00014-75-C-1177, November 1976.
2. J. Choma, Jr., "A Process-Oriented Model for the Simulation of Base Pushout in Integrated Bipolar Devices," IEEE Transactions on Electron Devices, Vol. ED-22, pages 1079-1086, December 1975.

APPENDIX E

CIRCUIT MODEL FOR NEUTRON-INDUCED
PERFORMANCE DEGRADATION IN BIPOLAR JUNCTION TRANSISTORS

CIRCUIT MODEL FOR NEUTRON-INDUCED
PERFORMANCE DEGRADATION IN BIPOLAR JUNCTION TRANSISTORS

J. Choma, Jr., Senior Member
IEEE

J. M. Oberholtzer

ABSTRACT:

This paper proposes the use of an existing large-signal circuits model to simulate bipolar transistor performance degradation induced by neutron irradiation. It is shown that only three radiation parameters are required to establish a model for neutron effects over the entire practical current and voltage ranges of bipolar transistor operation.

September, 1977

1.0 INTRODUCTION

The predominant effects of neutron displacement damage in silicon are an increase in carrier generation rate and a decrease in majority carrier concentration. In a bipolar junction transistor (BJT), these effects combine to produce current gain attenuation, degradation in gain-bandwidth product, enhanced base-collector leakage current, increased collector breakdown voltage, and increased collector saturation voltage [1]. Additionally, neutron displacement damage in a BJT may significantly perturb the nominal thermal characteristics of a bipolar circuit. Depending on circuit configuration, the nominal thermal behavior can either be aggravated or improved by neutron bombardment [2]-[3].

Traditionally, the performance of bipolar circuits immersed in a neutron environment is simulated by exploiting various damage constants which are enumerated from experimental device characterizations. In particular, gain, leakage current, and gain-bandwidth product are measured prior to and immediately following controlled neutron irradiation of a given bipolar device. This data is used to extrapolate simple relationships between pre-irradiated and irradiated values of various device parameters. An example of such a relationship is the Messenger-Spratt equation [4],

$$\frac{1}{\beta_{\phi}} = \frac{1}{\beta_0} + K_{\phi} \tau_{FO} \phi, \quad (1)$$

where β_{ϕ} is the irradiated value of static short-circuit current transfer ratio, β_0 , τ_{FO} is the transit time of minority carriers across the neutral base, ϕ is neutron fluence, and K_{ϕ} is the pertinent damage constant. Other device performance indices, such as gain-bandwidth product, breakdown voltage, and leakage current, are related to device neutron fluence exposure by expressions whose forms are analogous to (1).

Although neutron-induced damage assessment equations are useful both for simulating the dependence of irradiated electrical parameters on their pre-irradiated counterparts and for establishing a basis of neutron hardness screening, at least two fundamental objections can be raised if these equations are used exclusively in evaluating bipolar response to neutron irradiation.

First, the damage constant methodology can only simulate measured results. It cannot be applied to the problem of predicting the radiation response of bipolar transistors, because the damage constants are empirical performance barometers. These constants are not well-defined in terms of intrinsic physical or geometrical device properties but instead, they derive purely from experimental data.

A second shortcoming is that most of the damage constants invoked in a neutron radiation response exercise are sensitive functions of device injection level. For example, K_ϕ in (1) varies with the voltage and current at which gain β_0 is measured. The upshot of the matter is that most damage assessment equations are applicable only to the injection regime in which they are formulated. Attempts made to invoke these same equations to damage assessment at significantly lower or higher injection levels generally result in substantial analytical errors. It follows that the methodology in question conveys little, if any, understanding of the sensitivity of neutron radiation response with respect to the possibly wide injection range which a bipolar device encounters in a prescribed circuit application.

This paper presents a new bipolar neutron damage model which is uniformly applicable to the low-through-high injection range of BJT operation. The model is an extension of an existing circuits model which is capable of predicting large-signal transient responses to forcing inputs that can drive the transistor from low-to-high injection regimes. In addition to the model parameters pertinent to simulation and prediction of traditional electrical responses, only three additional parameters are required for an evaluation of the effects of neutron radiation. These parameters are independent of voltage and current and moreover, they can be related to damage constants which have been enumerated from a damage assessment appropriate to mid-injection operational regimes.

2.0 FUNDAMENTAL TRANSISTOR MODEL

The bipolar transistor circuit model diagrammed in Figure (1) is proposed as the foundation for neutron radiation response studies.⁽¹⁾ The model possesses all of the attributes of the classical Ebers-Moll [5] and Gummel-Poon [6] topologies and in addition, it provides the following simulation capabilities.

- (1). The effects of base-collector depletion layer width modulations arising out of collector junction voltage changes are incorporated. This phenomenon, known as the Early Effect [7], gives rise to current gain dependence on collector voltage. Analogously, an account is made of Inverse Early Effect, which produces inverse beta dependence on base-emitter voltage.
- (2). Low-injection forward current gain attenuation due to non-ideal diode currents flowing across the base-emitter junction is replicated by the model. In Figure (1), the lumped equivalent to the non-ideal base-emitter diode current is

$$I_{BEN} = I_{ER} (\epsilon^{V'_E/N_E V_{TE}} - 1), \quad (2)$$

where V_{TE} is junction thermal voltage, and I_{ER} and N_E relate implicitly to emitter efficiency, degree of emitter sidewall injection, and the recombination velocity at the base-emitter interface. Parameter N_E is always greater than or equal to unity. The diode current, I_{BCN} , mathematically parallels the form of (2) and allows for low-level inverse current gain attenuation for transistors operated in inverted or saturated modes.

(1) The model, which was developed by the author at the University of Pennsylvania, is embedded in the ISPICE computer-aided design program and is available on a timeshare network marketed by National CSS, Inc., Norwalk, Connecticut.

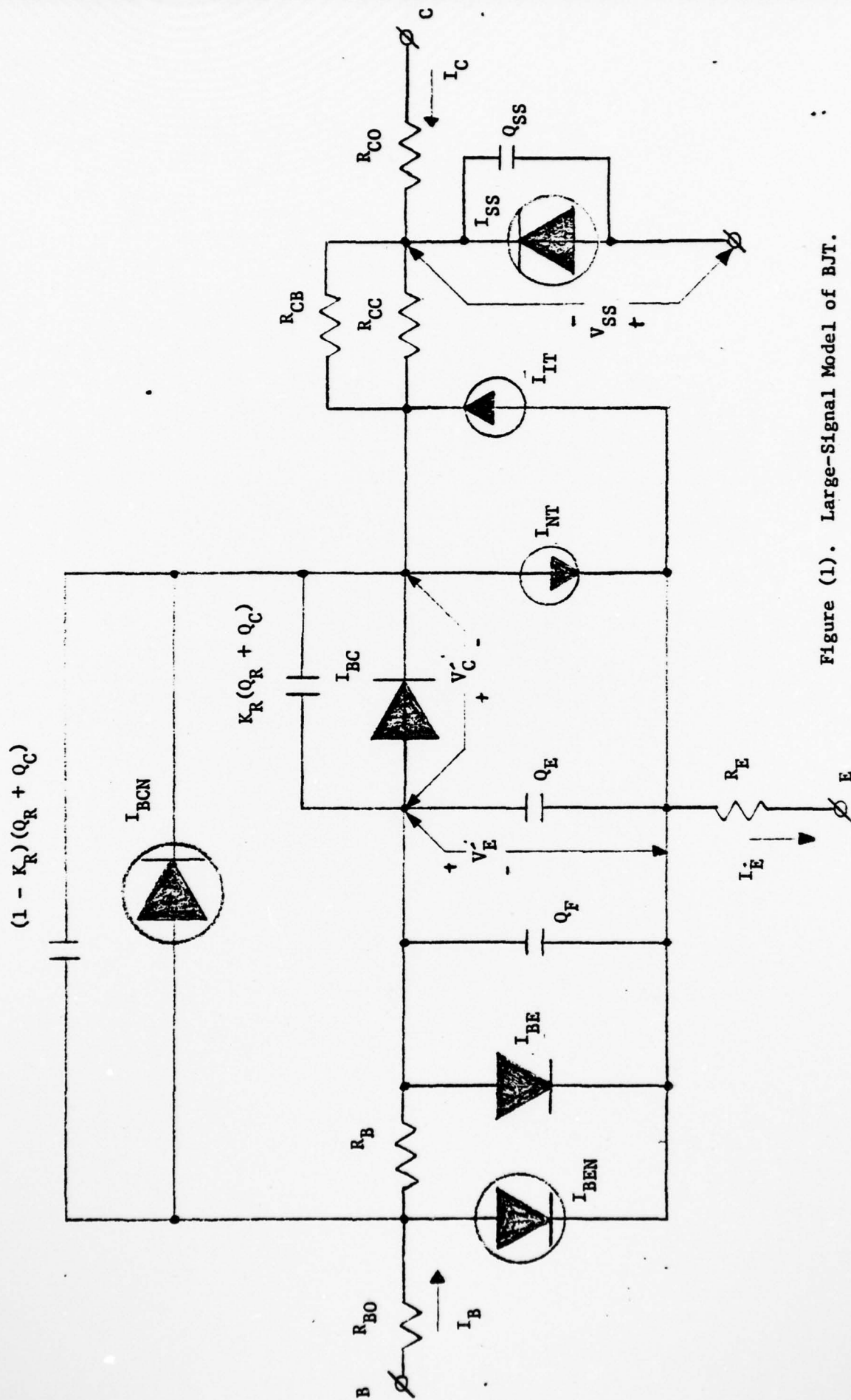


Figure (1). Large-Signal Model of BJT.

- (3). High-injection forward current gain degradation caused by conductivity modulation in both the base and quasi-saturated collector regions is incorporated in the model of Figure (1). The element germane to this simulation capability is

$$I_{NT} = \left(\frac{Q_{BO}}{Q_B} \right) I_S (\epsilon^{V'_E/V_{TE}} - 1), \quad (3)$$

where Q_B , the net majority charge in the effective base, has a value of Q_{BO} under zero bias ($V'_E = V'_C = 0$) conditions. The charge function, Q_B , which is the superposition of charge Q_E stored in the base-emitter transition layer, charge Q_C stored in the base-collector depletion region, and the charges (Q_F and Q_R) required to preserve space-charge neutrality in the face of charge injection across either junction, is given by

$$\frac{Q_B}{Q_{BO}} = (1 + \lambda_E) + \frac{\tau_F I_S (\epsilon^{V'_E/V_{TE}} - 1)}{Q_B} + \frac{\tau_R I_S (\epsilon^{V'_C/V_{TC}} - 1)}{Q_B} . \quad (4)$$

In (4),

$$\lambda_E = \frac{V'_E}{V_{ER}} + \frac{V'_C}{V_{CR}} , \quad (5)$$

where V_{ER} and V_{CR} are inverse and forward Early effect parameters, and τ_F (τ_R) is the forward (inverse) transit time of minority carriers in the field-neutral base. Because of base pushout phenomena, these transit times vary with device current and voltage [8]. Parameter I_S in (3) and (4) is directly proportional to the product of intrinsic carrier concentration and carrier diffusivity in the base, and it relates inversely to the total majority charge in the base region.

- (4). High-injection gain-bandwidth product (f_T) degradation caused by base pushout and conductivity modulation in the collector layer is a model feature. The model also addresses the related nonlinearity in effective collector resistance, ($R_{CC} + R_{CO}$).

- (5). The effects of static emitter crowding on the effective base resistance, $(R_{BO} + R_{BB})$, are embodied in the model. Excess phase and both static and dynamic conduction across the collector substrate interface are also included.
- (6). A first order approximation of the distributed effects of high-frequency excitation is introduced by way of the semi-empirical parameter, K_R ($K_R \leq 1$).

3.0 LOW-INJECTION CURRENT GAIN DEGRADATION

Under static forward bias operating conditions, all charge functions vanish, the substrate diode current, I_{SS} , is very nearly zero, and currents I_{BCN} , I_{BC} , and I_{IT} , which are exponential functions of the intrinsic base-collector junction voltage, are essentially zero. Accordingly, Figure (1) verifies that base current I_B is given by

$$I_B = I_{BE} + I_{BEN}, \quad (6)$$

where I_{BEN} is defined by (2) and

$$I_{BE} = \frac{I_S}{\beta_0} [e^{V_E/V_{TE}} - 1]. \quad (7)$$

In (7), β_0 is the maximum value of the static transfer ratio,

$$h_{FE} = \frac{I_C}{I_B}, \quad (8)$$

under the special condition of zero bias ($V_C' = 0$) across base-collector junction.

Returning to Figure (1), it is clear that under the conditions stipulated above, the collector current, I_C , is identical to the current, I_{NT} . From (3) and (4) it can be shown that

$$I_C = \frac{I_S (\epsilon^{V'_E/V_{TE}} - 1)}{\left(\frac{1 + \lambda_E}{2} \right) + \left\{ \left(\frac{1 + \lambda_E}{2} \right)^2 + Q_{FN} (\epsilon^{V'_E/V_{TE}} - 1) + Q_{RN} (\epsilon^{V'_C/V_{TC}} - 1) \right\}^{1/2}} \quad (9)$$

where

$$Q_{FN} \triangleq \frac{\tau_F I_S}{Q_{BO}} \quad (10)$$

$$Q_{RN} \triangleq \frac{\tau_R I_S}{Q_{BO}} \quad (11)$$

The term involving Q_{RN} in (9) is essentially zero, provided that the BJT is operated in its linear active domain. Moreover, for low-to-moderate injection levels, the term containing Q_{FN} is negligible, so that (9) collapses to

$$I_C \approx \left(\frac{I_S}{1 + \lambda_E} \right) \epsilon^{V'_E/V_{TE}} \quad (12)$$

In (12), it is assumed that the exponential term is much larger than unity. If this same reasonable assumption is invoked on (2), (8) can be shown to deliver

$$h_{FE} \approx \frac{\beta_o / (1 + \lambda_E)}{1 + \exp \left[\left(\frac{N_E - 1}{N_E} \right) \left(\frac{V_K - V'_E}{V_{TE}} \right) \right]} \quad (13)$$

with

$$V_K \triangleq \left(\frac{N_E}{N_E - 1} \right) V_{TE} \ln \left(\frac{\beta_o I_{ER}}{I_S} \right) \quad (14)$$

Figure (2) portrays the dependence of h_{FE} and V'_E , and hence the dependence of h_{FE} on the natural logarithm of collector current I_C . Recalling (5), the effect of parameter λ_E , as depicted in the figure, is to simulate the sensitivity of current gain with respect to the reverse biasing voltage applied at the collector. Observe then that for increasing V'_E , h_{FE} correctly approaches a constant at fixed collector junction voltage, provided that the contribution of V'_E to λ_E is insignificant in comparison to the contribution of V'_C . For decreasing forward bias, h_{FE} attenuates in such a way that at $V'_E = V_K$, h_{FE} is one-half of the current gain at moderate current levels. Notice that V_K is dependent on both I_{ER} and N_E , which implicitly relate to the characteristics of the base-emitter interface. Finally, N_E fixes the slope of the gain curve at $V'_E = V_K$. If $N_E = 1$, which infers only idealized diode current flow across the base-emitter junction, h_{FE} is constant over the addressed range of V'_E .

The preceding discussion applies to a BJT operated in a traditional, non-nuclear, electrical environment. When this environment is perturbed by significant neutron fluence, one can postulate that additional base current, say ΔI_B , must be supplied in order to maintain the collector current at its pre-irradiated level. Let this base current enhancement be expressed as

$$\Delta I_B = I_\phi \left[\epsilon^{V'_E/V_{TE}} - 1 \right] + I_{\phi 0} \left[\epsilon^{V'_E/N_E V_{TE}} - 1 \right], \quad (15)$$

where it is understood that I_ϕ is a function of the neutron energy imparted to the active region of the base-emitter junction. On the other hand, $I_{\phi 0}$ is parametrically related to the neutron energy absorbed by the emitter sidewalls, the emitter-base depletion region, and the surface of the depleted layer associated with the base-emitter junction.

Clearly, the induced increment in base current can be modeled by incorporating two additional current sources in the base-emitter circuit of Figure (1). Current I_{BEN} is placed in parallel with a source whose current is defined by the second term on the right hand side of (15), while the first term in this relationship is a diode in shunt with current I_{BE} in Figure (1). Notice, however, that these modifications infer a mere redefinition of parameters β_0 and I_{ER} . Specifically, β_0 and I_{ER} in the traditional model can be replaced by irradiated parameter values, β_ϕ and

AD-A062 790

TRW DEFENSE AND SPACE SYSTEMS GROUP REDONDO BEACH CALIF F/G 9/1
PROCESS-ORIENTED, HIGH-INJECTION CIRCUIT MODELS FOR INTEGRATED --ETC(U)
JAN 78 J CHOMA N00014-77-C-0043

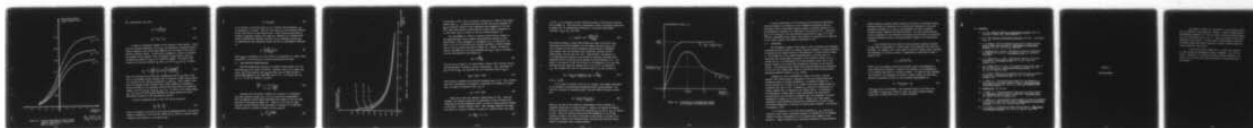
UNCLASSIFIED

TRW-78.4734.7-023-PT-2-V0

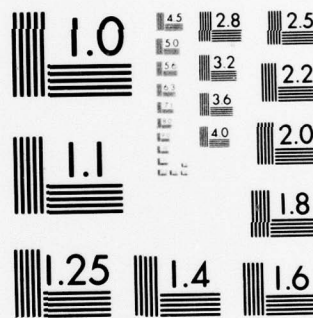
NL

4 OF 4

AD
A062790



END
DATE
FILMED
3-79
DDC



MICROCOPY RESOLUTION TEST CHART
NATIONAL BUREAU OF STANDARDS-1963-A

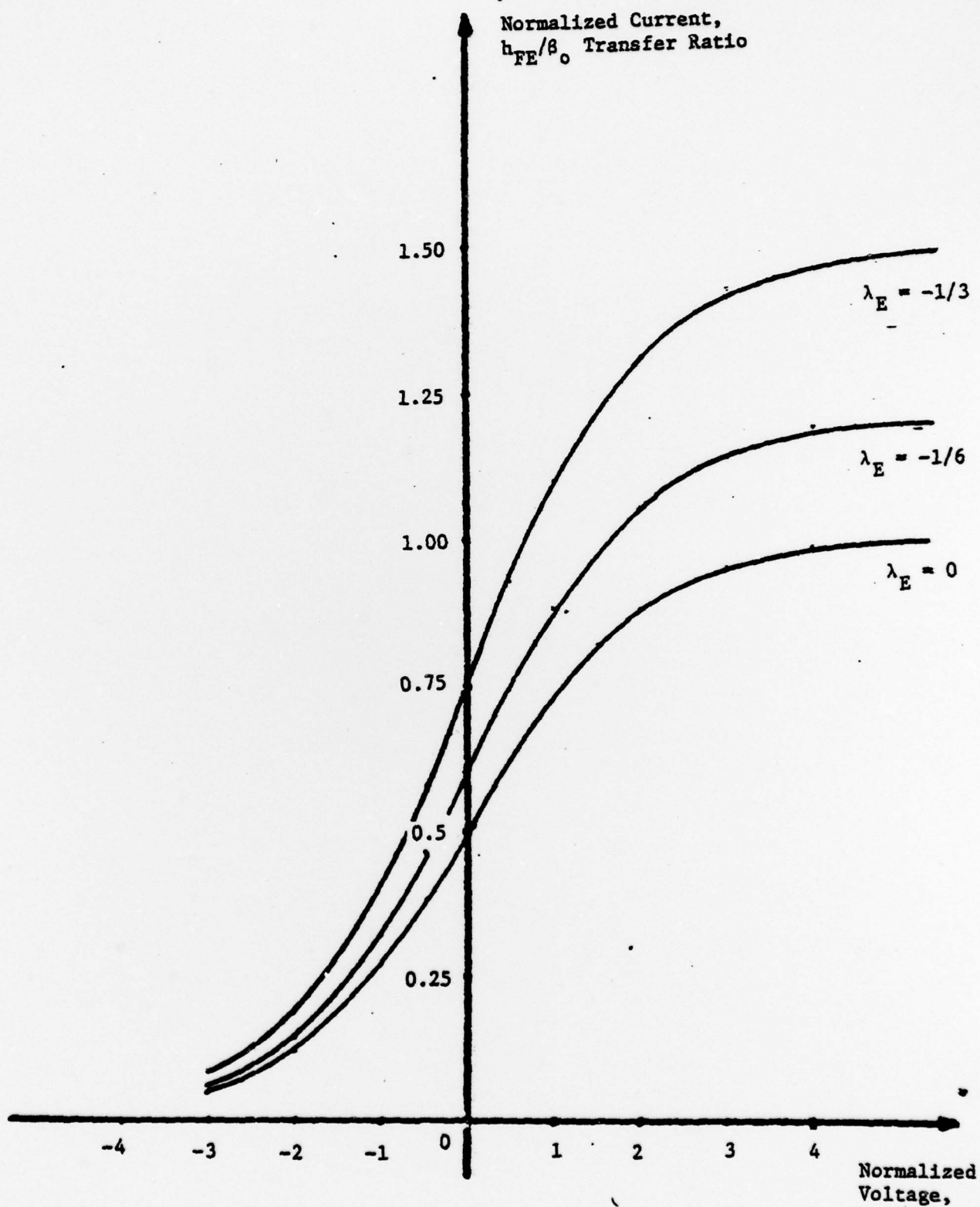


Figure (2). Forward Large-Signal, Static Current Transfer Characteristic Predicted by Model of Figure (1).

$$\left(\frac{N_E - 1}{N_E} \right) \left(\frac{V_E - V_K}{V_T} \right)$$

$I_{\phi R}$, respectively, such that

$$\beta_{\phi} = \frac{\beta_o}{1 + \beta_o I_{\phi} / I_S} \quad (16)$$

$$I_{\phi R} = I_{ER} + I_{\phi o}. \quad (17)$$

A number of noteworthy comments can be offered at this juncture. First, only two constant parameters, I_{ϕ} and $I_{\phi o}$, are required to establish neutron-induced changes in the current gain response over the range of very low-to-moderate injection levels. In particular, parameter I_{ϕ} serves to attenuate the maximum current transfer ratio at moderate current levels, while $I_{\phi o}$ influences the nature of h_{FE} in low injection regimes. The latter point becomes clear when one replaces I_{ER} and β_o in (14) by $I_{\phi R}$ and β_{ϕ} to obtain

$$V_{K\phi} = V_K + \left(\frac{N_E}{N_E - 1} \right) V_{TE} \ln \left[\frac{1 + I_{\phi o} / I_{ER}}{1 + \beta_o I_{\phi} / I_S} \right] \quad (18)$$

Thus, the base-emitter junction bias commensurate with an h_{FE} that is one-half of the maximum current transfer ratio at moderate current levels shifts as a function of the radiation parameters, I_{ϕ} and $I_{\phi o}$. Note, however, that while the maximum current transfer ratio always decreases in response to neutron irradiation, the half-gain junction bias level does not necessarily change, since if $I_{\phi o} / I_{ER} = \beta_o I_{\phi} / I_S$, $V_{K\phi} \equiv V_K$. In effect, the voltage change, $V_{K\phi} - V_K$, monitors the relative deposition of energy between the active and inactive portions of the base-emitter junction.

A second interesting point is that (16) can be written as

$$\frac{1}{\beta_{\phi}} = \frac{1}{\beta_o} + \frac{I_{\phi}}{I_S}, \quad (19)$$

which is precisely of the form of the classical Messenger-Spratt relationship. Indeed, a comparison of (1) and (19) infers the I_{ϕ} relates to neutron damage constant K_{ϕ} and fluence ϕ in accordance with

$$I_{\phi} = K_{\phi} \tau_{FO} I_S \phi. \quad (20)$$

It is critical to note that since I_{ϕ} is a constant model parameter, τ_{FO} is necessarily a constant. This is to say that τ_{FO} is the minority carrier transit time across a field-neutral base. Since a field-neutral base is ensured at moderate currents only under the condition of a strongly back-biased collector-base junction, and since τ_{FO} is inversely proportional to common-emitter gain bandwidth product f_T , (20) is meaningfully expressed as

$$I_{\phi} = \left(\frac{K_{\phi}}{2\pi f_{TMAX}} \right) I_S \phi, \quad (21)$$

where f_{TMAX} is understood to be the value of f_T appropriate to linear active operation of a BJT subjected to strong collector-base back bias.

4.0 HIGH-INJECTION CHARACTERISTICS

When the base-emitter junction is strongly forward biased, the term involving Q_{FN} in (9) cannot be ignored. Moreover, since N_E is larger than unity, I_{BE} is much greater than I_{BEN} and thus, the net base current is closely approximated by the right hand side of (7). It follows that for $V_C \ll 0$, (7) and (9) combine to produce

$$\frac{h_{FE}}{\beta_0} = \frac{1}{(1 + \lambda_E) + \frac{Q_{FN} I_C}{I_S}}. \quad (22)$$

Equation (22) is plotted in Figure (3), wherein it is understood that zero collector current ($I_C = 0$) is in one-to-one correspondence with the moderate current levels associated with regions on the far right hand side in the graph of Figure (2). Observe in (22) that the high-injection current transfer ratio attenuates to one-half of its moderate current value at a collector current, say I_K , given by

$$I_K = \frac{(1 + \lambda_E) Q_{BO}}{\tau_F}. \quad (23)$$

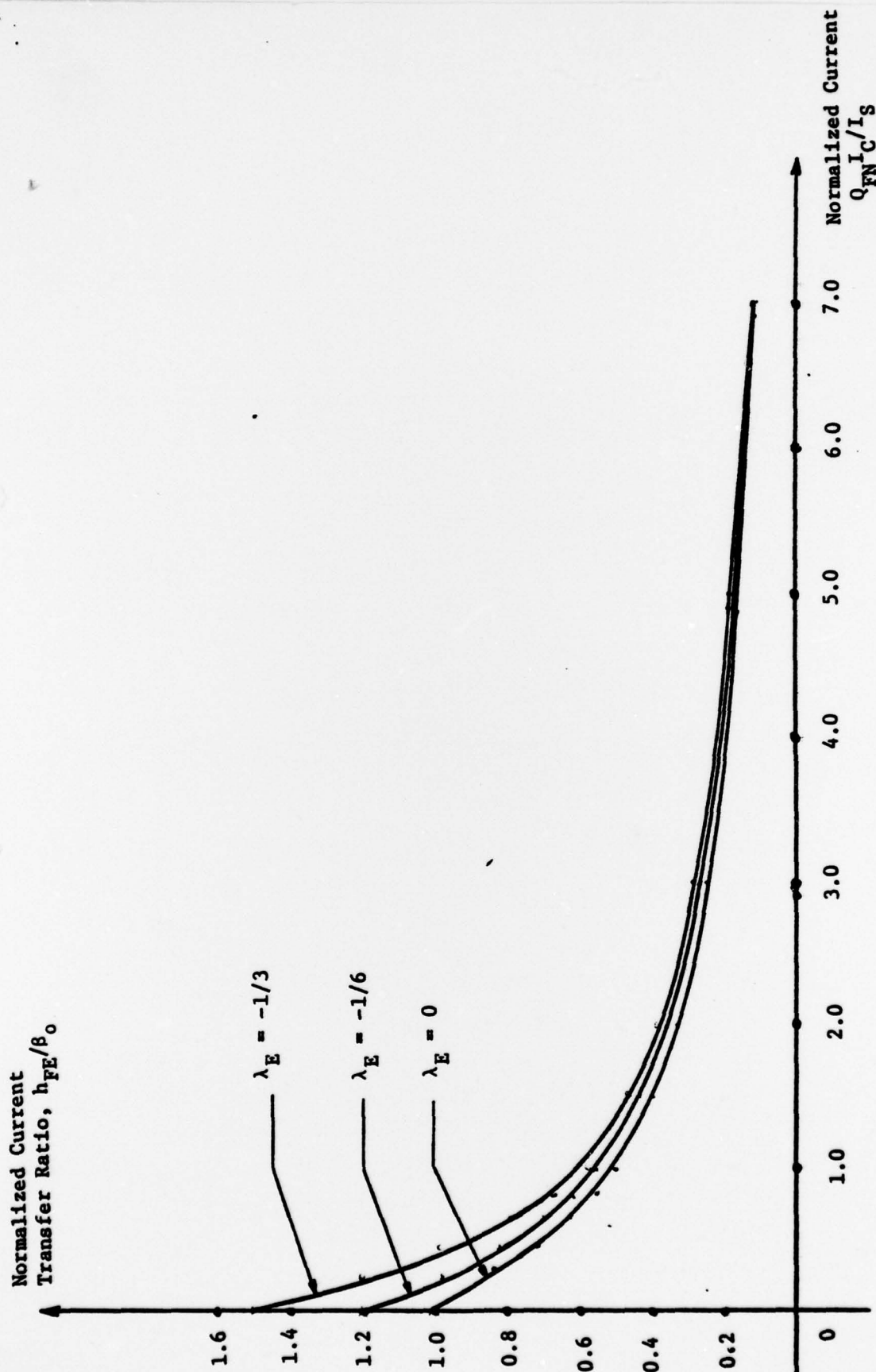


Figure (3). Forward Current Transfer Ratio At High-Injection Levels.

In arriving at (23), (10) is utilized to express I_K in terms of base region transit time, τ_F . It should be pointed out that the actual dependence of h_{FE} on collector current is more complicated than suggested by (22) and (23), since base pushout at high-injection levels incurs a dependence of τ_F (and hence, Q_{FN}) on current I_C and the voltage parameter, λ_E .

The development of a model to simulate neutron-induced changes in the high-injection current transfer characteristics derives from two observations. First, parameter β_0 attenuates to β_ϕ , as defined by (16). Thus, β_0 in (22) is replaced by β_ϕ , thereby incurring a uniform downward shift in the h_{FE} curves portrayed in Figure (3). Second, the majority carrier concentration in the base decreases from Q_{BO} to $Q_{B\phi}$ in accordance with the semi-empirical relationship [9]

$$Q_{B\phi} = \frac{Q_{BO}}{1 + K_B \phi}, \quad (24)$$

where K_B can be thought of as charge damage constant which reflects neutron-induced decreases in majority carrier concentration. Upon replacement of Q_{BO} in (10) by $Q_{B\phi}$, one concludes that the irradiated value of Q_{FN} is

$$Q_{FN\phi} = Q_{FN}(1 + K_B \phi), \quad (25)$$

which directly supplants pre-irradiated parameter Q_{FN} in (22). Note, however, that such a replacement of variables is equivalent to allowing the transit time to assume an irradiated value, $\tau_{F\phi}$, of

$$\tau_{F\phi} = \tau_F(1 + K_B \phi). \quad (26)$$

There are at least two important ramifications of (26). First and foremost, the equation allows for the simulation of neutron-induced perturbations in the gain-bandwidth product, as well as neutron-induced changes in the forward current transfer ratio. This statement exploits the simple fact that for collector currents in excess of a critical value, say $I_0(V'_C)$,

$$f_T = \frac{1}{2\pi\tau_F}, \quad I_C > I_0. \quad (27)$$

In (27), τ_F is a function of both collector current I_C and collector junction bias voltage, V_C' . This functional relationship, which is portrayed graphically by Figure (4), is mathematically defined by a so-called "base-pushout function," $B_F(I_C, V_C')$, such that

$$\tau_F = \tau_{FO} B_F(I_C, V_C') = \frac{B_F(I_C, V_C')}{2\pi f_{TMAX}} \quad (28)$$

The current parameter, $I_0(V_C')$ which defines the onset of BJT entry into high-injection operating regimes, and the pushout function, $B_F(I_C, V_C')$, can be related to such device processing characteristics as epitaxial layer doping, base and epitaxial layer geometries, minority carrier diffusivities, and the like [8], [10]. Alternatively, the behavior of τ_F in high-injection domains can be modeled by empirical equations whose parameters derive conveniently from measured f_T -characteristics [11]. The upshot of the matter is that (26) allows for the simulation of f_T over both moderate and high injection regimes since if τ_F in (27) is replaced by $\tau_{F\phi}$, (26) through (28) infer an irradiated value of f_T that is given by

$$f_{T\phi} = \frac{1}{2\pi\tau_{FO}(1 + K_B\phi)B_F(I_C, V_C')} = \frac{f_T}{1 + K_B\phi} \quad (29)$$

for $I_C > I_0(V_C')$.

It is useful to interject that for $I_C \leq I_0(V_C')$, (26) remains applicable to the problem of simulating gain-bandwidth product characteristics. For collector currents not exceeding $I_0(V_C')$, the base pushout function is unity and

$$f_T = \frac{1}{2\pi[\tau_{FO} + V_{TE}C_T/I_C]} \quad (30)$$

where C_T , the sum of the transition capacitances of both junctions, is nominally insensitive to neutron fluence. Clearly, the neutron irradiated value of low-current f_T is obtained by replacing τ_{FO} in (30) by $\tau_{F\phi}$, as defined by (26). Unlike the uniform neutron-incurred degradation of f_T at high collector currents, the effect of neutrons on low-current f_T is seen to be non-uniform, owing to the relatively small influence which neutron fluence exerts on transition layer storage dynamics.

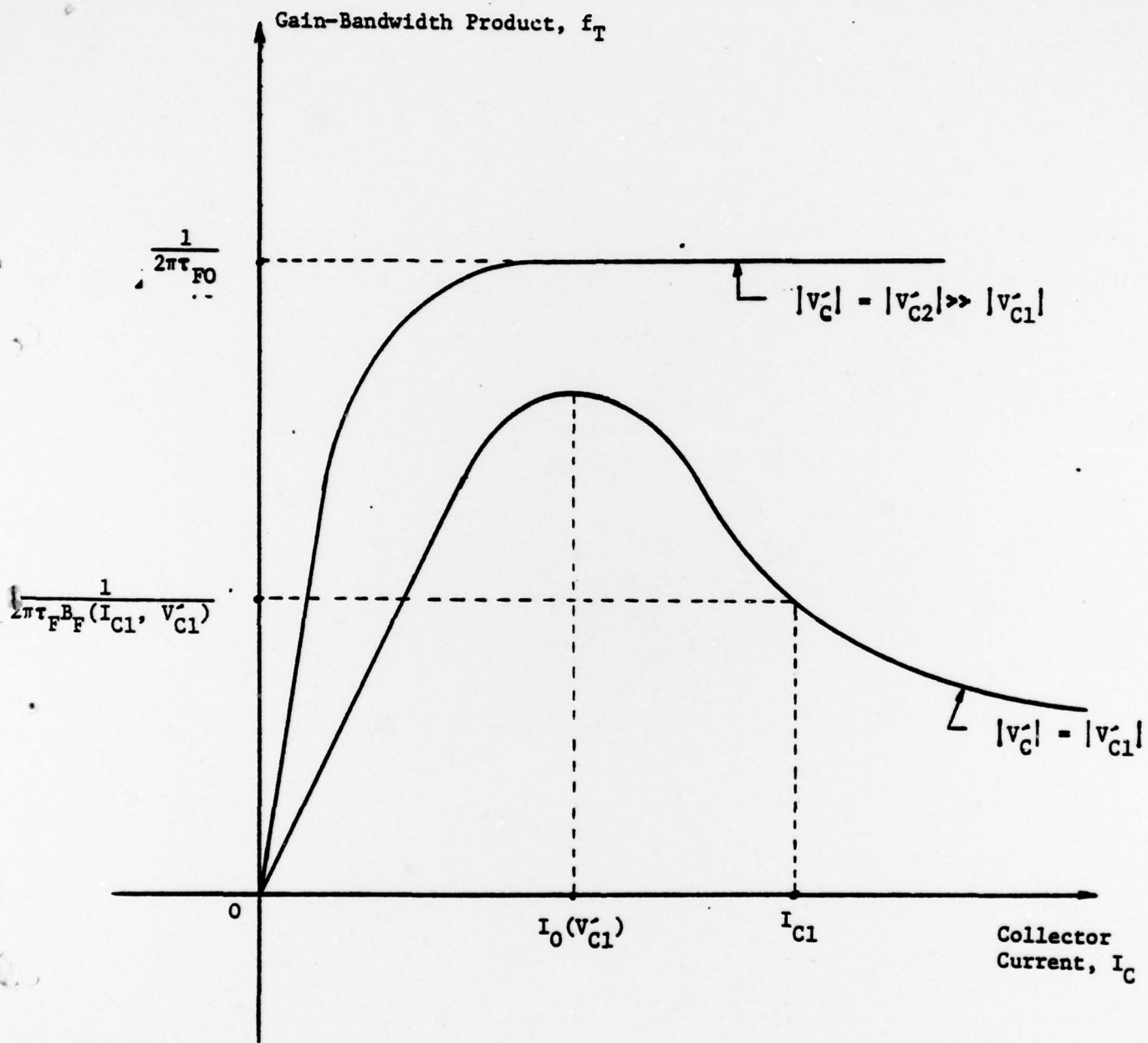


Figure (4). Common-Emitter Gain-Bandwidth Product as a Function of Voltage and Current.

A second ramification of (26) derives directly from the observation that this equation is predicated on the fundamental assumption that the irradiated value of base region majority charge is linearly related to its pre-irradiated counterpart by an expression of the form of (24). Since both Q_{RN} in (11) and Q_{FN} in (10) are inversely proportional to Q_{BN} , it is clear that the irradiated inverse transit time behaves in a manner that is identical to the forward transit time behavior prescribed by (26).

5.0 CONCLUSIONS

The fundamental premise of this paper is that an existing and reasonably accessible electrical model of a bipolar junction transistor is easily modified to incorporate the cognate effects of BJT exposure to a given neutron fluence, ϕ . The foundation for the required modifications is the fact that (1) additional base current must be supplied if the collector current of an irradiated BJT is to be maintained at its pre-irradiated value, and (2) the majority charge in the active base decreases in proportion to the neutron fluence. The additional base current and charge perturbation are stipulated by (15) and (24), respectively, which in turn define three neutron-related modeling parameters; namely, I_ϕ , $I_{\phi 0}$, and K_B .

Parameter I_ϕ can be determined in either of two ways. One way exploits (19), which entails a comparison of the pre-irradiated and post-irradiated values of the gain parameter β_0 , as defined in Figure (2). A second technique is to relate I_ϕ to a known current gain damage constant in accordance with (20) or (21). Parameter $I_{\phi 0}$ requires an investigation of current transfer ratio evidenced at low current levels. In particular, the base-emitter voltage (which closely approximates the base-emitter junction bias at low currents) is measured prior and subsequent to neutron irradiation to deduce $I_{\phi 0}$ by way of (18). Finally, K_B is most easily estimated by monitoring pre-irradiated and irradiated f_T at fixed current and voltage appropriate to operation in high-injection regimes. The equation of interest is (29).

It is important to note that while parameters I_ϕ , $I_{\phi 0}$, and K_B are constants, their correct utilization enables the simulation of the damaging effects of neutron bombardment over all forward active regimes of BJT operation. Indeed, parameter K_B is ostensibly applicable to gain-bandwidth

product studies of bipolar devices operated in inverted or saturated regimes. Although inverse BJT operation is not specifically addressed in this work, parameters analogous to I_ϕ and $I_{\phi 0}$ can presumably be found to simulate inverted current transfer ratio characteristics. The only problem inherent in this presumption is the difficulty encountered in monitoring pre-irradiated inverted performance without incurring permanent damage at the base-emitter interface.

It is believed that the theory of neutron effects modeling developed in this paper is applicable to a broad range of BJT simulation and prediction problems. For example, over a wide range of practical bipolar device operation, the dependence of collector current on temperature at fixed bias voltage is given by [12]

$$I_C = A T^M e^{-V_{GO}/V_{TE}}, \quad (31)$$

where V_{GO} is the bandgap voltage and constants A and M are determined by device fabrication processes. Clearly, M is critical to the determination of the thermal sensitivity of collector current. It turns out that published data related to the dependence of minority carrier mobility on base region impurity concentration infers [2] that M behaves approximately as

$$M \approx \ln(Q_{BO}/Q_{MO}) - M_0, \quad (32)$$

where Q_{MO} and M_0 are constants. The irradiated value of M evolves from replacement of Q_{BO} by $Q_{B\phi}$, whence by (31), the neutron-induced thermal sensitivity of collector current is easily discerned.

6.0 REFERENCES

1. F. Larin, Radiation Effects in Semiconductor Devices, New York: John Wiley & Sons, Inc., 1968, Chapter 9.
2. S. M. Sze, Physics of Semiconductor Devices, New York: John Wiley & Sons, Inc.
3. J. S. Brugler, "Silicon Transistor Biasing for Linear Collector Current Temperature Dependence," IEEE Journal of Solid-State Circuits, Vol. SC-2, pp. 57-58, June 1967.
4. G. Messenger and J. Spratt, "The Effects of Neutron Irradiation on Germanium and Silicon," Proceedings of IRE, pp. 1038-1044, June 1958.
5. J. J. Ebers and J. L. Moll, "Large-Signal Behavior of Junction Transistors," Proceedings of IRE, Vol. 42, pp. 1761-1772, December 1954.
6. H. K. Gummel and H. C. Poon, "An Integral Charge-Control Model of Bipolar Transistors," Bell System Technical Journal, Vol. 49, pp. 115-120, May-June 1970.
7. J. M. Early, "Effects of Space-Charge Layer Widening In Junction Transistors," Proceedings of IRE, Vol. 40, pp. 1401-1406, November 1952.
8. J. Choma, Jr., "A Process-Oriented Model for the Simulation of Base Pushout In Integrated Bipolar Devices," IEEE Transactions on Electron Devices, Vol. ED-22, pp. 1079-1086, December 1975.
9. Reference #1, pp. 157-169.
10. J. Choma, Jr., "Process-Oriented, High-Injection Circuit Models for Integrated Bipolar Junction Transistors," ONR Final Report, No. N00014-75-C-1177, November 1976.
11. J. Choma, Jr., "A Curve-Fitted Circuits Model for Bipolar Transistor f_T Roll-Off at High Injection Levels," IEEE Journal of Solid-State Circuits, Vol. SC-11, pp. 346-348, April 1976.
12. K. E. Kuijk, "A Precision Reference Voltage Source," IEEE Journal of Solid-State Circuits, Vol. SC-8, pp. 222-225, June 1973.

APPENDIX F

ACKNOWLEDGEMENTS

The number of people who contributed to this research project are too numerous to list herewith. However, I would be neglecting my professional obligations if I did not offer my personal congratulations for a job excellently done to Mr. E. J. Mock, who served as the senior engineer on this project. Mr. Mock almost single-handedly developed the PAREV program and worked diligently to ensure continuum among the various phases of this project.

I should also like to thank Mr. G. I. Haas, who supported Mr. Mock during the developmental phase of EQSOLVE. Last, but not least, I thank Mr. R. K. Ellis, the senior research engineer in my section, for bringing much needed experimental testing expertise to the program.